SUBTASK 1.10 – CO_2 STORAGE AND ENHANCED BAKKEN RECOVERY RESEARCH PROGRAM

Final Report

(for the period May 1, 2012, through May 31, 2014)

Prepared for:

AAD Document Control

National Energy Technology Laboratory
U.S. Department of Energy
626 Cochrans Mill Road
PO Box 10940, MS 921-107
Pittsburgh, PA 15236-0940

Cooperative Agreement No.: DE-FC26-08NT43291
DOE Technical Monitor: Andrea McNemar

Prepared by:

James A. Sorensen
Steven B. Hawthorne
Steven A. Smith
Jason R. Braunberger
Guoxiang Liu
Robert C.L. Klenner
Lisa S. Botnen
Edward N. Steadman
John A. Harju
Thomas E. Doll

Energy & Environmental Research Center
University of North Dakota
15 North 23rd Street, Stop 9018
Grand Forks, ND 58202-9018

2014-EERC-05-16 May 2014

EERC DISCLAIMER

LEGAL NOTICE This research report was prepared by the Energy & Environmental Research Center (EERC), an agency of the University of North Dakota, as an account of work sponsored by the U.S. Department of Energy (DOE) National Energy Technology Laboratory (NETL); the North Dakota Industrial Commission (NDIC); Marathon Oil Corporation; Continental Resources, Inc.; and TAQA North Ltd. Because of the research nature of the work performed, neither the EERC nor any of its employees makes any warranty, express or implied, or assumes any legal liability or responsibility for the accuracy, completeness, or usefulness of any information, apparatus, product, or process disclosed or represents that its use would not infringe privately owned rights. Reference herein to any specific commercial product, process, or service by trade name, trademark, manufacturer, or otherwise does not necessarily constitute or imply its endorsement or recommendation by the EERC.

ACKNOWLEDGMENT

This material is based upon work supported by DOE NETL under Award No. DE-FC26-08NT43291.

DOE DISCLAIMER

This report was prepared as an account of work sponsored by an agency of the United States Government. Neither the United States Government, nor any agency thereof, nor any of their employees, makes any warranty, express or implied, or assumes any legal liability or responsibility for the accuracy, completeness, or usefulness of any information, apparatus, product, or process disclosed, or represents that its use would not infringe privately owned rights. Reference herein to any specific commercial product, process, or service by trade name, trademark, manufacturer, or otherwise does not necessarily constitute or imply its endorsement, recommendation, or favoring by the United States Government or any agency thereof. The views and opinions of authors expressed herein do not necessarily state or reflect those of the United States Government or any agency thereof.

NDIC DISCLAIMER

This report was prepared by the EERC pursuant to an agreement partially funded by the Industrial Commission of North Dakota, and neither the EERC nor any of its subcontractors nor the North Dakota Industrial Commission nor any person acting on behalf of either:

(A) Makes any warranty or representation, express or implied, with respect to the accuracy, completeness, or usefulness of the information contained in this report or that the use of any information, apparatus, method, or process disclosed in this report may not infringe privately owned rights; or

(B) Assumes any liabilities with respect to the use of, or for damages resulting from the use of, any information, apparatus, method, or process disclosed in this report.

Reference herein to any specific commercial product, process, or service by trade name, trademark, manufacturer, or otherwise does not necessarily constitute or imply its endorsement, recommendation, or favoring by the North Dakota Industrial Commission. The views and opinions of authors expressed herein do not necessarily state or reflect those of the North Dakota Industrial Commission.

SUBTASK 1.10 – CO_2 STORAGE AND ENHANCED BAKKEN RECOVERY RESEARCH PROGRAM

ABSTRACT

Small improvements in productivity could increase technically recoverable oil in the Bakken Petroleum System by billions of barrels. The use of CO_2 for enhanced oil recovery (EOR) in tight oil reservoirs is a relatively new concept. The large-scale injection of CO_2 into the Bakken would also result in the geological storage of significant amounts of CO_2. The Energy & Environmental Research Center (EERC) has conducted laboratory and modeling activities to examine the potential for CO_2 storage and EOR in the Bakken. Specific activities included the characterization and subsequent modeling of North Dakota study areas as well as dynamic predictive simulations of possible CO_2 injection schemes to predict the potential CO_2 storage and EOR in those areas. Laboratory studies to evaluate the ability of CO_2 to remove hydrocarbons from Bakken rocks and determine minimum miscibility pressures for Bakken oil samples were conducted. Data from a CO_2 injection test conducted in the Elm Coulee area of Montana in 2009 were evaluated with an eye toward the possible application of knowledge gained to future injection tests in other areas. A first-order estimation of potential CO_2 storage capacity in the Bakken Formation in North Dakota was also conducted. Key findings of the program are as follows.

The results of the research activities suggest that CO_2 may be effective in enhancing the productivity of oil from the Bakken and that the Bakken may hold the ability to geologically store between 120 Mt and 3.2 Gt of CO_2. However, there are no clear-cut answers regarding the most effective approach for using CO_2 to improve oil productivity or the storage capacity of the Bakken. The results underscore the notion that an unconventional resource will likely require unconventional methods of both assessment and implementation when it comes to the injection of CO_2. In particular, a better understanding of the fundamental mechanisms controlling the interactions between CO_2, oil, and other reservoir fluids in these unique formations is necessary to develop accurate assessments of potential CO_2 storage and EOR in the Bakken. In addition, existing modeling and simulation software packages do not adequately address or incorporate the unique properties of these tight, unconventional reservoirs in terms of their impact on CO_2 behavior. These knowledge gaps can be filled by conducting scaled-up laboratory activities integrated with improved modeling and simulation techniques, the results of which will provide a robust foundation for pilot-scale field injection tests. Finally, field-based data on injection, fluid production, and long-term monitoring from pilot-scale CO_2 injection tests in the Bakken are necessary to verify and validate the findings of the laboratory- and modeling-based research efforts.

This subtask was funded through the EERC–U.S. Department of Energy (DOE) Joint Program on Research and Development for Fossil Energy-Related Resources Cooperative Agreement No. DE-FC26-08NT43291. Nonfederal funding was provided by the North Dakota Industrial Commission, Marathon Oil Corporation, Continental Resources Inc., and TAQA North, Ltd.

TABLE OF CONTENTS

Continued. . .

TABLE OF CONTENTS (continued)

LIST OF FIGURES

Continued. . .

LIST OF FIGURES (continued)

Continued. . .

LIST OF FIGURES (continued)

Continued. . .

LIST OF FIGURES (continued)

LIST OF TABLES

SUBTASK 1.10 – CO_2 STORAGE AND ENHANCED BAKKEN RECOVERY RESEARCH PROGRAM

EXECUTIVE SUMMARY

Total oil in place estimates for the Bakken Petroleum System range from 160 billion barrels (Bbbl) to over 900 Bbbl. Most estimates for primary recovery range from 3% to 6%, depending on reservoir characteristics. Therefore, small improvements in productivity could increase technically recoverable oil in the Bakken by billions of barrels. While the use of CO_2 in conventional reservoirs is a widely applied practice, its use for enhanced oil recovery (EOR) in tight oil reservoirs is a relatively new concept. If successful, the large-scale injection of CO_2 into the Bakken will not only increase oil productivity but will also result in the geological storage of significant amounts of CO_2. The Energy & Environmental Research Center (EERC) has conducted laboratory and modeling activities to examine the potential for CO_2 storage and EOR in the Bakken. Specific activities included 1) the characterization of rock samples from four different areas of the Bakken in North Dakota; 2) the creation of static geologic models for two of those areas, the Bailey and Grenora areas, and subsequent dynamic simulation modeling of possible CO_2 injection schemes to predict the potential CO_2 storage and EOR in those areas; 3) laboratory studies to evaluate the ability of CO_2 to remove hydrocarbons from Bakken shales and Middle Member lithofacies; 4) laboratory determination of minimum miscibility pressures for Bakken oil samples using an innovative technique; 5) evaluation of data from a CO_2 injection test conducted in the Elm Coulee area of Montana in 2009 and the possible application of knowledge gained to future injection tests in other areas; and 6) a first-order estimation of potential CO_2 storage capacity in the Bakken Formation in North Dakota. Key findings of the program include the following:

- Initial estimates of CO_2 storage resource using the methodology for estimating geologic storage potential in oil and gas reservoirs, as outlined in the U.S. Department of Energy (DOE) Carbon Sequestration Atlas of the United States, suggest that the Bakken in North Dakota may have a CO_2 storage resource ranging from 121 Mt to 3.2 Gt. This broad range indicates that more data are required to develop more accurate assessments of CO_2 storage potential in tight oil-bearing formations such as the Bakken.

- Results of dynamic simulation modeling of the Bailey area in Dunn County suggest that the injection of CO_2 could increase oil production by as much as 50%. They also indicate that a scheme that pairs two injection wells with a single production well was the most effective approach for EOR of the schemes modeled.

- Laboratory experimental studies indicate that CO_2 can remove over 90% of hydrocarbons from Bakken reservoir rocks and up to 60% from the shales in a time frame that ranges from hours to days in small-scale elution experiments. Diffusion appears to be the primary mechanism driving the observed hydrocarbon removal.

- In the Bakken, CO_2 flow will be dominated by fracture flow, and not significantly through the rock matrix. Fracture-dominated CO_2 flow could essentially eliminate the

displacement mechanisms responsible for increased recovery in conventional reservoirs. As such, other mechanisms, such as diffusion, must be optimized in tight reservoirs.

- The Elm Coulee injection test appeared to result in a delayed improvement in oil production. The improved oil production was not seen until 6 months after the test, but it lasted for a few months.

- Simulation results indicated that diffusion may play a significant role in moving oil from the reservoir matrix into the fracture network.

- The concept that diffusion plays a significant role in CO_2 movement in the Bakken, as indicated in the laboratory and modeling results, is also supported by the delayed improvement in oil production after the Burning Tree CO_2 injection test. This suggests that the role of diffusion in the behavior of CO_2 in the Bakken should be a subject for further research.

The results of the research activities suggest that CO_2 may be effective in enhancing the productivity of oil from the Bakken and that the Bakken may hold the ability to geologically store significant amounts of CO_2. However, there are no clear-cut answers regarding the most effective approach for using CO_2 to improve oil productivity or the storage capacity of the Bakken. The results underscore the notion that an unconventional resource will likely require unconventional methods of both assessment and implementation when it comes to the injection of CO_2. With that in mind, it is clear that additional knowledge is necessary to make informed decisions regarding the design and implementation of potential injection and production schemes. In particular, a better understanding of the fundamental mechanisms controlling the interactions between CO_2, oil, and other reservoir fluids in these unique formations is necessary to develop accurate assessments of potential CO_2 storage. Another issue that must be addressed is that existing modeling and simulation software packages do not adequately address or incorporate the unique properties (e.g., microfractures, high organic carbon content, combined diffusion, adsorption, and darcy flow or the physical interactions between the injected CO_2 and formation fluids) of these tight, unconventional reservoirs in terms of their impact on CO_2 behavior. These knowledge gaps can be filled by conducting scaled-up laboratory activities integrated with improved modeling and simulation techniques, the results of which will provide a robust foundation for pilot-scale field injection tests. Finally, field-based data on injection, fluid production, and long-term monitoring from pilot-scale CO_2 injection tests in the Bakken are necessary to verify and validate the findings of the laboratory- and modeling-based research efforts.

This subtask was funded through the EERC–DOE Joint Program on Research and Development for Fossil Energy-Related Resources Cooperative Agreement No. DE-FC26-08NT43291. Nonfederal funding was provided by the North Dakota Industrial Commission, Marathon Oil Corporation, Continental Resources Inc., and TAQA North, Ltd.

SUBTASK 1.10 – CO_2 STORAGE AND ENHANCED BAKKEN RECOVERY RESEARCH PROGRAM

INTRODUCTION AND BACKGROUND

Total oil in place reserve estimates for the Bakken Formation range from a minimum of 100 billion barrels (Bbbl) to 900 Bbbl (Nordeng and Helms, 2010; Continental Resources Inc., 2012). Most estimates for primary recovery range from approximately 3% to 6% (LeFever and Helms, 2008). With such low primary recovery factors associated with this massive resource, even small improvements in productivity will add billions of barrels to the recoverable resource. Also, by employing CO_2, the Bakken could prove to be a tremendous CO_2 storage resource. The Energy & Environmental Research Center (EERC) has conducted laboratory and modeling-based activities to evaluate strategies for improving the ultimate recovery of oil from the Bakken Petroleum System and determining the potential for carbon dioxide (CO_2) storage. CO_2 has been used for enhanced oil recovery (EOR) operations in conventional reservoirs for several decades. The project presented and discussed in this report examines the potential to use CO_2 for EOR in the Bakken Petroleum System. If implemented, large-scale injection of CO_2 into the Bakken for EOR will also lead to significant storage of CO_2 in the formation. With that in mind, the project also examined the data generated by the laboratory and modeling efforts in the context of potential CO_2 storage in a tight oil formation. The project was supported by financial contributions from Marathon Oil Corporation; Continental Resources Inc.; TAQA North, Ltd.; the North Dakota Industrial Commission (NDIC) Oil and Gas Research Council (OGRC); and the U.S. Department of Energy (DOE) National Energy Technology Laboratory (NETL). Additional in-kind support in the form of unpublished, confidential reservoir characterization and operational data was also provided by Marathon Oil Corporation and Continental Resources Inc. Core samples used for the laboratory characterization and experimental activities were provided by Marathon Oil Corporation and the North Dakota Geological Survey (NDGS).

Goals and Objectives

While the use of CO_2 in conventional reservoirs is a widely applied and well-understood practice (Jarrell and others, 2002), its use for EOR in tight oil reservoirs is a relatively new concept. In conventional reservoirs, vertical heterogeneity and relative permeability characteristics can have a significant effect on the effectiveness of an EOR scheme, and fracture networks are considered to be detrimental to EOR operations (Jarrell and others, 2002). In tight oil reservoirs such as the Bakken, which rely on a sustained fracture network for the bulk of their productivity, the conventional notions of positive and negative attributes may or may not apply. These same principles can also be applied to the concept of storing CO_2 in tight oil formations. The results of the project provide insight regarding the relationships of the Bakken system and injected CO_2 under reservoir conditions.

The ultimate goal of the project was to generate previously unavailable data and technical insight that will enable operators and other stakeholders to make informed decisions regarding the use of CO_2-based technologies for Bakken EOR and CO_2 storage. The objective of the project is to use new and existing reservoir characterization and laboratory analytical data (e.g.,

core analyses, well logs, oil analyses, etc.) and state-of-the-art modeling to determine the viability of using CO_2 for EOR in the Bakken Formation. If positive results are achieved, then the application of those results can have a significant positive effect on the ultimate recovery of oil from the vast Bakken resources of North Dakota and Montana. The results of the work provide insight regarding relationships between Bakken oil, key reservoir attributes, and CO_2 under reservoir conditions toward the efficient use of CO_2 for EOR and the ability of tight oil-bearing formations to geologically store CO_2.

Overview of the Bakken Play

The Bakken Formation is currently the most productive oil-producing formation in the Williston Basin and one of the most productive tight oil plays in North America. In the U.S. portion of the Williston Basin, it occurs in North Dakota and Montana, while in Canada, it occurs in Saskatchewan and Manitoba (Figure 1). Daily oil production in the North Dakota portion of the Bakken has been as high as 950,000 bbl/day (North Dakota Industrial Commission, 2013), and estimates of total oil in place across the entire Bakken Formation range from 100 Bbbl to 900 Bbbl (Nordeng and Helms, 2010; Continental Resources Inc., 2012). While the hydrocarbon resource within the Bakken Formation is tremendous, the Bakken is considered to be an unconventional oil play because it is typically characterized by very low porosity (<10%) and permeability (<0.1 mD).

With respect to stratigraphy, the Devonian–Mississippian-age Bakken Formation in the Williston Basin typically consists of three members: the Upper, Middle, and Lower Bakken (Figure 2). In some locations, the lower shale is underlain by a unit with variable lithology referred to as the Pronghorn Member. Lithologically, the upper and lower members of the

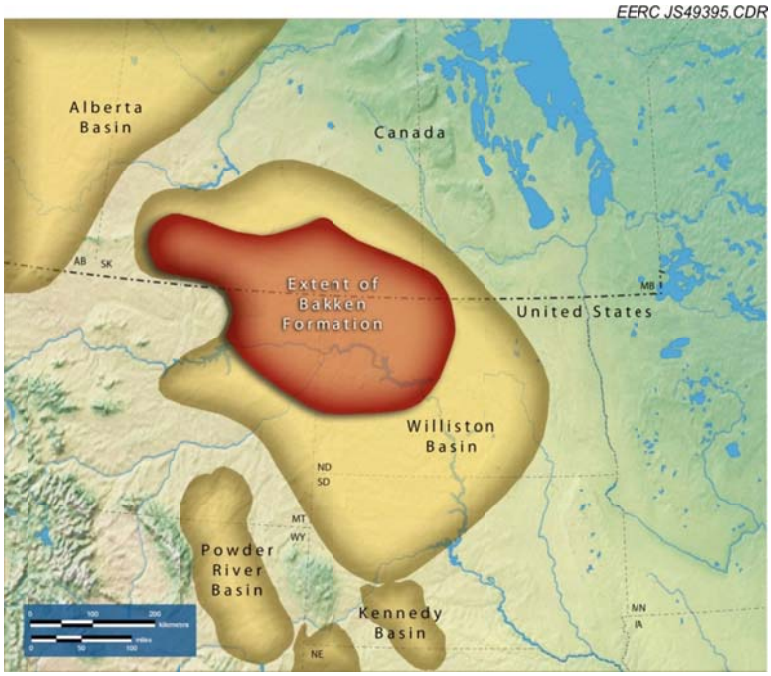

Figure 1. Map of the extent of the Bakken Formation in the Williston Basin.

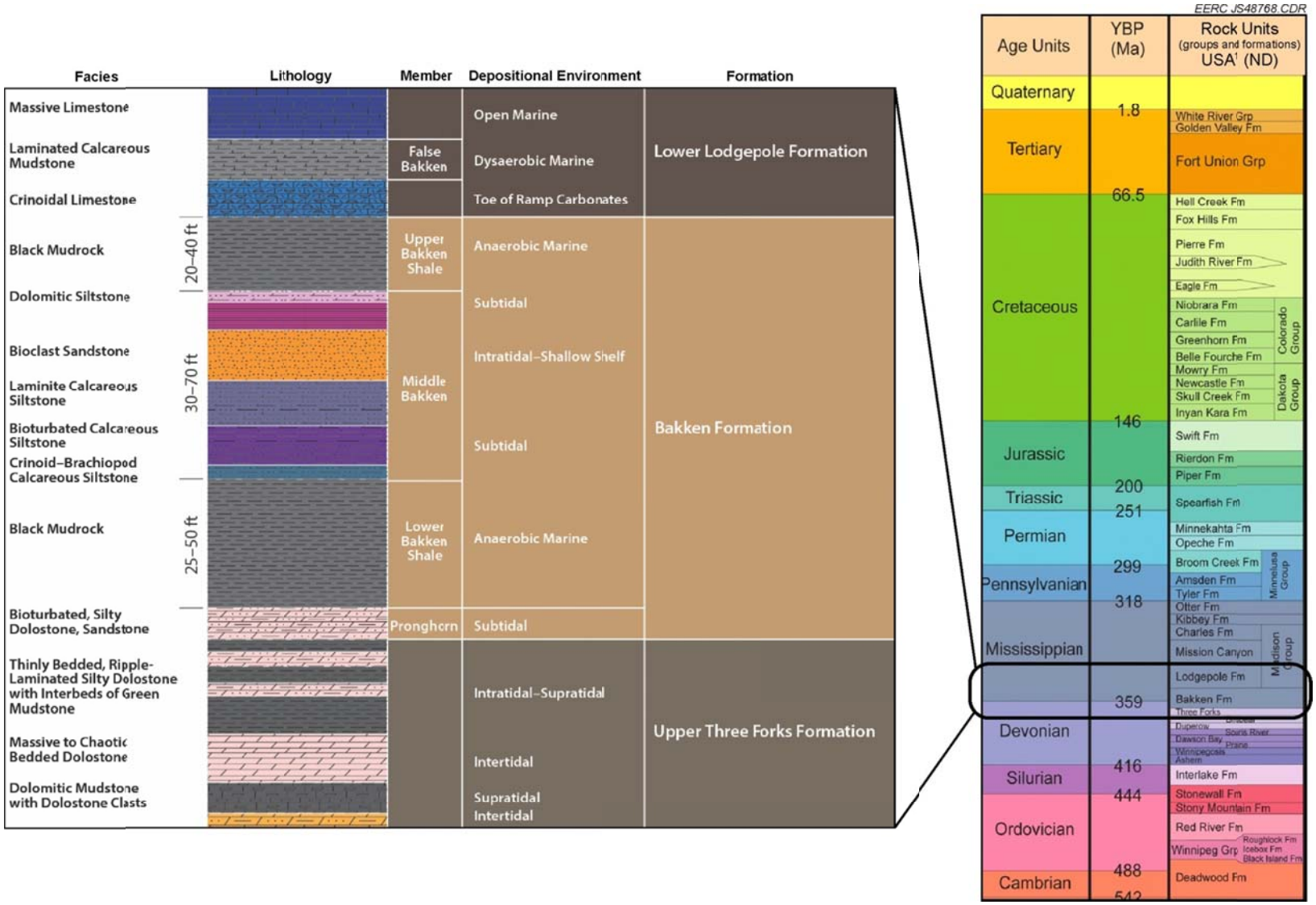

Figure 2. Stratigraphic column for rocks of the Williston Basin in North Dakota and generalized stratigraphy of the Bakken Formation in North Dakota (modified from Sonnenberg and others, 2011).

Bakken are dominated by shales rich in organic carbon that act as the source rock for oil reservoirs in the Middle Bakken and Pronghorn Members. The lithology of the Middle Bakken varies widely from clastics (including shales, silts, and sandstones) to carbonates, with five distinct lithofacies typically being identified in the North Dakota portion of the Williston Basin (Nordeng and others, 2010), although in some areas, there may be more than five and in other areas fewer. In general, all of these rocks are characterized by low porosity and permeability (Pittman and others, 2001). The geomechanical properties of the various Bakken members and lithofacies are a key component of their ability to serve as productive oil reservoirs, as those properties will dictate the size, frequency, pattern, and orientation of fracture networks (natural and artificial) at both the micro- and macroscale.

Challenges with Respect to CO_2 Storage

The obvious primary challenge of using the Bakken Formation, or any tight oil formation, as a target for large-scale storage of CO_2 is the characteristic low porosity and low permeability of the formation. The tight nature of the Bakken Formation will present challenges to both CO_2 injectivity and storage capacity. Furthermore, the presence of complex, heterogeneous lithologies (including organic-rich, oil-saturated shales) will complicate the ability to understand and predict the effectiveness of various mechanisms (e.g., diffusion, sorption, dissolution, etc.) that will be acting on CO_2 mobility and storage.

Prior to this project, there were no published studies that focused on the potential for CO_2 storage in tight oil formations. However, some work has been published on the potential storage capacity of tight, natural gas-rich shale formations, including studies on gas shales in Kentucky (Nutall and others, 2005), Texas (Uzoh and others, 2010), and the Appalachian region (Godec and others, 2011). The authors of those studies assumed that the CO_2 storage, and subsequent methane recovery, in organic-rich gas shales will be controlled by similar adsorption and desorption mechanisms as CO_2 storage and methane recovery in coal seams. In those cases, the sorptive capacity of the organic content in the shales plays a prominent role in estimating their potential CO_2 storage capacity. Unfortunately, those approaches may have limited applicability to the Bakken for two reasons. First, much of the formation is actually comprised of a combination of organic-rich shales, tight carbonates, and clastics; second, the Bakken is saturated with oil and brine as opposed to gas. The diversity of lithology and presence of oil and brine may substantially limit the effects of sorptive mechanisms on CO_2 storage as compared to the gas shale formations that have been examined in the current literature. To accurately assess the potential for tight oil formations to store CO_2, it is necessary to develop a better understanding of the fundamental mechanisms and unique formation properties (e.g., tight matrix, microfractures, high organic carbon content, etc.) controlling the interactions between CO_2 and the rocks and fluids of those tight oil formations.

Challenges with Respect to Recovery Factors

Recent total oil in place estimates for the Bakken Petroleum System range from 100 Bbbl to over 900 Bbbl. Most estimates for primary recovery range from 3% to 6%, depending on reservoir characteristics. When considering these low primary recovery factors in the context of such a large resource, it is clear that just small improvements in productivity could increase

technically recoverable oil in the Bakken by billions of barrels. The challenges of EOR within the Bakken have to do with the mobility of traditional fluids (i.e., reservoir fluids and injected water vs. CO_2, polymers, or surfactants) through natural or induced fractures relative to very low matrix permeability and the aversion of exposing swelling clays to water, which can reduce permeability and damage the formation. Further, the oil-wet nature of much of the Bakken system will dramatically minimize the effectiveness and utility of waterflooding. With these issues in mind, the use of CO_2 as a fluid for EOR in the Bakken may be effective.

The use of CO_2 for EOR in conventional reservoirs began in West Texas in the 1970s and has since been applied at locations around the world (Jarrell and others, 2002). However, its use for EOR in tight oil reservoirs is a relatively new concept. In conventional reservoirs, vertical heterogeneity, wettability, gravity, and relative permeability characteristics can have a significant effect on the effectiveness of an EOR scheme, and fracture networks could be detrimental to EOR operations (Jarrell and others, 2002). However, tight oil reservoirs, such as the Bakken, rely on natural and hydraulically induced fracture networks for their productivity. Because of the tight matrix, dominance of fractures, and oil-wet nature of the Bakken, the conventional notion of positive and negative attributes of a candidate injection reservoir may or may not apply. With respect to CO_2, fracture networks will be the primary means of its movement throughout the reservoir, and their characteristics will control the contact time that CO_2 has with the oil in the reservoir.

PROGRAM APPROACH

The EERC has conducted a research program to determine the viability of using CO_2 for EOR and carbon storage in the Bakken Formation. The key elements of the program include the development and integration of new and existing reservoir characterization and laboratory analytical data (e.g., core analyses, well logs, oil analyses, etc.) and static and dynamic modeling. The technical aspects of the project are divided according to six primary areas of activity, specifically 1) detailed geological characterization of selected Bakken reservoirs, with an emphasis on understanding the nature of naturally occurring fracture networks; 2) characterization of Bakken oils from the selected reservoirs; 3) laboratory investigations of the ability of CO_2 to diffuse into and remove hydrocarbons from Bakken rocks; 4) static model development and dynamic simulation of potential CO_2 injection scenarios; 5) evaluation of data from a pilot-scale CO_2 injection test in a Bakken well in Montana in 2009; and 6) a first-order, reconnaissance-level estimation of potential CO_2 storage capacity in the Bakken. This report will provide an overview of the project approach, results, and anticipated next steps.

In 2012, the EERC initiated a suite of experimental and modeling activities as well as a review of relevant historical data and literature to examine the potential for CO_2 EOR in the Bakken. Four study areas in North Dakota and one in Montana (Figure 3) were selected for various levels of examination (depending on the availability of data and/or samples). In North Dakota, those areas include the Bailey and Murphy Creek oil fields of Dunn County, the Rival oil field of Burke County, and the Grenora oil field of Williams County. The reservoir characterization and laboratory-based activities were conducted using data and samples from the North Dakota study areas, and subsequent modeling activities were focused on those fields as

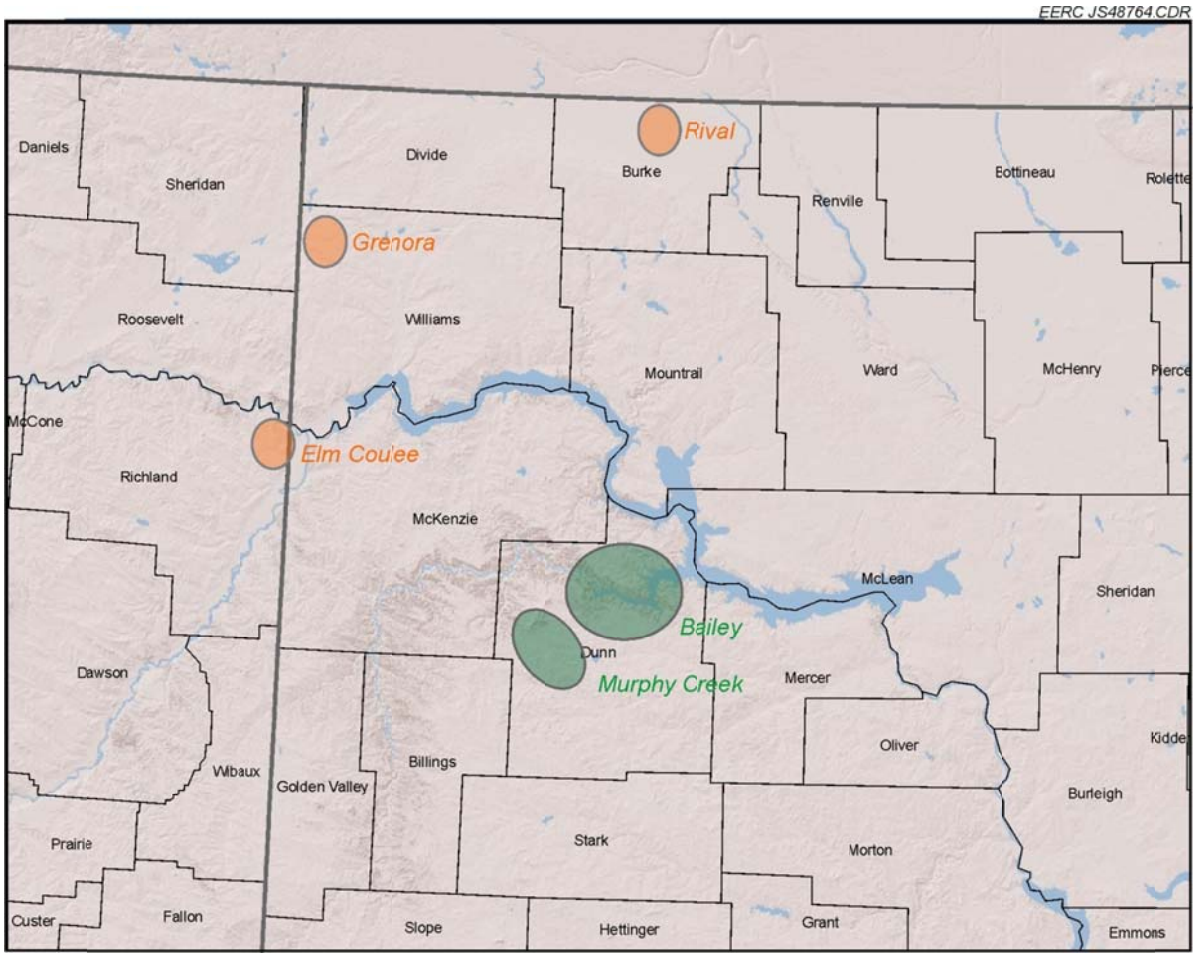

Figure 3. Map of the study areas.

well. The North Dakota fields were chosen to represent thermally mature (Bailey and Murphy Creek) and thermally immature (Rival and Grenora) portions of the Bakken. The Elm Coulee area was examined with respect to a pilot-scale CO_2 EOR test that was conducted there in 2009.

To consider the potential use of CO_2 for EOR in the Bakken, all of the ways in which CO_2 can, or may, interact with the system need to be examined. The research program included activities (graphically represented in Figure 4) that develop an understanding of:

- How CO_2 interacts with the rock matrix.
- The nature of both macroscale and microscale fractures within the reservoir.
- The roles that fractures play in moving the CO_2 in and the oil out of the matrix.
- The effects that CO_2 will have on Bakken oil under reservoir conditions (temperatures and pressures) with respect to miscibility, swelling, and diffusion.

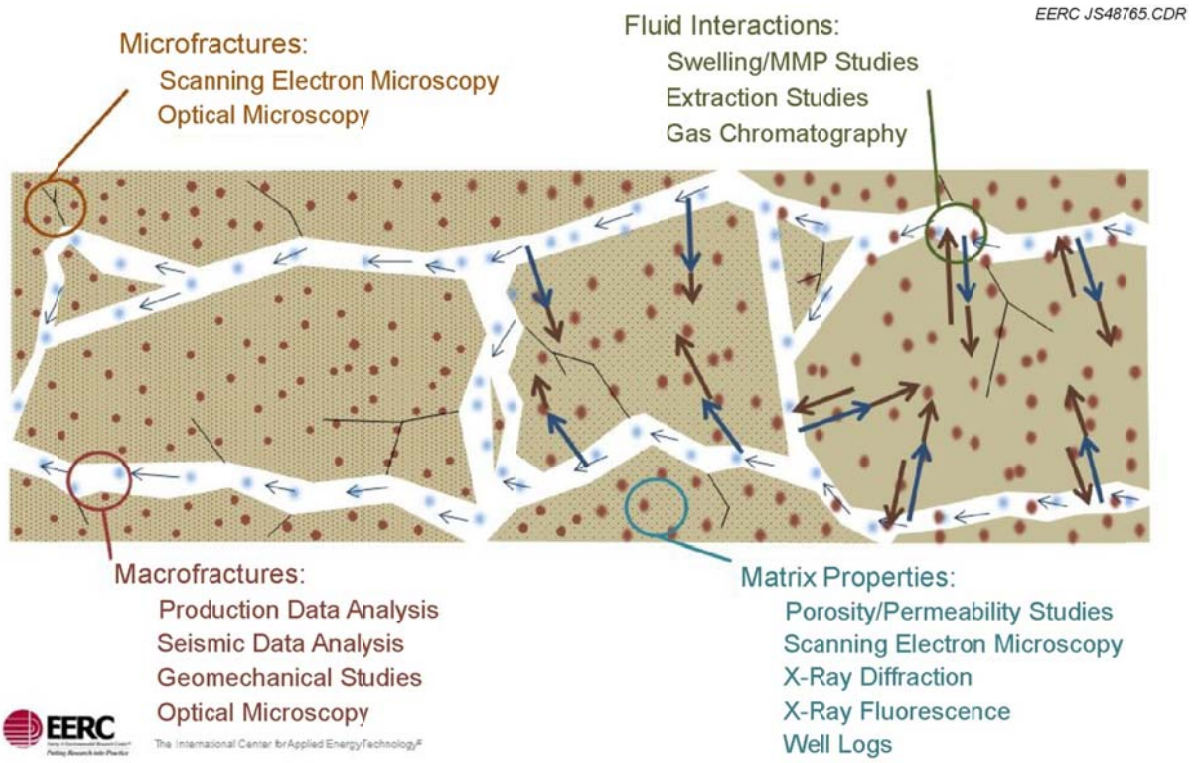

Figure 4. Aspects of the Bakken reservoir system that were evaluated under the Bakken CO_2 Enhanced Recovery Research Program.

Although it was not the subject of detailed characterization and modeling, data from the Elm Coulee pilot-scale CO_2 EOR field test were examined with the intent of providing insight with respect to lessons learned that might be applied to future CO_2 injection efforts in the Bakken.

RESERVOIR CHARACTERIZATION APPROACH AND RESULTS

Approach to Reservoir Characterization

Detailed knowledge of reservoir properties (e.g., lithology, total organic carbon, water saturation, mineralogy, natural fractures, etc.) can be used to identify and exploit relationships between those properties and CO_2 storage/oil productivity. Data describing reservoir rock and fluid properties for a given location are crucial for predicting the ability to store CO_2 and the effectiveness of any EOR scheme. The North Dakota Bakken study reservoirs were characterized from the perspective of properties considered most likely to affect storage and EOR. Laboratory techniques that may be applied include the following:

- Optical microscopy and thin-section analysis
- X-ray fluorescence (XRF) for bulk chemical analysis

- X-ray diffraction (XRD) for bulk mineral analysis
- Scanning electron microscopy (SEM) to provide high-magnification images of rock samples for analysis of microfractures (Figure 5) and rock fabric and determination of minerals (Figure 6)
- Energy-dispersive spectroscopy (EDS) to provide quantitative elemental analysis and determination of minerals
- Porosity determination through the use of a helium gas porosimeter
- Permeability to air
- Geomechanical testing of core plugs, including key parameters such as Young's modulus, Poisson's ratio, and peak strength

Working with the participating operators, the study areas were chosen and site-specific characterization work plans developed. Development of the work plan began by identifying and evaluating existing characterization data (both publicly available and confidential data from the operator) from wells in the study area. Existing well logs, production history, and core data were compiled and evaluated. Wells with core in the study area were then selected for detailed laboratory characterization as part of the research program. The specific characterization work plan for each study area varied to some extent, depending on the data gaps that were identified and the work that was required to fill those gaps. For instance, a study well may already have had

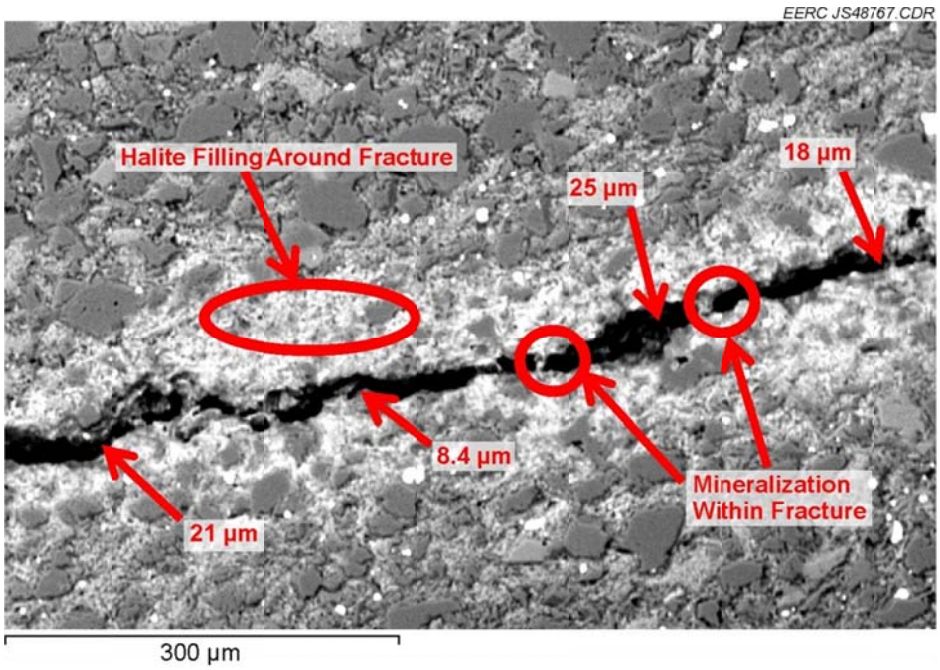

Figure 5. Example of an SEM-based evaluation of a microfracture in a Middle Bakken rock sample.

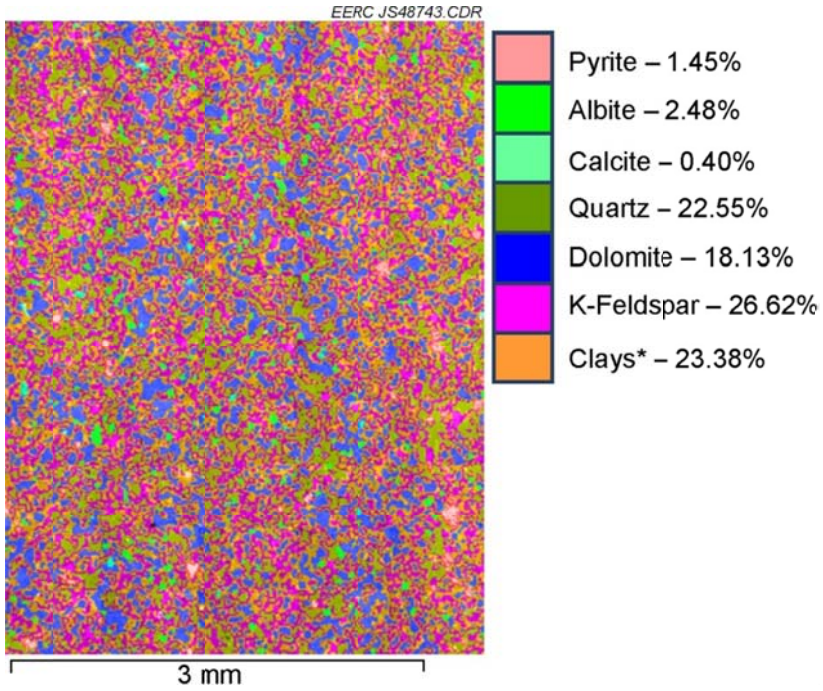

Figure 6. Example of an SEM mineral map. This mineral map is for a portion of a thin section from Rival area Lithofacies 4 (L4) in core collected from NDIC-9001.

extensive geomechanical data and thin-section descriptions but limited XRD, XRF, and SEM data. In that case, the EERC efforts targeted those analyses. The results of the previous characterization efforts and the new characterization results were combined, examined holistically in the context of potential CO_2 EOR and storage, and integrated into the modeling efforts. With respect to reservoir characterization, this report primarily presents and discusses the results of the EERC efforts. Although well file data and operator confidential data were incorporated into the modeling efforts, they are generally not specifically presented in this report.

Reservoir Fracture Characterization

The majority of oil production within unconventional reservoir systems such as the Bakken can be attributed to fractures. The oil-productive fracture networks in the Bakken are primarily attributed to hydraulic fracturing processes that are applied to create large fractures within the formation. Although artificially induced fractures are thought to be the dominant means of fluid movement in the Bakken, long-term pressure rate transient analysis of production history data suggests that natural fractures play a significant role in production (Kurtoglu and others, 2013). Open fractures that are present in situ will hold oil and can increase reservoir permeability if connected naturally or because of hydraulic fracturing operations. Hydraulic fracturing can also open natural fractures as the energy of the fracturing operation will follow the paths of least resistance. Thus the fracture network of a hydraulically fractured well in a reservoir with a high degree of natural fracturing will have a larger fracture surface area and, therefore, greater productivity as compared to a non-naturally fractured reservoir. Understanding the nature of fractures (e.g., fracture width, fracture length, orientation, and distribution) in a reservoir is

necessary to develop accurate predictions of how and where fluids will flow within that reservoir.

When considering the use of CO_2 injection as a means of EOR and CO_2 storage in the Bakken, understanding the nature of fractures is crucial because they can have both positive and negative effects on a CO_2-based EOR scheme. A fracture network in the reservoir that has a high frequency of fractures (i.e., closely spaced) and that does not extend far beyond the wellbore (i.e., short to moderate length) may maximize the surface area of rock that comes into contact with CO_2, thus serving as a means of exposing more oil-saturated rock to the beneficial effects of CO_2. It may be easier to maintain pressure in such a system, thus optimizing the effects of miscible CO_2 on the target reservoir and improving oil production. However, a fracture network that is characterized by long, wide fractures will most likely act as a thief zone for the injected CO_2, serving as conduits that allow CO_2 to quickly migrate away from the well's productive area of influence. Such a fracture network would also make it difficult to maintain the higher pressures that are necessary for an optimal CO_2 EOR operation. Conducting quantitative and semiquantitative fracture analysis on samples from the different facies within a Bakken reservoir will provide insight that will support our understanding of the nature of the fracture network in that reservoir, which, in turn, can be used to predict the effects of those fractures on CO_2 movement and EOR.

The Bakken Formation is made up of a series of complex lithofacies with variable distribution and properties. Understanding the presence and nature of fractures within and across the various lithofacies is critical to developing an accurate model of a Bakken reservoir and predicting the effectiveness of CO_2 injection for storage and EOR. Fracture analyses were conducted on core from each of the four North Dakota study areas to assist in understanding the natural fracture networks of the Bakken Formation. These analyses used a suite of fracture-logging techniques that includes a combination of EERC-developed techniques as well as additional techniques described in the literature.

During fracture logging, several parameters were measured. Those measurements served as a basis for the creation of fracture intensity logs. The fracture intensity logs were then used in the reservoir-modeling efforts of this project. The fracture-logging data include quantitative and qualitative data. The quantitative data include fracture length, fracture aperture (width), and fracture orientation (with respect to a 180° scale). These direct measurements are utilized to derive the qualitative data, which include whether a fracture is open or closed, and designate a generic orientation (three categories including horizontal, shallow dipping, and steeply dipping) for each fracture. Fracture analysis data from core samples representing the North Dakota study areas are provided in Appendix A.

Determining whether a fracture is naturally occurring or induced as part of the core collection and handling process is the single most important task when conducting a fracture analysis. Mineralization within a fracture is the most common indicator of a fracture being natural. Figure 7 shows an example of a calcite-filled fracture in a core sample from one of the Rival area wells. Fractures that are mineralized also assist in determining the in situ aperture. Stylolites, steeply dipping fractures, and fractures associated with local folding or faulting are

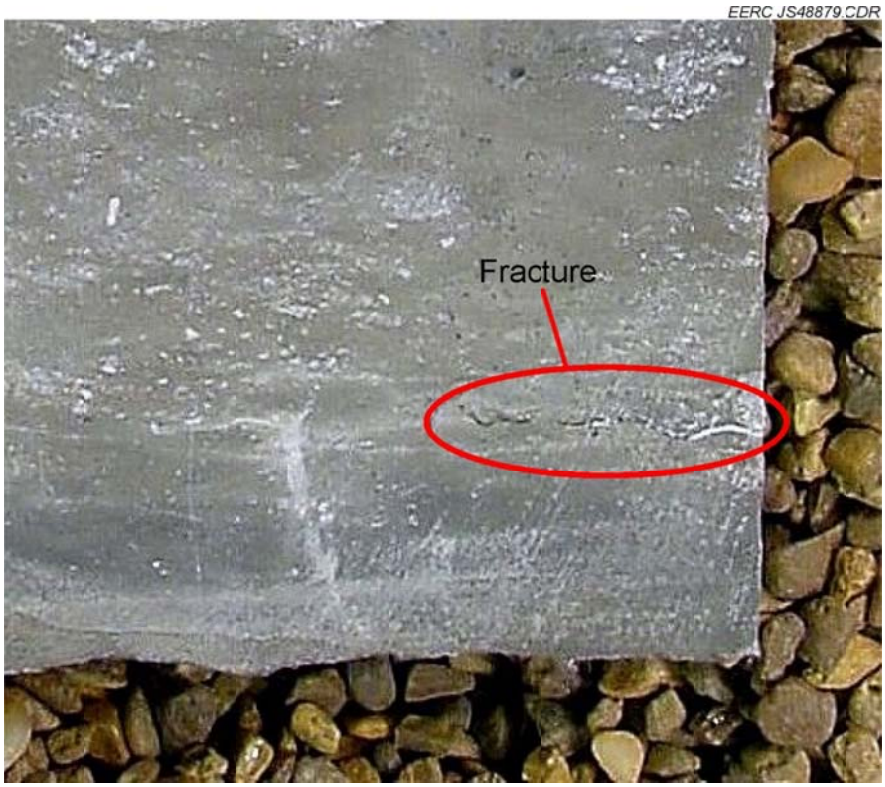

Figure 7. Photograph of a calcite-filled, shallow-dipping fracture within a Middle Bakken core from NDIC-8850 in the Rival study area.

also indications that a fracture is natural (Nelson, 2001). Induced fractures can include bedding planes that opened because of destressing, rotational core breaks during the coring process, and/or mechanical breaks such as hammer strikes that occur when the core was being removed from the core barrels (Nelson, 2001). The fractures logged during core viewing were measured for aperture, when possible, and orientation or dip.

The fracture apertures were measured using the feeler gauge method which can accurately measure apertures as low as 0.0015 inches. Fractures that were too tight for the thinnest feeler gauge to measure, but an opening could still be seen, the aperture was estimated as having a 0.0001-inch aperture. The aperture measurement of core fractures is referred to as unstressed, which typically will be larger than actually present at in situ conditions.

The orientation of each fracture was measured using a standard protractor to determine the dip angle on a 90° scale. Even though the core is typically not orientated, this measurement can still be used as the dip angle for modeling purpose. Graphs of orientation data were created to illustrate the amount of shallowly dipping (<15°) versus steeply dipping (>15°) fractures. These graphs were also used to illustrate different fracture sets within separate lithofacies of the Middle Bakken in the study areas.

While naturally occurring macrofractures (i.e., those that are visible to the naked eye in core samples) are obviously a major component of a Bakken reservoir's fracture network, microfractures also play a significant role. For instance, microfractures are known to account for much of the porosity and permeability in some of the Middle Bakken lithofacies and make significant contributions to long-term oil production in the Dunn County area (Kurtoglu and others, 2013). Microfractures were identified and characterized in thin-section samples from Middle Bakken core for each of the North Dakota study areas. The application of SEM and ultraviolet fluorescence (UVF) techniques were used to identify the microfractures and examine them for signs of being naturally occurring or induced (Figures 8 and 9). As with macrofractures, the presence of mineralization (e.g., calcite or pyrite) or clay filling in a microfracture is an indicator that it is naturally occurring. Sharp, straight edges are indicators that a microfracture is induced. In the case of those that were considered to be naturally occurring, the microfractures were further measured for aperture and length using SEM techniques (Figure 5), and their relative orientation was noted. Those data were then provided to the modeling team for application to the development of their static reservoir models.

Summary of Key Observations for Rival Area Characterization

While two wells in the Rival oil field penetrate the Bakken, neither of those wells had Bakken core collected. Therefore, the two closest (both within 5 miles) wells to the Rival Field that had Bakken core were characterized. Figure 10 shows the locations of those wells relative to the Rival Field. In both wells, seven distinct lithofacies were identified through macroscopic description of the core. For this report, the lithofacies are designated L1 at the base of the Middle Member of the Bakken (contact on the Lower Bakken shale) to L7 at the top of the Middle

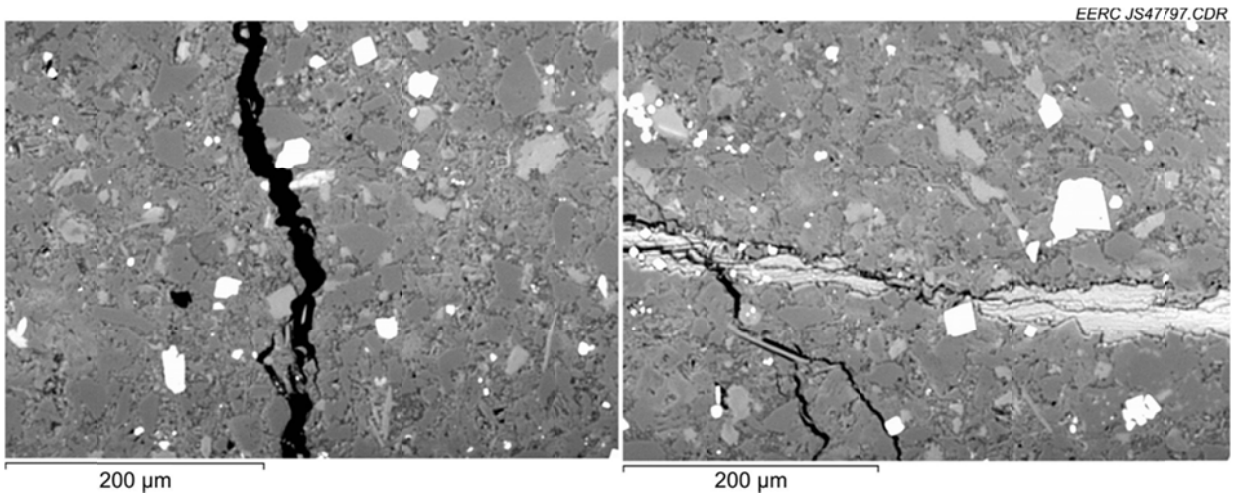

Figure 8. Microfractures in L7 from NDIC-8850. The image on the left shows a microfracture with no indications of mineralization or clay filling, suggesting that it may have been artificially induced through the drilling or sampling process. The image on the right shows a microfracture that has been partially filled by calcite, indicating that it likely formed naturally within the reservoir.

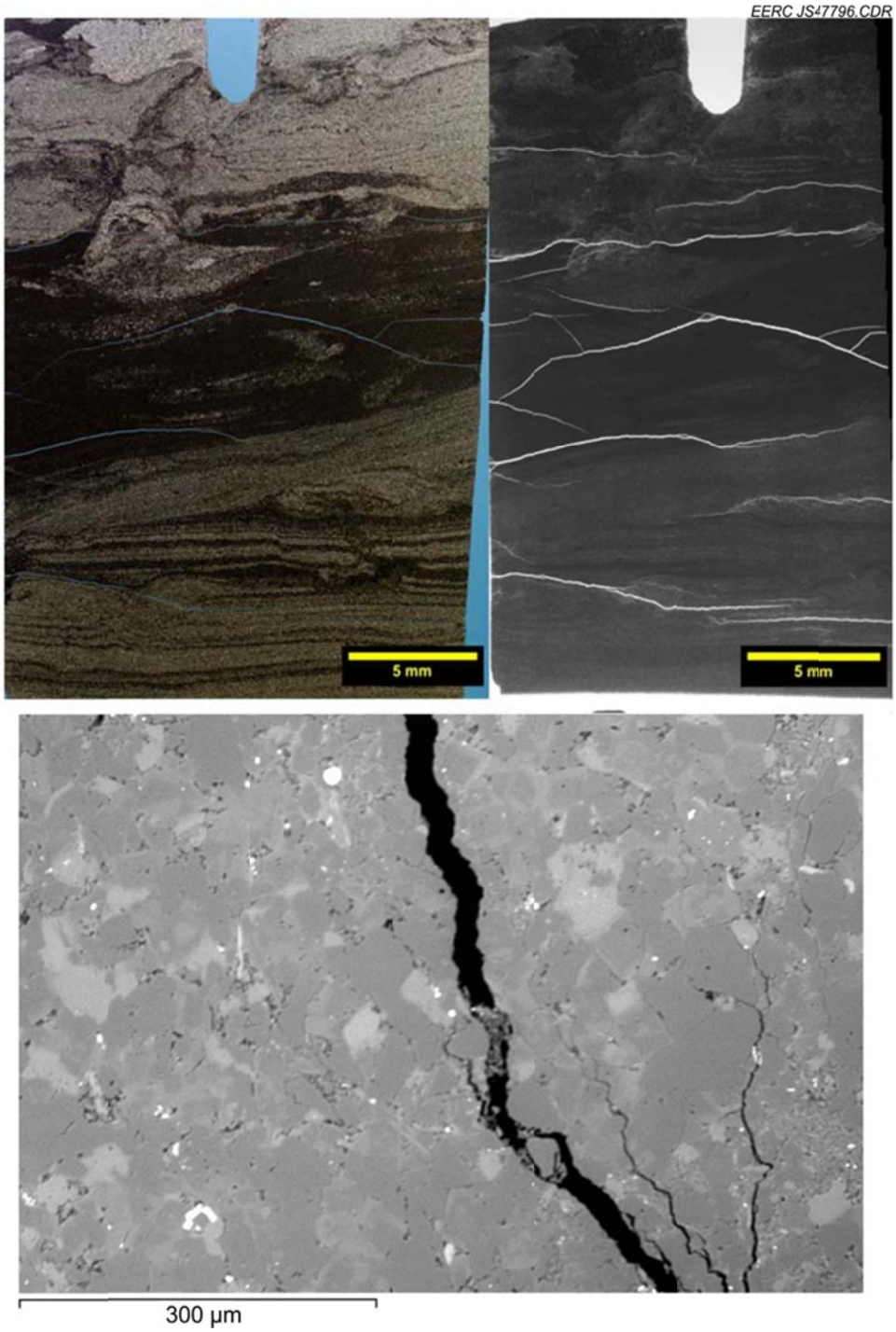

Figure 9. Images of microfractures in L8 from NDIC-20552. The top two images are (left to right) transmission and fluorescence whole-slide images of a thin section from L8 in NDIC-20552. While a few fractures are easily visible in the transmitted-light image in the upper left, several additional microfractures can be seen in the fluorescent-light image in the upper right. However, closer examination of these fractures using SEM techniques showed no indications of mineralization or clay filling in any of the microfractures.

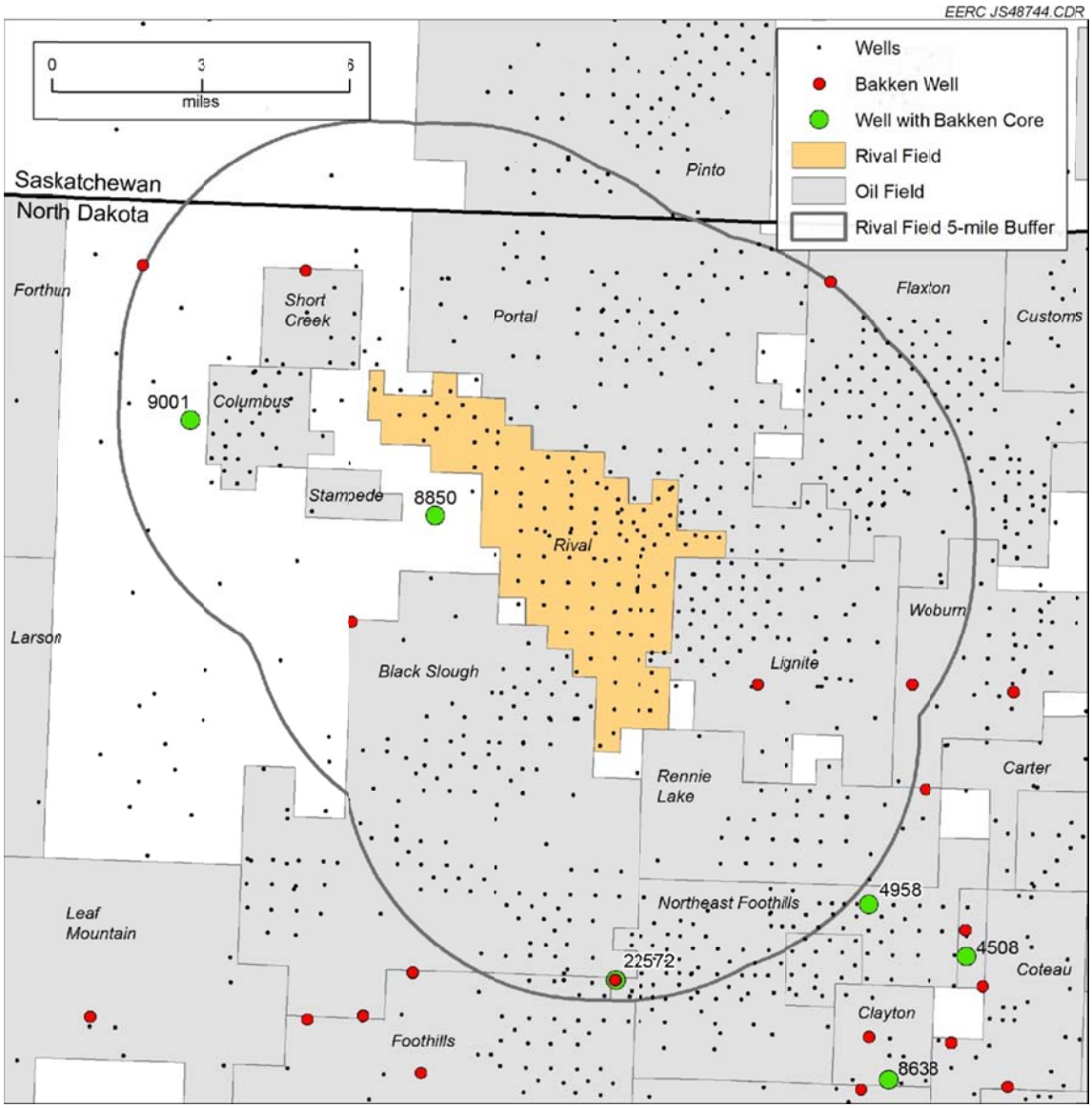

Figure 10. Location of wells sampled near the Rival Field.

Member (contact on the Upper Bakken shale). These designations are not necessarily correlative to similar Middle Bakken lithofacies designations that are commonly used throughout published literature on Bakken stratigraphy. In this report, they are strictly used to orient the reader within the context of the relative stratigraphic position within the core. A summary of the key observations and data regarding porosity, grain density, and dominant mineral phases identified for each sample collected as well as a summary of geomechanical results for selected samples from the Rival area cores are provided in Appendix A. Key observations for the Rival area characterization are as follows.

The lithofacies in the two Rival study area wells appear to be fairly correlative. Both wells have a relatively thick argillaceous siltstone at the base (L1). The primary difference in L1 between the two wells is that L1 in NDIC-8850 exhibits a more massive character in contrast to a more bioturbated L1 to the west in NDIC-9001. Throughout the area, L2 appears to be a calcite-rich siltstone, L3 is a bioturbated siltstone, and L4 is a 2- to 3-foot-thick, laminated, dolomitic siltstone. This is particularly noteworthy because it has been recognized that the predominantly laminated lithofacies within the Middle Bakken Member are thought to be the more productive intervals. Many companies are known to specifically target the laminated intervals for their horizontal drilling programs. Similarity in appearance of L4 between the two wells is shown in Figure 11. Examination by UVF indicated no presence of microfractures in L4 in either well. This is interesting because the literature and observations of laminated zones in the other study areas suggest that, at least in oil-productive areas of the Bakken, the laminated lithofacies tend to be more fractured, both with respect to macrofractures and microfractures.

Some differences in mineralogy between the two Rival area wells can be observed. Specifically, L4 in NDIC-9001 appears to have nearly twice as much feldspar when compared to L4 in NDIC-8850. Both wells show L5 to be a bioturbated siltstone, L6 to be a thin dolostone, and L7 to be a more massive dolostone.

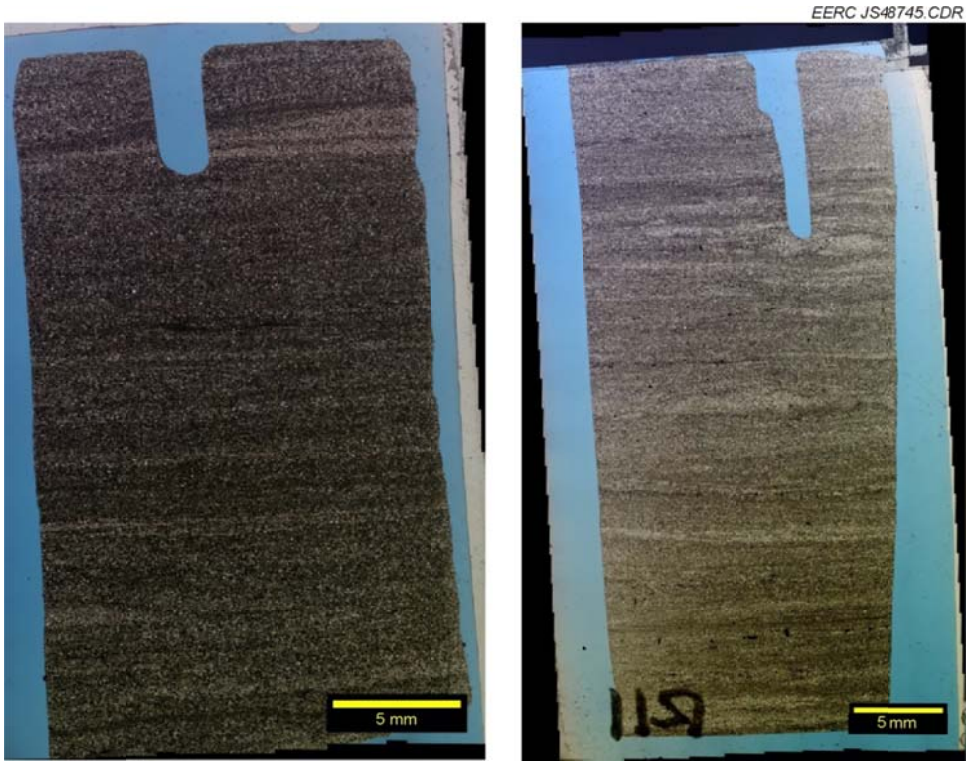

Figure 11. Transmitted-light images of thin sections from L4 in the Rival study area; sample from NDIC-8850 on the left and a sample from NDIC-9001 on the right. The laminated character of these samples is clearly represented in these images.

Summary of Key Observations for Grenora Area Samples

At the time of this project, there were no Bakken wells in the Grenora oil field proper, but one of the industry partners considered the Grenora area to be a high-priority location for evaluation of the Bakken. Of the three wells in the Grenora study area (Figure 12), NDIC-20552 is the closest to the legally defined Grenora Field, located approximately 1 mile south of the field. It is worth noting that this well is distinctive from the other two in that it contains eight identifiable lithofacies (from L1 at the base to L8 at the top of the Middle Bakken), whereas the others appear to contain only seven. Because of its close proximity to the Grenora Field, a brief summary description of the eight lithofacies identified in NDIC-20552 is provided as follows. L1 is a massive to bioturbated fossiliferous siltstone. Lithofacies L2 through L7 alternate between

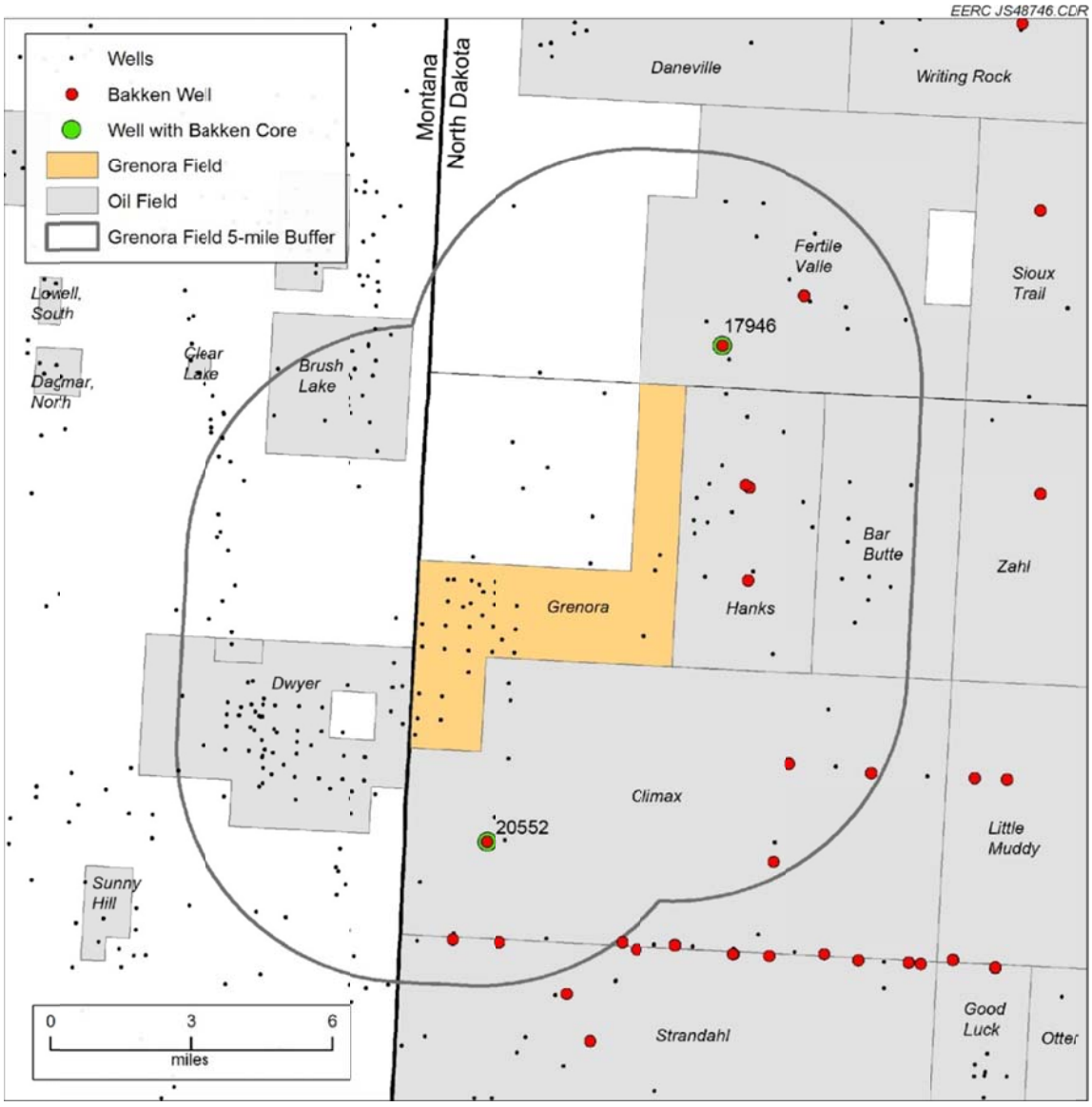

Figure 12. Location of wells sampled near the Grenora Field.

bioturbated siltstone and laminated siltstone, with the laminated zones generally being thinner than the bioturbated zones. L5 through L7 appear to become more dolomitized as one moves up the core, until finally at the top of the Middle Member of the Bakken, L8 appears as a dolomitic siltstone. As with the evaluation of Rival cores, these designations are not necessarily correlative to similar Middle Bakken lithofacies designations that are commonly used throughout published literature on Bakken stratigraphy. In this report, they are strictly used to orient the reader within the context of the relative stratigraphic position within the cores that were evaluated in Grenora area.

Figure 13 shows a cross section of the Bakken from three wells in the Grenora study area. Both NDIC-20844 and NDIC-17946 have seven lithofacies that appear to be somewhat correlative, with some subtle differences in fabric and mineralogy. Generally speaking, the Middle Bakken in the Grenora area appears to be significantly more dolomitic than the Rival area. The lithofacies in the Grenora area appear to be generally more variable than was observed in the Rival area and the Dunn County areas. This variability and lack of an easily correlatable, thick, laminated zone makes the selection of a suitable horizontal drilling target more challenging. The cores from the Grenora area are generally more fractured than those from the Rival and the Dunn County areas (Figure 14). This may be due to the presence of structure that is known to occur in the Grenora area. The presence of dolomite also facilitates the development of fractures as dolomite tends to fracture more easily than calcite. The presence of structure and dolomite may be linked. The existence of a fracture network caused by structure or tectonic activity along the Brockton–Froid fault (which runs near the Grenora Field) may have facilitated fluid migration through the Bakken. Such fluid migration may have supported diagenesis, creating dolomite rhombs and further enhanced natural fracturing of the formation.

Summary of Key Observations for Murphy Creek and Bailey (Dunn County) Area Samples

While the Murphy Creek and Bailey Fields are separated by approximately 6 miles (Figure 15), the characterization activities indicated that the depositional environment and associated diagenetic histories were similar. Specifically, the number of lithofacies and their general character were such that the observations for those fields have been summarized together and are collectively referred to as the Dunn County study area.

The Bakken in the Dunn County study area includes both the upper and lower shales and five distinct lithofacies within the middle member. Figure 16 shows a cross section of the Bakken lithofacies in the Dunn County study area. Because the middle member is the target for horizontal drilling, it is the focus of the characterization and modeling efforts described in this paper. The full suite of characterization data generated from the Rogne 44-34H core (representing the Murphy Creek area) and the Burbank BIA 23-8 well (representing the Bailey area) is provided in Appendix B. The five middle member lithofacies observed in the study area are briefly described as follows.

The Middle Bakken lithofacies are numbered 1 through 5, with L5 at the top and L1 at the bottom. L5 is a massive, dense, mottled, dolomitic siltstone. Helium gas porosimeter measurements on core plugs showed L5 porosity ranging from 0.28% to 5.5%.

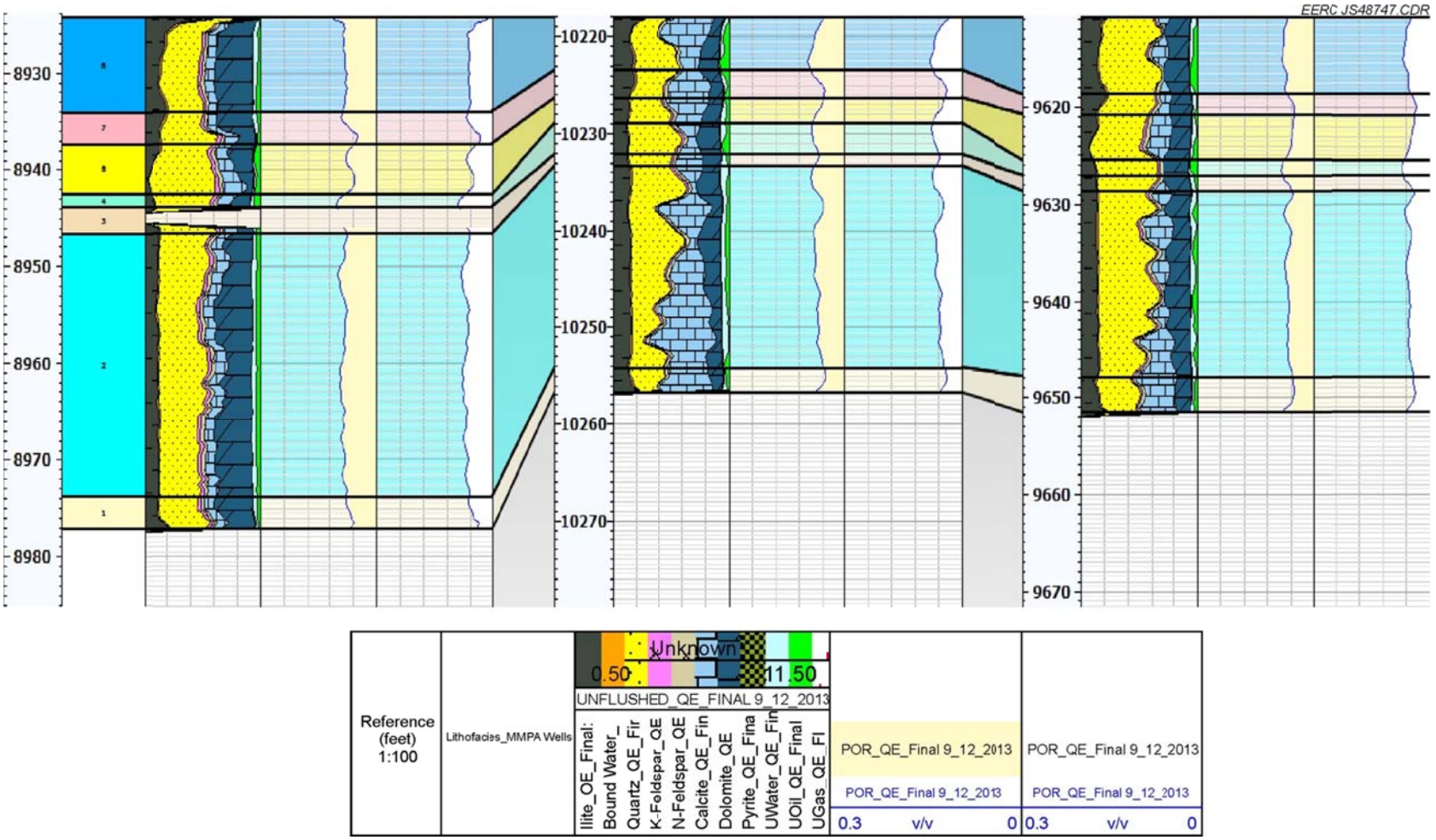

Figure 13. Cross section showing the thickness of Middle Bakken lithofacies in the Grenora study area. The well logs shown, from left to right, represent NDIC-17946, NDIC-20844, and NDIC-20552, respectively.

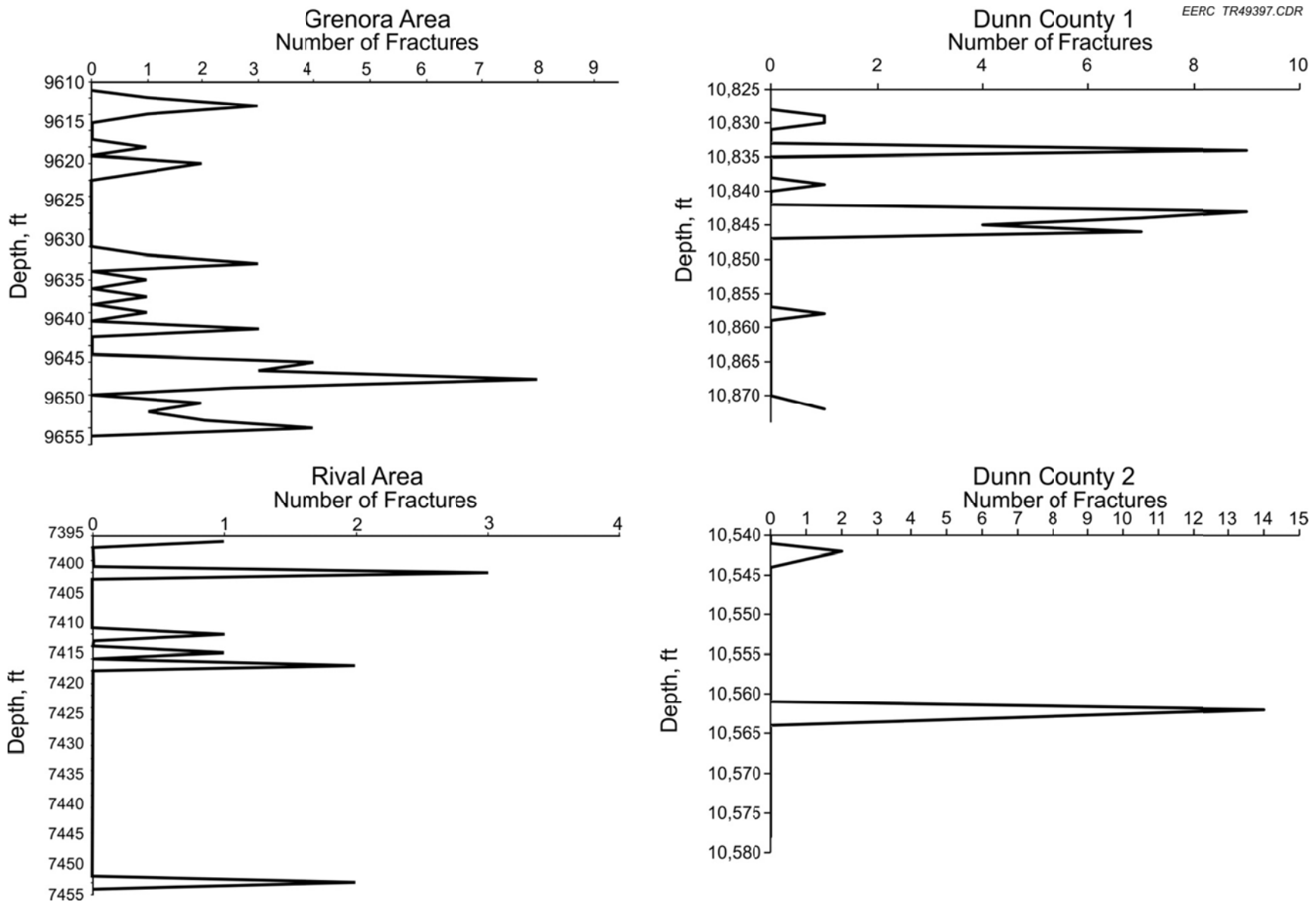

Figure 14. Fracture intensity graphs from Grenora, Rival, and Dunn County cores.

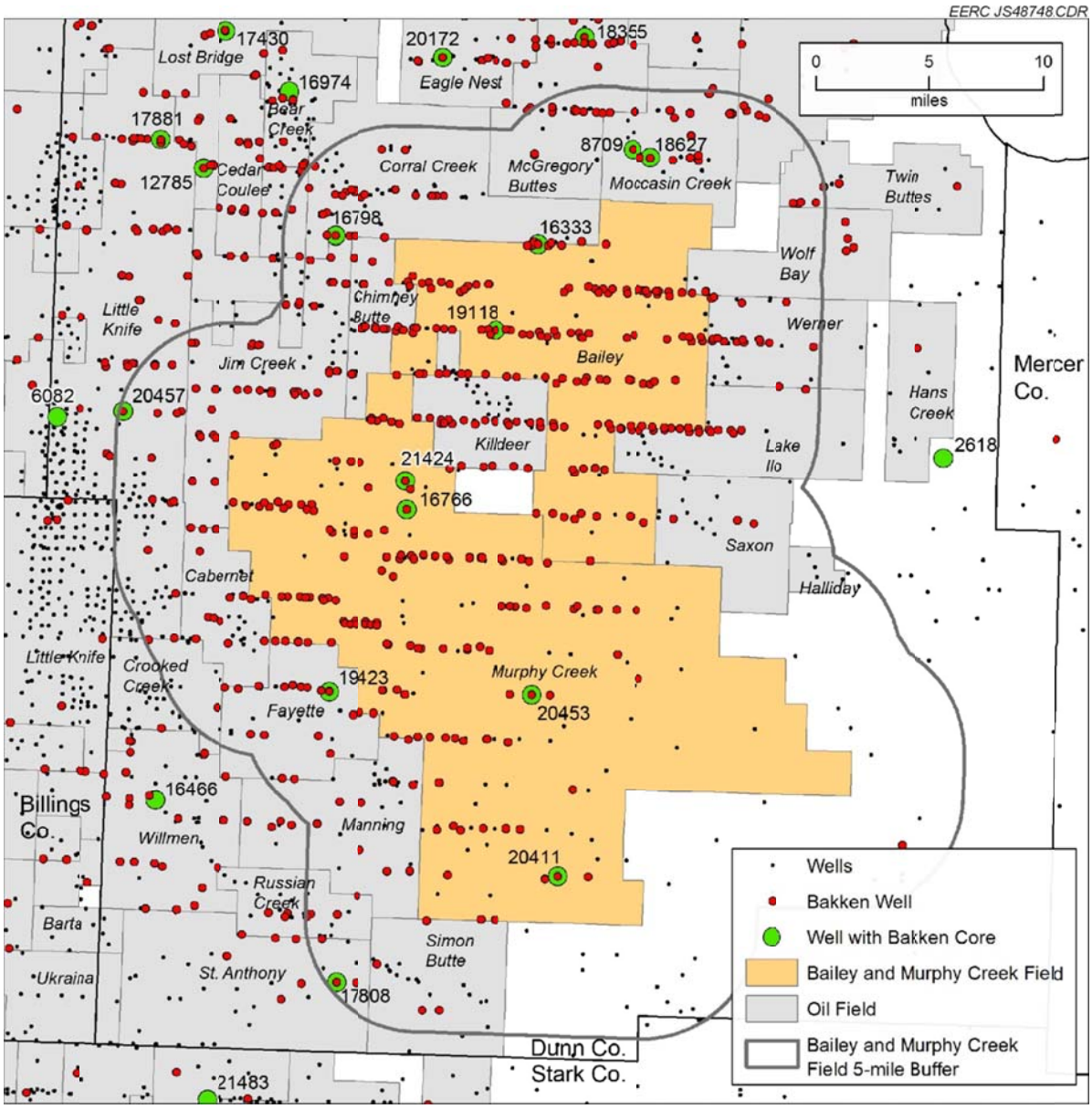

Figure 15. Map of the Dunn County study area.

L4 in the Dunn County study area, which is often referred to as the "packstone facies," ranges in thickness from just 2 feet in the southwest portion of the study area to over 12 feet in the central and northern portions. This lithofacies is considered by some to be one of the more oil-productive zones within the middle member of the Bakken. Generally speaking, in the Dunn County area, L4 can be divided into carbonate-dominated zones in the bottom half of the zone overlain by a 1- to 3-ft-thick zone of laminated, sometimes bioturbated, fine-grained sandstone, which, in turn, is topped by another carbonate packstone. Thin-section, XRD, and SEM analyses indicated that calcite is the dominant mineral (approaching 80% in some samples) in L4. Clays generally account for less than 1% of the mineral content, with illite being the

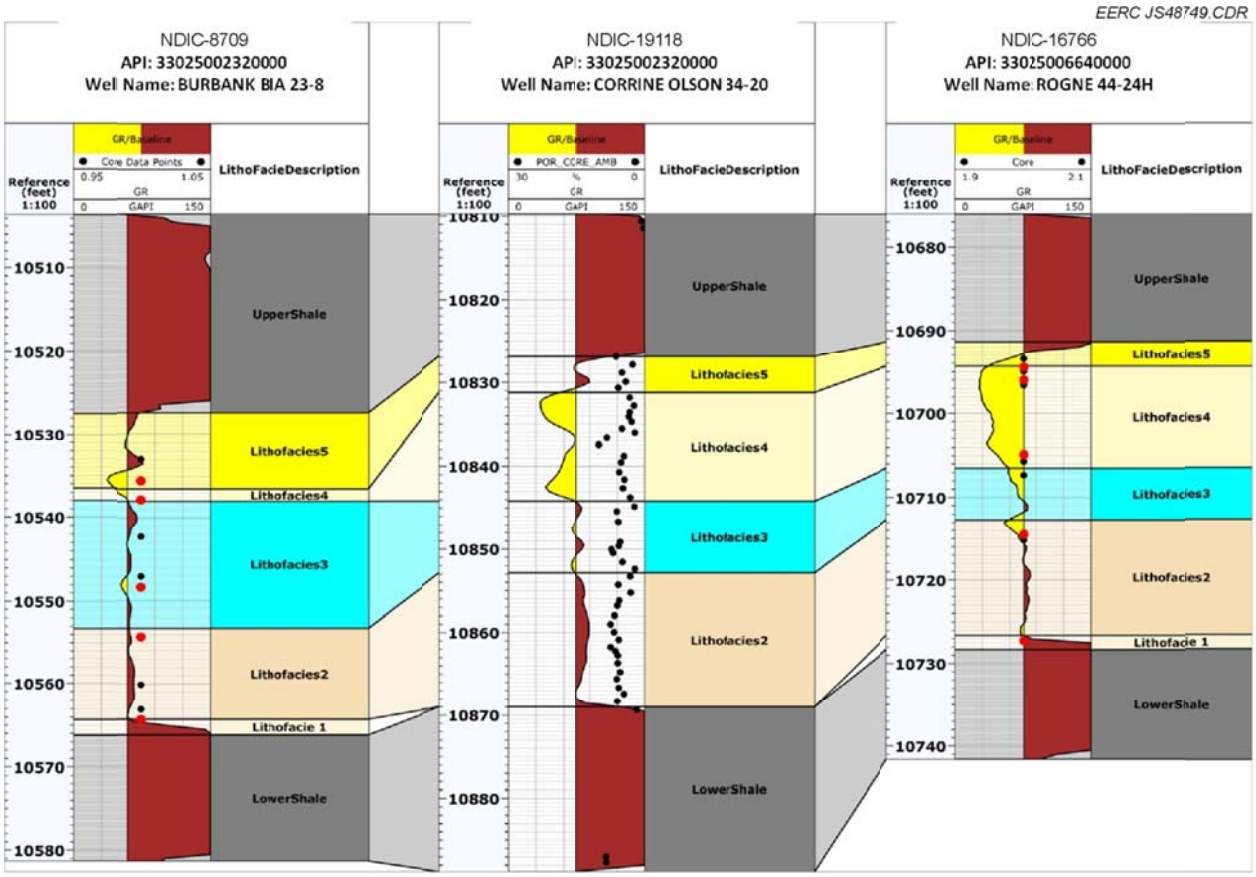

Figure 16. Cross section showing the thickness of Bakken lithofacies in the Dunn County study area.

primary clay. Porosity in the carbonate-dominated zones of L4 is observed only within fractures. Helium gas porosimeter measurements on core plugs showed L4 porosity ranging from 0.77% to 1.41%. Thin-section analysis indicated that observed porosity was limited to microfractures, with SEM measurements of microfracture aperture ranging from 2.4 to 8 µm.

Sometimes referred to as the "laminated facies," L3 in the Dunn County study area is an interbedded, sandy and silty dolostone and argillaceous dolomitic mudstone. In the Dunn County area, the laminated facies is often the drilling target for the horizontal leg of Bakken wells. Along with L4, L3 is considered to be an important zone of oil productivity within the Bakken. The thickness of the laminated facies in the Dunn County area ranges from 7 to 15 ft, with the thickest occurrence being in the southwest portion of the study area. Thin-section, XRD, and SEM analyses indicated that quartz is the dominant mineral (approaching 50% in some samples) in L3, with calcite and dolomite cements accounting for up to 30% of the mineral content. Clays generally account for less than 10% of the mineral content. Illite accounts for a majority of the clay, although some smectite and chlorite were identified. Thin-section analysis showed that the laminated facies includes intraparticle, interparticle, and fracture types of porosity. Many of these features are shown in the SEM-generated mineral map in Figure 17. Helium gas porosimeter

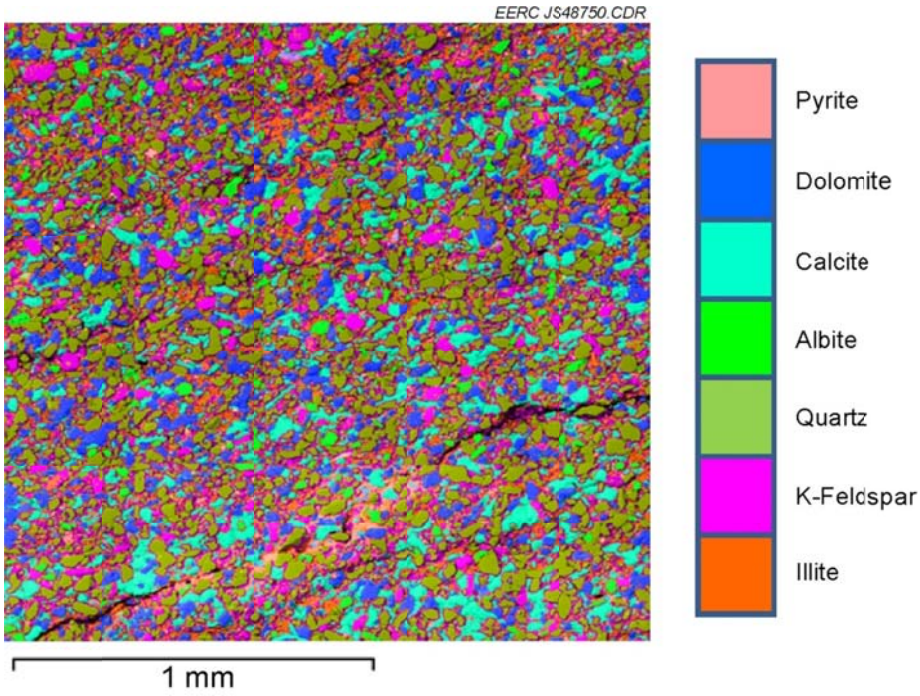

Figure 17. SEM-generated mineral map of sample from L3 in the Bailey Field of Dunn County. Porosity is represented by black. Microfracture porosity is the dominant form of porosity in this sample.

measurements on core plugs showed L3 porosity ranging from 3.2% to 5.03%. Thin-section analysis indicated that observed porosity was limited to microfractures, with SEM measurements of microfracture aperture ranging from 3 to 17 μm.

It is important to note that L3 can be further subdivided into two or three different zones, depending on the well. These subzones are marked by changes in porosity (as seen in well log data, most noticeably in the gamma log) and are observed in core as zones where laminations become more numerous and uniform toward the base of L3. Understanding the relative thickness and distribution of these more highly laminated zones is important when predicting the movement of injected CO_2. The laminated zones not only display slightly higher porosity, but also are generally geomechanically weaker than other Bakken lithofacies and, therefore, more prone to fracturing during the well stimulation process. This combination of characteristics suggests that CO_2 will move more easily through this portion of the reservoir, a phenomenon that must be considered when designing an EOR scheme.

L2 is a brownish gray argillaceous siltstone that is sometimes referred to as the "burrowed" lithofacies because of its moderately to strongly bioturbated nature. In the Dunn County study area, it ranges from 11 to 16 ft in thickness, with the thickest occurrence being in the center of the area. Thin-section, XRD, and SEM analyses indicate that quartz and illite are generally the dominant minerals in L2, although some thin sections were dominated by calcite. Figure 18 shows an SEM-generated mineral map that illustrates the relative abundance of illite clay, which

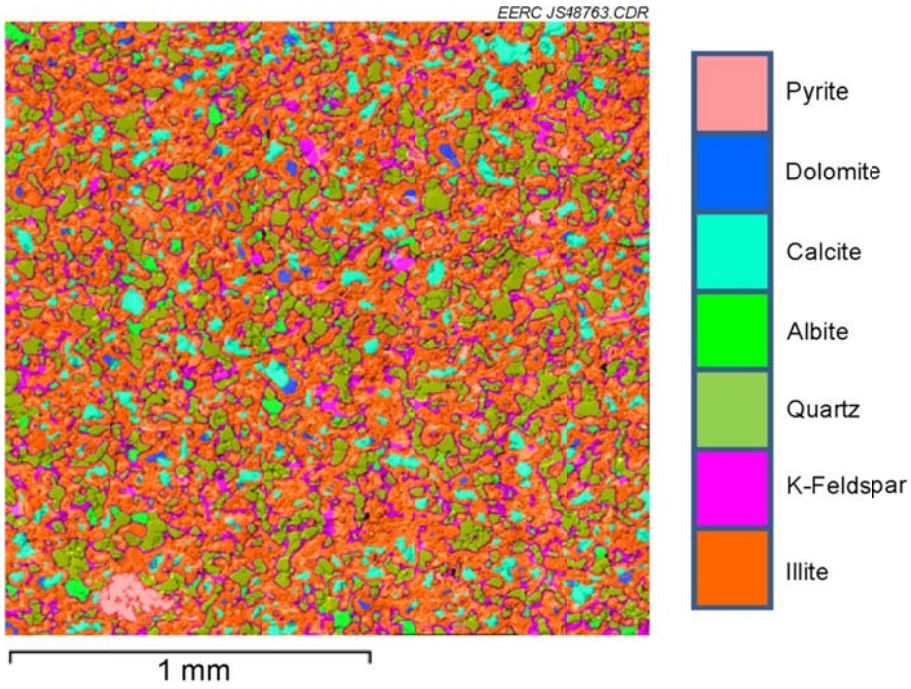

Figure 18. SEM-generated mineral map for a sample of Middle Bakken L2 in the Bailey Field of Dunn County. The abundance of illite clay present in L2 as compared to L3 should be noted. Only a very few interparticle points of porosity, represented by black, are visible in this sample.

is a nonswelling clay, in L2. Helium gas porosimeter measurements on core plugs showed L2 porosity ranging from 1.32% to 3.75%. Thin-section analysis indicated that observed porosity was limited to microfractures, with SEM measurements of microfracture aperture ranging from 3 to 17 μm.

L1 is a transitional facies from the anoxic environment that deposited the Lower Bakken black shale into a normal marine setting. In the Dunn County study area, it is an argillaceous siltstone ranging in thickness from very thin (less than 1.5 ft) in the north and south to nonexistent in the center. Thin-section and XRD analyses show that it is dominated by quartz and calcite, including bioclasts, with occasional dolomite and feldspar occurrence and trace amounts of pyrite and muscovite. Illite is the dominant clay, comprising as much as 10% of the mineral composition. The fabric of L1 is generally massive, dense, and somewhat mottled in appearance. Helium gas porosimeter measurements on core plugs showed L1 porosity to range from 2.73% to 3.87%. Thin-section analysis indicated that observed porosity was limited to microfractures, with SEM measurements of microfracture aperture ranging from 5 to 10 μm.

Observed Differences in the Middle Member of the Bakken Formation in the North Dakota Study Areas

While the four North Dakota study areas for characterization were selected in part to determine if thermal maturity had a significant effect on reservoir characteristics that might impact CO_2 EOR and storage, the final selection of specific areas was made in close

collaboration with the project's industry partners. The areas that were selected for characterization were areas that had been identified as being of high priority by their respective operators. At the time the project was proposed in 2011, relatively few successful Bakken wells had been drilled in the thermally immature portion of North Dakota. This meant that there were fewer thermally immature Bakken fields to choose from and that the selection of the Rival and Grenora areas was largely driven by the exploration priorities of one of the partner companies as opposed to production history. Conversely, thousands of successful wells had been drilled in the thermally mature portion of the basin, and there were many fields to choose from. This translated into the selection of fields representing the thermally mature part of the basin that had both significant amounts of characterization data and production history. As the results of the characterization activities were evaluated and compared, a few significant differences were observed. Figure 19 provides a summary overview of the characteristics of the Middle Bakken lithofacies observed in the Dunn County, Grenora, and Rival areas.

The lithofacies in the Grenora area appear to be generally more variable (i.e., more variability in attributes between wells in the area) than was observed in the Rival and Dunn County areas. The increased variability made correlation of lithofacies within the Grenora area more difficult and increased the uncertainty of key reservoir properties (e.g., porosity, permeability, etc.) distribution. This variability and lack of an easily correlatable, thick, laminated zone make the choosing of a suitable horizontal drilling target, and subsequent CO_2 injection target, in the Grenora area more challenging.

Generally speaking, the Middle Bakken in the Grenora and Rival areas appears to be significantly more dolomitic than the Bailey and Murphy Creek areas. For example, XRD results indicate that both the Rival and Grenora Middle Bakken samples had an average of 22.8% dolomite, while the Middle Bakken samples from the Bailey and Murphy Creek areas had an average of 11.4% and 4.5% dolomite, respectively. The published literature suggests that amongst Bakken fields, the Elm Coulee Field in Montana is known for being highly dolomitic and that the dolomitization in that field is likely due to depositional environment and/or diagenetic factors (Sonnenberg and Pramudito, 2009). The proximity of the Grenora area to the Elm Coulee area in Montana (Grenora is approximately 45 miles north of Elm Coulee) suggests that the elevated dolomite occurrence in the Grenora area may be related to the same regional depositional environment and/or diagenetic trends that affected Elm Coulee. While the Rival area is another 90 miles to the east and north of Grenora, the fact that both areas displayed more distinctly dolomitic lithofacies may suggest that they had similar depositional environments and/or diagenetic histories.

One of the thoughts behind the comparison of thermally mature to thermally immature areas of the Bakken was that the thermally mature areas might have more natural fractures than the immature areas. This is because the expulsion of oil that takes place as a result of the transformation process of kerogen to oil can result in the overpressurization of the formation, thereby inducing the development of fractures. A comparison of the fracture analysis data collected for the four study areas showed that all four areas had a significant amount of naturally occurring fractures in at least one lithofacies. The presence of structure in all four areas makes it difficult to definitively attribute the presence of those fractures to thermal maturity.

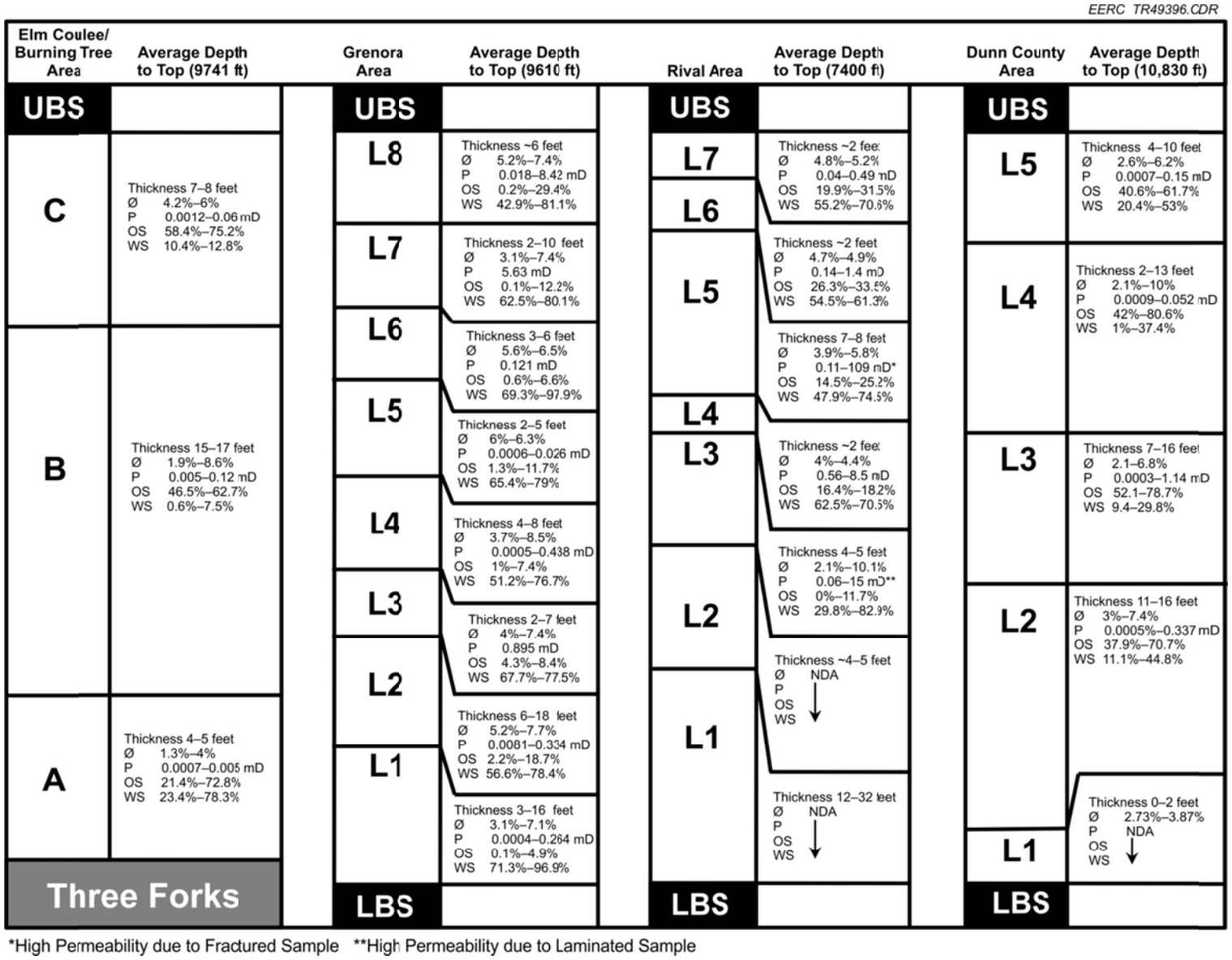

Figure 19. Summary overview of the characteristics of the Middle Bakken lithofacies observed in the Elm Coulee, Grenora, Dunn County, and Rival areas. Lithofacies designations for the North Dakota areas are location-specific and are not necessarily correlative between different areas. The lithofacies designations for the Elm Coulee/Burning Tree area are based on Alexandre and others (2011).

BUILDING STATIC GEOLOGIC MODELS AND DYNAMICALLY MODELING POTENTIAL EOR SCHEMES

CO_2 EOR processes are expected to be very different in tight reservoirs compared to conventional reservoirs. During CO_2 EOR in conventional reservoirs, CO_2 flows through the permeable rock, and oil is mobilized by a combination of oil swelling, reduced viscosity, hydrocarbon stripping, and CO_2 flushing. In the Bakken, CO_2 flow will be dominated by fracture flow, and not significantly through the rock matrix, so fractures must be a major component of any Bakken reservoir model that will be used for dynamic simulations. However, diffusion of CO_2 from the fracture system into the matrix may have a significant effect on CO_2 storage and oil recovery; therefore, understanding the nature of the matrix is also vital to predicting the effectiveness of CO_2-based EOR and storage in the Bakken. As such, the EERC's approach to modeling for this project includes robust multimineral petrophysical analysis (MMPA) to account for the distribution of matrix properties and the creation of a discrete fracture network (DFN) to account for the role of fractures in the reservoir system.

MMPA can use well log data and core data to provide an estimate of residual and producible hydrocarbons, effective porosity, and lithofacies-based permeabilities. MMPA is calibrated to core analytical data (e.g., thin-section and XRD analyses) and well log-based bulk density, matrix density, porosity, and irreducible water saturation data. The DFN is created using log data and data generated by macro- and microfracture analyses. The EERC combines MMPA and DFN results to establish a dual-porosity–dual-permeability model for the study reservoir.

Static and dynamic modeling activities were conducted using industry-standard software provided by Computer Modelling Group (CMG) and Schlumberger Carbon Services (SCS). The modeling activities were conducted on existing computer hardware at the EERC. Modeling hardware at the EERC includes a high-performance computer cluster that is designed and dedicated to serve the needs of advanced reservoir modeling and simulations. As with other components of the research program, the EERC worked closely with the operating partner to tailor the modeling activities for a specific study area to fit with the previous and/or ongoing efforts of that partner.

Static Modeling Approach

Of the four North Dakota Bakken fields that were characterized, two were selected to be the focal points for static and dynamic modeling efforts. A portion of the Bailey Field in Dunn County was selected to represent a thermally mature area of the Bakken. The thermally immature area of the Bakken was represented by a portion of the Grenora Field in Williams County. These fields were selected for modeling because they had the largest, most detailed publicly available data sets of the four characterized fields. A significant amount of confidential characterization data was also provided by one of the partner companies for a well in the Bailey Field, further supporting its selection for detailed modeling activities. The creation of the static geologic models for the Bailey and Grenora study areas took place in a stepwise manner, starting with the development of a structural model, followed by the creation of matrix petrophysical and fracture petrophysical modeling. The types of data that were used to create the models include a variety of well log, stratigraphic, XRD, SEM, and routine core analysis data (e.g., effective porosity,

permeability, bulk volume and density, grain volume and density). MMPA was performed to derive mineral volumes, saturations of clay-bound and unbound water, saturations of oil, and porosity.

Structural surfaces of the upper, middle, and lower members of the Bakken Formation in each field were created from the well correlation process using gamma ray (GR) logs followed by geostatistical interpretation. Once the structural model was established, efforts were then focused on the creation of petrophysical models. Two different petrophysical models are required to support realistic dynamic modeling of a CO_2 EOR scheme, a matrix petrophysical model and a fracture petrophysical model. The matrix and fracture petrophysical models are ultimately integrated to create a dual-porosity–dual-permeability model upon which dynamic simulations of CO_2 injection and fluid production are conducted. An overview of the steps taken to create the petrophysical models is provided as follows.

Matrix Petrophysical Modeling

The complex nature of the unconventional Bakken reservoir requires an understanding of the way CO_2 will fundamentally interact with all of the key elements of the reservoir matrix. Specifically, an accurate model of the minerals, clays, and fluid saturations is critical to predict the interactions that CO_2 will have with the reservoir system. The primary steps for developing the matrix petrophysical model can be categorized as data preparation, selection of key wells, synthetic well log creation, lithofacies correlation, incorporation of core data, MMPA, and petrophysical modeling. The first step of data preparation included the collection and placement of well logs into a Techlog database that allowed for efficient management of the log data and evaluation of data for log analysis and quality control purposes. The Techlog application included core data, core photos, thin-section photos, and MMPA precomputational analysis from well files and log headers. Techlog was also used to pick formation tops and lithofacies tops for the vertical portions of wells in the study area. Data preparation also included the use of Petrel for managing and manipulating data on wells and well deviations, well tops, well logs, mud logs, and results generated within Techlog.

Once the Techlog and Petrel databases had been established for each study area, a set of key wells was selected for detailed well log analysis that would ultimately lead to MMPA. Of the dozens of wells in each study area (72 in Bailey and 30 in Grenora), a much smaller subset of wells in each area had sufficient data for MMPA and served as key wells for analysis. Key wells were identified as those wells having a suite of GR, bulk density (RHOB), photoelectron effect (PEF), sonic (DT), neutron porosity (NPHI), resistivity (RT), and flushed-zone resistivity (RXO) logs. In some cases wells that were initially identified as being key were later identified as having bad PEF, DT, or RHOB log data and were removed from the list of key wells. In the Bailey Field, the Corrine Olson well had the largest and most detailed suite of core analysis data among the key wells. Its data were used for calibration of core analytical data to well logs. In the Grenora Field, there were three wells (NDIC-17946, NDIC-20844, and NDIC-20552) with essentially equal amounts of core analysis data, so all three were used for core-to-log calibration. Not all of the key wells had PEF or DT logs, the lack of which could adversely affect the results of MMPA. Synthetic logs were, therefore, created using Techlog. Synthetic DT logs were created for five of the key wells, while eight synthetic PEF logs were created. Once a full suite of logs

had been established for each of the key wells, then it was possible to correlate the primary Bakken middle member lithofacies in each of the study areas.

After the middle member lithofacies had been correlated, core data were integrated into the static geologic model. XRD data from core samples taken from the calibration wells were used to predefine the mineral solver. A RockView geochemical log was used for MMPA calibration and validation. Core lithofacies descriptions were also incorporated, and core data were depth-shifted as part of the quality control (QC) process for finalizing MMPA results. The core data were shifted based on core gamma measurements as compared to the well gamma log.

The use of MMPA is an approach that goes beyond simply assigning properties to a facies. MMPA is typically conducted to determine the complexity of oil and gas reservoirs and the effects of overall mineral content on fluid movement and production estimates. It is a more robust and rigorous means of assigning a multitude of properties to a given lithofacies, particularly with respect to mineral composition and fluid saturations and the relationships between those aspects of a reservoir. Mineral composition ultimately determines the physical parameters of the rocks and can be used as a tool to determine the overall characteristics of the reservoir and the depositional environment. Logs used in the inversion process typically include GR, neutron porosity, bulk density, formation resistivity, flushed zone resistivity, sonic, and photoelectric factor. The Quanti.Elan module in Techlog was used to calculate MMPA from the key well log data and determine the overall quantity and volume of different mineral components in each wellbore. This mineral volume calculation aids in determining the stratigraphy and the overall correlation from one wellbore to another, thus describing the geologic structure for property distribution in the 3-D model. MMPA can also help determine the interaction of bulk mineral volume and CO_2. Other key properties calculated by the MMPA process include pore fluid volumes and the calculation of effective and total porosity. An example of an output from MMPA is shown in Figure 20, which is a correlation cross section created from the 12 vertical key wells in the Bailey Field, with the Corrine Olson well results on the far right of the image.

Upon completion of MMPA, the reservoir properties were imported into Petrel for the creation of the matrix petrophysical model for the Bakken in the respective study area. Petrel was then used to conduct variogram data analysis and geostatistically populate effective porosity, permeability, and oil and water saturation properties. Figure 21 illustrates an example of the distribution of effective porosity and permeability for the matrix petrophysical model of one of the lithofacies in the Bailey study area.

Fracture Petrophysical Modeling

Because the matrix of the Bakken is characterized by low porosity and permeability, fracture networks are crucial to successfully producing oil from a Bakken reservoir. Fracture networks will also serve as the primary pathway for CO_2 movement within the reservoir; therefore, a fracture petrophysical model is essential to predict the effectiveness of a CO_2 storage and EOR scheme. The process to create a fracture petrophysical model includes core viewing to conduct macroscale fracture analyses, laboratory analysis to characterize macrofractures and microfractures, definition of fracture sets, and the creation of a DFN.

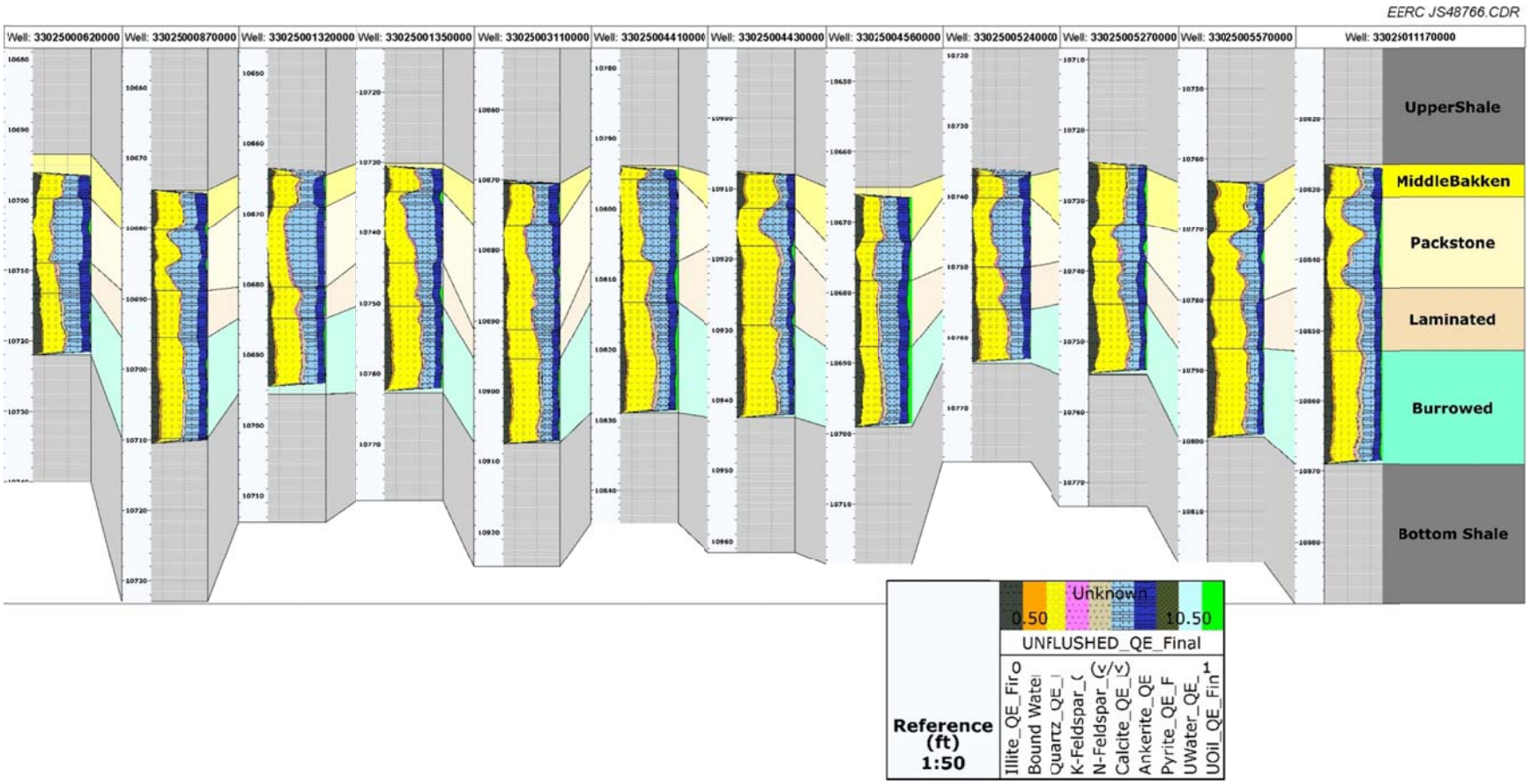

Figure 20. MMPA results for the 12 vertical key wells in the Bailey area, with the Corrine Olson well on the far right.

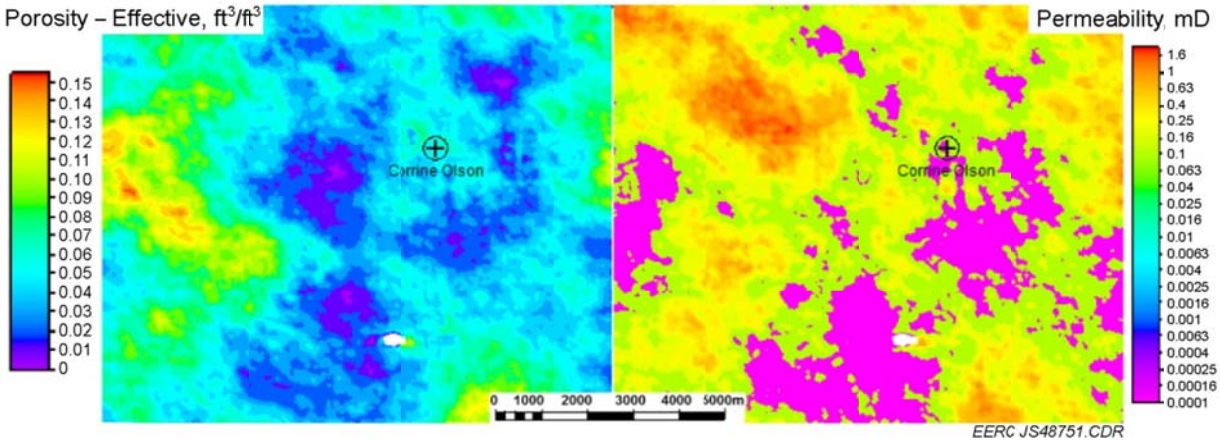

Figure 21. Example of key matrix petrophysical model properties, showing the distribution of effective porosity and permeability for one of the lithofacies in the Bailey study area. The area of the model shown is approximately 10 km × 12 km.

Core from three wells in each study area were available for analyses to support the creation of the fracture petrophysical models for Bailey (Corrine Olson, Burbank BIA 23-8, and Rogne 44-34H) and Grenora (NDIC-17946, NDIC-20552, and NDIC-20844). Middle Bakken core samples from all six of these wells were visually described for facies and examined for macrofracture analysis. Macrofracture analyses were conducted according to methodologies described in Nelson (2001) and U.S. Bureau of Reclamation (1998). Those analyses resulted in the creation of fracture intensity logs (number of fractures per foot of core), quantitative measurements of aperture, and qualitative data on orientation (shallow dipping versus steeply dipping) for the Middle Bakken Member of the Bakken in each of the six wells. An example of a fracture intensity log is provided in Figure 22. SEM was also used in a similar workflow to identify and characterize microfractures for aperture. Since SEM samples represent a small piece of the reservoir and few samples were analyzed, microfracture length and orientation were assumed from the closed fractures measured during the core macrofracture analysis.

Once macrofracture and microfracture properties have been measured and evaluated for the core, fracture sets can be defined for the reservoir. Fracture intensity logs are first normalized over the stratigraphic intervals represented in each structural model, assigning a fracture density, aperture, length, and orientation for each fracture set. Two fracture sets were assigned to each stratigraphic zone, resulting in 12 total fracture sets in Grenora, represented in six of the eight Middle Bakken zones. The Bailey model had fractures in all four zones in the Middle Bakken, thus having eight fracture sets. Set one represents the vertical-dipping fractures and Set two the horizontal-dipping fractures. Both fracture sets have a dip azimuth parallel to the maximum horizontal stress (S_{Hmax}). Fractures with a dip azimuth perpendicular to S_{Hmax} were assumed to be closed and thus were not included in the DFN modeling.

Petrel was used for DFN modeling. First the structural models that were created for the study areas were clipped down to a drill spacing unit (DSU). The DSU encompassed a 2.6-square-mile area in the northwestern portion of the Bailey study area and the southeastern

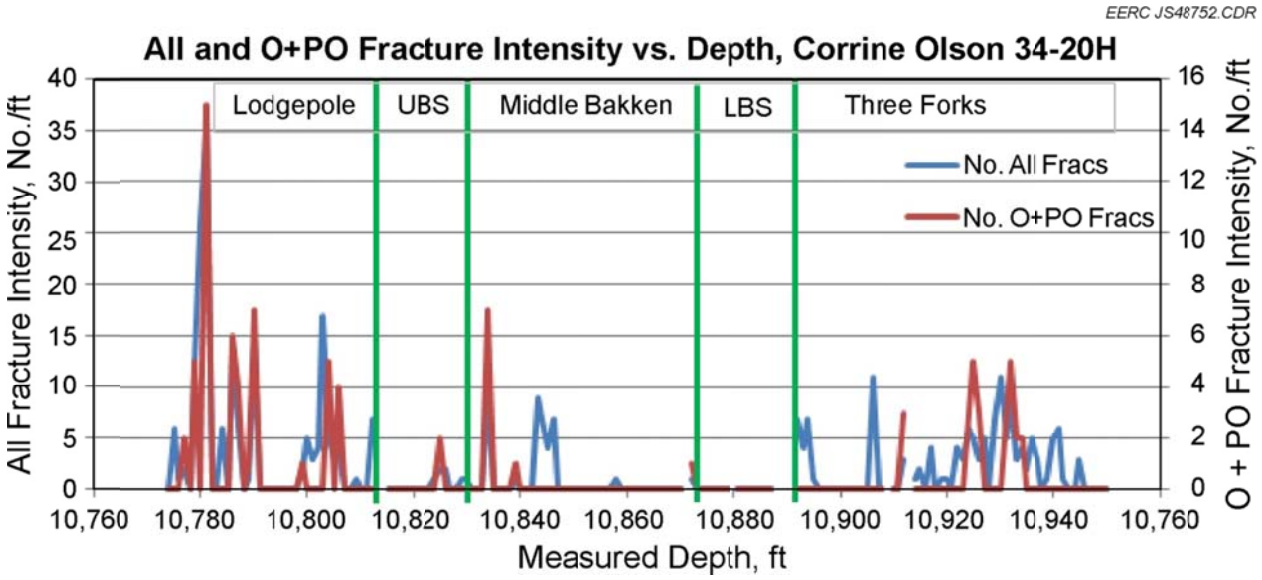

Figure 22. Fracture intensity log for the Corrine Olson well in the Bailey Field (O + PO refers to the combined number of fractures that were either open or partially open).

portion of the Grenora study area, respectively. This size was chosen to save overall computation time during DFN modeling and subsequent upscaling before dynamic simulation. The normalized fracture set data were imported into the Petrel DFN modeling process which was followed to build the desired fracture sets in each stratigraphic zone for both the Grenora and Bailey models (Figures 23 and 24). Macrofractures were represented by the discrete fractures and microfractures by the implicit fractures during DFN modeling within Petrel. Resulting DFN models were then upscaled to create dual-porosity–dual-permeability models (Figure 25), which were passed on for dynamic simulation.

The Bakken reservoir system is represented by both matrix and fracture flow which have drastically different reservoir properties, especially when quantifying porosity and permeability. A single-porosity–single-permeability model would overestimate the matrix reservoir properties and underestimate the fracture reservoir properties. The Middle Bakken matrix porosity is average, while the permeability is very low; in contrast, the fracture porosity is very low and the permeability high. In addition, applying relative permeability curves during simulation leads to more problems to solve when building a single-porosity–single-permeability model. Thus a dual-porosity–dual-permeability model was built for both the Grenora and Bailey Fields. The DFN represented by discrete and implicit fracture sets is upscaled into the same mesh as the matrix petrophysical model. The Oda upscale process was used to bin the fractures into the cells as defined by the mesh. Then the fracture properties were all summed within a cell and considered to be part of the fracture flow. The resulting properties are created from this upscale process: fracture porosity; fracture permeability in the I, J, and K directions and a fracture spacing coefficient. Following the upscale process, fracture properties are combined with all the matrix properties and exported to Computer Modelling Group Ltd. (CMG) for dynamic simulation.

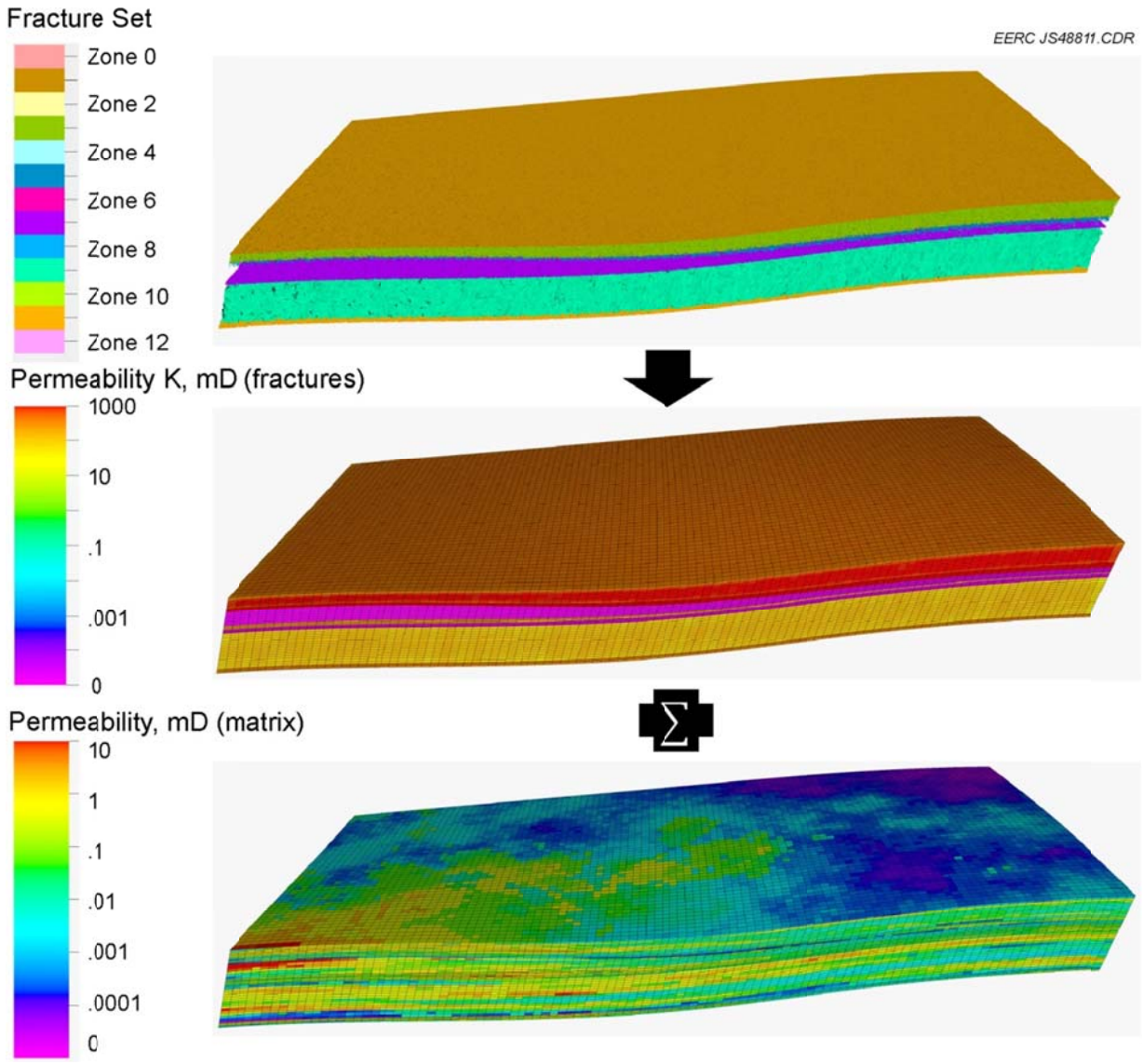

Figure 23. Fracture and matrix models are integrated to create the dual-porosity–dual-permeability model for the Grenora DSU.

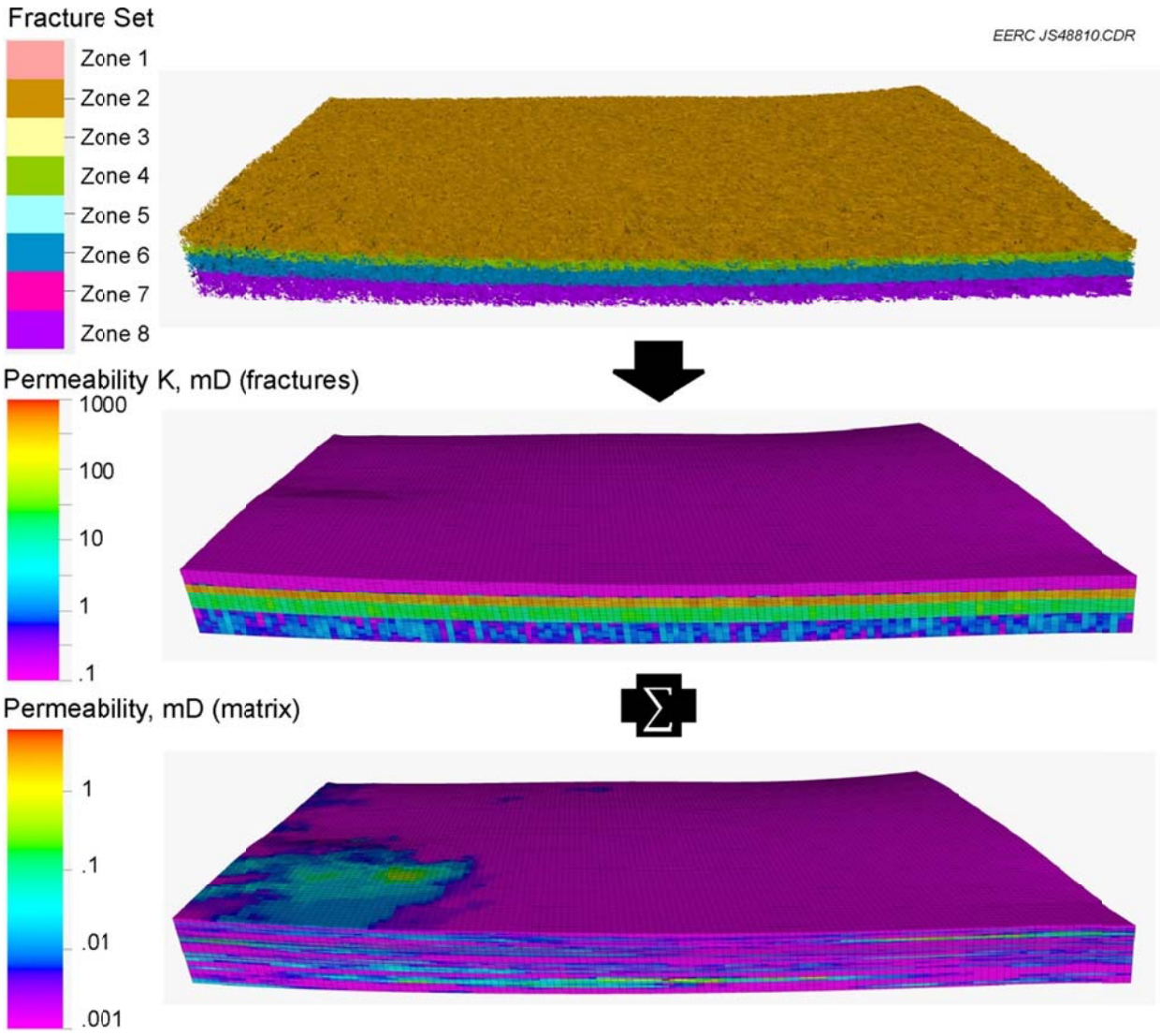

Figure 24. Fracture and matrix models are integrated to create the dual-porosity–dual-permeability model for the Bailey DSU.

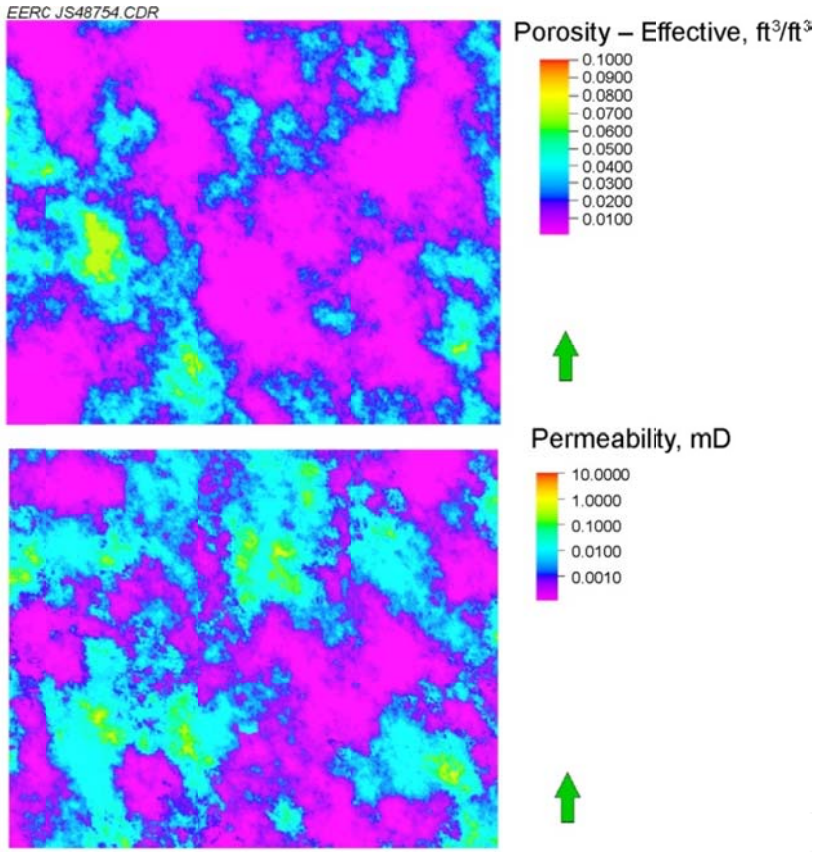

Figure 25. Example of dual-porosity–dual-permeability distribution in one of the lithofacies in the Bailey Field model.

Dynamic Simulations Modeling Approach

A two-stage approach was conducted for petrophysical and static modeling of the Bakken reservoirs. As described above, the first step was to design a single-porosity–single-permeability model of the study area from the data available. Lessons learned from this study were then applied to construct a dual-porosity–dual-permeability model to better understand the reservoir processes involved in coupled matrix/fracture flow in the next stage. While this initial model was being developed, advanced laboratory tests and fracture analyses were performed in order to guide the construction of an unconventional dual-porosity–dual-permeability model.

As described in previous sections, the model was constructed with available data, which included geophysical well logs, routine core analysis, and stratigraphy derived from viewing subsurface core. MMPA was designed to incorporate both matrix and fracture properties into one set of reservoir properties. Thus the reservoir permeability properties will include fracture flow up to 300 times the values measured in the matrix alone. This model was clipped down to an optimized near-wellbore model and used for dynamic simulation. Since this single-porosity–single-permeability model combined the matrix and fracture properties, the sensitivity of two sets of relative permeability curves (matrix system and fracture system) were analyzed to determine the incremental oil based on the relative permeability changes.

To address the system's response to CO_2 injection for oil production, four cases were evaluated based on the near-wellbore single-porosity–single-permeability model for the Bailey area. The results of these cases were used to more accurately build models for simulations that utilize dual-porosity–dual-permeability models for both Bailey and Grenora areas.

GEOLOGICAL MODELING DEVELOPMENT FOR SINGLE-POROSITY–SINGLE-PERMEABILITY SIMULATIONS

A single-porosity–single-permeability geocellular model of the Bailey Field study area (Figure 26) was built based on a database containing geophysical well logs, well information, stratigraphy, routine core analysis data, XRD, XRF, SEM, and UVF. The study area covers 38 square miles and includes 72 wells. A total of 13 key vertical wells were used in MMPA and stratigraphic correlation of lithofacies. Three of the key wells (Rogne, Burbank, and Corrine Olson wells) had preserved subsurface core, which was described and sampled for routine, special, and fracture core analysis. Correlated well logs showing the occurrence and thickness of the Middle Bakken lithofacies at the three key wells are shown in Figure 27. Routine analysis provided petrographic interpretation, grain and bulk densities, porosity, permeability, XRD, and XRF analysis. Special core analysis included SEM work to better understand mineral composition and the natural fracture system. A UVF technique was also used to identify naturally occurring fracture patterns, joint angles, fracture diagenesis, and hints toward improved understanding of natural vs. induced fractures.

The model was divided into four distinct lithofacies that were evident by sequence stratigraphy in understanding mechanical zones, ichnology, and biostratigraphic correlation among subsurface cores, MMPA, and fracture analysis. A structural model was built based on these four lithofacies and capped on top by the Upper Bakken shale and on the bottom by the Lower Bakken shale. These six zones were represented by a grid cell size of 33 × 33 ft laterally by an average of 0.5 to 1.0 ft vertically (Figure 28). The study area model has a total of 50 million cells. Well logs were upscaled into the structural model, and data analysis was performed to develop variograms for major, minor, and vertical ranges: 6300, 5000, and 3 ft, respectively. These small variogram ranges introduce strong heterogeneity into the model both laterally and vertically. Geostatistical methods were then used to populate water saturation, effective porosity, and permeability into the structural model. Pressure and temperature were determined based on bottomhole parameters derived from drillstem tests within the study area.

A fine-scale, near-wellbore model was clipped from the study area model to test CO_2 EOR by performing numerical simulation. The selection of the clipped model was based on a workflow to first understand connected volumes based on effective porosity and permeability cutoffs and then choose two wells that contain higher permeabilities from the inclusion of natural fracture properties into the matrix model. The model size is 6800 × 1800 ft laterally by 40 ft thick, with a grid cell size of 33 × 33 ft laterally by an average of 1 ft thick for 50 layers (Figure 26). The total cell count for the near-wellbore model is 610,000.

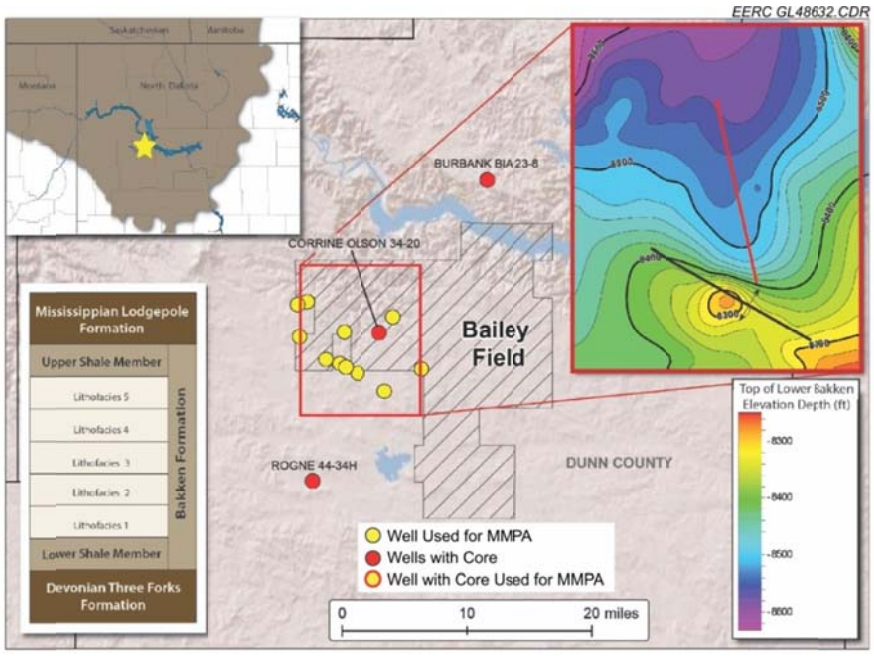

Figure 26. Bailey Field study area shown with static model boundary outlined in red and structure top of Middle Bakken on inset. 13 key wells used in MMPA are represented by yellow dots, while the wells with core are shown as red dots.

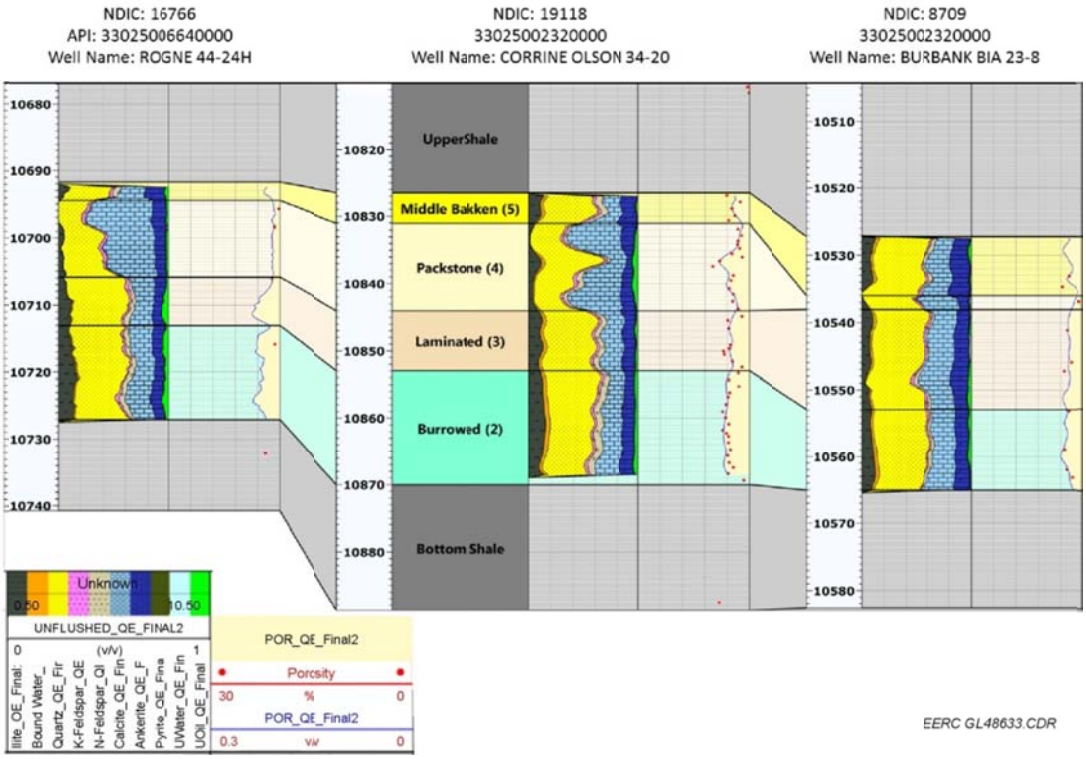

Figure 27. Three wells with subsurface core that were sampled to better understand both the matrix and fracture reservoir characteristics and petrophysical properties.

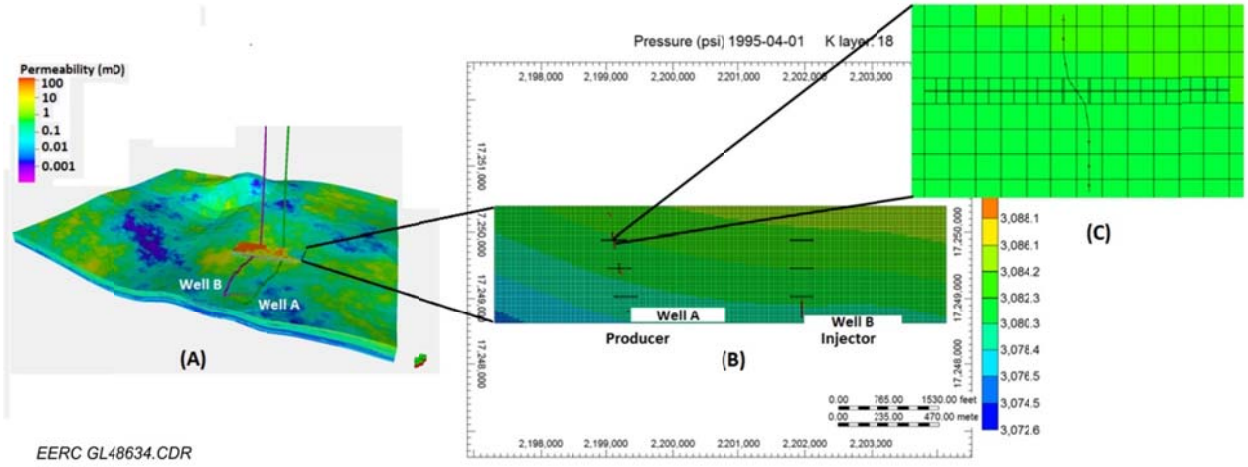

Figure 28. (A) Bailey Field study area, clipped near-wellbore model, and a pair of wells for the simulation. Zones 2 through 5 are shown with individual layers at a minimum thickness of 0.5 ft. This model has a total of 50 million cells. The fine-scale wellbore model is clipped from the much larger static model. Cell sizes are 10 × 10 ft laterally and an average of 1 ft thick. The permeability property is shown and represents a combination of both matrix and natural fracture data. (B) Three stages of hydraulic fracture for each horizontal well in the wellbore model. (C) Zoom-in of the grids and hydraulic fracture in the model. Both wells are perforated only through the hydraulic fractures.

CO_2 Injection Simulations Using Single-Porosity–Single-Permeability Model

As discussed, injecting CO_2 into the Bakken Formation was simulated using the fine-scale, near-wellbore model. In this study, a pair of existing horizontal wells with a spacing of 3000 ft was selected based on the connected volume between wells that allows the fluids to communicate with each other (Figure 28A). In this simulated case, Well A was designated as a producer and Well B as a CO_2 injector. However, only 1800 ft of the horizontal wells is modeled in both the injection and production wells. It is assumed that these results and the percent increase can be extrapolated to the entire length of each well. Based on characterization results, two 3-stage hydraulic fractures were incorporated into each of the 1800-ft sections of both the CO_2 injection and oil production wells (Figure 28B). The hydraulic fracture dimensions are 300 ft in length by 2 ft wide, and the permeability of the cells is 100 times higher than the surrounding cells. The CO_2 injection and oil production wells were only perforated in the cells that passed through the hydraulic fractures located in the Middle Bakken zones.

After the near-wellbore model had been prepared for simulation, the remaining steps of the dynamic modeling workflow were followed (Figure 29) (Gorecki and others, 2013). The workflow introduces several techniques: 1) grid-size sensitivity analysis for possible coarse grid resolution, which produces identical results of finer grids; 2) numerical tuning for simulation speedup and minimizing low-mass material balance error caused by numerical methods; 3) property/parameter sensitivity analysis to address the influence on model output; 4) operational optimization including varying factors such as well spacing, injection rate, CO_2

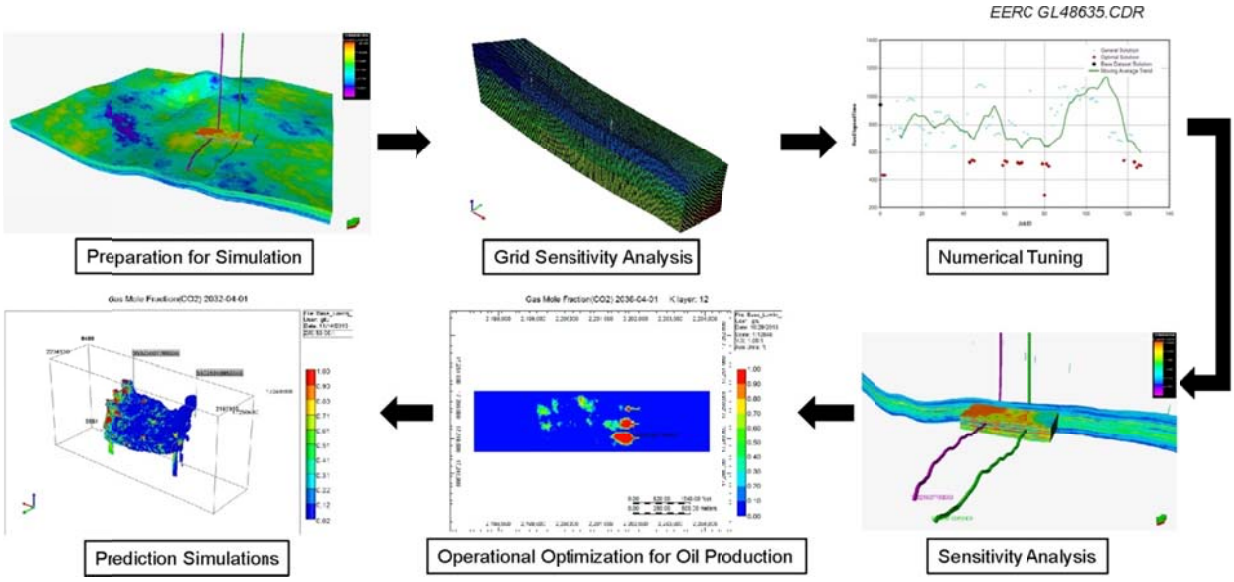

Figure 29. Dynamic simulation workflow.

recycle, etc., which potentially increases the oil production during predictive simulations; and 5) prediction simulations, which may be executed based on the net present value to optimize the prediction even after history matching if any applicable records can be used.

The fluid model used in the simulation system was calculated based on laboratory oil compositional analysis and a swelling test. A total of 40 components were combined into five components (CO_2, N_2–C_1, C_2–C_3, C_4–C_6, C_7–C_{36+}) to generate the equation-of-state (EOS) parameters for the simulation (Kurtoglu, 2013). Two 3-phase relative permeability curves were used, one that approximates the matrix relative permeability and one that approximates the fracture relative permeability to test the sensitivity for flow from each on the model. The parameters used to generate the curves based on the Brooks–Corey equations are listed in Table 1 (Kurtoglu and others, 2012). Capillary pressure was neglected in the simulations because of the lack of laboratory test data.

Table 1. Parameters Used to Generate Relative Permeability Curves for Matrix and Fracture Systems in the CMG Simulator by Brooks–Corey Equations

Matrix System				Fracture System			
Water–Oil		Gas–Oil		Water–Oil		Gas–Oil	
Krw	0.024	Krg	0.096	Krw	0.400	Krg	0.500
Krow	0.103	Krog	0.106	Krow	0.800	Krog	0.800
Swr	0.531	Slg	0.730	Swr	0.050	Slg	0.100
Sorw	0.211	Sgr	0.000	Sorw	0.050	Sgr	0.000
Nw	1.500	Ng	2.000	Nw	1.500	Ng	2.000
No	2.500	Nog	2.500	No	2.000	Nog	2.000

The CO_2 was also allowed to dissolve into brine to mimic the nature of the system. The aqueous density and viscosity of the fluids were, respectively, correlated by using the Rowe and Chou (1970) and Kestin and others (1981) methods with varying temperatures and pressures of the saline system over the location and depth. Henry's law constant was correlated by Harvey's method to determine the solubility of CO_2 in the brine (Harvey, 1996).

To test CO_2 recovery, a total of four cases were designed to address the potential for CO_2 EOR in the Bakken (Table 2). Cases 1 and 2 investigate oil production without CO_2 injection. Cases 3 and 4 introduced continuous CO_2 injection to investigate the potential to enhance recovery to above cases without CO_2 injection. The bottomhole pressure (BHP) maximum was set on the injection well not to exceed 20% more than the initial reservoir BHP. All of the dynamic simulations were performed using CMG's software package (www.cmgl.ca/) on a 184-core, high-performance, parallel computing cluster. The results of all four single-porosity–single-permeability simulation cases are shown in Table 2.

Results and Discussion of Simulations Using Single-Porosity–Single-Permeability Model

The results of the four cases, including oil production, CO_2 storage, and net CO_2 utilization, are listed in Table 2. Net CO_2 utilization was calculated by dividing the total stored CO_2 by incremental oil produced during the production periods. By comparing the oil production, 58% more oil was produced with CO_2 injection in Case 3 than the production without CO_2 injection in Case 1. This results in an increase in the cumulative oil production from 839 bbl in Case 1 to 1323 bbl in Case 3. The cases that used fracture relative permeability curves experienced a similar increase when CO_2 injection was utilized, with oil production in Case 4 (2680 bbl) 43% higher than Case 2 (1869 bbl), which had no CO_2 injection (Figure 5 and Table 2). By comparing the cases based on fracture or matrix relative permeability, the cumulative oil production was two to three times higher from fracture relative permeability in Cases 2 and 4 than the results using matrix relative permeability in Cases 1 and 3 (Table 2 and Figure 30). This explains the resulting lowered CO_2 net utilization of cases based on fracture when compared to the matrix. With respect to CO_2 storage, the matrix relative permeability case was observed to be more than twice as effective at storing CO_2 as the fracture relative permeability case.

Table 2. Results for All Four Cases Run Using the Single-Porosity–Single-Permeability Model

Case No.	RPT*	CO_2 Recycle	Injection Rate, Mscf/day	Produced Oil, bbl	Oil Change, %	Incremental Oil, bbl	Stored CO_2, Mscf	Net Utilization, Mscf/bbl
1	Matrix	No	N/A	839	N/A	N/A	N/A	N/A
2	Fracture	No	N/A	1869	N/A	N/A	N/A	N/A
3	Matrix	Yes	10	1323	58	484	11,213	23.17
4	Fracture	Yes	10	2680	43	811	4750	5.86

* Relative permeability curves (matrix or fracture systems).

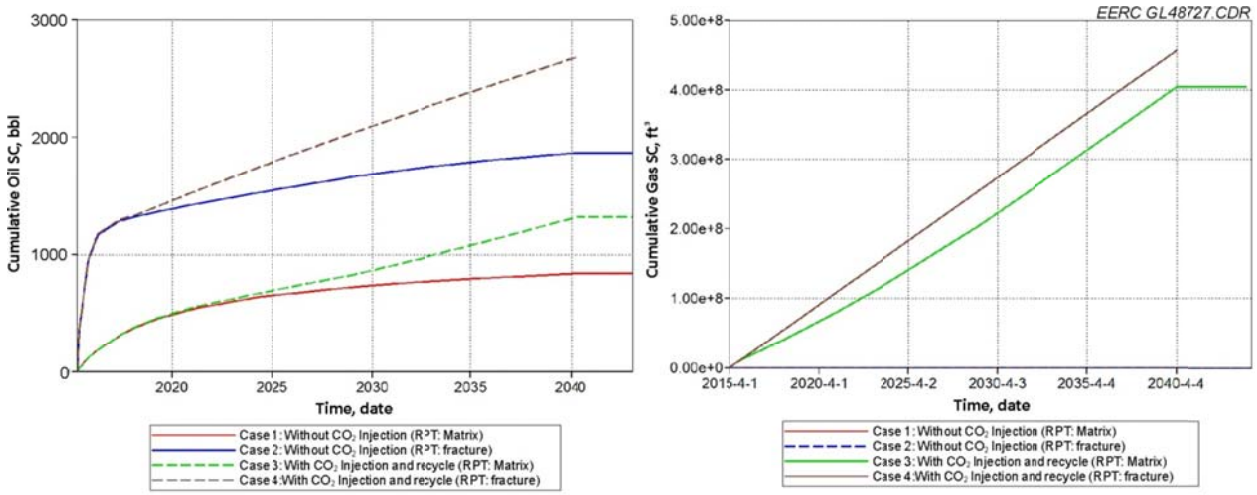

Figure 30. Results for the four cases. Left: Cumulative oil production over time. Right: Cumulative CO_2 injection (SC stands for surface condition).

The results of the simulations using the single-porosity–single-permeability models show that tight oil formations have the potential to serve as targets for CO_2 storage. They also suggest that CO_2 injection may play a significant role in increasing oil production. Results of this study indicate that production can be enhanced by 43% to 58% compared to cases without CO_2 injection. Since a single-porosity–single-permeability model was used, relative permeability curves that represent the fractures and matrix were both tested to determine the effects of this variable on the outcome. The results indicated that both CO_2 storage and CO_2 EOR are very sensitive to relative permeability, and that results varied over 100% between the two curves. This result underscores the notion that understanding the movement of CO_2 from the fracture network into the formation matrix is critical to achieving maximum storage capacity and EOR. This case study for CO_2 storage in the Bakken Formation provides a basic guideline to address CO_2-based EOR. Oil production results based on the relative permeability of the matrix or fracture used in the model are quite sensitive and lead to the 100% to 170% oil production difference. As such, it will be very important to have a good understanding of the contribution to flow from both the matrix and the fractures and to accurately understand the relative permeability of each portion. These sensitivities will be further addressed in the dual-porosity–dual-permeability model.

Simulations Using Dual-Porosity–Dual-Permeability Models (Bailey and Grenora Fields)

The injection of CO_2 into portions of the Bailey and Grenora Fields was simulated using the dual-porosity–dual-permeability geological model. In this study, the premise for both locations was that three horizontal wells were drilled through the reservoir zone of the Middle Bakken members (Figure 31). The middle well was designed as a producer, and the wells on both sides were used as injectors. In some cases, just the right-side well was opened for CO_2 injection to address a paired well performance. The distances between each of the three wells were fixed at 600 ft.

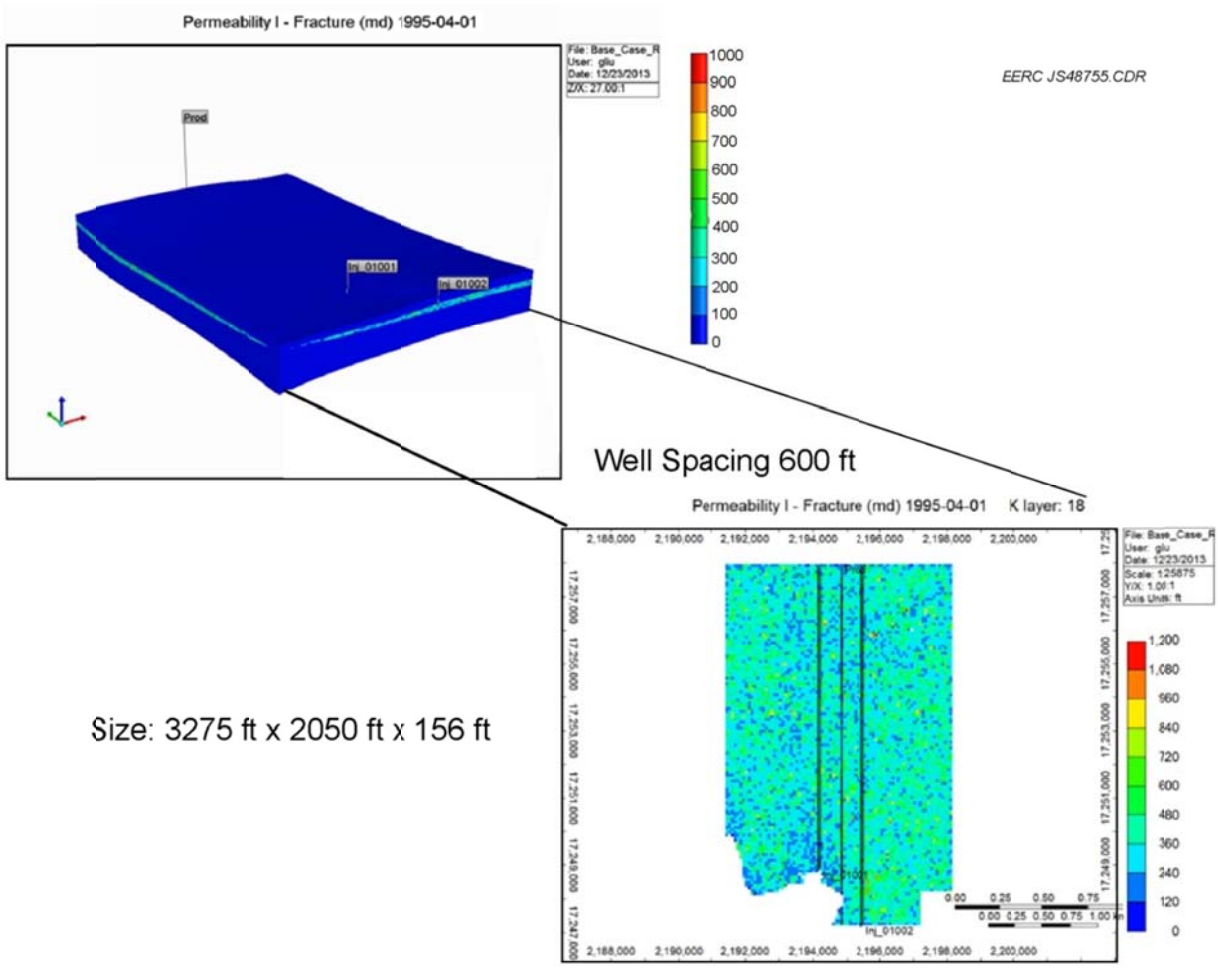

Figure 31. Geological model and well placements (Bailey Field).

After the dual-porosity–dual-permeability geological model had been prepared for simulation, the remaining steps of the dynamic modeling workflow were followed (Figure 29) (Gorecki and others, 2013). The PVT model and relative permeability parameters for matrix and fractures are the same as the setting used in the single-porosity–single-permeability models described above. The fluid model used in the simulation system was calculated based on laboratory oil compositional analysis and swelling test data that were provided by an operating partner. A total of 40 components were combined into five components (CO_2, N_2–C_1, C_2–C_3, C_4–C_6, C_7–C_{36+}) to generate the EOS parameters for the simulation (Kurtoglu, 2013). Three-phase relative permeability curves for matrix and fracture generated by one of the operating partners were applied to the simulations simultaneously. The parameters used to generate the curves based on the Brooks–Corey equations were the same as those used in the single-porosity–single-permeability model, listed in Table 1. As with the single-porosity–single-permeability model simulations, capillary pressure was neglected in the simulations because of the lack of laboratory test data.

The CO_2 was also allowed to dissolve into brine to mimic the nature of the saline system for CO_2 injection. The aqueous density and viscosity of the fluids were correlated by using the Rowe and Chou (1970) and Kestin and others (1981) methods, respectively, with varying temperatures and pressures of the saline system over the location and depth. Henry's law constant was correlated by Harvey's method to determine the solubility of CO_2 in the brine (Harvey, 1996).

To test CO_2 recovery in three scenarios, a total of six cases were designed to address factors such as CO_2 injection strategies and well configurations (Table 3) in the Bailey Field. Scenario 1 focused on the comparison of oil production and CO_2 injection results between the cases with one injector and one producer and two injectors and one producer. Scenario 2 added the diffusion phenomenon to the simulation to test the oil flowing out from the matrix to the fracture for EOR (Table 3). Scenario 3 opened production without CO_2 injection for 14 months and then added CO_2 injection to stimulate oil flow to the producer. The BHP constraint of the injection well was 20% more than the local BHP, which is less than the maximum pore pressure for injection. For the simulation of the Grenora Field, one case was tested based on the same settings of Case 2 of the Bailey Field (Table 4).

All of the dynamic simulations were performed using the CMG software package (www.cmgl.ca/) on a 184-core, high-performance, parallel computing cluster. The simulation time was started from April 1, 2015, to April 1, 2040. The CO_2 net utilization was calculated by a 5-year interval for the cases (Table 3). Results of the simulation of the Grenora Field are reported for just the first 200 days in Table 4.

Results and Discussion of Simulations Using Dual-Porosity–Dual-Permeability Model

The results of the injection and production simulations that were run using the single-porosity–single-permeability models indicated that CO_2 storage in tight oil formations is possible and that, in some cases, CO_2 injection could substantially improve oil production from the reservoir. The next step in the modeling process was to run the most promising CO_2 injection and EOR scenarios identified in the single-porosity–single-permeability simulations through the dual-porosity–dual-permeability models. The dual-porosity–dual-permeability models are thought to more accurately represent the Bakken reservoirs. Running the most promising injection and EOR scenarios through the dual-porosity–dual-permeability models provides additional, refined insight to the potential effectiveness of these approaches and will support the development of an optimal field test design.

The results of the five injection and production cases that were run in the dual-porosity–dual-permeability model, including oil production, CO_2 storage, and net CO_2 utilization for each case, are provided in Table 3. All five cases simulated schemes that included combinations of injection and production wells. Cases 4 and 5 start with a 14-month period of production without CO_2 injection (to represent a period of primary recovery); followed by a period of CO_2 injection (to represent a period of secondary recovery). A comparison of the relative effectiveness of the different injector–producer scenarios simulated in the dual-porosity–dual-permeability model is provided as follows.

Table 3. Results for the Six Cases for the Bailey Field Using the Dual-Porosity–Dual-Permeability Model

Results Summary											
Case	Well Settings	Diffusion Included	Production Before Injection	Time of Injection, years	CO_2 Injected, Mscf	CO_2 Produced, Mscf	CO_2 Stored, Mscf	% of HCPV	Oil Produced Before Injection, bbl	Oil Produced, total bbl	CO_2 Utilization Mscf/bbl
1	One injector One producer	No	No	5	183,000	118,000	64,800	0.30	NA	28,000	2.31
				10	365,000	247,000	118,000	0.55	NA	52,800	2.23
				15	548,000	381,000	167,000	0.77	NA	76,000	2.19
2	Two injectors One producer	No	No	5	365,000	264,000	101,000	0.47	NA	43,500	2.33
				10	731,000	564,000	167,000	0.78	NA	73,500	2.27
				15	1,100,000	874,000	222,000	1.03	NA	103,000	2.17
				20	1,460,000	1,190,000	274,000	1.27	NA	128,000	2.14
				25	1,830,000	1,500,000	322,000	1.50	NA	151,000	2.13
3	Two injectors One producer	Yes	No	5	365,000	264,000	101,000	0.47	NA	47,500	2.13
				10	731,000	564,000	167,000	0.78	NA	80,700	2.07
				15	1,100,000	874,000	222,000	1.03	NA	110,000	2.03
				20	1,460,000	1,180,000	276,000	1.28	NA	136,000	2.03
4	One injector One producer	No	Yes (1.17 yr)	5	1,770,000	1,230,000	535,000	2.49	5390	48,700	12.37
5	Two injectors One producer	No	Yes (1.17 yr)	2	1,340,000	901,000	437,000	2.03	5390	59,500	7.35

Table 4. Results for the One Case for the Grenora Field

Well Settings	Two injectors and one producer
Diffusion Included	No
Production Before Injection	No
Time, days	200
CO_2 Stored, Mscf	28,848
Oil Produced, bbl	3918
CO_2 Net Utilization, Mscf/bbl	13.58

By comparing the oil production over time in Case 1, it appears that 89% more oil was produced over the course of 10 years of injection than was produced in 5 years of injection and that 171% more was produced in 15 years of injection than was produced in 5 years (Table 3 and Figure 32). Case 1 results also show that CO_2 utilization decreased as the injection periods became longer, which further supports the observation that the EOR operation became more efficient as time went on. For the other cases, the results show a similar tendency that CO_2 storage and oil production substantially increases over time with CO_2 injection regardless of whether one injector or two injectors were used in the simulation. However, for cumulative oil production in a specific time period, the results with two injectors definitely showed more productivity than the case with one injector. This increasing percentage dropped over the time period. For example, for the first 5 years of production, the increase is 56% by comparing Cases 1 and 2, and then this number dropped to 33% after 15 years of production. This observation also applied to the amounts of CO_2 stored (Table 3 and Figure 32). In general, these results suggest that an EOR scheme that pairs two injectors with one producer will have lower CO_2 utilization rates and produce more oil than a single injector–producer scheme. It also appears that the incremental recovery and efficiency improve with longer periods of injection.

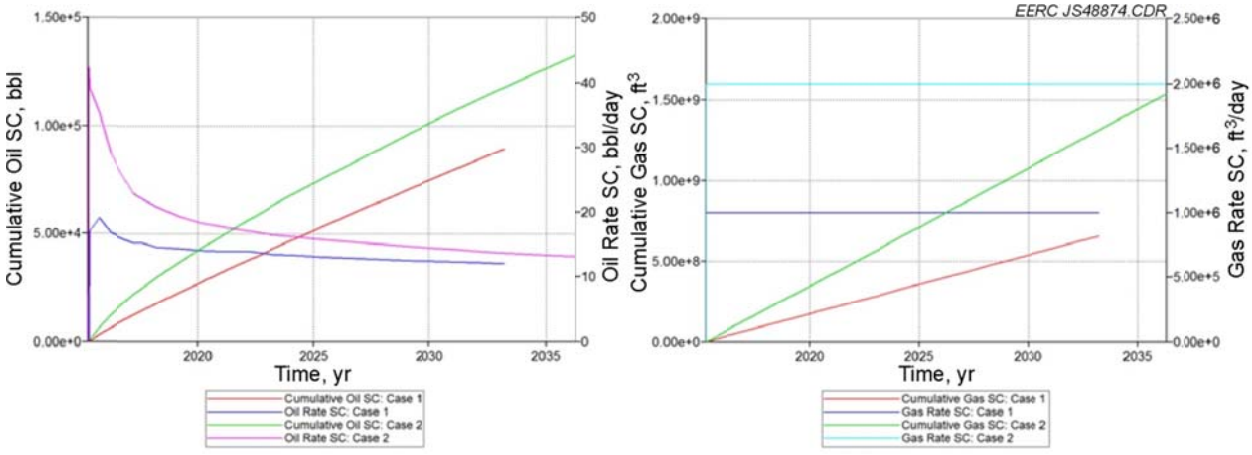

Figure 32. Results of Cases 1 and 2: Cumulative oil production and oil production rate (left) and cumulative CO_2 and CO_2 injection rate (right).

The case with diffusion behavior included as part of the simulation (Case 3) shows better oil production than the case without this phenomenon (Case 2). The likely reason for this result is that much of the oil in the matrix was mobilized by CO_2 (Table 3 and Figure 33), a phenomenon supported by laboratory data generated by experiments conducted as part of this research program and described in the next section of this report. However, this diffusion-driven enhancement is not obvious in the beginning of the production period because that period is dominated by fracture flow, which primarily explains why the enhancement of the case with diffusion is increasing over time. Specifically, results for the 10-year period show that production is about 10% more in Case 3 than it is in Case 2, even though the amount of injected CO_2 is the same (Table 3 and Figure 32). Regarding the effect of diffusion on CO_2 storage, these modeling results suggest that it has minimal effect, although integration of experimentally derived diffusion data in future modeling efforts may show otherwise. With respect to the time frame for CO_2 breakthrough in the production well, the cases with two injectors are about 10 days, which is faster than the 18-day breakthrough observed in the case with one injector (Figure 34).

Cases 4 and 5 included a 14-month period of primary oil production before beginning CO_2 injection. Case 4 results show that the oil production in the first 5 years is greater than one in Case 1 (Table 3 and Figure 35), primarily because the production period is longer in Case 4 and more CO_2 is injected for enhancing recovery because more oil is being produced than in Case 1.

This also explains why the CO_2 utilization factor is greater than the utilization factors for cases without a period of primary production before injection (Table 3). Adding a second injector in Case 5 resulted in 22% more oil being produced, and significantly less CO_2 stored, as compared to Case 4 (Table 3 and Figure 33).

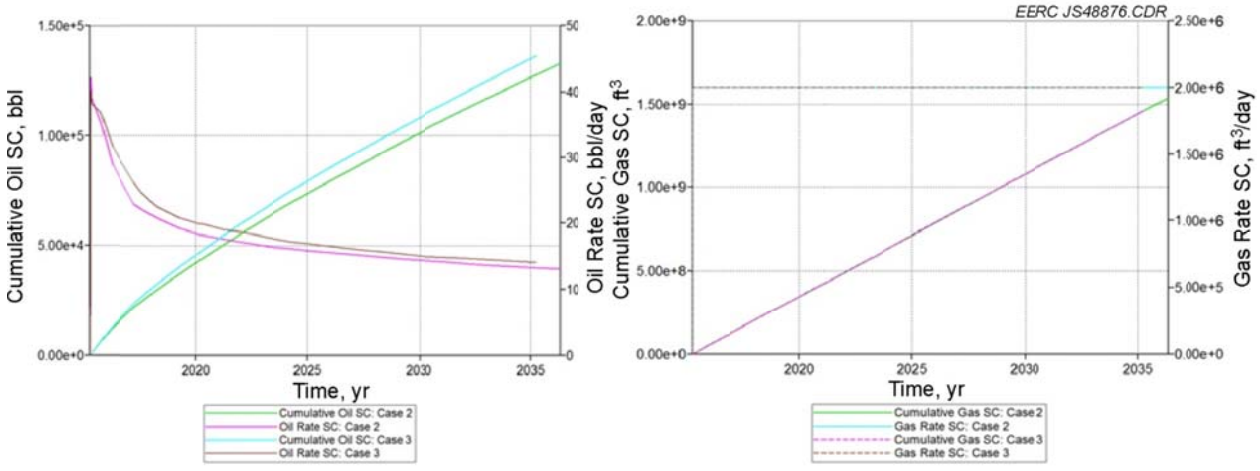

Figure 33. Results of Cases 2 and 3: Cumulative oil production and oil production rate (left) and cumulative CO_2 and CO_2 injection rate (right).

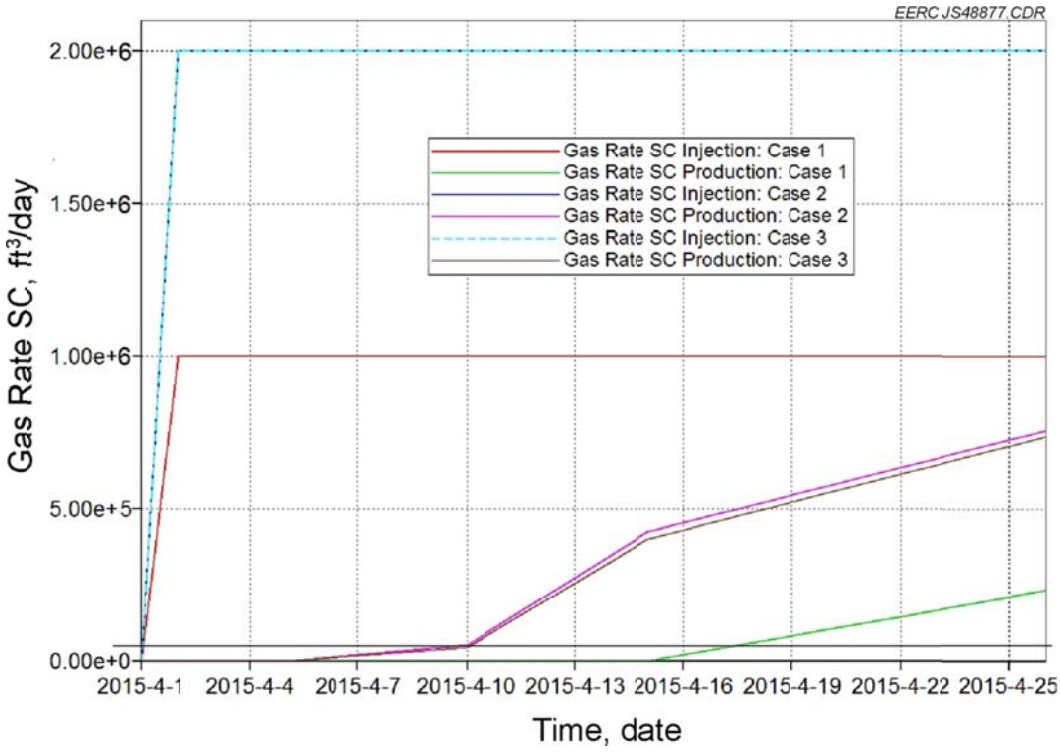

Figure 34. CO_2 breakthrough on production well for Cases 1, 2, and 3.

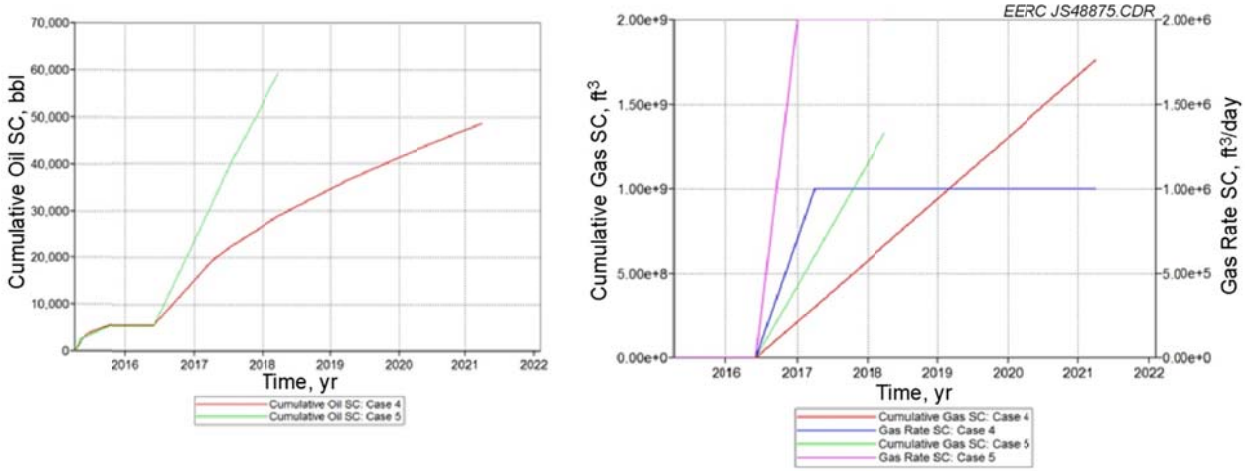

Figure 35. Results of Cases 4 and 5: Cumulative oil production (left) and cumulative CO_2 and CO_2 injection rate (right).

Summary of Key Observations from CO_2 Injection and EOR Simulations

The first round of CO_2 injection–oil production simulations were run using the single-porosity–single-permeability models. Initial simulation results indicated that not only is CO_2 injection into the Bakken feasible, but the potential for storage and EOR may be significant, with some scenarios showing the potential to produce over 50% more oil as compared to production without CO_2 injection. Some of the injection–production scenarios were then simulated using a dual-porosity–dual-permeability model to provide further insight regarding their potential effectiveness in the field. Those results suggest that an EOR scheme that pairs two injectors with one producer will produce more oil than a single injector–producer scheme. They also indicate that patience may be rewarded, with the incremental recovery and efficiency improving with longer periods of injection.

The results of one of the dual-porosity–dual-permeability simulation runs indicated that diffusion may play a significant role in moving oil from the reservoir matrix into the fracture network. This modeling result is supported by the results of the laboratory-based CO_2 hydrocarbon elution experiments from Bakken rock samples, which also showed that well over 50% of hydrocarbons could be mobilized from the matrix in a reasonable amount of time. While these modeling results might suggest that diffusion does not appear to significantly affect the amount of CO_2 stored, it is important to note that these modeling exercises may not accurately account for all of the interactions that might occur between CO_2 and these organic-rich rocks. An improved knowledge of those interactions, and their integration into future modeling activities, may show that the CO_2 storage capacity of the Bakken is actually higher than what is shown in these results.

However, it is important to note that the high degree of complexity in the Bakken static models means that a single round of Bakken reservoir simulations will take several days to weeks to run. This limits the number of injection scenarios and cases that can be simulated over the course of a given project. These limitations precluded the running of enough simulations to do any robust sensitivity analyses or optimization studies on any of the potential CO_2 injection–EOR scenarios. Future studies of CO_2 storage and EOR in the Bakken should include robust sensitivity analysis of the well placement, well spacing and operational optimization, diffusion analysis based on the potential formations, hydraulic fracture optimization based on the dual-porosity–dual-permeability system, and sequential multiwell huff ‘n’ puff investigations. Such efforts would provide tremendous insight into the design and implementation of field-based pilot tests.

OIL CHARACTERIZATION RESULTS

The Effects of CO_2 on Bakken Oil

The challenges of EOR within the Bakken have to do with the mobility of traditional fluids (i.e., reservoir fluids and injected water vs. CO_2, polymers, or surfactants) through natural or induced fractures relative to very low matrix permeability and the effects of exposing swelling clays to water, which can reduce permeability and damage the formation. Further, the oil-wet nature of much of the Bakken system will dramatically minimize the effectiveness and utility of

waterflooding. With these issues in mind, the use of CO_2 as a fluid for EOR in the Bakken may be effective. To predict the performance of CO_2 EOR in the Bakken, the program included a suite of experimental activities to help quantify phase behavior and fluid property under reservoir conditions. As with the reservoir characterization efforts, the specific oil–CO_2 interaction data (i.e., minimum miscibility pressure [MMP]) were determined within the context of previously generated oil property data and in close consultation with the operating partners. The data generated by these activities not only provided insight regarding the effects of CO_2 on Bakken oil but were ultimately integrated into the dynamic simulation modeling of potential CO_2 EOR injection and production schemes.

Rapid and Simple Determination of MMP (expedited MMP)

Methods to determine MMP of crude oil (e.g., slim tube, rising bubble) can be costly, slow, and subject to operational variations. In contrast, vanishing interfacial tension (VIT) methods rely on a more fundamental definition of miscibility, i.e., the conditions at which there is no interfacial tension (IFT) between the two fluids. IFT is determined at different injection fluid pressures, yielding an IFT/pressure curve which is extrapolated to zero IFT, with the pressure intercept being MMP. Determining IFT requires measuring the oil height in a capillary tube (with accurately known internal diameter) and the density of both fluid phases at each experimental condition. The requirement for density determinations adds complexity and cost because of the densitometer required as well as the need to transfer both fluids to the densitometer at each pressure step without affecting the oil composition in the experimental system (Ayirala and Rao, 2011).

Fortunately, it is not necessary to measure IFT at several pressures to determine when the IFT goes to zero since a plot of the oil height in the capillary versus pressure will intercept the pressure axis at the same value as the IFT data. That is, both zero IFT and zero capillary rise height occur at the same pressure. This approach yields linear plots (rather than the curves from IFT versus pressure data), and no density measurements are needed, which greatly reduces instrument cost and experimental complexity. The need to transfer fluids to the densitometer is eliminated, assuring a constant oil composition during experiments, and only a few grams of oil is needed. The rising capillary approach to estimating MMP is based on determining when the surface tension between the bulk crude oil and the overlying CO_2 phase goes to zero. This is measured by placing the oil in a view cell (the viewing window is ca. ¾ inches in diameter) and sequentially adding CO_2 starting from ambient up to when the oil level in the capillary can no longer be observed to be above the level of the bulk oil in the bottom of the cell. Each sequential pressure addition of CO_2 results in a very rapid change in the capillary height, so a new data point is produced with each pressure step. The method uses three capillaries with different diameters so that three full sets of data can be generated from each experimental run. Figure 36 is an example of the data that are generated by this method. The pressure at which the three lines converge on a zero value for height is considered to be the MMP value for CO_2 in that particular oil sample.

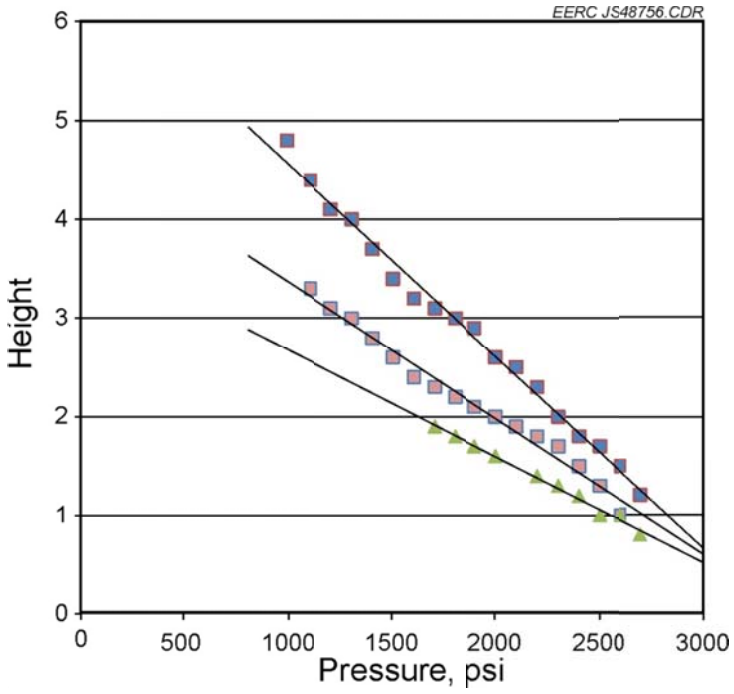

Figure 36. Example of data generated by the capillary rise approach for MMP determination.

Prior to adding the CO_2, the cell and oil are preheated to the reservoir temperature (110°C for Bakken experiments) in an oven with high-precision temperature controls. Figure 37 shows the view cell within which the MMP experiment is conducted and the chamber loaded with a Bakken oil sample and the three capillaries.

As part of this project, samples of "dead" oil (i.e., oil that had not been specially collected and preserved to retain dissolved gases) and "live" oil (i.e., oil that had been specially collected and preserved to retain dissolved gases and was, therefore, considered to be representative of the oil in the reservoir) were subjected to MMP tests. The dead oil experiments were largely used to develop the method. While a detailed discussion of the dead oil results is not particularly insightful with respect to the MMP in an actual Bakken reservoir, the resulting MMP values were sufficiently in line with MMP values for other oils reported in the literature and through communication with operator partners about Bakken MMP values derived by slim-tube tests to move forward with the more complicated live oil MMP experiments. The MMP value for two different samples of live Bakken oil obtained by the rising-capillary test were approximately 3180 and 3196 psi, respectively, which agree very well with the values determined by the commercial partner using EOS.

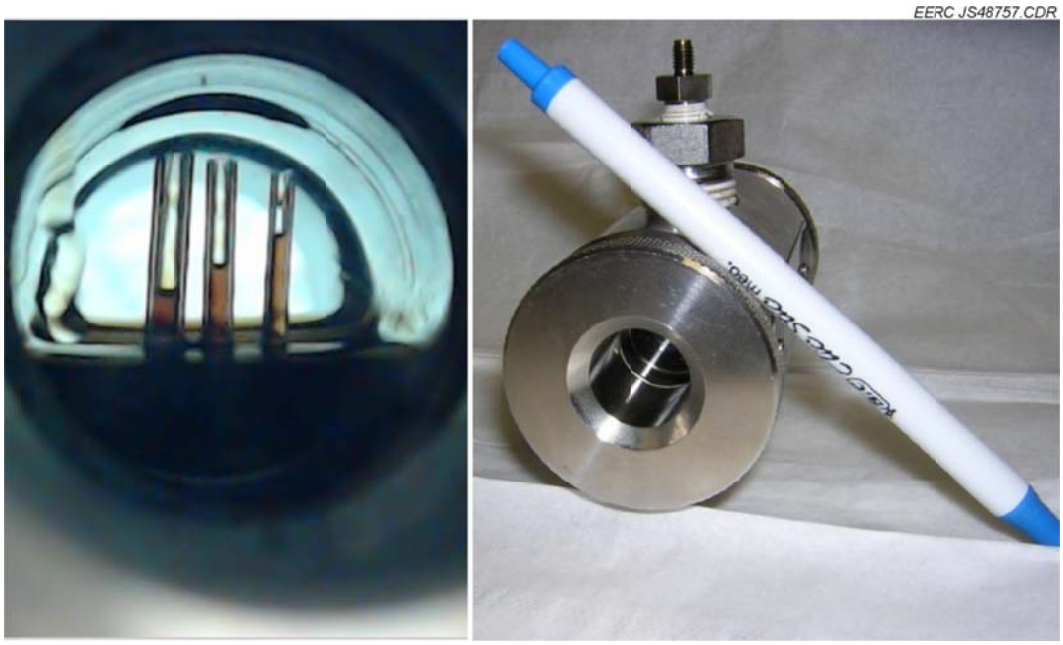

Figure 37. Photos of Bakken oil and three capillaries within the view cell chamber (left) and the view cell chamber (right).

With this simplified approach, MMP determinations can be rapidly and cost-effectively determined, allowing the effects of multiple parameters on MMP to be investigated. For example, MMP values could be tracked during the entire production of a reservoir, rather than relying on only the MMP value originally determined. Questions such as, What happens to the MMP values in the reservoir as the oil/gas ratio changes?, can efficiently be investigated by exposing produced oil to various hydrocarbon gas compositions, rather than relying only on predictive modeling correlations.

HYDROCARBON ELUTION EXPERIMENTS ON BAKKEN SAMPLES

Preliminary CO_2 extraction/exposure experiments of Bakken reservoir rock show that oil recovery may be driven by exposure time more than the CO_2 quantity used in tight, hydraulically fractured formations. In essence, the data indicate that oil recovery mechanisms shift from sweeping the oil through the reservoir rock (as in permeable reservoirs) to much slower processes where the CO_2 first flows into the fractures and surrounds the unfractured rock portions, followed by recovery mechanisms that are more limited by CO_2 exposure time than CO_2 volume. Given the difficulty in generating reproducible relative permeability data for tight formations and the many questions surrounding the relevance and applicability of conventionally derived relative permeability data to unconventional reservoir rocks, a series of CO_2 extraction/exposure experiments on Bakken rock samples were conducted to provide previously unavailable insight regarding the ability of CO_2 to mobilize oil in the Bakken. The EERC conducted CO_2 extraction/exposure experiments on samples of Upper, Middle, and Lower Bakken rocks. The purpose of the investigations was to gain a better understanding of the

mechanisms that control CO_2 EOR from the matrix within tight reservoirs in order to provide insights on how to better design and manage CO_2 EOR efforts. Understanding these mechanisms will also provide insight as to the extent that tight oil-bearing formations such as the Bakken may serve as targets for CO_2 storage.

The basis for the approach that was taken in these experimental activities is that CO_2-based EOR and storage mechanistic processes will be very different for these tight formations from those that control CO_2 storage and recovery of oil from conventional reservoirs. From an oil recovery standpoint, CO_2-induced processes that are important to EOR in conventional (i.e., permeable) formations, including oil swelling, lowered oil viscosity, and the formation of multiple-contact, miscible mixed CO_2–oil phases are likely to also enhance oil recovery from tight formations (Jarrell and others, 2002). However, the displacement mechanism of oil production caused by the action of CO_2 flowing through conventional reservoir rock matrix will not likely apply to tight formations. In tight formations, the bulk CO_2 is expected to flow through natural and produced fractures but not significantly through the nonfractured rock matrix. Thus oil remaining in the unfractured rock will not experience significant sweeping (displacement) flow of CO_2 from injection to production areas but will only see CO_2 that permeates into the rock after the CO_2 first fills the fracture spaces.

This section reports the results of CO_2 exposure experiments designed to mimic the proposed mechanisms in an effort to better understand and, hopefully, to better exploit these processes to enhance EOR in the Bakken play (Hawthorne and others, 2013). It is important to note that these investigations focus solely on processes that control the transport of oil from the rock matrix into the CO_2-filled fractures but do not address subsequent engineering, completion, and production steps needed to move the hydrocarbons to the production well.

Conceptual steps for the use of CO_2 for EOR and storage in the Bakken include the following: 1) CO_2 flows into and through the fractures; 2) unfractured rock matrix is exposed to CO_2 at fracture surfaces; 3) CO_2 permeates the rock initially driven by pressure, carrying some hydrocarbon inward, but the oil is also swelling and extruding some oil out of the pores; 4) oil migrates to the bulk CO_2 in the fractures via swelling and reduced viscosity; and 5) as the CO_2 pressure gradient gets smaller, oil production is slowly driven by concentration gradient diffusion from pores into the bulk CO_2 in the fractures.

To investigate these concepts, rock samples from the Middle Bakken (low permeability), Upper and Lower Bakken (very low permeability), and a conventional reservoir (high permeability) were exposed to CO_2 at Bakken conditions of 110°C and 5000 psi (230°F, 34.5 MPa) to determine the effects of CO_2 exposure time on hydrocarbon production. Varying geometries of each rock ranging from small (mm) “chips” to 1 cm-diameter rods were exposed for up to 96 hours, and mobilized hydrocarbons were collected for analysis.

Mechanistic Considerations for Hydrocarbon Elution Experiments

As noted above, it is likely that the flow patterns of CO_2 (and other EOR fluids) will be substantially different in conventional reservoirs (where CO_2 flows through the rock matrix and sweeps the oil out in a manner mimicked by the sand-packed and oil-saturated slim tube) and

unconventional, tight, hydraulically fractured reservoirs (CO_2 is expected to flow most rapidly through the major and minor fractures) but not significantly through the unfractured rock matrix.

The proposed conceptual mechanisms for CO_2 EOR in tight hydraulically fractured systems are shown in Figure 38. During the initial phases of CO_2 injection (Step 1), the CO_2 flows rapidly through fractures but not through the rock matrix itself. The CO_2 then begins to permeate the rock matrix driven by the pressure gradient caused by CO_2 injection (Step 2). The initial permeation of CO_2 into the rock matrix could potentially reduce oil production by carrying oil near the surface deeper into the rock matrix. Conversely, the oil swelling caused by the CO_2 could yield increases of oil during the pressurization process. As CO_2 continues to permeate the rock, the oil will increasingly migrate to the rock surface (and into the fractures) based on swelling and lowered viscosity caused by the CO_2 (Step 3). The CO_2 pressure then begins to equalize throughout the rock matrix (Step 4). At this point, oil swelling and lowered viscosity and the possible formation of a CO_2–oil miscible phase continue to enhance oil mobilization. Finally, as pressure equilibrium is approached, concentration-driven diffusion of hydrocarbons in CO_2 from the rock interior to the bulk CO_2 in the fractures may become the dominating process.

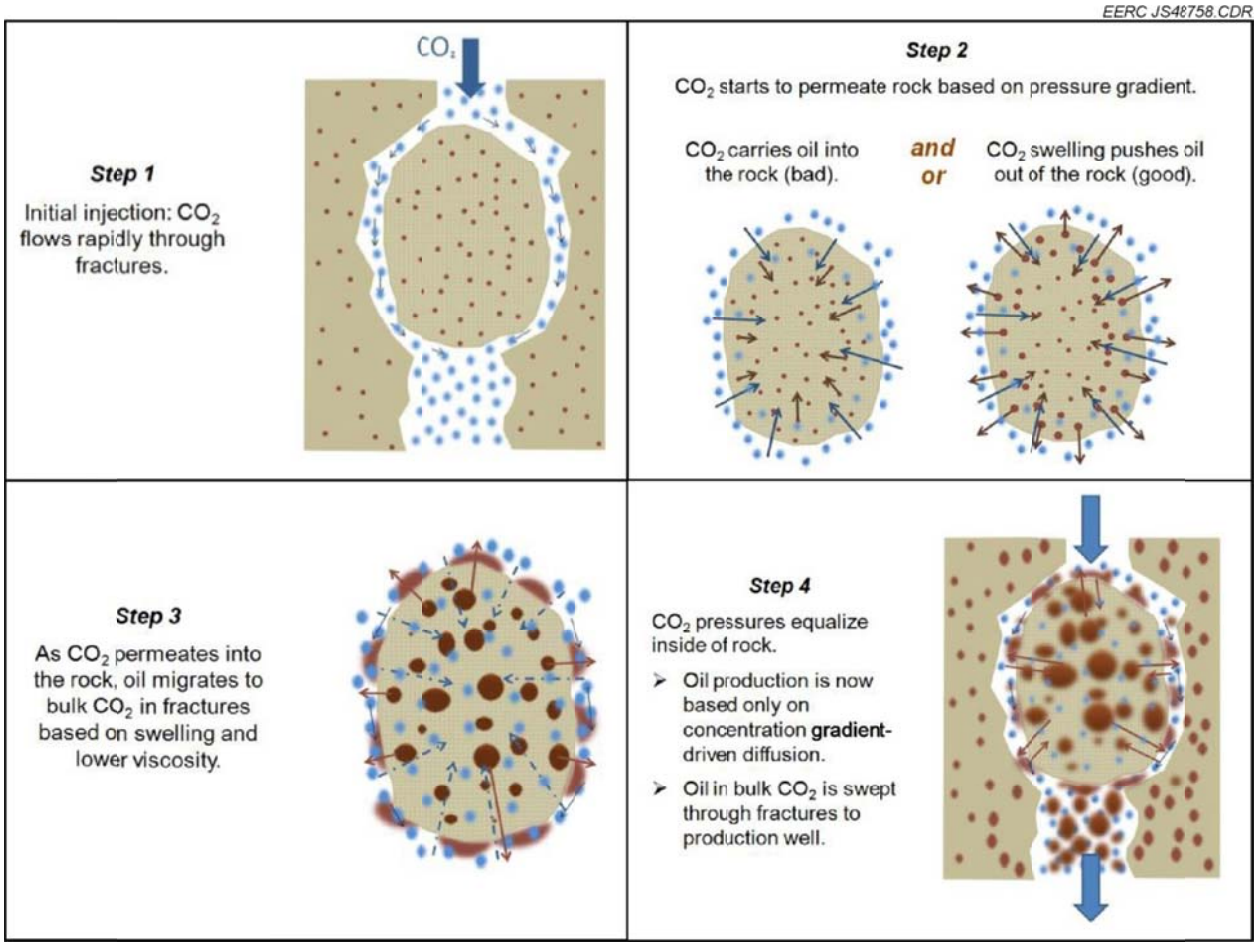

Figure 38. Conceptual steps for CO_2 EOR in fractured tight reservoirs. The individual steps are described in the text.

As in any chemical/physical process, there are two overall controlling factors that must be satisfied, i.e., the thermodynamics of the process (Is CO_2 capable of mobilizing oil in tight formations under the temperature/pressure conditions of that reservoir?) and the kinetics of that process (Does the mobilization of the oil occur rapidly enough to be useful?). The experiments reported here are an attempt to answer those two fundamental questions.

Hydrocarbon Elution Test Samples

Samples were obtained from two locations in the Bakken Formation. Samples of Middle Bakken reservoir rock and both upper and lower source shales from the same borehole in a thermally mature area of the formation in North Dakota were provided by an operator. Middle and Lower Bakken samples from another well were also obtained from the North Dakota Geological Survey core library, also representing a thermally mature region. In the regions sampled, Middle Bakken porosities range from 4.5% to 8.1% and permeabilities from 0.002 to 0.04 mD (Kurtoglu and others, 2013). Values for the porosity and permeability of lower and upper shales are not available, but permeability is expected to be orders of magnitude lower compared to Middle Bakken reservoir rock. A sample from a conventional sandstone reservoir was also obtained to act as a reference sample that would display the "fastest" CO_2-enhanced scenario under the experimental conditions used. Typical values in that region of the conventional reservoir are ca. 25% porosity and ca. 800 to 1100 mD permeability.

Different geometries (Figure 39) were prepared from the bulk samples, including 3–4-cm-long round rods made with a ca. 1-cm coring bit, 3–4-cm-long × ca. 9 × 9-mm square rods cut with a high-pressure water jet, 2–3-mm-thick × ca. 9 × 9-mm squares ("chicklets") by flaking of the square rods along existing fracture planes, and smaller particles prepared by crushing the samples to pass a 3.5-mm sieve. Crude oil samples were also obtained from similar locations for use as calibration standards.

Hydrocarbon Elution Experimental Methods

All CO_2 exposures were performed at reservoir conditions of 5000 psi and 110°C. Exposures were performed using an ISCO Model 210 SFX extractor, with the high-pressure CO_2 supplied by an ISCO Model 260D syringe pump set to deliver a constant 5000 psi of CO_2 to the extraction unit. Rock samples were placed into the 10-mL sample cell shown in Figure 2. It should be noted that the 5- to 8-gram samples were not sealed to the cell wall in any way (in contrast to what would be done, for example, for a high-pressure permeation test), so that the CO_2 was free to flow around the pieces of rock samples rather than being forced through the rock matrix, in order to mimic the fracture flow dominance anticipated in tight hydraulically fractured systems. CO_2 entered through the top of the cell and exited through the bottom of the cell to pass through a heated flow restrictor that controlled the CO_2 flow (measured as liquid CO_2 at the pump) at 1.5 mL/minute. The heated outlet of the restrictor was placed in a vial containing 15 mL of methylene chloride to collect the produced hydrocarbons. CO_2 outlet flow could be continuous (dynamic mode) or stopped (static mode) as controlled by a shut-off valve located between the extraction cell outlet and the outlet restrictor. More detailed descriptions of the CO_2 exposure instrumentation and operation are provided by Hawthorne (1990).

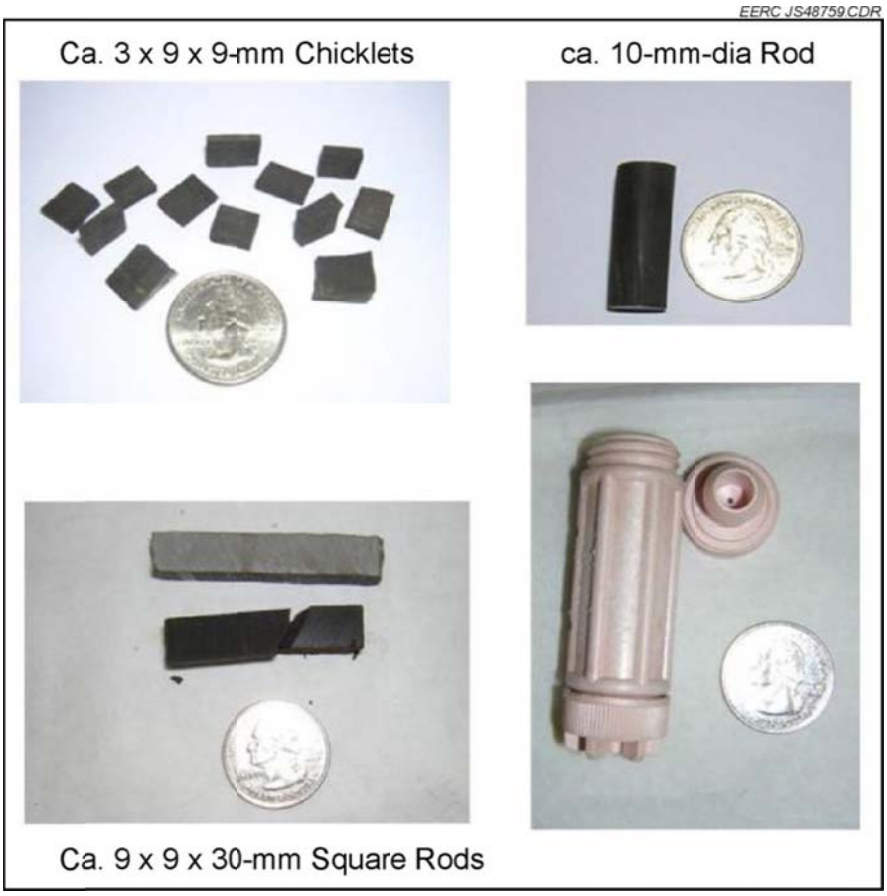

Figure 39. Typical reservoir and source rock samples prepared for CO_2 exposure. Samples are placed in the 10-mL extraction vessel (15 mm i.d. × 57 mm long, lower right), and exposed to CO_2 as described in the text.

Produced hydrocarbons (C7+) collected at the restrictor outlet were analyzed using capillary gas chromatography coupled with a flame ionization detector (GC–FID) using tetradecylbenzene as a quantitative internal standard and the Bakken crude oils as calibration standards. After the CO_2 exposures were completed, the residual rock samples were crushed to a powder and extracted with a 1:2 acetone/methylene chloride solvent with the aid of sonication for several hours. Replicate extractions were performed until no more significant hydrocarbon could be extracted. The sum of all the collected CO_2 extracts and rock residue solvent extracts was considered to be 100% of the hydrocarbon in the rock matrix.

Results of the Hydrocarbon Elution Experimental Activities

Initial 96-hour Exposures with Static (nonflowing) CO_2

Because of the low permeability of the Bakken reservoir and source rocks, it was expected that hydrocarbon recovery using CO_2 would be very slow, even with the small rock samples being exposed. Therefore, the initial hydrocarbon mobilization experiments were conducted for

96 hours. For the first day, the sample was pressurized to 5000 psi (110°C) under static (nonflowing) conditions for 50 minutes, followed by a 10-minute dynamic sweep with CO_2 to collect the mobilized hydrocarbons as described above. Approximately 15 mL of dense CO_2 (ca. 2 cell void volumes) swept the cell during the 10-minute dynamic collection step (instrumentation automatically maintained the CO_2 pressure and temperature at 5000 psi and 110°C, regardless of whether the CO_2 flow was static or dynamic). This 1-hour sequence was repeated for 7 hours, then followed by longer static exposures with 10-minute collections of the mobilized hydrocarbons at 24, 48, 72, and 96 hours. The remaining rock residue was then solvent-extracted to determine residual hydrocarbons as described above.

Results of the 96-hour exposures are shown in Figure 40. As might be expected based on its high permeability, hydrocarbons were rapidly recovered to nearly 100% from the conventional reservoir rock square rod sample. These results clearly demonstrated that even though the CO_2 is not flushing through the reservoir rock, but is only surrounding it (followed by the recovery mechanisms discussed above), the hydrocarbon recovery is not only rapid but highly efficient. Surprisingly, the recoveries from the Middle Bakken were also high and quite rapid from the square rod. While it took only ca. 2 hours to recover 90% from the conventional reservoir square rod, 90% recovery was achieved by ca. 4 hours from the Middle Bakken square rod. Also, recovery rates from the smaller Middle Bakken chicklets were essentially the same as from the conventional square rod sample.

As would be expected, recovery from the even tighter Lower Bakken sample was much slower from the square rods, and only ca. 60% of the hydrocarbon was recovered in 96 hours, still surprisingly high considering the very low permeability of this source shale. In addition, hydrocarbon recovery in 96 hours from the Lower Bakken shale increased to >80% as the thinner chicklets were exposed to the CO_2, as would be expected since smaller particles require less time for CO_2 mobilization of interior hydrocarbons, as proposed in Figure 1 and the related mechanistic discussion.

Hydrocarbon Recovery under Dynamic (flowing) CO_2 Conditions

Since the times involved to achieve such high recoveries in a reservoir are likely to be much too long to be practical, and since even very small (e.g., 1%) increases in oil recovery represent a tremendous amount of additional oil produced, additional shorter exposures were performed under dynamic (flowing CO_2) conditions using the operator-provided Lower, Middle, and Upper Bakken samples obtained from a single borehole. CO_2 flow was continuous during the first 7 hours of extraction, then static from 7 to 24 hours, followed by a 1-hour dynamic collection of the produced hydrocarbons. In order to obtain data to investigate the very early exposure steps outlined in Figure 1, samples were collected from 0 to 10, 10 to 30, and 30 to 60 minutes followed by hour-long collection periods.

As shown in Figure 4, recovery from the Upper and Lower Bakken round rods is very slow and only achieves ca. 40% after 24 hours of CO_2 exposure. As noted for the other Middle Bakken sample in Figure 3, recovery from the Middle Bakken round rod is nearly as fast as that from the permeable conventional reservoir round rod, demonstrating that on the centimeter scale,

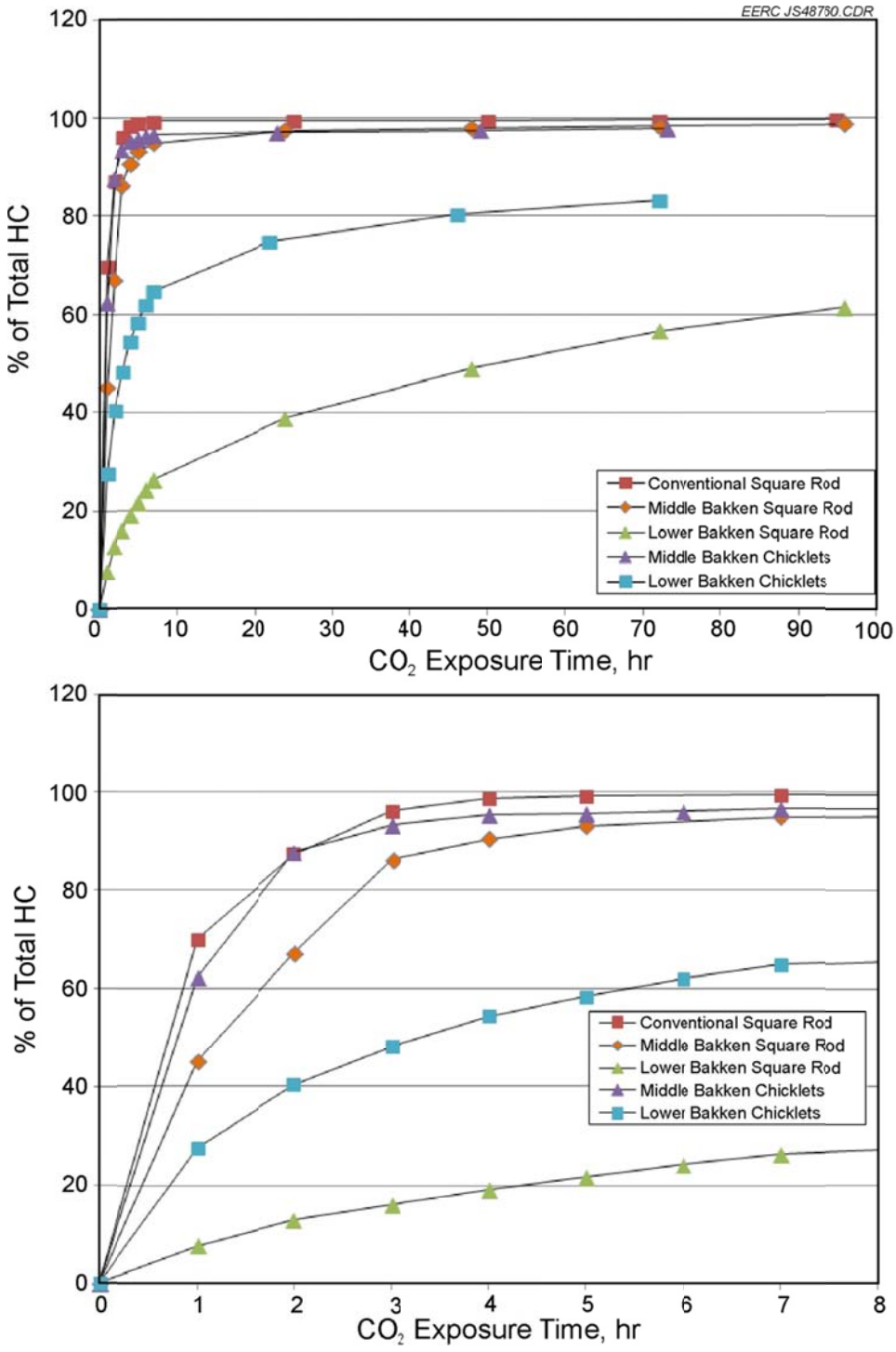

Figure 40. CO_2 mobilization of hydrocarbons from Middle Bakken, Lower Bakken, and a conventional reservoir rock with 96 hours of exposure at 5000 psi and 110°C. The lower plot has the time scale expanded to show hydrocarbon recovery during the first 8 hours of exposure. "Square rod" indicates a ca. 9 × 9 × 40-mm rectangular rod, and "chicklets" indicates ca. 3 × 9 × 9-mm flat squares.

CO_2 is fairly efficient at recovering hydrocarbons from the rock interior. As expected based on mass transfer consideration in the very low permeability Upper and Lower Bakken shales, increasing the surface area by grinding to <3.5 mm dramatically raises the recovery rates, with nearly complete hydrocarbon recovery achieved after 24 hours of CO_2 exposure (Figure 41).

Effect of Hydrocarbon Molecular Weight on Recovery Rates with CO_2

Bulk effects of CO_2 dissolving into the oil in the rock matrix (i.e., swelling and lowered viscosity) would be expected to show little molecular weight preference in the recovered hydrocarbons. In contrast, recovery processes that involve mobilizing hydrocarbons into the CO_2 would favor lighter hydrocarbons both because they have higher solubility than higher-molecular-weight hydrocarbons and because formation of a new miscible phase of mixed CO_2–hydrocarbons favors lower- over higher-molecular-weight hydrocarbons. Therefore, it is useful to observe the molecular weight distribution in the hydrocarbons recovered during the CO_2 exposures. As shown in Figure 42 for the round rod samples, there is a great degree of preference for CO_2 recovery of lighter versus heavier hydrocarbons, as is especially evident from the tighter Upper and Lower Bakken shales. For example, the C7 hydrocarbons are recovered ca. 10-fold faster than the C20 hydrocarbons from the Upper and Lower Bakken shales. Although the same range of hydrocarbons could not be observed from the Middle Bakken sample (because of their loss during transport and storage of the core sample), some preference for lighter hydrocarbons is also observed for the Middle Bakken sample. The implications of these results are discussed as follows.

Implications of the Results of Hydrocarbon Elution Experiments

The experimental results discussed above support the overall mechanism proposed in Figure 1 for hydrocarbon recovery from tight formations. Some interpretations of these results in reference to the steps described in Figure 1 include the following:

- Step 1: Since the rock samples are not sealed in the extraction vessel, the step of flowing the CO_2 around the sample rather than through the rock matrix should be valid to represent fractured, tight systems such as the Bakken.

- Step 2: Since there is no apparent lag in oil recovery, even when samples are collected during the first 10 minutes of exposure, the concern that the initial pressurization could reduce hydrocarbon production by carrying hydrocarbons into the rock matrix does not seem to be significant. Similarly, the absence of an especially fast recovery in the first few minutes indicates that the initial oil swelling is not a significant recovery mechanism (although it should be noted that these observations on small samples may not be relevant in the actual reservoir conditions).

- Step 3: While both oil swelling and lowered oil viscosity caused by CO_2 dissolving into the oil are likely to enhance recovery, the high degree of preference to produce lower-molecular-weight hydrocarbons, shown in Figure 42, demonstrates that mobilization of hydrocarbons into the CO_2 (rather than dissolution of CO_2 into the bulk oil) is a

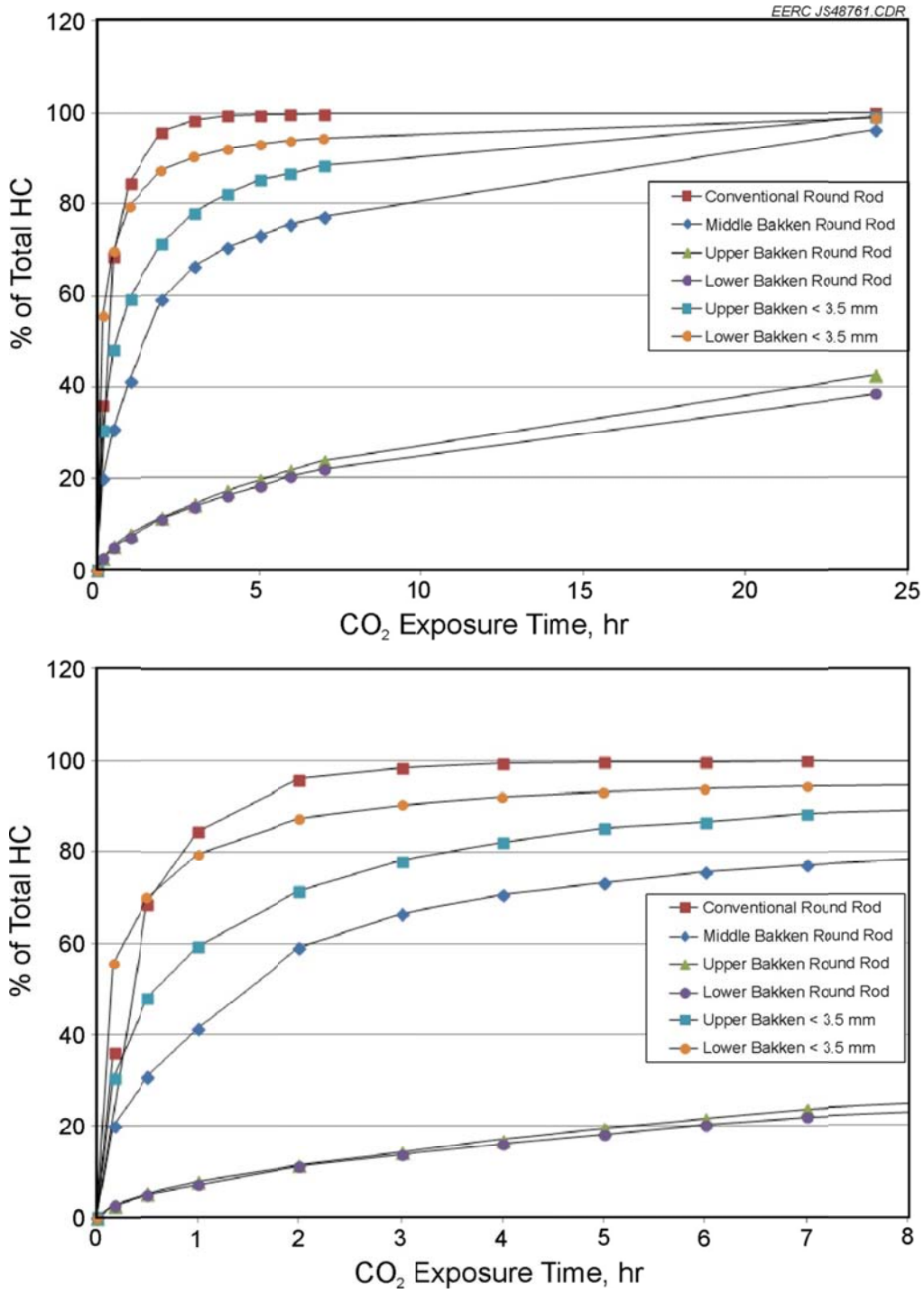

Figure 41. CO_2 mobilization of hydrocarbons from Upper Bakken, Middle Bakken, Lower Bakken (all from the same borehole), and a conventional reservoir rock with 24 hours of CO_2 exposure at 5000 psi and 110°C. The lower plot has the time scale expanded to show hydrocarbon recovery during the first 8 hours of exposure. "Round rods" refer to cylinders with a diameter of ca. 10 mm × ca. 40 mm long; "<3.5 mm" indicates rock crushed to pass a 3.5-mm screen.

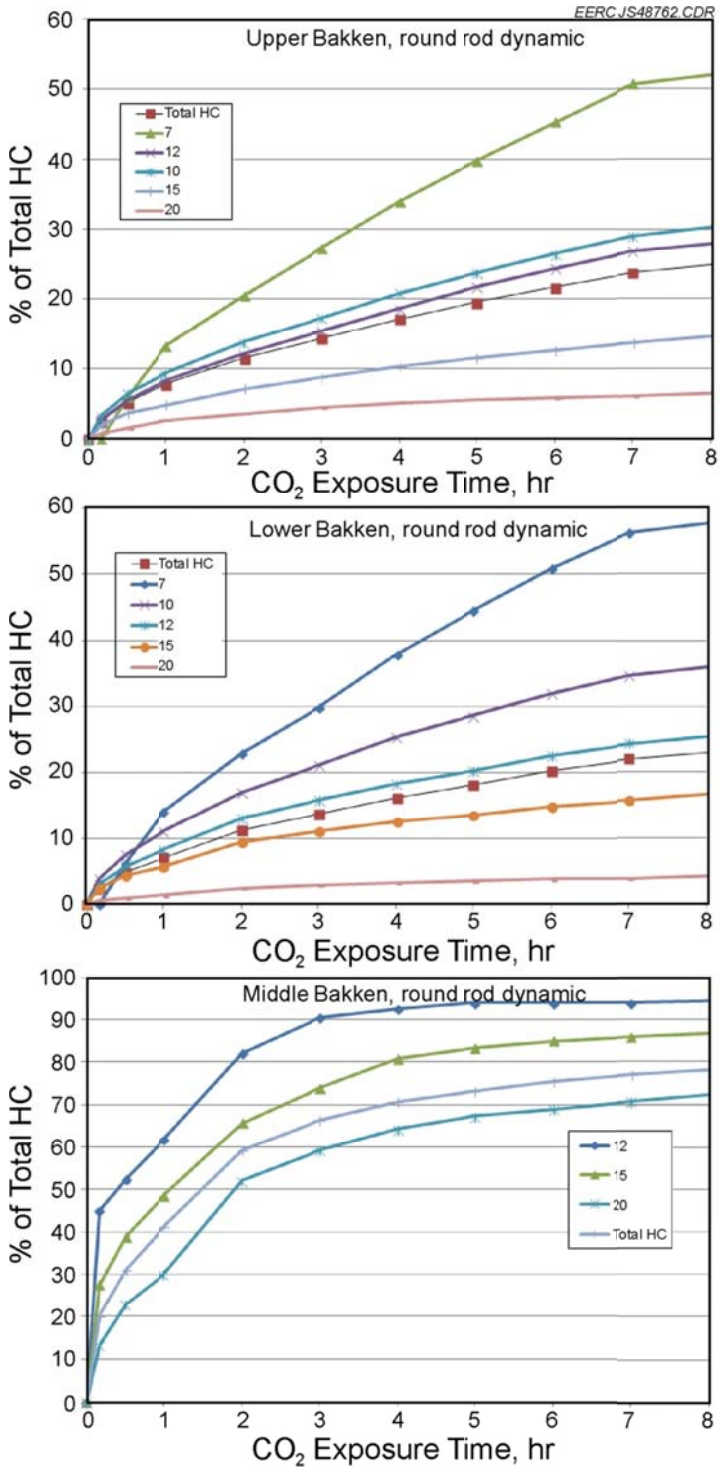

Figure 42. Recovery rates of different-molecular-weight alkanes under dynamic CO_2 exposures (5000 psi, 110°C) from ca. 10-mm-diameter × 40-mm-long round rods of Upper, Middle, and Lower Bakken source and reservoir rocks from a single borehole. The "7" indicates the total C7 alkanes as defined by chromatographic retention times. The same definition applies to the other carbon numbers shown. "Total HC" indicates the total hydrocarbon mass recovered regardless of molecular weight.

dominant recovery process. This could be from solvation of the oil hydrocarbons into the bulk CO_2 phase and/or generation of a new miscible mixed CO_2–hydrocarbon phase, since both of these processes select for lighter hydrocarbons (the 5000-psi exposures are substantially above the MMP for Bakken oils of ca. 2800 psi).

- Step 4: The exponential decrease in recovery rates with time and the large effect on sample particle size both support a mass transfer-limited transport of hydrocarbons from the interior of the rock to the bulk CO_2 at the surface, but speculation on the exact mechanism is difficult based on the available experimental results. However, the overall lesson is that the more surface area per mass of rock that can be accessed by CO_2, the faster the hydrocarbons will be recovered.

Estimation of Potential CO_2 Storage Capacity of the Bakken in North Dakota

One of the goals of this program was to develop a first-order, reconnaissance-level estimate of the potential CO_2 storage capacity of the Bakken Formation in North Dakota. There are currently no published studies that address the potential CO_2 storage capacity of any tight oil formations, such as the Bakken. However, some work has been published on the potential storage capacity of natural gas-rich shale formations, including studies on the Devonian gas shales of Kentucky (Nutall and others, 2005), the Barnett shale of Texas (Uzoh and others, 2010), and the Marcellus shale in the eastern United States (Godec and others, 2011). The approach that has been taken in those studies has been to assume that the CO_2 storage, and subsequent methane recovery, in organic-rich gas shales will be controlled by essentially the same adsorption and desorption mechanisms as CO_2 storage and methane recovery in coal seams. In those cases, the sorptive capacity of the organic content in the shales is assumed to play a significant role in determining the CO_2 storage capacity of those shales. Unfortunately those approaches have limited applicability to the Bakken, since most of the Bakken Formation is not organic-rich shale but, rather, oil- and brine-saturated tight carbonates and clastics, as discussed in the sections above. With these characteristics in mind, published methods to estimate the storage capacity of oil reservoirs may be more applicable to estimating the potential storage capacity of the Bakken.

To develop first-order CO_2 storage capacity estimates for the Bakken in North Dakota, an approach was used that estimates the amount of CO_2 needed for EOR in the Bakken. Specifically, the methodologies for estimating CO_2 storage capacity in oil formations based on production and volumetrics as presented in the *Carbon Sequestration Atlas of the United States and Canada* (U.S. Department of Energy, 2007) were applied to the Bakken Formation in North Dakota. In both of these approaches, it is assumed that the stored amount of CO_2 would be equal to the purchased quantity. Through the EOR process, the gross mass (volume) would be greater. The results of these CO_2 storage capacity estimation efforts are presented in Table 5.

$$G_{CO2} = Ah_n\emptyset_e(1 - S_{wi})Bp_{CO2std}E_{oil/gas} \quad \text{[Eq. 1]}$$

Table 5. Estimated CO_2 Storage Capacity Results for the Bakken in North Dakota

Scenario	ND OOIP, stb	Incremental Recovery Factor	Net Utilization Factor, ft^3/bbl	Mass of CO_2 Storage, tons
1	170,000,000,000	0.04	8000	3,155,200,000
2	170,000,000,000	0.04	5000	1,972,000,000
3	10,500,000,000	0.04	8000	194,880,000
4	10,500,000,000	0.04	5000	121,800,000
	ND Cum. Production	Recovery Factor	Rounded OOIP	
3 and 4	732,000,000	0.07	10,500,000,000	

The first method, referred to as the volumetrics method, is largely based on estimating the OOIP of the Bakken according to known reservoir properties. Specifically, the product of the area (A), net thickness (h_n), average effective porosity (φ_e), original hydrocarbon saturation (1-initial water saturation, expressed as a fraction [S_{wi}]), and the initial oil (or gas) formation volume factor (B) yield the OOIP. The storage efficiency factor ($E_{oil/\,gas}$) is derived from local CO_2 EOR experience or reservoir simulation as standard volume of CO_2 per volume of OOIP. Using OOIP data from Nordeng and others (2010) for North Dakota, an estimate of a 4% increase in oil recovery (4% of OOIP) and two utilization factors, the mass of CO_2 needed for a Bakken EOR effort (i.e., the potential CO_2 storage capacity of the Bakken in North Dakota) ranges from 1.9 to 3.2 billion tons (Scenarios 1 and 2).

A second approach, generally applied to mature oil fields or those for which key reservoir property data are unavailable, to determining OOIP is to use cumulative production divided by a recovery factor (e.g., 36%). In the case of the Bakken in North Dakota, a recovery factor of 7% was used along with a cumulative production of 732,000,000 bbl. This approach results in a predicted OOIP of 10.5 billion bbl and a corresponding CO_2 storage capacity for the Bakken ranging from 121 to 194 Mt.

The estimates using the reservoir property-based OOIP approach are likely too high because the U.S. Department of Energy (DOE) method was developed based on knowledge derived from decades of studies and experience related to CO_2 injection, utilization, and storage in conventional oil reservoirs. While the OOIP of the Bakken is known to be high (LeFever and Helms, 2008; Continental Resources Inc., 2012), the extremely tight nature of the formation may adversely affect injectivity and storage efficiency and thus reduce the storage capacity estimates. It is possible that the negative impact of the tight porosity and permeability may be at least somewhat positively offset by the potential adsorption of CO_2 into the high-organic-content shales of the Bakken. However, the extent of that impact is unknown because of the lack of field-scale data on CO_2 behavior in tight oil formations, which is why two utilization factors (5 mcf/bbl and 8 mcf/bbl) were used in the estimation exercise. Alternatively, the estimates using the cumulative production approach are likely too low. Having just started in the mid-2000s, the Bakken play in North Dakota is still in its early stages of development, and the effects on CO_2 storage estimation are twofold. First, the North Dakota Department of Mineral Resources has estimated that Bakken production will likely continue for at least another 20 to 30 years. This

means that the cumulative production numbers used in this CO_2 storage capacity exercise are likely only a small fraction of what the ultimate cumulative production of oil from the Bakken will be, and therefore the capacity estimates likely represent too small a fraction of the CO_2 storage resource. Also, because the play is in the early stages, there are only a few wells for which long-term decline curve data are available. The lack of such decline curve data means that operators and regulators are still in the process of determining the typical estimated ultimate recovery (EUR) of a Bakken well. Reported Bakken EUR values have been rising over the past few years, which again would strongly suggest that the CO_2 storage capacity estimates based on current cumulative production are too low.

Since the high end of the estimated storage capacity range may be too high, and the low end is likely too low, it is clear that more data from laboratory- and field-based research efforts are required to develop improved CO_2 storage capacity estimates for tight oil formations. Future evaluations of CO_2 storage potential in tight oil formations like the Bakken may consider using a hybrid method that combines some elements of the shale gas capacity methods with elements of the oilfield methods.

Evaluation of a Field-Based Pilot-Scale CO_2 Injection Test in the Elm Coulee Area, Montana

Overview of the Elm Coulee Area

The Elm Coulee area in Richland County, Montana, is one of the first areas to see prolific oil production from the middle member of the Bakken Formation. Oil production from the Elm Coulee Bakken play began in 2000, and it continues to be one of the most oil-productive areas in Montana, with approximately 50,000 barrels of oil per day produced in 2012 (Montana Board of Oil and Gas Conservation, 2013). As with the Bakken play in North Dakota, the application of horizontal drilling combined with hydraulic fracturing technologies were the critical components that enabled operators to economically produce oil from the Middle Bakken in Elm Coulee. In fact, for decades the Bakken Formation was known to hold tremendous amounts of oil throughout the Williston Basin (LeFever, 2006), but its unconventional nature discouraged most operators from trying to exploit it. This paradigm changed in the early 2000s when a number of successful Middle Bakken wells were brought online in the Elm Coulee area through the use of horizontal drilling and hydraulic fracturing. The Elm Coulee success prompted Williston Basin operators to rethink their Bakken assets and was the forerunner to the tremendous Bakken production that occurs in North Dakota today. As might be expected, the fact that the Elm Coulee play is one of the first productive Middle Bakken plays also means that it will be among the first to be considered for the application of EOR techniques. It is with EOR in mind that in 2009 three companies (Continental Resources, Enerplus, and XTO) jointly conducted a pilot-scale CO_2 injection test in the Burning Tree–State 36-2H well (hereafter referred to in this report as the Burning Tree well) in the north central part of the Elm Coulee Field (Figure 43).

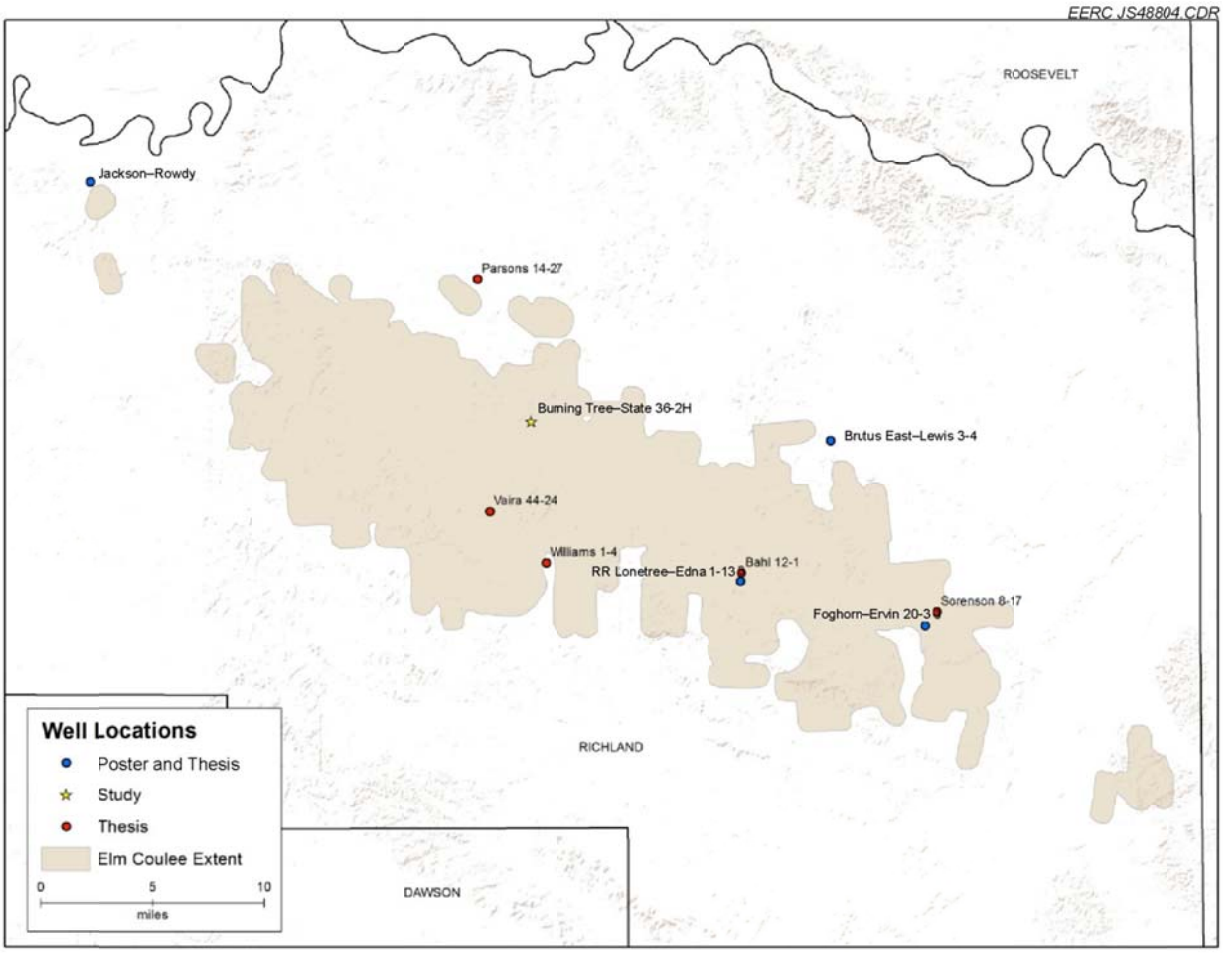

Figure 43. The Elm Coulee Field in Richland County, Montana, including the names and location of wells for which characterization data were available.

As part of the effort to understand the behavior of CO_2 in a Bakken reservoir and the potential effectiveness of CO_2 for Bakken EOR, the EERC has evaluated publicly available and confidential data from the Elm Coulee pilot field test. The purpose of that evaluation was to identify key knowledge gained from the test that may be applied to possible future CO_2 injection tests in other parts of the Bakken.

Basic Overview of the 2009 Elm Coulee CO_2 Injection Test

The Burning Tree well was drilled and completed in March and April 2000. The top of the Bakken in the Elm Coulee area at the Burning Tree well location is approximately 9740 ft. The horizontal leg of the well was drilled into the middle member of the Bakken, which at that location is approximately 40 ft thick and dominated by sandy to silty dolostones. The well was drilled with a horizontal lateral leg 1592 ft in length, completed with 5.5 inches of cemented production casing, perforating approximately 813 ft of the wellbore (leaving about 380 ft of the heal and 390 ft of the toe unperforated), and stimulated using a single-stage, hydraulic fracturing

operation with 20–40 sand proppant (Figure 44). The initial oil production of the well was 196 bbl/day of 40.1° API (American Petroleum Institute) gravity crude, but by August 2008, that had dropped to between 30 and 40 bbl/day. This sort of decline was typical of Elm Coulee Bakken wells, and in 2008, a consortium of three operator companies decided to conduct a field test to examine the potential for CO_2 to improve oil recovery in the Burning Tree well.

A CO_2 huff 'n puff scheme was chosen for the Burning Tree test. A huff 'n' puff scheme is an approach by which CO_2 is injected into a single well (the "huff"), after which the well is then closed for a period of time (referred to as the "soak" period), and then allowed to produce again (the "puff"). Huff 'n' puff tests can be an effective means of evaluating the response of a reservoir to CO_2, both with respect to EOR and CO_2 storage. The approach is economically attractive because relatively small volume injections can yield adequate results to determine the efficacy of a larger-scale CO_2 injection. However, while hundreds of CO_2-based huff 'n' puff

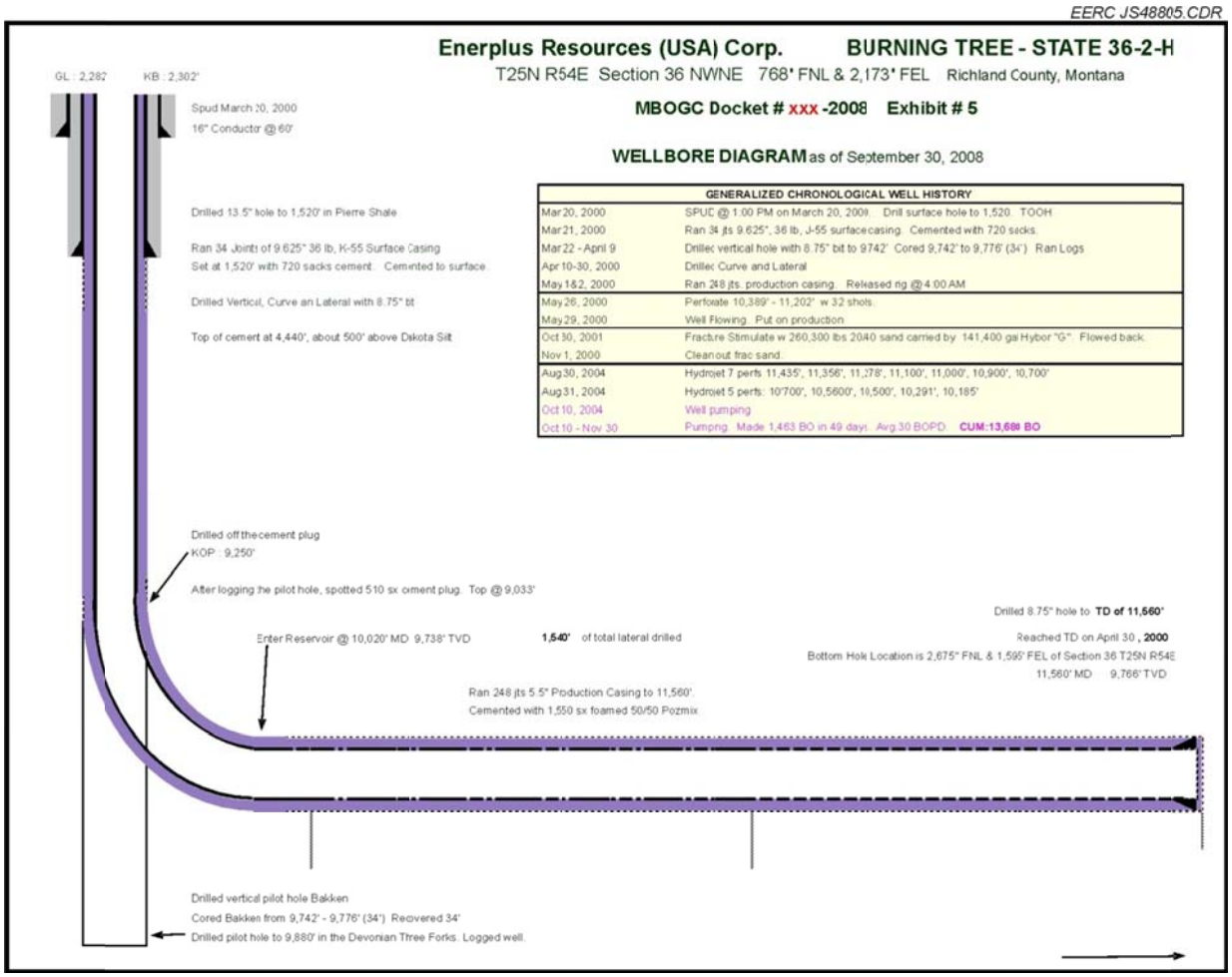

Figure 44. Wellbore diagram for the Burning Tree–State 36-2-H well, as presented to the Montana Board of Oil and Gas Conservation.

tests have been conducted around the world in conventional reservoirs (Mohammed-Singh and others, 2006), the literature indicates that very few have been conducted in tight oil formations such as the Bakken. In this regard, the Burning Tree CO_2 huff 'n' puff test was a pioneering effort.

Over the course of a 45-day period between January 16, 2009, and February 28, 2009, approximately 45,000 mcf (2570 tons) of CO_2 were injected into the Burning Tree well. The maximum injection pressure was 1848 psi BHP. While the average daily injection rate was approximately 1000 mcf/day, the actual injection operation was intermittent, with injection rates ranging from 0 to 3000 mcf/day. Specific reasons for the intermittent nature of the injection operations were not provided in any of the materials reviewed, but the intermittence may have been due to operational issues related to the trucked nature of the CO_2 source and, possibly, even related to severe winter weather conditions. After injection, the well was capped and the CO_2 was allowed to soak for 64 days, from March 1 to May 3, 2009. On May 4, the well was opened and allowed to flow freely. Daily oil, water, and gas production data for the Burning Tree well for the period from May 3 to October 19, 2009, were examined. After rapidly climbing to a peak oil production of over 160 bbl/day 8 days after the well was brought back into production, the oil production settled into an average of about 20 bbl/day during the first 30 days after the end of the soak period. By the end of June 2009, the well was no longer flowing and was put on pump. The average oil production over the following 3 months rose slightly to about 22 bbl/day, with a range of about 15 to 25 bbl/day. By the end of September, the range of daily oil production was from 20 to 30 bbl/day, which was still below the preinjection range of 30 to 40 bbl/day. By the end of 2009, average daily oil production had risen to nearly 28 bbl/day. Oil production continued to slowly rise in early 2010, reaching a peak postinjection high approaching 44 bbl/day in March 2010, which is a higher rate of production than was achieved during any of the 14 months immediately prior to the injection test. While oil production from the Burning Tree well remained above 35 bbl/day throughout the summer of 2010, by November of that year, it was back down to less than 30 bbl/day and has continued to decline. By the end of November 2013 (the latest month for which data were available) production had declined to slightly less than 15 bbl/day. Figure 45 shows the monthly oil production history of the Burning Tree well from June 2000 to November 2013. Figure 46 shows the monthly oil production from February 2008 to November 2013.

Typical "successful" CO_2 huff 'n' puff operations in conventional wells see a dramatic improvement in oil production immediately following the soak that often takes several weeks, or even months, to return to preinjection rates (Mohammed-Singh and others, 2006). When compared to conventional huff 'n' puff tests, particularly when looking at the first 6 months of data after the soak, the Burning Tree huff 'n' puff test might not be considered successful. However, the Bakken is an unconventional play. In the Elm Coulee area, the porosity of the middle member of the Bakken commonly ranges from 4% to 6% and the permeability typically ranges from 0.06 to 0.12 mD (Almanza, 2012), and the play, therefore, requires the artificial generation of fracture networks to enable hydrocarbons to flow to wells. When viewed through a "conventional" lens, a reservoir that is highly fractured with a tight matrix is not an ideal candidate for any type of CO_2-based EOR. But that is why the Burning Tree test should be viewed in the context of a pioneer and judged accordingly. It is true that other than in the first

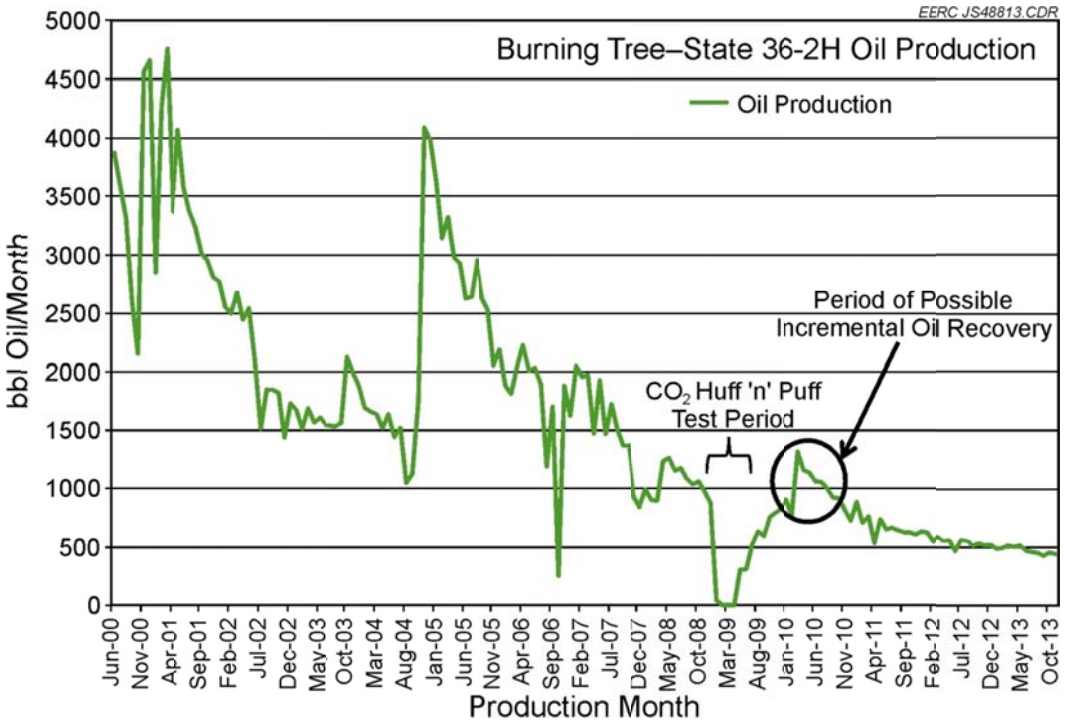

Figure 45. Monthly oil production from the Burning Tree well over the course of its entire operational history from June 2000 to November 2013.

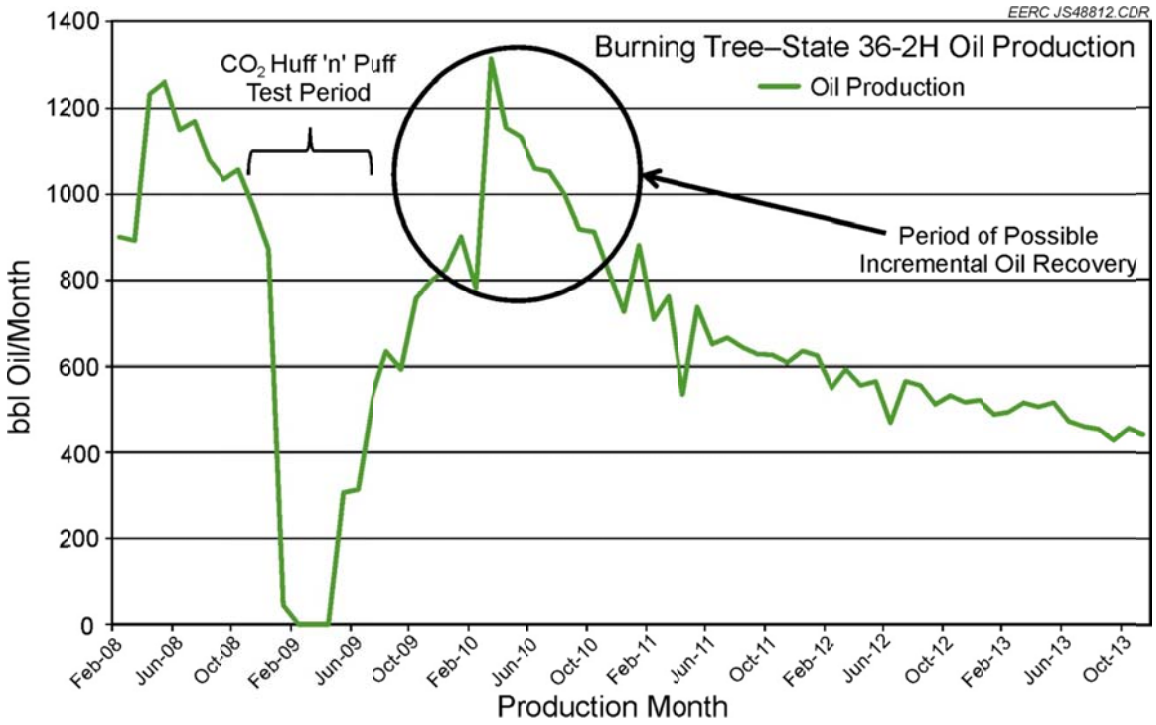

Figure 46. Monthly oil production from the Burning Tree well from February 2008 to November 2013.

few days, which saw an initial spike in fluid production that was likely the result of pressure buildup as opposed to any miscibility-related effects of CO_2, the Burning Tree well did not see a dramatic increase in oil production. But CO_2 was successfully injected and reservoir fluids produced from this tight, unconventional formation. When a longer view is taken, there was a period (January to March 2010) that saw a gradual increase in oil productivity, and though it was delayed and certainly not dramatic, this improved productivity, which lasted for another several months through the summer of 2010, might be attributable to the injection of CO_2.

Unfortunately, the nature of the data that were available for this assessment makes it difficult to determine how much of that improvement may be related to the CO_2 or if it is actually associated with other operational factors that have nothing to do with the CO_2. Gaps in the CO_2 monitoring data were perhaps the most significant limitation to fully assessing the effect of CO_2 on the Burning Tree reservoir. While there are gas analysis data that showed approximately 50% of the CO_2 injection volume was recovered from May 2009 to August 2009, no further testing results for CO_2 in produced fluids from the Burning Tree well were found. Furthermore, it appears that during the test period, no offset producing wells were operated or monitored in a way that could shed light on possible migration of the injected CO_2 (e.g., there are no CO_2 analysis data from any of the producing wells in the vicinity of the Burning Tree well). The lack of well testing and sampling for CO_2 in offset wells negatively impacts the mass balance to evaluate mobilized oil and the CO_2 movement within that portion of the Elm Coulee reservoir. There are also no data that provide insight on where the CO_2 may have left the wellbore. The well completion data indicate that the initial perforated interval received a hydraulic fracturing treatment, but the later hydro-jetted intervals appear to have not been stimulated, so it is difficult to speculate on where in the wellbore the CO_2 may have entered the reservoir.

Comparison of Elm Coulee Geology to Dunn County Geology

Of the North Dakota areas evaluated over the course of this program, it appears that the Dunn County area is the most attractive area with respect to a future CO_2 injection test. Therefore the Elm Coulee information was evaluated not only in terms of the effectiveness of CO_2 on the productivity of the Burning Tree well, but also in the context of how it may or may not be relevant to a potential Dunn County injection test.

The Elm Coulee and Dunn County areas are separated by approximately 80 miles. As parts of the same continuous sedimentary formation, the Bakken rocks in Elm Coulee and Dunn County of course share many similarities. But as might be expected, there are also many significant differences between the geology of the Bakken in the Elm Coulee and the Dunn County areas. A brief discussion of the geological characteristics of the Bakken Formation in the Elm Coulee area as compared to the Dunn County area is provided below.

- The Bakken in the Elm Coulee area is approximately 1000 ft shallower than it is in the Bailey area, although with the top of the Bakken occurring at around 9700 ft depth from surface in the Elm Coulee area, it is still considered to be a deep reservoir.

- With respect to structure, the Dunn County area has notable anticlinal and synclinal structure and is bisected by the Heart River fault, whereas the Elm Coulee area appears to have a single, subtle fold along its east–west axis (Figure 47).

- The thicknesses of Upper and Middle Bakken in the area of the Burning Tree well are generally fairly similar to those in the Dunn County area, with the Upper Bakken being about 6 to 10 ft thick and the Middle Bakken averaging between 40 and 45 ft thick. However, in the Elm Coulee area, the Middle Bakken thins toward the west, eventually to a thickness of only 5 ft.

- The Lower Bakken shale is absent from the southern half of the Elm Coulee area (Figure 48), including the area of the Burning Tree well (Figure 49), whereas the Lower Bakken is present throughout the Dunn County area where it is consistently about 12 ft thick.

- Both areas generally have multiple distinct lithofacies present in the Middle Bakken, including a laminated zone.

- The number of lithofacies present in Elm Coulee declines as the formation pinches out towards the west, until there are only one or two distinct Middle Bakken lithofacies present (Figure 50).

- The Dunn County area generally has five distinct lithofacies present across the entire area.

- The porosity of the Middle Bakken is reasonably similar in both areas, with the Elm Coulee porosity typically ranging from 3% to 6% and the Dunn County porosity typically ranging from 2% to 7%.

- The permeability of the Middle Bakken in the two areas is widely variable, depending on the lithofacies, but generally speaking, the areas appear to have similar permeability ranges and distribution.

- Both the Elm Coulee and Bailey area Bakken are considered to be thermally mature (Sonnenberg and Pramudito, 2009; Nordeng and others, 2010; Meissner, 1984). As such a significant amount of natural fracturing has occurred as a result of the expulsion of oil from kerogen, and the reservoirs initial pressures are considered to be overpressured relative to the typical pressure gradient in their respective parts of the Williston Basin.

- The lithology of the Middle Bakken in Elm Coulee is dominated by dolomite, whereas the lithology of the Middle Bakken in the Dunn County area is more of a mixed system of calcite-dominated carbonates and clastics (Alexandre and others, 2011; Almanza, 2011).

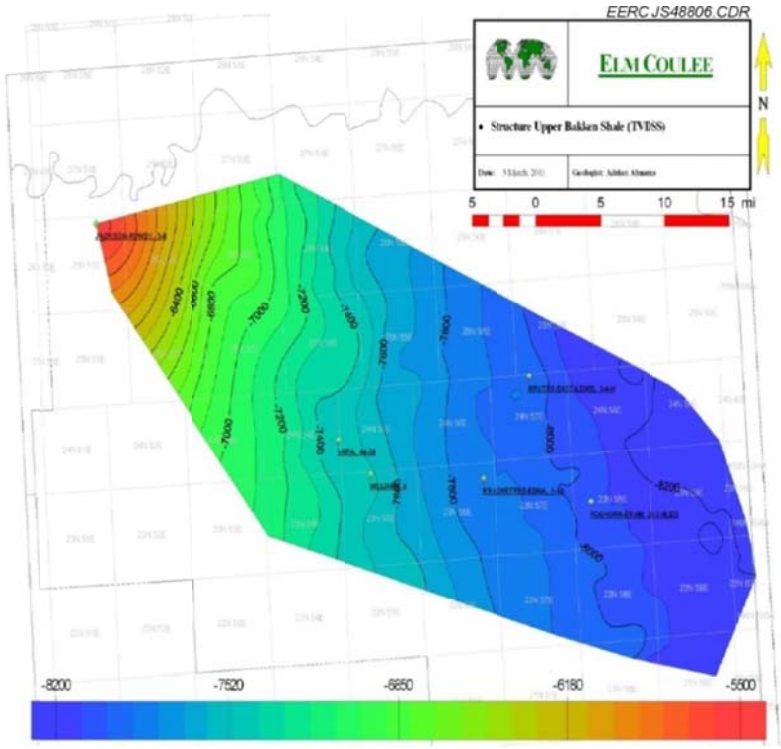

Figure 47. Structure map of the Upper Bakken shale in the Elm Coulee area (Almanza, 2011).

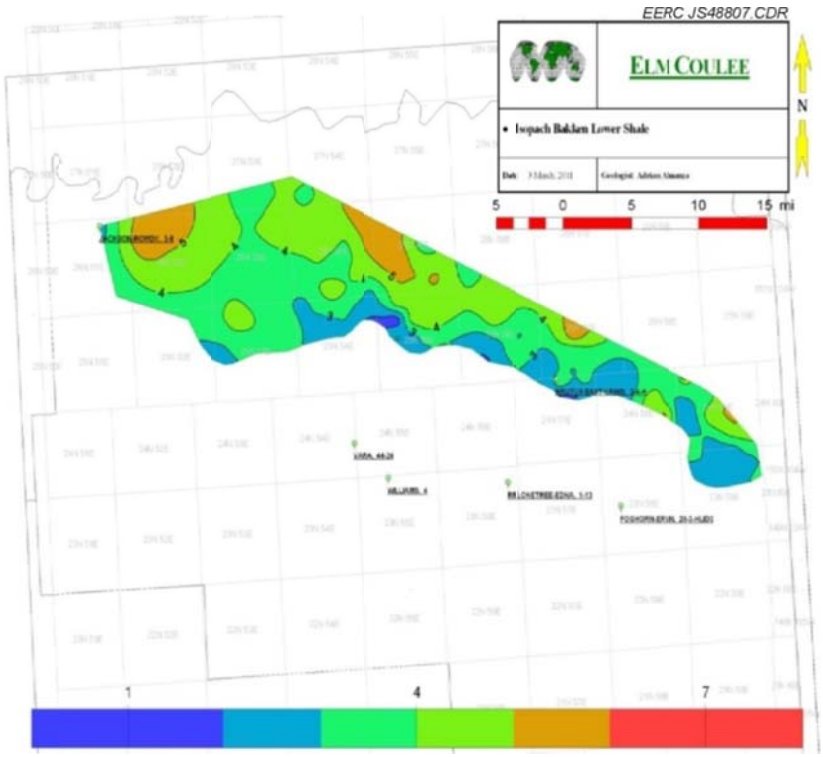

Figure 48. Isopach of the Lower Bakken shale in the Elm Coulee area (Almanza, 2011).

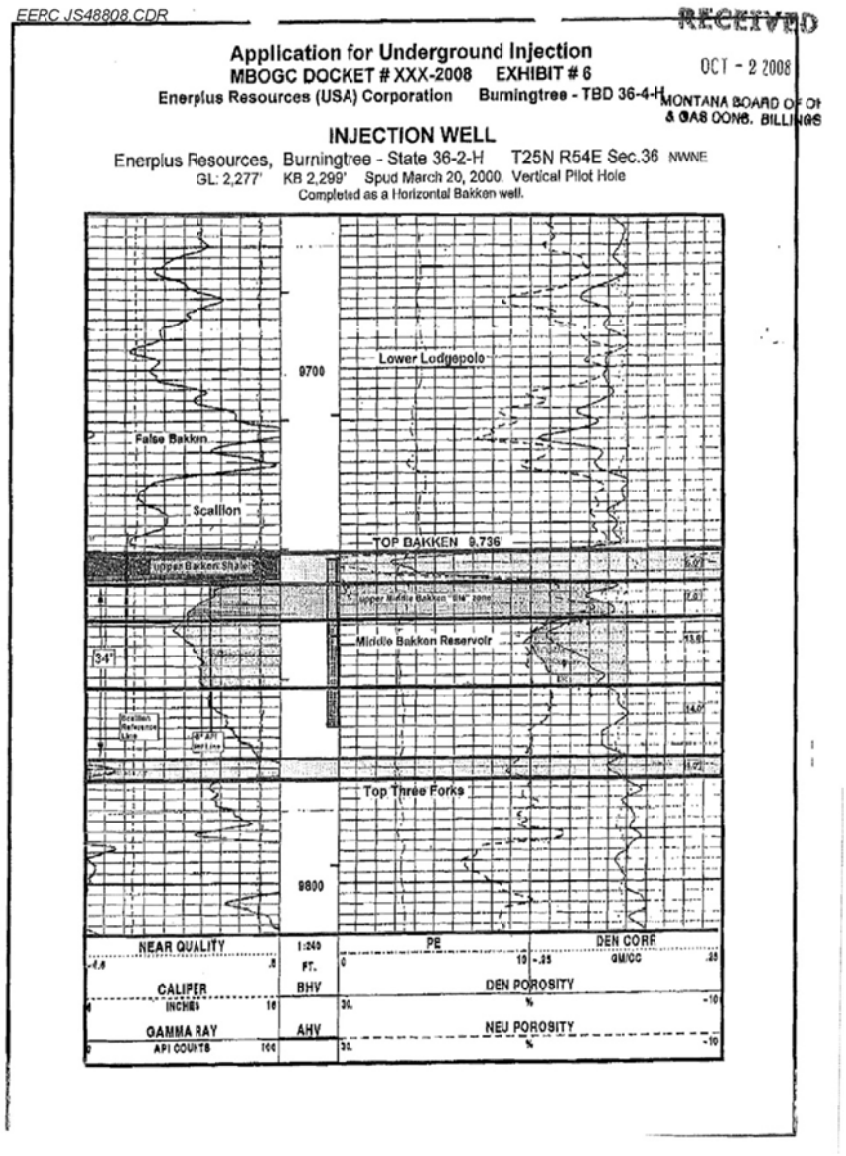

Figure 49. Well log of the Lower Lodgepole, Bakken, and Upper Three Forks Formations from the Burning Tree well. The absence of a Lower Bakken shale unit should be noted.

- Oil saturations in the Elm Coulee area are, on average, lower (ranging from 21% to 72%) than in the Dunn County area (ranging from 38% to 81%), although they may be considered to be comparable on a well-by-well basis.

While there are significant differences in the geology of the Bakken Formation in the Elm Coulee area and the Dunn County area, most notably the absence of the Lower Bakken shale in much of Elm Coulee and the dominance of dolomite in the Elm Coulee Middle Bakken, these differences would not likely make one area more or less suitable for CO_2 EOR than the other. Since CO_2 is buoyant, the absence of a sealing shale underlying the Middle Bakken target

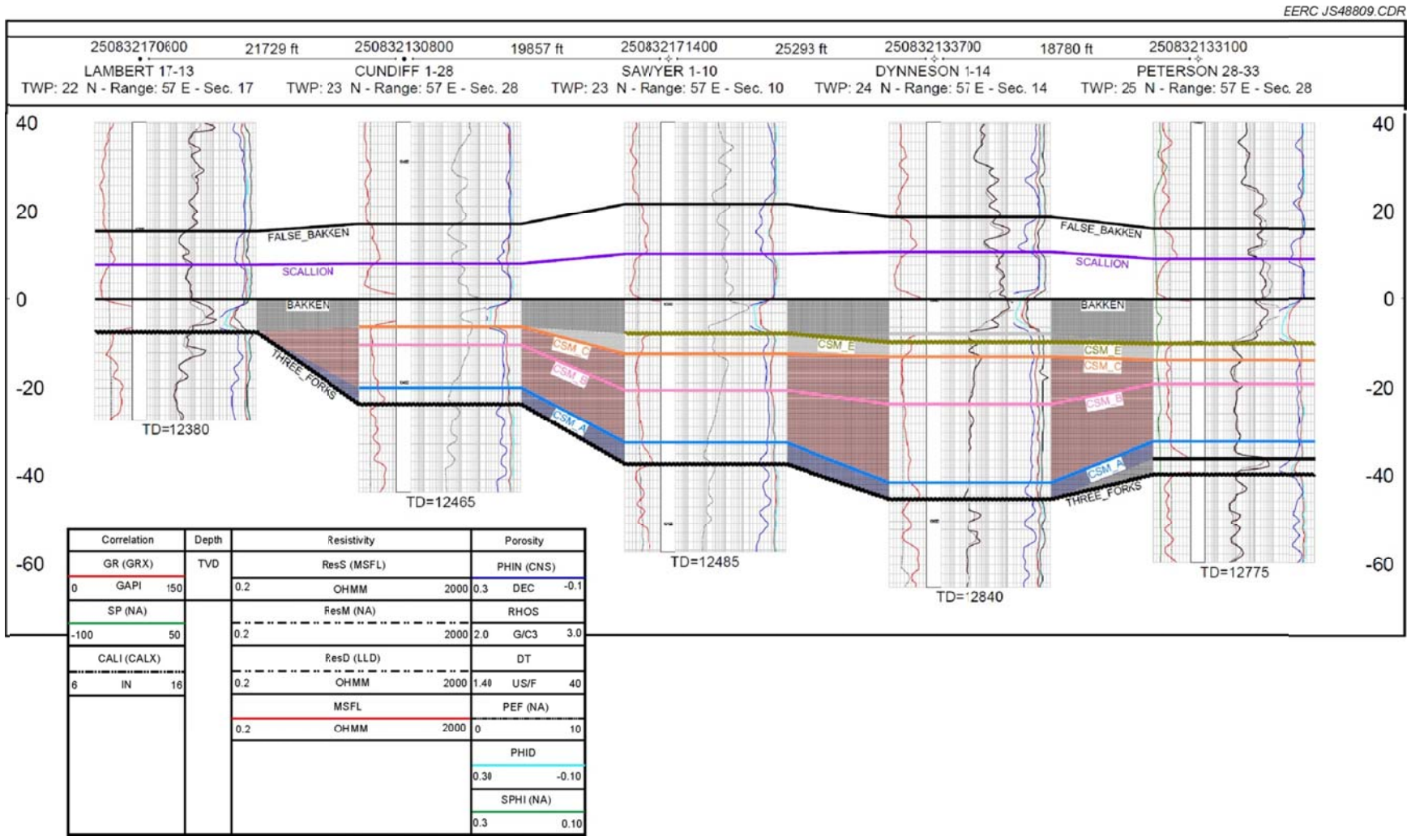

Figure 50. East–west stratigraphic cross section of the Elm Coulee area (Almanza, 2011) from Peterson-28-33 in the east to Lambert-17-13 in the west (The absence of the Lower Bakken shale unit in the four western wells and the thinning of the Middle Bakken towards the west should be noted).

injection zone would not likely be a factor in affecting its movements. While the Middle Bakken in the Dunn County area is less dominated by carbonates (particularly with respect to dolomite) and carbonates may be more reactive to CO_2, there are many successful CO_2 EOR operations in carbonate reservoirs.

Applicability of Burning Tree Test Results to Potential Tests in Dunn County

One of the primary aspects of how CO_2 in the Burning Tree well might behave as compared to a Dunn County well is the nature of the fracture network in the respective wells. Reservoir fluid flow in both the Elm Coulee and Dunn County areas is significantly influenced, if not controlled by, fracture networks (both naturally occurring and induced). With respect to naturally occurring fractures, although the type of detailed fracture analysis data that were developed for the Dunn County area were not found to be available for the Elm Coulee area, generally speaking, the literature suggests that the areas do not appear to be significantly different with respect to naturally occurring fractures. This is supported by the fact that both areas are thermally mature and have some structural elements and by the qualitative descriptions of Elm Coulee Bakken core. However, it is important to note that as one of the first hydraulically fractured Middle Bakken oil wells, the geometry of the hydraulically induced fracture network of the Burning Tree well is likely to be much different from the geometry of the induced fracture network of most Dunn County wells.

There are a few key aspects of the Burning Tree well that make it substantially different from a majority of North Dakota Bakken wells, including those in Dunn County. At a length of 1592 ft, the Burning Tree horizontal lateral is significantly shorter than the typical North Dakota lateral length, which may be 5 to 10 times longer. As mentioned above, the Burning Tree well was hydraulically fractured using a single-stage stimulation operation. This means that the geometry of the fracture network in the Burning Tree well will be substantially different from any multistage hydraulically fractured well. In Dunn County, many of the older Middle Bakken wells were stimulated using single-stage hydraulic fracturing. However, many of those wells had openhole completions so their single-stage induced-fracture networks would likely be different from that of the Burning Tree well, which had cemented, perforated, production casing. Understanding the geometry of the induced fractures in the Burning Tree well and trying to apply them to North Dakota wells is further complicated by the fact that only the middle 800 ft of the Burning Tree lateral was perforated during the initial hydraulic fracturing operation in 2001, and hydrojetting was done at several intervals along most of the length of the horizontal leg 3 years later in 2004. When considered together, all of these engineering aspects of the Burning Tree well severely limit the extent to which the observations and results from the Burning Tree CO_2 injection may be applied to other potential Bakken CO_2 injection tests.

Key Lessons of the Burning Tree CO_2 Huff 'n' Puff Test in Elm Coulee

As described above, the CO_2 huff 'n' puff test conducted at the Burning Tree well in the Elm Coulee area of Montana was one of the first such tests not only in the Bakken Formation, but in any tight, unconventional oil reservoir. As such, it was a pioneering effort and the value of the observations and lessons learned generated by the consortium of operators who conducted that test cannot be overstated. Those key lessons include the following:

- It has been demonstrated that CO_2 can be injected into the Bakken Formation at rates that may be considered to be reasonable for both potential EOR and storage operations.

- Although the amount of CO_2 stored and incremental oil produced as a result of the CO_2 injection may not be economically or technically significant, it appears that some incremental oil may have been produced. Unfortunately, the available data did not yield insight regarding the amount of CO_2 that may have remained in the reservoir.

- The delayed timing and relatively muted nature of the incremental oil production suggests that different mechanisms of interaction between CO_2 and the reservoir may be at play in the Bakken (particularly with respect to the tight matrix) as compared to a conventional reservoir. This observation with respect to timing and nature of reservoir response may be indicative of the role that diffusion may play, as has been indicated in the laboratory-scale CO_2 hydrocarbon elution studies conducted as part of this research program.

- The Burning Tree huff 'n' puff test, as conceived, implemented, and reported, has not discouraged research or the planning of other field-based efforts to determine the effectiveness of using CO_2 injection for simultaneous EOR and CO_2 storage in the Bakken and other tight oil formations.

One of the primary goals of the evaluation of the Burning Tree huff 'n' puff observations and data was to develop recommendations for potential future CO_2 injection tests in the Bakken Petroleum System. While the most useful application of specific data from this test to any future test would require a site-specific comparison and evaluation, some broadly applicable recommendations include the following:

- Any field-based project must include thorough planning and adequate budget.

- The geological understanding of the Bakken reservoir and laboratory analysis of live crude oil, formation water and gas, and fresh core samples is critical to understanding interactions between CO_2 within the Bakken reservoir and will aid in the design of pilot and long-term CO_2 storage and EOR projects.

- CO_2 injection rates should be consistent, and methodologies should be utilized to evaluate injection distribution along the length of the wellbore. Injection volume must be adequate for the technical evaluation of a pilot project.

- Well testing and sampling of CO_2 in the offset producing wells within the field during and after the injection test should be incorporated into the project design. A determination of mass balance to evaluate mobilized oil and the movement and disposition of CO_2 within the reservoir is critical, particularly with respect to determining storage capacity.

- Data gathering should be rigorous and well-documented.

SUMMARY AND RECOMMENDATIONS FOR FUTURE WORK

The Bakken CO_2 Enhanced Recovery and Storage Program was conducted over the course of 2012 and 2013. The objective of the program was to use new and existing reservoir characterization and laboratory analytical data (e.g., core analyses, well logs, oil analyses, etc.) coupled with state-of-the-art modeling to determine the viability of using CO_2 for EOR in the Bakken Formation. The research activities generated the following key results:

- A first-order estimate of the potential CO_2 storage capacity of the Bakken Formation in North Dakota suggests that it may range from 120 million tons to over 3 billion tons of CO_2. This broad range suggests that additional laboratory experimental studies and field test data, are needed to better determine the storage capacity of tight oil-bearing formations.

- The current CO_2 capacity estimation methodologies may be somewhat limited in their applicability to tight oil formations because they have unique reservoir properties relative to other conventional CCS targets. A methodology that considers the effects of those unique properties, such as high total organic content, as part of the equation should be developed for future CO_2 storage capacity estimations of tight oil formations. The development of a hydrid method that combines some elements of the shale gas capacity methods used by Nutall et al. (2005) with elements of the U.S. DOE methodology for oil fields may be an appropriate area of research since tight oil formations have increasingly become the focus of exploration in the past several years.
- CO_2 extraction studies on samples of Middle and Lower Bakken rocks indicate that CO_2 can remove over 90% of hydrocarbons from Middle Bakken reservoir rocks and over 60% of hydrocarbons from Lower Bakken shales in small-scale experiments.

- A rising capillary approach appears to offer a cost-effective, quick-turnaround means of evaluating the effects of CO_2 on Bakken oil under a broad range of conditions, including changes in pressure, temperature, and hydrocarbon gas (i.e. methane, ethane, etc.) content.

- In the Bakken, CO_2 flow will be dominated by fracture flow, and not significantly through the rock matrix. Fracture-dominated CO_2 flow could essentially eliminate the displacement mechanisms responsible for increased recovery in conventional reservoirs. As such, other mechanisms must be optimized in tight reservoirs such as the Bakken.

- Because fractures will play a dominant role in CO_2 flow through the Bakken, determining whether a fracture or microfracture in core is naturally occurring in the reservoir or was induced by the collection process is essential to developing an accurate understanding of the natural fracture network in any given reservoir. A variety of techniques, including SEM, UVF, and standard optical microscopy, showed promise with respect to identifying and describing microfractures.

- Static petrophysical models were created of the Middle Bakken in the Bailey and Grenora areas. The modeling efforts included the development of both a single

porosity/single permeability model and a dual porosity/dual permeability model for both areas. Both models followed the same workflow, however data sets did vary, particularly with respect to the number and nature of the lithofacies (Grenora had more lithofacies zones and a somewhat more robust fracture network). Also, PVT and relative permeability data specific to Grenora were not available. The same values for those parameters that were used in Bailey were applied in Grenora, which is not likely an accurate assumption. So while a comparison can be made, there may be limitations to its applicability.

- Dynamic simulation modeling of CO_2 injection was conducted using the Bailey and Grenora models. A variety of schemes were simulated, and results suggest that CO_2-based EOR may be technically possible. Specifically, some of the simulated schemes showed increases in oil production by as much as 40 to 50% as a result of CO_2 injection, although actual increases would likely be lower.

- The CO_2 utilization factor (reported as mcf of CO_2 injected per barrel of oil produced) is perhaps the best output parameter by which to compare the Bailey and Grenora areas with respect to CO_2 storage and EOR potential. The simulations indicate that the Grenora Bakken reservoir had a CO_2 utilization factor that was 5 to 6 times greater than the Bailey Bakken reservoir. This suggests that injection and EOR in the Bailey reservoir will be more efficient from an EOR standpoint than in the Grenora reservoir. The more fractured nature, complex lithofacies, and higher water saturation found in the Grenora Bakken as compared to the Bailey Bakken may be the primary reasons for the differences in the simulation results. However, many questions remain regarding the precise role that fractures will play, and the timeframe and economic viability of CO_2-based EOR in the Bakken.

- Those results suggest that an EOR scheme that pairs two injectors with one producer will produce more oil than a single injector-producer scheme. They also indicate that patience may be rewarded, with the incremental recovery and efficiency improving with longer periods of injection.

- The results of the static and dynamic modeling efforts underscored the importance of having detailed knowledge of both the natural fracture network and induced hydraulic fractures (at both the macro- and microscales) when predicting the effectiveness of CO_2 injection for EOR in the Bakken.

- The results of one of the dual porosity/dual permeability simulation runs indicated that diffusion may play a significant role in moving oil from the reservoir matrix into the fracture network. This modeling result is supported by the results of the laboratory-based CO_2 hydrocarbon elution experiments from Bakken rock samples which also showed that as much as 90% of hydrocarbons could be mobilized from the Middle Bakken matrix in a reasonable amount of time. Furthermore, these laboratory and modeling results are also supported by an analysis of the results from the pilot-scale huff ‘n puff test conducted in the Burning Tree well in Elm Coulee, Montana. The oil production data from the Burning Tree well, which shows that it took several months

for the oil production rate to climb and remain above the pre-injection rates, also supports the notion that diffusion is an important mechanism controlling the mobility and disposition of CO_2 within a tight oil reservoir.

The results of the research activities suggest that CO_2 may be effective in enhancing the productivity of oil from the Bakken. However, there is no clear-cut answer regarding the most effective approach for using CO_2 to improve productivity. It is likely that an unconventional resource will require unconventional methods for EOR and CO_2 storage. With that in mind, it is clear that additional knowledge is necessary to make informed decisions regarding the design and implementation of potential injection and production schemes. Some of the key questions that came out of the research presented in this report include the following:

- How far into the matrix can CO_2 penetrate Bakken rocks (lower and middle) at larger scales? What is the time frame of that penetration? Does the CO_2 affect the porosity and/or permeability of the matrix?

- Is it possible to identify natural microfractures in the Lower Bakken shale?

- How do the fracture networks behave as reservoir pressures are depleted, and how does that behavior impact reservoir permeability and production? How would CO_2-based EOR and affiliated pressure changes affect reservoir and fracture permeability?

- How can an improved understanding of microfractures be incorporated into the development of a DFN within a static model? How can data on microfractures be integrated into dual-porosity–dual-permeability models?

- How much of the injected CO_2 can be recycled, and how much is permanently stored in the formation?

- How well, if at all, do the lessons learned on Bakken rocks translate to rocks of the Three Forks Formation?

With these questions in mind, the EERC is planning a second phase of the Bakken CO_2 Enhanced Recovery and Storage Project. The objective of Phase II is to refine the techniques and approaches developed under Phase I and apply them to the development and implementation of a pilot-scale injection test in the field. The technical aspects of Phase II will be divided according to three primary areas of technical activity, specifically 1) refined understanding of hydrocarbon extraction from tight rock matrix, 2) detailed microfracture characterization, and 3) participation in a pilot-scale CO_2 injection test in a Bakken reservoir.

For future work, more field and laboratory experience such as detailed decline curve analysis, CO_2 core flooding upscaling, natural fracture measurements, relative permeability tests under Bakken reservoir conditions of the study area, and the inclusion of a dual-porosity–dual-permeability model may be added to the modeling and simulation processes to better understand the comprehensive mechanisms of CO_2 EOR and storage in the unconventional Bakken

Formation. These efforts may help to improve the operational design and optimization of future laboratory and simulation efforts and a potential pilot project.

ACKNOWLEDGMENTS

The authors thank Marathon Oil Corporation, Continental Resources Inc., and the North Dakota Geological Survey (NDGS) for providing the samples used in these investigations. The authors also thank Schlumberger Carbon Services for providing the Petrel software package and Computer Modelling Group Ltd. for providing simulation software packages for use in this research. Financial support from U.S. Department of Energy National Energy Technology Laboratory Cooperative Agreement No. DE-FC26-08NT43291, OGRC, Marathon Oil, Continental Resources, and TAQA North is also gratefully acknowledged. We also want to acknowledge the efforts and contributions made by the following individuals, without whose support much of the work presented here would not have been possible: Terry Kovacevich, Basak Kurtoglu, and Bill Zogg of Marathon Oil; Archie Taylor and Sam Amadi of Continental Resources; Ed Murphy, Julie LeFever, and Stephen Nordeng of NDGS; Ron Ness of the North Dakota Petroleum Council; and Lynn Helms of the North Dakota Department of Mineral Resources.

REFERENCES

Alexandre, C.S., Sonnenberg, S., and Sarg, J., 2011, Reservoir characterization of Elm Coulee Field, Richland County, Montana: Poster presentation at American Association of Petroleum Geologist Annual Convention and Exhibition, Houston, Texas, April 10–13, 2011.

Almanza, A., 2011, Integrated three-dimensional geological model of the Devonian Bakken Formation Elm Coulee Field, Williston Basin: Richland County, Montana: M.S. thesis, Colorado School of Mines.

Ayirala, S.C., and Rao, D.N., 2011, Comparative evaluation of a new gas/oil miscibility determination technique: Journal of Canadian Petroleum Technology, September/October, p. 71–81.

Continental Resources, Inc., 2012. Bakken and Three Forks: www.contres.com/operations/bakken-and-three-forks (accessed May 30, 2013).

Godec, M., Kuuskraa, V., Van Leeuwen, T., Melzer, L.S., and Wildgust, N., 2011, CO_2 storage in depleted oil fields—the worldwide potential for carbon dioxide enhanced oil recovery: Energy Procedia, v. 4, p. 2162–69.

Gorecki, C.D., Liu, G., Bailey, T.P., Sorensen, J.A., Klapperich, R.J., Braunberger, J.R., Steadman, E.N., and Harju, J.A., 2013, The role of static and dynamic modeling in the Fort Nelson CCS project: Energy Procedia, v. 37, p. 3733–3741, ISSN 1876-6102, http://dx.doi.org/10.1016/j.egypro.2013.06.268.

Harvey, A.H., 1996, Semiempirical correlation for Henry's constants over large temperature ranges: Journal of the American Institute of Chemical Engineering, v. 42, p. 1491.

Hawthorne, S., 1990, Analytical-scale supercritical fluid extraction. Analytical chemistry, v. 62, no. 11, p. 633–642, June 1, 1990.

Hawthorne, S.B., Gorecki, C.D., Sorensen, J.A., Steadman, E.N., and Harju, J.A., 2013, Hydrocarbon mobilization mechanisms from Upper, Middle, and Lower Bakken reservoir rocks exposed to CO_2: SPE Unconventional Resources Conference, Calgary, Alberta, November 5–7, SPE 167200-MS.

Jarrell, P.M., Fox, C.E., Stein, M.H., and Webb, S.L., 2002, Practical aspects of CO_2 flooding: SPE Monograph v. 22, Henry L. Doherty Series, Richardson, Texas, 220 p.

Kestin, J., Khalifa, H.E., and Correia, R.J., 1981, Tables of dynamic and kinematic viscosity of aqueous NaCI solutions in the temperature range 20°–150°C and the pressure range 0.1–35 MPa: Journal of Physical and Chemical Reference Data, v. 10, p. 71–87.

Kurtoglu, B., 2013, Integrated reservoir characterization and modeling in support of enhanced oil recovery for Bakken: Ph.D. dissertation, Colorado School of Mines, 2013.

Kurtoglu, B., Sorensen, J., Braunberger, J., Smith, S., and Kazemi, H., 2013, Geologic characterization of a Bakken reservoir for potential CO_2 EOR: Presented at 2013 Unconventional Resources Technology Conference, Denver, Colorado, August 12–14, Paper URTeC 1619698.

Kurtoglu, B., Nelson, R., and Brehm, J., 2012, EERC & Marathon CO_2 enhanced bakken recovery research: Technical presentation, Grand Forks, North Dakota, November 26.

LeFever, J., and Helms, L., 2008, Bakken Formation reserve estimates: North Dakota Geological Survey white paper, Bismarck, North Dakota, North Dakota Geological Survey, March, p. 6.

Meissner, F.F., 1984, Petroleum geology of the Bakken Formation, Williston Basin, North Dakota and Montana, in G. Demaison and R.J. Murris, eds., Petroleum geochemistry and basin evaluation: AAPG Memoir 35, p. 159–179.

Mohammed-Singh, L., Singhai, A.K., and Sim, S., 2006, Screening criteria for carbon dioxide huff 'n' puff operations: SPE 100044.

Murphy, E.C., Nordeng, S.H., Juenker, B.J., and Hoganson, J.W., 2009, North Dakota stratigraphic column: Miscellaneous Series 91.

Nelson, R.A., 2001, Geologic analysis of naturally fractured reservoirs, 2nd Ed.: Gulf Professional Publishing.

Nordeng, S.H., LeFever, J.A., Anderson, F.J., Bingle-Davis, M., and Johnson, E.H., 2010, An examination of the factors that impact oil production from the middle member of the Bakken Formation in Mountrail County, North Dakota: North Dakota Geological Survey, RI-109.

Nordeng, S.H., and Helms, L.D., 2010, Bakken source system – Three Forks Formation assessment: North Dakota Department of Mineral Resources, April.

North Dakota Industrial Commission, 2013, Director's cut, North Dakota production statistics: www.dmr.nd.gov/oilgas/directorscut-2013-05-15.pdf (accessed November 30, 2013).

Nuttall, B.C., Eble, C.F., Drahovzal, J.A., and Bustin, M.R., 2005, Analysis of Devonian black shales in Kentucky for potential carbon dioxide sequestration and enhanced natural gas production: Kentucky Geological Survey Final Report to U.S. Department of Energy, 120 p.

Pittman, J.K., Price, L.C., and LeFever, J.A., 2001, Diagenesis and fracture development in the Bakken Formation, Williston Basin—implications for reservoir quality in the middle member: U.S. Geologic Survey Professional Paper 1653.

Rowe, A.M., and Chou, J.C.S., 1970, Pressure-volume-temperature-concentration relation of aqueous NaCl solutions: Journal of Chemical Engineering Data, v. 15, no. 1, pp. 61–66.

Sonnenberg, S., and Pramudito, A., 2009, Petroleum geology of the giant Elm Coulee Field, Williston Basin: AAPG Bulletin, v. 93, p. 1127–1153.

U.S. Bureau of Reclamation, 1998, Engineering Geology Field Manual, 2nd Ed., Vol. I: U.S. Government Printing Office.

U.S. Department of Energy, 2007, Carbon sequestration atlas of the United States and Canada: U.S. Department of Energy Office of Fossil Energy, March, www.precaution.org/lib/carbon_sequestration_atlas.070601.pdf.

Uzoh, C., Han, J., Hu, L.W., Siripatrachai, N., Osholake, T., and Chen, X., 2010, Economic optimization analysis of the development process on a field in the Barnett Shale Formation: EME 580 Final Report.

APPENDIX A

FRACTURE ANALYSIS OF THE MIDDLE BAKKEN FORMATION ON NORTH DAKOTA STUDY AREAS FOR CO_2 STORAGE AND ENHANCED OIL RECOVERY

EERC Energy & Environmental Research Center® Putting Research into Practice UND THE UNIVERSITY OF NORTH DAKOTA	**Applied Geology Laboratory**		ID: 116978
	Well Name: NDIC No. 8850	Middle Bakken 7	Rival Field
	American Petroleum Institute (API) No.: 33-013-00867-00-03	Lithology: Silty dolostone	Depth: 7397.5'

SAMPLE PHOTOGRAPH

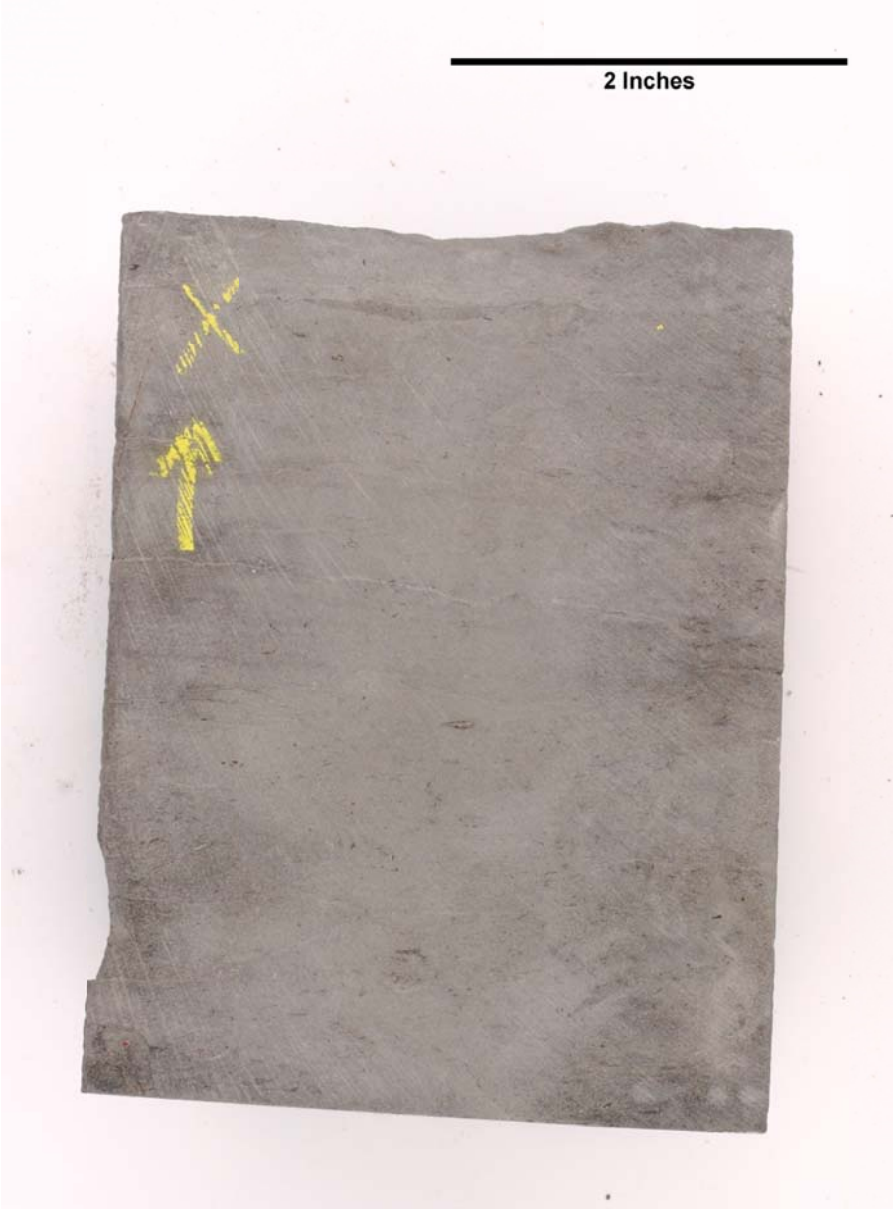

PHYSICAL PROPERTIES

Porosity and Grain Density by Core Laboratories

Pycnometer Effective Porosity, vol%	Grain Density, g/cm^3
6.68	2.763

EERC Energy & Environmental Research Center® Putting Research into Practice UND THE UNIVERSITY OF NORTH DAKOTA	**Applied Geology Laboratory**		ID: 116978
	Well Name: NDIC No. 8850	Middle Bakken 7	Rival Field
	American Petroleum Institute (API) No.: 33-013-00867-00-03	Lithology: Silty dolostone	Depth: 7397.5'

PHOTOMICROGRAPHS

Transmission

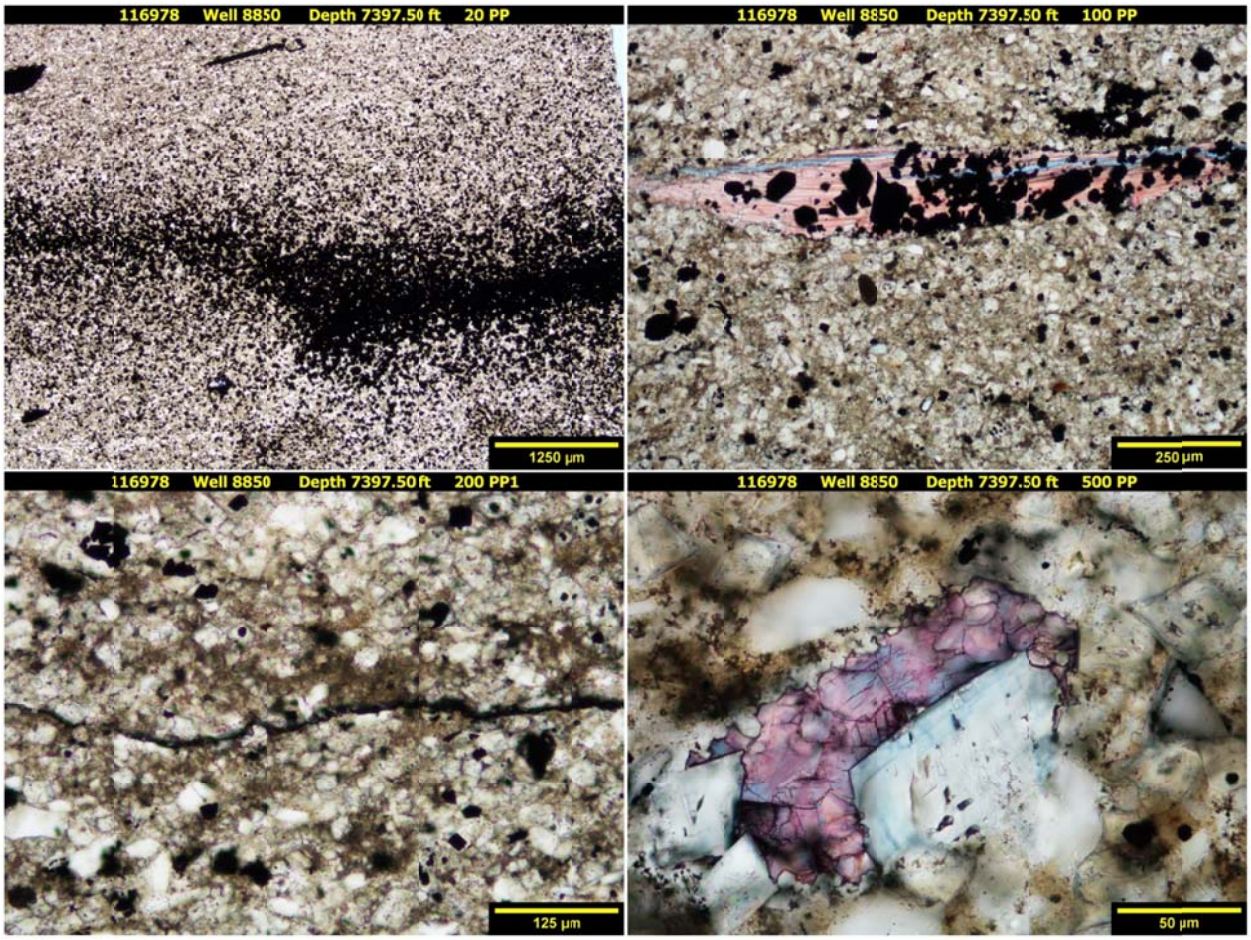

The sample from a depth of 7397.50 ft shows a silty dolostone. It is a predominately massive sample having some faint bioturbation features. Very fine grained, angular to subangular, monocrystalline quartz and feldspar grains with trace amounts of muscovite are disseminated throughout. Extensive anhederal to euhedral dolomitization (trace ferroan) has occurred throughout the sample. Only trace calcareous skeletal grains remain. Disseminated pore-filling and replacement pyrite grains are present. Zonally high concentrations of pyrite exists creating horizontal bands across the entire sample; many allochems have been completely pyritized. Clay is found disseminated at small quantities, and occasionally concentrated with burrowing structures. Filled and unfilled fractures are detected. Open fractures, predominately horizontal, observed are likely the result of the sampling process. Filled fractures have a variety of orientations and are cemented by a combination of clays, carbonates, pyrite, and organics. Organics observed are typically associated with pyrite. No particle-based porosity is observed using standard petrographic techniques.

EERC Energy & Environmental Research Center® Putting Research into Practice UND THE UNIVERSITY OF NORTH DAKOTA	**Applied Geology Laboratory**		ID: 116978
	Well Name: NDIC No. 8850	Middle Bakken 7	Rival Field
	American Petroleum Institute (API) No.: 33-013-00867-00-03	Lithology: Silty dolostone	Depth: 7397.5'

Reflection

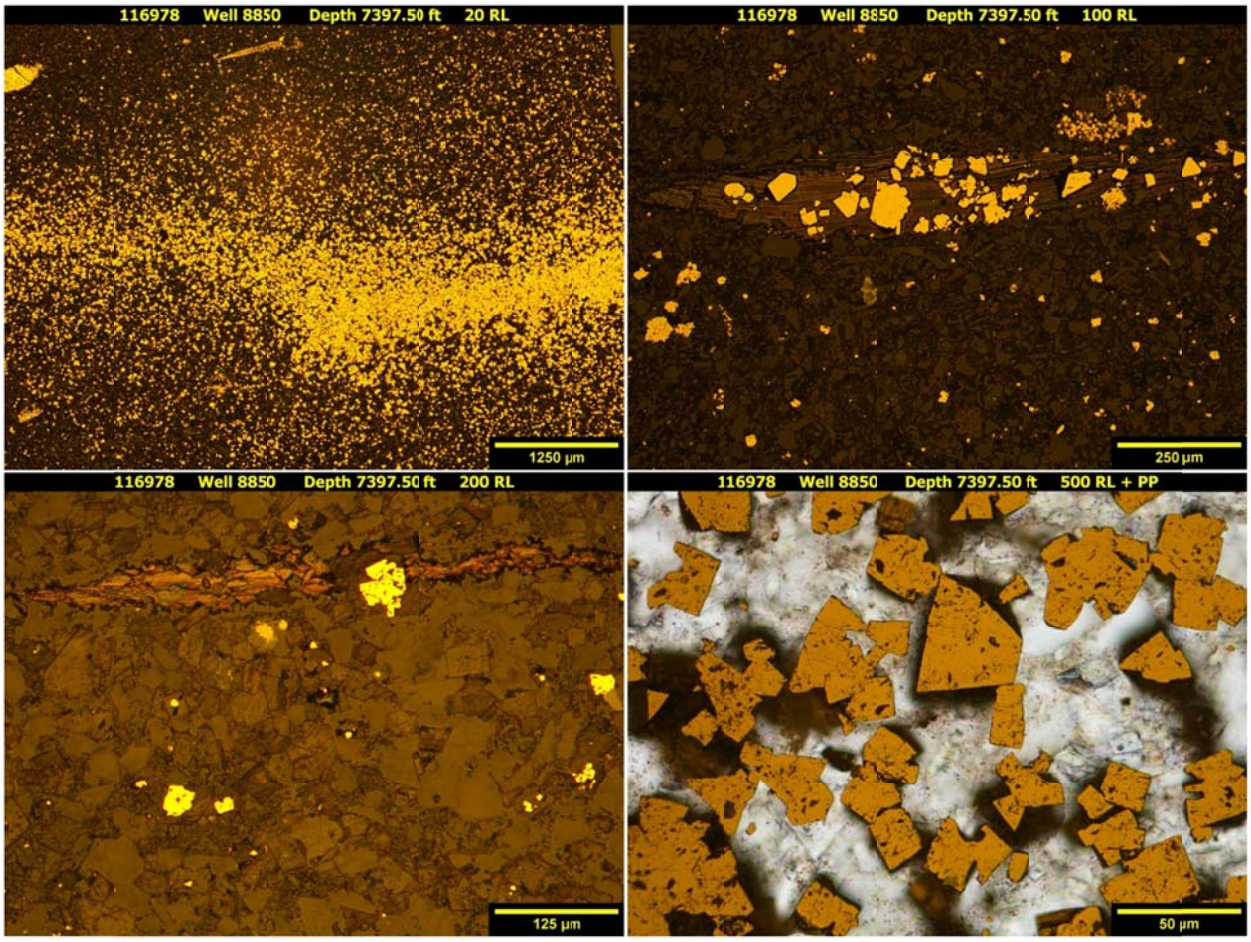

The sample from a depth of 7397.50 ft displays both prevalent euhedral and frambodial pyrite growth. This diagenetic feature acts as a pore filler and as grain replacement. Euhedral grains are very fine grained and individual frambodial grains are observed at a fraction of that size. A high concentration of euhedral pyrite grains creates a band or lamination. Nearly complete pyritization of skeletal and non-skeletal grains and organics have occurred at some localities. Organics observed are typically associated with both euhedral and framboidal pyrite.

EERC Energy & Environmental Research Center® Putting Research into Practice UND THE UNIVERSITY OF NORTH DAKOTA	**Applied Geology Laboratory**		ID: 116978
	Well Name: NDIC No. 8850	Middle Bakken 7	Rival Field
	American Petroleum Institute (API) No.: 33-013-00867-00-03	Lithology: Silty dolostone	Depth: 7397.5'

Transmission and Fluorescence Whole-Slide Images

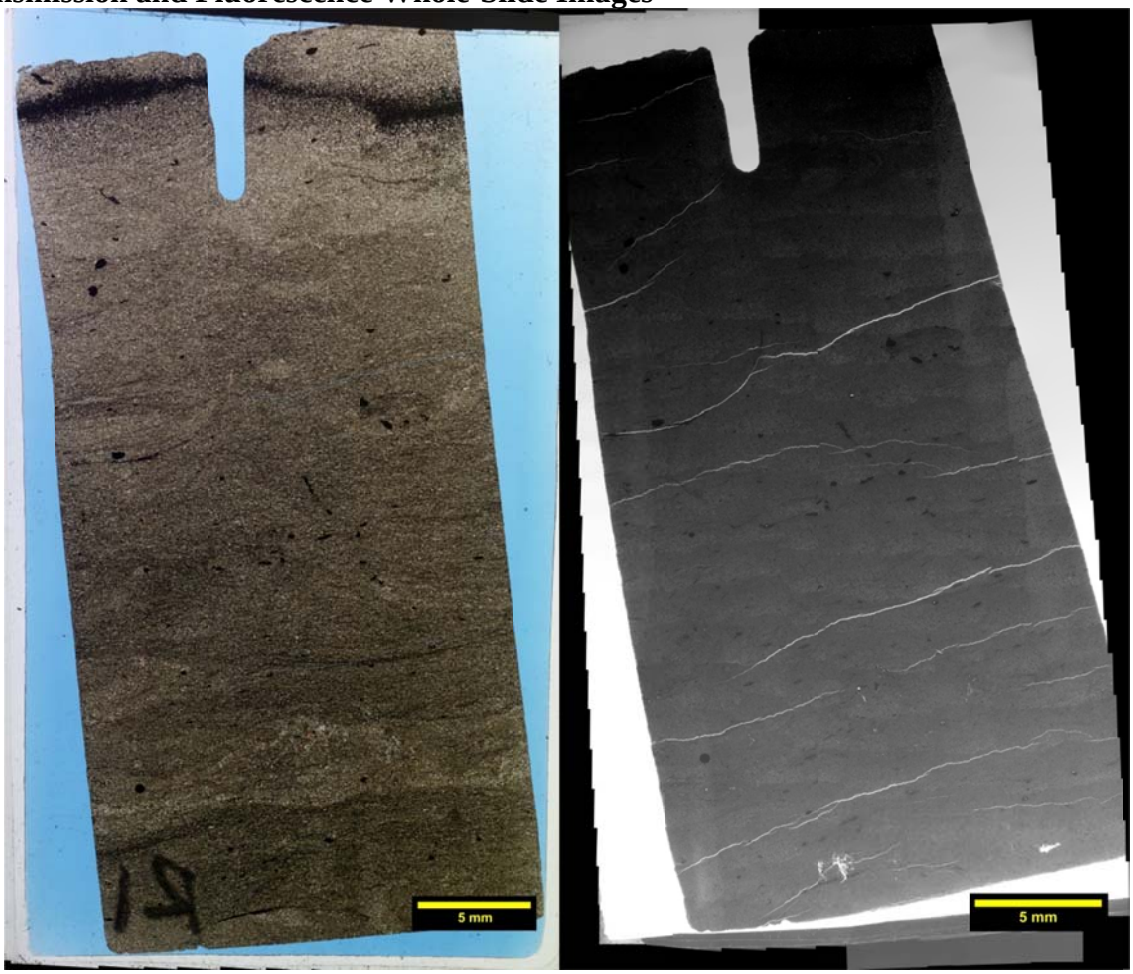

The image collected from a depth of 7397.50 ft is a slightly bioturbated, largely massive sample. Effective porosity is reported at 6.68 vol%. Extensive interlocking anhedral to euhedral dolomitization and pyritization has occurred, perhaps revealing a more advanced diagenetical history. These diagenetic events along with moderate clay content and very fine grain sizes are limiting factors of pore size (<30 µm) and distribution. No natural fractures are observed. All observed fractures are likely the result of sampling process, but may give insight to how the rock would perform under stress.

EERC Energy & Environmental Research Center® Putting Research into Practice UND THE UNIVERSITY OF NORTH DAKOTA	**Applied Geology Laboratory**		ID: 116978
	Well Name: NDIC No. 8850	Middle Bakken 7	Rival Field
	American Petroleum Institute (API) No.: 33-013-00867-00-03	Lithology: Silty dolostone	Depth: 7397.5'

X-Ray Fluorescence (XRF) BULK CHEMICAL COMPOSITION

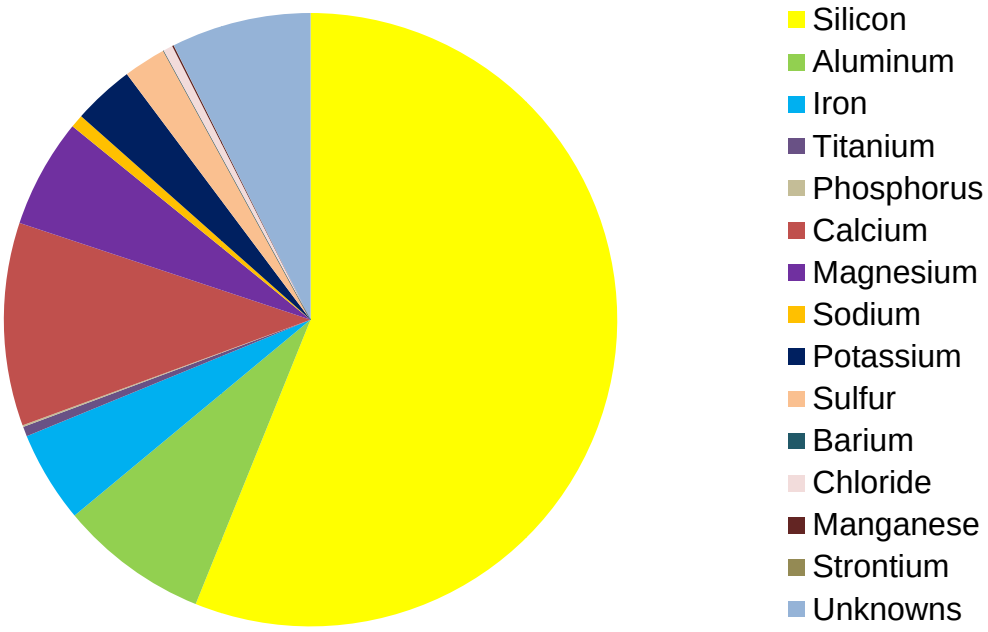

Element	Reporting Convention (Oxide)	Weight %
Si (silicon)	SiO_2	56.11
Al (aluminum)	Al_2O_3	7.87
Fe (iron)	Fe_2O_3	4.83
Ti (titanium)	TiO_2	0.51
P (phosphorus)	P_2O_5	0.09
Ca (calcium)	CaO	10.71
Mg (magnesium)	MgO	5.75
Na (sodium)	Na_2O	0.69
K (potassium)	K_2O	3.23
S (sulfur)	SO_3	2.26
Ba (barium)	BaO	0.00
Cl (chloride)	Cl	0.51
Mn (manganese)	MnO	0.08
Sr (strontium)	SrO	0.01
Unknowns	Due to the presence of carbonates	7.36
Total		100.01

EERC Energy & Environmental Research Center® Putting Research into Practice UND THE UNIVERSITY OF NORTH DAKOTA	**Applied Geology Laboratory**		ID: 116978
	Well Name: NDIC No. 8850	Middle Bakken 7	Rival Field
	American Petroleum Institute (API) No.: 33-013-00867-00-03	Lithology: Silty dolostone	Depth: 7397.5'

X-RAY DIFFRACTION (XRD) MINERAL PHASE DISTRIBUTION

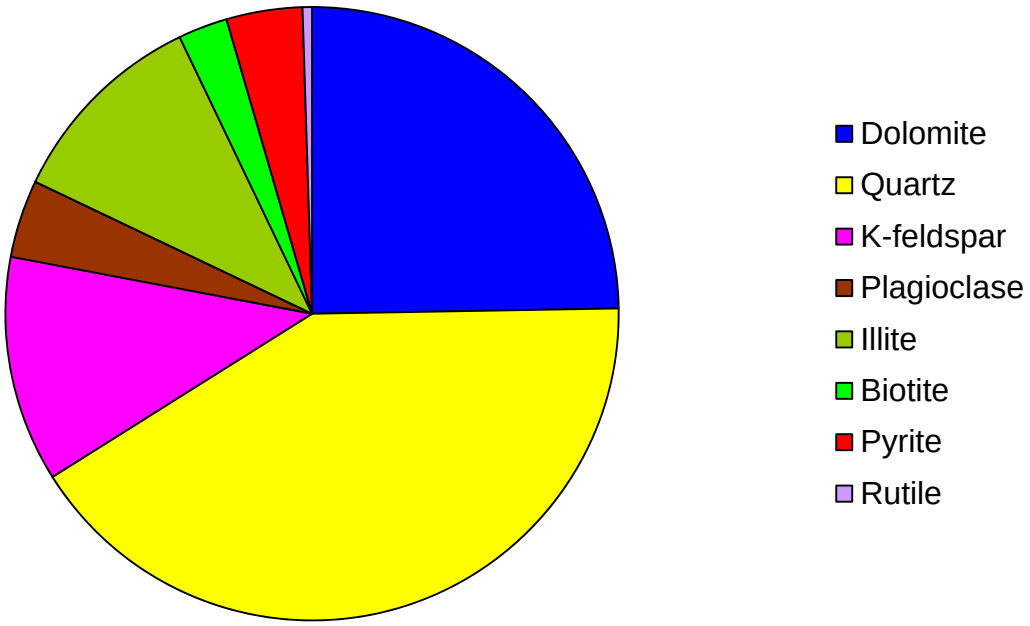

Mineral Phase	Formula	Weight %
Dolomite	$CaMg(CO_3)_2$	24.7
Quartz	SiO_2	41.3
K-feldspar	$KAlSi_3O_8$	11.9
Plagioclase	$Na_{0.5}Ca_{0.5}Al_{1.5}Si_{2.5}O_8$	4.1
Illite	$(K,H_3O)(Al,Mg,Fe)_2(Si,Al)_4O_{10}[(OH)_2,(H_2O)]$	10.8
Biotite	$K(Mg,Fe)_3[(OH)_2AlSi_3O_{10}]$	2.6
Pyrite	FeS_2	4.0
Rutile	TiO_2	0.5

EERC Energy & Environmental Research Center® Putting Research into Practice UND THE UNIVERSITY OF NORTH DAKOTA	**Applied Geology Laboratory**		ID: 116978
	Well Name: NDIC No. 8850	Middle Bakken 7	Rival Field
	American Petroleum Institute (API) No.: 33-013-00867-00-03	Lithology: Silty dolostone	Depth: 7397.5'

SCANNING ELECTRON MICROSCOPY (SEM)

Observed Minerals

Mineral Phase	Mineral Phase
Calcite	Dolomite
Quartz	K-feldspar
Rutile	Illite
Pyrite	Albite
Apatite	Biotite

High-Magnification Backscattered Electron (BSE) Image Annotated with Examples of Mineral Phases Identified

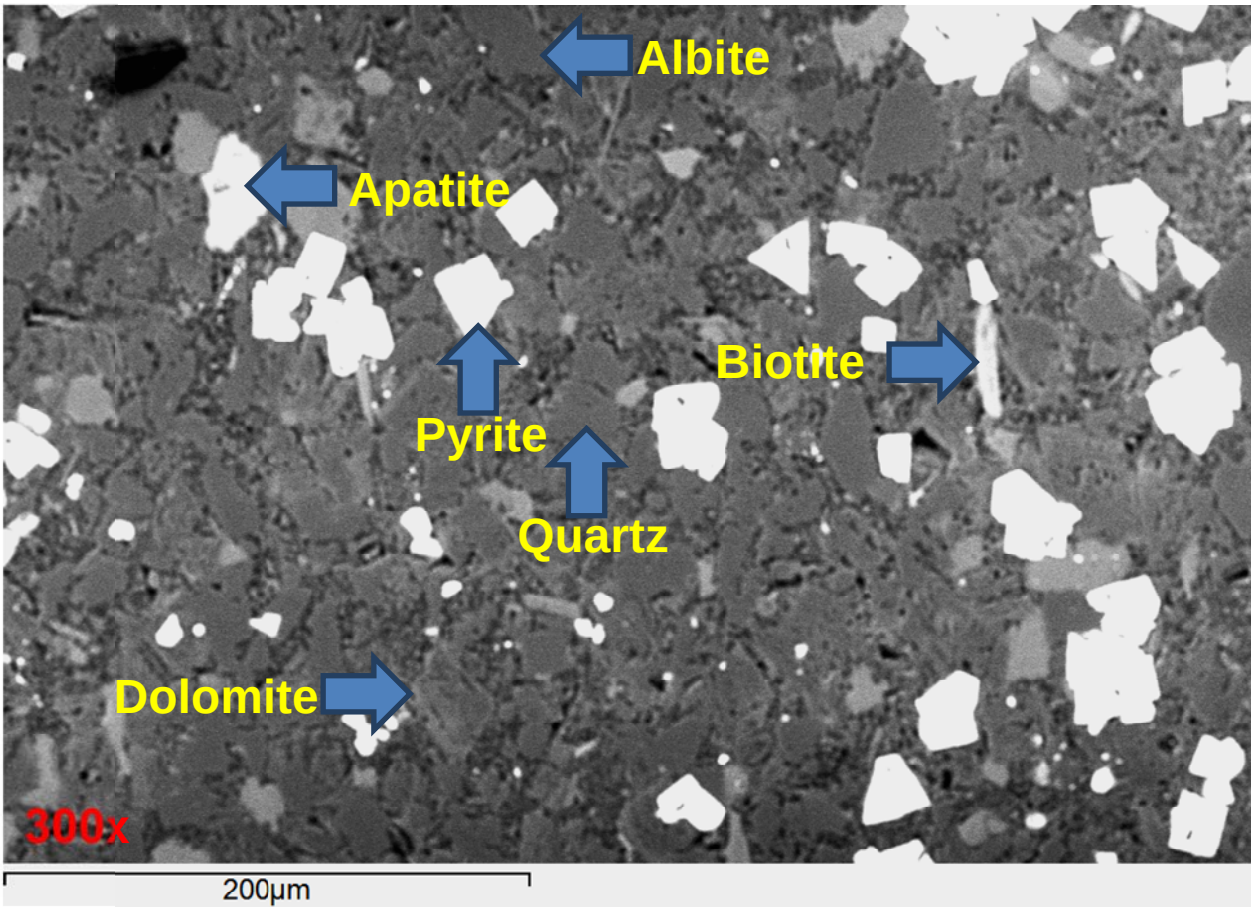

Additional High-Magnification BSE Images

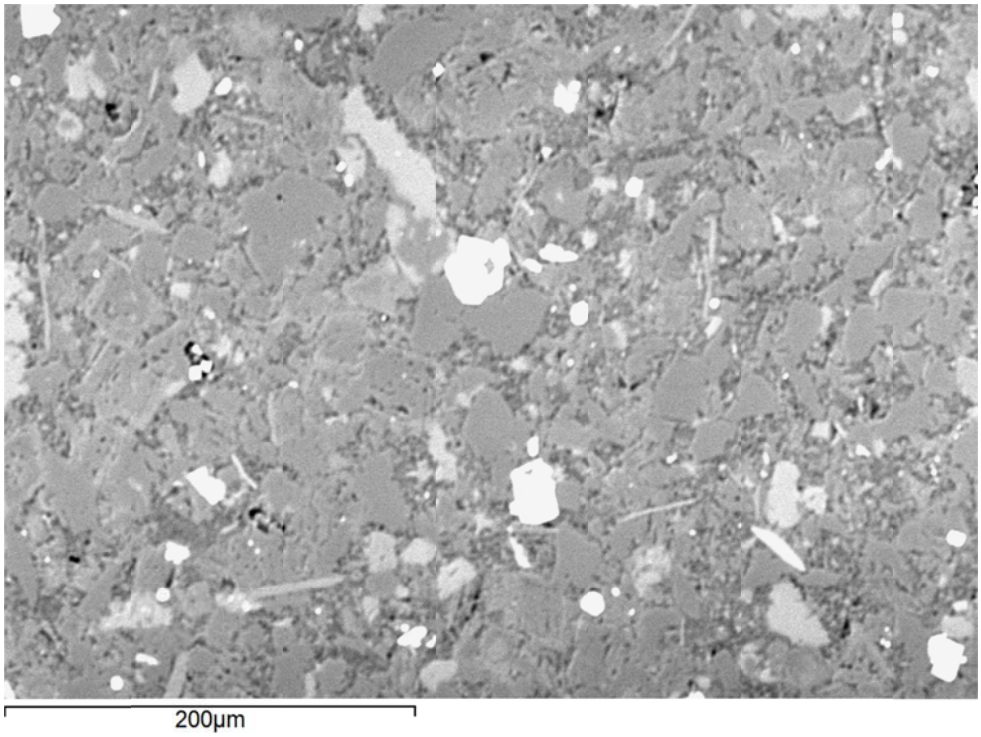

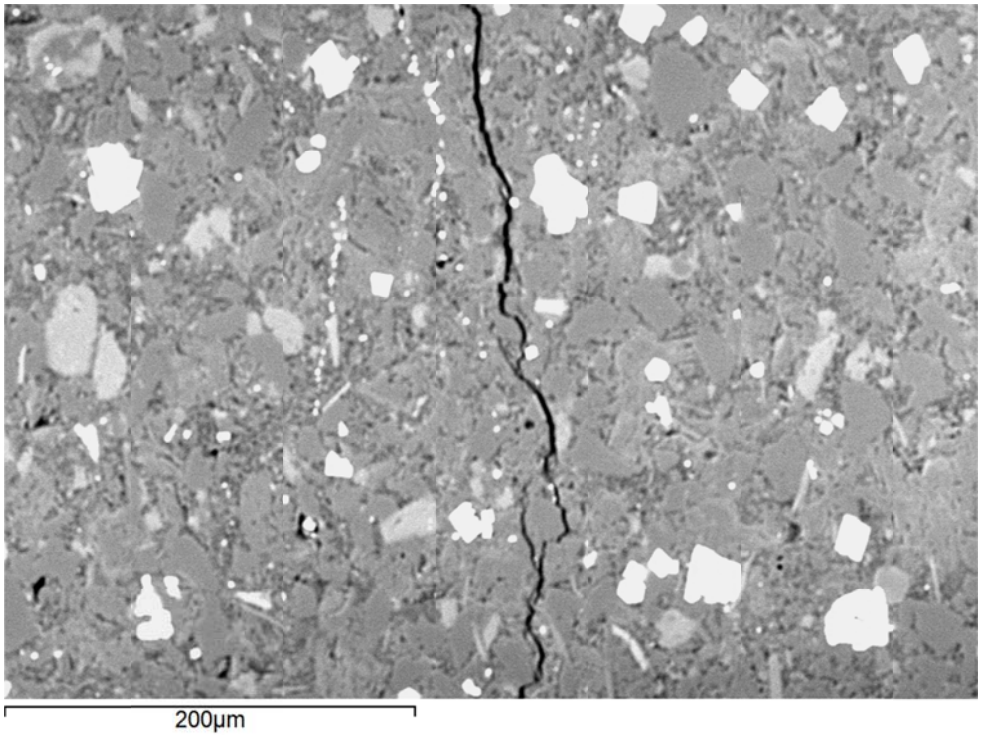

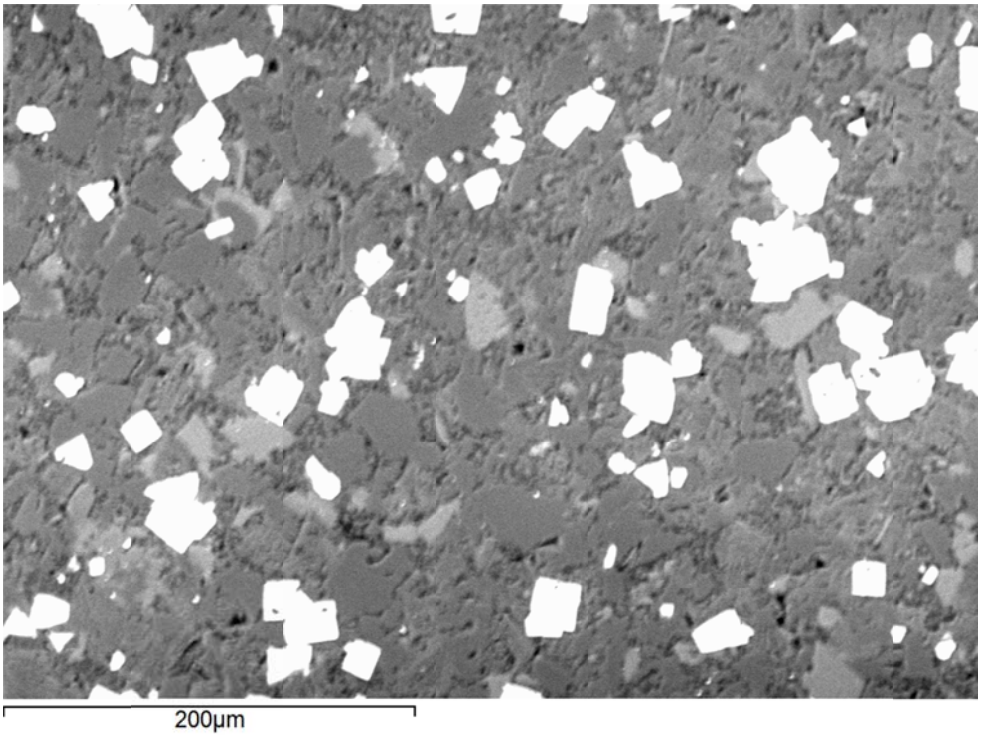
200µm

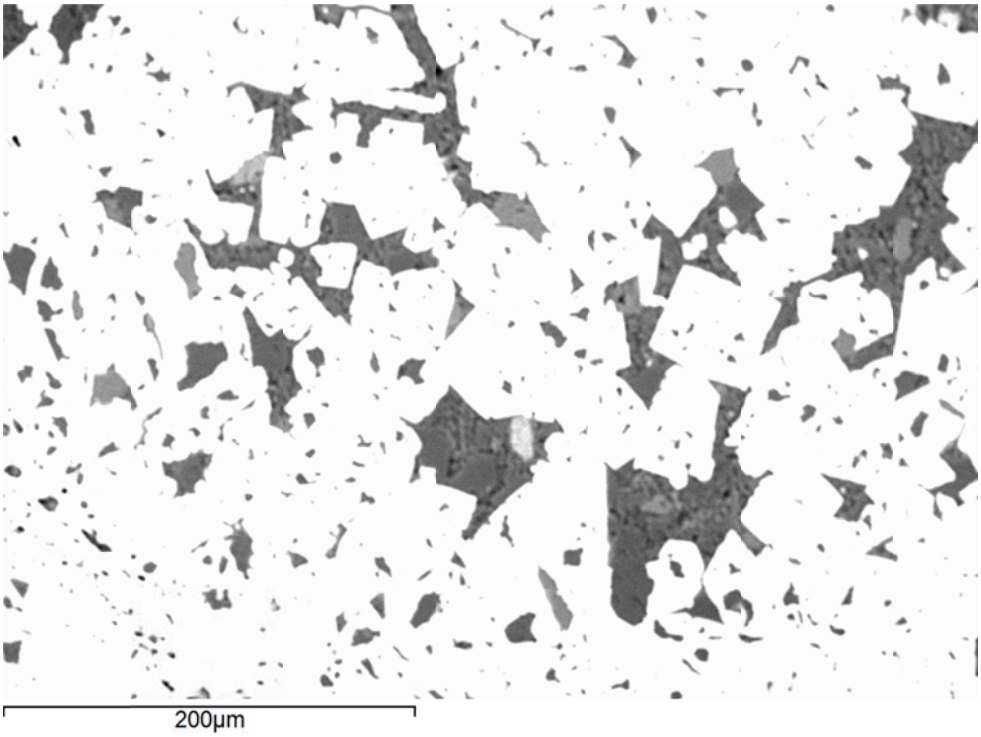
200µm

EERC Energy & Environmental Research Center® Putting Research into Practice UND THE UNIVERSITY OF NORTH DAKOTA	**Applied Geology Laboratory**		ID: 116978
	Well Name: NDIC No. 8850	Middle Bakken 7	Rival Field
	American Petroleum Institute (API) No.: 33-013-00867-00-03	Lithology: Silty dolostone	Depth: 7397.5'

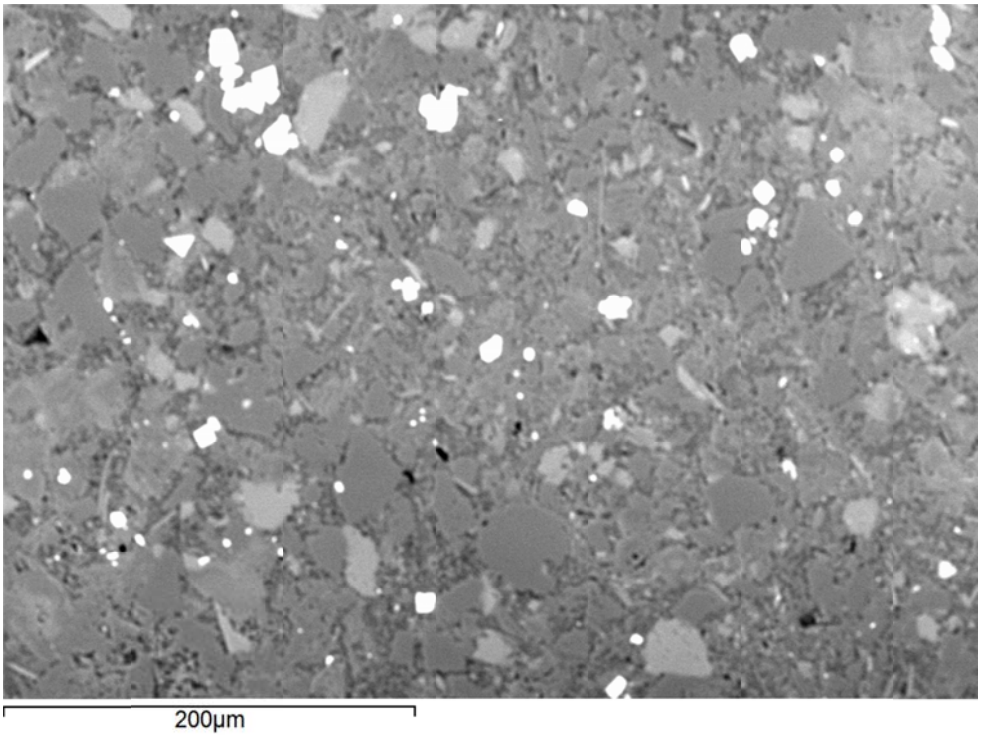

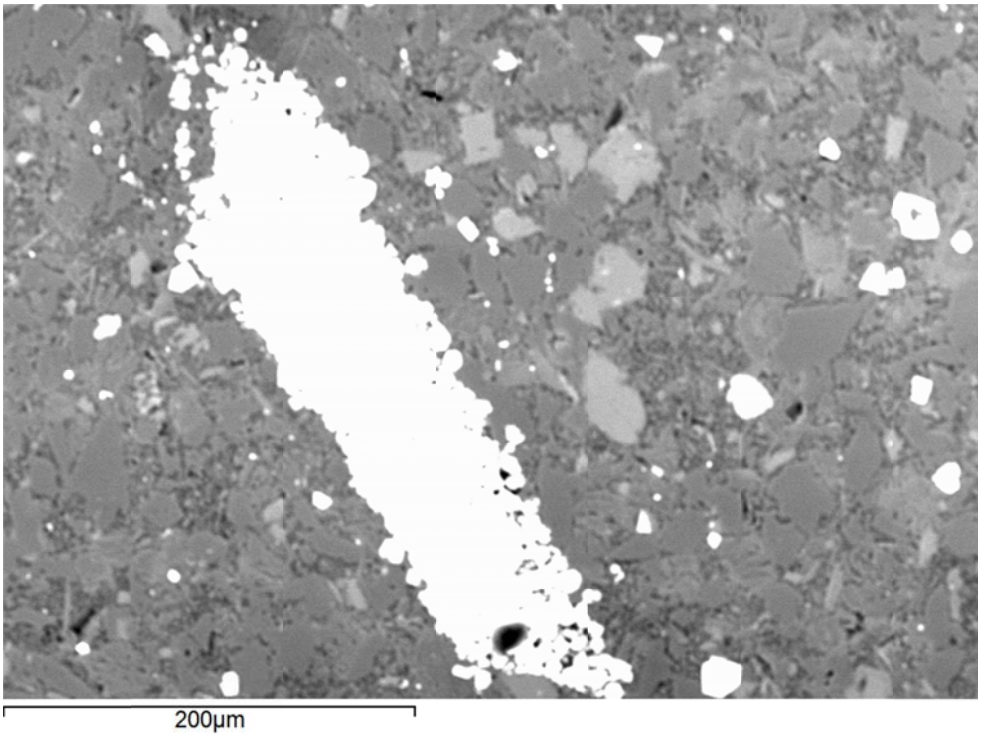

EERC Energy & Environmental Research Center® Putting Research into Practice UND THE UNIVERSITY OF NORTH DAKOTA	**Applied Geology Laboratory**		ID: 116978
	Well Name: NDIC No. 8850	Middle Bakken 7	Rival Field
	American Petroleum Institute (API) No.: 33-013-00867-00-03	Lithology: Silty dolostone	Depth: 7397.5'

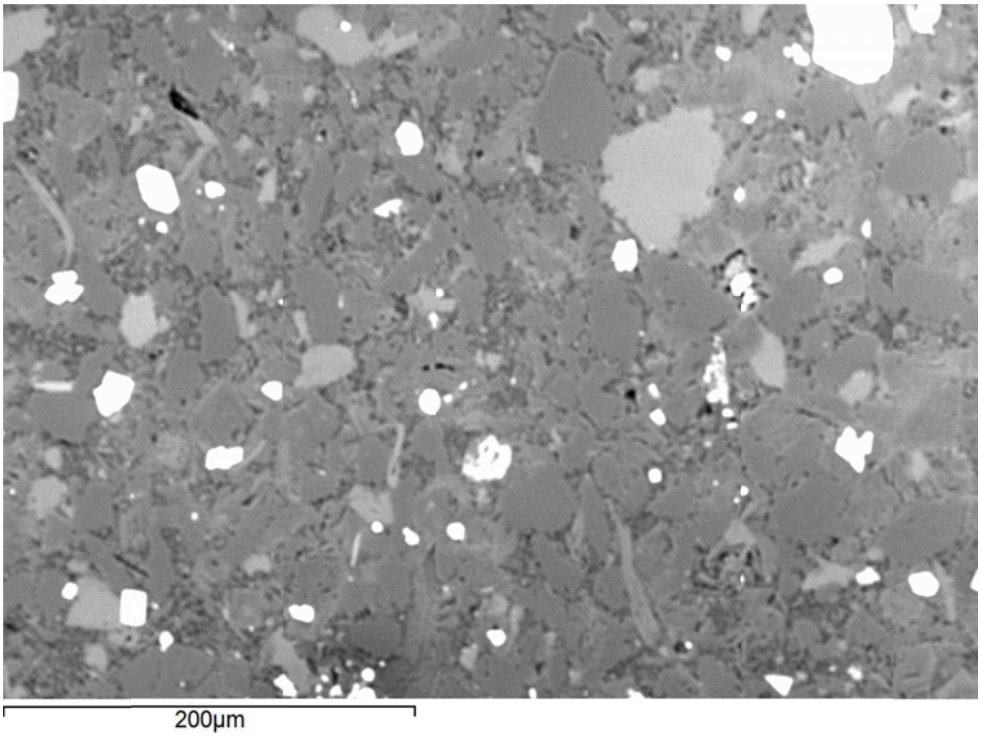

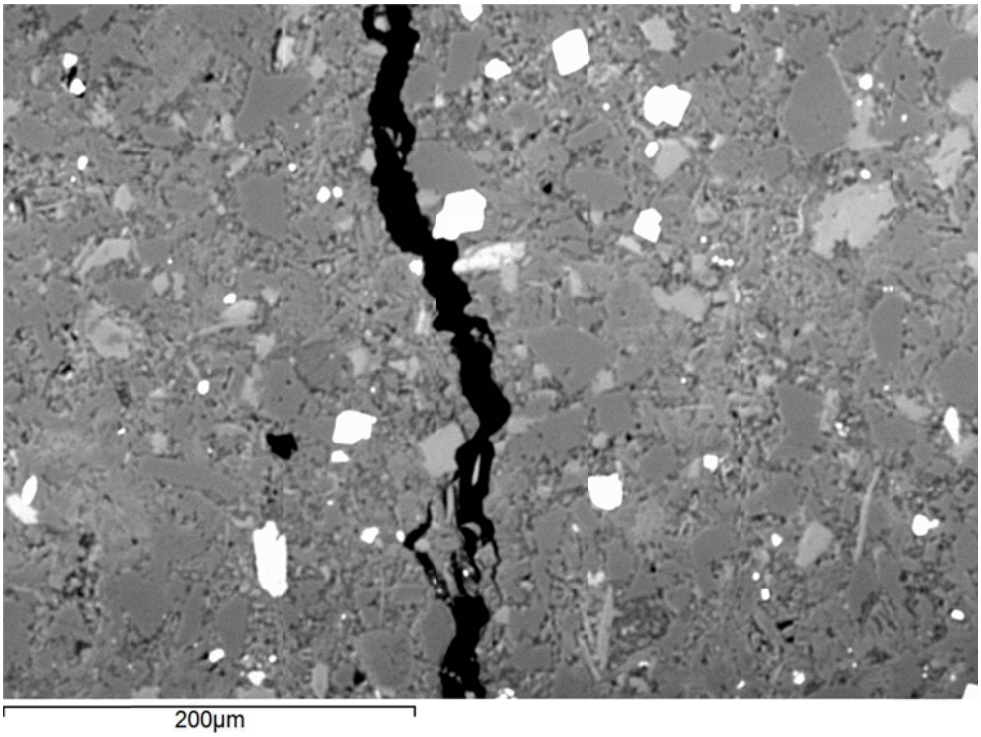

EERC Energy & Environmental Research Center® Putting Research into Practice UND THE UNIVERSITY OF NORTH DAKOTA	**Applied Geology Laboratory**		ID: 116978
	Well Name: NDIC No. 8850	Middle Bakken 7	Rival Field
	American Petroleum Institute (API) No.: 33-013-00867-00-03	Lithology: Silty dolostone	Depth: 7397.5'

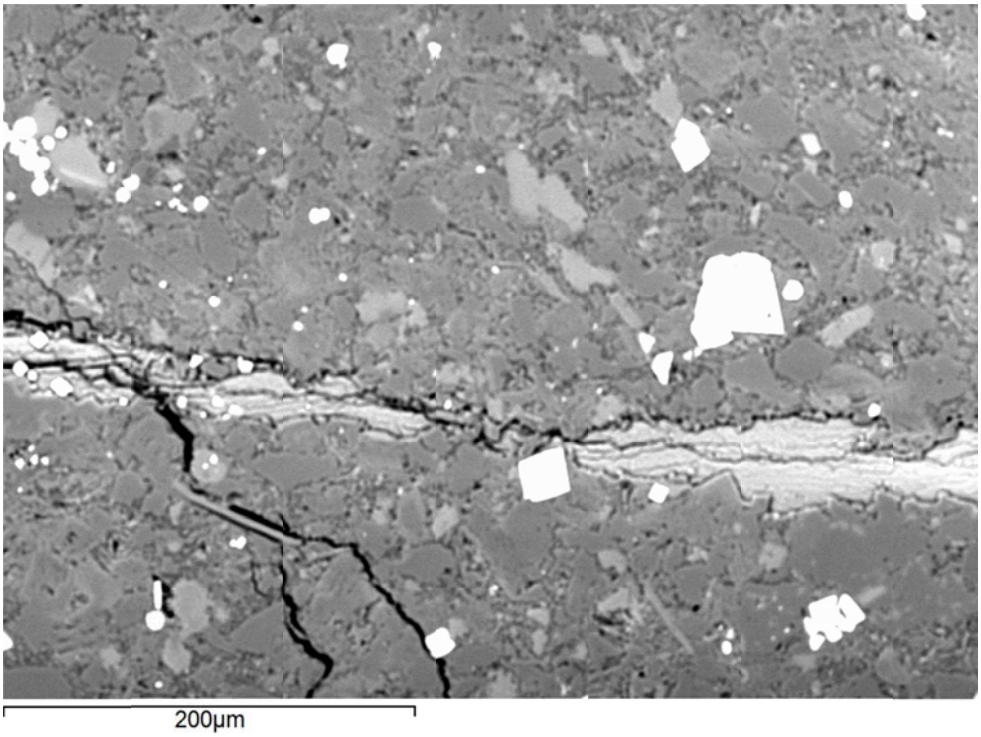

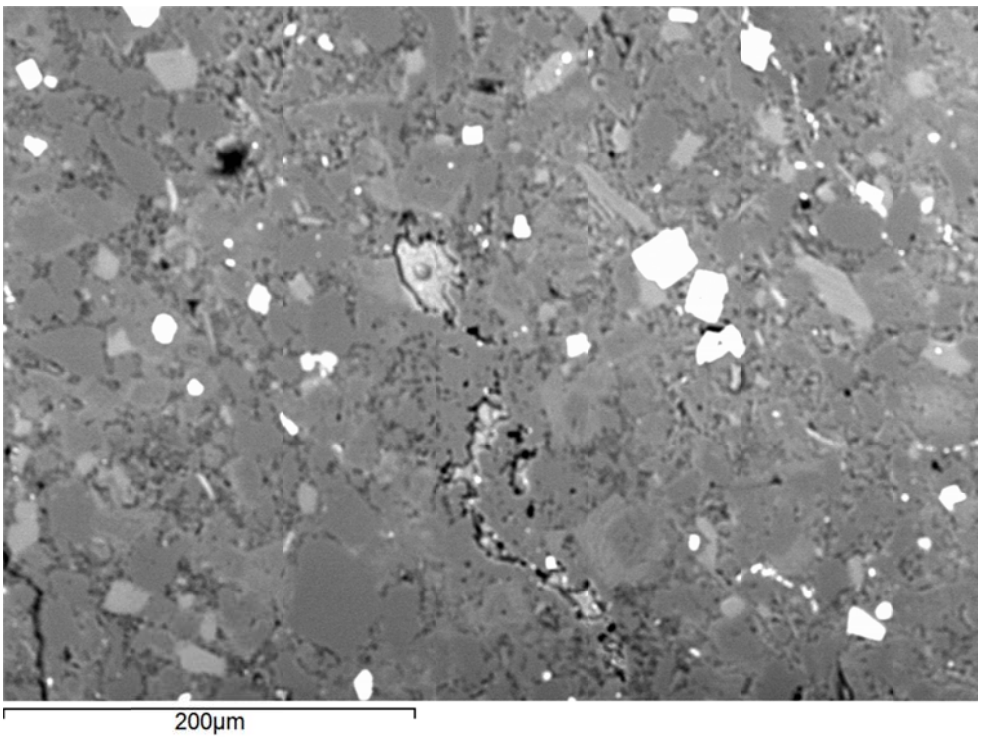

	Applied Geology Laboratory		ID: 116978
	Well Name: NDIC No. 8850	Middle Bakken 7	Rival Field
	American Petroleum Institute (API) No.: 33-013-00867-00-03	Lithology: Silty dolostone	Depth: 7397.5'

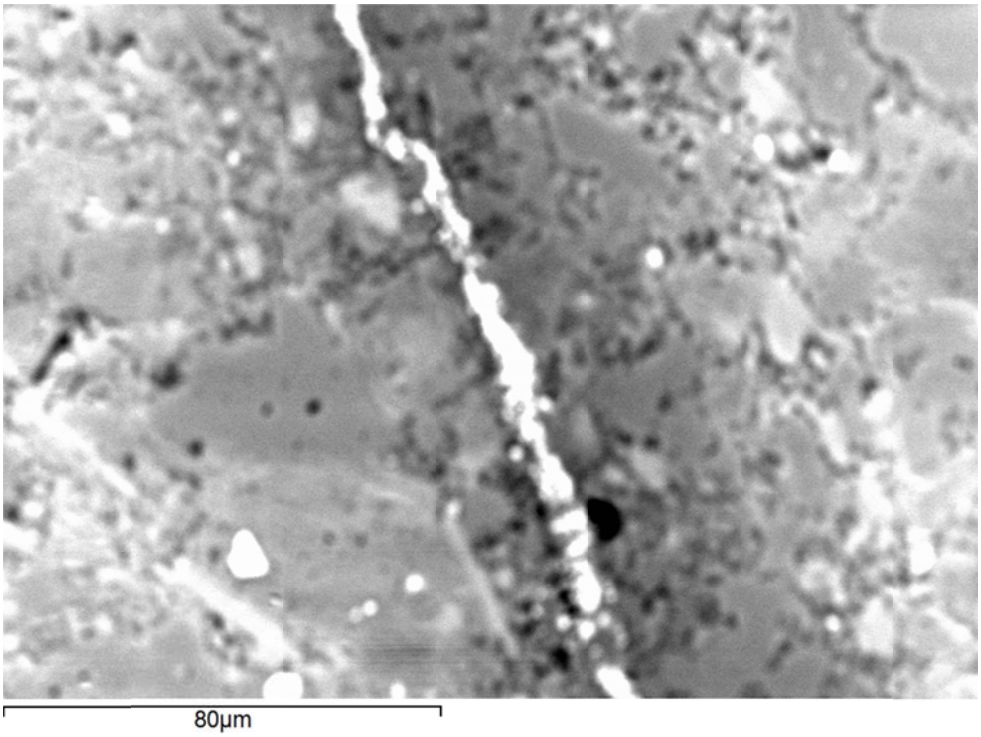

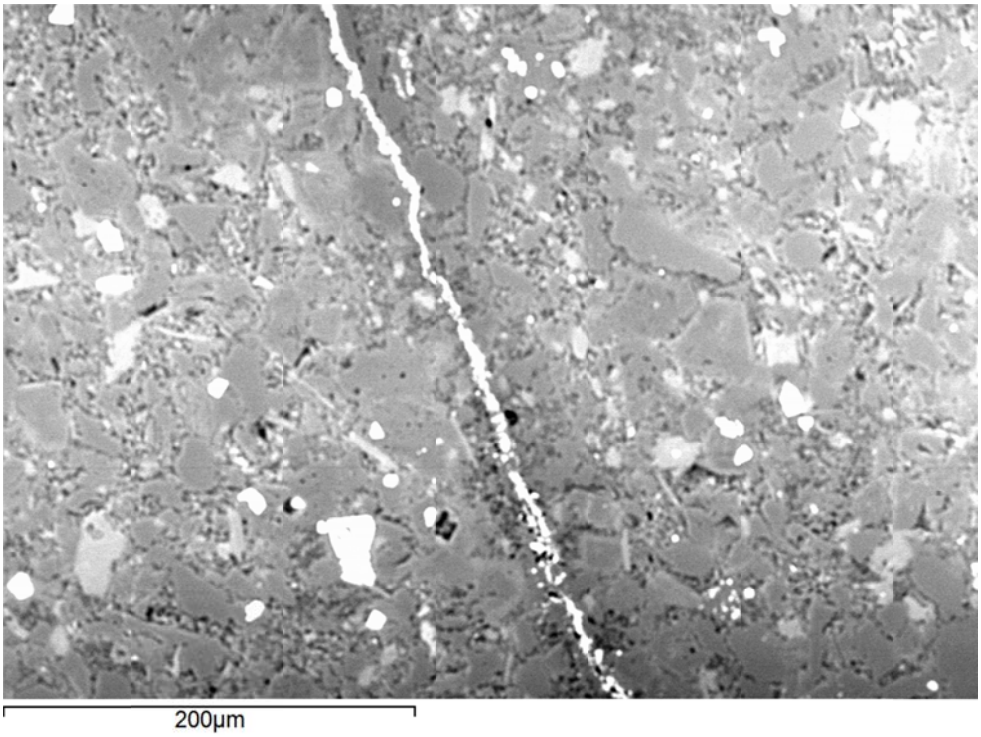

	Applied Geology Laboratory		ID: 116978
	Well Name: NDIC No. 8850	Middle Bakken 7	Rival Field
	American Petroleum Institute (API) No.: 33-013-00867-00-03	Lithology: Silty dolostone	Depth: 7397.5'

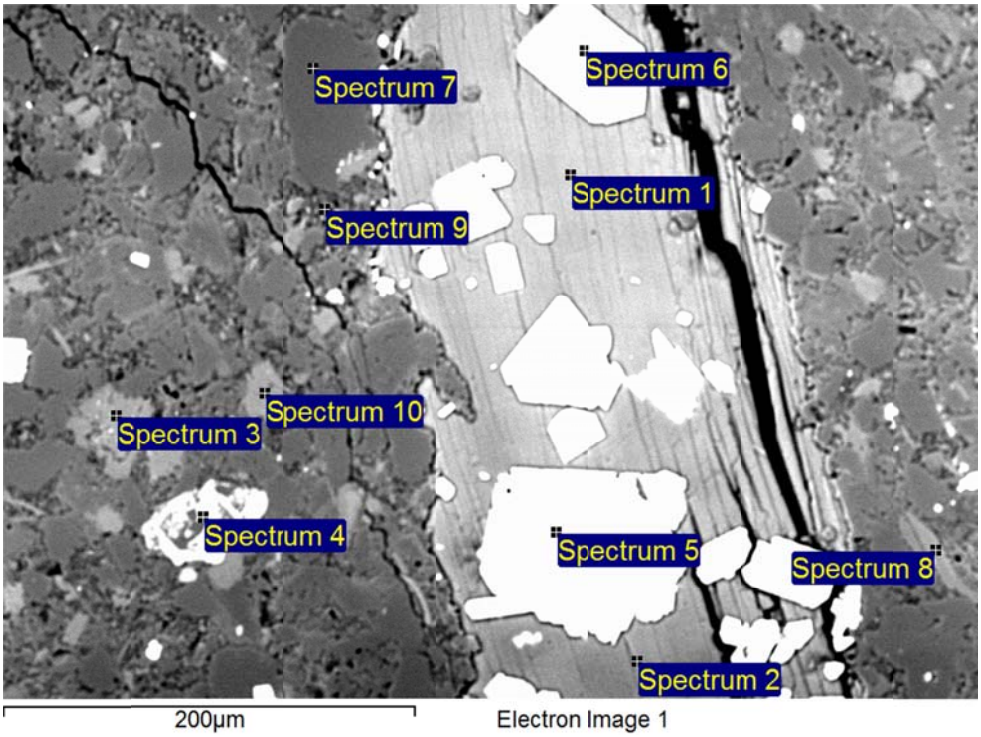

(No plain image was in the Excel file.)

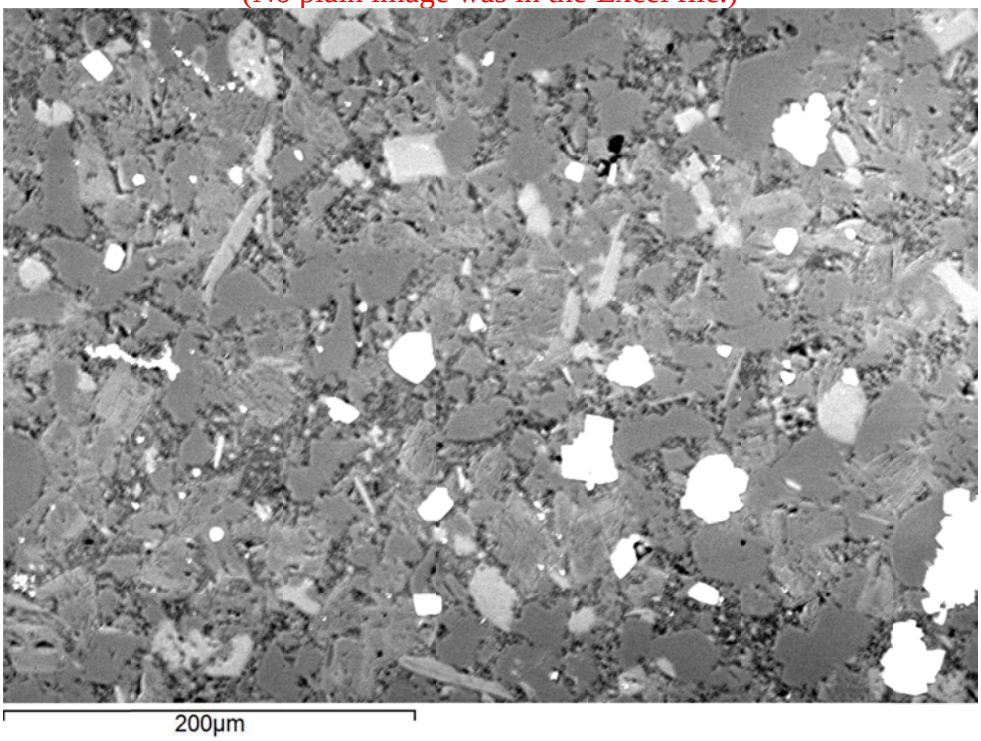

EERC Energy & Environmental Research Center® Putting Research into Practice UND THE UNIVERSITY OF NORTH DAKOTA	**Applied Geology Laboratory**		ID: 116978
	Well Name: NDIC No. 8850	Middle Bakken 7	Rival Field
	American Petroleum Institute (API) No.: 33-013-00867-00-03	Lithology: Silty dolostone	Depth: 7397.5'

SEM Mineral Map Image Overlaid on BSE Image with Mineral Phase 2D Area Percentages

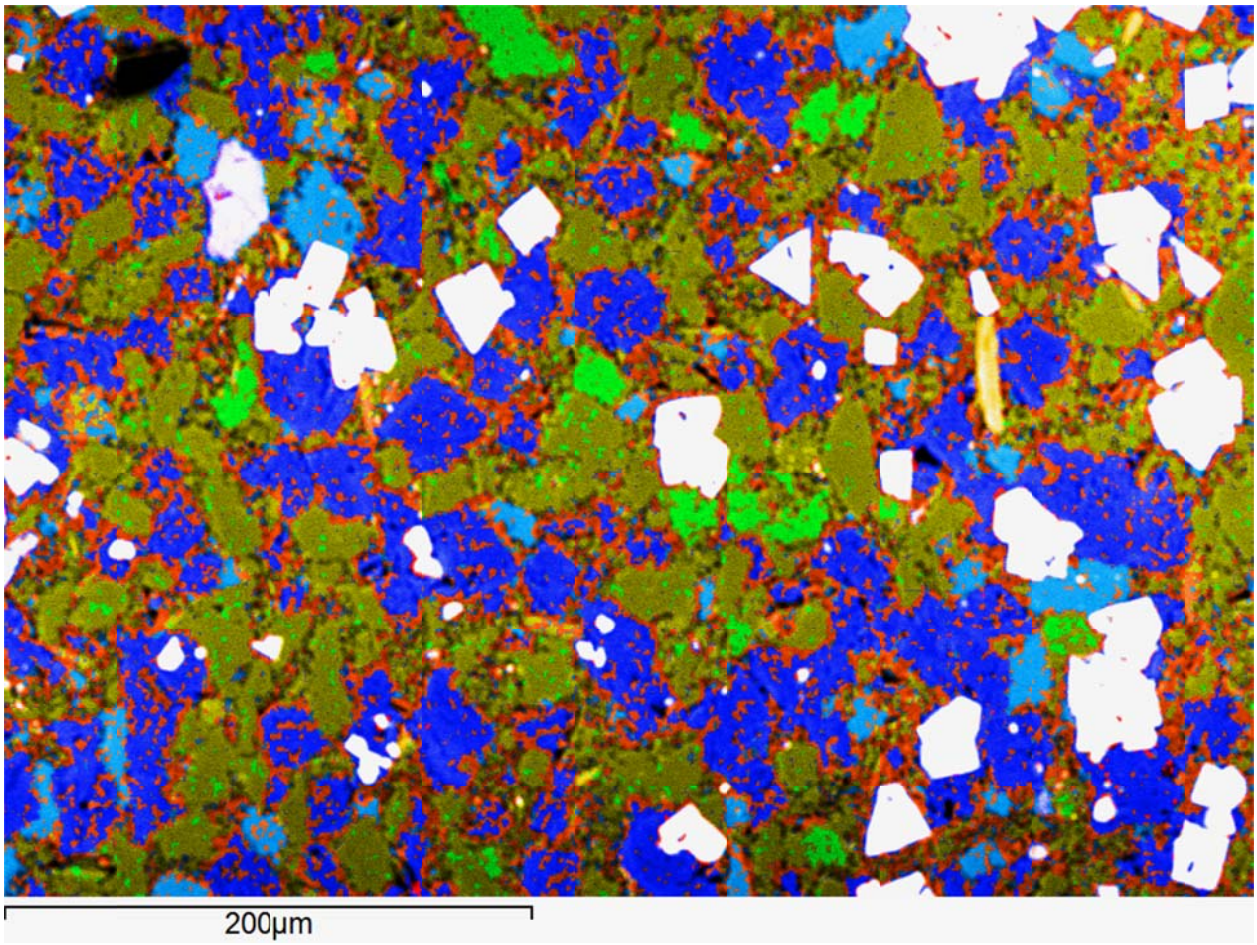

This page intentionally left blank.

EERC Energy & Environmental Research Center® Putting Research into Practice UND THE UNIVERSITY OF NORTH DAKOTA	**Applied Geology Laboratory**		ID: 116979
	Well Name: NDIC No. 8850	Middle Bakken 6	Rival Field
	API No.: 33-013-00867-00-02	Lithology: Silty dolostone	Depth: 7400.8'

SAMPLE PHOTOGRAPH

PHYSICAL PROPERTIES

Porosity and Grain Density by Core Laboratories

Pycnometer Effective Porosity, vol%	Grain Density, g/cm^3
6.11	2.748

EERC Energy & Environmental Research Center® Putting Research into Practice UND THE UNIVERSITY OF NORTH DAKOTA	**Applied Geology Laboratory**		ID: 116979
	Well Name: NDIC No. 8850	Middle Bakken 6	Rival Field
	API No.: 33-013-00867-00-02	Lithology: Silty dolostone	Depth: 7400.8'

PHOTOMICROGRAPHS

Transmission

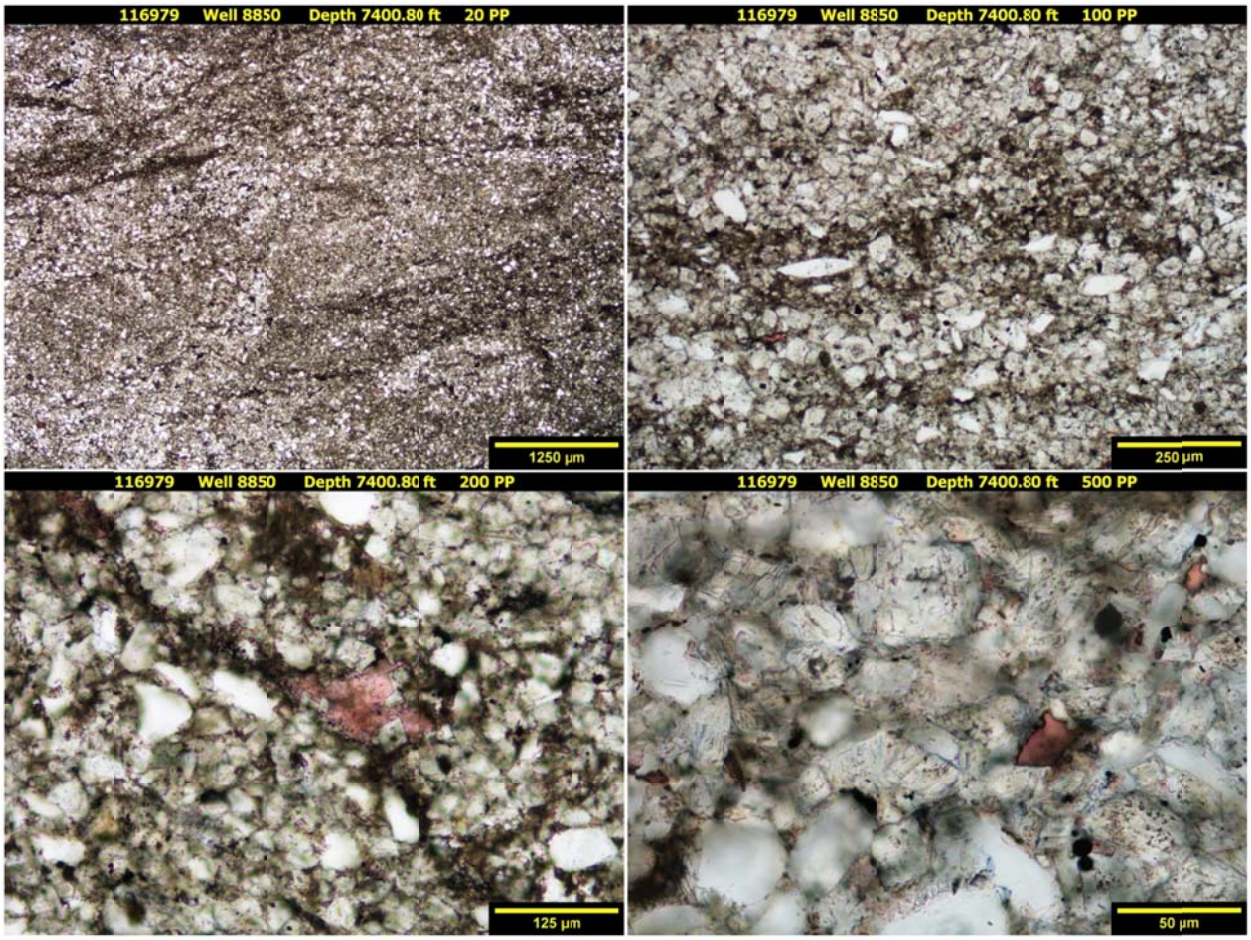

The sample from a depth of 7400.80 ft shows a silty dolostone. A mild degree of bioturbation and faint wavy laminations are present. Very fine grained, angular to subrounded, monocrystalline quartz grains and trace amounts of muscovite are disseminated throughout. Extensive anhederal to euhedral dolomitization has occurred throughout the sample. Very rare calcareous grains remain. Disseminated pore-filling and replacement pyrite grains are present at much lesser quantities than in other samples within the well. An additional matrical component is clay, found at mild quantities shown as faint, wavy laminations and lenses because of burrowing. Randomly-oriented filled and unfilled fractures are detected. Open fractures, predominately horizontal, observed are likely the result of the sample process. A combination of clays, carbonates, pyrite, and organics cement the remaining fractures. Organics are rarely observed and typically associated with pyrite. A trace amount of intra-particle porosity is observed using standard petrographic techniques.

EERC Energy & Environmental Research Center® Putting Research into Practice UND THE UNIVERSITY OF NORTH DAKOTA	**Applied Geology Laboratory**		ID: 116979
	Well Name: NDIC No. 8850	Middle Bakken 6	Rival Field
	API No.: 33-013-00867-00-02	Lithology: Silty dolostone	Depth: 7400.8'

Reflection

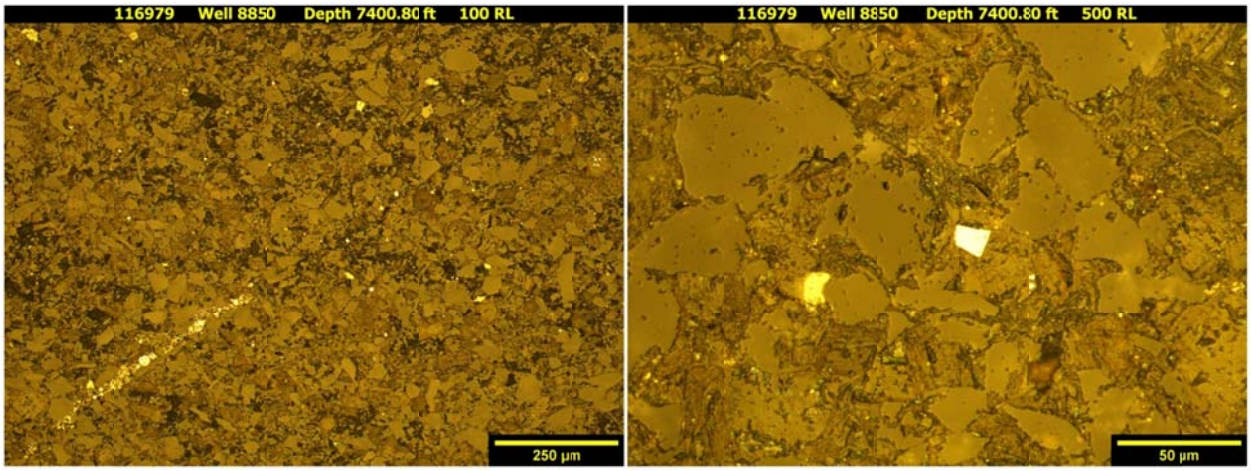

The sample from a depth of 7400.80 ft displays minor amounts of both euhedral and frambodial pyrite growth. Trace amounts of euhedral pyrite exists. Predominantly tiny individual spherical framboidal pyrite is observed as organic replacement. Very little skeletal or non-skeletal grain replacement has occurred. Euhedral grains are very fine grained and individual frambodial grains are observed at a fraction of that size. Organics observed are typically associated with both euhedral and framboidal pyrite.

EERC Energy & Environmental Research Center® Putting Research into Practice UND THE UNIVERSITY OF NORTH DAKOTA	**Applied Geology Laboratory**		ID: 116979
	Well Name: NDIC No. 8850	Middle Bakken 6	Rival Field
	API No.: 33-013-00867-00-02	Lithology: Silty dolostone	Depth: 7400.8'

Transmission and Fluorescence Whole-Slide Images

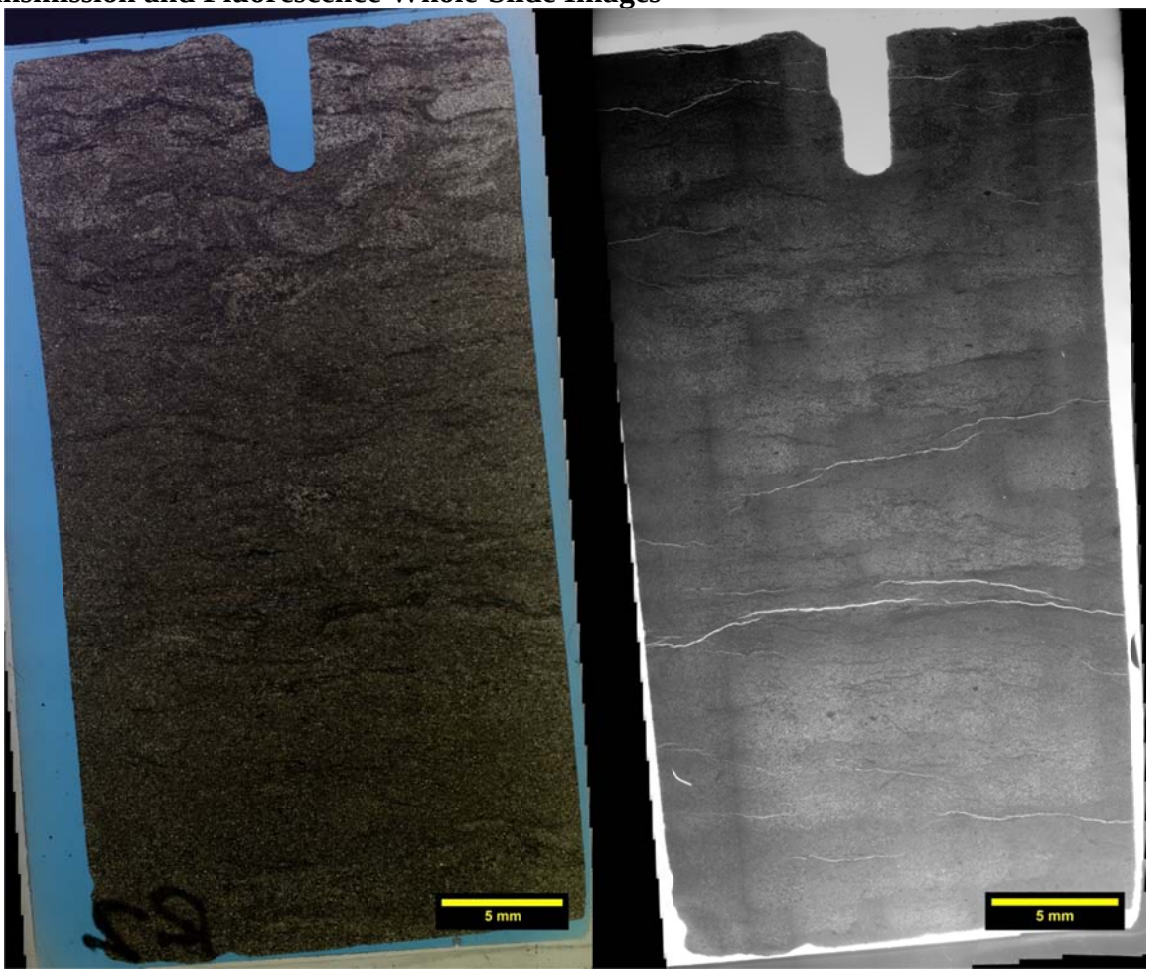

Images issues. The image collected from a depth of 7400.80 ft is moderately bioturbated, silty dolostone. Effective porosity is reported at 6.11 vol%. Extensive interlocking, mainly anhedral to euhedral, dolomitization and pyritization has occurred. These diagenetic events along with moderate clay content and very fine grain sizes are limiting factors of pore size (<30 µm) and distribution. No natural open fractures are observed. All observed fractures are likely the result of sampling process, but may give insight to how the rock would perform under stress.

EERC Energy & Environmental Research Center® Putting Research into Practice UND THE UNIVERSITY OF NORTH DAKOTA	**Applied Geology Laboratory**		ID: 116979
	Well Name: NDIC No. 8850	Middle Bakken 6	Rival Field
	API No.: 33-013-00867-00-02	Lithology: Silty dolostone	Depth: 7400.8'

XRF BULK CHEMICAL COMPOSITION

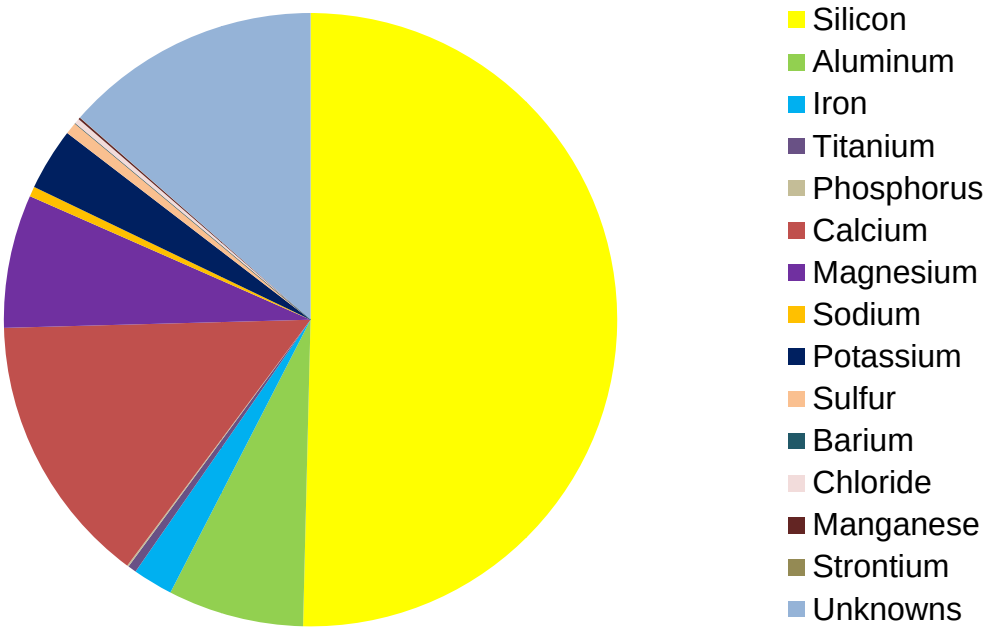

Element	Reporting Convention (Oxide)	Weight %
Si (silicon)	SiO_2	50.39
Al (aluminum)	Al_2O_3	7.17
Fe (iron)	Fe_2O_3	2.11
Ti (titanium)	TiO_2	0.45
P (phosphorus)	P_2O_5	0.08
Ca (calcium)	CaO	14.38
Mg (magnesium)	MgO	7.03
Na (sodium)	Na_2O	0.53
K (potassium)	K_2O	3.29
S (sulfur)	SO_3	0.65
Ba (barium)	BaO	0.00
Cl (chloride)	Cl	0.28
Mn (manganese)	MnO	0.10
Sr (strontium)	SrO	0.01
Unknowns	Due to the presence of carbonates	13.54
Total		100.01

EERC Energy & Environmental Research Center® Putting Research into Practice UND THE UNIVERSITY OF NORTH DAKOTA	**Applied Geology Laboratory**		ID: 116979
	Well Name: NDIC No. 8850	Middle Bakken 6	Rival Field
	API No.: 33-013-00867-00-02	Lithology: Silty dolostone	Depth: 7400.8'

XRD MINERAL PHASE DISTRIBUTION

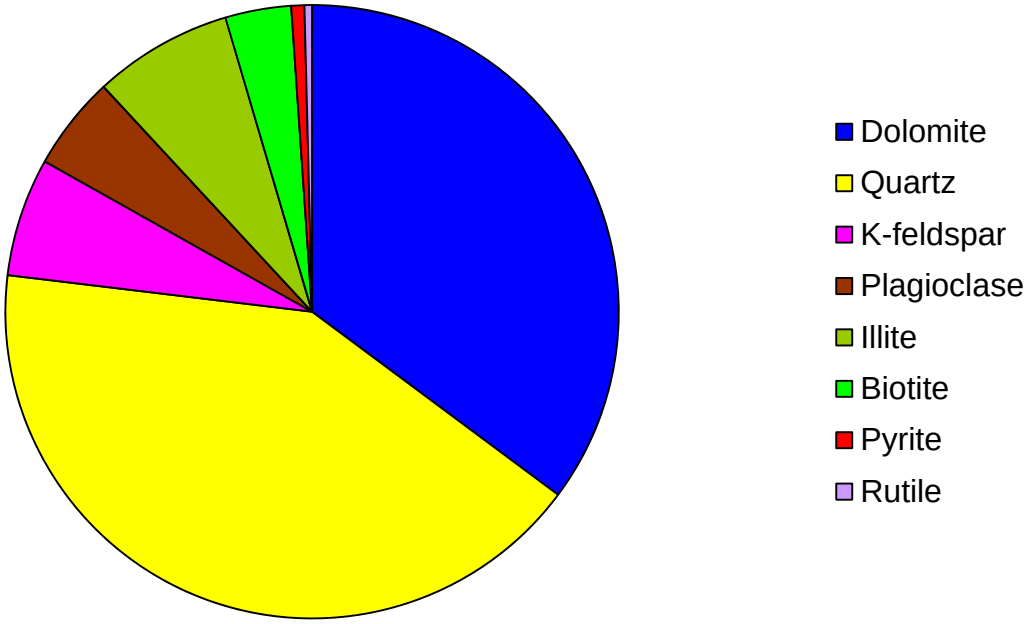

Mineral Phase	Formula	Weight %
Dolomite	$CaMg(CO_3)_2$	35.5
Quartz	SiO_2	42.1
K-feldspar	$KAlSi_3O_8$	6.3
Plagioclase	$Na_{0.5}Ca_{0.5}Al_{1.5}Si_{2.5}O_8$	5.0
Illite	$(K,H_3O)(Al,Mg,Fe)_2(Si,Al)_4O_{10}[(OH)_2,(H_2O)]$	7.4
Biotite	$K(Mg,Fe)_3[(OH)_2AlSi_3O_{10}]$	3.5
Pyrite	FeS_2	0.7
Rutile	TiO_2	0.4

EERC Energy & Environmental Research Center® Putting Research into Practice UND THE UNIVERSITY OF NORTH DAKOTA	**Applied Geology Laboratory**		ID: 116979
	Well Name: NDIC No. 8850	Middle Bakken 6	Rival Field
	API No.: 33-013-00867-00-02	Lithology: Silty dolostone	Depth: 7400.8'

SEM

Observed Minerals

Mineral Phase	Mineral Phase
Quartz	Zircon
Calcite	Apatite
Illite	Rutile
K-feldspar	Albite
Dolomite	Biotite
Pyrite	

High-Magnification BSE Image Annotated with Examples of Mineral Phases Identified

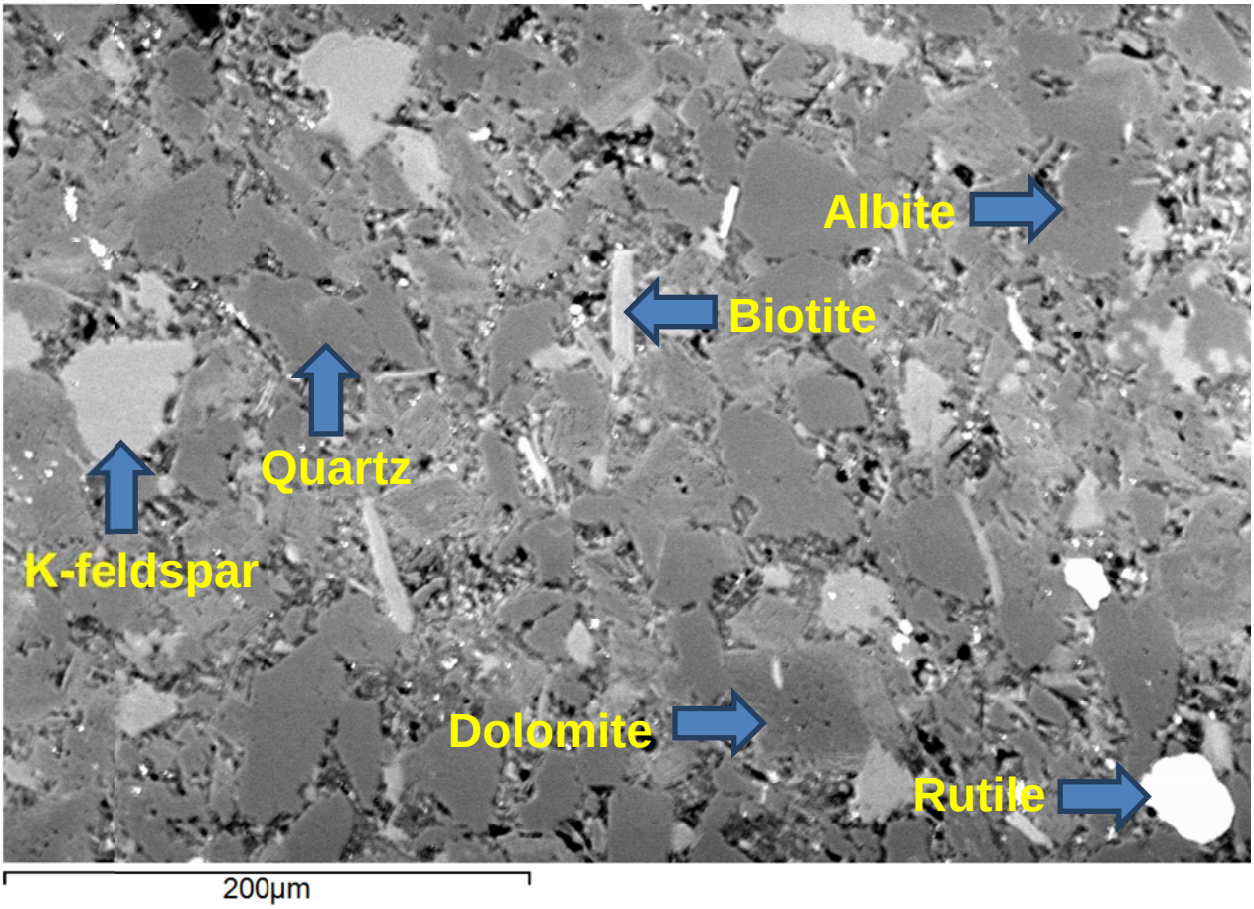

Additional High-Magnification BSE Images

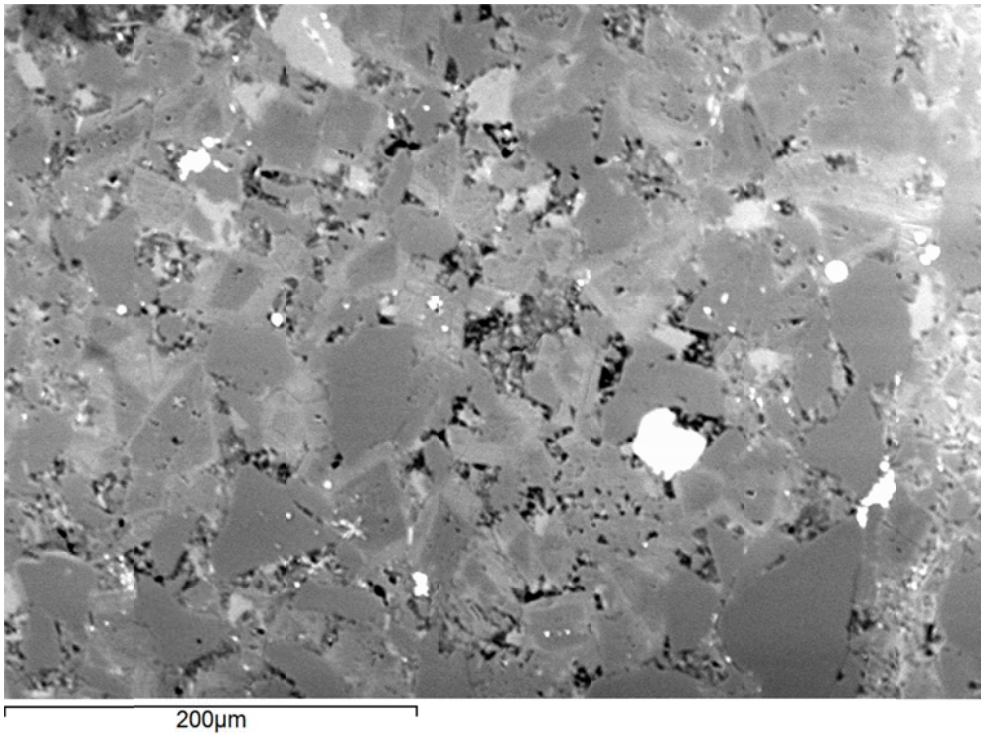

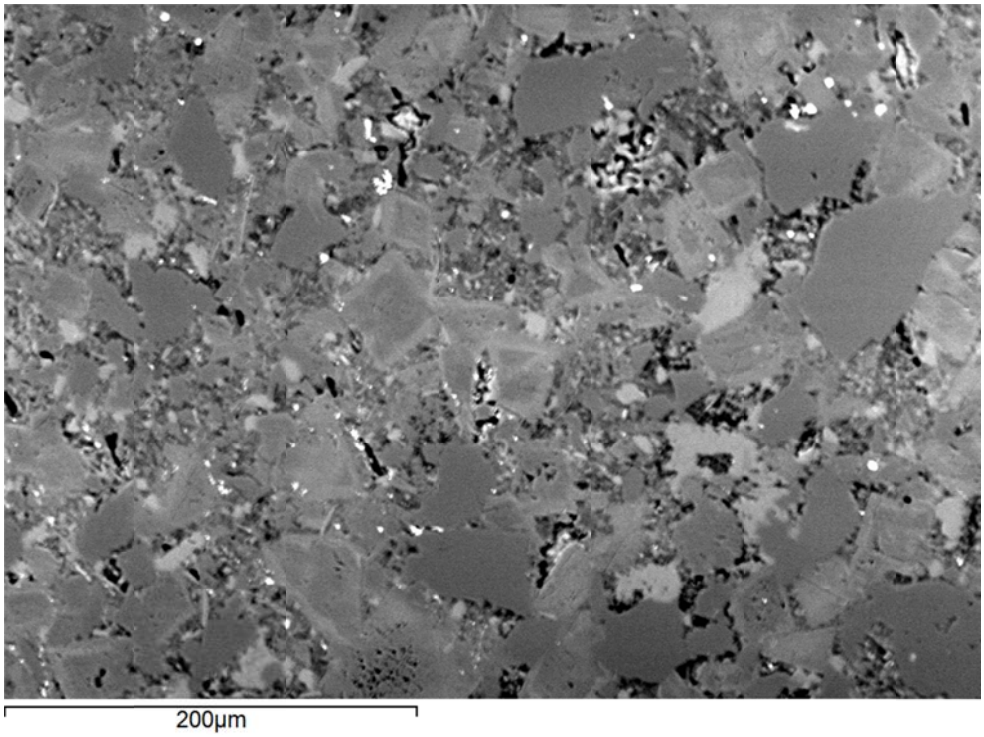

	Applied Geology Laboratory		ID: 116979
EERC Energy & Environmental Research Center® Putting Research into Practice UND THE UNIVERSITY OF NORTH DAKOTA	Well Name: NDIC No. 8850	Middle Bakken 6	Rival Field
	API No.: 33-013-00867-00-02	Lithology: Silty dolostone	Depth: 7400.8'

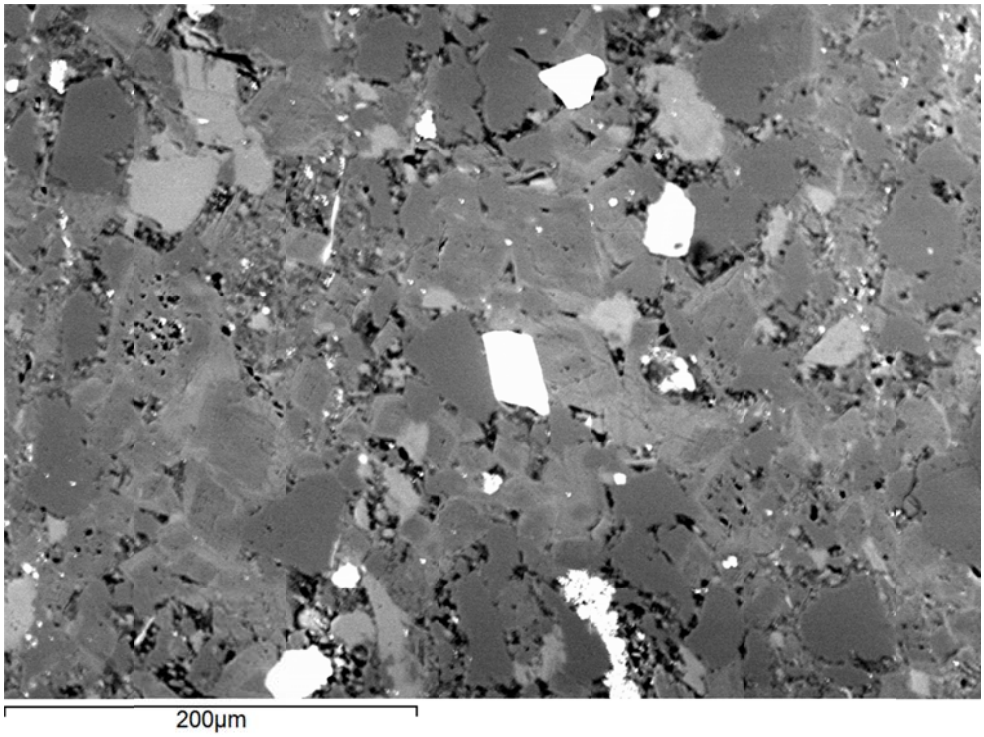

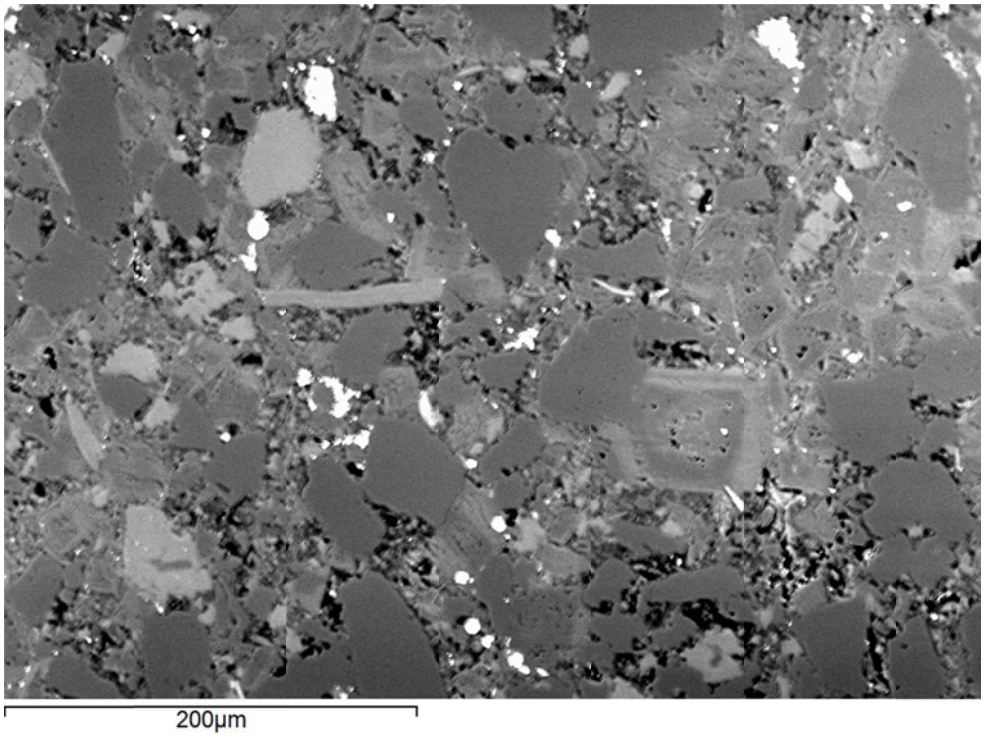

EERC Energy & Environmental Research Center® Putting Research into Practice UND THE UNIVERSITY OF NORTH DAKOTA	**Applied Geology Laboratory**		ID: 116979
	Well Name: NDIC No. 8850	Middle Bakken 6	Rival Field
	API No.: 33-013-00867-00-02	Lithology: Silty dolostone	Depth: 7400.8'

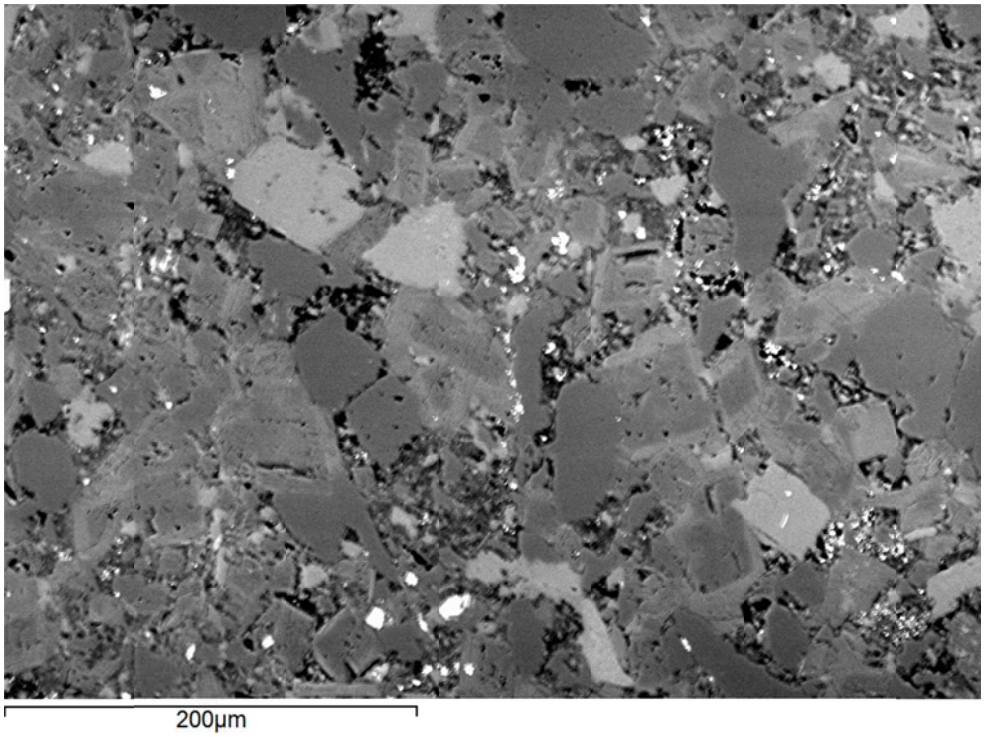

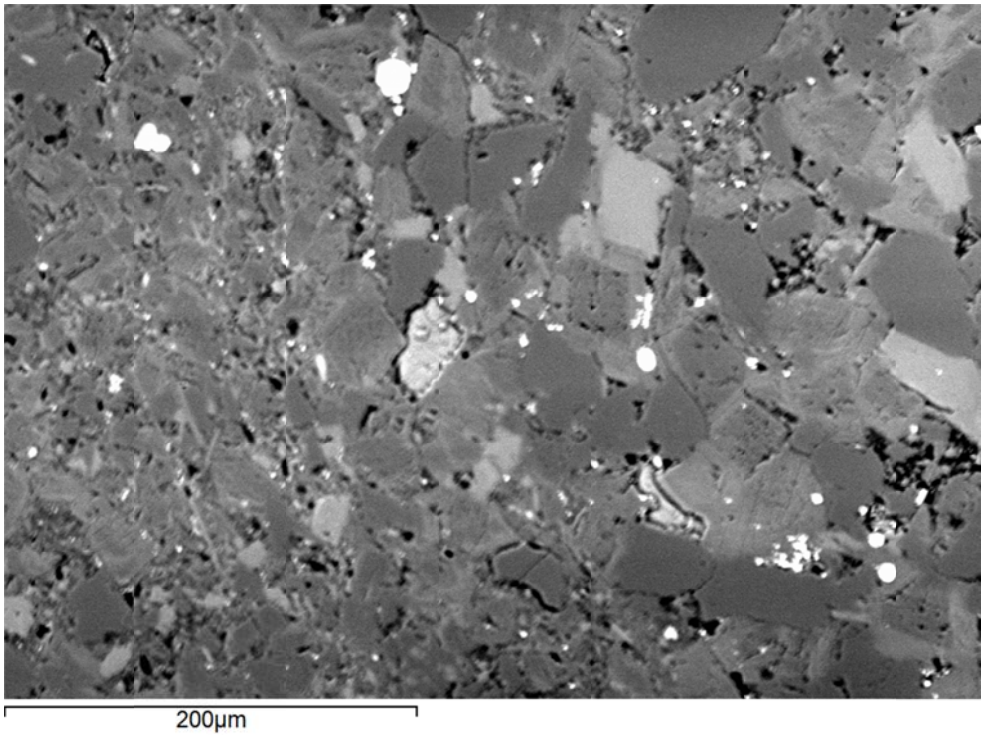

EERC Energy & Environmental Research Center® Putting Research into Practice UND THE UNIVERSITY OF NORTH DAKOTA	**Applied Geology Laboratory**		ID: 116979
	Well Name: NDIC No. 8850	Middle Bakken 6	Rival Field
	API No.: 33-013-00867-00-02	Lithology: Silty dolostone	Depth: 7400.8'

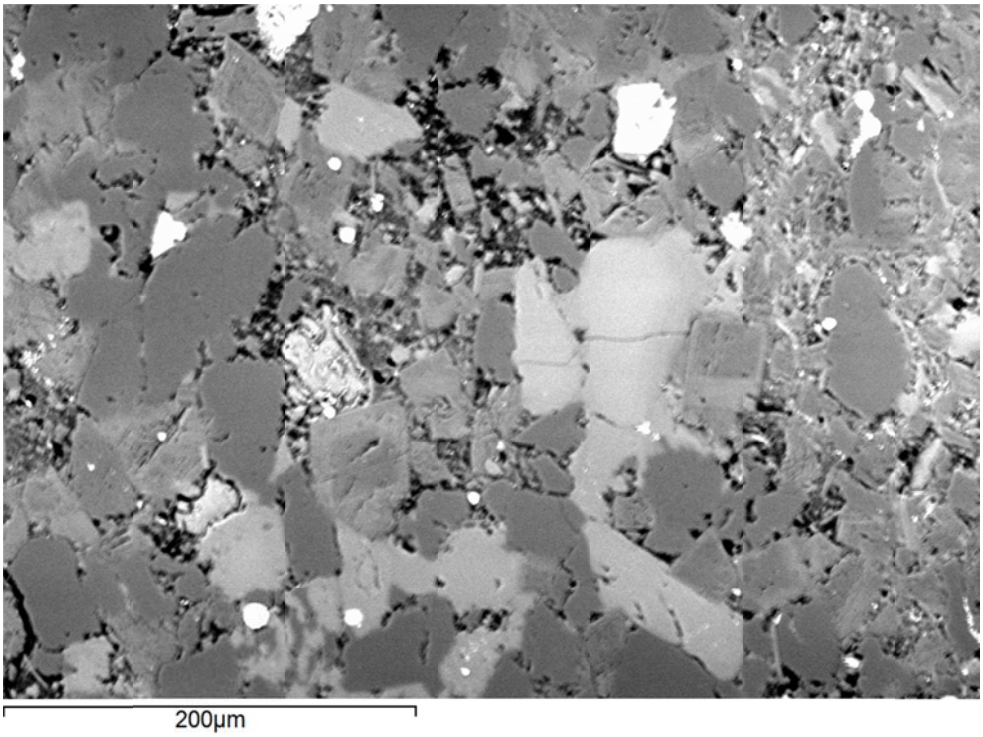

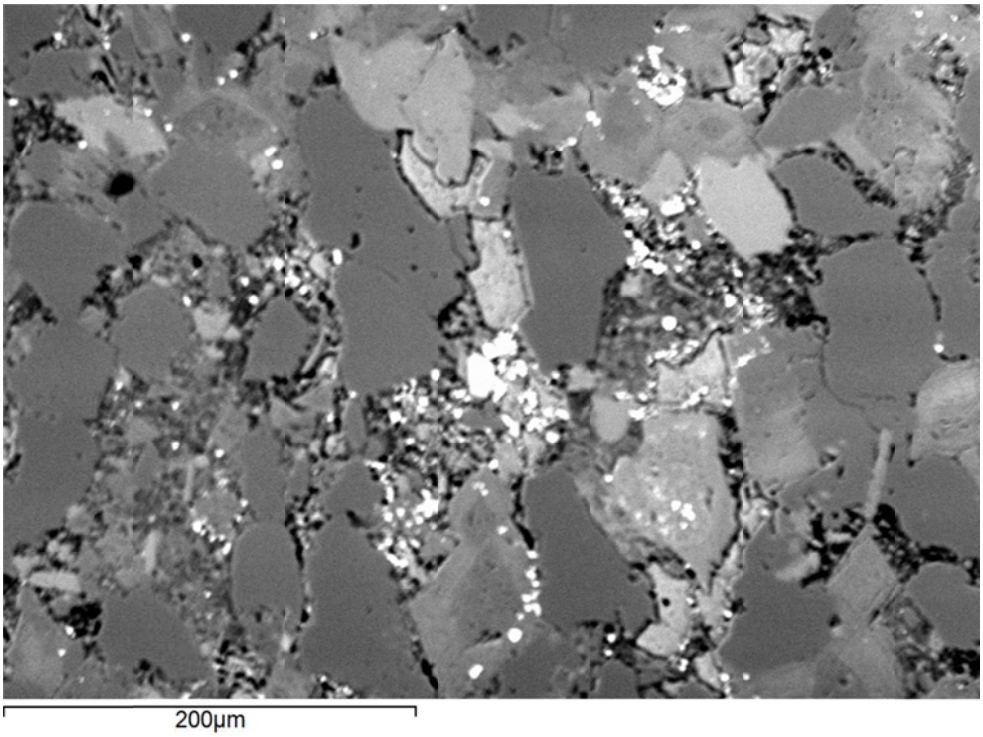

EERC Energy & Environmental Research Center® Putting Research into Practice UND THE UNIVERSITY OF NORTH DAKOTA	**Applied Geology Laboratory**		ID: 116979
	Well Name: NDIC No. 8850	Middle Bakken 6	Rival Field
	API No.: 33-013-00867-00-02	Lithology: Silty dolostone	Depth: 7400.8'

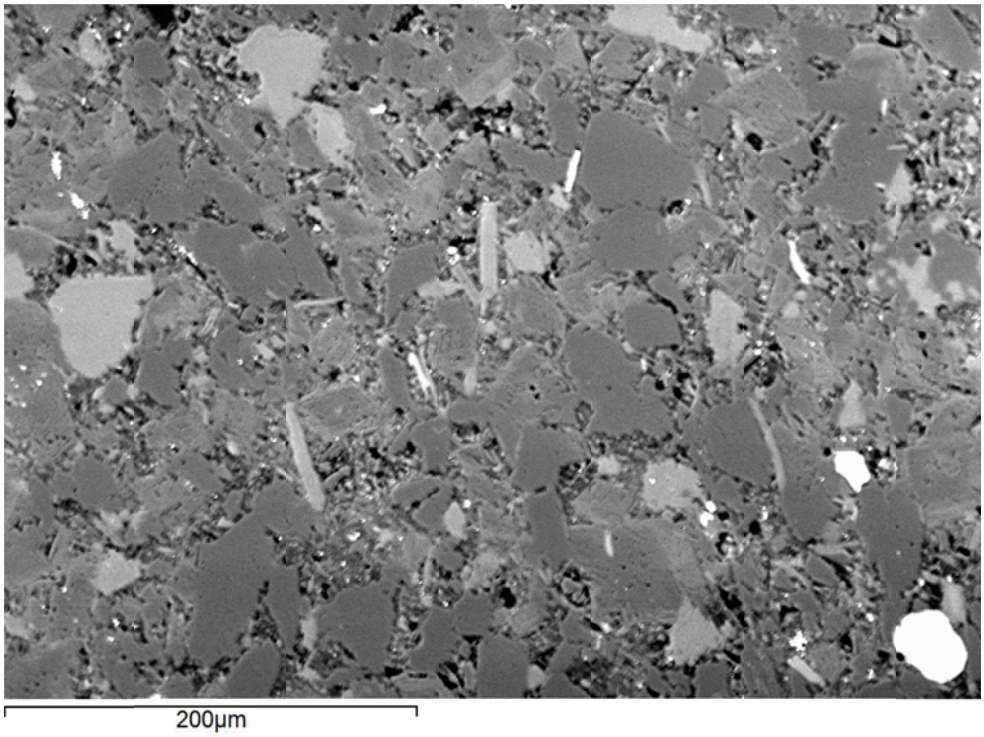

EERC Energy & Environmental Research Center® Putting Research into Practice UND THE UNIVERSITY OF NORTH DAKOTA	**Applied Geology Laboratory**		ID: 116979
	Well Name: NDIC No. 8850	Middle Bakken 6	Rival Field
	API No.: 33-013-00867-00-02	Lithology: Silty dolostone	Depth: 7400.8'

SEM Mineral Map Image Overlaid on BSE Image with Mineral Phase 2D Area Percentages

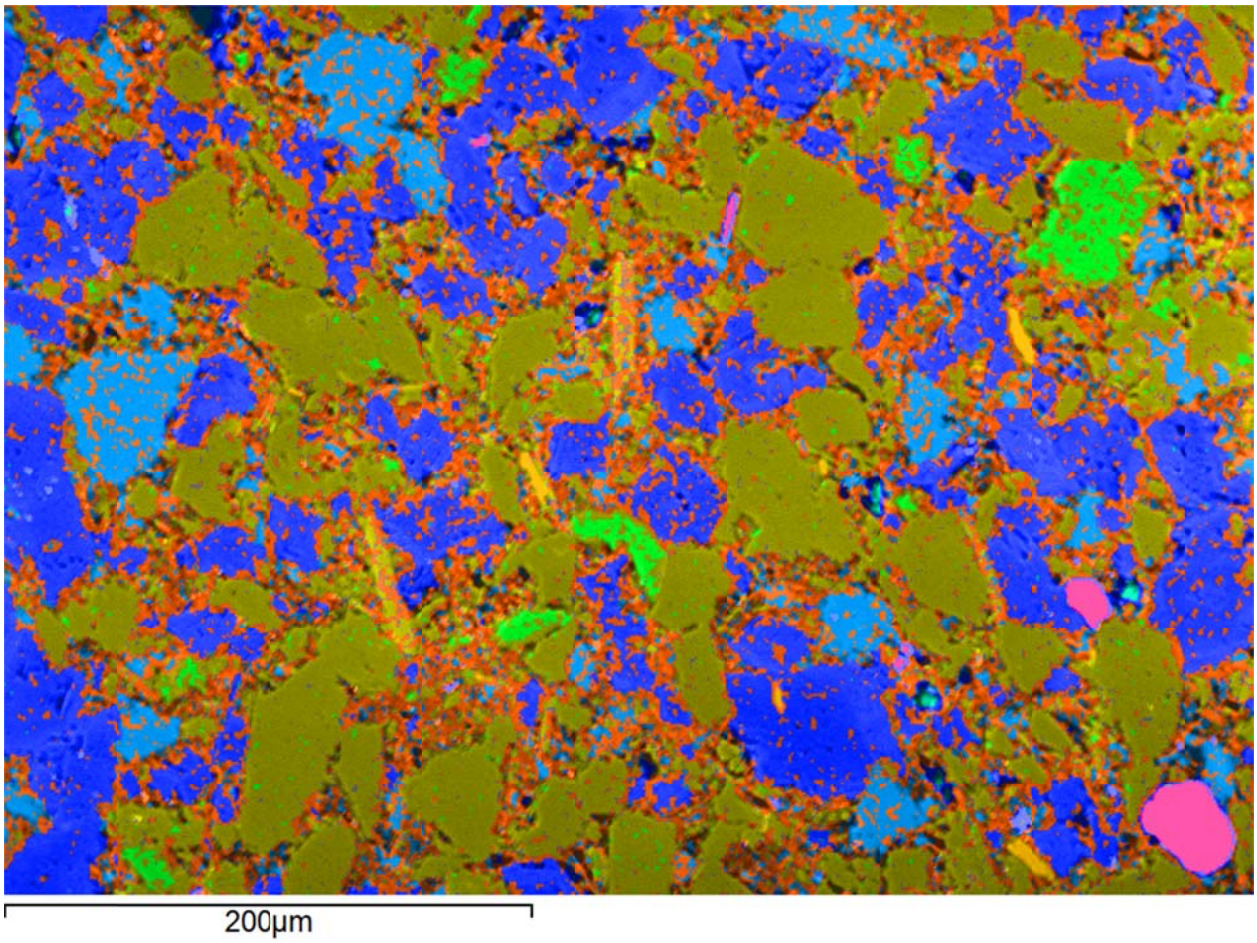

This page intentionally left blank.

EERC Energy & Environmental Research Center® Putting Research into Practice UND THE UNIVERSITY OF NORTH DAKOTA	**Applied Geology Laboratory**		ID: 116980
	Well Name: NDIC No. 8850	Middle Bakken 5	Rival Field
	API No.: 33-013-00867-00-01	Lithology: Dolomitic siltstone	Depth: 7407.3'

SAMPLE PHOTOGRAPH

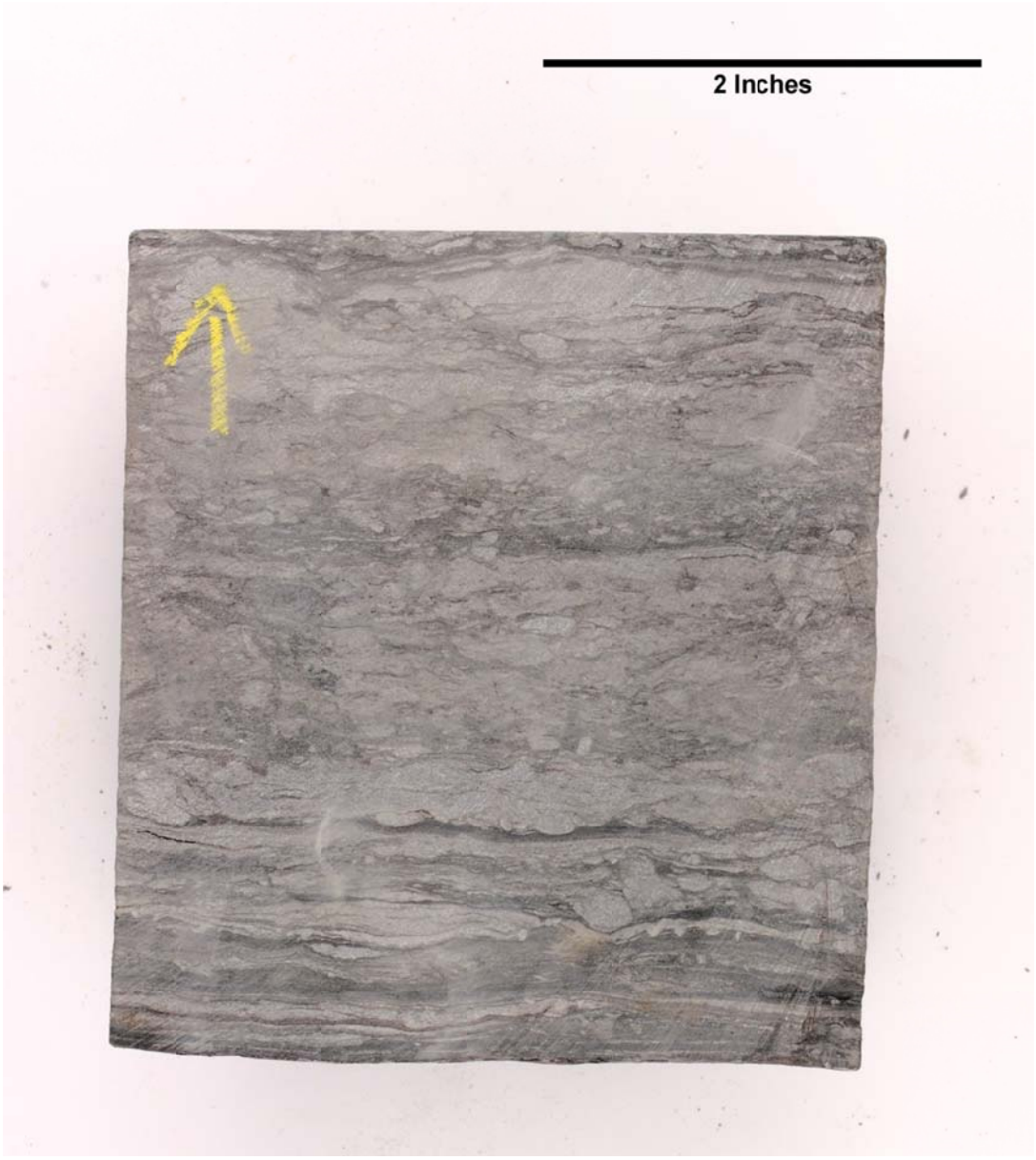

PHYSICAL PROPERTIES

Porosity and Grain Density by Core Laboratories

Pycnometer Effective Porosity, vol%	Grain Density, g/cm^3
6.84	2.706

EERC Energy & Environmental Research Center® Putting Research into Practice UND THE UNIVERSITY OF NORTH DAKOTA	**Applied Geology Laboratory**		ID: 116980
	Well Name: NDIC No. 8850	Middle Bakken 5	Rival Field
	API No.: 33-013-00867-00-01	Lithology: Dolomitic siltstone	Depth: 7407.3'

PHOTOMICROGRAPHS

Transmission

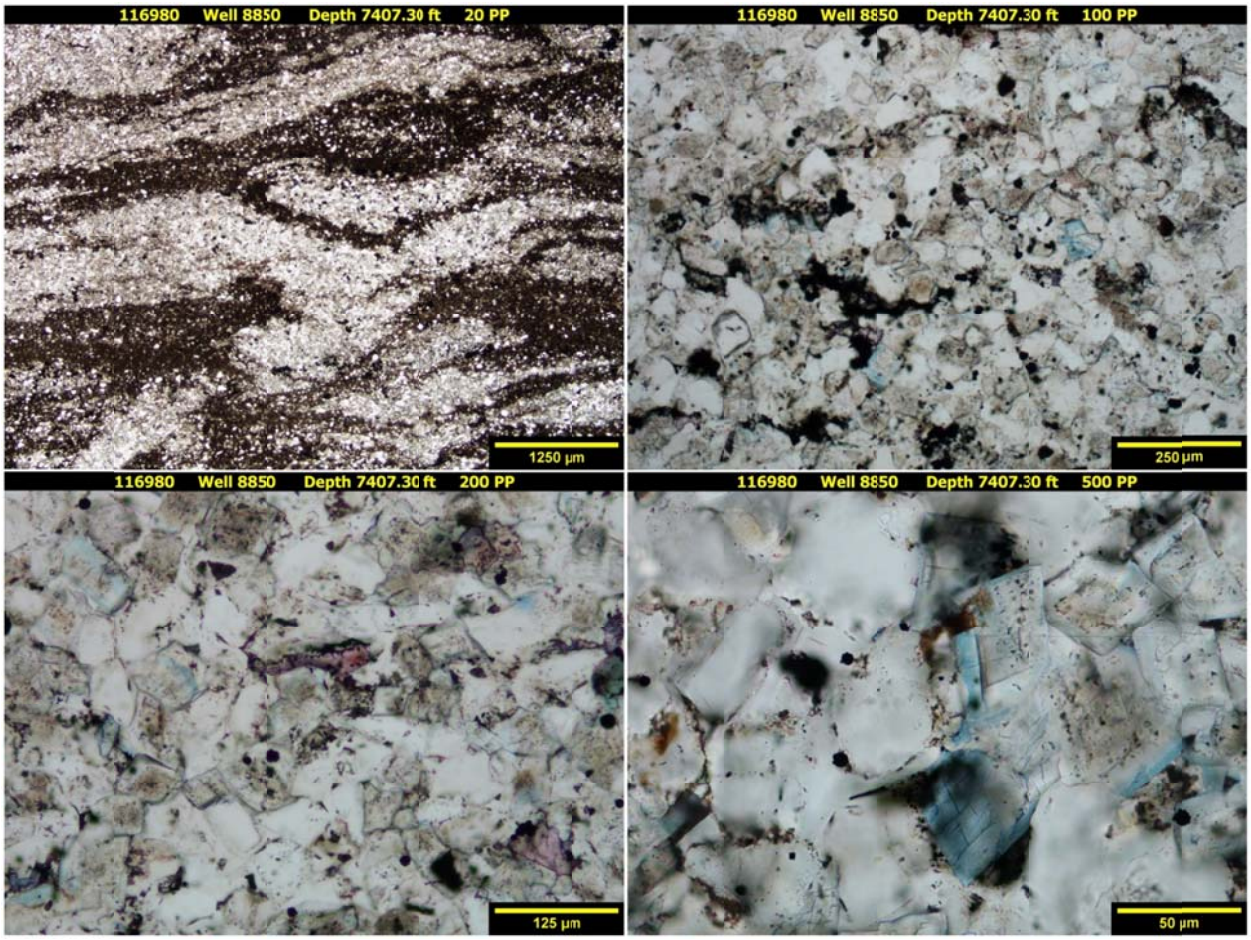

The sample from a depth of 7407.30 ft shows a dolomitic siltstone. A high degree of bioturbation is present. Very fine grained, subangular to subrounded, monocrystalline quartz grains having moderately high overgrowths at a few localities where quartz grains are concentrated. Trace amounts of muscovite and feldspars are disseminated throughout. Extensive anhederal to euhedral dolomitization has occurred throughout the sample. Very fine to fine-grained crystalline, partially ferroan dolomite is noted. Very rare calcareous grains remain. Disseminated pore-filling and replacement pyrite grains are observed throughout, concentrating in some areas. An abundant mineralogical component is clay, found throughout the sample creating a variety of burrowing features. Randomly-oriented filled and unfilled fractures are detected. Open fractures, predominately horizontal, observed are likely the result of the sample process. A combination of clays, carbonates, pyrite, and organics cement the remaining fractures. Organics are observed as tiny globs typically associated with pyrite. A trace amount of inter-particle porosity is observed using standard petrographic techniques.

	Applied Geology Laboratory		ID: 116980
EERC Energy & Environmental Research Center® Putting Research into Practice UND THE UNIVERSITY OF NORTH DAKOTA	Well Name: NDIC No. 8850	Middle Bakken 5	Rival Field
	API No.: 33-013-00867-00-01	Lithology: Dolomitic siltstone	Depth: 7407.3'

Reflection

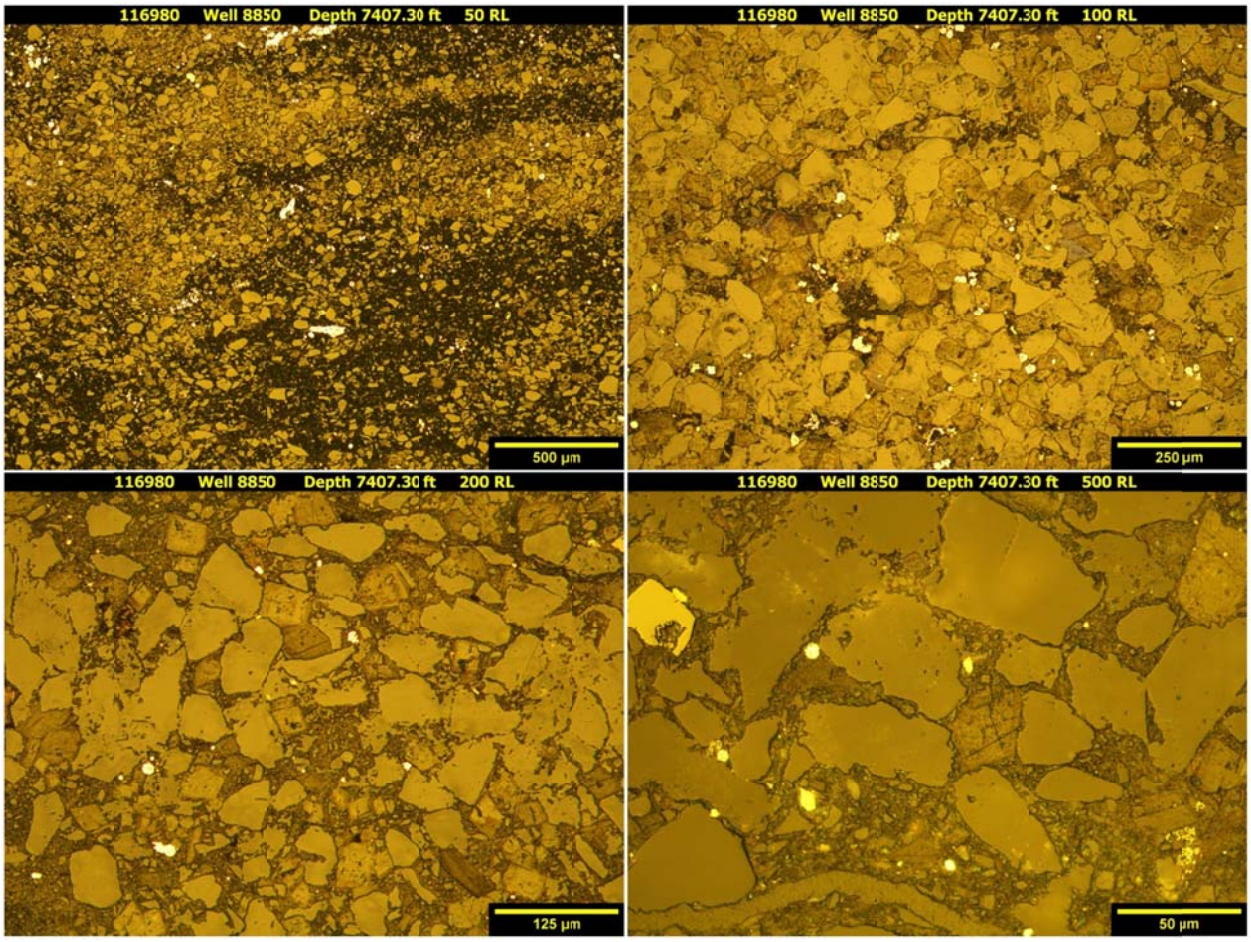

The sample from a depth of 7407.30 ft displays both euhedral and frambodial pyrite disseminated growth. This diagenetic mineral acts as a pore filler and a grain replacer. Euhedral grains are very fine grained and individual frambodial grains are observed at a fraction of that size. Framboidal pyrite predominately is shown as individual spheres; rarely is there an assemblage of spheres to create a larger, more mature grouping. Nearly complete pyritization of precursor grains and organics have occurred at some localities. Organics observed are typically associated with both euhedral and framboidal pyrite.

EERC Energy & Environmental Research Center® Putting Research into Practice UND THE UNIVERSITY OF NORTH DAKOTA	**Applied Geology Laboratory**		ID: 116980
	Well Name: NDIC No. 8850	Middle Bakken 5	Rival Field
	API No.: 33-013-00867-00-01	Lithology: Dolomitic siltstone	Depth: 7407.3'

Transmission and Fluorescence Whole-Slide Images

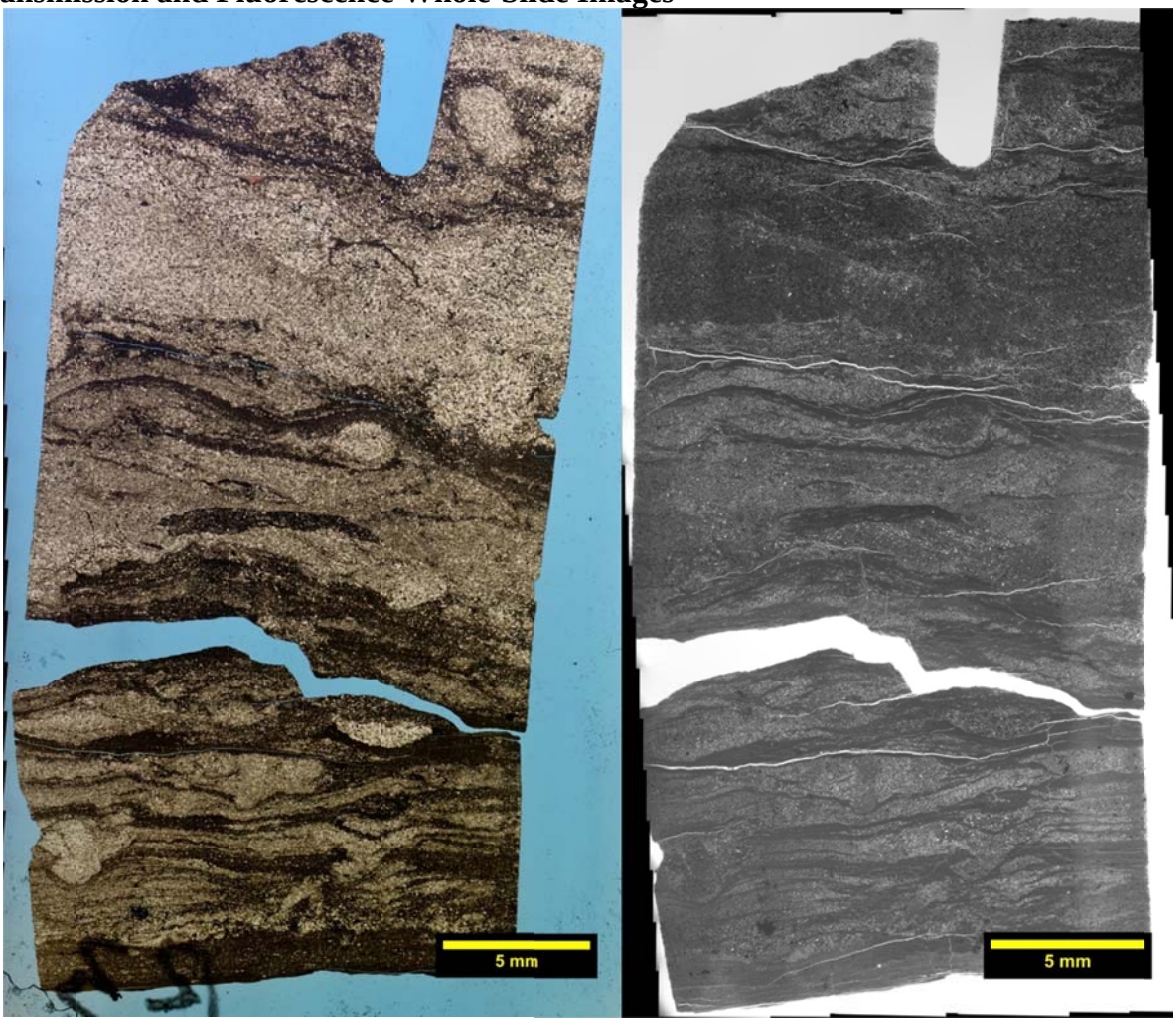

The image collected at a depth of 7407.30 ft shows a predominantly bioturbated sample. Effective porosity is reported at 6.84 vol%. Inter-particle-based micro-porosity exists throughout the sample, typically concentrating within larger grained quartz and dolomite-rich zones. Lesser amounts of porosity are noted within areas of smaller grains and clay concentrations. Extensive interlocking anhedral to euhedral dolomitization and dispersed pyritization has occurred. These diagenetic events and very fine grain sizes are limiting factors of pore size and distribution. No natural open fractures are likely observed. All observed fractures are likely the result of sampling process, but may give insight to how the rock would perform under stress.

EERC Energy & Environmental Research Center® Putting Research into Practice UND THE UNIVERSITY OF NORTH DAKOTA	**Applied Geology Laboratory**		ID: 116980
	Well Name: NDIC No. 8850	Middle Bakken 5	Rival Field
	API No.: 33-013-00867-00-01	Lithology: Dolomitic siltstone	Depth: 7407.3'

XRF BULK CHEMICAL COMPOSITION

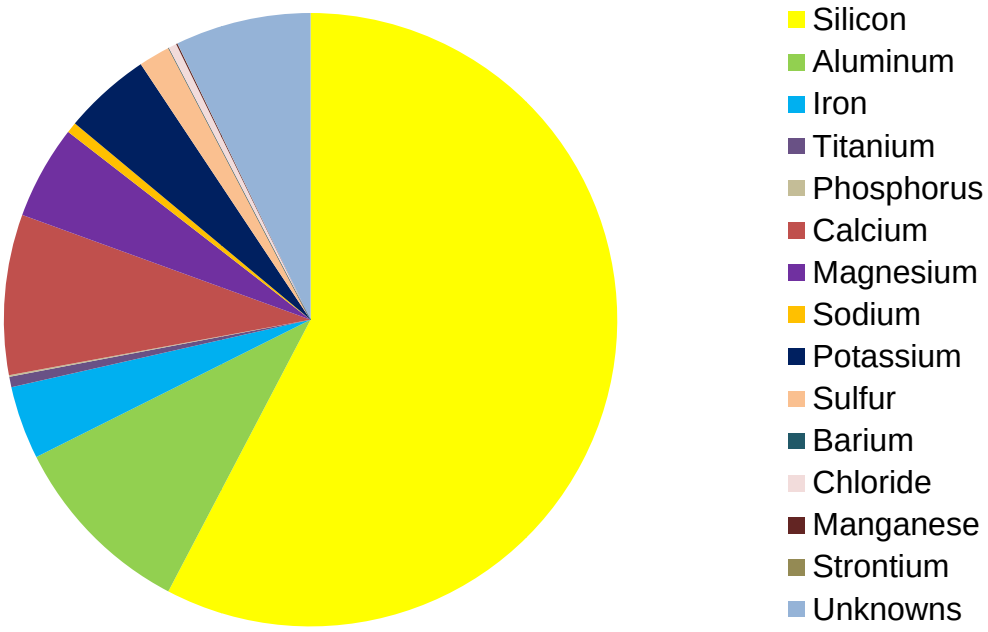

Element	Reporting Convention (Oxide)	Weight %
Si (silicon)	SiO_2	57.68
Al (aluminum)	Al_2O_3	9.95
Fe (iron)	Fe_2O_3	3.85
Ti (titanium)	TiO_2	0.55
P (phosphorus)	P_2O_5	0.09
Ca (calcium)	CaO	8.45
Mg (magnesium)	MgO	4.94
Na (sodium)	Na_2O	0.56
K (potassium)	K_2O	4.62
S (sulfur)	SO_3	1.67
Ba (barium)	BaO	0.00
Cl (chloride)	Cl	0.44
Mn (manganese)	MnO	0.07
Sr (strontium)	SrO	0.01
Unknowns	Due to the presence of carbonates	7.14
Total		100.02

EERC Energy & Environmental Research Center® Putting Research into Practice UND THE UNIVERSITY OF NORTH DAKOTA	**Applied Geology Laboratory**		ID: 116980
	Well Name: NDIC No. 8850	Middle Bakken 5	Rival Field
	API No.: 33-013-00867-00-01	Lithology: Dolomitic siltstone	Depth: 7407.3'

XRD MINERAL PHASE DISTRIBUTION

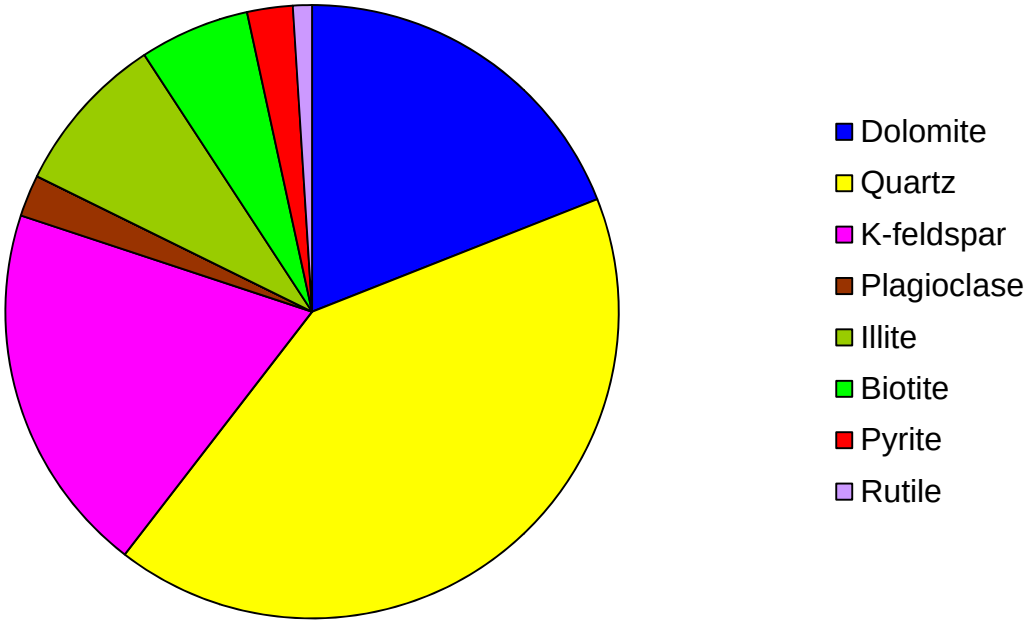

Mineral Phase	Formula	Weight %
Dolomite	$CaMg(CO_3)_2$	19.0
Quartz	SiO_2	41.4
K-feldspar	$KAlSi_3O_8$	19.6
Plagioclase	$Na_{0.5}Ca_{0.5}Al_{1.5}Si_{2.5}O_8$	2.2
Illite	$(K,H_3O)(Al,Mg,Fe)_2(Si,Al)_4O_{10}[(OH)_2,(H_2O)]$	8.5
Biotite	$K(Mg,Fe)_3[(OH)_2AlSi_3O_{10}]$	5.8
Pyrite	FeS_2	2.4
Rutile	TiO_2	1.0

EERC Energy & Environmental Research Center® Putting Research into Practice UND THE UNIVERSITY OF NORTH DAKOTA	**Applied Geology Laboratory**		ID: 116980
	Well Name: NDIC No. 8850	Middle Bakken 5	Rival Field
	API No.: 33-013-00867-00-01	Lithology: Dolomitic siltstone	Depth: 7407.3'

SEM

Observed Minerals

Mineral Phase	Mineral Phase
Calcite	Apatite
Quartz	Pyrite
Zircon	Albite
Rutile	Dolomite
K-feldspar	

High-Magnification BSE Image Annotated with Examples of Mineral Phases Identified

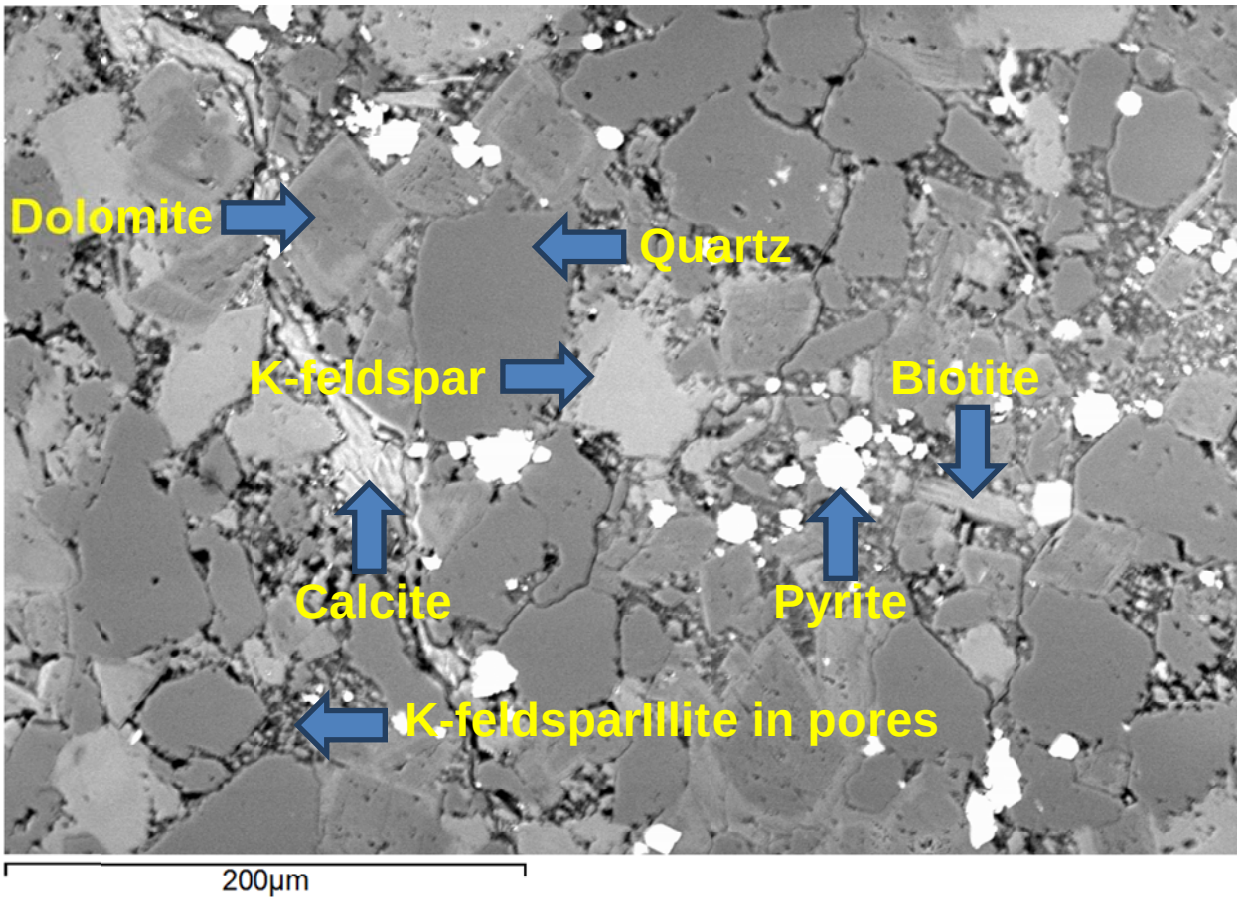

Additional High-Magnification BSE Images

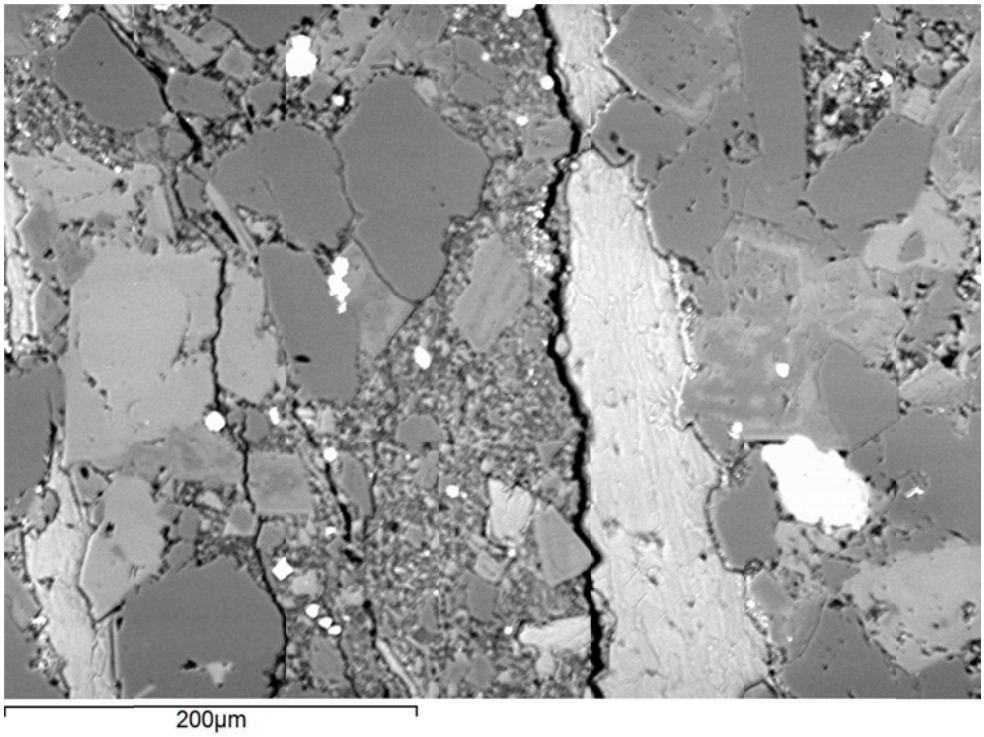

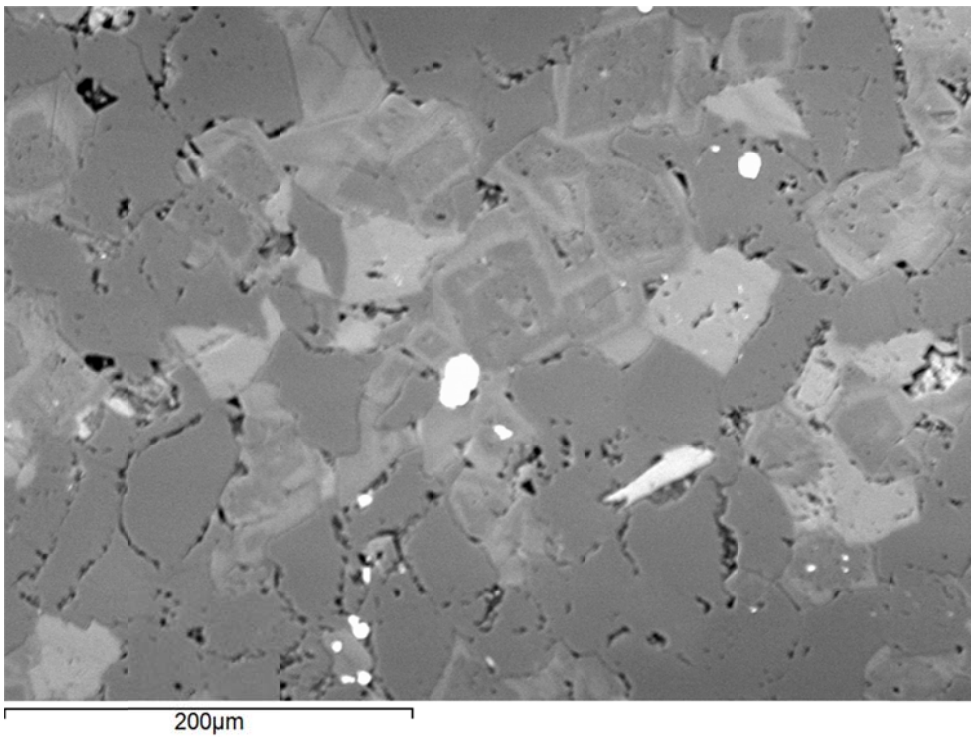

	Applied Geology Laboratory		ID: 116980
EERC Energy & Environmental Research Center® Putting Research into Practice UND THE UNIVERSITY OF NORTH DAKOTA	Well Name: NDIC No. 8850	Middle Bakken 5	Rival Field
	API No.: 33-013-00867-00-01	Lithology: Dolomitic siltstone	Depth: 7407.3'

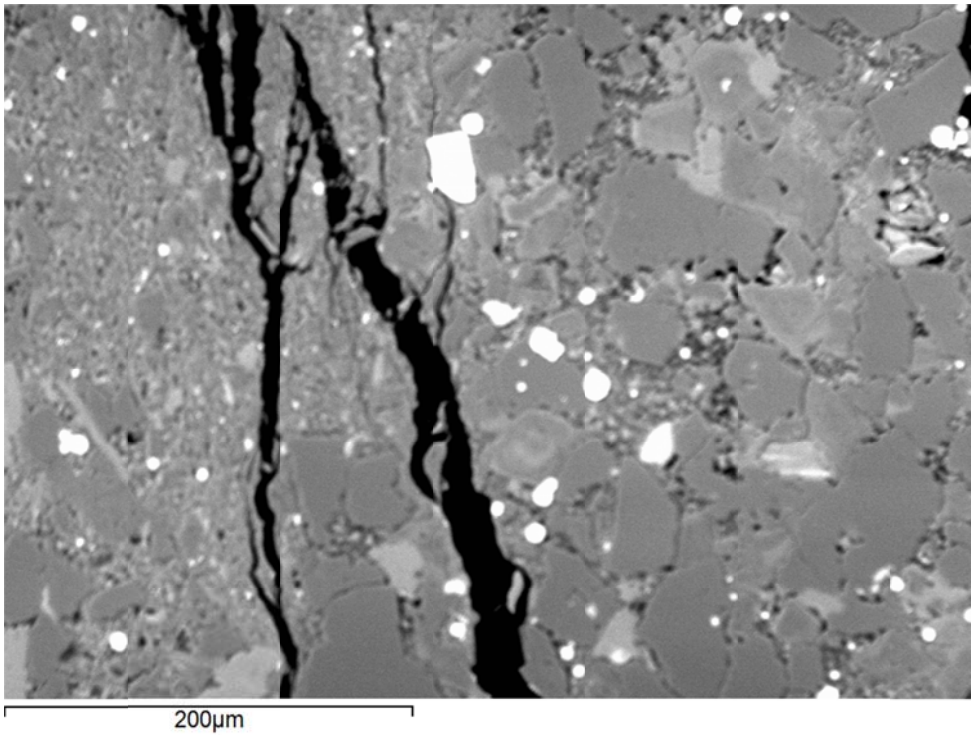

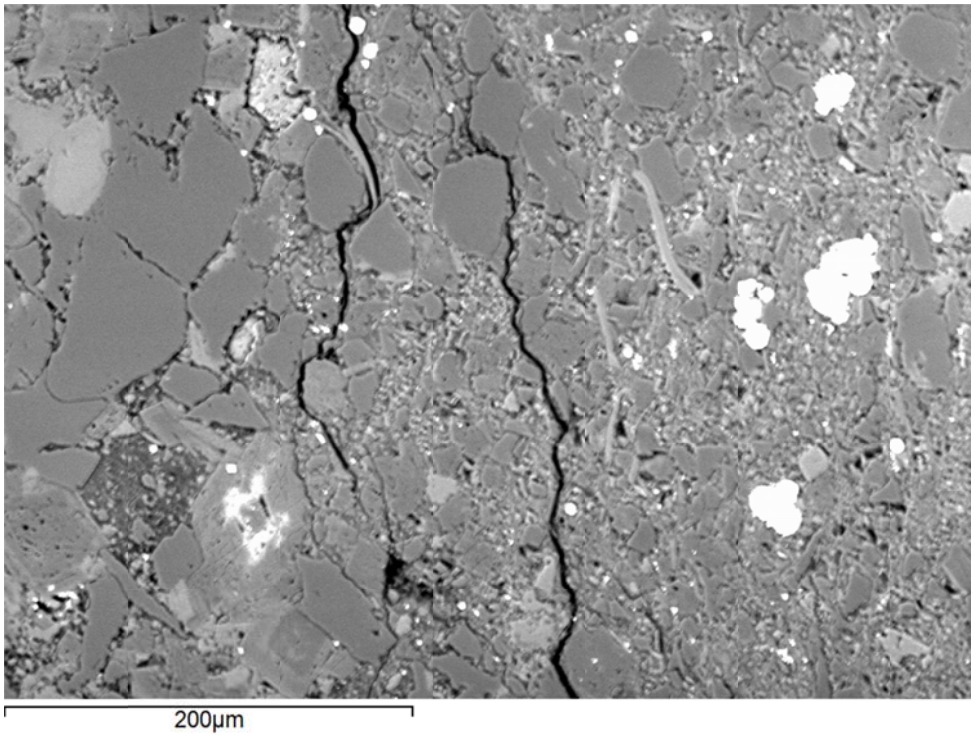

	Applied Geology Laboratory		ID: 116980
EERC Energy & Environmental Research Center® Putting Research into Practice UND THE UNIVERSITY OF NORTH DAKOTA	Well Name: NDIC No. 8850	Middle Bakken 5	Rival Field
	API No.: 33-013-00867-00-01	Lithology: Dolomitic siltstone	Depth: 7407.3'

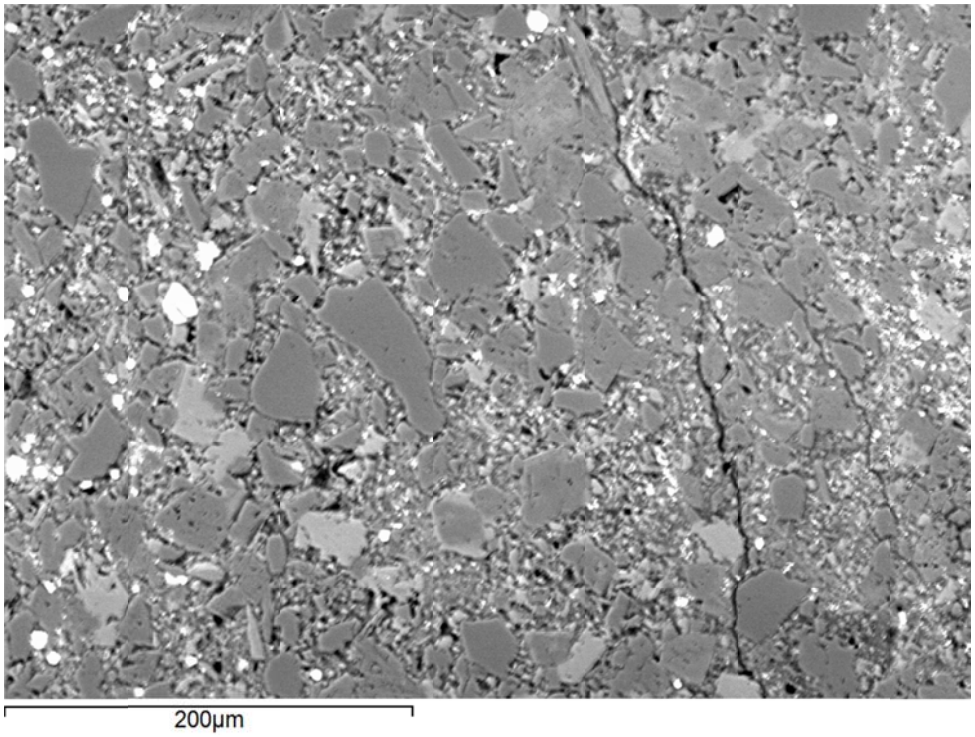

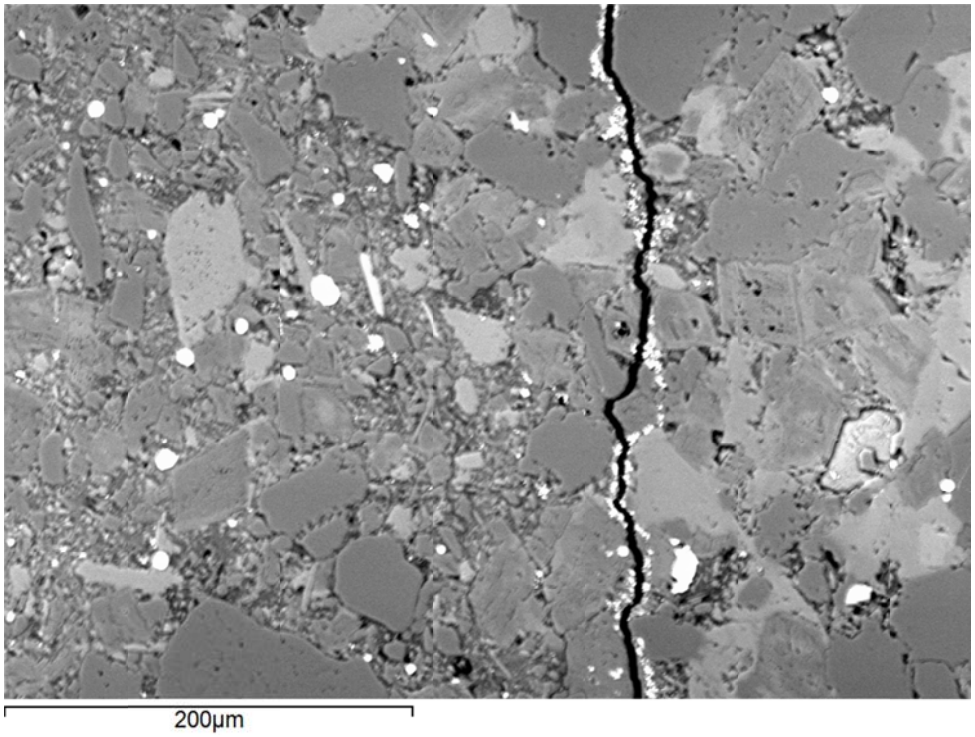

	Applied Geology Laboratory		ID: 116980
EERC Energy & Environmental Research Center® Putting Research into Practice UND THE UNIVERSITY OF NORTH DAKOTA	Well Name: NDIC No. 8850	Middle Bakken 5	Rival Field
	API No.: 33-013-00867-00-01	Lithology: Dolomitic siltstone	Depth: 7407.3'

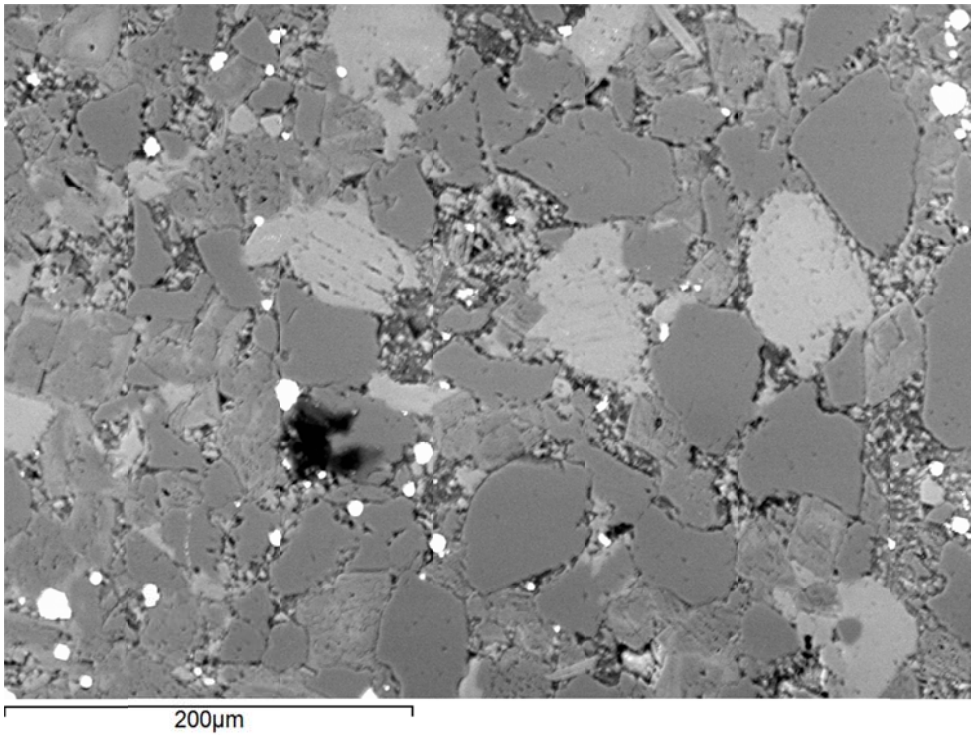

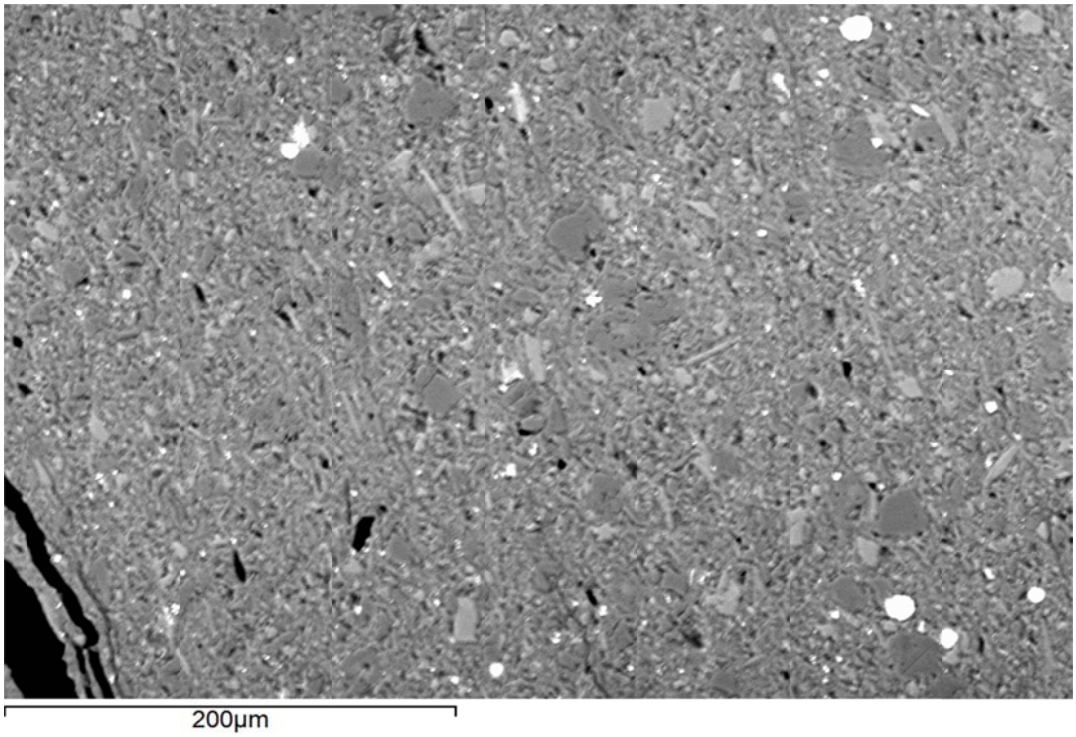

This page intentionally left blank.

EERC Energy & Environmental Research Center® Putting Research into Practice UND THE UNIVERSITY OF NORTH DAKOTA	**Applied Geology Laboratory**		ID: 116981
	Well Name: NDIC No. 8850	Middle Bakken 4	Rival Field
	API No.: 33-013-00867-00-00	Lithology: Dolomitic, argillaceous siltstone	Depth: 7410.0'

SAMPLE PHOTOGRAPHY

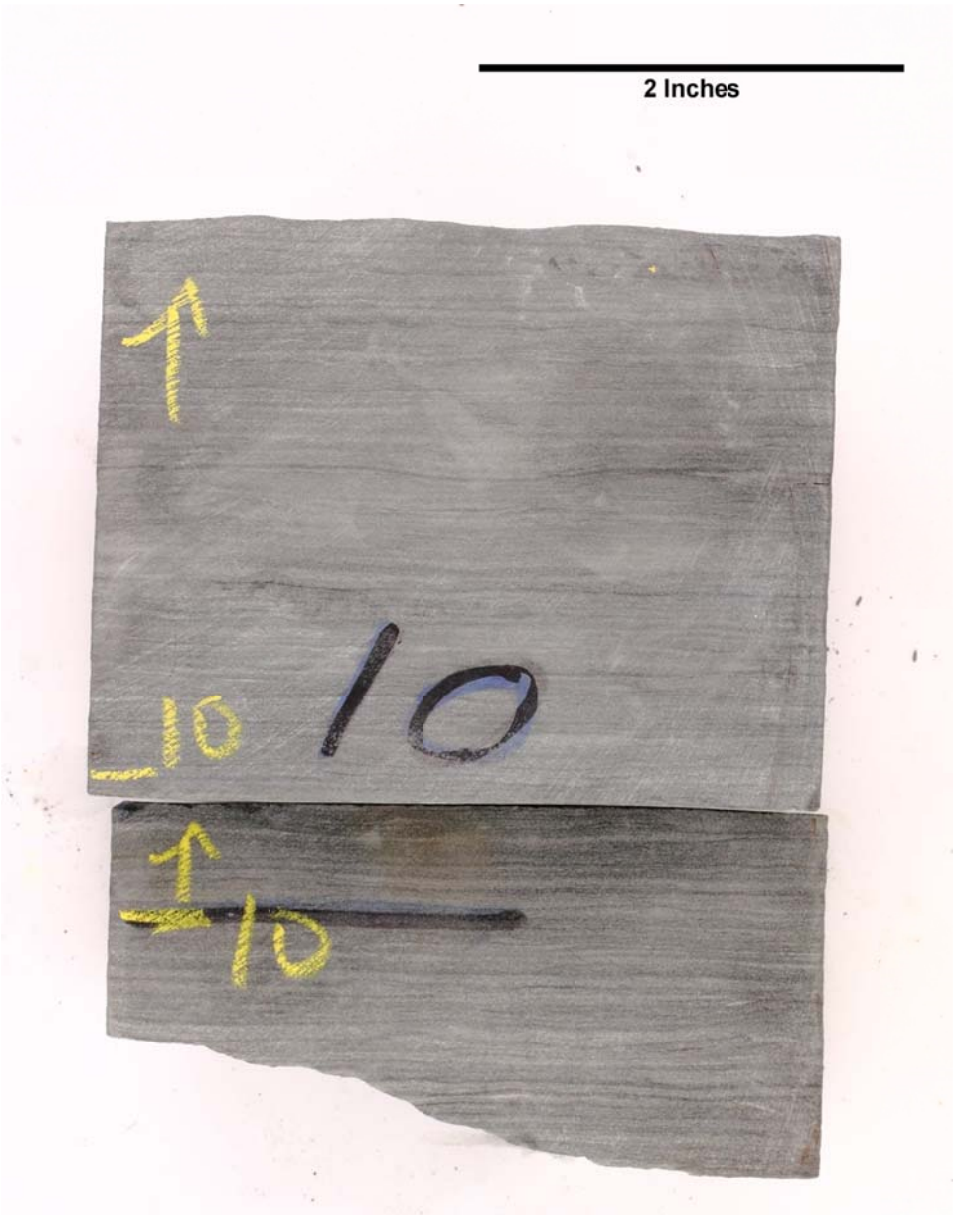

PHYSICAL PROPERTIES

Porosity and Grain Density by Core Laboratories

Pycnometer Effective Porosity, vol%	Grain Density, g/cm^3
3.67	2.741

	Applied Geology Laboratory		ID: 116981
	Well Name: NDIC No. 8850	Middle Bakken 4	Rival Field
	API No.: 33-013-00867-00-00	Lithology: Dolomitic, argillaceous siltstone	Depth: 7410.0'

PHOTOMICROGRAPHS

Transmission

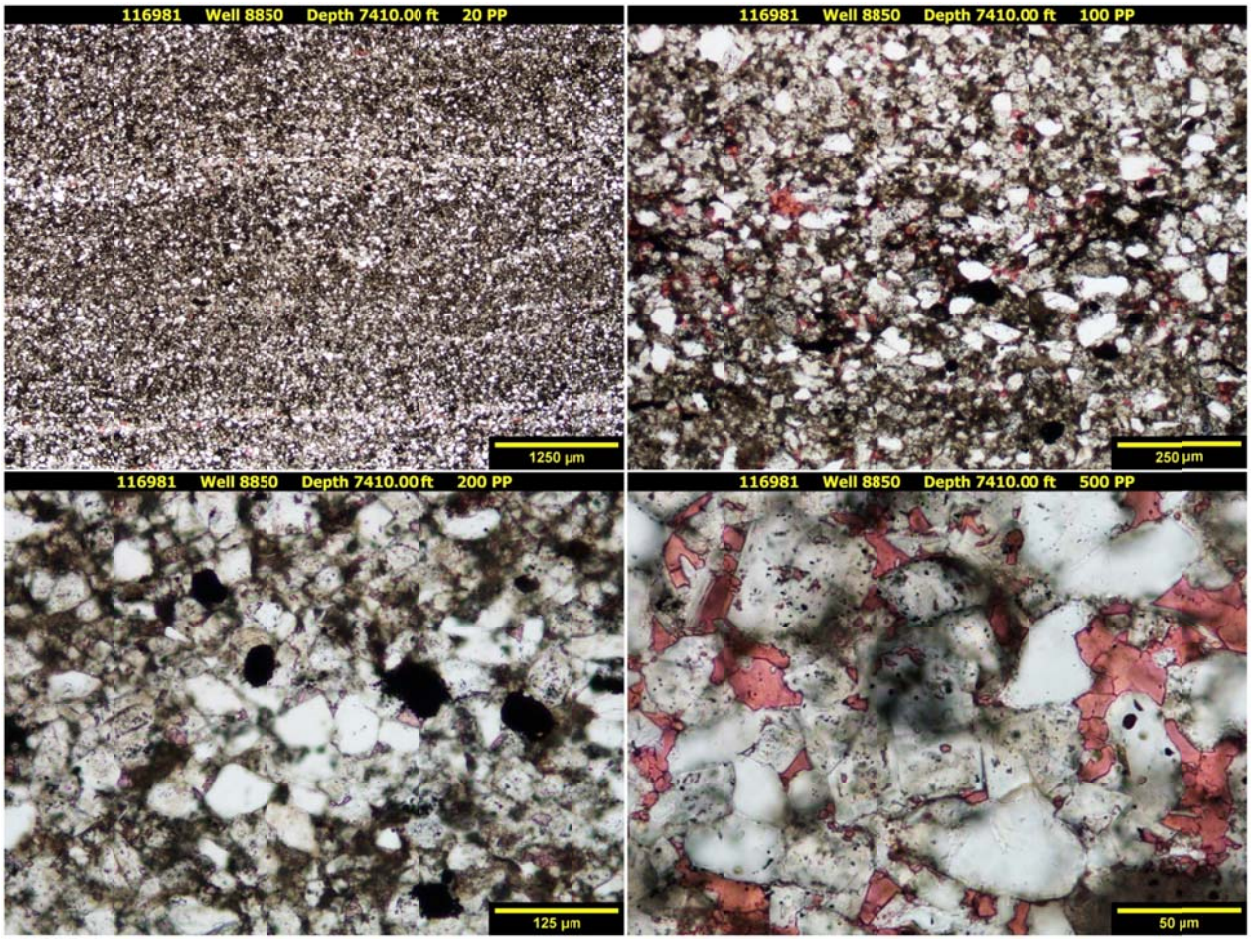

The sample from a depth of 7410.00 ft shows a dolomitic, argillaceous siltstone. A slight degree of bioturbation and well-defined horizontal-to-slightly wavy laminations are present. Very fine grained, angular to subrounded, monocrystalline quartz grains and trace amounts of muscovite and feldspars are disseminated throughout. Anhederal to euhedral dolomitization has occurred throughout the sample. Very rare calcareous non-skeletal grains and sparry cement remain. Disseminated pore-filling and replacement pyrite grains are observed. Matrical clay is common, found throughout at inconsistent quantities creating laminations. Organics are observed and typically associated with pyrite. No fractures or porosity are observed using standard petrographic techniques.

	Applied Geology Laboratory		ID: 116981
EERC Energy & Environmental Research Center® Putting Research into Practice UND THE UNIVERSITY OF NORTH DAKOTA	Well Name: NDIC No. 8850	Middle Bakken 4	Rival Field
	API No.: 33-013-00867-00-00	Lithology: Dolomitic, argillaceous siltstone	Depth: 7410.0'

Reflection

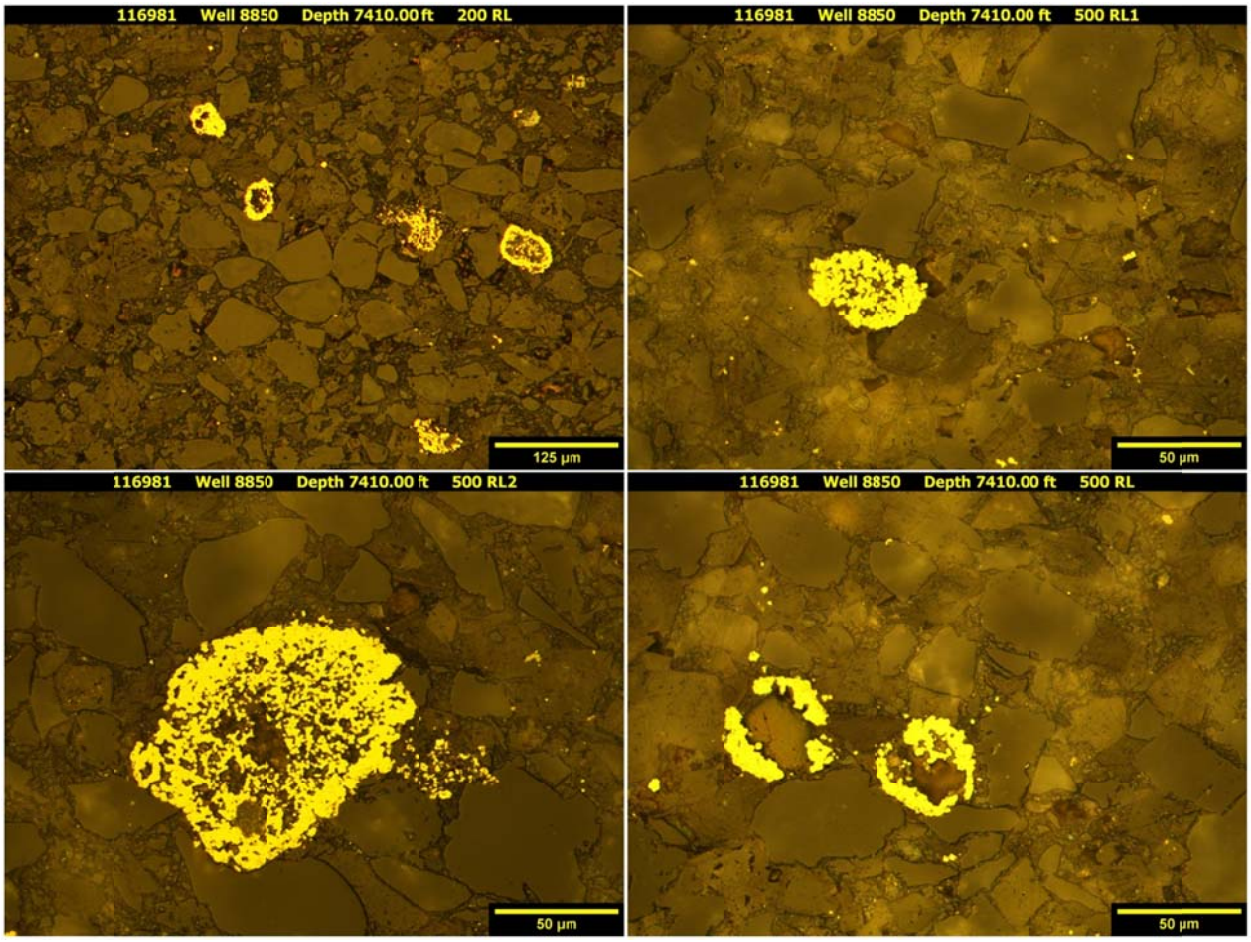

The sample from a depth of 7410.00 ft displays both euhedral and frambodial pyrite mineralization. This diagenetic mineral acts as a pore filler and a grain replacer. Framboidal pyrite predominately is shown as individual spheres; rarely is there an assemblage of spheres to create a larger, more mature grouping. Nearly complete pyritization of precursor grains and organics have occurred rarely. Organics observed are typically associated with both euhedral and framboidal pyrite.

EERC Energy & Environmental Research Center® Putting Research into Practice UND THE UNIVERSITY OF NORTH DAKOTA	**Applied Geology Laboratory**		ID: 116981
	Well Name: NDIC No. 8850	Middle Bakken 4	Rival Field
	API No.: 33-013-00867-00-00	Lithology: Dolomitic, argillaceous siltstone	Depth: 7410.0'

Transmission and Fluorescence Whole-Slide Images

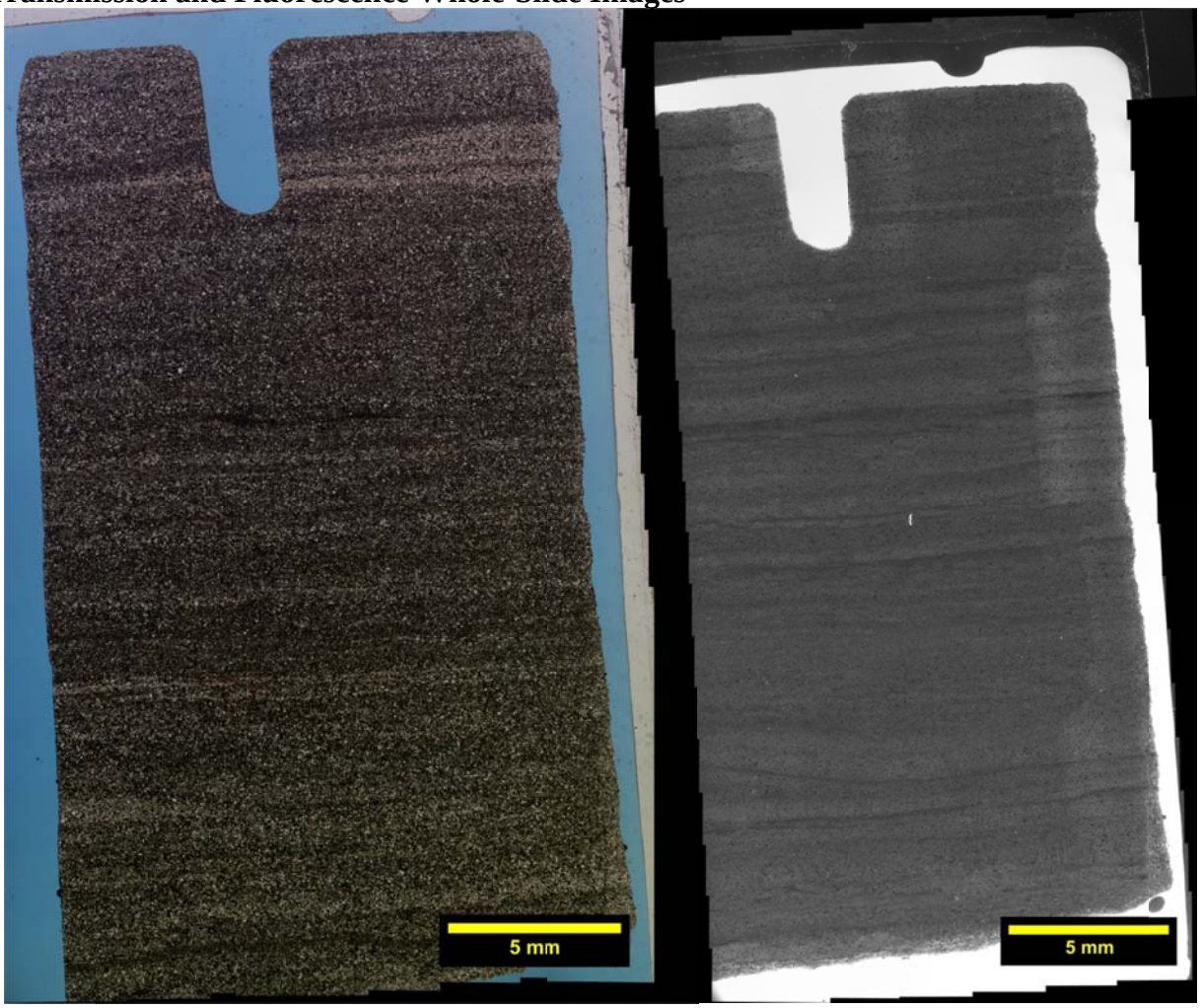

The image collected from a depth of 7410.00 ft shows a laminated sample. Effective porosity is reported at 3.67 vol%. Inter-particle-based porosity mainly exists within quartz and euhedral dolomite-rich laminations. Lesser amounts of porosity re noted within areas of small, mostly anhedral, dolomite grains and clay concentrations. Pore sizes appear to be very small (<30 µm). No natural or induced fractures are observed.

	Applied Geology Laboratory		ID: 116981
	Well Name: NDIC No. 8850	Middle Bakken 4	Rival Field
	API No.: 33-013-00867-00-00	Lithology: Dolomitic, argillaceous siltstone	Depth: 7410.0'

XRF BULK CHEMICAL COMPOSITION

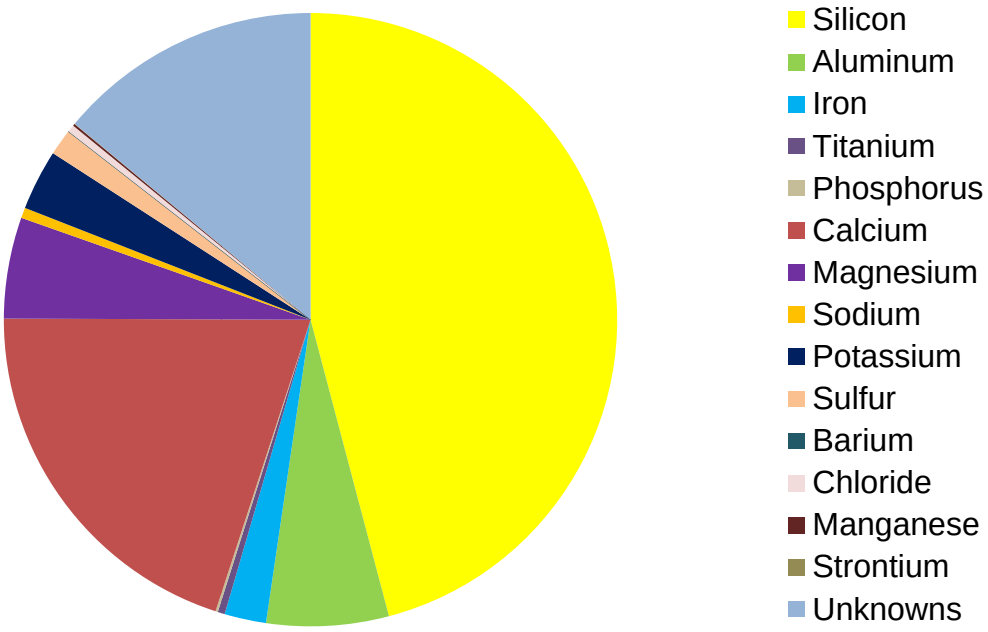

Element	Reporting Convention (Oxide)	Weight %
Si (silicon)	SiO_2	45.88
Al (aluminum)	Al_2O_3	6.44
Fe (iron)	Fe_2O_3	2.20
Ti (titanium)	TiO_2	0.37
P (phosphorus)	P_2O_5	0.12
Ca (calcium)	CaO	20.05
Mg (magnesium)	MgO	5.33
Na (sodium)	Na_2O	0.55
K (potassium)	K_2O	3.20
S (sulfur)	SO_3	1.38
Ba (barium)	BaO	0.00
Cl (chloride)	Cl	0.39
Mn (manganese)	MnO	0.11
Sr (strontium)	SrO	0.02
Unknowns	Due to the presence of carbonates	13.96
Total		100.00

EERC	Applied Geology Laboratory		ID: 116981
	Well Name: NDIC No. 8850	Middle Bakken 4	Rival Field
	API No.: 33-013-00867-00-00	Lithology: Dolomitic, argillaceous siltstone	Depth: 7410.0'

XRD MINERAL PHASE DISTRIBUTION

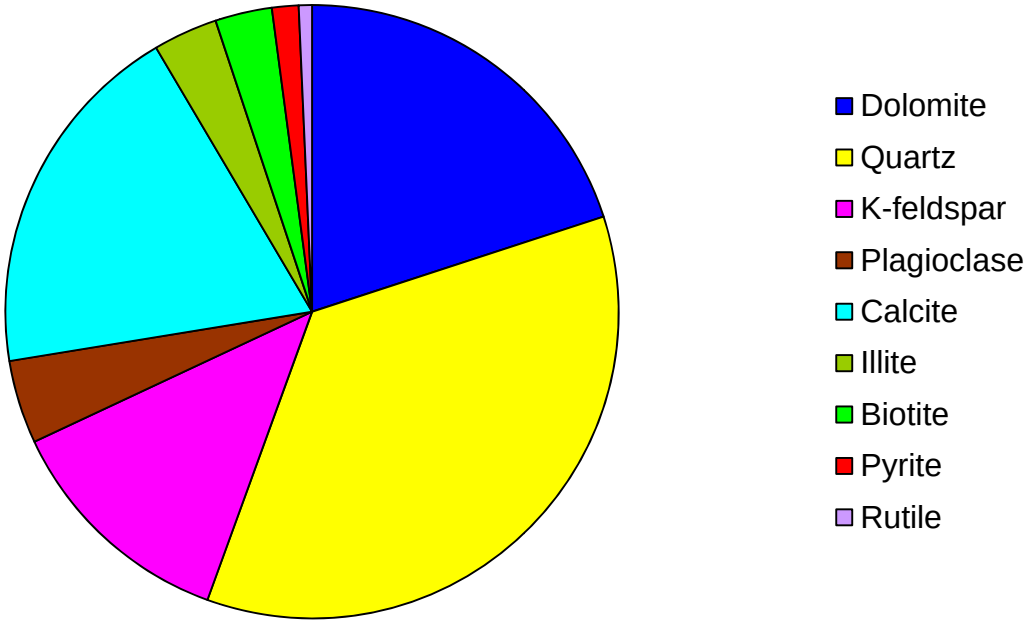

Mineral Phase	Formula	Weight %
Dolomite	$CaMg(CO_3)_2$	20.0
Quartz	SiO_2	35.6
K-feldspar	$KAlSi_3O_8$	12.5
Plagioclase	$Na_{0.5}Ca_{0.5}Al_{1.5}Si_{2.5}O_8$	4.4
Calcite	$CaCO_3$	19.1
Illite	$(K,H_3O)(Al,Mg,Fe)_2(Si,Al)_4O_{10}[(OH)_2,(H_2O)]$	3.4
Biotite	$K(Mg,Fe)_3[(OH)_2AlSi_3O_{10}]$	3.0
Pyrite	FeS_2	1.4
Rutile	TiO_2	0.7

EERC Energy & Environmental Research Center® Putting Research into Practice UND THE UNIVERSITY OF NORTH DAKOTA	**Applied Geology Laboratory**		ID: 116981
	Well Name: NDIC No. 8850	Middle Bakken 4	Rival Field
	API No.: 33-013-00867-00-00	Lithology: Dolomitic, argillaceous siltstone	Depth: 7410.0'

SEM

Observed Minerals

Mineral Phase	Mineral Phase
Calcite	Apatite
Dolomite	Rutile
Quartz	Zircon
Pyrite	Biotite
Illite	Albite
K-feldspar	

High-Magnification BSE Image Annotated with Examples of Mineral Phases Identified

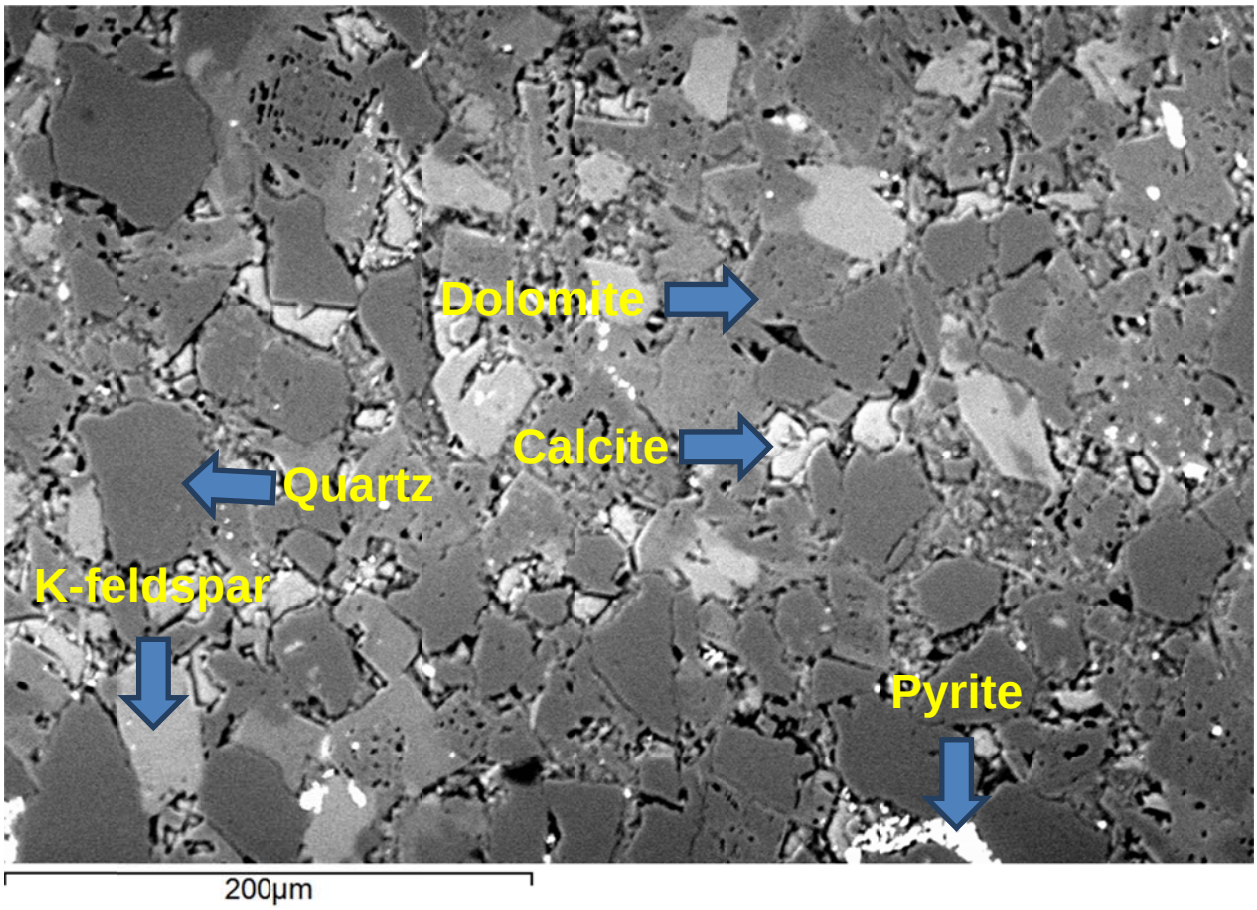

Additional High-Magnification BSE Images

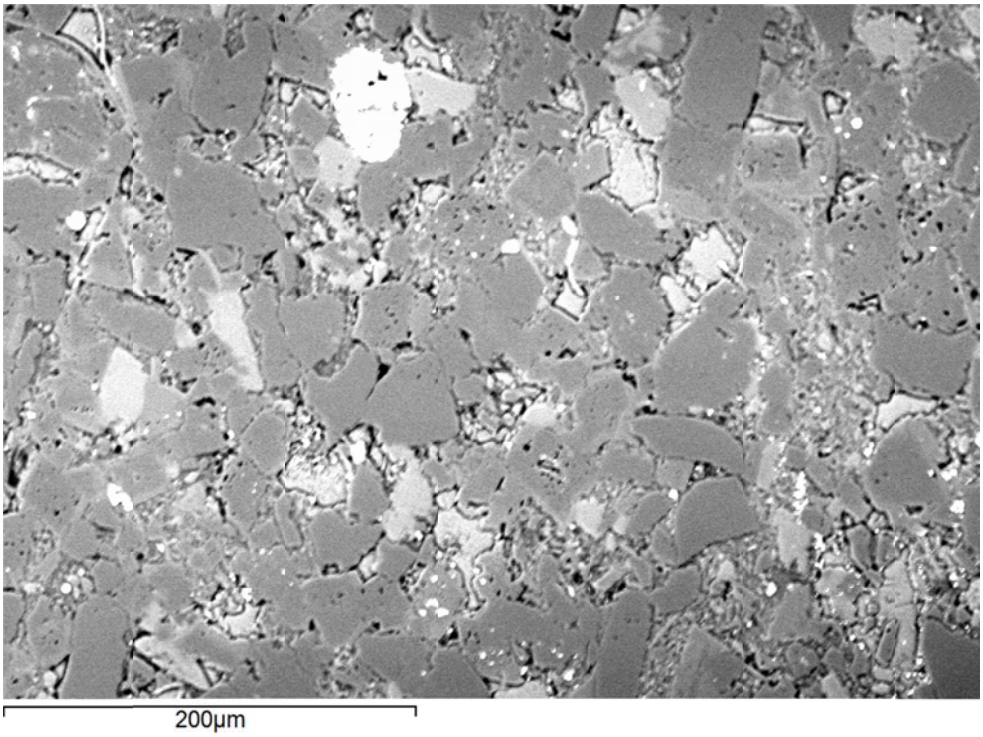

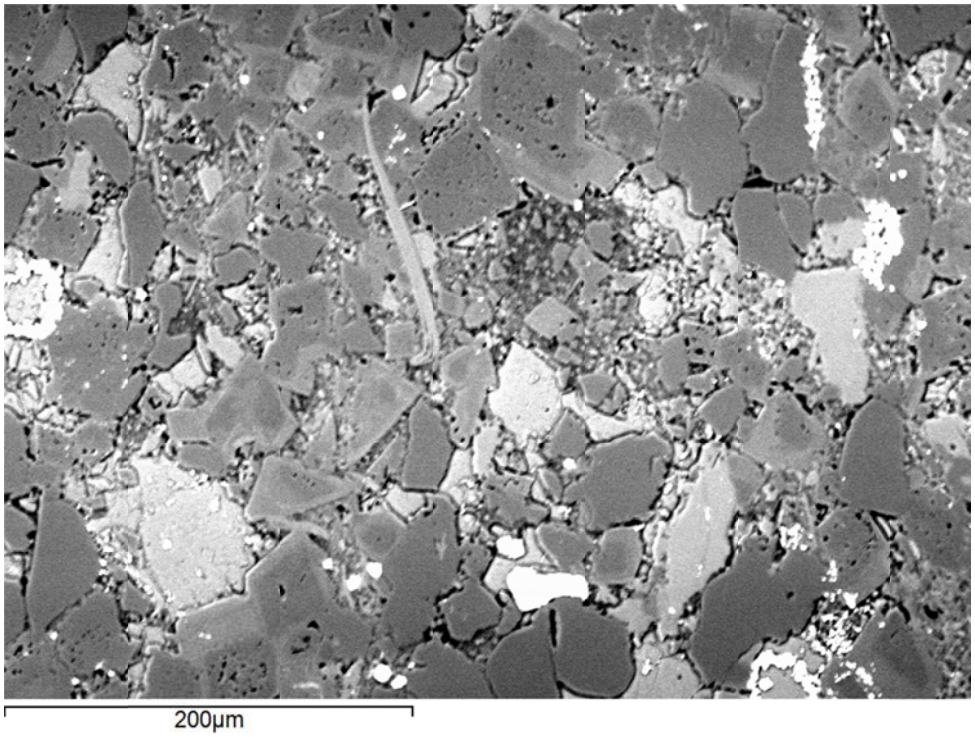

EERC Energy & Environmental Research Center® Putting Research into Practice UND THE UNIVERSITY OF NORTH DAKOTA	**Applied Geology Laboratory**		ID: 116981
	Well Name: NDIC No. 8850	Middle Bakken 4	Rival Field
	API No.: 33-013-00867-00-00	Lithology: Dolomitic, argillaceous siltstone	Depth: 7410.0'

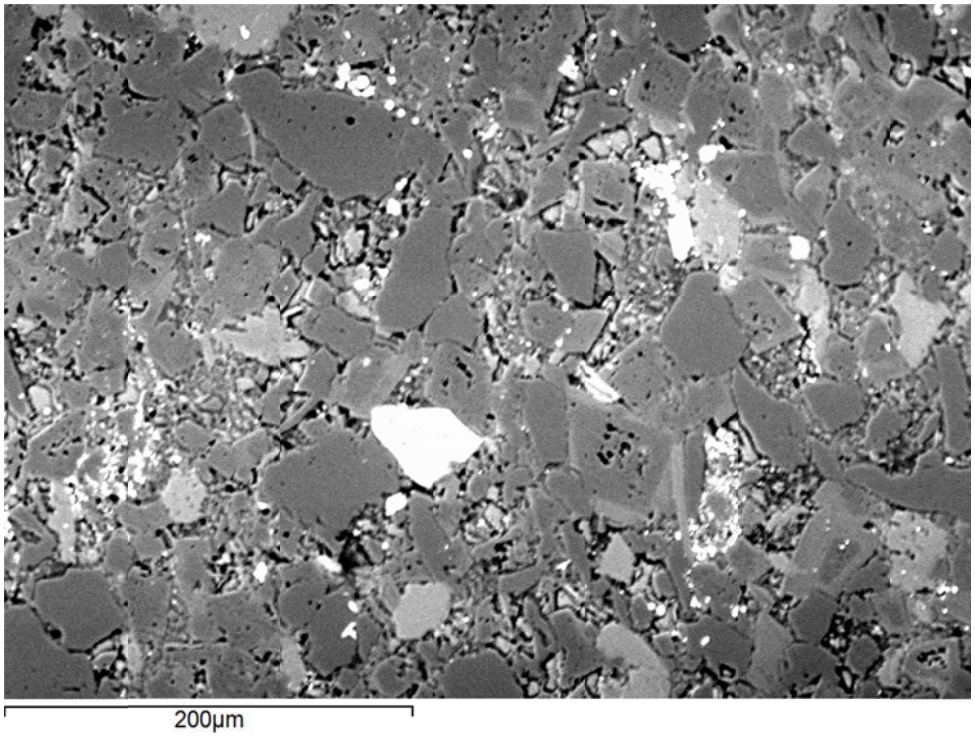

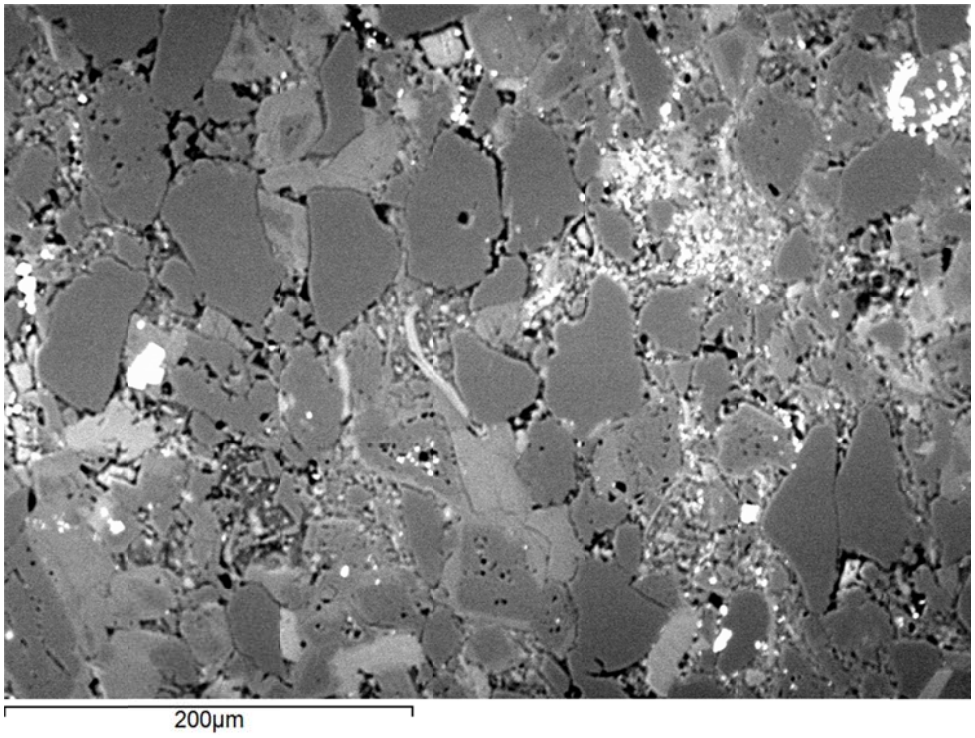

EERC Energy & Environmental Research Center® Putting Research into Practice UND THE UNIVERSITY OF NORTH DAKOTA	**Applied Geology Laboratory**		ID: 116981
	Well Name: NDIC No. 8850	Middle Bakken 4	Rival Field
	API No.: 33-013-00867-00-00	Lithology: Dolomitic, argillaceous siltstone	Depth: 7410.0'

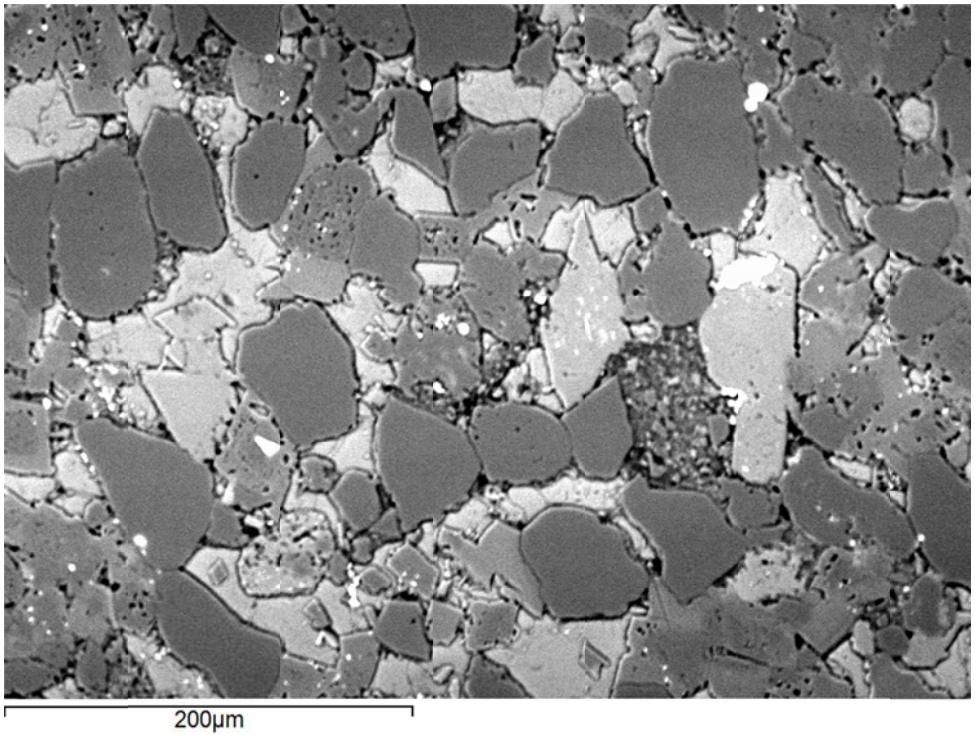

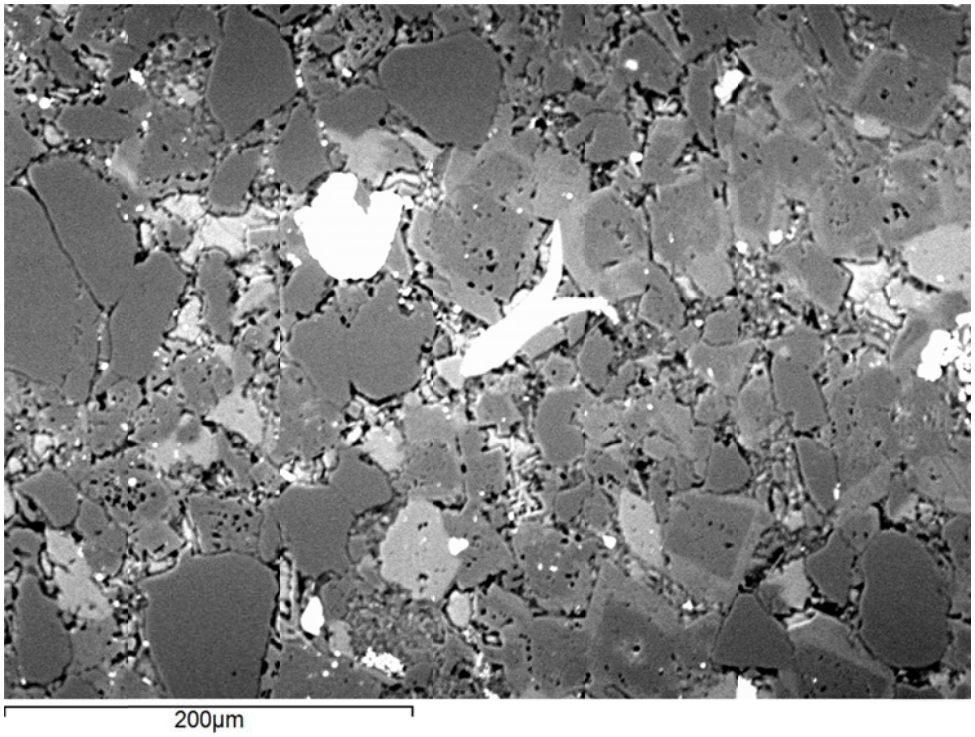

EERC Energy & Environmental Research Center® Putting Research into Practice UND THE UNIVERSITY OF NORTH DAKOTA	**Applied Geology Laboratory**		ID: 116981
	Well Name: NDIC No. 8850	Middle Bakken 4	Rival Field
	API No.: 33-013-00867-00-00	Lithology: Dolomitic, argillaceous siltstone	Depth: 7410.0'

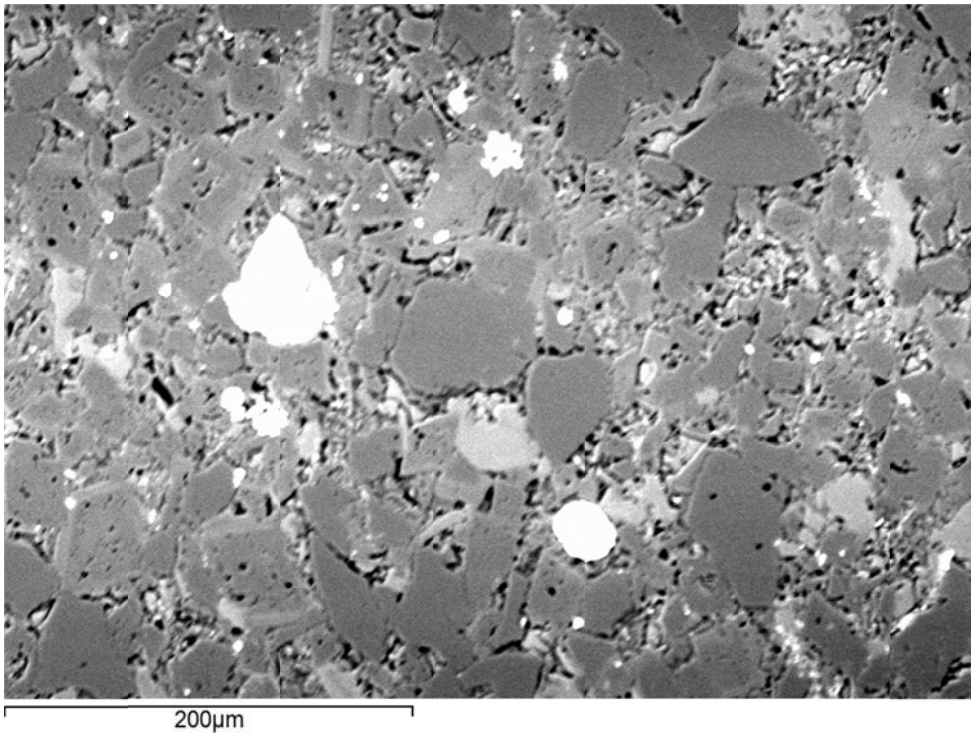

Applied Geology Laboratory		ID: 116981
Well Name: NDIC No. 8850	Middle Bakken 4	Rival Field
API No.: 33-013-00867-00-00	Lithology: Dolomitic, argillaceous siltstone	Depth: 7410.0'

SEM Digital Composite Mineral Map Image Overlaid on BSE Image with Mineral Phase 2D Area Percentages

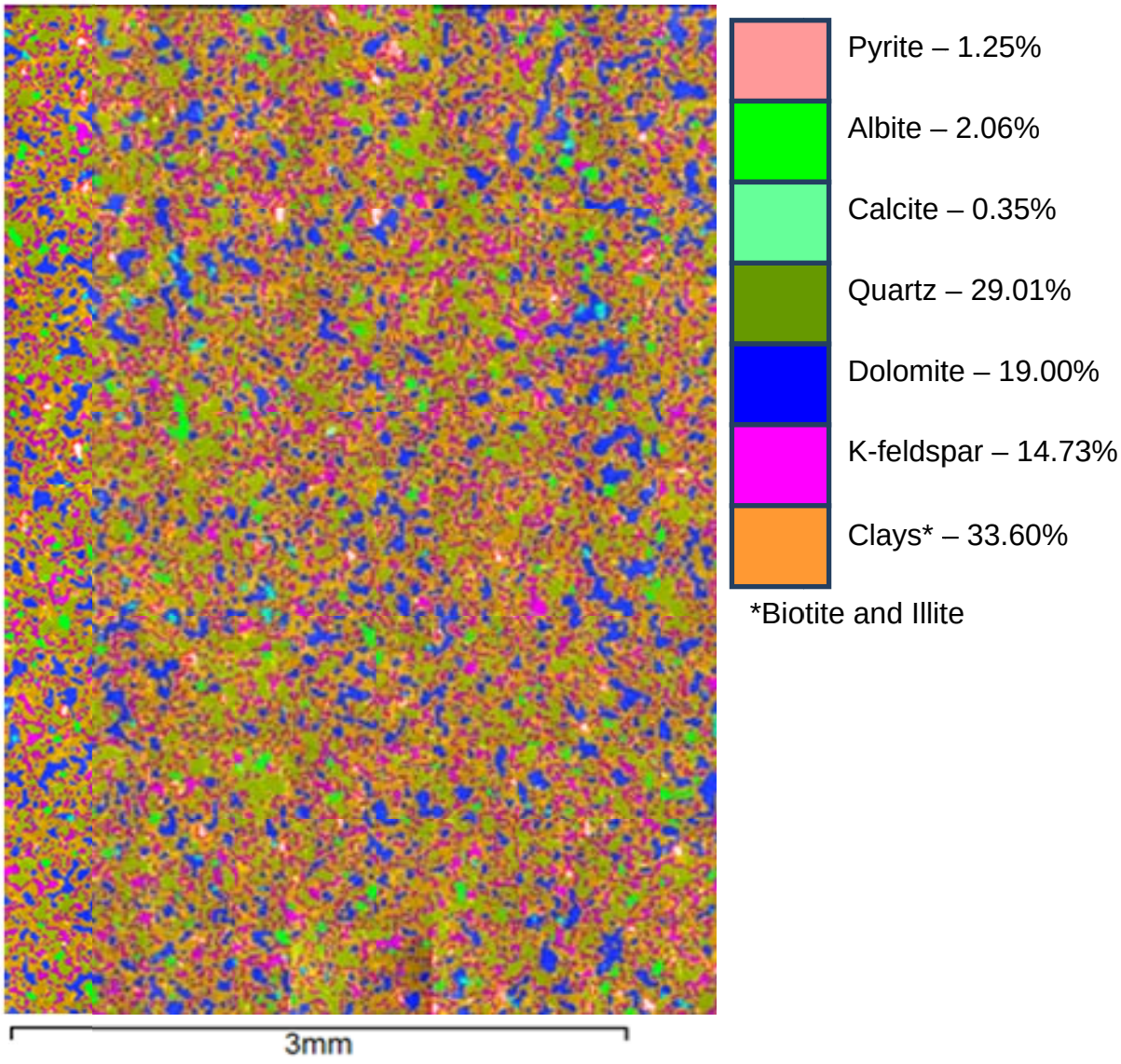

EERC Energy & Environmental Research Center® Putting Research into Practice UND THE UNIVERSITY OF NORTH DAKOTA	**Applied Geology Laboratory**		ID: 116981
	Well Name: NDIC No. 8850	Middle Bakken 4	Rival Field
	API No.: 33-013-00867-00-00	Lithology: Dolomitic, argillaceous siltstone	Depth: 7410.0'

SEM Mineral Map Image Overlaid on BSE Image with Mineral Phase 2D Area Percentages

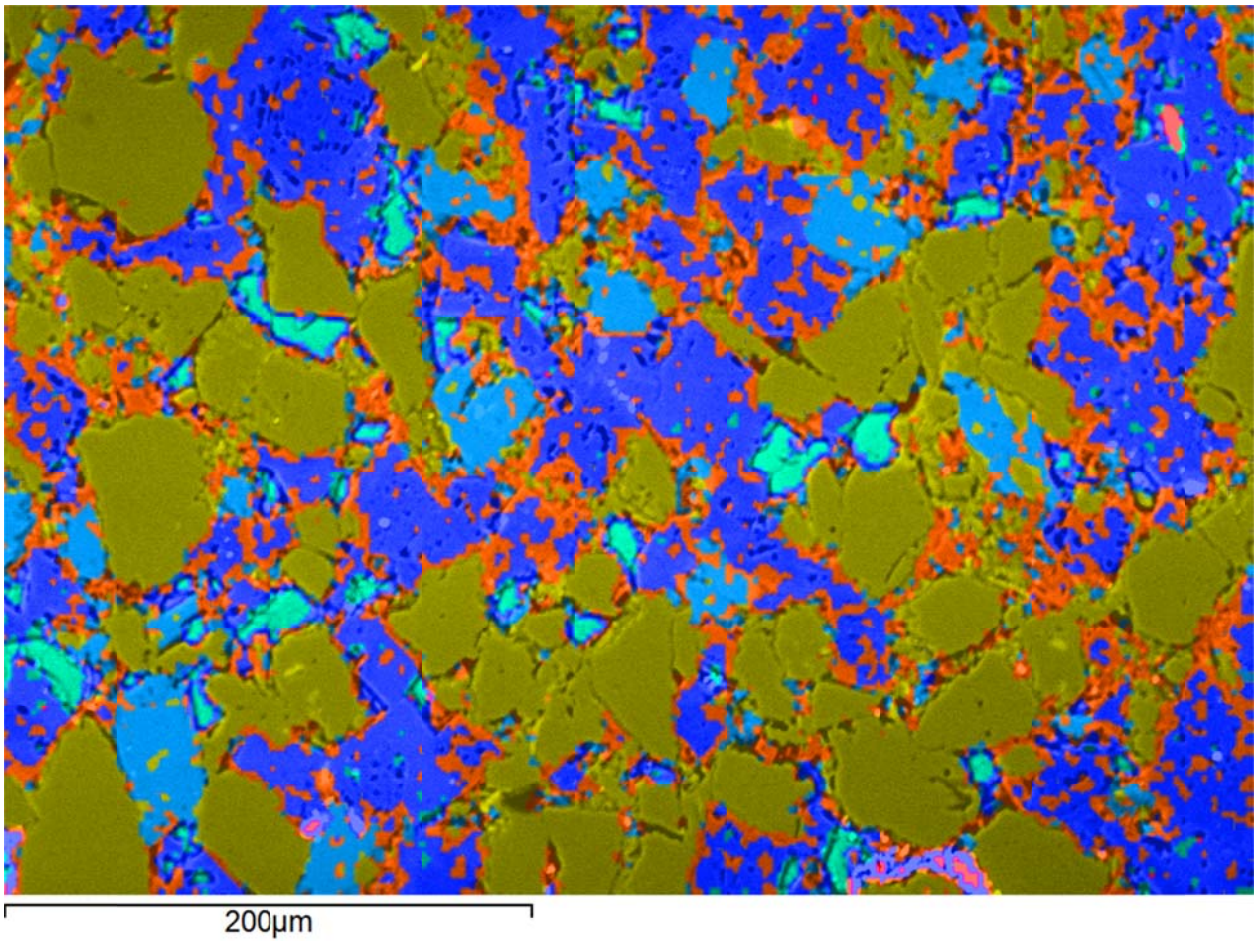

This page intentionally left blank.

EERC Energy & Environmental Research Center® Putting Research into Practice UND THE UNIVERSITY OF NORTH DAKOTA	**Applied Geology Laboratory**		ID: 116982
	Well Name: NDIC No. 8850	Middle Bakken 3	Rival Field
	API No.: 33-013-00867-00-01	Lithology: Dolomitic siltstone	Depth: 7412.5'

SAMPLE PHOTOGRAPH

PHYSICAL PROPERTIES

Porosity and Grain Density by Core Laboratories

Pycnometer Effective Porosity, vol%	Grain Density, g/cm^3
9.88	2.728

	Applied Geology Laboratory		ID: 116982
EERC Energy & Environmental Research Center® Putting Research into Practice UND THE UNIVERSITY OF NORTH DAKOTA	Well Name: NDIC No. 8850	Middle Bakken 3	Rival Field
	API No.: 33-013-00867-00-01	Lithology: Dolomitic siltstone	Depth: 7412.5'

PHOTOMICROGRAPHS

Transmission

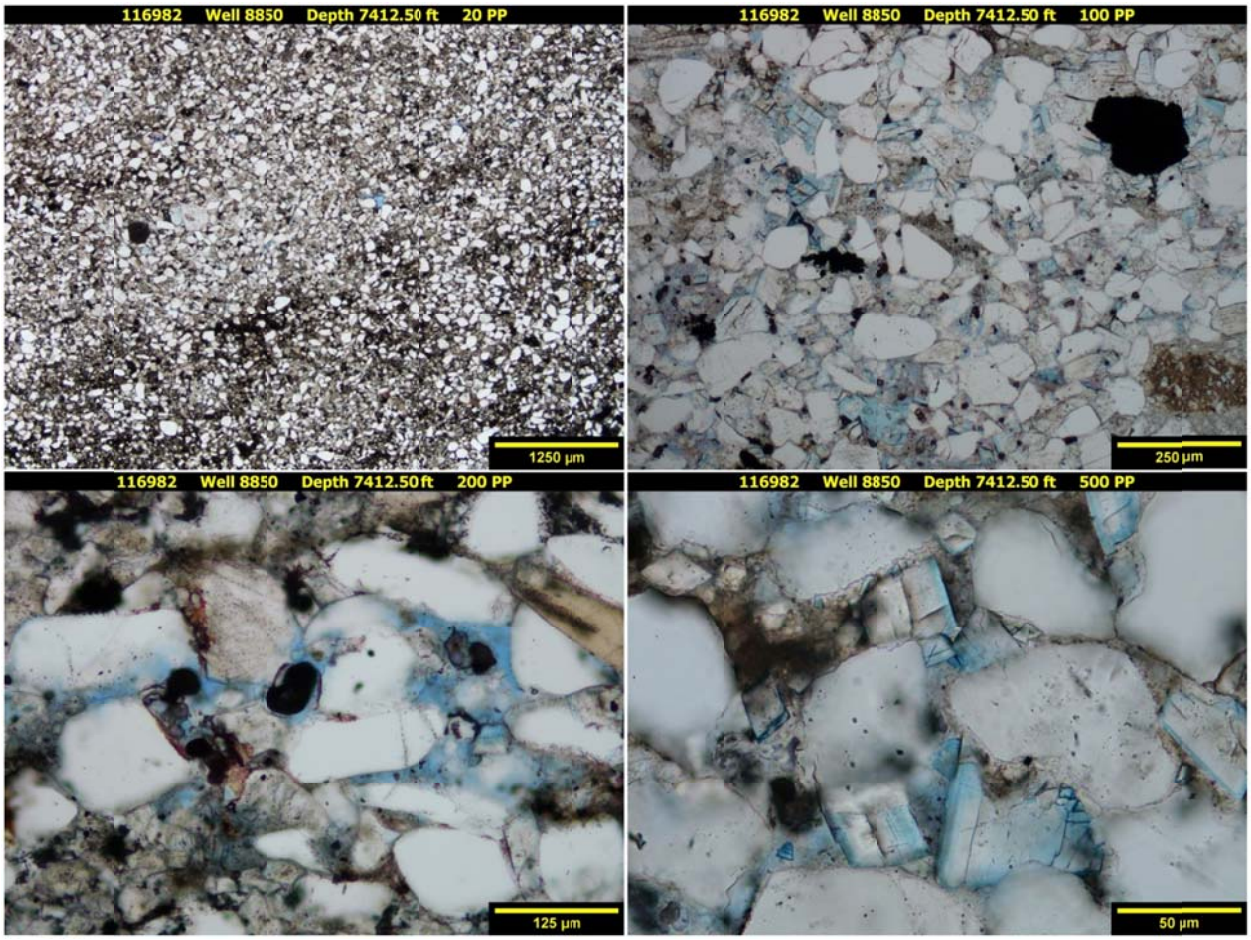

The sample from a depth of 7412.50 ft shows a dolomitic siltstone. A large degree of bioturbation and very faint wavy laminations are present. Very fine grained, subangular to subrounded, monocrystalline quartz grains and trace amounts of muscovite, rutile, and feldspars are disseminated throughout. Extensive anhederal to euhedral dolomitization has occurred throughout the sample. Very fine to fine-grained crystalline partially ferroan dolomite is noted. No calcareous skeletal or non-skeletal grains remain. Disseminated pore-filling and replacement pyrite grains are observed throughout, concentrating in some areas. An additional mineralogical component is clay, found at moderate quantities creating faint, wavy laminations and lenses. No fractures are detected. Organics are observed as tiny globs typically associated with pyrite. A greater than average (for Middle Bakken) amount of inter-particle porosity is observed using standard petrographic techniques.

	Applied Geology Laboratory		ID: 116982
	Well Name: NDIC No. 8850	Middle Bakken 3	Rival Field
	API No.: 33-013-00867-00-01	Lithology: Dolomitic siltstone	Depth: 7412.5'

Reflection

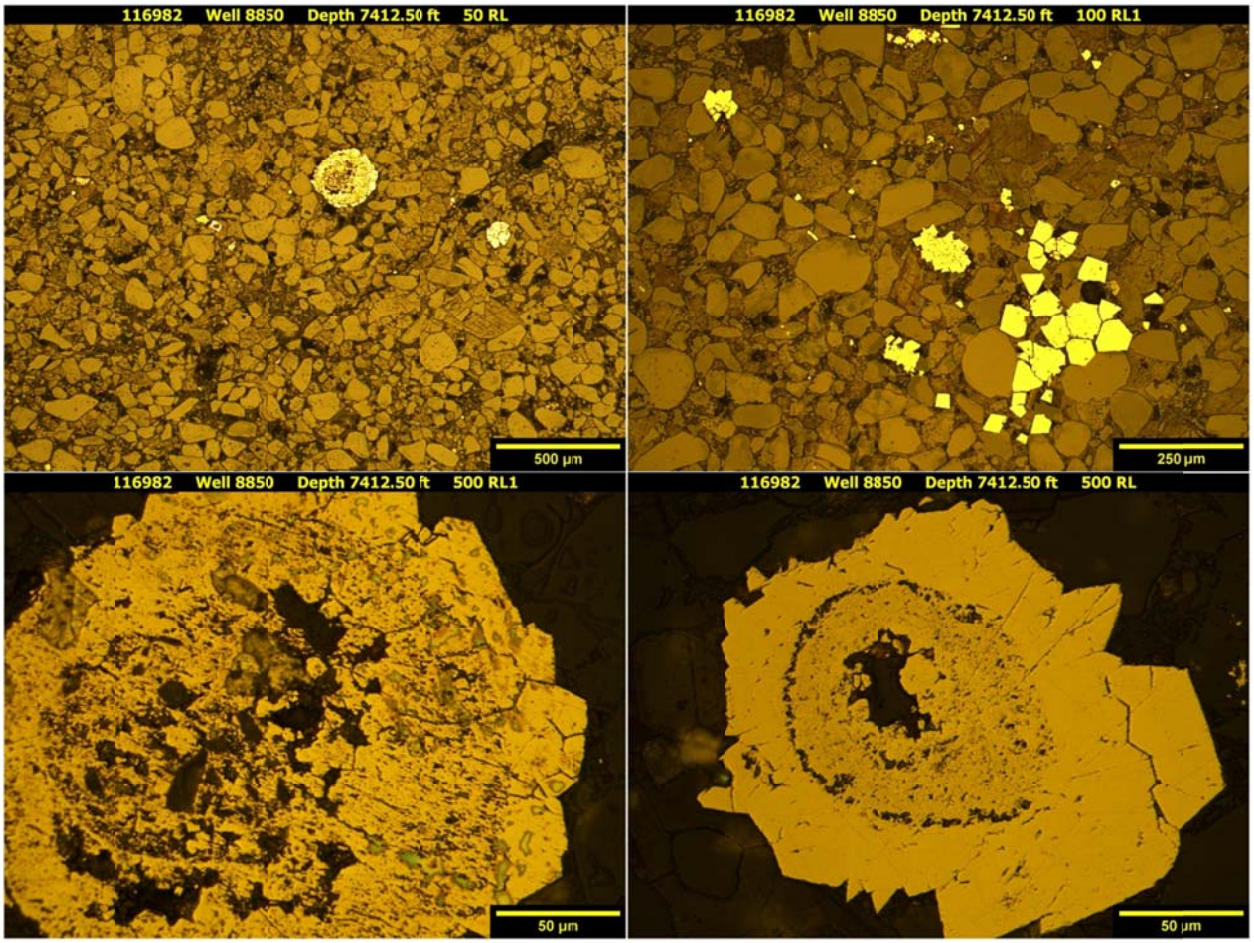

The sample from a depth of 7412.50 ft displays a lesser pyrite presence. Mostly euhedral and trace quantities of frambodial pyrite growth are detected; both pore-filling and as grain replacement are observed. Euhedral grains are very fine grained and individual frambodial grains are observed at a fraction of that size. Trace framboidal pyrite is immature, displaying no larger sphere assemblages. Occasional complete to nearly complete pyritization of precursor grains and organics have occurred.

EERC Energy & Environmental Research Center® Putting Research into Practice UND THE UNIVERSITY OF NORTH DAKOTA	**Applied Geology Laboratory**		ID: 116982
	Well Name: NDIC No. 8850	Middle Bakken 3	Rival Field
	API No.: 33-013-00867-00-01	Lithology: Dolomitic siltstone	Depth: 7412.5'

Transmission and Fluorescence Whole-Slide Images

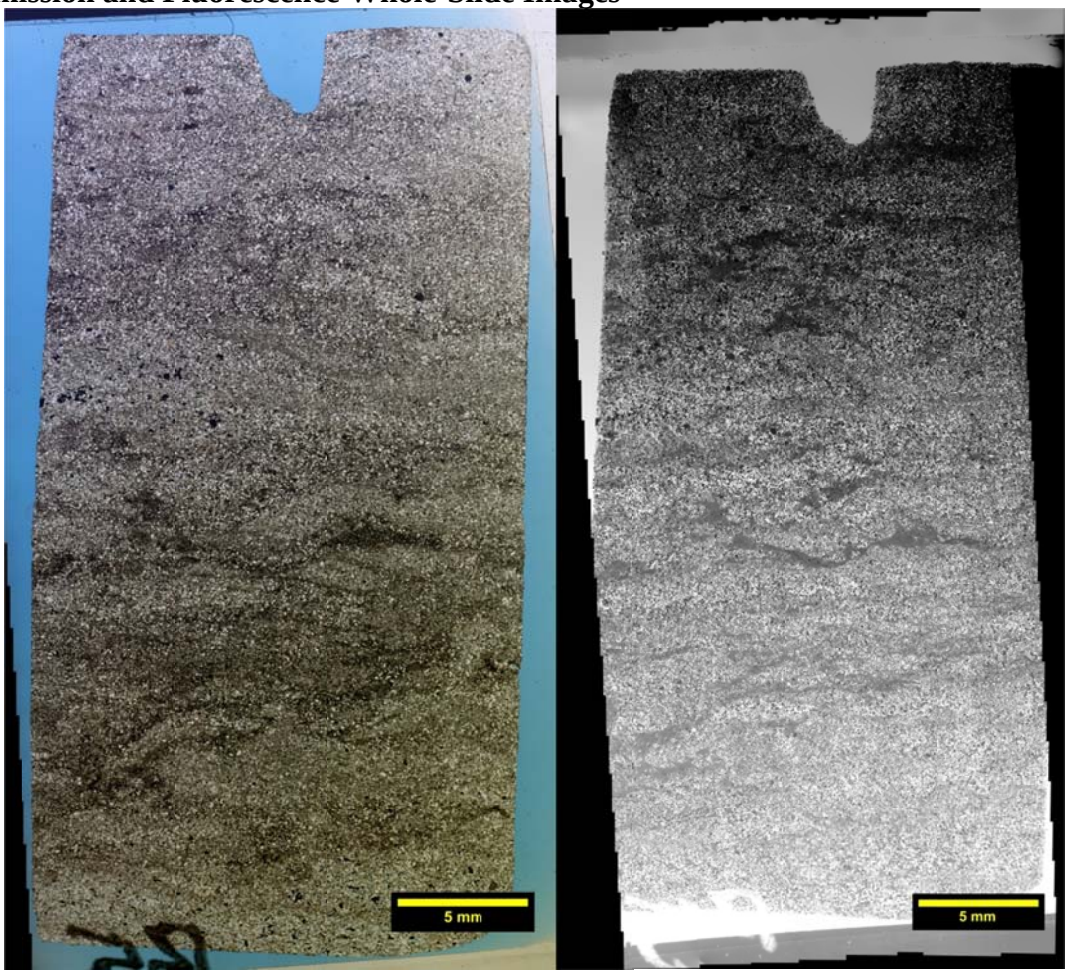

Images issues. The image collected from a depth of 7412.50 ft is moderately bioturbated dolomitic siltstone. Effective porosity is reported at 9.88 vol%. Extensive interlocking anhedral to euhedral dolomitization and pyritization has occurred. Slight variability in grain sizes, mineral dissolution, and clay-free zones enable the highest observed porosity within this sample set. No natural or induced fractures are noted.

EERC Energy & Environmental Research Center® Putting Research into Practice UND THE UNIVERSITY OF NORTH DAKOTA	**Applied Geology Laboratory**		ID: 116982
	Well Name: NDIC No. 8850	Middle Bakken 3	Rival Field
	API No.: 33-013-00867-00-01	Lithology: Dolomitic siltstone	Depth: 7412.5'

XRF BULK CHEMICAL COMPOSITION

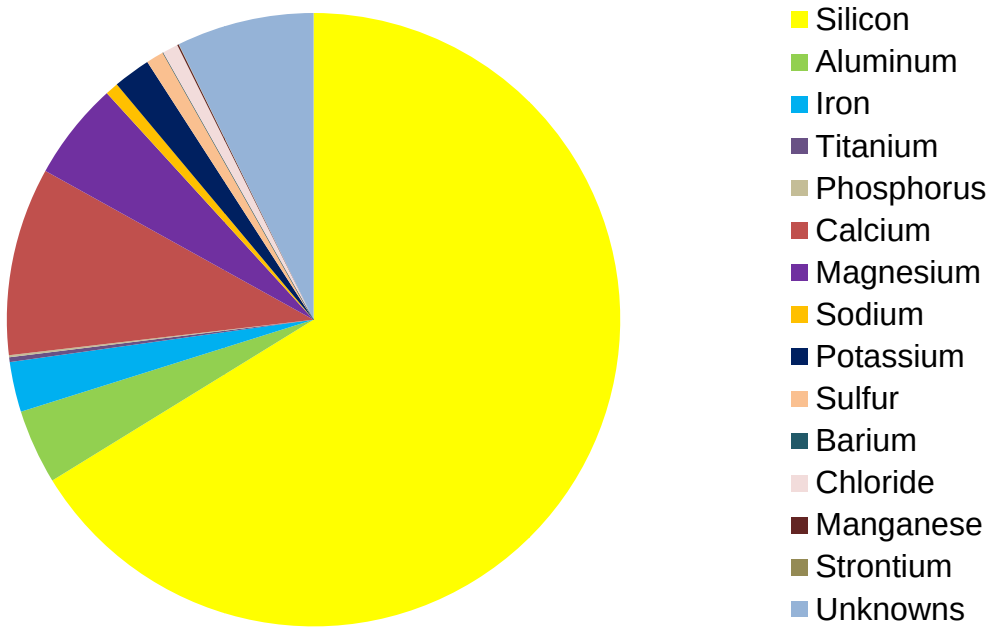

Element	Reporting Convention (Oxide)	Weight %
Si (silicon)	SiO_2	66.22
Al (aluminum)	Al_2O_3	3.93
Fe (iron)	Fe_2O_3	2.64
Ti (titanium)	TiO_2	0.25
P (phosphorus)	P_2O_5	0.11
Ca (calcium)	CaO	9.91
Mg (magnesium)	MgO	5.17
Na (sodium)	Na_2O	0.69
K (potassium)	K_2O	1.97
S (sulfur)	SO_3	0.95
Ba (barium)	BaO	0.00
Cl (chloride)	Cl	0.83
Mn (manganese)	MnO	0.08
Sr (strontium)	SrO	0.01
Unknowns	Due to the presence of carbonates	7.24
Total		100.00

EERC Energy & Environmental Research Center® Putting Research into Practice UND THE UNIVERSITY OF NORTH DAKOTA	**Applied Geology Laboratory**		ID: 116982
	Well Name: NDIC No. 8850	Middle Bakken 3	Rival Field
	API No.: 33-013-00867-00-01	Lithology: Dolomitic siltstone	Depth: 7412.5'

XRD MINERAL PHASE DISTRIBUTION

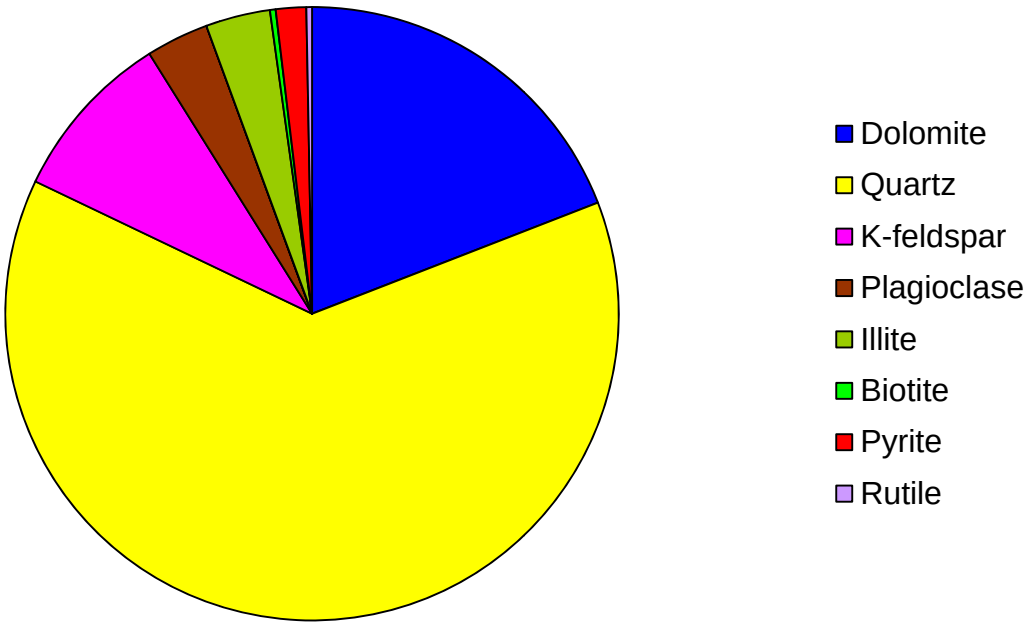

Mineral Phase	Formula	Weight %
Dolomite	$CaMg(CO_3)_2$	19.1
Quartz	SiO_2	63.0
K-feldspar	$KAlSi_3O_8$	9.0
Plagioclase	$Na_{0.5}Ca_{0.5}Al_{1.5}Si_{2.5}O_8$	3.3
Illite	$(K,H_3O)(Al,Mg,Fe)_2(Si,Al)_4O_{10}[(OH)_2,(H_2O)]$	3.4
Biotite	$K(Mg,Fe)_3[(OH)_2AlSi_3O_{10}]$	0.3
Pyrite	FeS_2	1.6
Rutile	TiO_2	0.3

EERC Energy & Environmental Research Center® Putting Research into Practice UND THE UNIVERSITY OF NORTH DAKOTA	**Applied Geology Laboratory**		ID: 116982
	Well Name: NDIC No. 8850	Middle Bakken 3	Rival Field
	API No.: 33-013-00867-00-01	Lithology: Dolomitic siltstone	Depth: 7412.5'

SEM

Observed Minerals

Mineral Phase	Mineral Phase
Quartz	Illite
K-feldspar	Zircon
Dolomite	Biotite
Pyrite	Apatite
Rutile	

High-Magnification BSE Image Annotated with Examples of Mineral Phases Identified

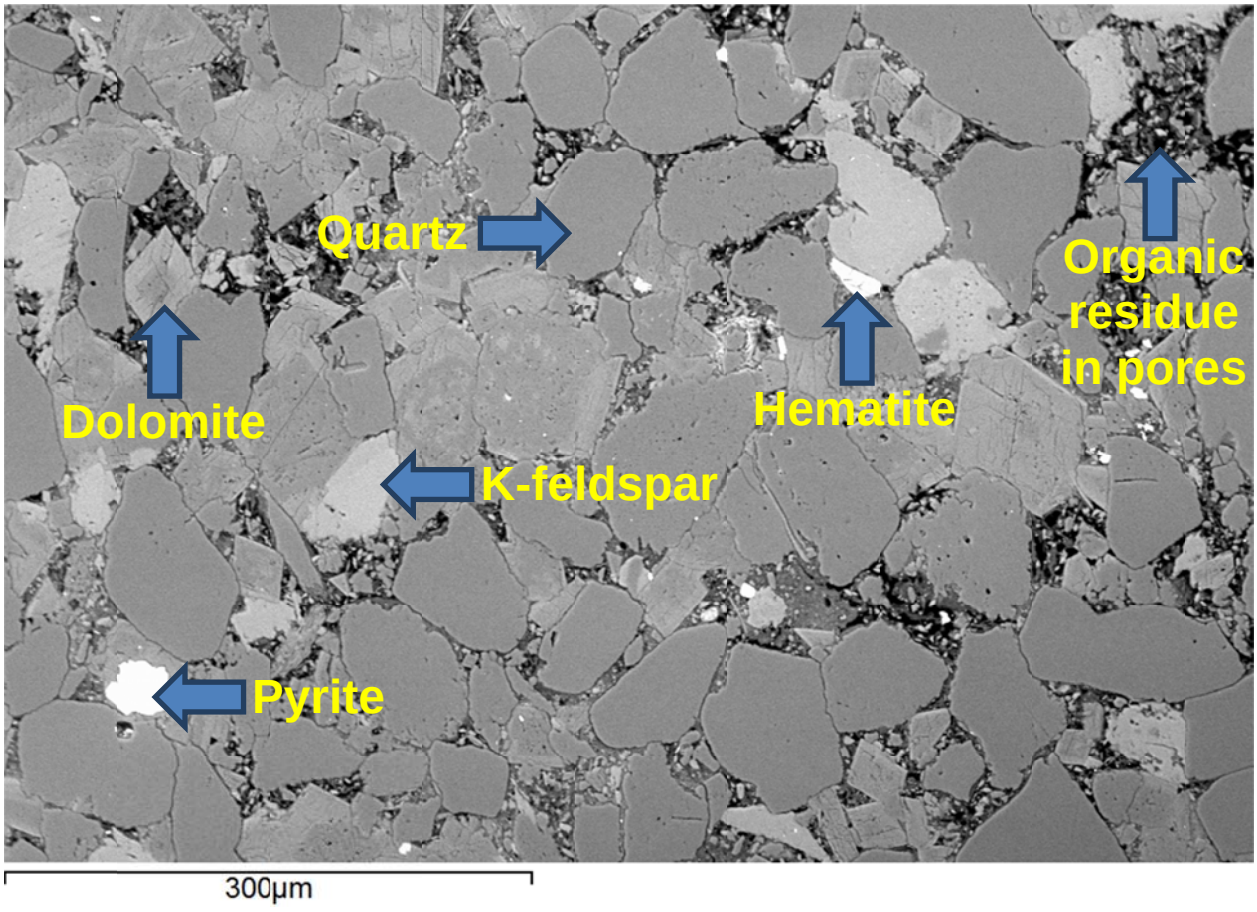

Additional High-Magnification BSE Images

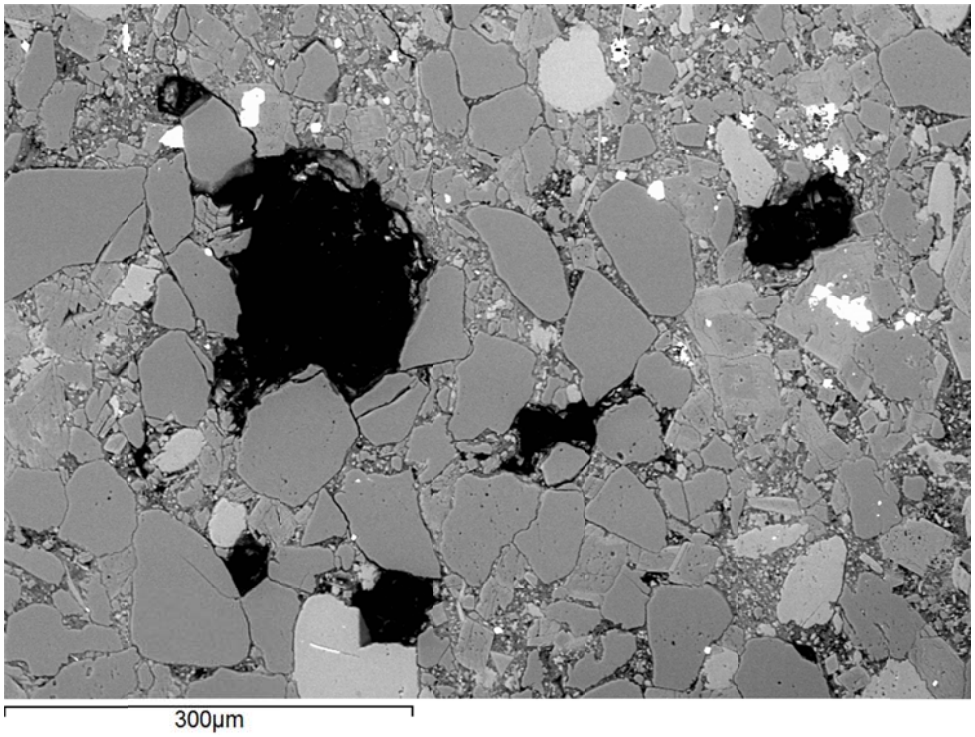

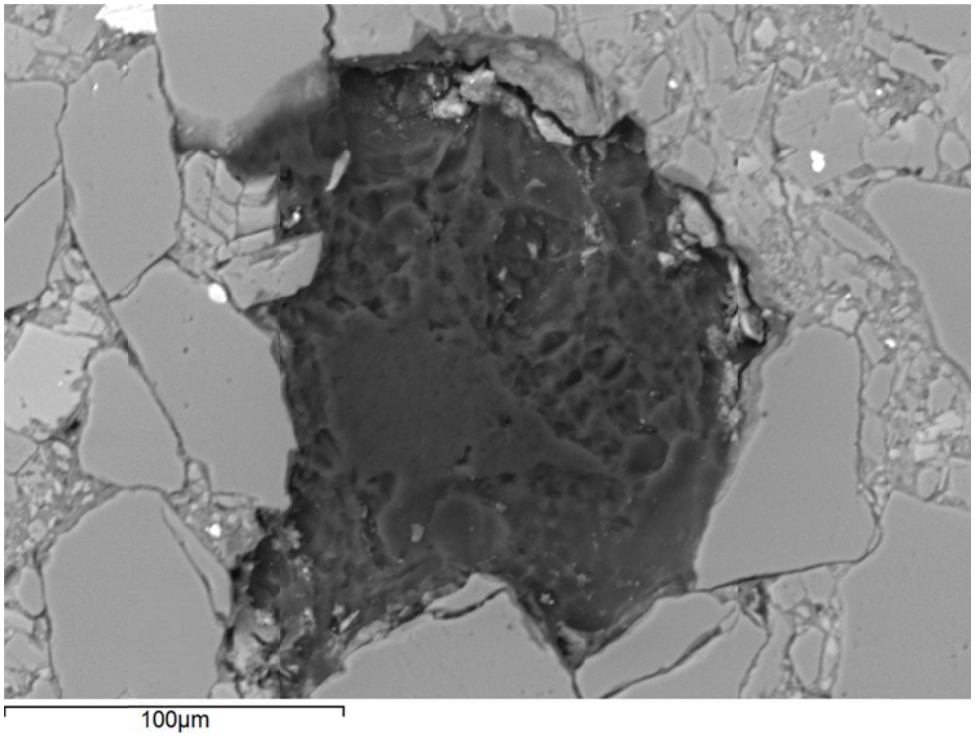

EERC Energy & Environmental Research Center® Putting Research into Practice UND THE UNIVERSITY OF NORTH DAKOTA	**Applied Geology Laboratory**		ID: 116982
	Well Name: NDIC No. 8850	Middle Bakken 3	Rival Field
	API No.: 33-013-00867-00-01	Lithology: Dolomitic siltstone	Depth: 7412.5'

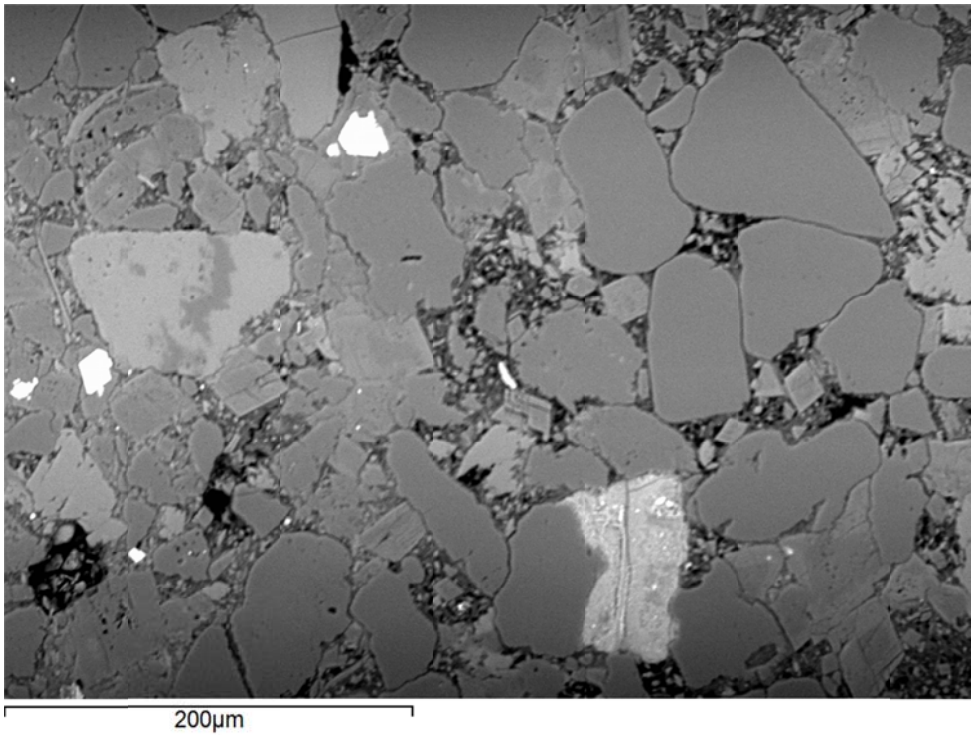

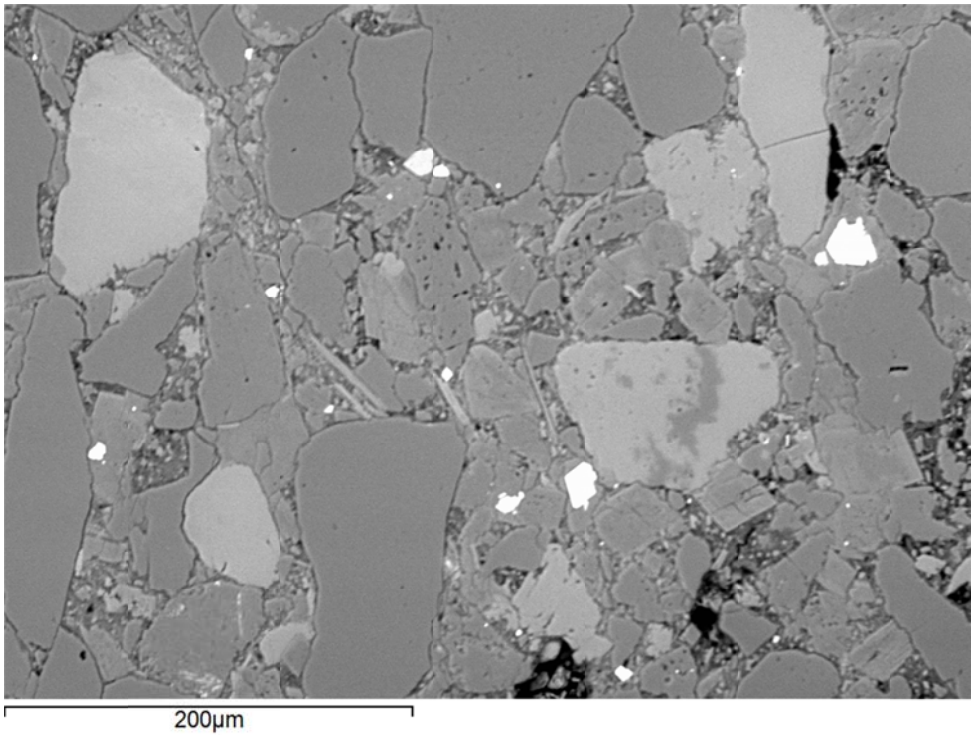

	Applied Geology Laboratory		ID: 116982
EERC Energy & Environmental Research Center® Putting Research into Practice UND THE UNIVERSITY OF NORTH DAKOTA	Well Name: NDIC No. 8850	Middle Bakken 3	Rival Field
	API No.: 33-013-00867-00-01	Lithology: Dolomitic siltstone	Depth: 7412.5'

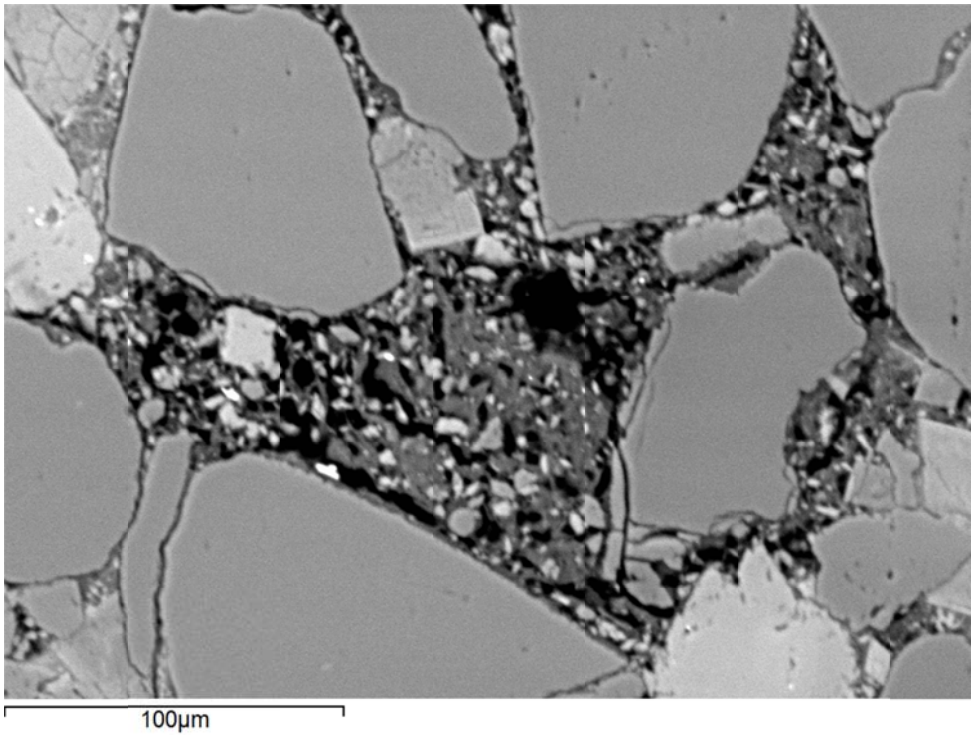

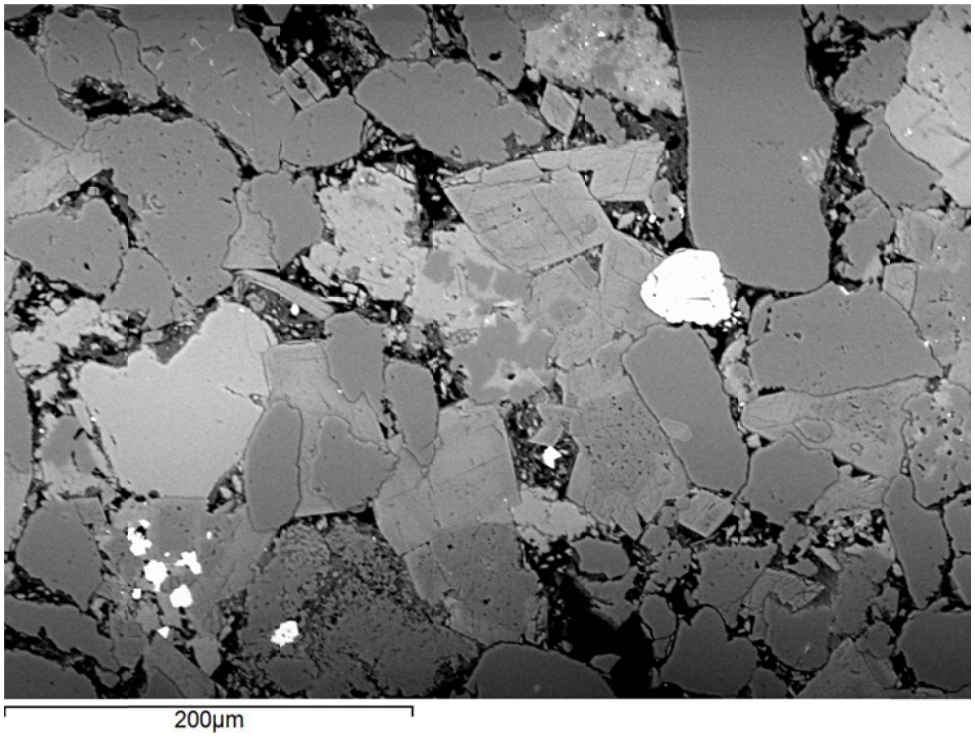

	Applied Geology Laboratory		ID: 116982
	Well Name: NDIC No. 8850	Middle Bakken 3	Rival Field
	API No.: 33-013-00867-00-01	Lithology: Dolomitic siltstone	Depth: 7412.5'

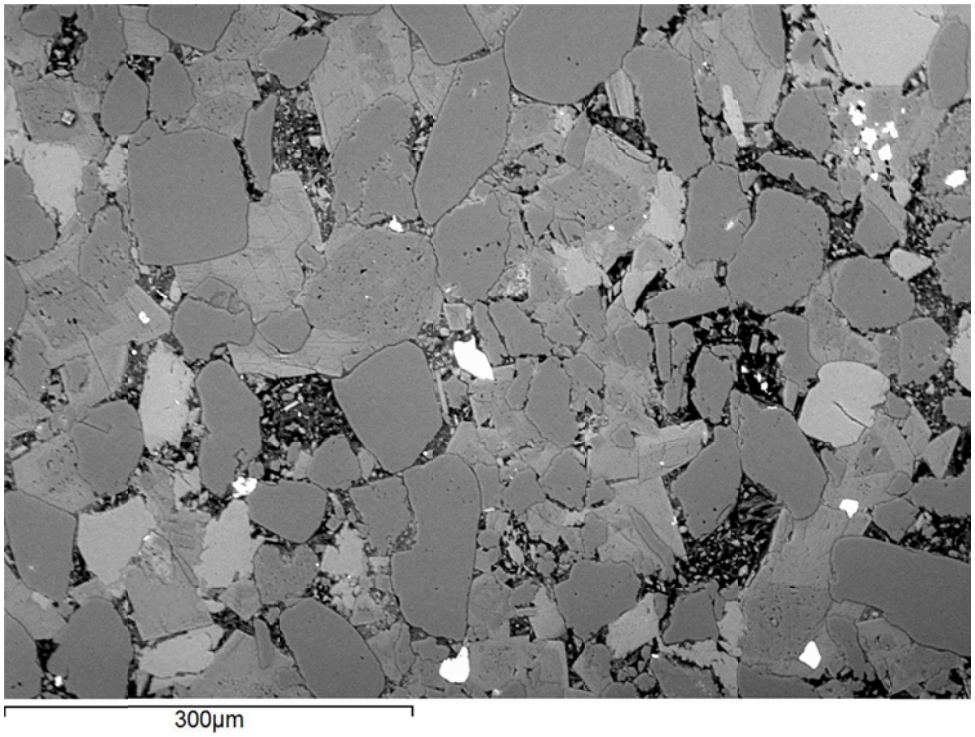

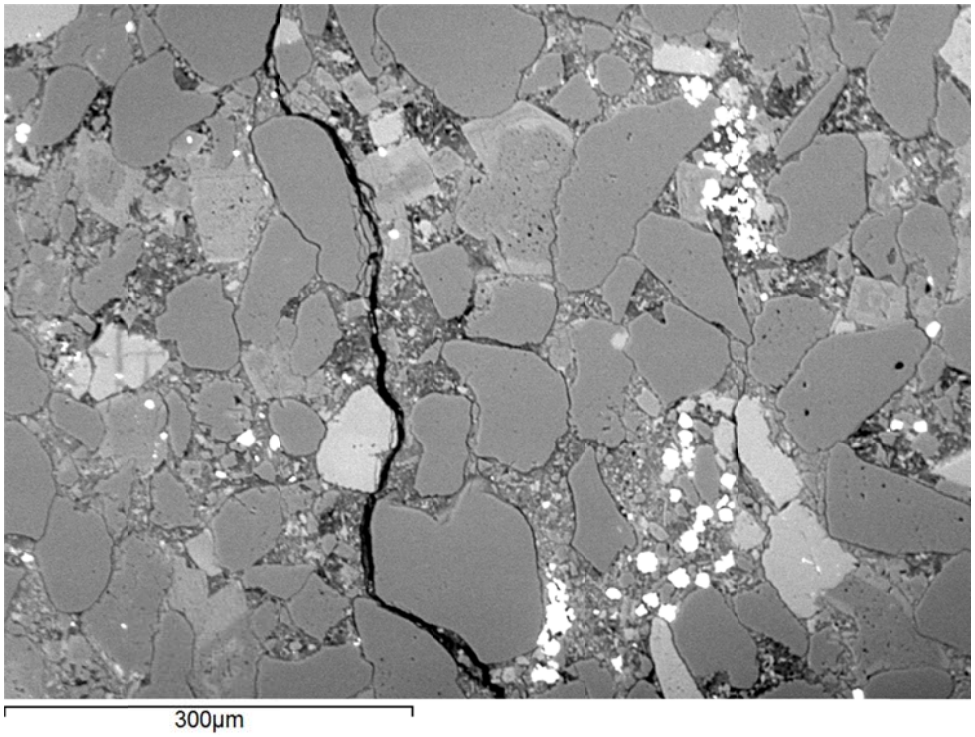

	Applied Geology Laboratory		ID: 116982
	Well Name: NDIC No. 8850	Middle Bakken 3	Rival Field
	API No.: 33-013-00867-00-01	Lithology: Dolomitic siltstone	Depth: 7412.5'

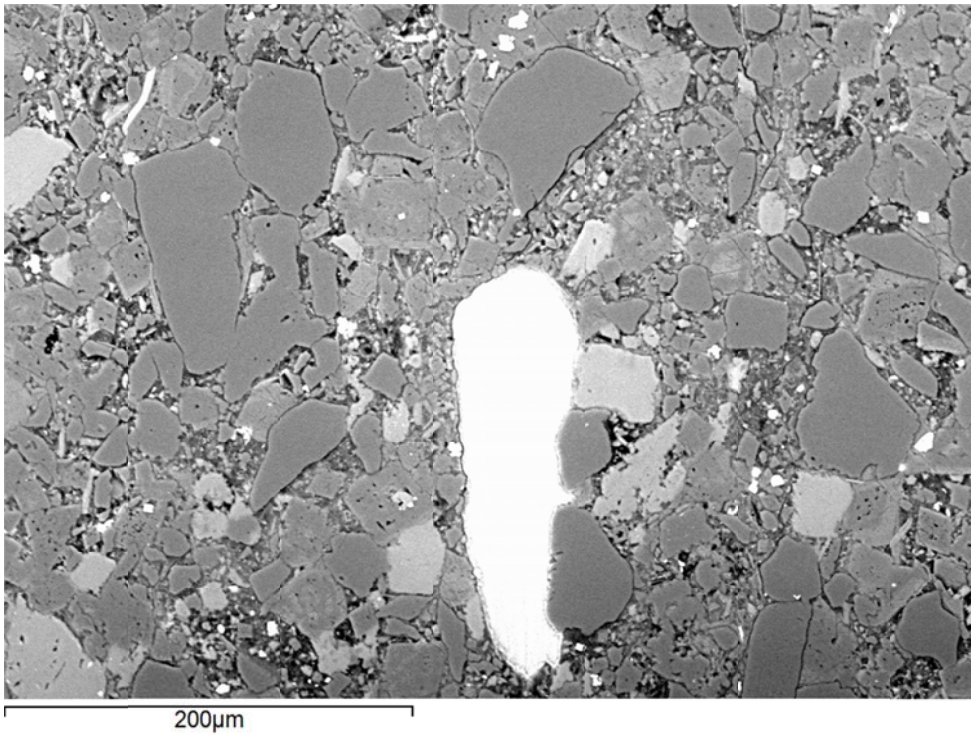

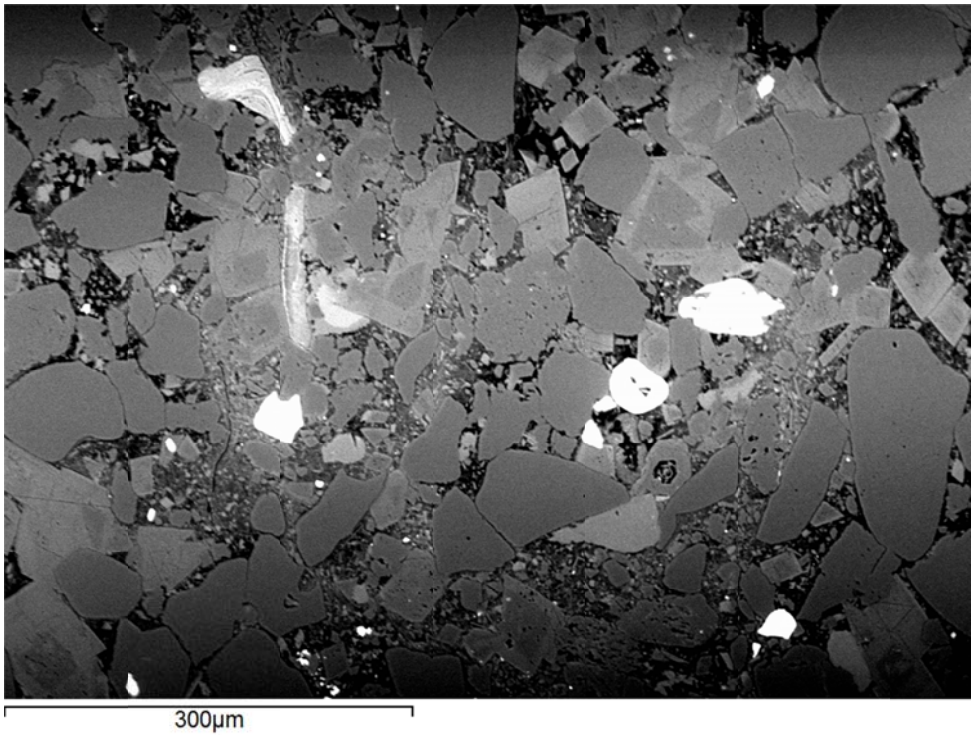

EERC Energy & Environmental Research Center® Putting Research into Practice UND THE UNIVERSITY OF NORTH DAKOTA	**Applied Geology Laboratory**		ID: 116982
	Well Name: NDIC No. 8850	Middle Bakken 3	Rival Field
	API No.: 33-013-00867-00-01	Lithology: Dolomitic siltstone	Depth: 7412.5'

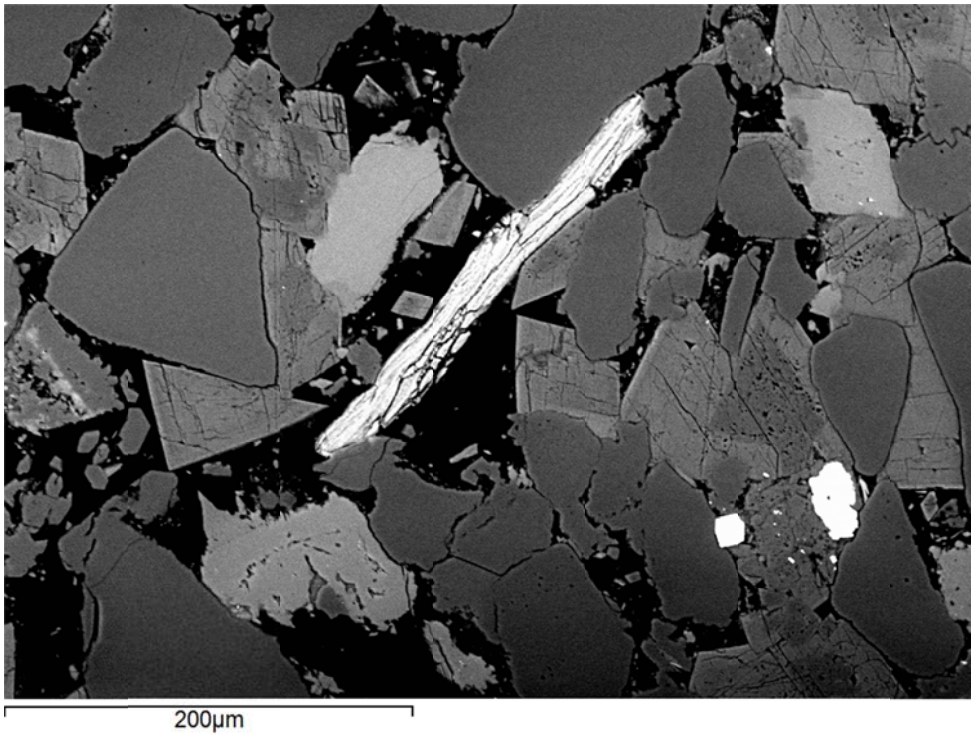

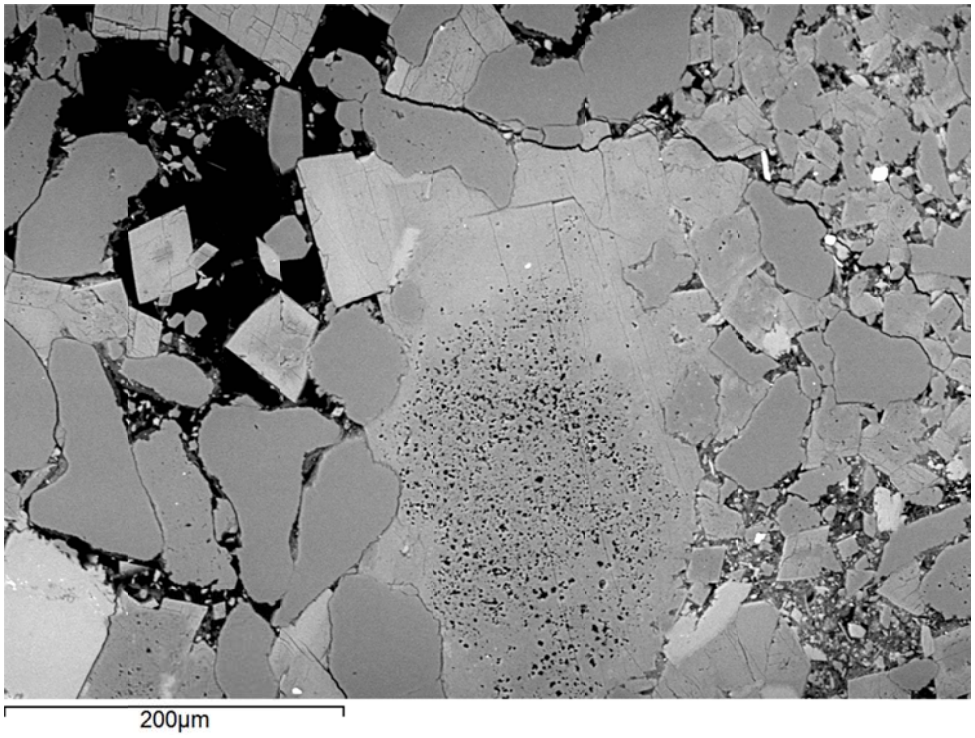

This page intentionally left blank.

EERC Energy & Environmental Research Center® Putting Research into Practice UND THE UNIVERSITY OF NORTH DAKOTA	**Applied Geology Laboratory**		ID: 116983
	Well Name: NDIC No. 8850	Middle Bakken 2	Rival Field
	API No.: 33-013-00867-00-02	Lithology: Calcareous to dolomitic siltstone	Depth: 7420.0'

SAMPLE PHOTOGRAPH

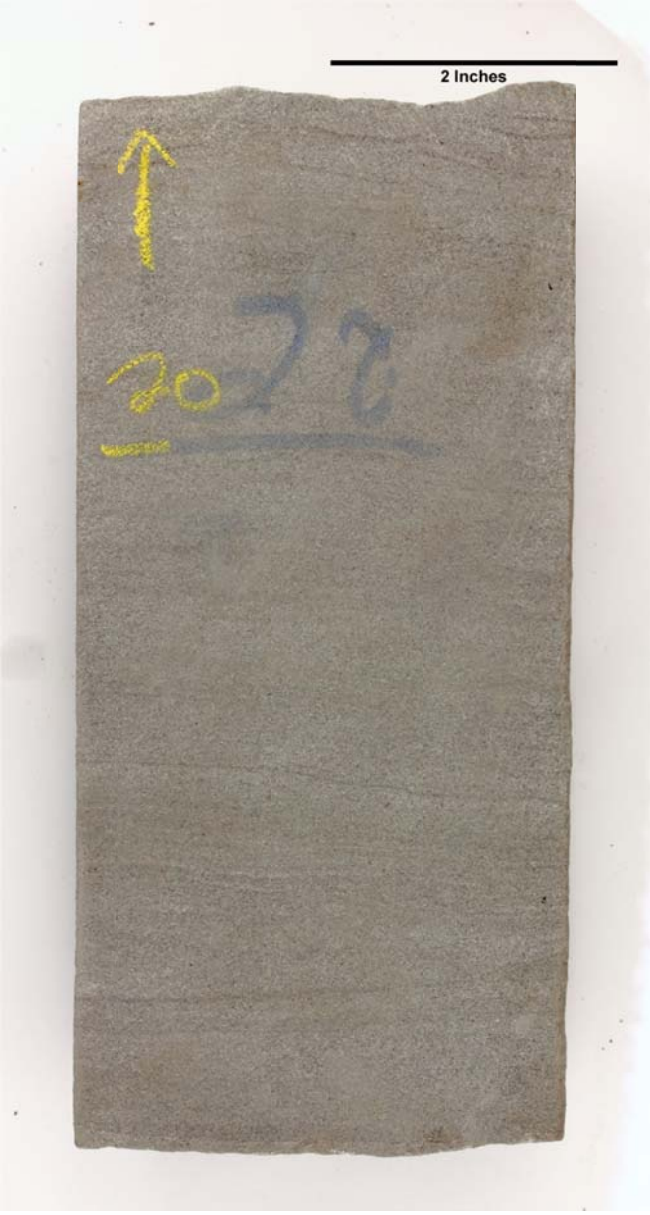

EERC Energy & Environmental Research Center® Putting Research into Practice UND THE UNIVERSITY OF NORTH DAKOTA	**Applied Geology Laboratory**		ID: 116983
	Well Name: NDIC No. 8850	Middle Bakken 2	Rival Field
	API No.: 33-013-00867-00-02	Lithology: Calcareous to dolomitic siltstone	Depth: 7420.0'

PHOTOMICROGRAPHS

Transmission

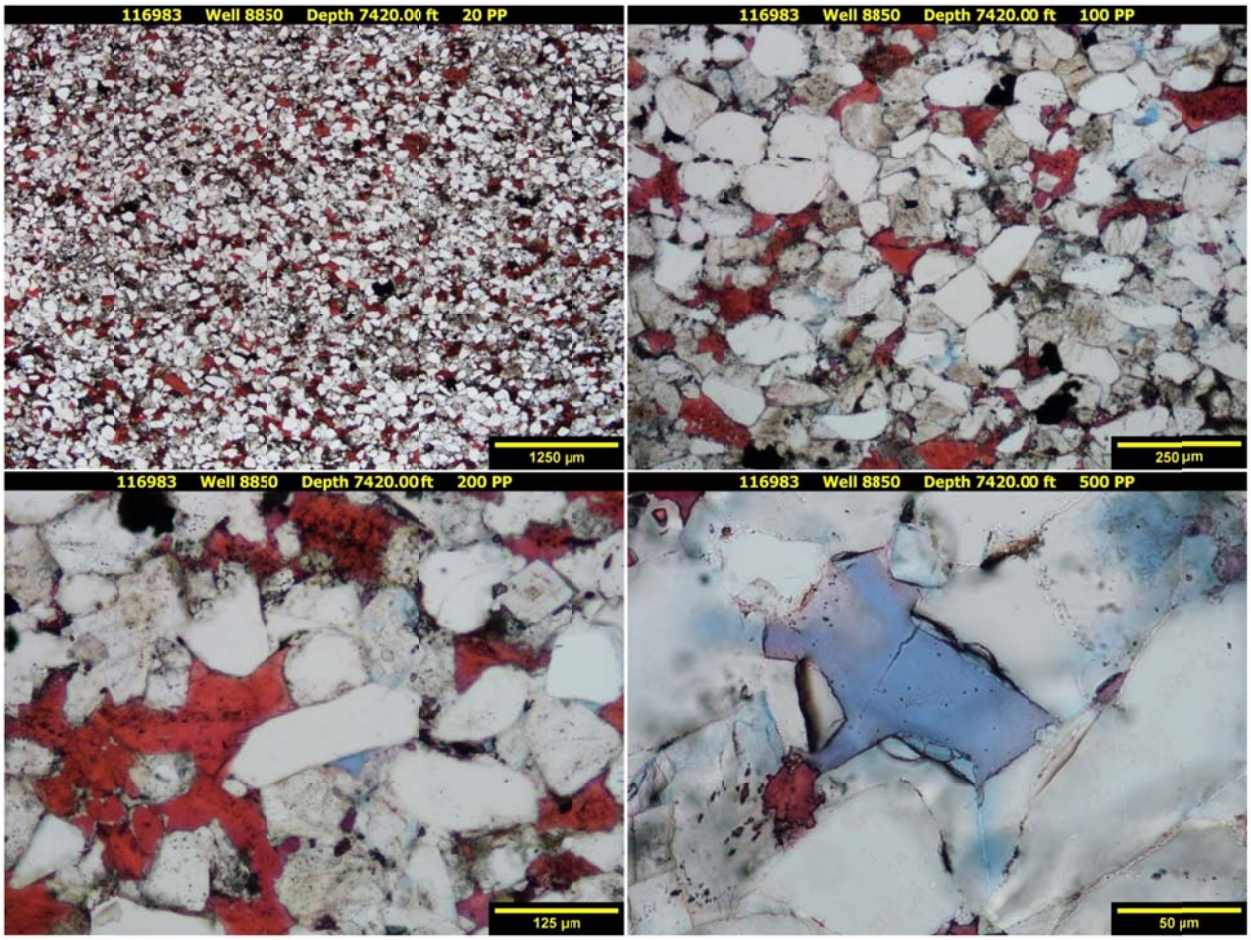

The sample captured at a depth of 7420.00 ft is a calcareous to dolomitic siltstone. It is a very massive sample expressing only slight bedding features and no bioturbation. Very fine grained, subangular to subrounded, monocrystalline quartz grains are present. Trace amounts of muscovite, rutile, and feldspars are disseminated throughout. Anhederal to euhedral dolomitization has occurred throughout the sample. Rare skeletal and non-skeletal calcite remains. Disseminated pore-filling and replacement pyrite grains exist throughout. Cementing agents are composed of a combination of clays, dolomite, and sparry calcite. Organics detection is rare and is usually associated with pyrite grains. Small occurrences of inter-particle-based porosity are detected, likely because of dolomitization. No fractures are detected.

	Applied Geology Laboratory		ID: 116983
EERC Energy & Environmental Research Center® Putting Research into Practice UND THE UNIVERSITY OF NORTH DAKOTA	Well Name: NDIC No. 8850	Middle Bakken 2	Rival Field
	API No.: 33-013-00867-00-02	Lithology: Calcareous to dolomitic siltstone	Depth: 7420.0'

Reflection

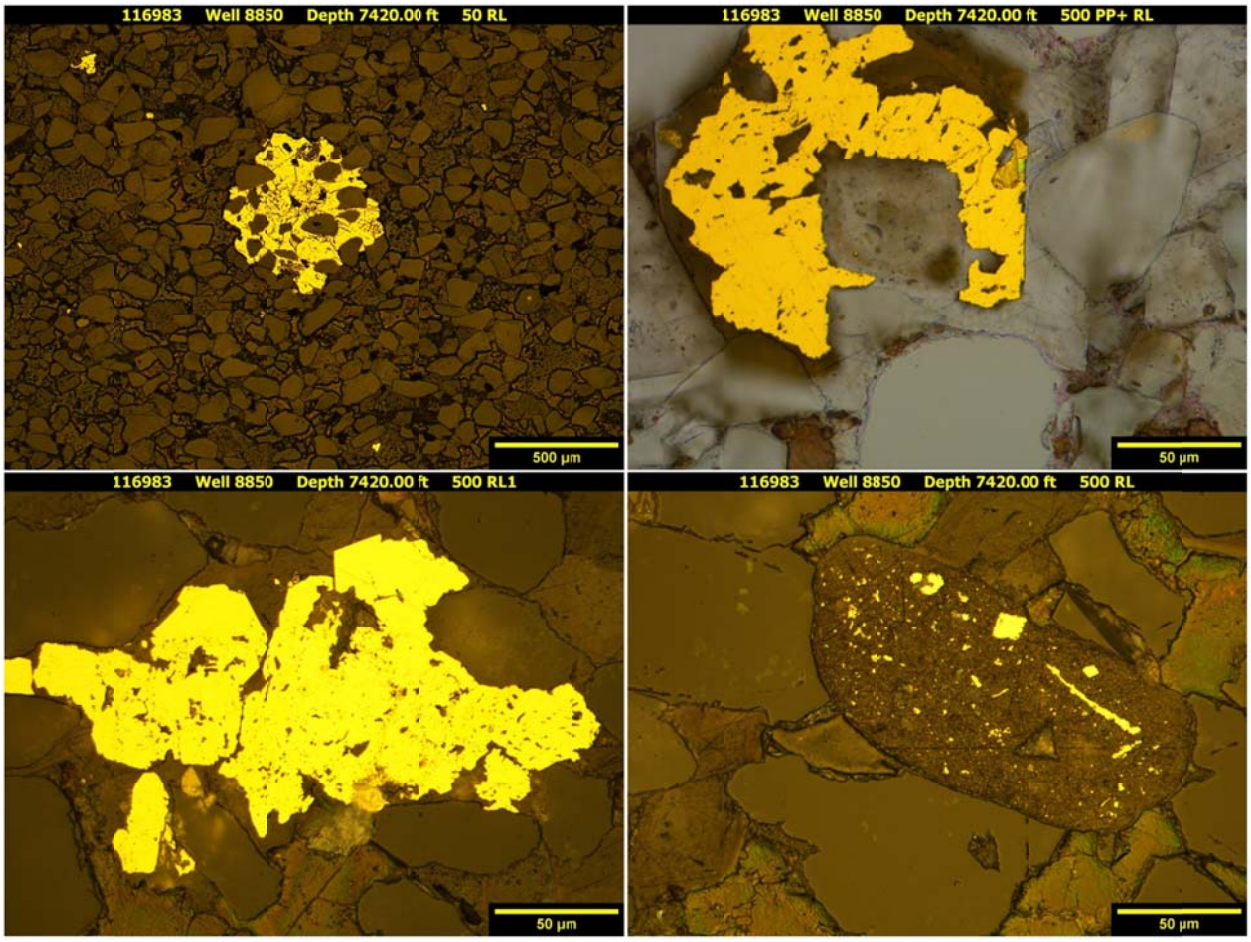

The sample from a depth of 7420.00 ft displays only euhedral pyrite growth. This diagenetic mineral acts predominantly as a pore filler and occasional grain replacer. Observed are carbonate clasts with euhedral pyrite inclusions.

EERC Energy & Environmental Research Center® Putting Research into Practice UND THE UNIVERSITY OF NORTH DAKOTA	**Applied Geology Laboratory**		ID: 116983
	Well Name: NDIC No. 8850	Middle Bakken 2	Rival Field
	API No.: 33-013-00867-00-02	Lithology: Calcareous to dolomitic siltstone	Depth: 7420.0'

Transmission and Fluorescence Whole-Slide Images

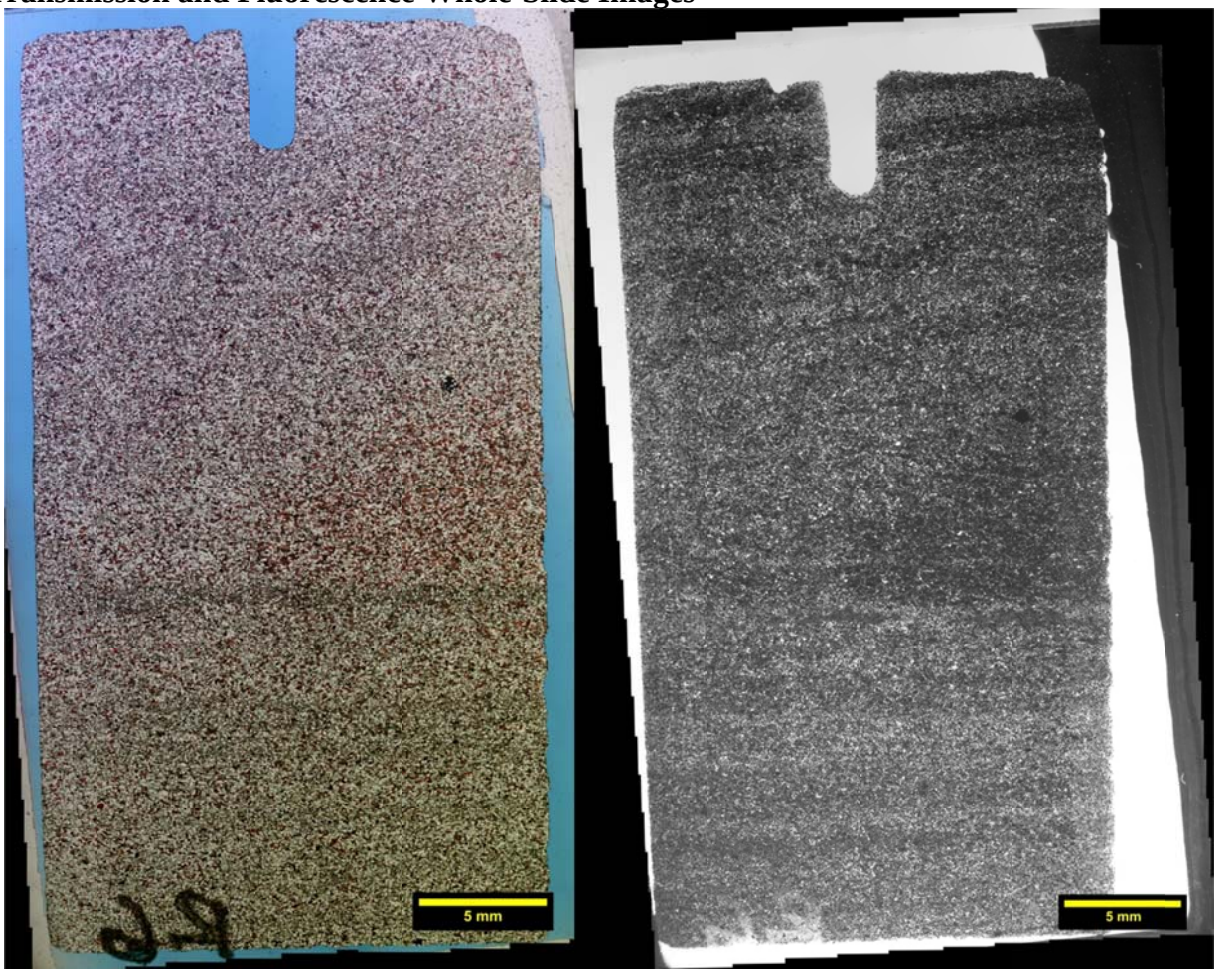

The sample at a depth of 7420.0 ft is a massive sample expressing only slight bedding features. Inter-particle micro-porosity is dispersed throughout, concentrating within zones of higher dolomite. Conversely, zones of higher calcite show less porosity. The center right of the images (reddish in the transmission image) best displays this. Extremely fined grained, mostly anhedral dolomite laminations and small quartz grains are located near the top and bottom of the sample. These carbonate laminations reduce the connectivity of pores. No natural or induced fractures are observed.

EERC Energy & Environmental Research Center® Putting Research into Practice UND THE UNIVERSITY OF NORTH DAKOTA	**Applied Geology Laboratory**		ID: 116983
	Well Name: NDIC No. 8850	Middle Bakken 2	Rival Field
	API No.: 33-013-00867-00-02	Lithology: Calcareous to dolomitic siltstone	Depth: 7420.0'

XRF BULK CHEMICAL COMPOSITION

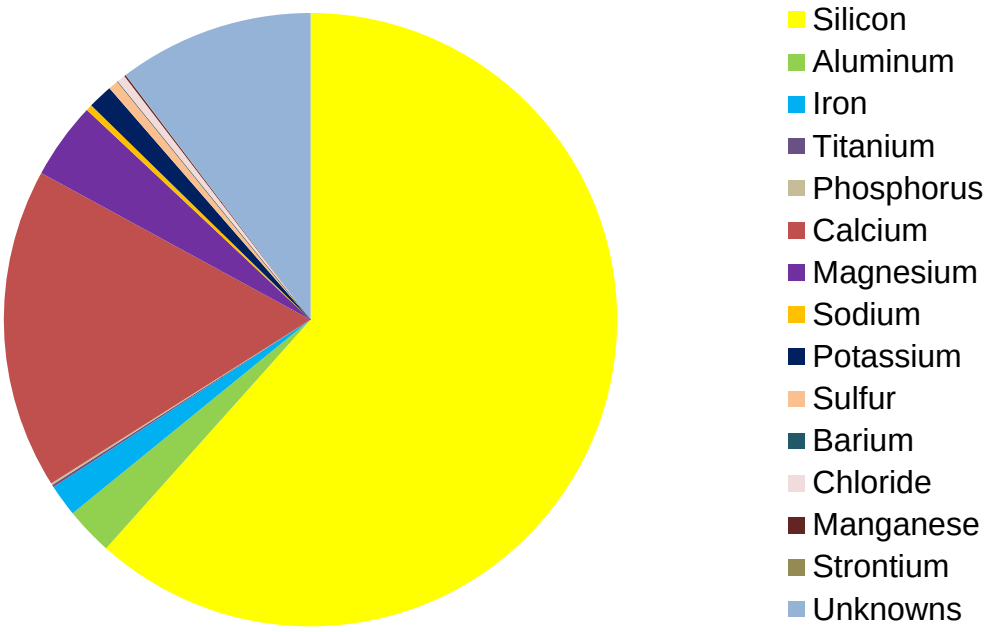

Element	Reporting Convention (Oxide)	Weight %
Si (silicon)	SiO_2	61.62
Al (aluminum)	Al_2O_3	2.51
Fe (iron)	Fe_2O_3	1.69
Ti (titanium)	TiO_2	0.13
P (phosphorus)	P_2O_5	0.10
Ca (calcium)	CaO	16.90
Mg (magnesium)	MgO	4.05
Na (sodium)	Na_2O	0.33
K (potassium)	K_2O	1.30
S (sulfur)	SO_3	0.55
Ba (barium)	BaO	0.00
Cl (chloride)	Cl	0.45
Mn (manganese)	MnO	0.08
Sr (strontium)	SrO	0.01
Unknowns	Due to the presence of carbonates	10.29
Total		100.01

EERC Energy & Environmental Research Center® Putting Research into Practice UND THE UNIVERSITY OF NORTH DAKOTA	**Applied Geology Laboratory**		ID: 116983
	Well Name: NDIC No. 8850	Middle Bakken 2	Rival Field
	API No.: 33-013-00867-00-02	Lithology: Calcareous to dolomitic siltstone	Depth: 7420.0'

XRD MINERAL PHASE DISTRIBUTION

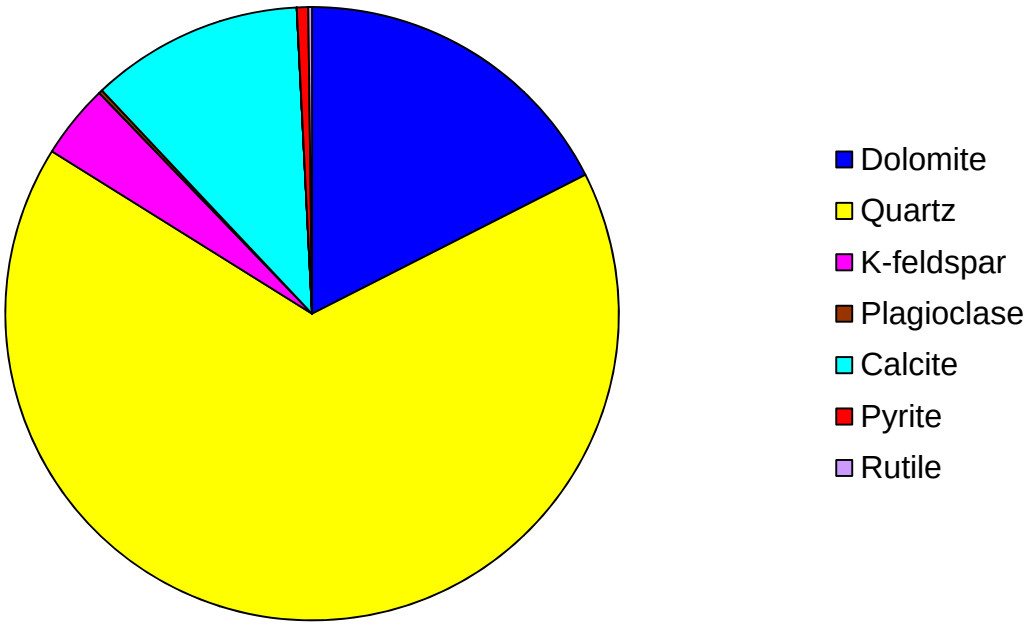

Mineral Phase	Formula	Weight %
Dolomite	$CaMg(CO_3)_2$	17.5
Quartz	SiO_2	66.3
K-feldspar	$KAlSi_3O_8$	3.9
Plagioclase	$Na_{0.5}Ca_{0.5}Al_{1.5}Si_{2.5}O_8$	0.2
Calcite	$CaCO_3$	11.2
Pyrite	FeS_2	0.6
Rutile	TiO_2	0.2

Applied Geology Laboratory		ID: 116983
Well Name: NDIC No. 8850	Middle Bakken 2	Rival Field
API No.: 33-013-00867-00-02	Lithology: Calcareous to dolomitic siltstone	Depth: 7420.0'

SEM

Observed Minerals

Mineral Phase	Mineral Phase
Calcite	Apatite
Quartz	Illite
Dolomite	Pyrite
K-feldspar	Zircon
Rutile	Albite

High-Magnification BSE Image Annotated with Examples of Mineral Phases Identified

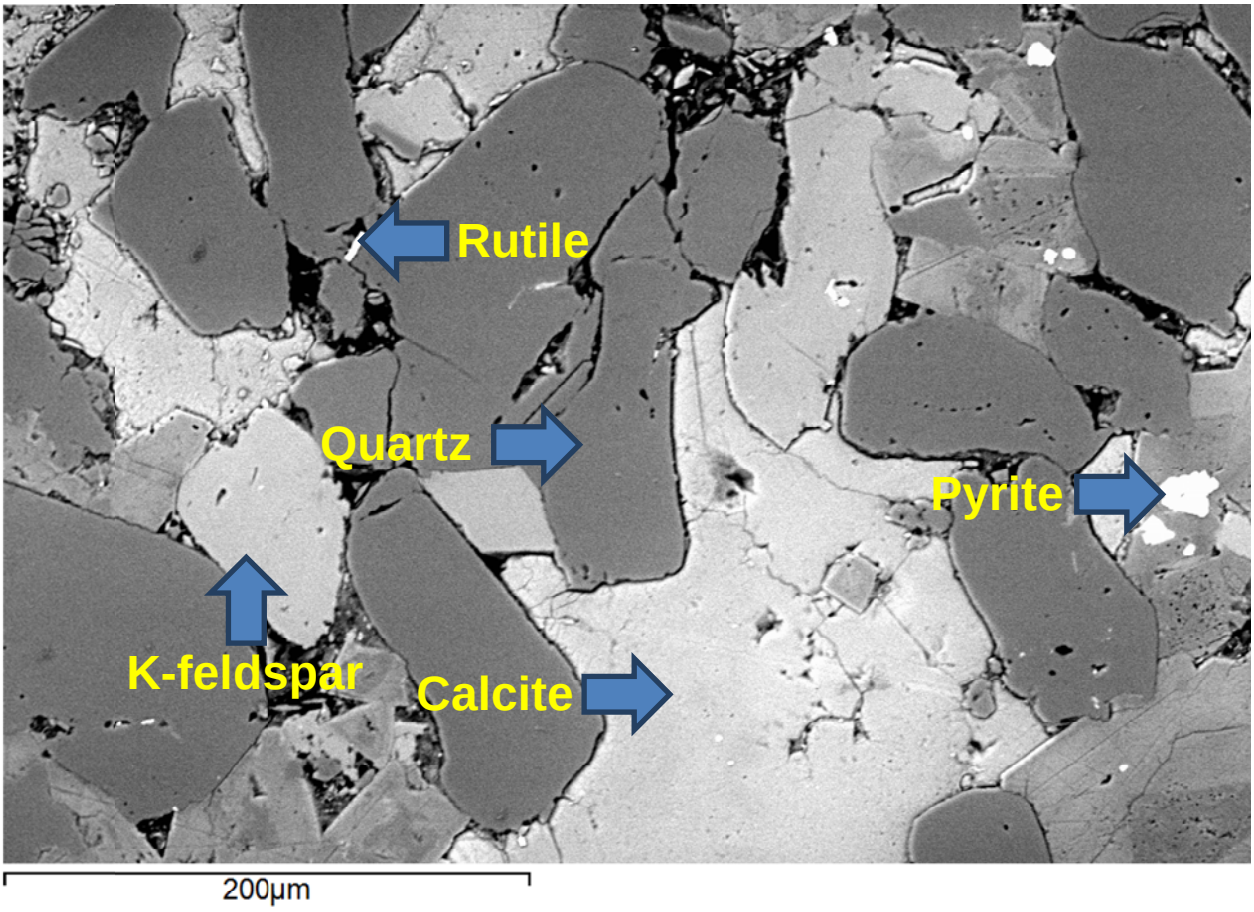

Additional High-Magnification BSE Images

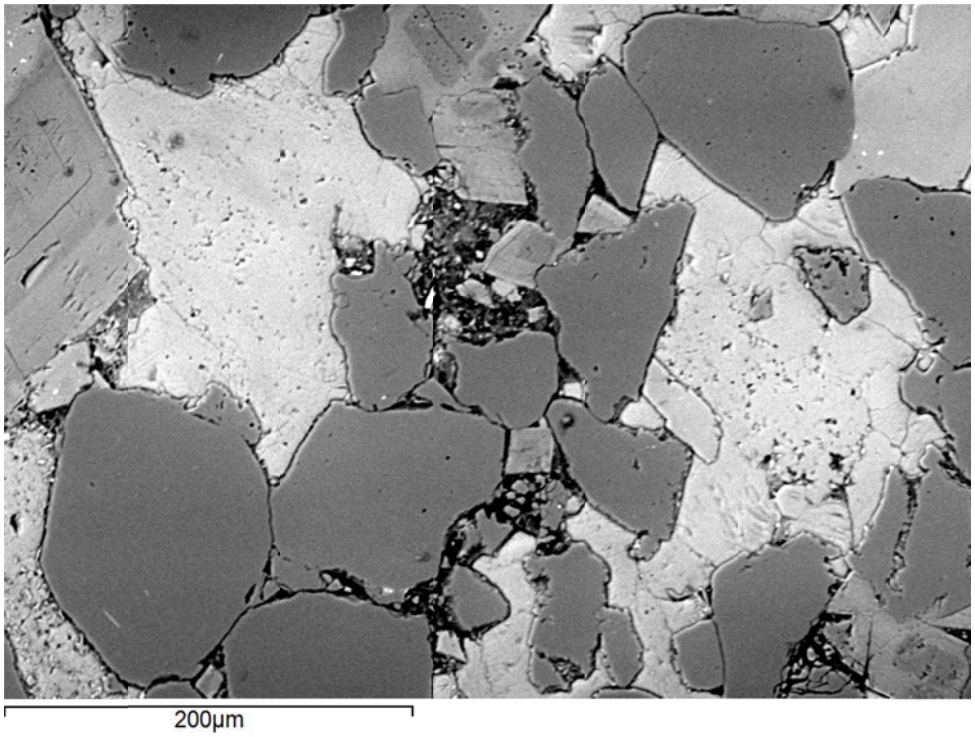

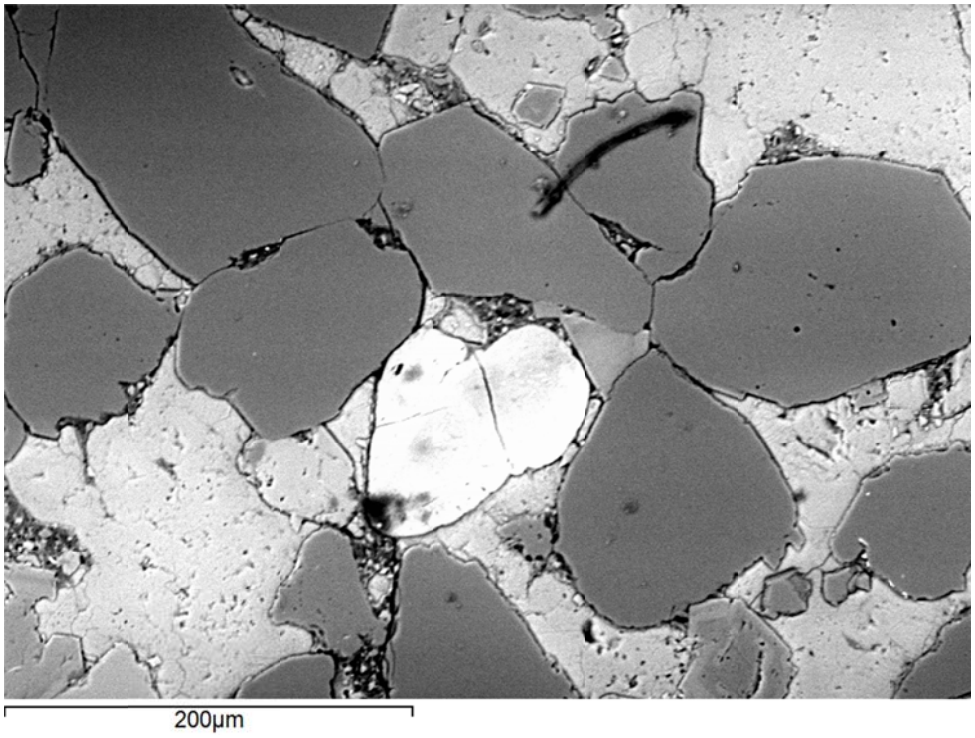

	Applied Geology Laboratory		ID: 116983
	Well Name: NDIC No. 8850	Middle Bakken 2	Rival Field
	API No.: 33-013-00867-00-02	Lithology: Calcareous to dolomitic siltstone	Depth: 7420.0'

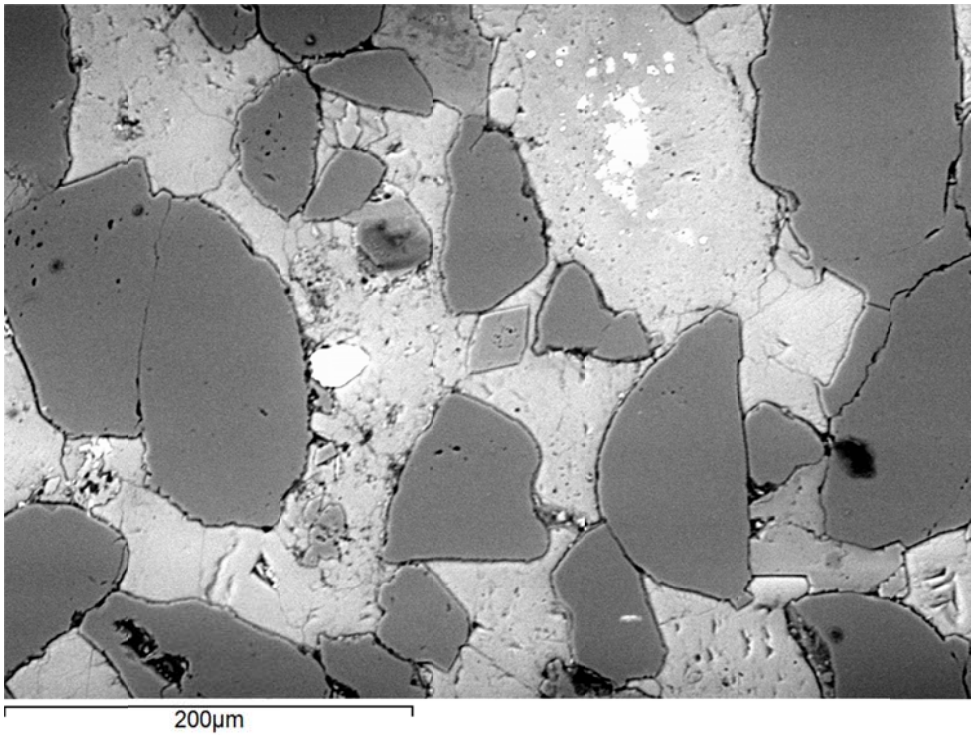

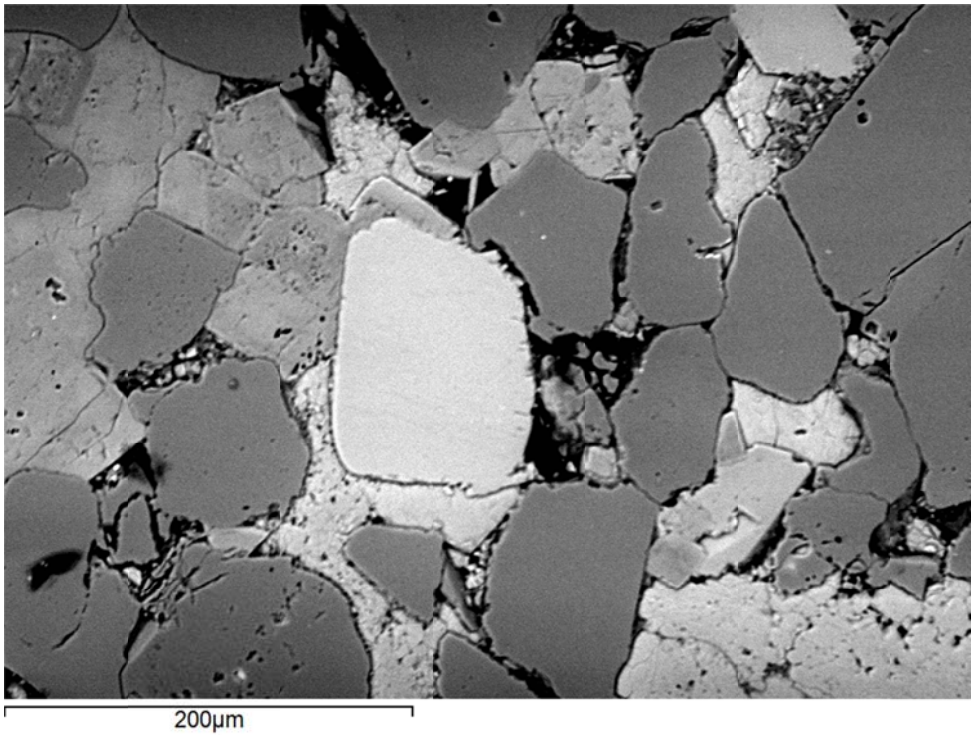

	Applied Geology Laboratory		ID: 116983
	Well Name: NDIC No. 8850	Middle Bakken 2	Rival Field
	API No.: 33-013-00867-00-02	Lithology: Calcareous to dolomitic siltstone	Depth: 7420.0'

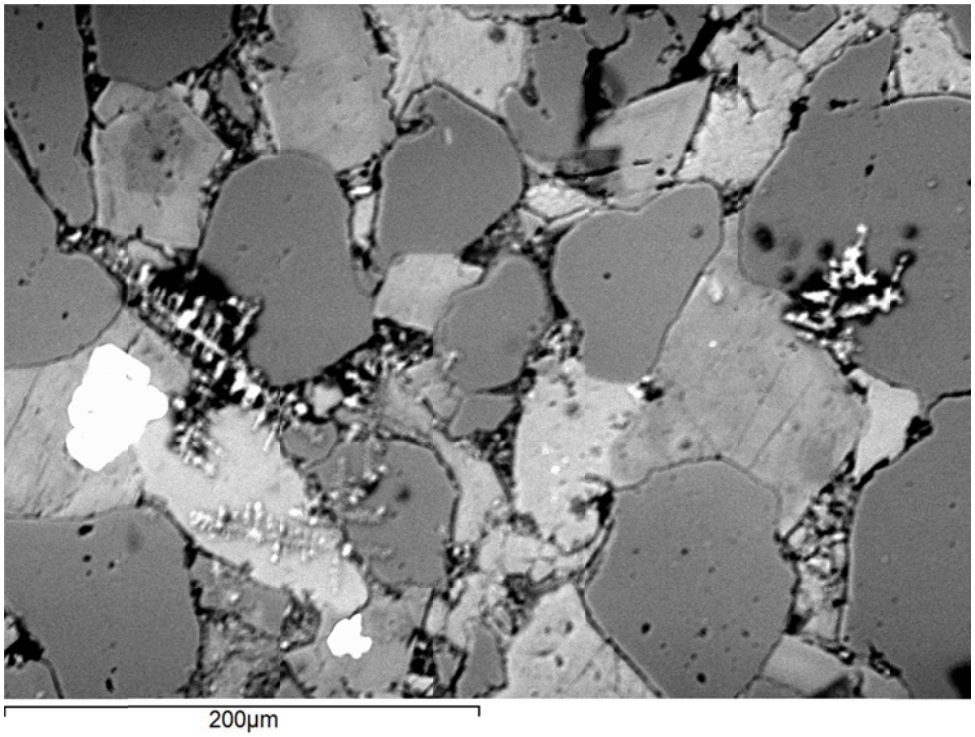

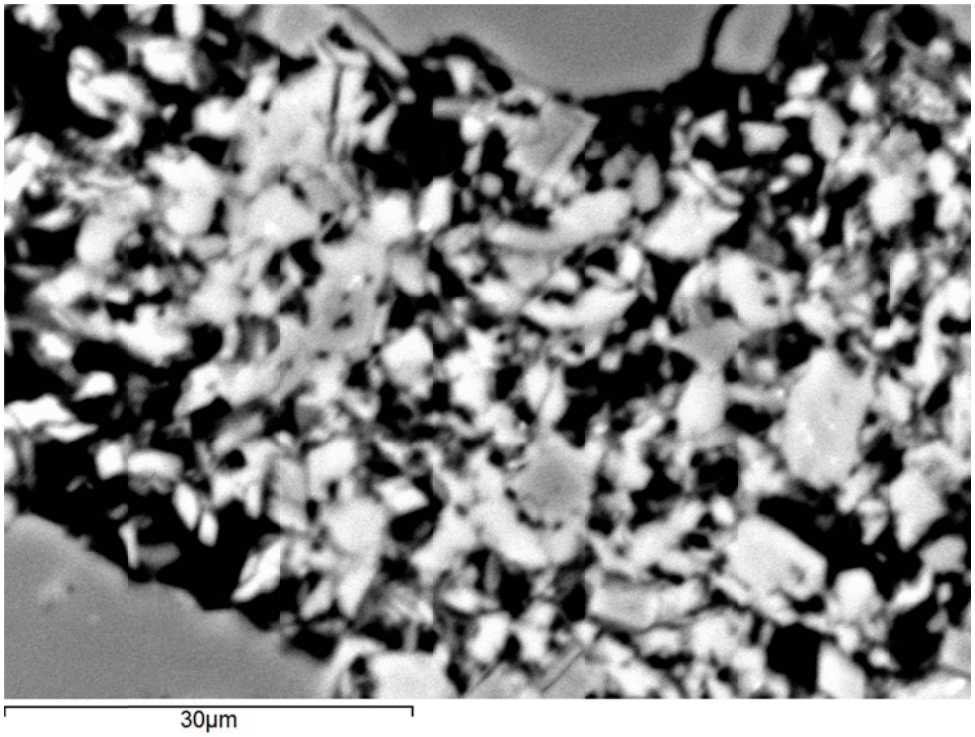

	Applied Geology Laboratory		ID: 116983
	Well Name: NDIC No. 8850	Middle Bakken 2	Rival Field
	API No.: 33-013-00867-00-02	Lithology: Calcareous to dolomitic siltstone	Depth: 7420.0'

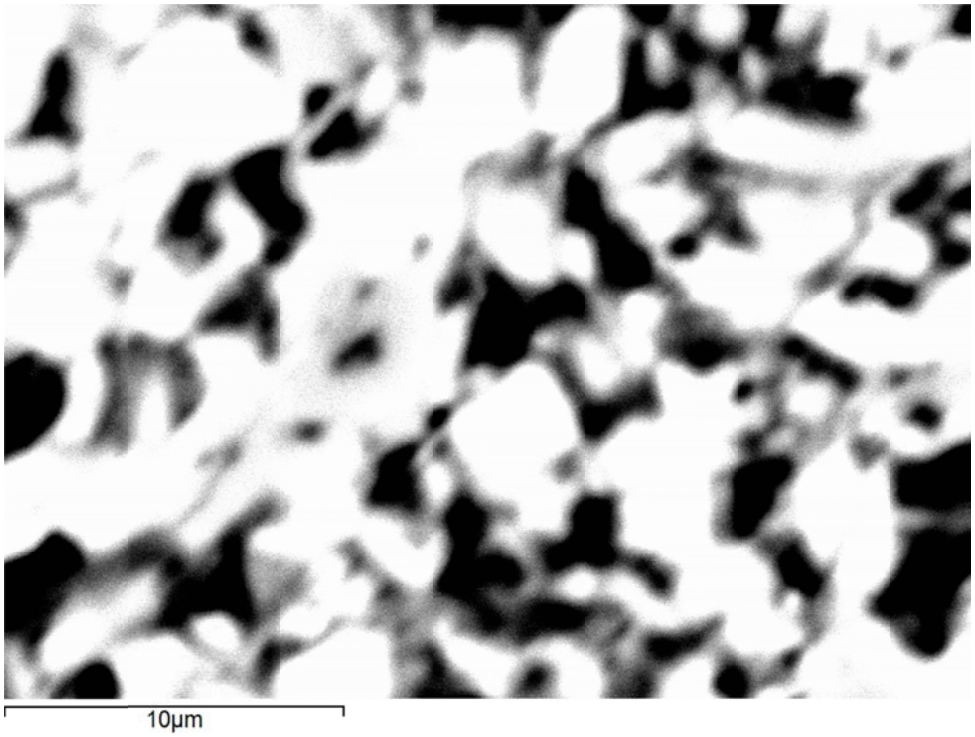

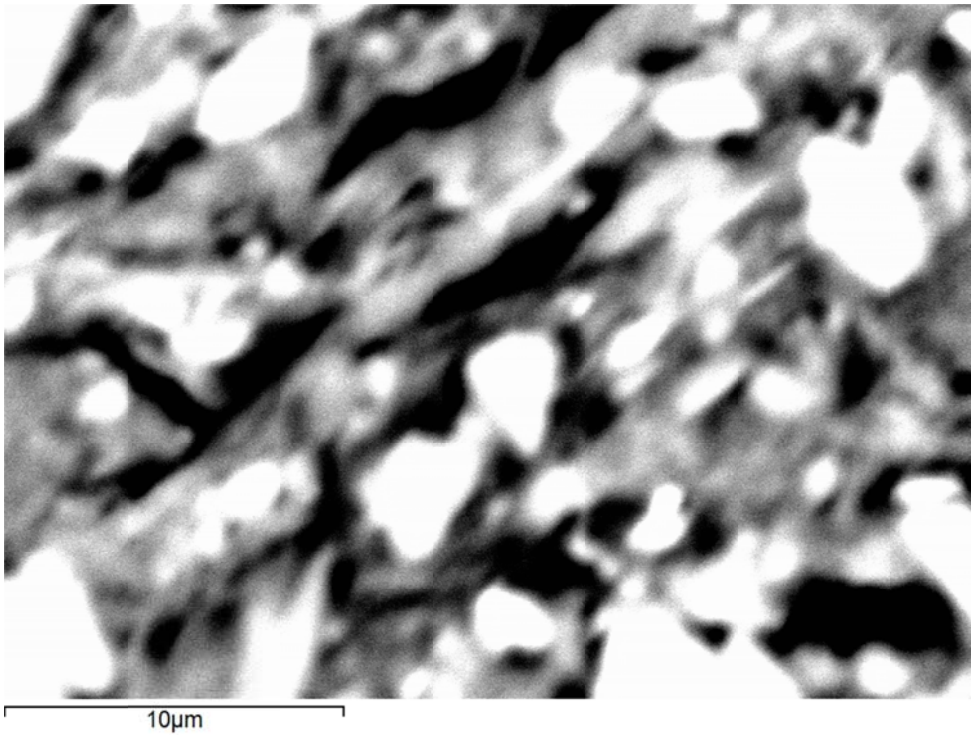

This page intentionally left blank.

EERC Energy & Environmental Research Center® Putting Research into Practice UND THE UNIVERSITY OF NORTH DAKOTA	**Applied Geology Laboratory**		ID: 116984
	Well Name: NDIC No. 8850	Middle Bakken 1	Rival Field
	API No.: 33-013-00867-00-03	Lithology: Calcareous, argillaceous siltstone	Depth: 7450.0'

SAMPLE PHOTOGRAPH

EERC Energy & Environmental Research Center® Putting Research into Practice UND THE UNIVERSITY OF NORTH DAKOTA	**Applied Geology Laboratory**		ID: 116984
	Well Name: NDIC No. 8850	Middle Bakken 1	Rival Field
	API No.: 33-013-00867-00-03	Lithology: Calcareous, argillaceous siltstone	Depth: 7450.0'

PHOTOMICROGRAPHS

Transmission

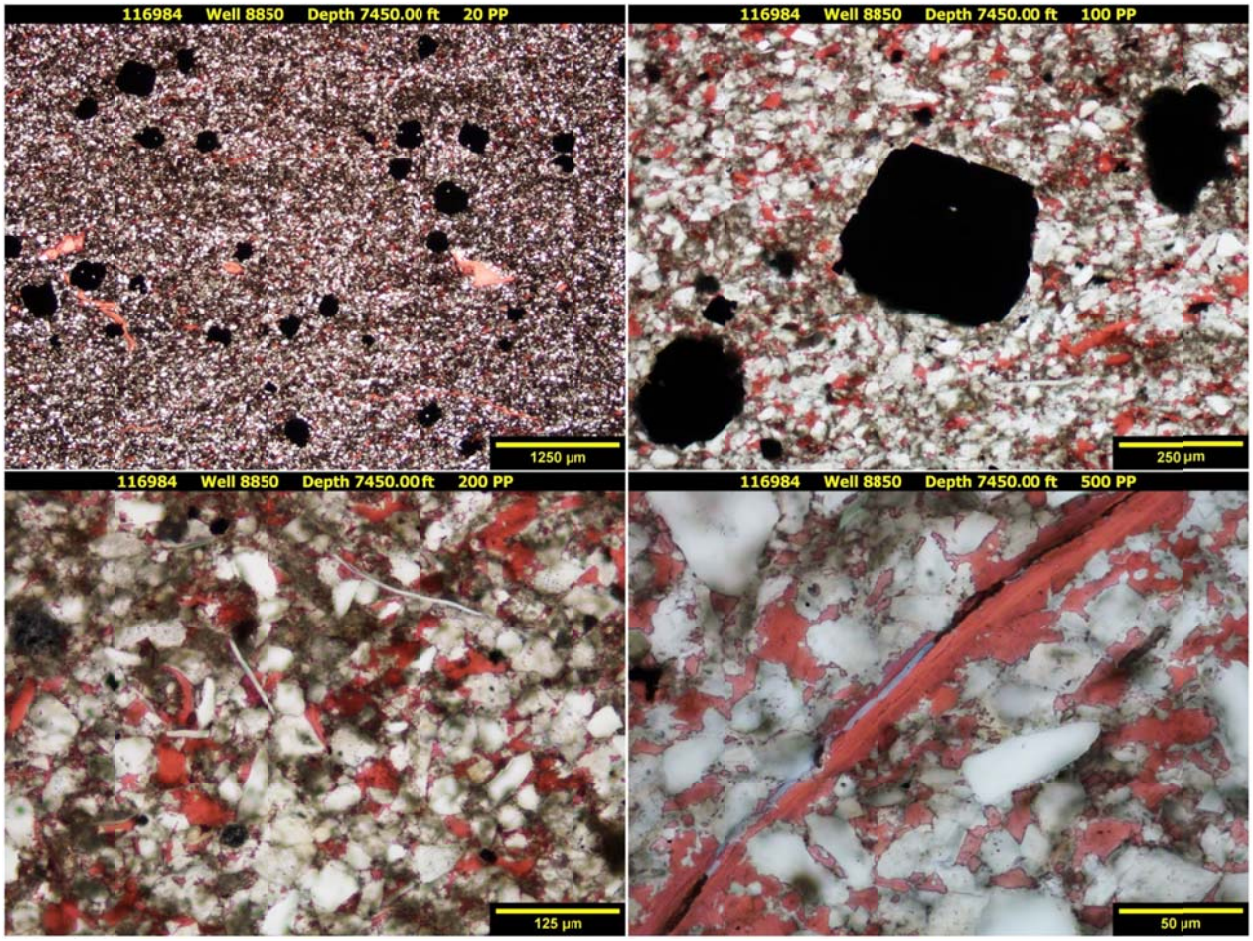

The sample captured at a depth of 7450.00 ft is a calcareous, argillaceous siltstone. It is a massive sample expressing moderate bedding structures (faint burrowing is observed). Very fine grained, angular to subrounded, monocrystalline quartz grains and trace amounts of muscovite are disseminated throughout. Anhederal to euhedral dolomitization has occurred throughout the sample. Abundant fine-grained crystalline dolomite occurs as replacement of largely lime mud. Skeletal and non-skeletal calcite remains. Disseminated medium-size replacement pyrite grains are zonally concentrated, forming a faint band. The matrix is composed of a combination of clays, micro- to cryptocrystalline dolomite, and sparry calcite. Organics detection is rare and is usually associated with pyrite grains. Trace occurrences of particle-based porosity are detected. No fractures are detected.

	Applied Geology Laboratory		ID: 116984
EERC Energy & Environmental Research Center® Putting Research into Practice UND THE UNIVERSITY OF NORTH DAKOTA	Well Name: NDIC No. 8850	Middle Bakken 1	Rival Field
	API No.: 33-013-00867-00-03	Lithology: Calcareous, argillaceous siltstone	Depth: 7450.0'

Reflection

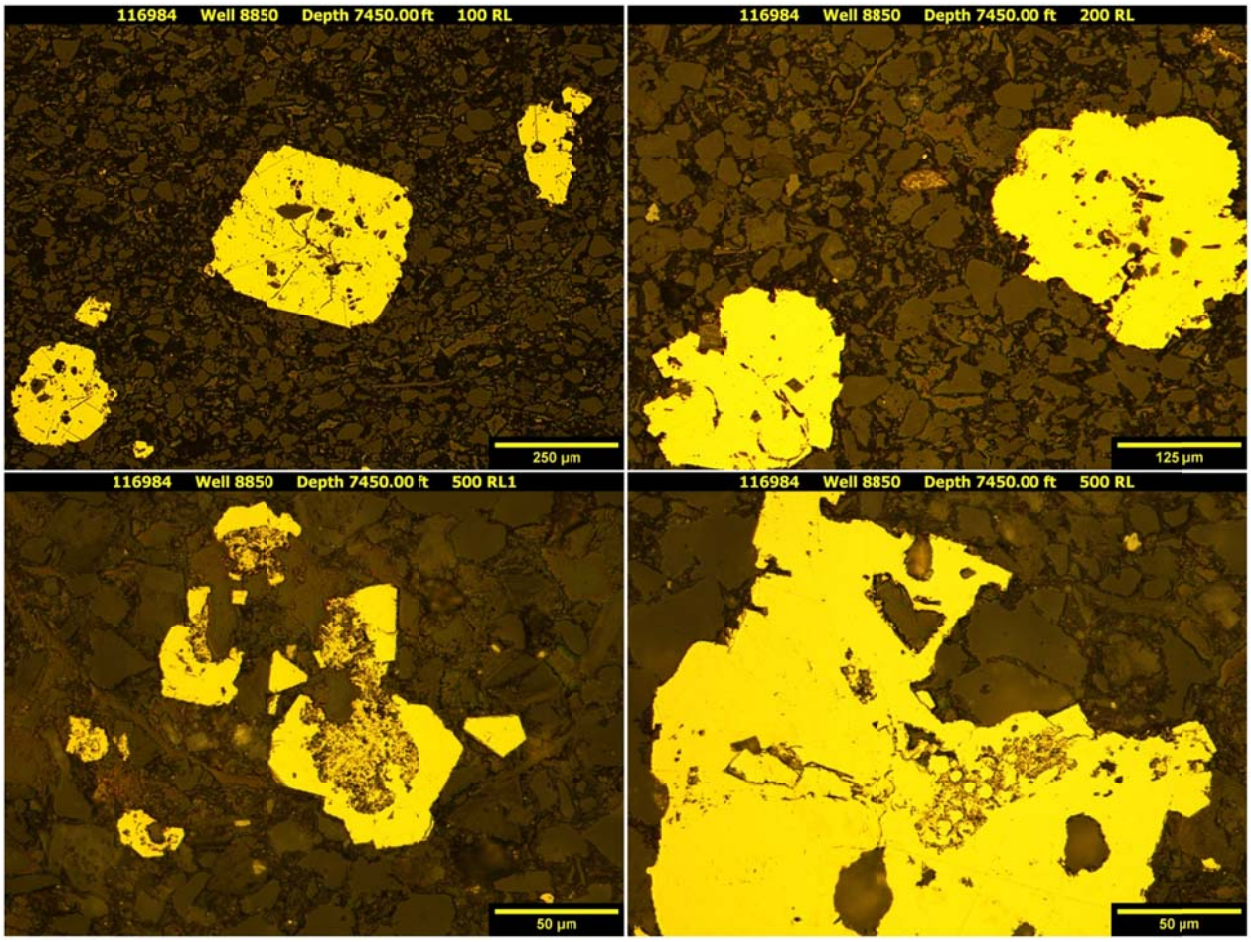

The sample from a depth of 7450.00 ft displays only euhedral pyrite mineralization. This diagenetic growth likely acts as both a pore filler and as grain replacement. Euhedral grains are very fine to medium-grained. A higher horizontal concentration of euhedral pyrite grains creates a weak band or faint lamination.

EERC Energy & Environmental Research Center® Putting Research into Practice UND THE UNIVERSITY OF NORTH DAKOTA	**Applied Geology Laboratory**		ID: 116984
	Well Name: NDIC No. 8850	Middle Bakken 1	Rival Field
	API No.: 33-013-00867-00-03	Lithology: Calcareous, argillaceous siltstone	Depth: 7450.0'

Transmission and Fluorescence Whole-Slide Images

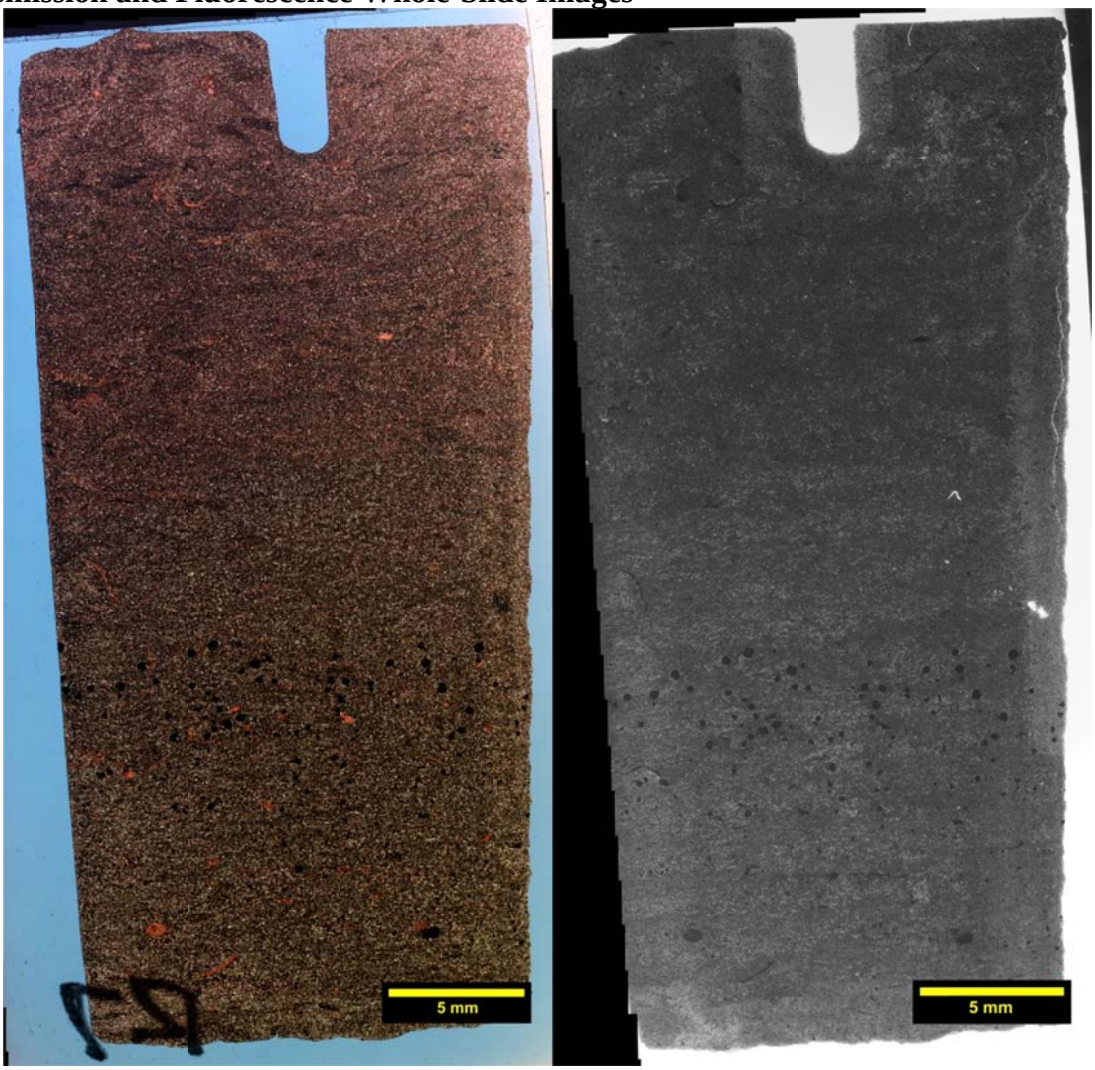

The sample at a depth of 7450.0 ft is a massive sample expressing only slight bedding features. Very little inter-particle micro-porosity is observed. This tightness is because of the small grain sizes and abundant carbonate cements. Trace macro-porosity is observed (middle-right side). This location was occupied by organics. Some of that organic was removed during the sample preparation process, leaving noticeable pore space. No natural fractures are observed. A vertical induced fracture is noted.

EERC Energy & Environmental Research Center® Putting Research into Practice UND THE UNIVERSITY OF NORTH DAKOTA	**Applied Geology Laboratory**		ID: 116984
	Well Name: NDIC No. 8850	Middle Bakken 1	Rival Field
	API No.: 33-013-00867-00-03	Lithology: Calcareous, argillaceous siltstone	Depth: 7450.0'

XRF BULK CHEMICAL COMPOSITION

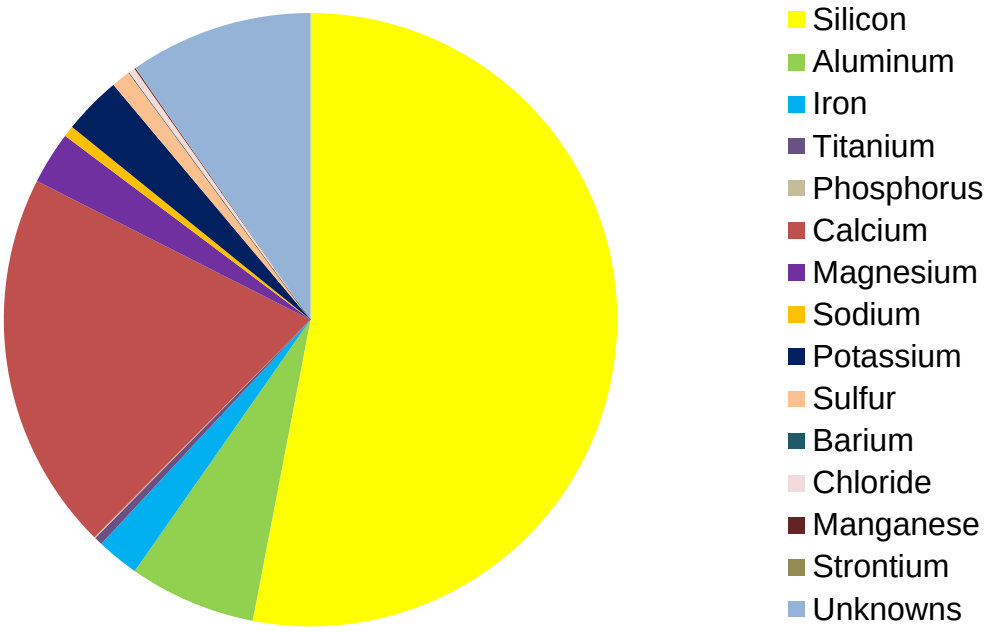

Element	Reporting Convention (Oxide)	Weight %
Si (silicon)	SiO_2	53.03
Al (aluminum)	Al_2O_3	6.69
Fe (iron)	Fe_2O_3	2.24
Ti (titanium)	TiO_2	0.43
P (phosphorus)	P_2O_5	0.06
Ca (calcium)	CaO	20.03
Mg (magnesium)	MgO	2.76
Na (sodium)	Na_2O	0.59
K (potassium)	K_2O	3.07
S (sulfur)	SO_3	1.03
Ba (barium)	BaO	0.00
Cl (chloride)	Cl	0.34
Mn (manganese)	MnO	0.06
Sr (strontium)	SrO	0.02
Unknowns	Due to the presence of carbonates	9.66
Total		100.01

EERC Energy & Environmental Research Center® Putting Research into Practice UND THE UNIVERSITY OF NORTH DAKOTA	**Applied Geology Laboratory**		ID: 116984
	Well Name: NDIC No. 8850	Middle Bakken 1	Rival Field
	API No.: 33-013-00867-00-03	Lithology: Calcareous, argillaceous siltstone	Depth: 7450.0'

XRD MINERAL PHASE DISTRIBUTION

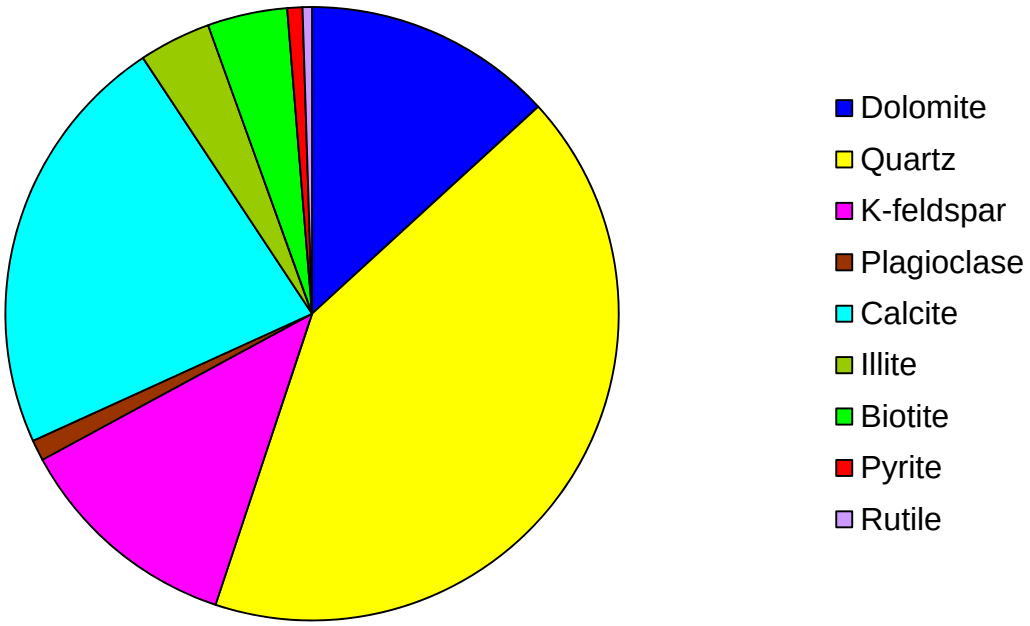

Mineral Phase	Formula	Weight %
Dolomite	$CaMg(CO_3)_2$	13.2
Quartz	SiO_2	41.9
K-feldspar	$KAlSi_3O_8$	12.0
Plagioclase	$Na_{0.5}Ca_{0.5}Al_{1.5}Si_{2.5}O_8$	1.1
Calcite	$CaCO_3$	22.5
Illite	$(K,H_3O)(Al,Mg,Fe)_2(Si,Al)_4O_{10}[(OH)_2,(H_2O)]$	3.8
Biotite	$K(Mg,Fe)_3[(OH)_2AlSi_3O_{10}]$	4.2
Pyrite	FeS_2	0.8
Rutile	TiO_2	0.5

Applied Geology Laboratory		ID: 116984
Well Name: NDIC No. 8850	Middle Bakken 1	Rival Field
API No.: 33-013-00867-00-03	Lithology: Calcareous, argillaceous siltstone	Depth: 7450.0'

SEM

Observed Minerals

Mineral Phase	Mineral Phase
Calcite	Rutile
Quartz	Zircon
Pyrite	Albite
K-feldspar	Chromite
Dolomite	Apatite
Illite	Monazite
Biotite	

High-Magnification BSE Image Annotated with Examples of Mineral Phases Identified

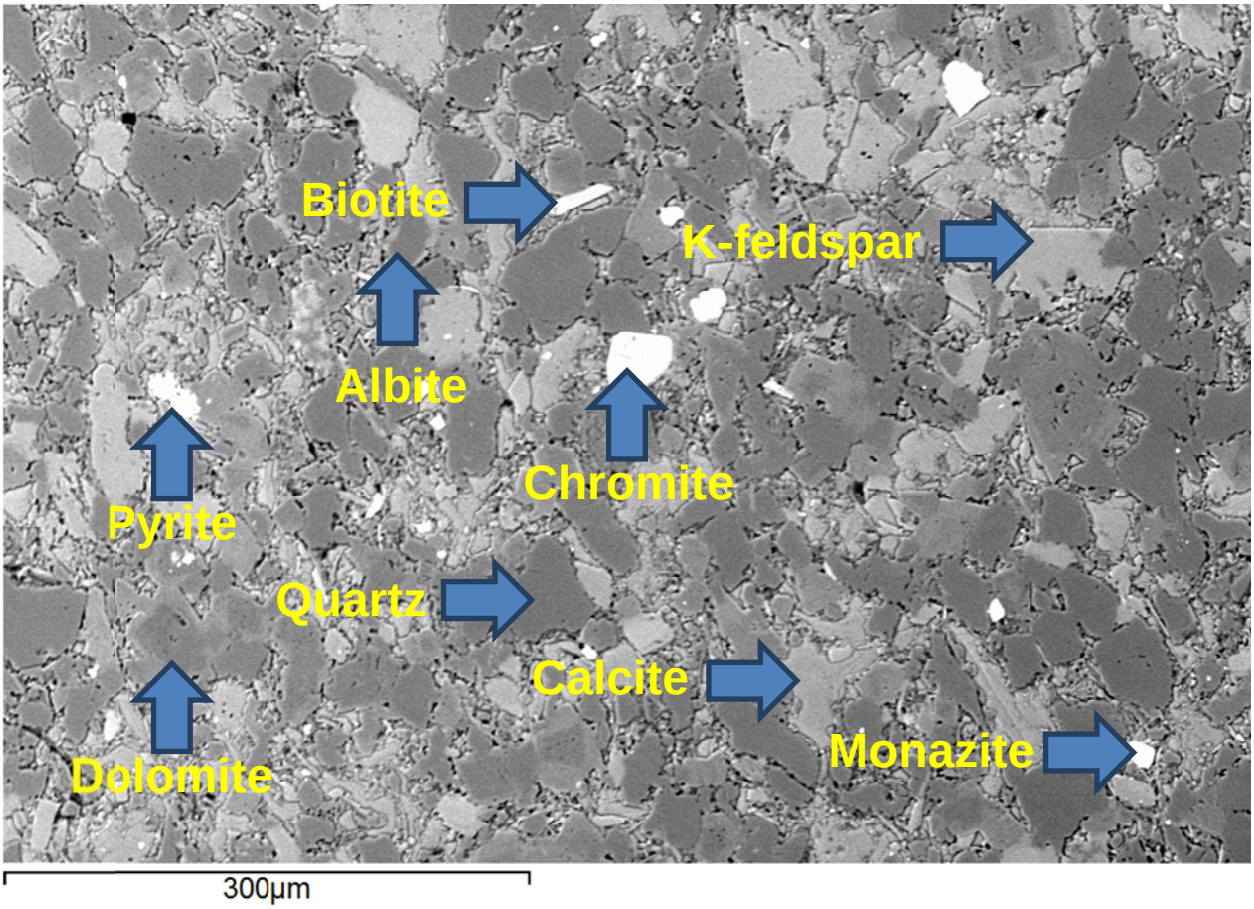

Additional High-Magnification BSE Images

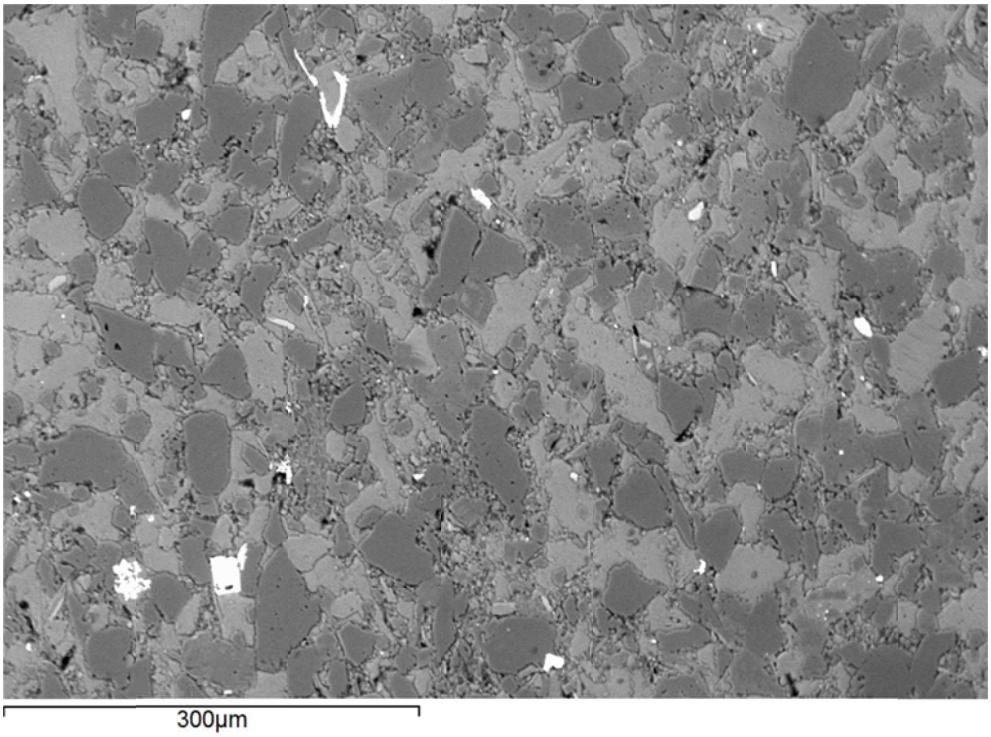

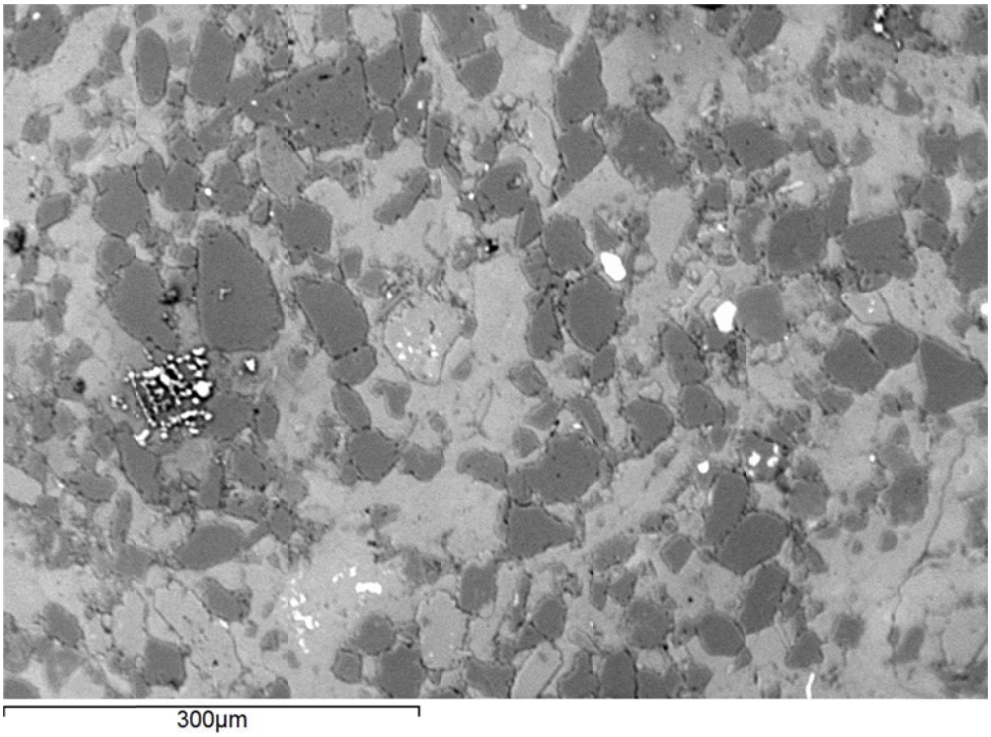

EERC Energy & Environmental Research Center® Putting Research into Practice UND THE UNIVERSITY OF NORTH DAKOTA	**Applied Geology Laboratory**		ID: 116984
	Well Name: NDIC No. 8850	Middle Bakken 1	Rival Field
	API No.: 33-013-00867-00-03	Lithology: Calcareous, argillaceous siltstone	Depth: 7450.0'

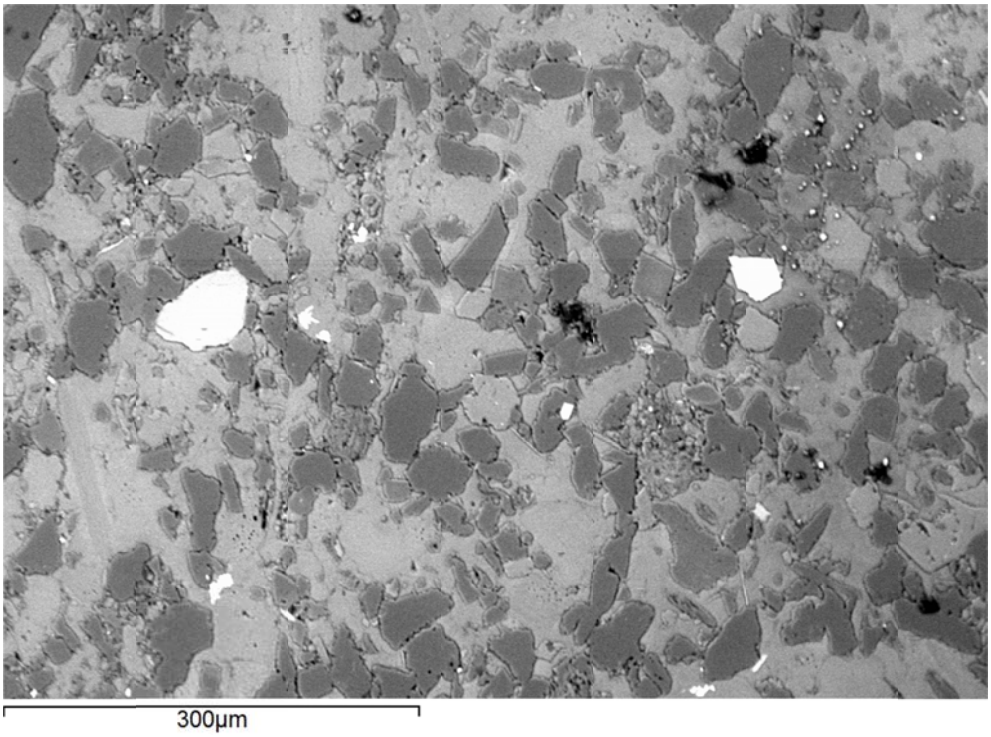

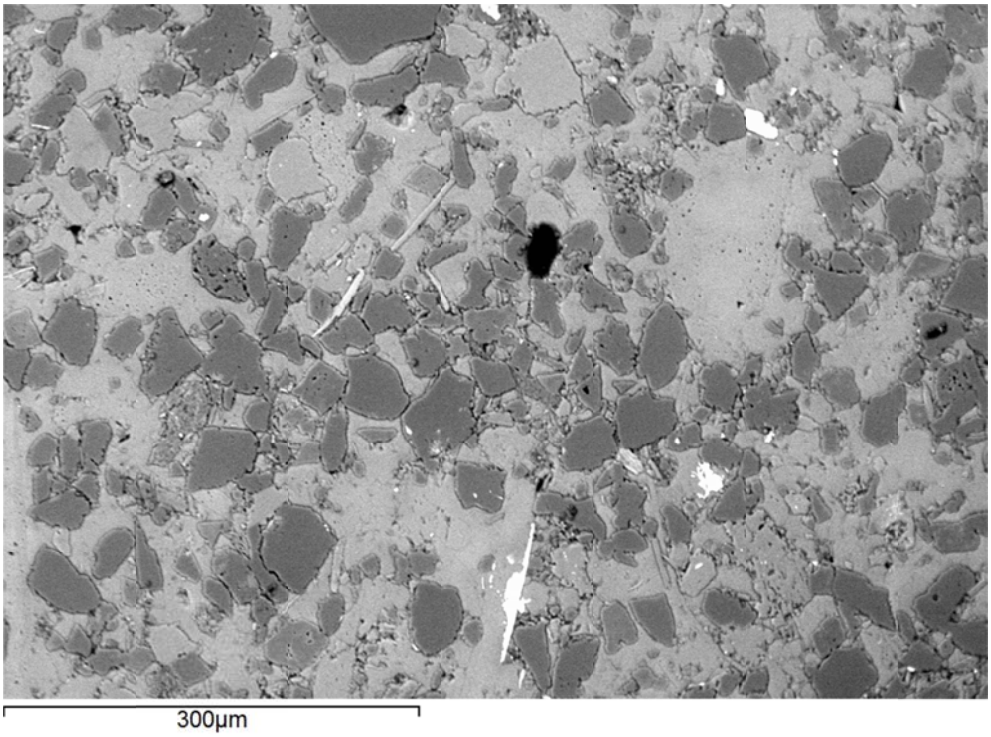

EERC Energy & Environmental Research Center® Putting Research into Practice UND THE UNIVERSITY OF NORTH DAKOTA	**Applied Geology Laboratory**		ID: 116984
	Well Name: NDIC No. 8850	Middle Bakken 1	Rival Field
	API No.: 33-013-00867-00-03	Lithology: Calcareous, argillaceous siltstone	Depth: 7450.0'

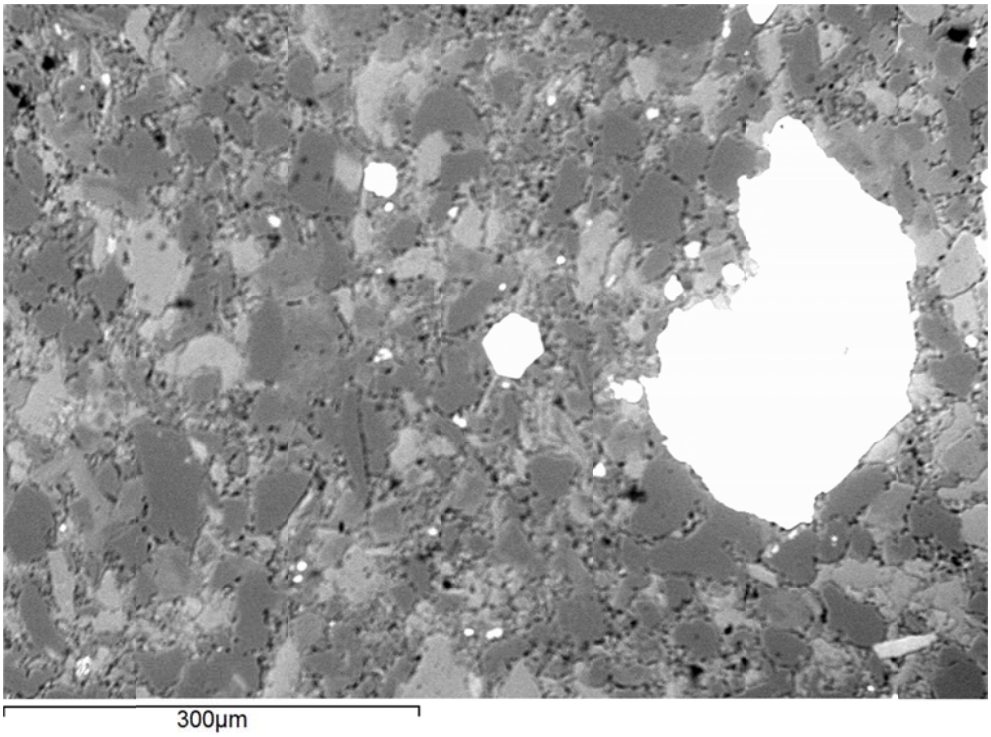

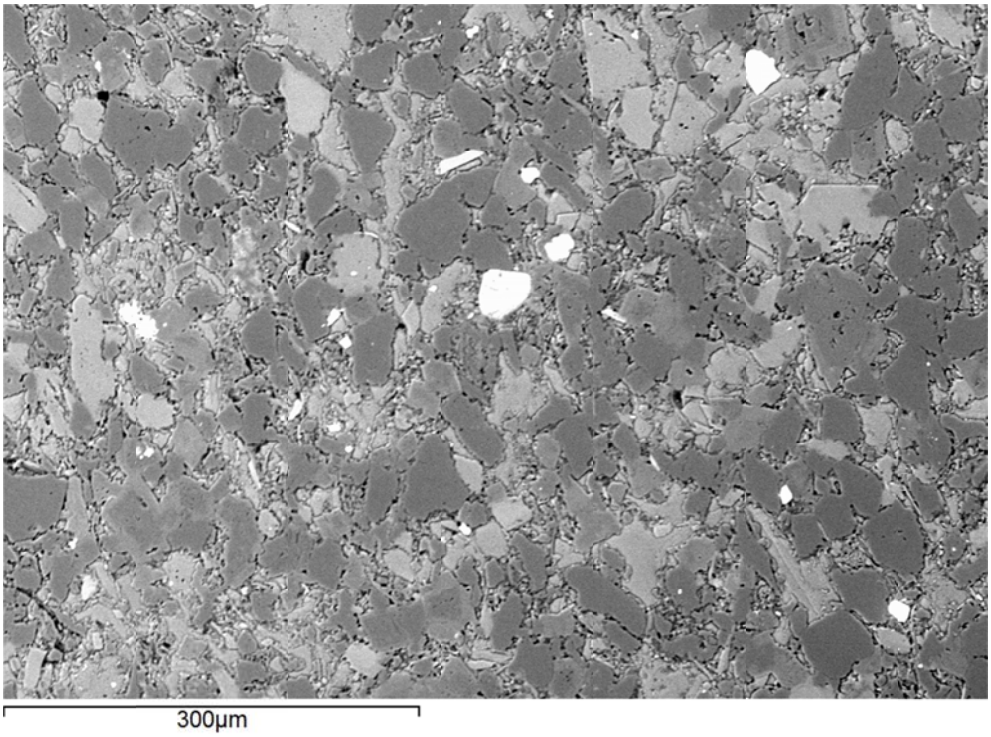

EERC Energy & Environmental Research Center® Putting Research into Practice UND THE UNIVERSITY OF NORTH DAKOTA	**Applied Geology Laboratory**		ID: 116984
	Well Name: NDIC No. 8850	Middle Bakken 1	Rival Field
	API No.: 33-013-00867-00-03	Lithology: Calcareous, argillaceous siltstone	Depth: 7450.0'

SEM Mineral Map Image Overlaid on BSE Image with Mineral Phase 2D Area Percentages

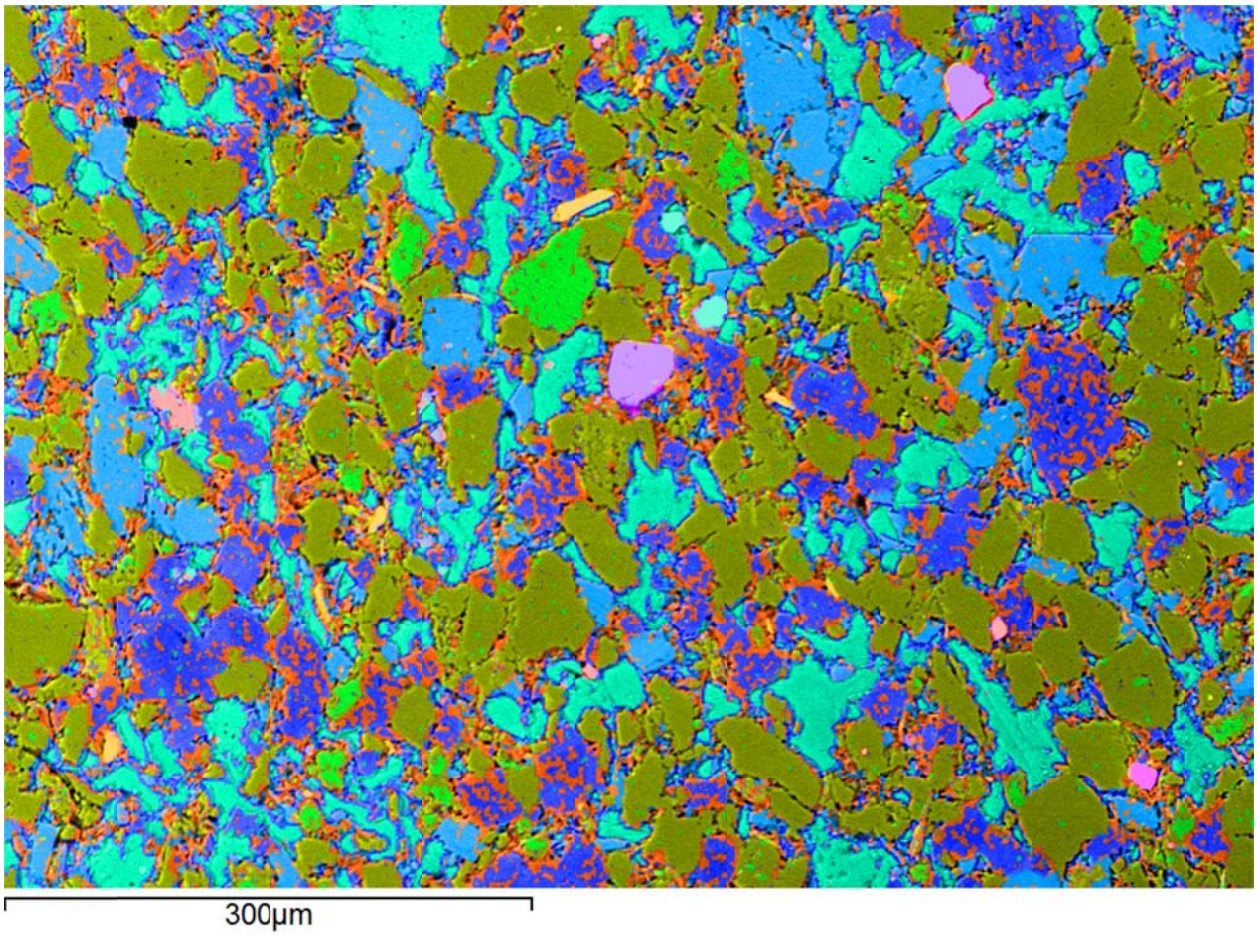

This page intentionally left blank.

EERC Energy & Environmental Research Center® Putting Research into Practice UND THE UNIVERSITY OF NORTH DAKOTA	**Applied Geology Laboratory**		ID: 116988
	Well Name: NDIC No. 9001	Middle Bakken 7	Rival Field
	API No.: 33-013-00877-00-00	Lithology: Silty, argillaceous dolostone	Depth: 7381.0'

SAMPLE PHOTOGRAPH

PHYSICAL PROPERTIES

Porosity and Grain Density by Core Laboratories

Pycnometer Effective Porosity, vol%	Grain Density, g/cm^3
6.11	2.761

EERC Energy & Environmental Research Center® Putting Research into Practice UND THE UNIVERSITY OF NORTH DAKOTA	**Applied Geology Laboratory**		ID: 116988
	Well Name: NDIC No. 9001	Middle Bakken 7	Rival Field
	API No.: 33-013-00877-00-00	Lithology: Silty, argillaceous dolostone	Depth: 7381.0'

PHOTOMICROGRAPHS

Transmission

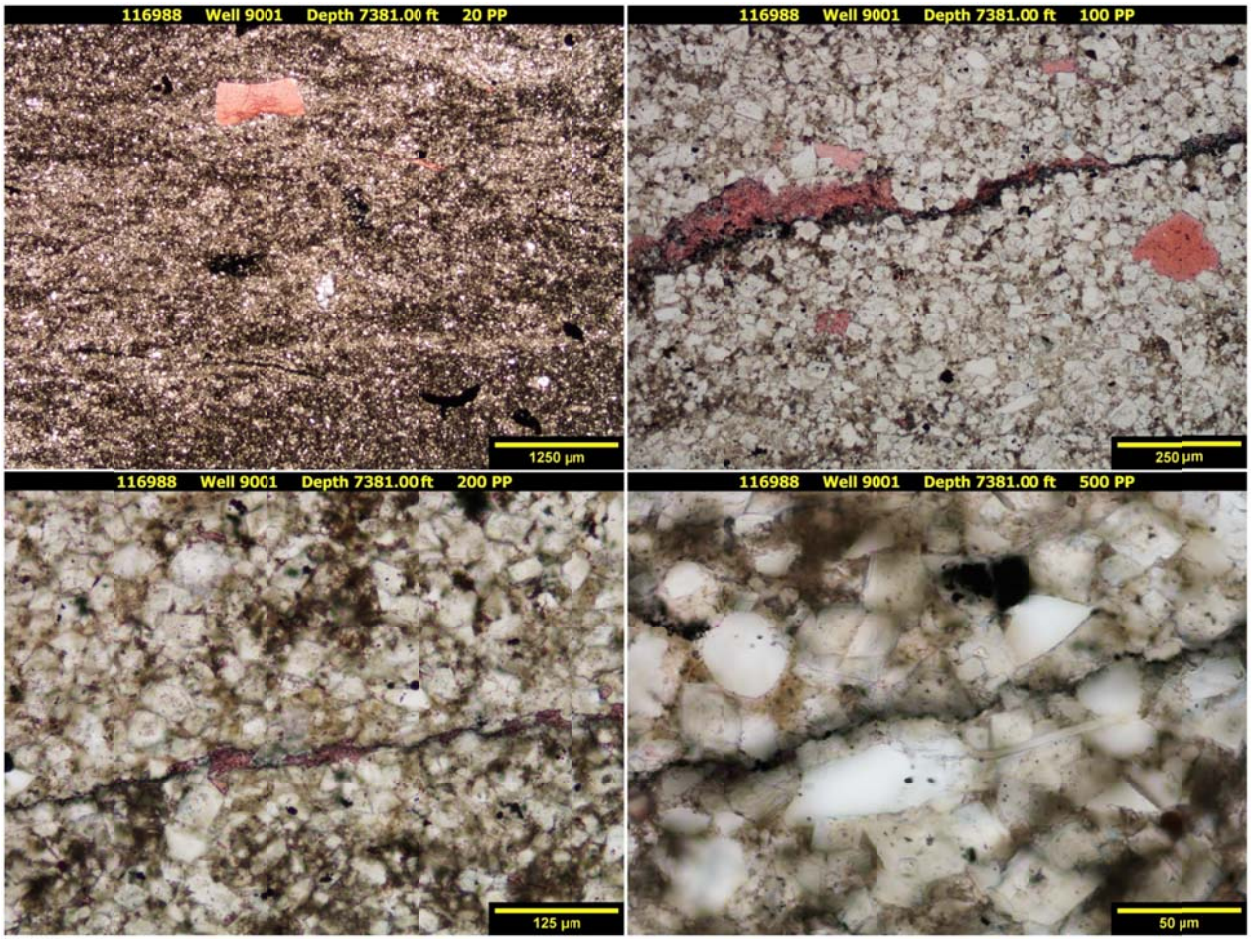

The sample from a depth of 7381.00 ft shows a silty, argillaceous dolostone. Some burrowing and wavy laminations are observed but the sample is largely massive. Very fine grained, angular to subangular, monocrystalline quartz and feldspar grains and trace amounts of muscovite are disseminated throughout. Extensive anhederal to euhedral dolomitization has occurred throughout the sample. Abundant fine-grained crystalline dolomite occurs as replacement of precursor carbonate grains and mud. Occasional sparry calcite cement and skeletal and non-skeletal grains remain. Disseminated pore-filling and replacement pyrite grains are observed throughout at small quantities. The matrix is composed of a combination of clays and micro- to cryptocrystalline dolomite and occasional calcite cement. Horizontal fractures are detected. Open fractures are likely because of the sampling process. Fractures filled with calcite, organics, clays, and pyrite are short and non-connecting. Additional organics are observed as globular and lensing features typically associated with pyrite. Other than potential open fractures, no porosity is observed using standard petrographic techniques.

EERC Energy & Environmental Research Center® Putting Research into Practice UND THE UNIVERSITY OF NORTH DAKOTA	**Applied Geology Laboratory**		ID: 116988
	Well Name: NDIC No. 9001	Middle Bakken 7	Rival Field
	API No.: 33-013-00877-00-00	Lithology: Silty, argillaceous dolostone	Depth: 7381.0'

Reflection

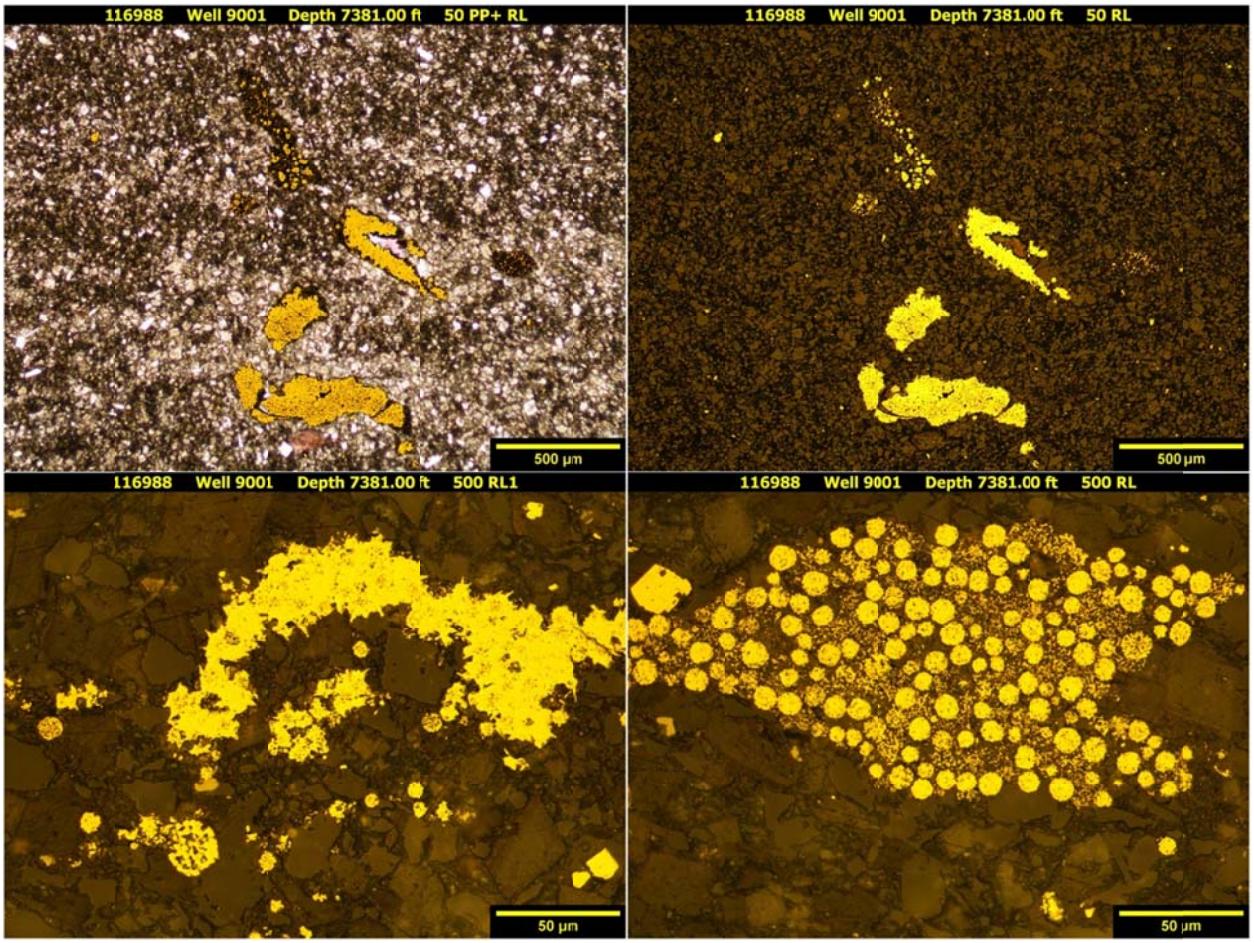

The sample from a depth of 7381.00 ft displays both euhedral and framboidal pyrite grains. Within this sample euhedral grains are typically replacing calcareous skeletal and non-skeletal grains. Partial to nearly complete pyritization of these precursor grains and organics have occurred. Framboidal grains are normally found within precursor pore and organic spaces. Occasional aggregates of semi-mature framboidal pyrite spheres are observed Organics observed are typically associated with framboidal pyrite.

EERC Energy & Environmental Research Center® Putting Research into Practice UND THE UNIVERSITY OF NORTH DAKOTA	**Applied Geology Laboratory**		ID: 116988
	Well Name: NDIC No. 9001	Middle Bakken 7	Rival Field
	API No.: 33-013-00877-00-00	Lithology: Silty, argillaceous dolostone	Depth: 7381.0'

Transmission and Fluorescence Whole-Slide Images

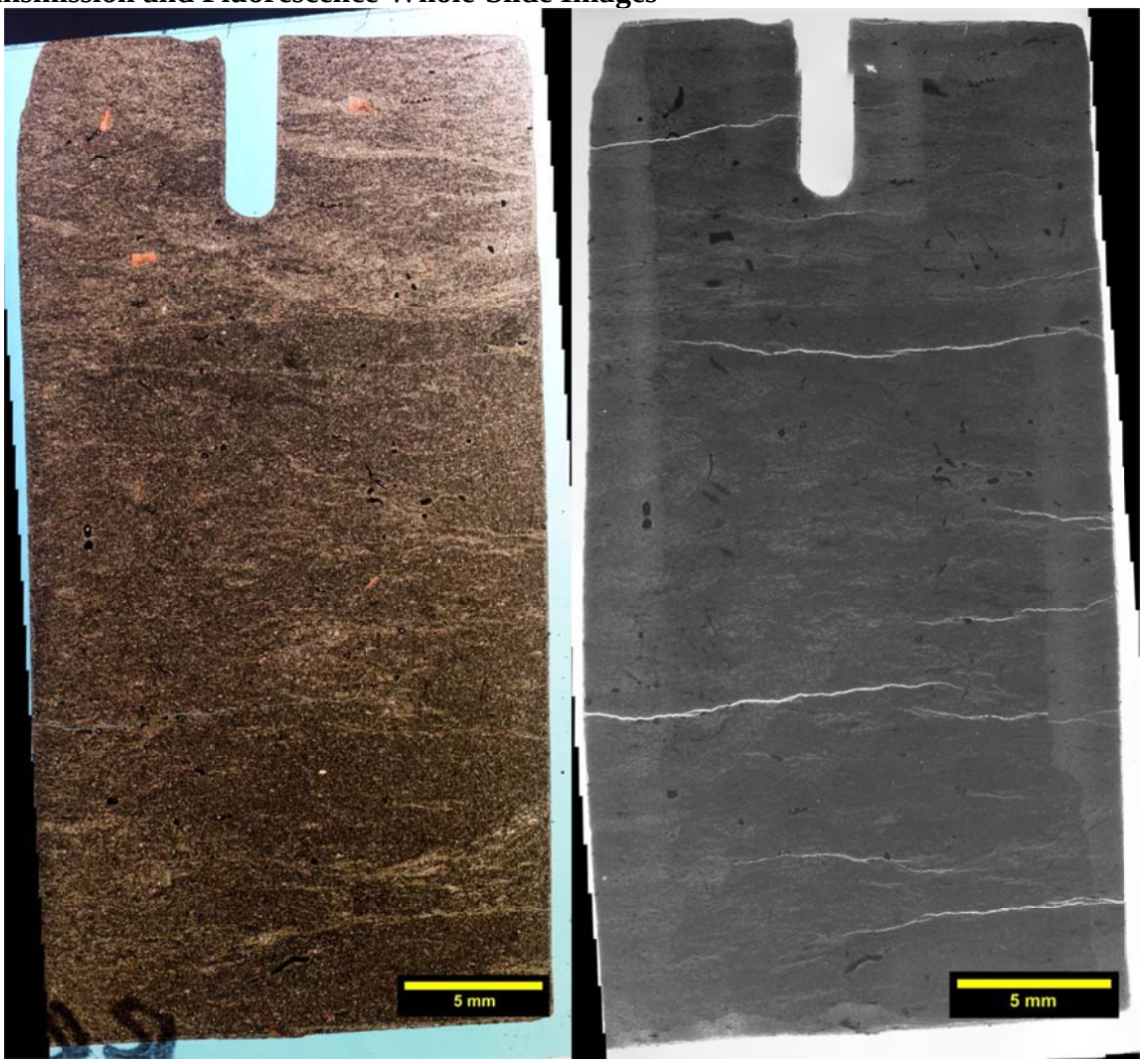

Image issues? The image collected from a depth of 7381.00 ft is a predominately massive silty, argillaceous dolostone. Effective porosity is reported at 6.11 vol%. Extensive interlocking anhedral to euhedral dolomitization and pyritization has occurred. These diagenetic events along consistent very fine grain sizes (except for skeletal and skeletal calcite grains and pyrite) and zonal concentrations of clay are limiting factors of pore size (<30 µm) and distribution. No naturally-occurring open fractures are observed. Induced horizontal fractures are likely the product of the sampling process. Though unnatural, they may provide insight to structural stability within this interval.

EERC Energy & Environmental Research Center® Putting Research into Practice UND THE UNIVERSITY OF NORTH DAKOTA	**Applied Geology Laboratory**		ID: 116988
	Well Name: NDIC No. 9001	Middle Bakken 7	Rival Field
	API No.: 33-013-00877-00-00	Lithology: Silty, argillaceous dolostone	Depth: 7381.0'

XRF BULK CHEMICAL COMPOSITION

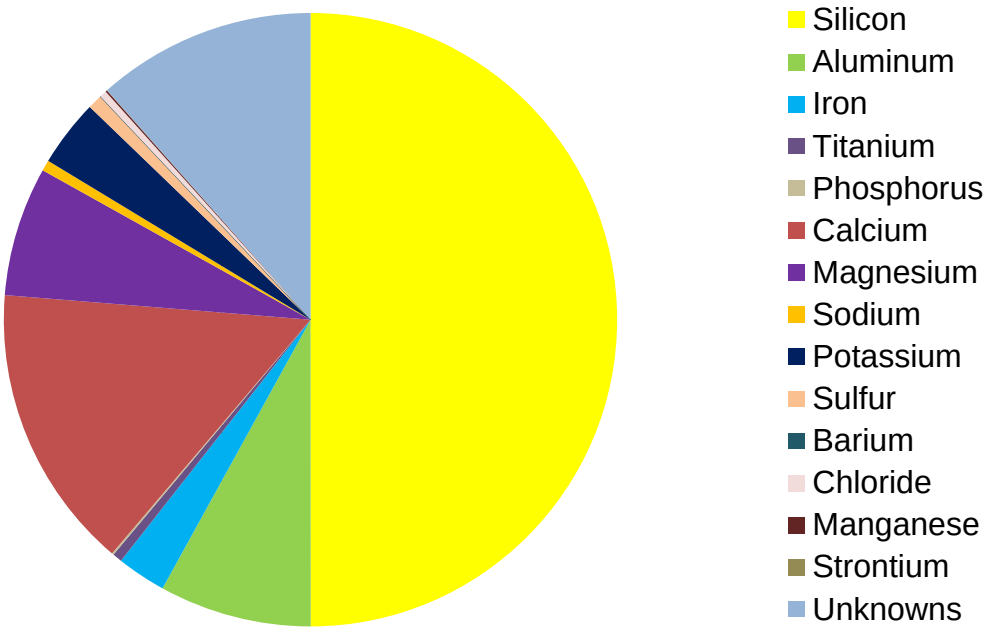

Element	Reporting Convention (Oxide)	Weight %
Si (silicon)	SiO_2	49.99
Al (aluminum)	Al_2O_3	8.02
Fe (iron)	Fe_2O_3	2.59
Ti (titanium)	TiO_2	0.51
P (phosphorus)	P_2O_5	0.10
Ca (calcium)	CaO	15.07
Mg (magnesium)	MgO	6.82
Na (sodium)	Na_2O	0.57
K (potassium)	K_2O	3.54
S (sulfur)	SO_3	0.77
Ba (barium)	BaO	0.00
Cl (chloride)	Cl	0.37
Mn (manganese)	MnO	0.09
Sr (strontium)	SrO	0.01
Unknowns	Due to the presence of carbonates	11.55
Total		100.00

EERC Energy & Environmental Research Center® Putting Research into Practice UND THE UNIVERSITY OF NORTH DAKOTA	**Applied Geology Laboratory**		ID: 116988
	Well Name: NDIC No. 9001	Middle Bakken 7	Rival Field
	API No.: 33-013-00877-00-00	Lithology: Silty, argillaceous dolostone	Depth: 7381.0'

XRD MINERAL PHASE DISTRIBUTION

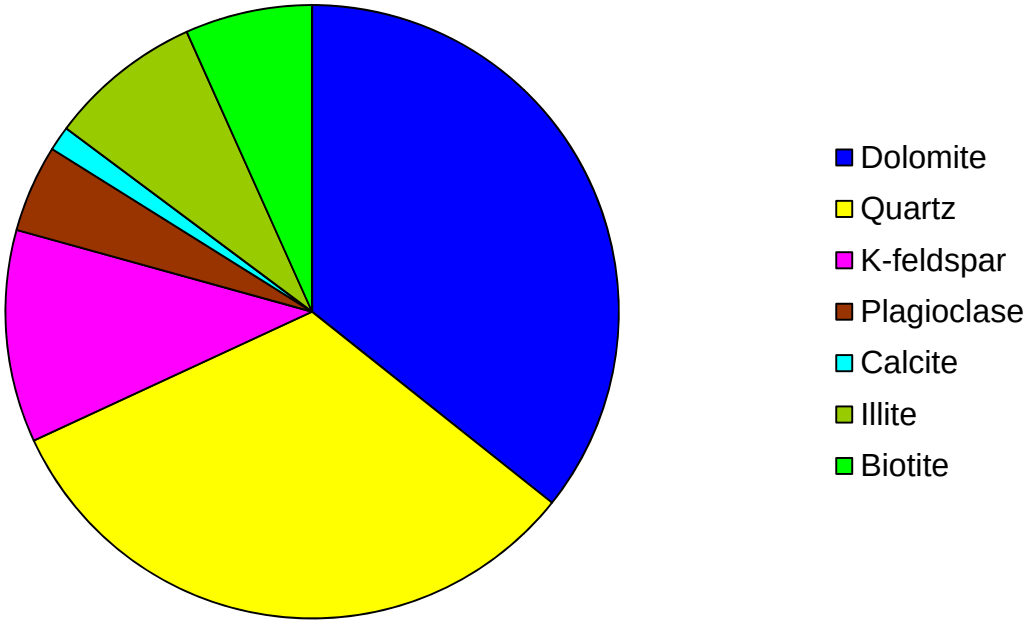

Mineral Phase	Formula	Weight %
Dolomite	$CaMg(CO_3)_2$	35.7
Quartz	SiO_2	32.4
K-feldspar	$KAlSi_3O_8$	11.2
Plagioclase	$Na_{0.5}Ca_{0.5}Al_{1.5}Si_{2.5}O_8$	4.6
Calcite	$CaCO_3$	1.3
Illite	$(K,H_3O)(Al,Mg,Fe)_2(Si,Al)_4O_{10}[(OH)_2,(H_2O)]$	8.1
Biotite	$K(Mg,Fe)_3[(OH)_2AlSi_3O_{10}]$	6.7

EERC Energy & Environmental Research Center® Putting Research into Practice UND THE UNIVERSITY OF NORTH DAKOTA	**Applied Geology Laboratory**		ID: 116988
	Well Name: NDIC No. 9001	Middle Bakken 7	Rival Field
	API No.: 33-013-00877-00-00	Lithology: Silty, argillaceous dolostone	Depth: 7381.0'

SEM

Observed Minerals

Mineral Phase	Mineral Phase
Calcite	Biotite
Pyrite	Dolomite
Quartz	Rutile
Apatite	Albite
K-feldspar	Zircon
Illite	

High-Magnification BSE Image Annotated with Examples of Mineral Phases Identified

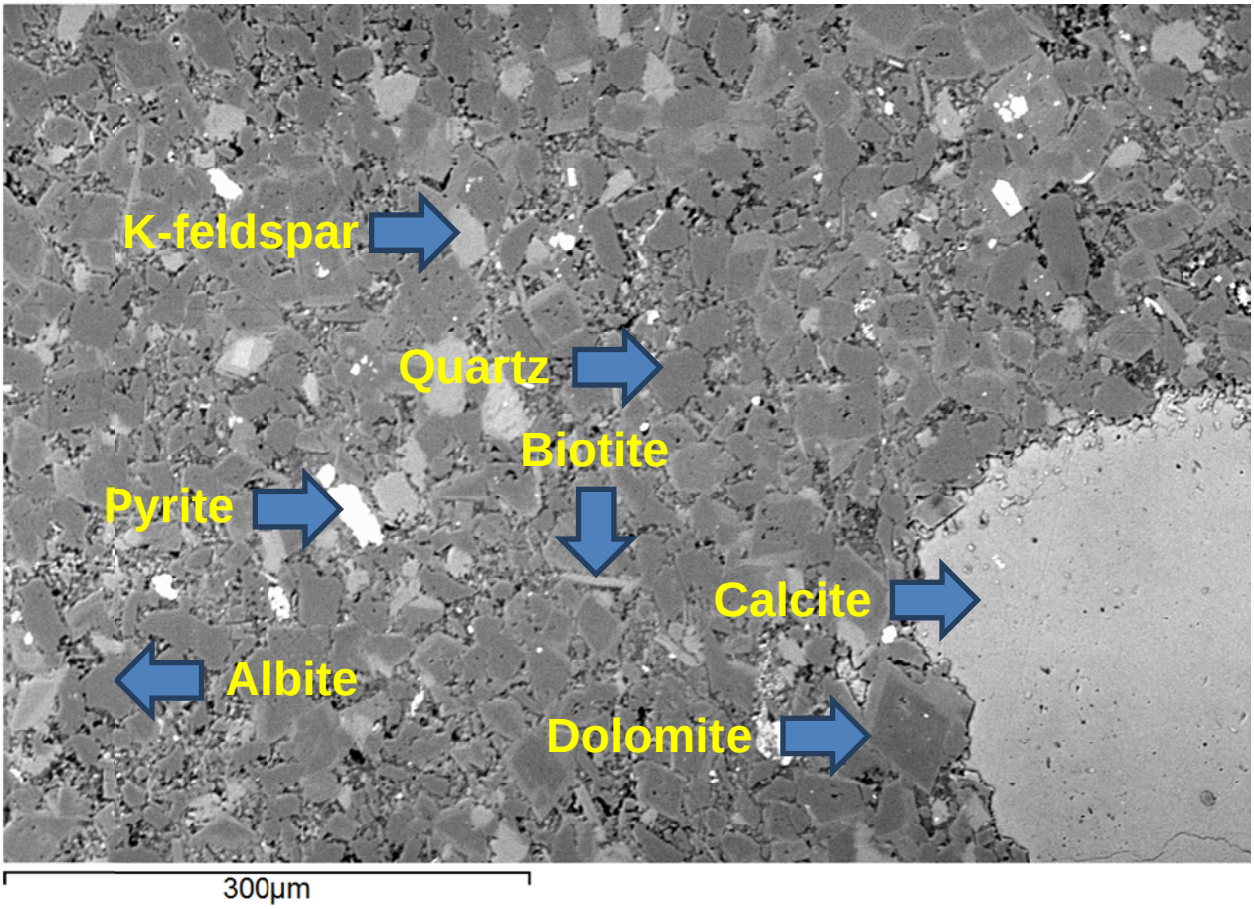

	Applied Geology Laboratory		ID: 116988
	Well Name: NDIC No. 9001	Middle Bakken 7	Rival Field
	API No.: 33-013-00877-00-00	Lithology: Silty, argillaceous dolostone	Depth: 7381.0'

Additional High-Magnification BSE Images

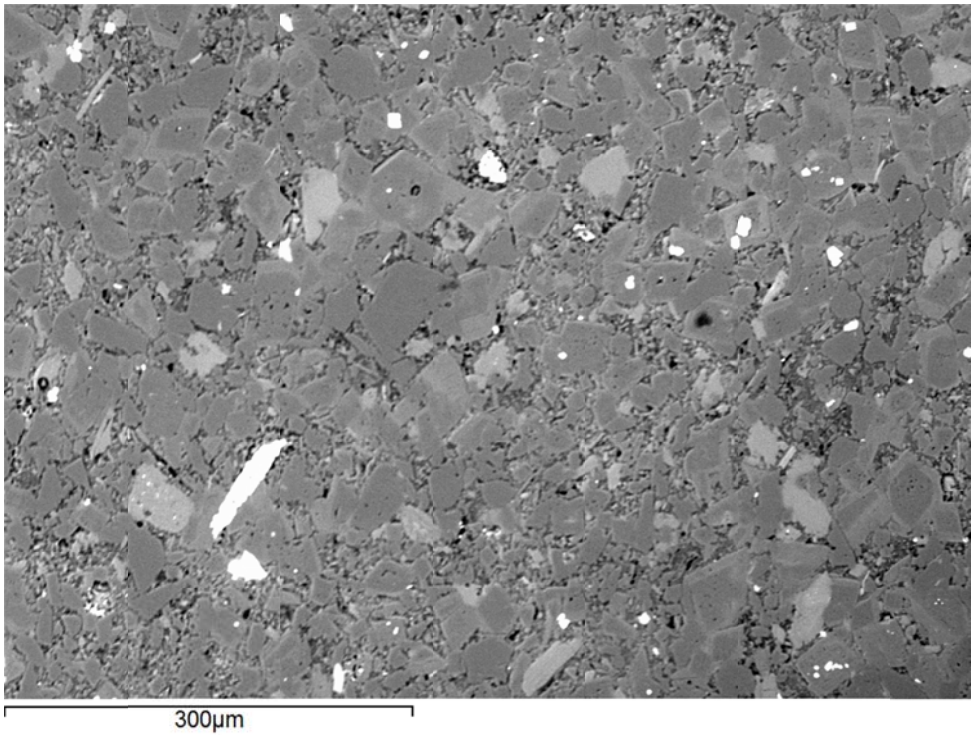

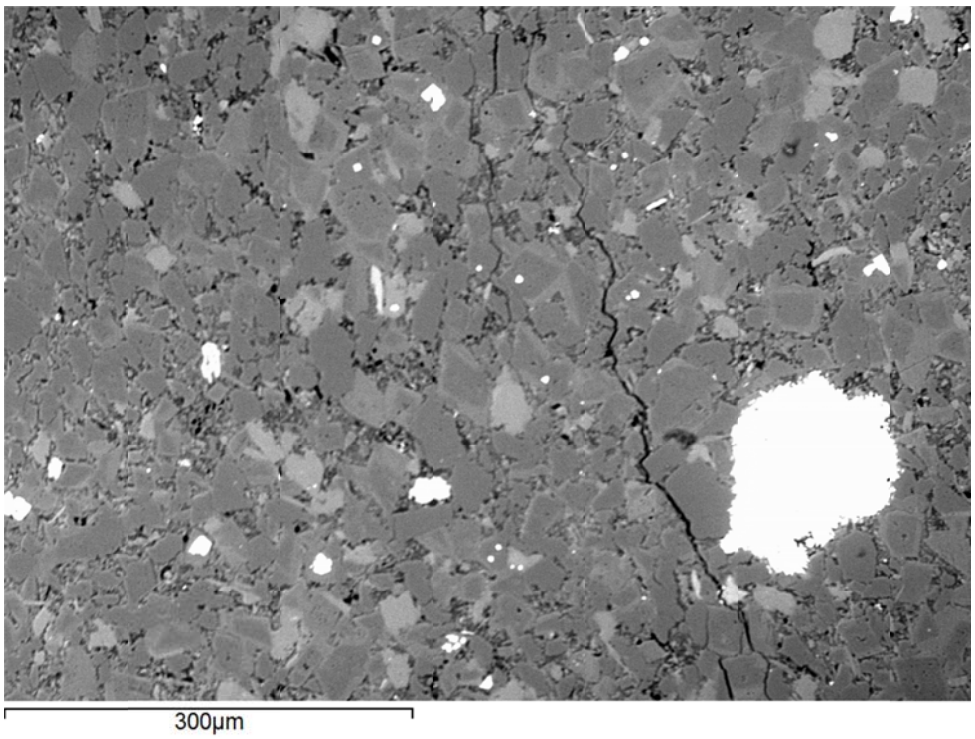

	Applied Geology Laboratory		ID: 116988
	Well Name: NDIC No. 9001	Middle Bakken 7	Rival Field
	API No.: 33-013-00877-00-00	Lithology: Silty, argillaceous dolostone	Depth: 7381.0'

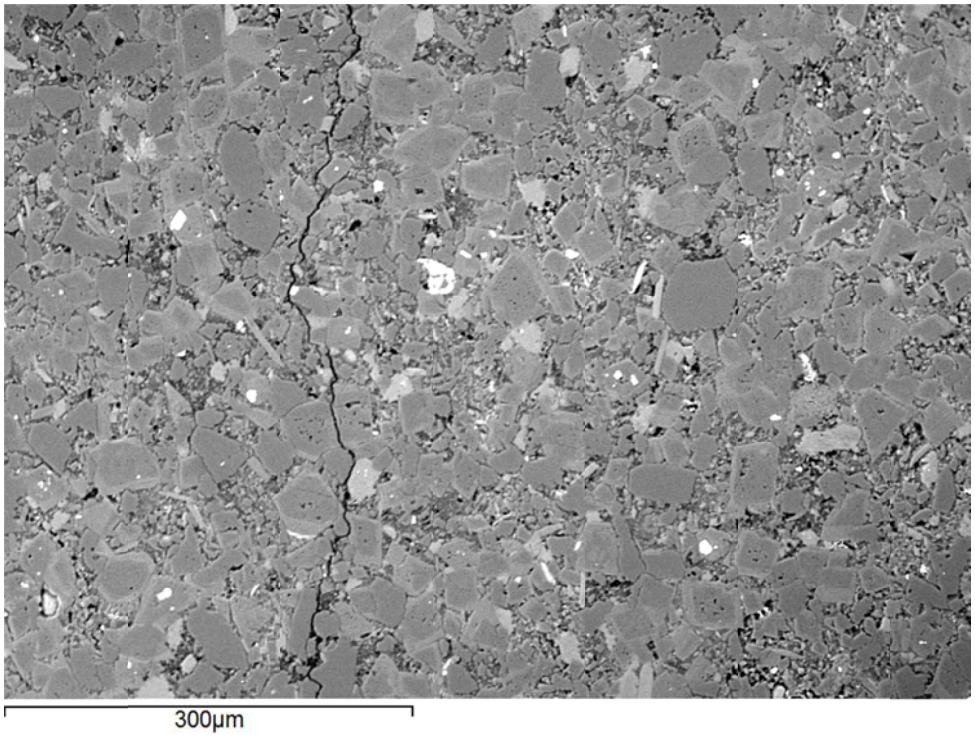

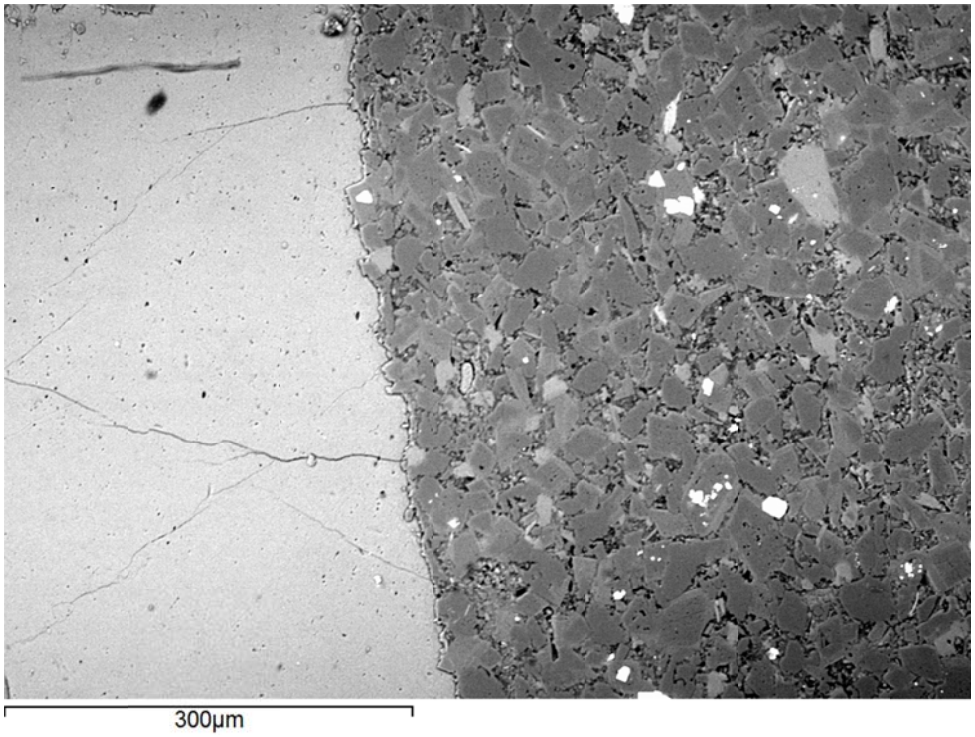

	Applied Geology Laboratory		ID: 116988
EERC Energy & Environmental Research Center® Putting Research into Practice UND THE UNIVERSITY OF NORTH DAKOTA	Well Name: NDIC No. 9001	Middle Bakken 7	Rival Field
	API No.: 33-013-00877-00-00	Lithology: Silty, argillaceous dolostone	Depth: 7381.0'

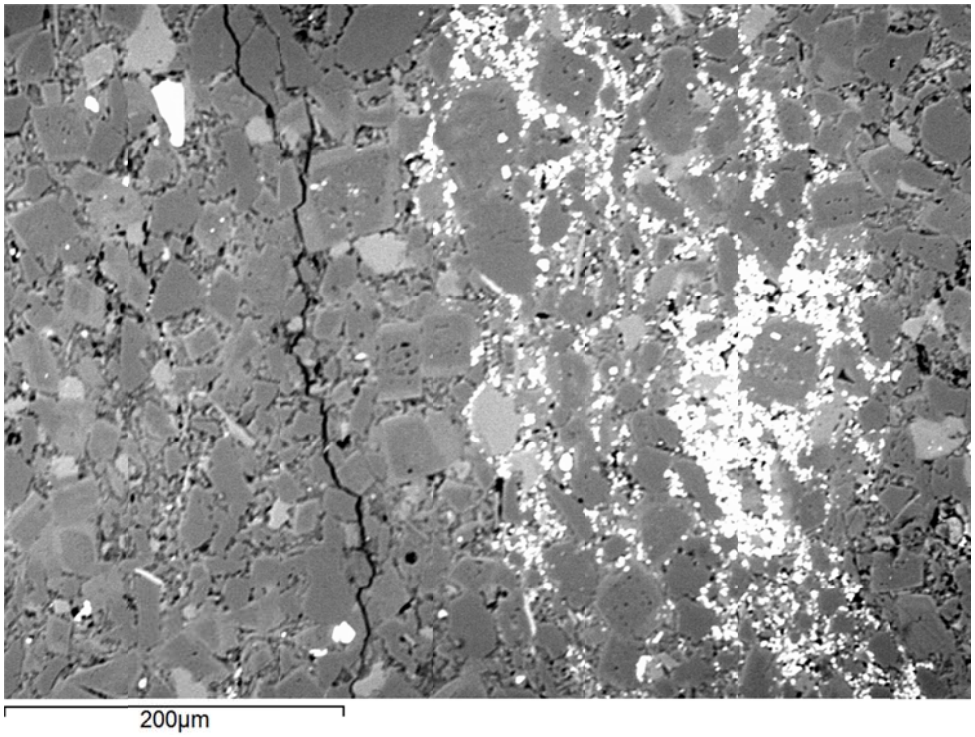

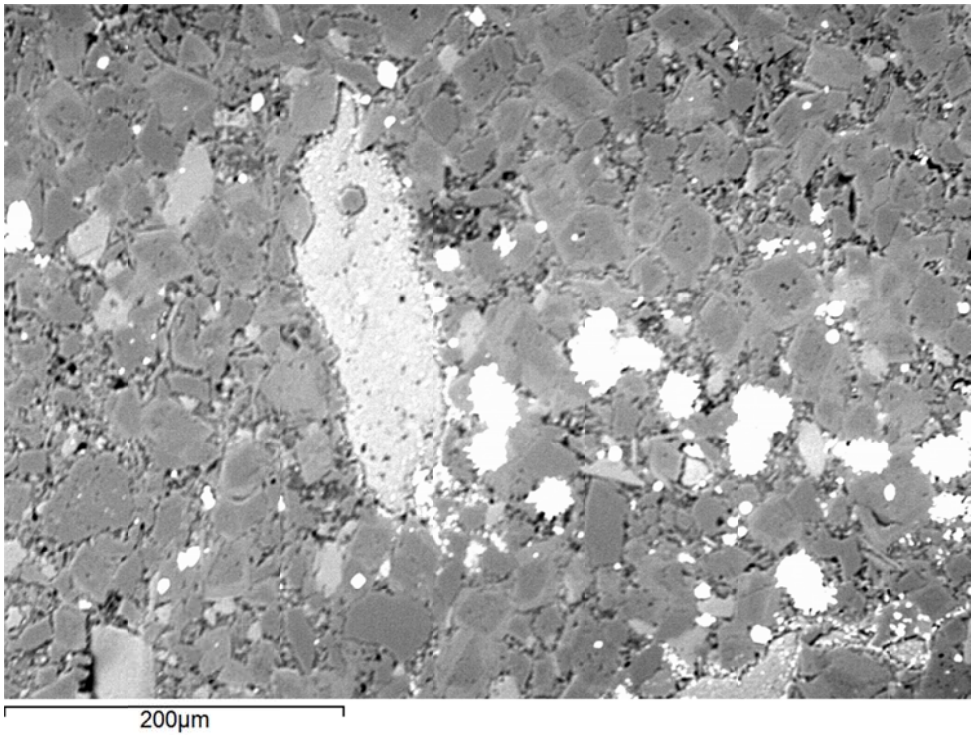

Applied Geology Laboratory		ID: 116988
Well Name: NDIC No. 9001	Middle Bakken 7	Rival Field
API No.: 33-013-00877-00-00	Lithology: Silty, argillaceous dolostone	Depth: 7381.0'

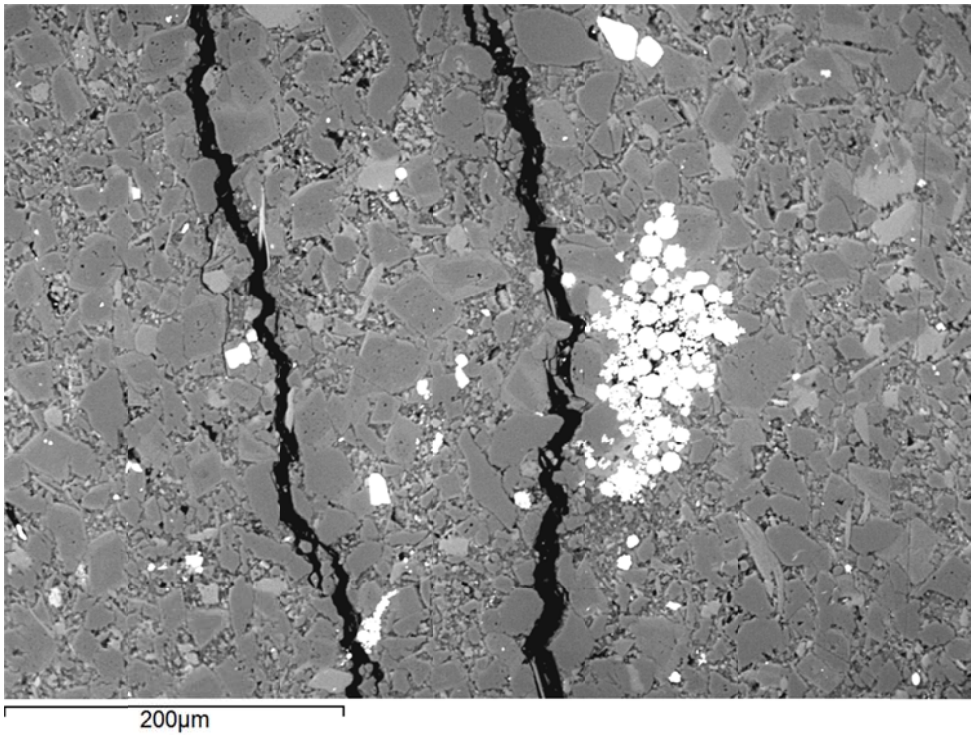

EERC Energy & Environmental Research Center® Putting Research into Practice UND THE UNIVERSITY OF NORTH DAKOTA	**Applied Geology Laboratory**		ID: 116988
	Well Name: NDIC No. 9001	Middle Bakken 7	Rival Field
	API No.: 33-013-00877-00-00	Lithology: Silty, argillaceous dolostone	Depth: 7381.0'

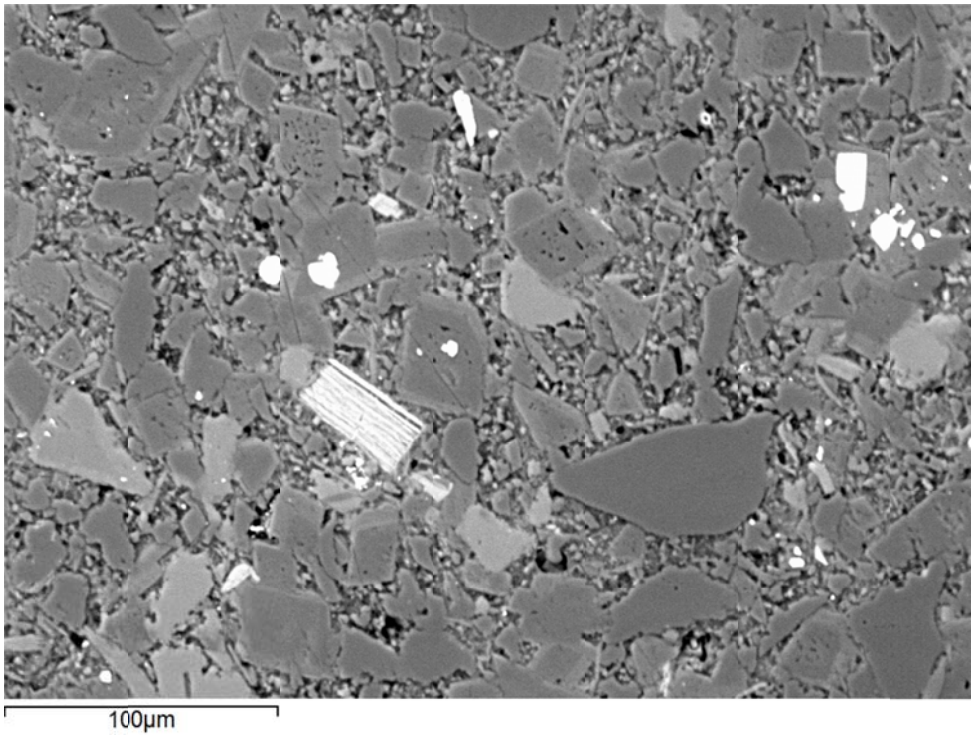

EERC Energy & Environmental Research Center® Putting Research into Practice UND THE UNIVERSITY OF NORTH DAKOTA	**Applied Geology Laboratory**		ID: 116988
	Well Name: NDIC No. 9001	Middle Bakken 7	Rival Field
	API No.: 33-013-00877-00-00	Lithology: Silty, argillaceous dolostone	Depth: 7381.0'

SEM Mineral Map Image Overlaid on BSE Image with Mineral Phase 2D Area Percentages

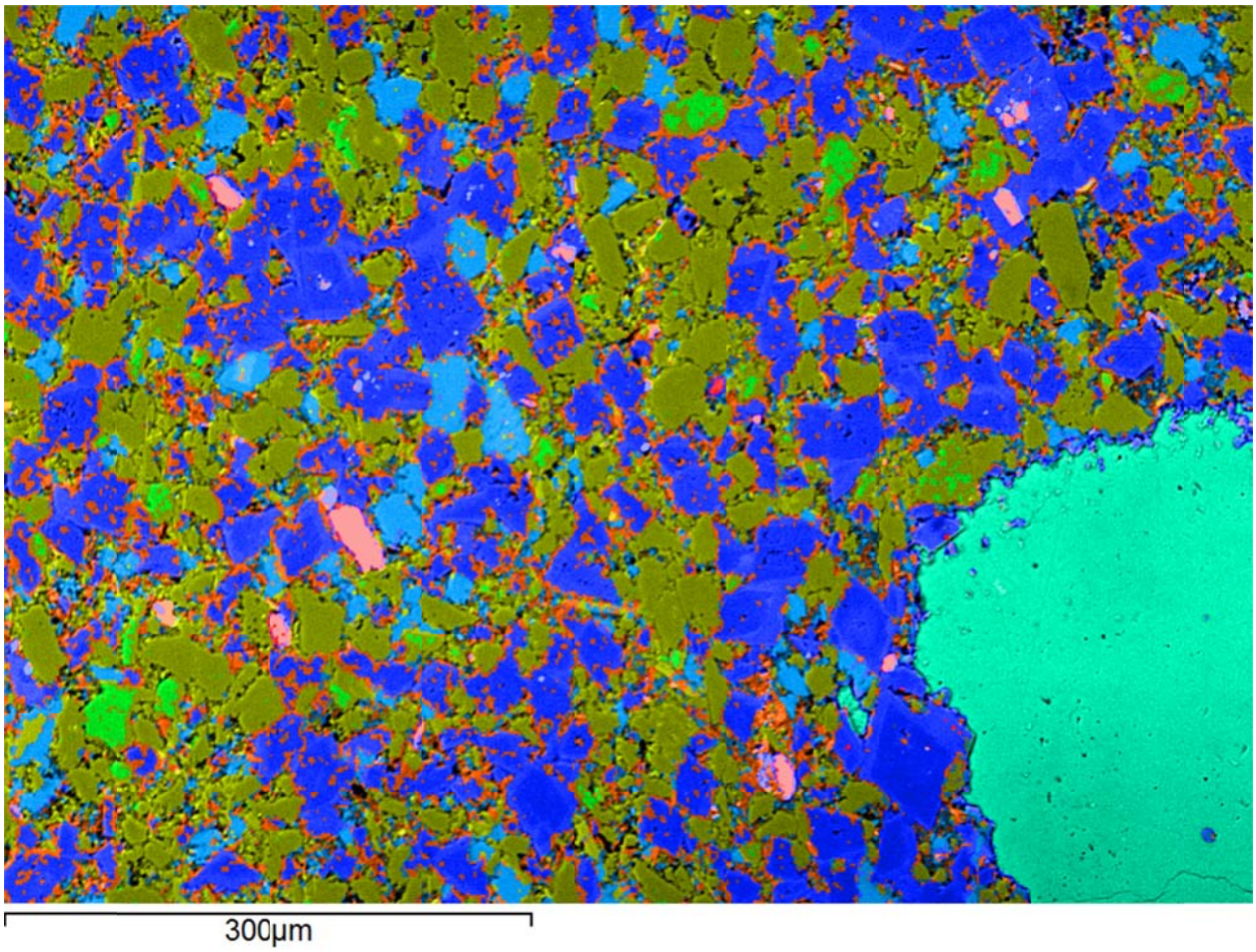

This page intentionally left blank.

EERC Energy & Environmental Research Center® Putting Research into Practice UND THE UNIVERSITY OF NORTH DAKOTA	**Applied Geology Laboratory**		ID: 116989
	Well Name: NDIC No. 9001	Middle Bakken 6	Rival Field
	API No.: 33-013-00877-00-01	Lithology: Argillaceous, silty dolostone	Depth: 7382.7'

SAMPLE PHOTOGRAPH

PHYSICAL PROPERTIES

Porosity and Grain Density by Core Laboratories

Pycnometer Effective Porosity, vol%	Grain Density, g/cm^3
5.11	2.749

EERC Energy & Environmental Research Center® Putting Research into Practice UND THE UNIVERSITY OF NORTH DAKOTA	**Applied Geology Laboratory**		ID: 116989
	Well Name: NDIC No. 9001	Middle Bakken 6	Rival Field
	API No.: 33-013-00877-00-01	Lithology: Argillaceous, silty dolostone	Depth: 7382.7'

PHOTOMICROGRAPHS

Transmission

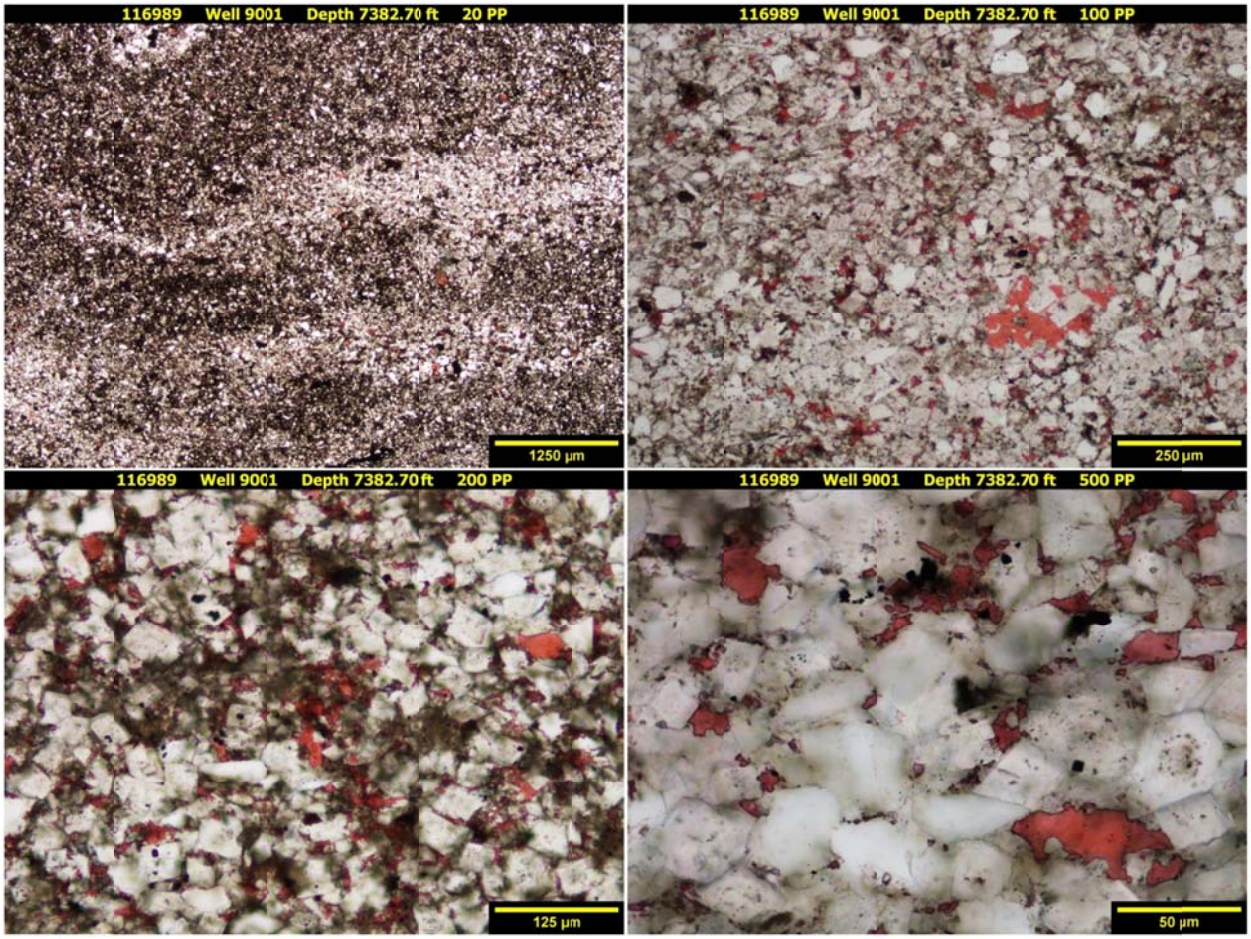

The sample from a depth of 7382.70 ft shows an argillaceous, silty dolostone. Moderate burrowing and few wavy laminations are observed. Very fine grained, angular to subangular, monocrystalline quartz grains and trace amounts of muscovite are disseminated throughout. Extensive anhederal to euhedral dolomitization has occurred throughout the sample. Abundant fine-grained crystalline dolomite occurs as replacement of precursor carbonate grains and mud. Occasional sparry calcite cement and skeletal grains remain. Disseminated pore-filling and replacement pyrite grains are observed throughout at small quantities. The matrix is composed of a combination of clays and micro- to cryptocrystalline dolomite and occasional calcite cement. Multiple, predominately horizontal, fractures are detected. These fractures are likely because of the sampling process. Organics are observed as globular and lensing features. Other than potential open fractures, no porosity is observed using standard petrographic techniques.

EERC Energy & Environmental Research Center® Putting Research into Practice UND THE UNIVERSITY OF NORTH DAKOTA	**Applied Geology Laboratory**		ID: 116989
	Well Name: NDIC No. 9001	Middle Bakken 6	Rival Field
	API No.: 33-013-00877-00-01	Lithology: Argillaceous, silty dolostone	Depth: 7382.7'

Reflection

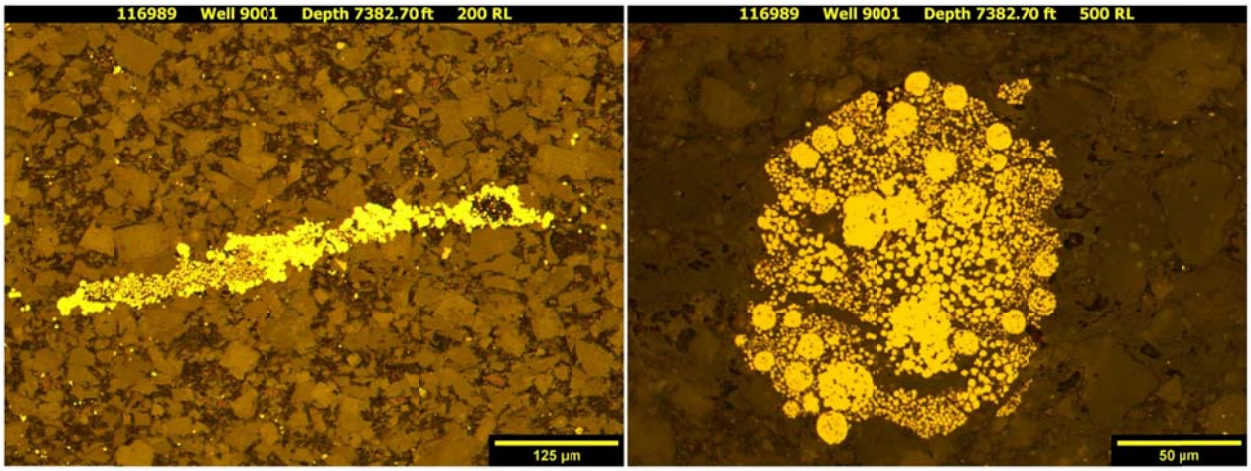

The sample from a depth of 7382.70 ft displays a moderate combination of disseminated framboidal and euhedral pyrite growth. This diagenetic mineral acts as a grain replacer and pore filler. Euhedral mineralization typically replaces calcareous skeletal and non-skeletal grains, but it also appears to fill micropores. Nearly complete pyritization of precursor grains and organics have occurred at some localities. Framboidal pyrite predominately is shown as individual spheres; rarely is there an assemblage of spheres to create a larger more mature sphere grouping. Organics observed are typically associated with both euhedral and framboidal pyrite.

EERC Energy & Environmental Research Center® Putting Research into Practice UND THE UNIVERSITY OF NORTH DAKOTA	**Applied Geology Laboratory**		ID: 116989
	Well Name: NDIC No. 9001	Middle Bakken 6	Rival Field
	API No.: 33-013-00877-00-01	Lithology: Argillaceous, silty dolostone	Depth: 7382.7'

Transmission and Fluorescence Whole-Slide Images

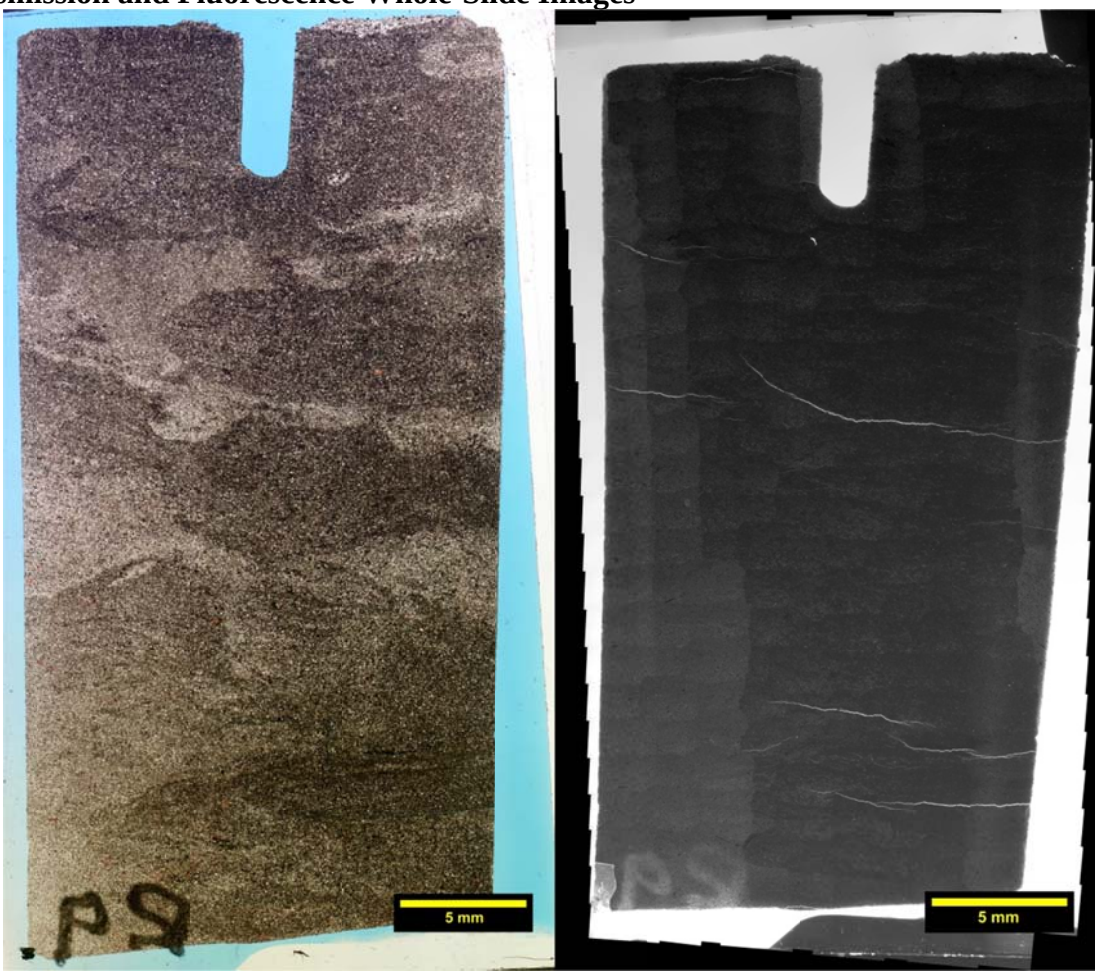

Image issues? The image collected from a depth of 7382.70 ft is a bioturbated silty dolostone. Effective porosity is reported at 5.11 vol%. Extensive interlocking anhedral to euhedral dolomitization and pyritization has occurred. These diagenetic events along consistent very fine grain sizes (except for skeletal and skeletal calcite grains and pyrite) and zonal concentrations of clay are limiting factors of pore size (<30 µm) and distribution. No naturally-occurring open fractures are observed. Induced horizontal fractures are likely the product of the sampling process. Though unnatural, they may provide insight to structural stability within this interval.

	Applied Geology Laboratory		ID: 116989
EERC Energy & Environmental Research Center® Putting Research into Practice UND THE UNIVERSITY OF NORTH DAKOTA	Well Name: NDIC No. 9001	Middle Bakken 6	Rival Field
	API No.: 33-013-00877-00-01	Lithology: Argillaceous, silty dolostone	Depth: 7382.7'

XRF BULK CHEMICAL COMPOSITION

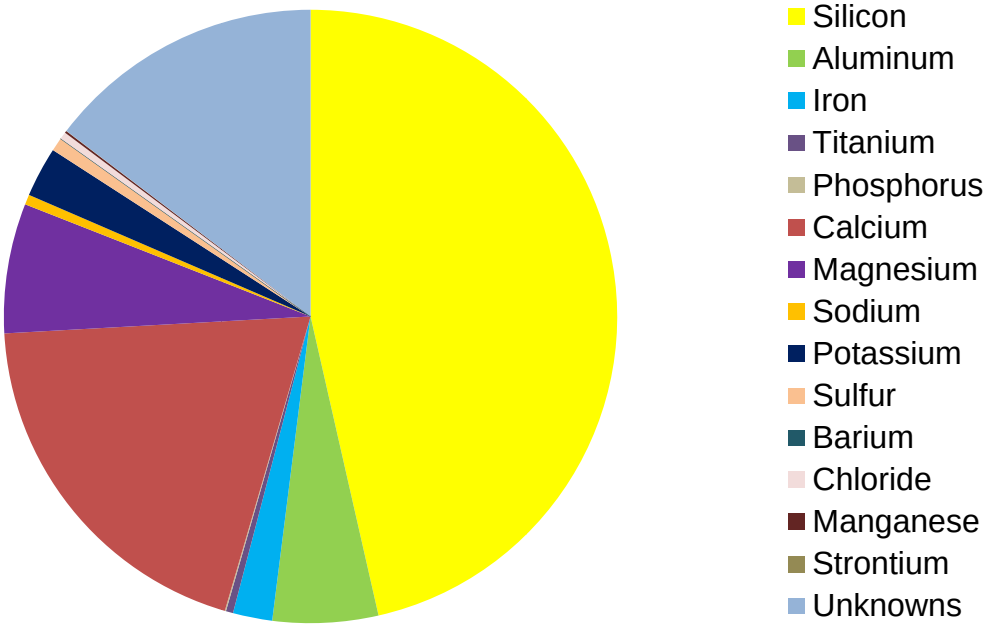

Element	Reporting Convention (Oxide)	Weight %
Si (silicon)	SiO_2	46.43
Al (aluminum)	Al_2O_3	5.56
Fe (iron)	Fe_2O_3	2.07
Ti (titanium)	TiO_2	0.38
P (phosphorus)	P_2O_5	0.06
Ca (calcium)	CaO	19.61
Mg (magnesium)	MgO	6.84
Na (sodium)	Na_2O	0.53
K (potassium)	K_2O	2.64
S (sulfur)	SO_3	0.72
Ba (barium)	BaO	0.00
Cl (chloride)	Cl	0.38
Mn (manganese)	MnO	0.11
Sr (strontium)	SrO	0.01
Unknowns	Due to the presence of carbonates	14.65
Total		99.99

EERC Energy & Environmental Research Center® Putting Research into Practice UND THE UNIVERSITY OF NORTH DAKOTA	**Applied Geology Laboratory**		ID: 116989
	Well Name: NDIC No. 9001	Middle Bakken 6	Rival Field
	API No.: 33-013-00877-00-01	Lithology: Argillaceous, silty dolostone	Depth: 7382.7'

XRD MINERAL PHASE DISTRIBUTION

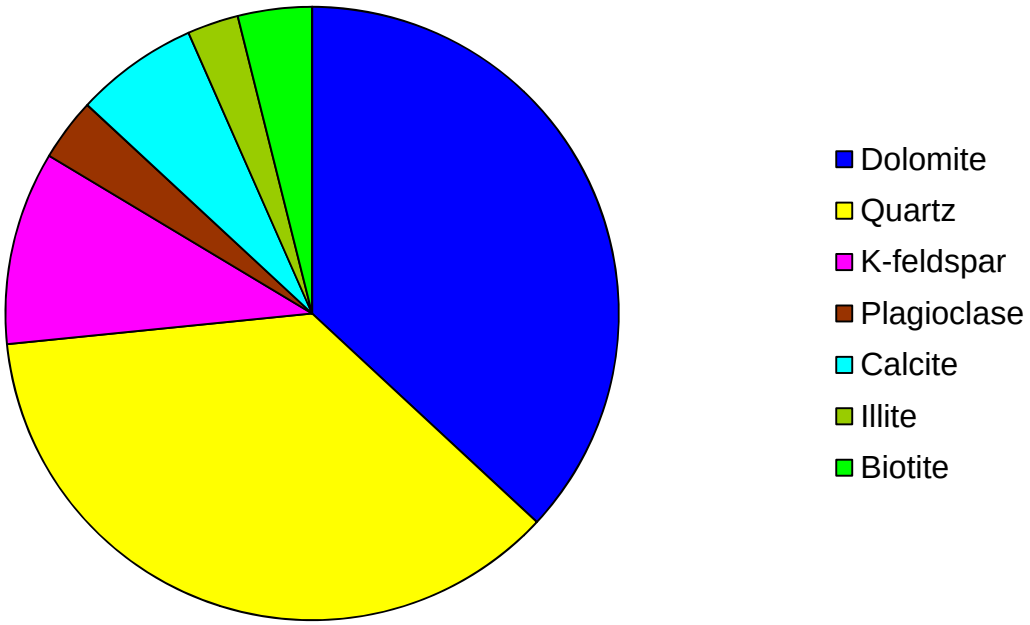

Mineral Phase	Formula	Weight %
Dolomite	$CaMg(CO_3)_2$	36.9
Quartz	SiO_2	36.5
K-feldspar	$KAlSi_3O_8$	10.2
Plagioclase	$Na_{0.5}Ca_{0.5}Al_{1.5}Si_{2.5}O_8$	3.3
Calcite	$CaCO_3$	6.5
Illite	$(K,H_3O)(Al,Mg,Fe)_2(Si,Al)_4O_{10}[(OH)_2,(H_2O)]$	2.7
Biotite	$K(Mg,Fe)_3[(OH)_2AlSi_3O_{10}]$	3.9

EERC Energy & Environmental Research Center® Putting Research into Practice UND THE UNIVERSITY OF NORTH DAKOTA	**Applied Geology Laboratory**		ID: 116989
	Well Name: NDIC No. 9001	Middle Bakken 6	Rival Field
	API No.: 33-013-00877-00-01	Lithology: Argillaceous, silty dolostone	Depth: 7382.7'

SEM

Observed Minerals

Mineral Phase	Mineral Phase
Calcite	Dolomite
Pyrite	Rutile
K-feldspar	Apatite
Quartz	Zircon
Illite	Albite
Biotite	

High-Magnification BSE Image Annotated with Examples of Mineral Phases Identified

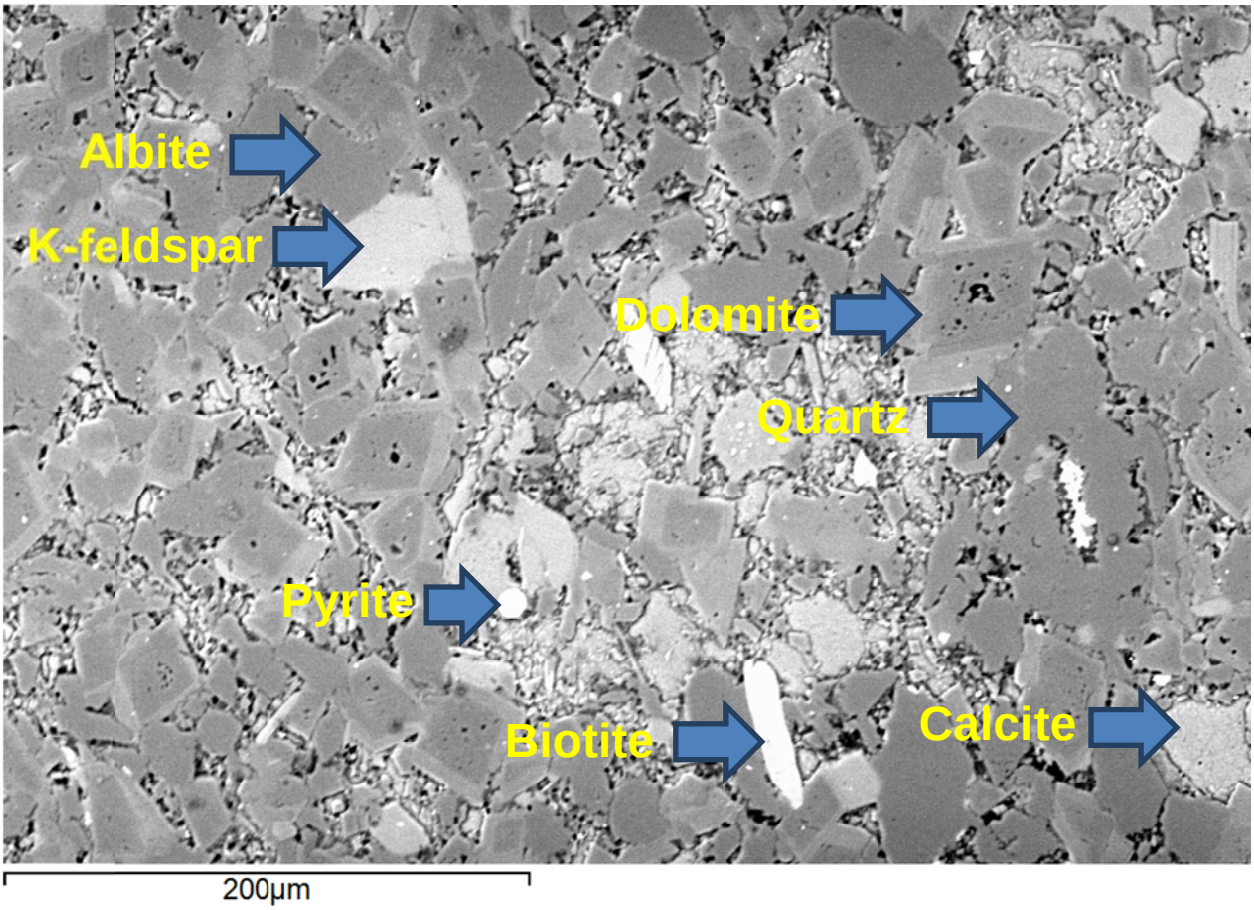

Additional High-Magnification BSE Images

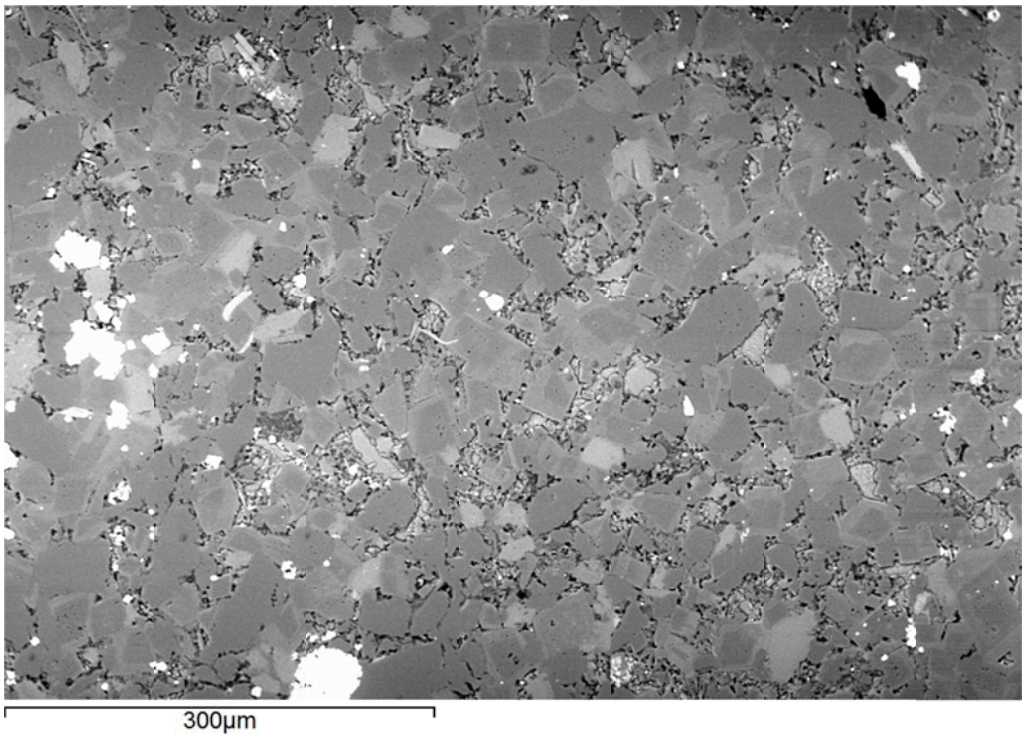

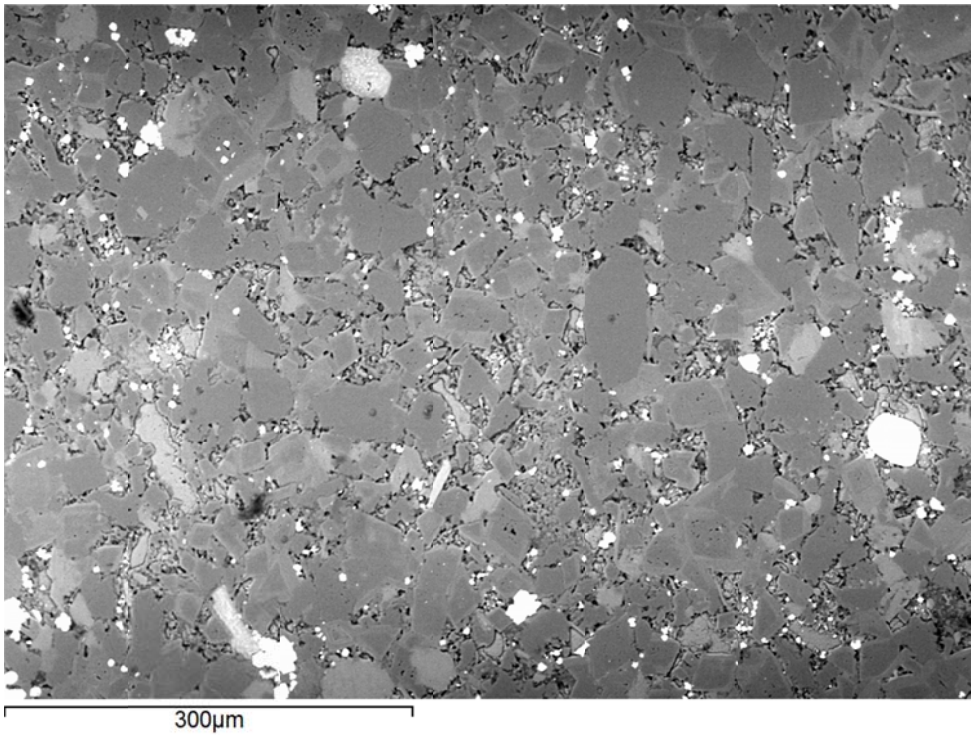

	Applied Geology Laboratory		ID: 116989
	Well Name: NDIC No. 9001	Middle Bakken 6	Rival Field
	API No.: 33-013-00877-00-01	Lithology: Argillaceous, silty dolostone	Depth: 7382.7'

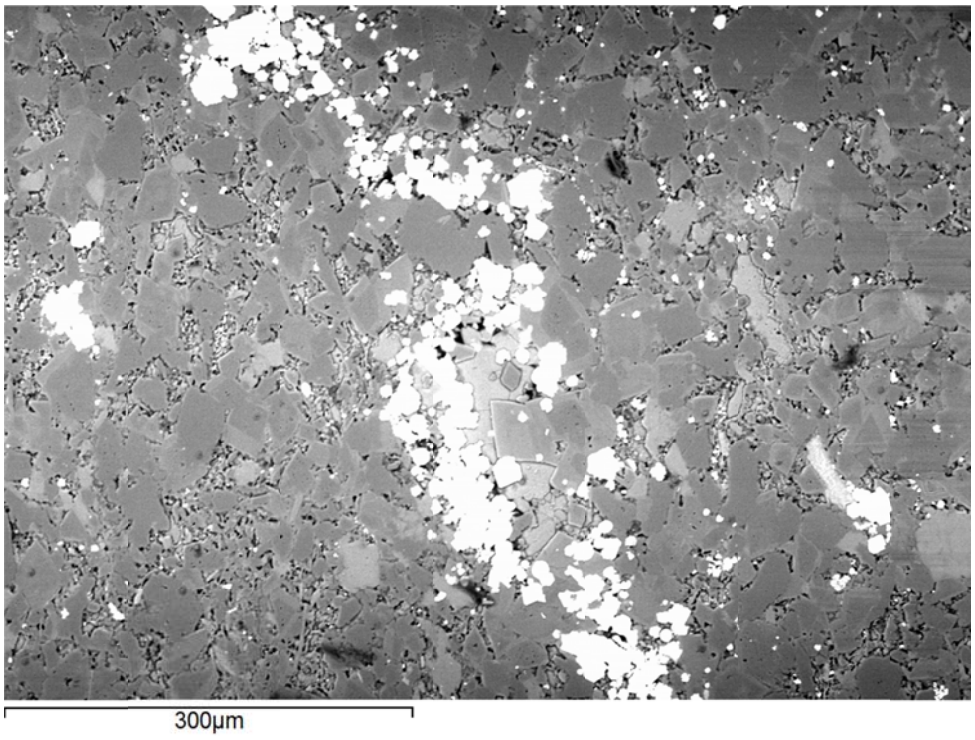

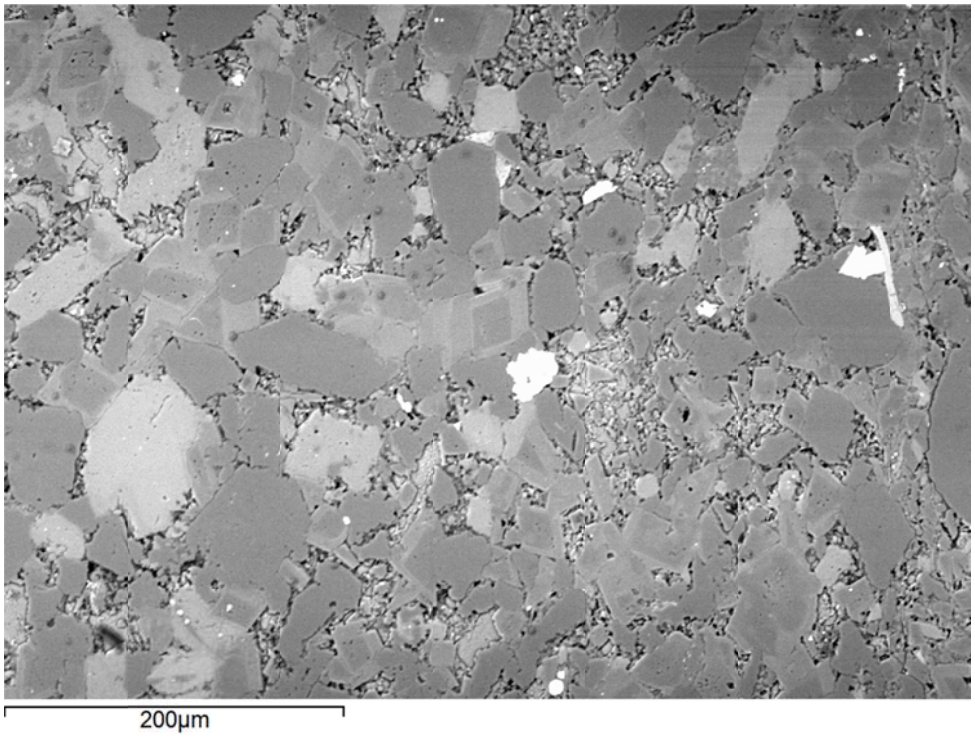

EERC Energy & Environmental Research Center® Putting Research into Practice UND THE UNIVERSITY OF NORTH DAKOTA	**Applied Geology Laboratory**		ID: 116989
	Well Name: NDIC No. 9001	Middle Bakken 6	Rival Field
	API No.: 33-013-00877-00-01	Lithology: Argillaceous, silty dolostone	Depth: 7382.7'

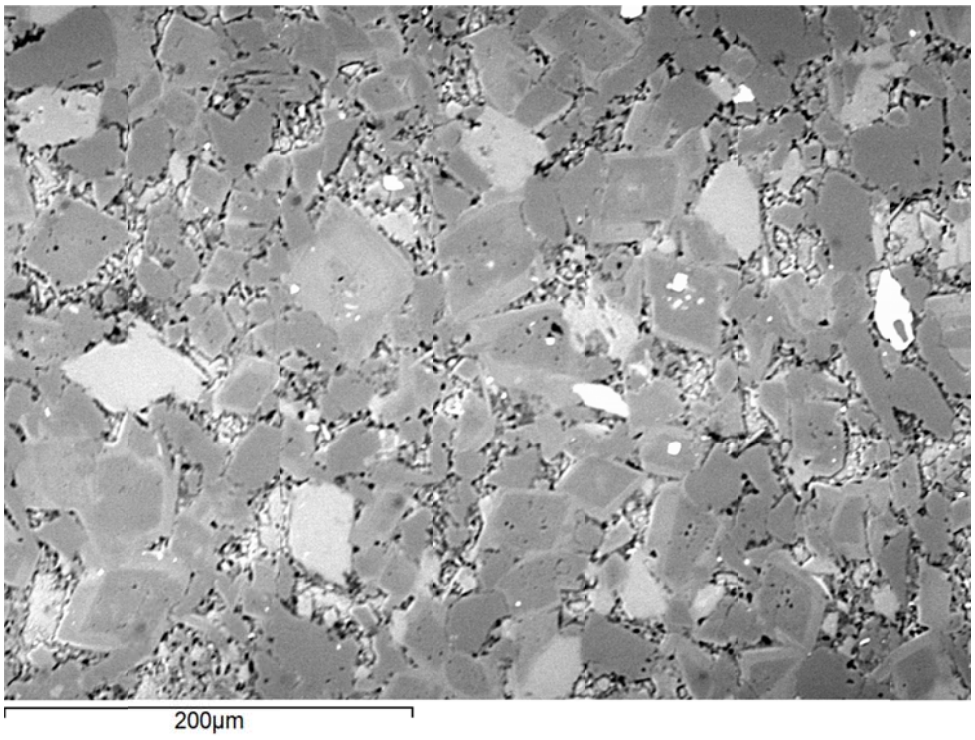

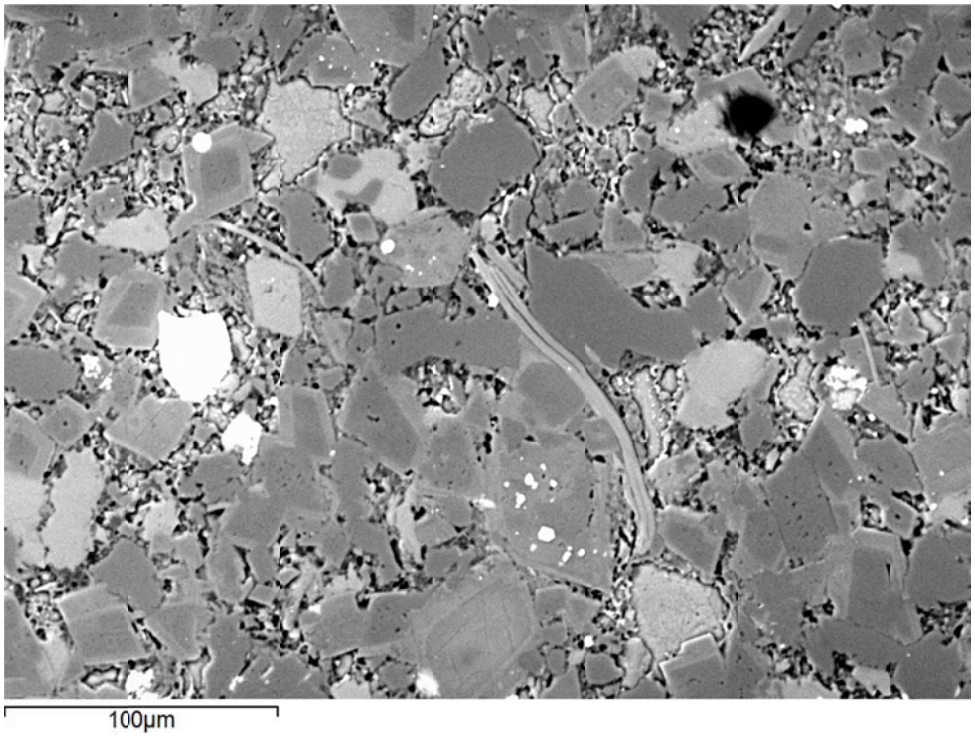

EERC Energy & Environmental Research Center® Putting Research into Practice UND THE UNIVERSITY OF NORTH DAKOTA	**Applied Geology Laboratory**		ID: 116989
	Well Name: NDIC No. 9001	Middle Bakken 6	Rival Field
	API No.: 33-013-00877-00-01	Lithology: Argillaceous, silty dolostone	Depth: 7382.7'

SEM Mineral Map Image Overlaid on BSE Image with Mineral Phase 2D Area Percentages

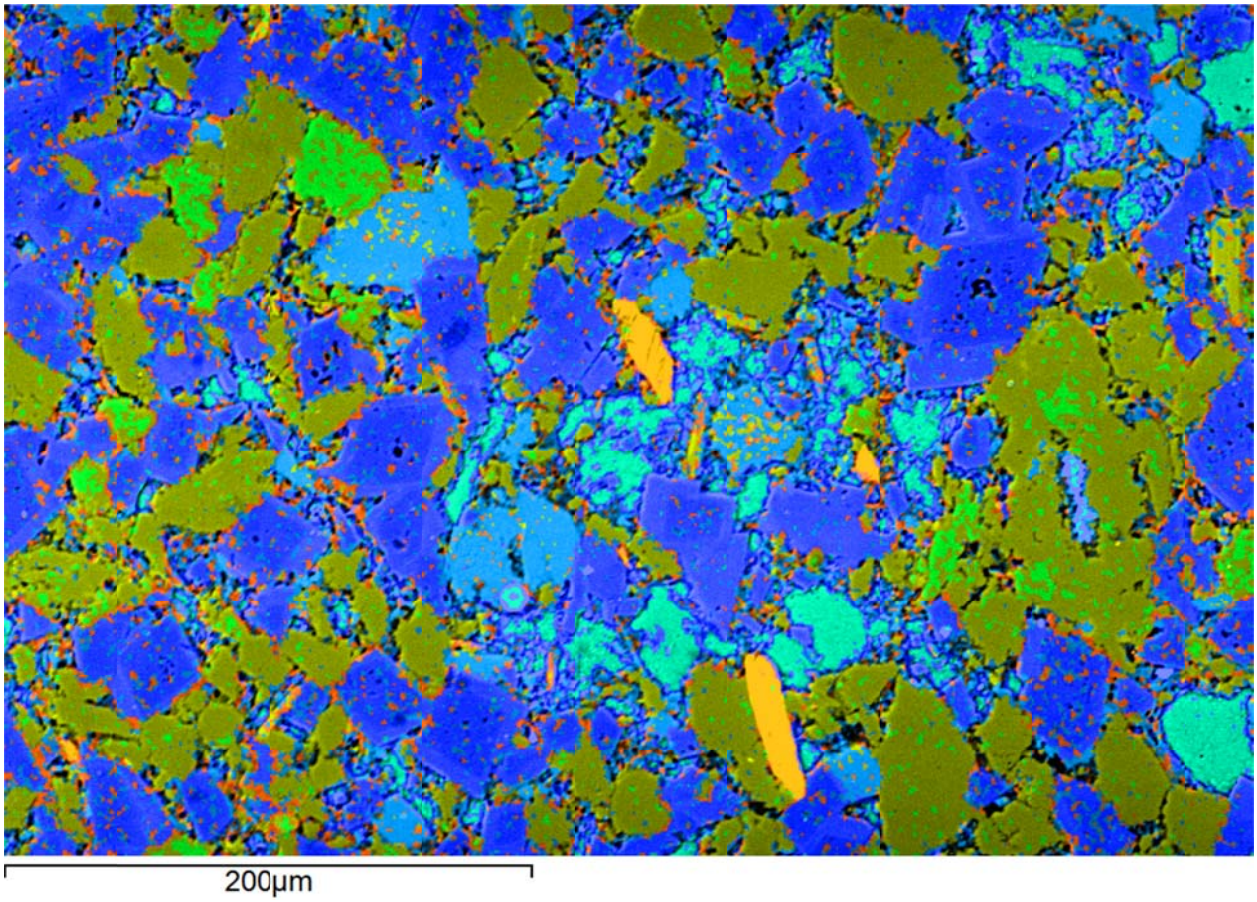

This page intentionally left blank.

EERC Energy & Environmental Research Center® Putting Research into Practice UND THE UNIVERSITY OF NORTH DAKOTA	**Applied Geology Laboratory**		ID: 116990
	Well Name: NDIC No. 9001	Middle Bakken 5	Rival Field
	API No.: 33-013-00877-00-02	Lithology: Argillaceous, dolomitic siltstone	Depth: 7385.3'

SAMPLE PHOTOGRAPH

PHYSICAL PROPERTIES

Porosity and Grain Density by Core Laboratories

Pycnometer Effective Porosity, vol%	Grain Density, g/cm^3
6.74	2.735

EERC Energy & Environmental Research Center® Putting Research into Practice UND THE UNIVERSITY OF NORTH DAKOTA	**Applied Geology Laboratory**		ID: 116990
	Well Name: NDIC No. 9001	Middle Bakken 5	Rival Field
	API No.: 33-013-00877-00-02	Lithology: Argillaceous, dolomitic siltstone	Depth: 7385.3'

PHOTOMICROGRAPHS

Transmission

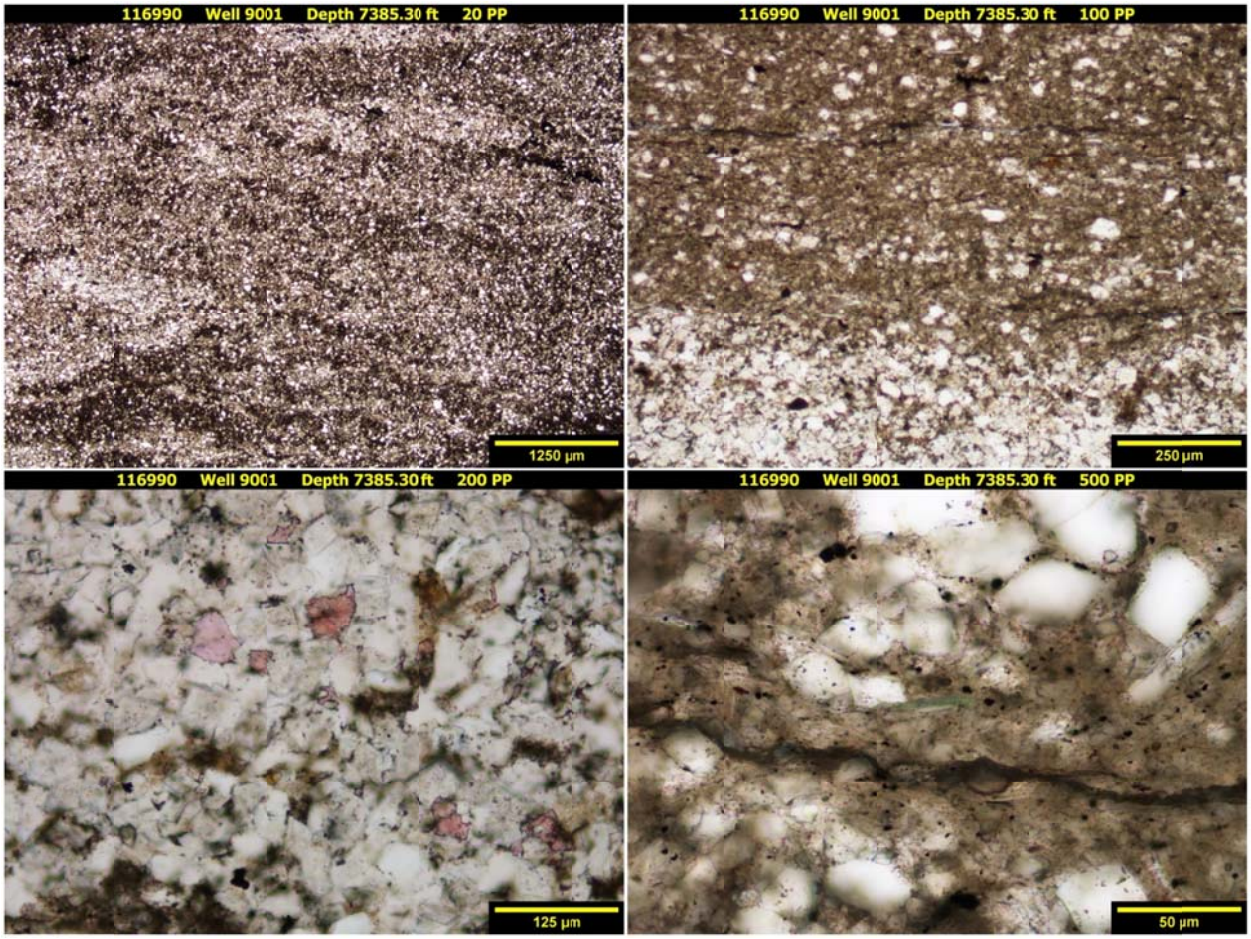

The sample from a depth of 7385.30 ft shows an argillaceous, dolomitic siltstone. Strong evidence of burrowing and wavy laminations is observed. Very fine grained, angular to subrounded, monocrystalline quartz grains and trace amounts of muscovite are disseminated throughout. Muscovite orientation is random, furthering bioturbation evidence and differing lithological strengths. Extensive anhederal to euhedral dolomitization has occurred throughout the sample. Abundant fine-grained crystalline dolomite occurs as replacement of precursor carbonate grains. Very little calcite remains. Disseminated pore-filling and replacement pyrite grains are observed throughout. The matrix is composed of a combination of clays and micro- to cryptocrystalline dolomite. No skeletal grains are observed. Multiple, predominately horizontal, fractures are detected. These fractures are likely because of the sampling process. Organics are observed as globular and lensing features. Other than potential open fractures, no porosity is observed using standard petrographic techniques.

EERC Energy & Environmental Research Center® Putting Research into Practice UND THE UNIVERSITY OF NORTH DAKOTA	**Applied Geology Laboratory**		ID: 116990
	Well Name: NDIC No. 9001	Middle Bakken 5	Rival Field
	API No.: 33-013-00877-00-02	Lithology: Argillaceous, dolomitic siltstone	Depth: 7385.3'

Reflection

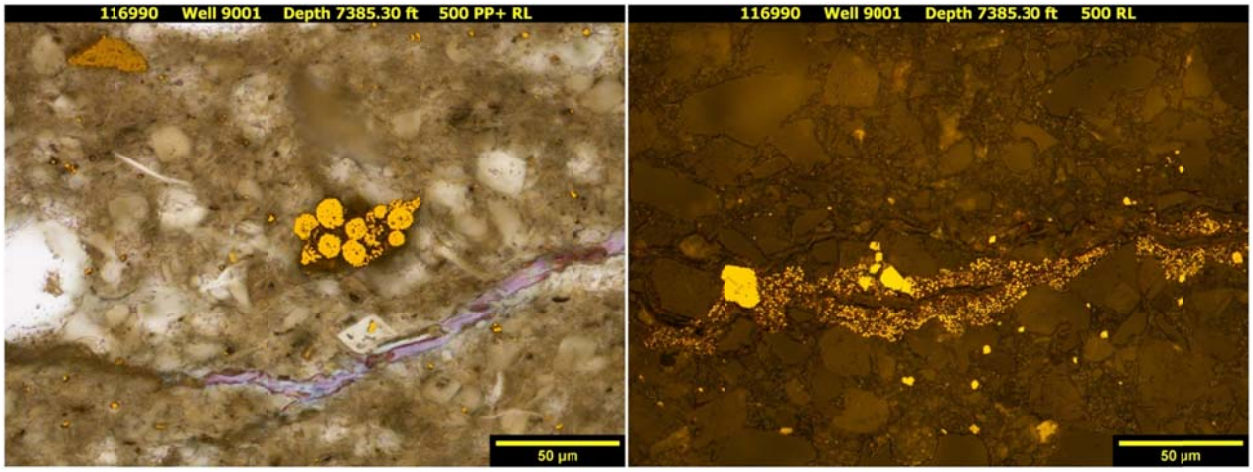

The sample from a depth of 7385.30 ft displays a combination of disseminated framboidal and euhedral pyrite growth. This diagenetic mineral acts as a grain replacer and pore filler. Euhedral grains are very fine grained and usually significantly larger than the framboidal pyrite. Framboidal pyrite predominately is shown as individual spheres; rarely is there an assemblage of spheres to create a larger more mature grouping. Occasionally, euhedral and framboidal grains lie together; typically they will lie away from each other. Nearly complete pyritization of precursor grains and organics have occurred at some localities. Organics observed are typically associated with both euhedral and framboidal pyrite.

EERC Energy & Environmental Research Center® Putting Research into Practice UND THE UNIVERSITY OF NORTH DAKOTA	**Applied Geology Laboratory**		ID: 116990
	Well Name: NDIC No. 9001	Middle Bakken 5	Rival Field
	API No.: 33-013-00877-00-02	Lithology: Argillaceous, dolomitic siltstone	Depth: 7385.3'

Transmission and Fluorescence Whole-Slide Images

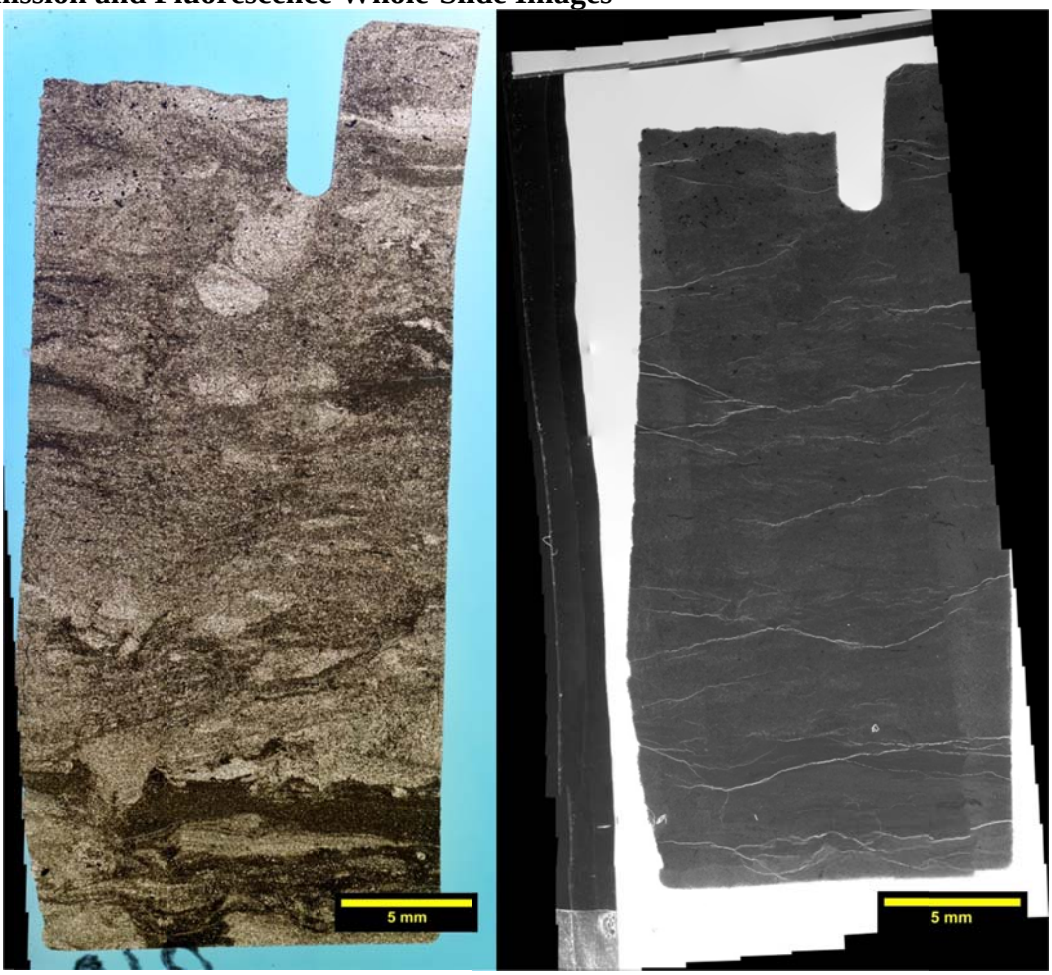

Image issues? The image collected from a depth of 7385.30 ft is a highly bioturbated dolomitic siltstone. Effective porosity is reported at 6.74 vol%. Extensive interlocking anhedral to euhedral dolomitization and pyritization has occurred. Zonal concentrations of clay and connectedness of quartz and dolomitic grains contributed to limiting of pore size (<30 µm) and distribution. No naturally-occurring open fractures are observed. Induced horizontal fractures are likely the product of the sampling process. Though unnatural, they may depict areas of structural weakness as stress is applied.

EERC Energy & Environmental Research Center® Putting Research into Practice UND THE UNIVERSITY OF NORTH DAKOTA	**Applied Geology Laboratory**		ID: 116990
	Well Name: NDIC No. 9001	Middle Bakken 5	Rival Field
	API No.: 33-013-00877-00-02	Lithology: Argillaceous, dolomitic siltstone	Depth: 7385.3'

XRF BULK CHEMICAL COMPOSITION

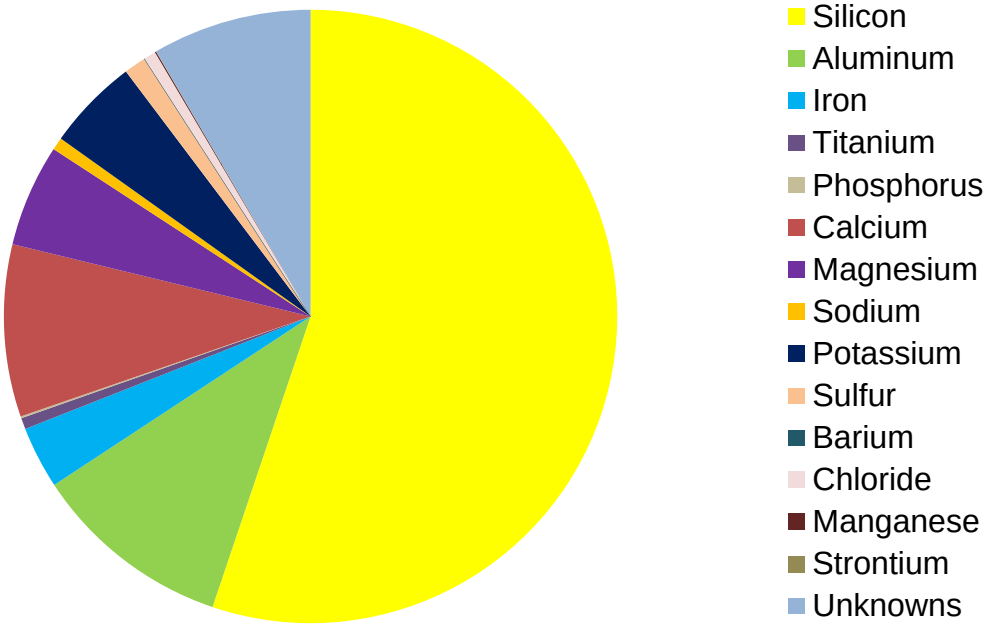

Element	Reporting Convention (Oxide)	Weight %
Si (silicon)	SiO_2	55.18
Al (aluminum)	Al_2O_3	10.57
Fe (iron)	Fe_2O_3	3.28
Ti (titanium)	TiO_2	0.59
P (phosphorus)	P_2O_5	0.10
Ca (calcium)	CaO	9.08
Mg (magnesium)	MgO	5.40
Na (sodium)	Na_2O	0.66
K (potassium)	K_2O	4.87
S (sulfur)	SO_3	1.17
Ba (barium)	BaO	0.00
Cl (chloride)	Cl	0.64
Mn (manganese)	MnO	0.07
Sr (strontium)	SrO	0.01
Unknowns	Due to the presence of carbonates	8.39
Total		100.01

EERC Energy & Environmental Research Center® Putting Research into Practice UND THE UNIVERSITY OF NORTH DAKOTA	**Applied Geology Laboratory**		ID: 116990
	Well Name: NDIC No. 9001	Middle Bakken 5	Rival Field
	API No.: 33-013-00877-00-02	Lithology: Argillaceous, dolomitic siltstone	Depth: 7385.3'

XRD MINERAL PHASE DISTRIBUTION

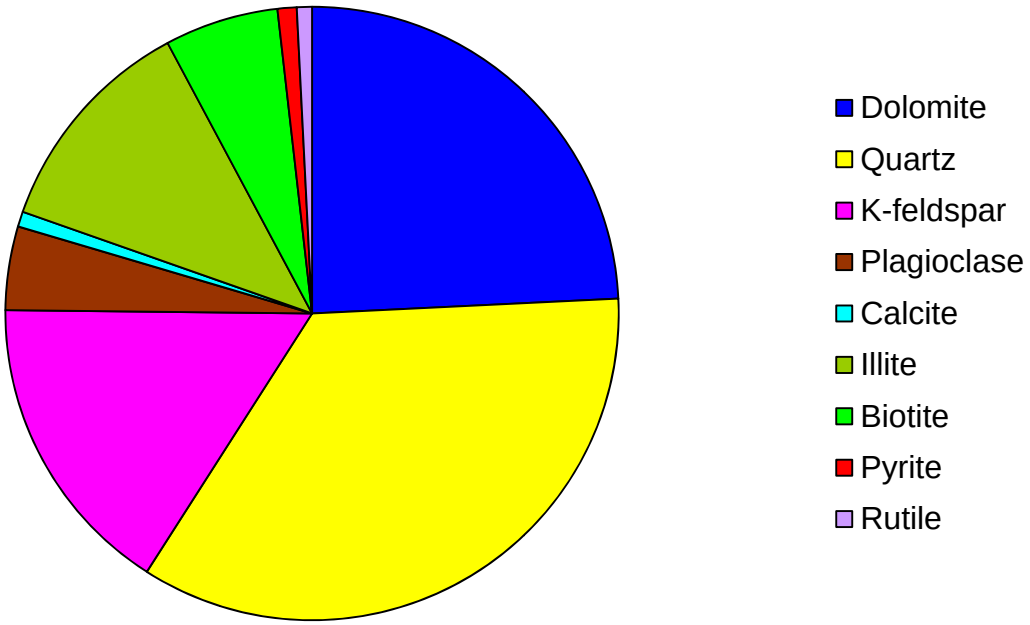

Mineral Phase	Formula	Weight %
Dolomite	$CaMg(CO_3)_2$	24.2
Quartz	SiO_2	34.8
K-feldspar	$KAlSi_3O_8$	16.1
Plagioclase	$Na_{0.5}Ca_{0.5}Al_{1.5}Si_{2.5}O_8$	4.4
Calcite	$CaCO_3$	0.8
Illite	$(K,H_3O)(Al,Mg,Fe)_2(Si,Al)_4O_{10}[(OH)_2,(H_2O)]$	11.8
Biotite	$K(Mg,Fe)_3[(OH)_2AlSi_3O_{10}]$	6.0
Pyrite	FeS_2	1.0
Rutile	TiO_2	0.8

Applied Geology Laboratory		ID: 116990
Well Name: NDIC No. 9001	Middle Bakken 5	Rival Field
API No.: 33-013-00877-00-02	Lithology: Argillaceous, dolomitic siltstone	Depth: 7385.3'

SEM

Observed Minerals

Mineral Phase	Mineral Phase
Calcite	Illite
Quartz	Biotite
Pyrite	K-feldspar
Albite	Dolomite
Rutile	Apatite

High-Magnification BSE Image Annotated with Examples of Mineral Phases Identified

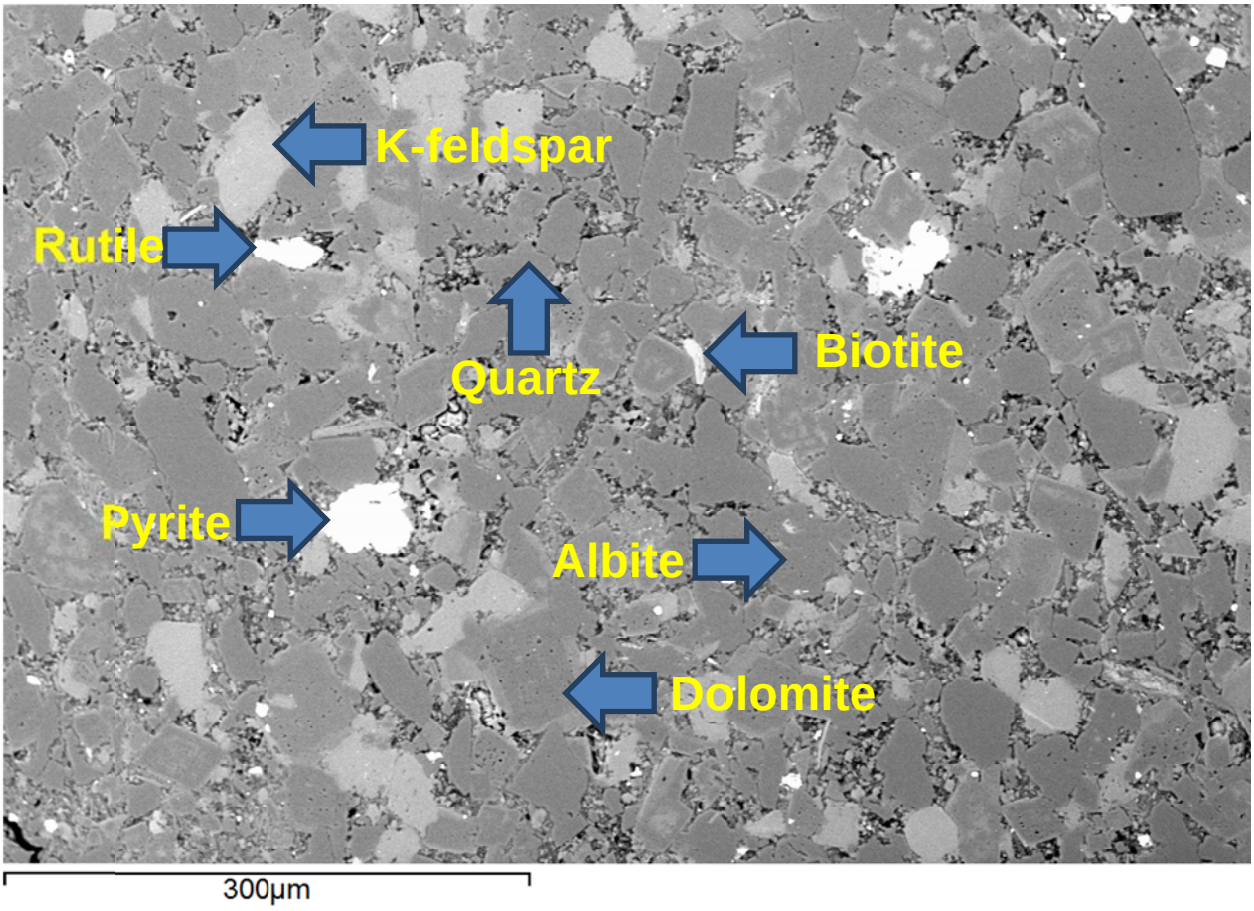

EERC Energy & Environmental Research Center® Putting Research into Practice UND THE UNIVERSITY OF NORTH DAKOTA	**Applied Geology Laboratory**		ID: 116990
	Well Name: NDIC No. 9001	Middle Bakken 5	Rival Field
	API No.: 33-013-00877-00-02	Lithology: Argillaceous, dolomitic siltstone	Depth: 7385.3'

Additional High-Magnification BSE Images

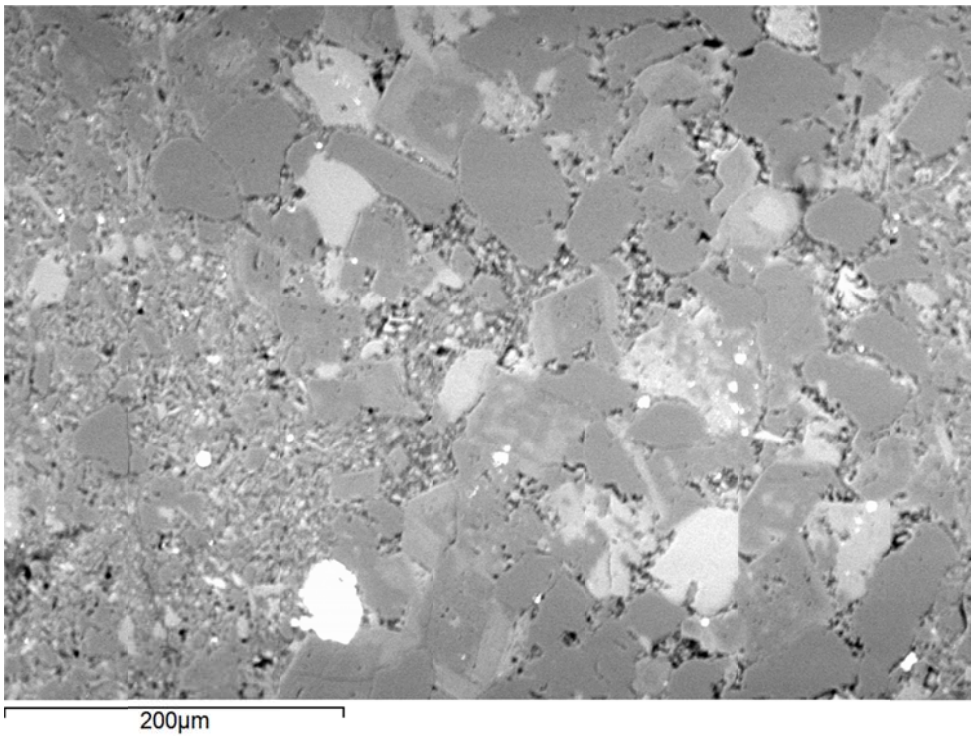

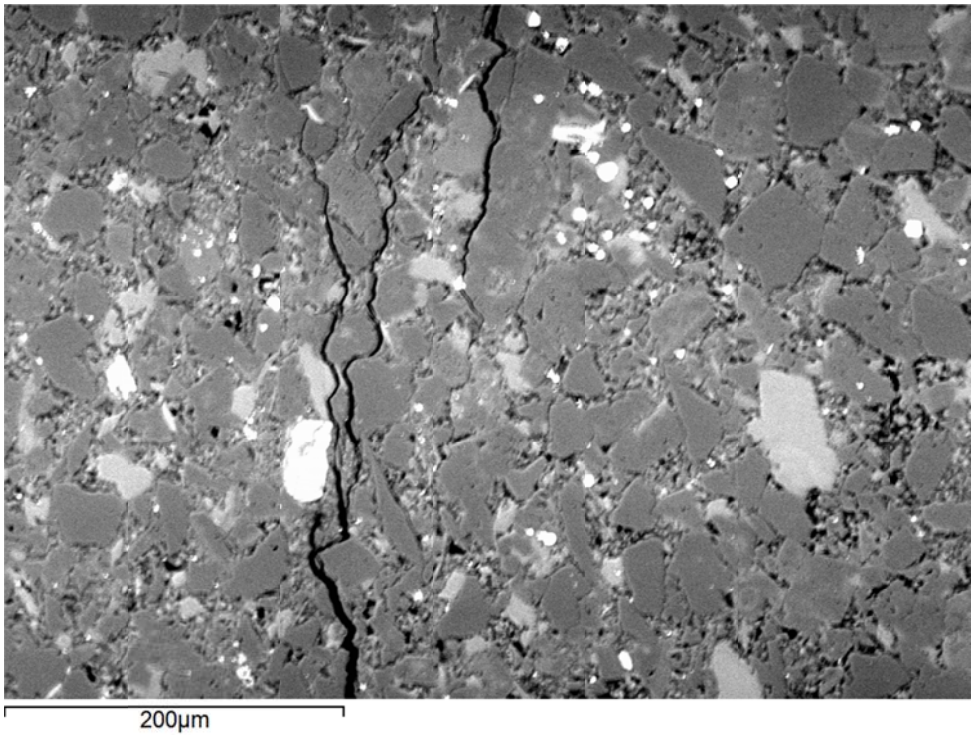

EERC Energy & Environmental Research Center® Putting Research into Practice UND THE UNIVERSITY OF NORTH DAKOTA	**Applied Geology Laboratory**		ID: 116990
	Well Name: NDIC No. 9001	Middle Bakken 5	Rival Field
	API No.: 33-013-00877-00-02	Lithology: Argillaceous, dolomitic siltstone	Depth: 7385.3'

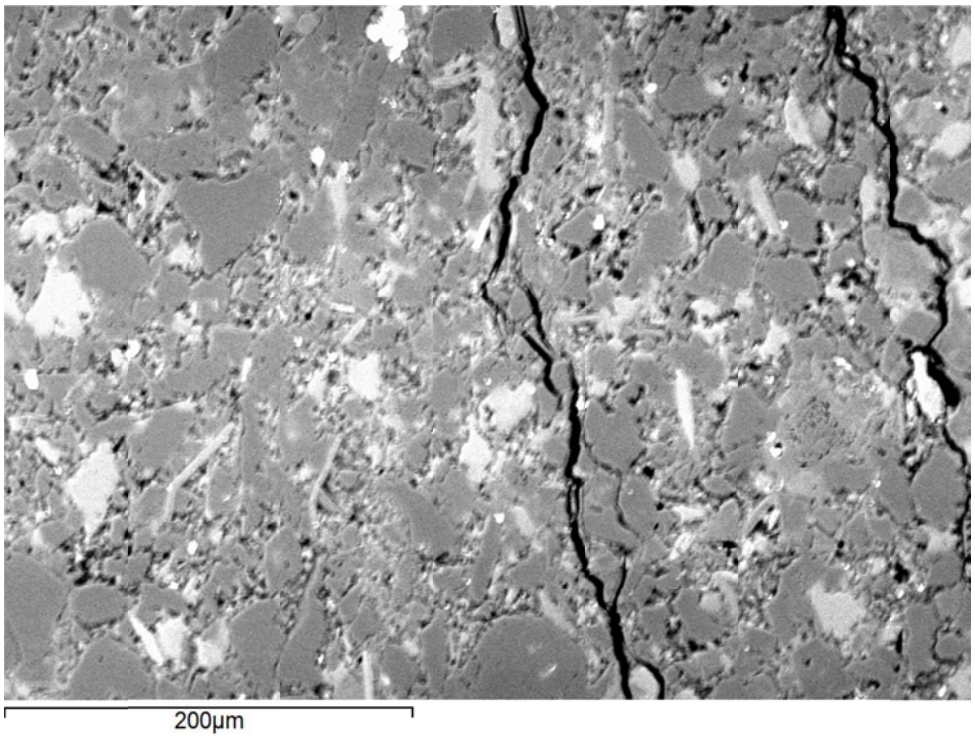

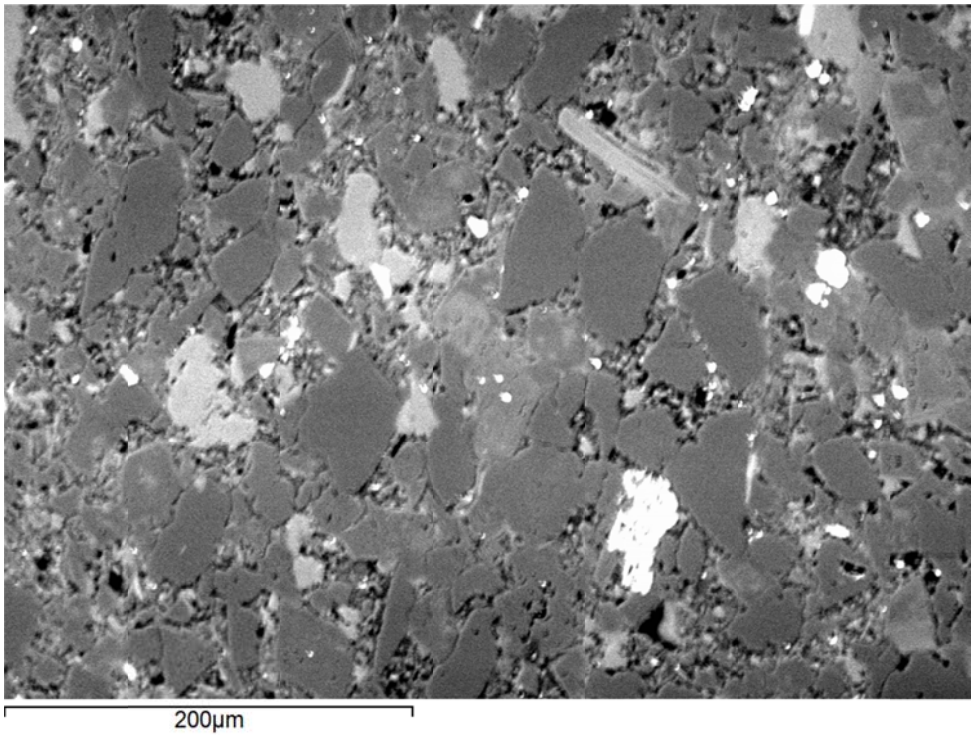

EERC Energy & Environmental Research Center® Putting Research into Practice UND THE UNIVERSITY OF NORTH DAKOTA	**Applied Geology Laboratory**		ID: 116990
	Well Name: NDIC No. 9001	Middle Bakken 5	Rival Field
	API No.: 33-013-00877-00-02	Lithology: Argillaceous, dolomitic siltstone	Depth: 7385.3'

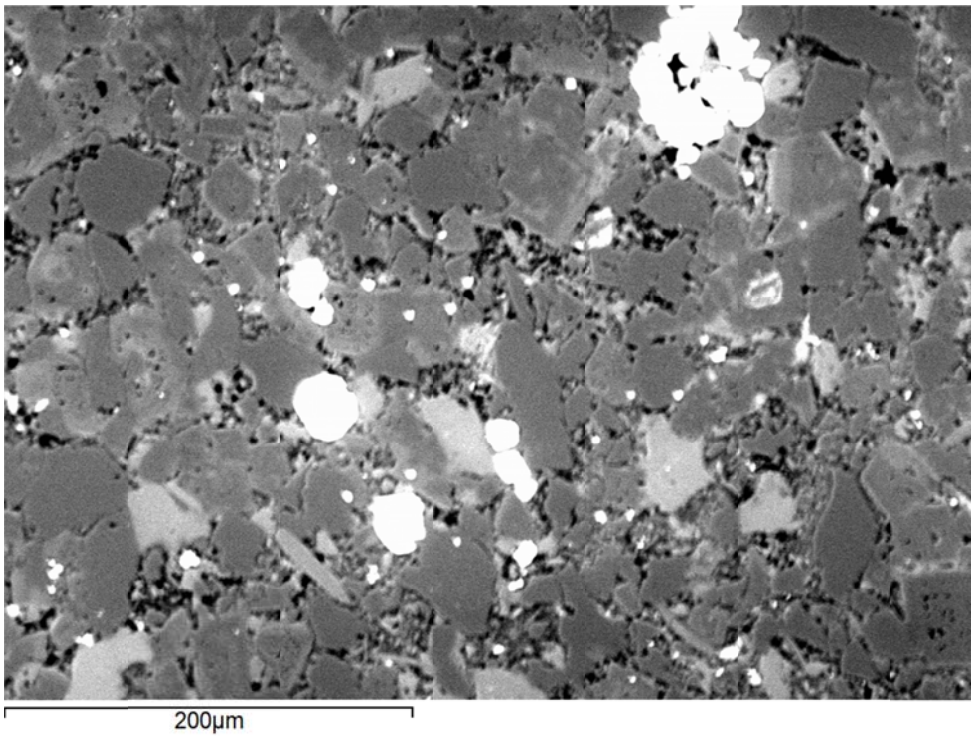

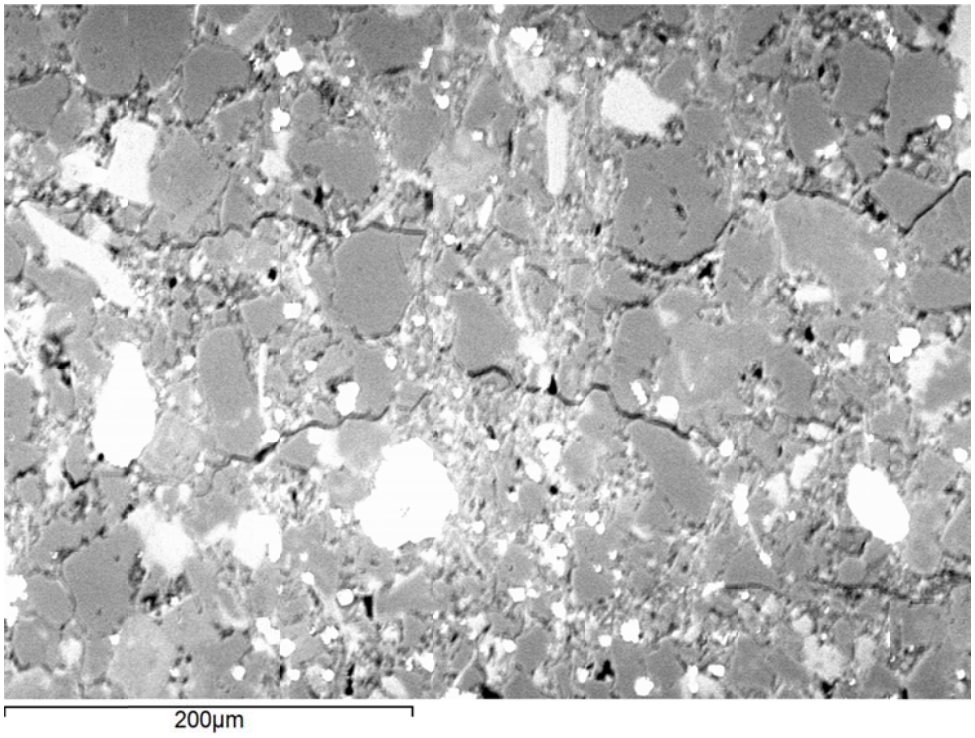

	Applied Geology Laboratory		ID: 116990
	Well Name: NDIC No. 9001	Middle Bakken 5	Rival Field
	API No.: 33-013-00877-00-02	Lithology: Argillaceous, dolomitic siltstone	Depth: 7385.3'

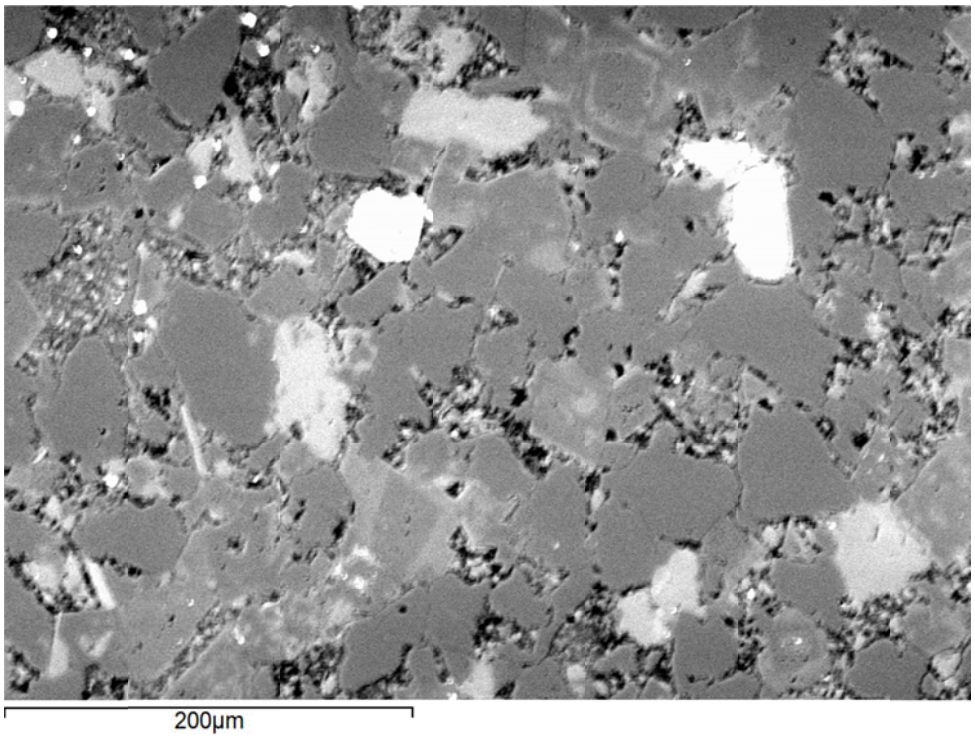

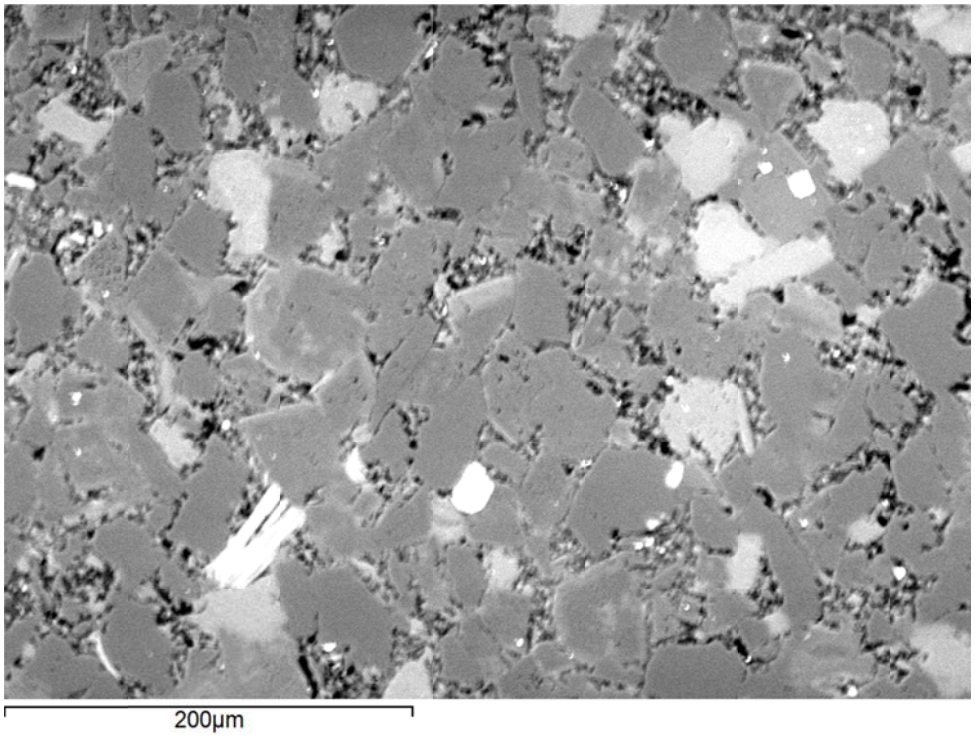

	Applied Geology Laboratory		ID: 116990
	Well Name: NDIC No. 9001	Middle Bakken 5	Rival Field
	API No.: 33-013-00877-00-02	Lithology: Argillaceous, dolomitic siltstone	Depth: 7385.3'

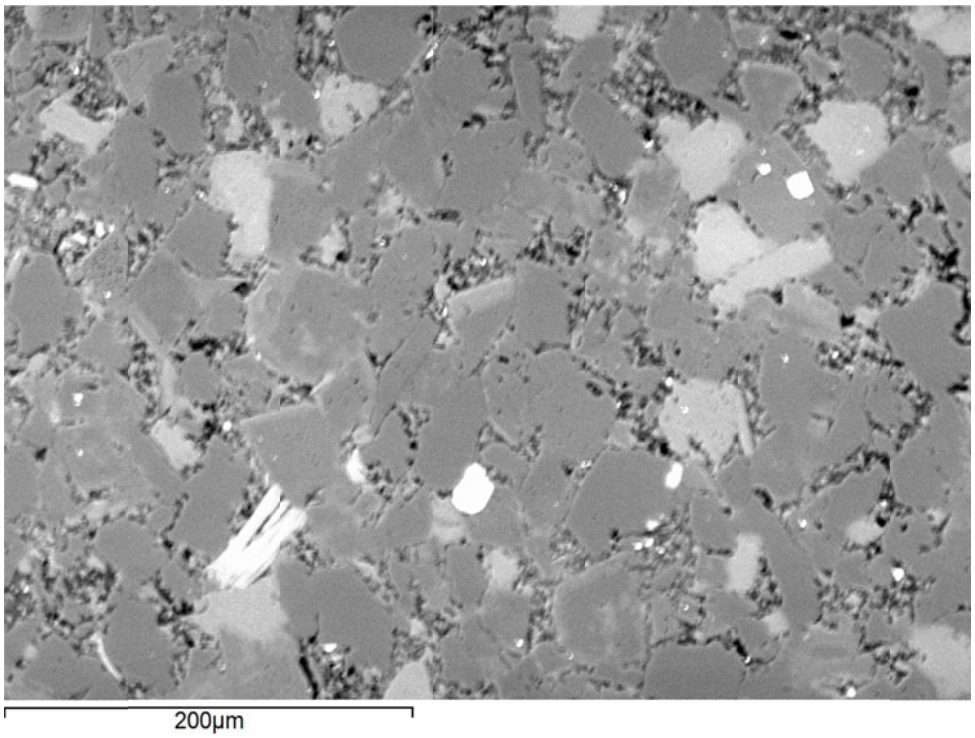

EERC Energy & Environmental Research Center® Putting Research into Practice UND THE UNIVERSITY OF NORTH DAKOTA	**Applied Geology Laboratory**		ID: 116990
	Well Name: NDIC No. 9001	Middle Bakken 5	Rival Field
	API No.: 33-013-00877-00-02	Lithology: Argillaceous, dolomitic siltstone	Depth: 7385.3'

SEM Mineral Map Image Overlaid on BSE Image with Mineral Phase 2D Area Percentages

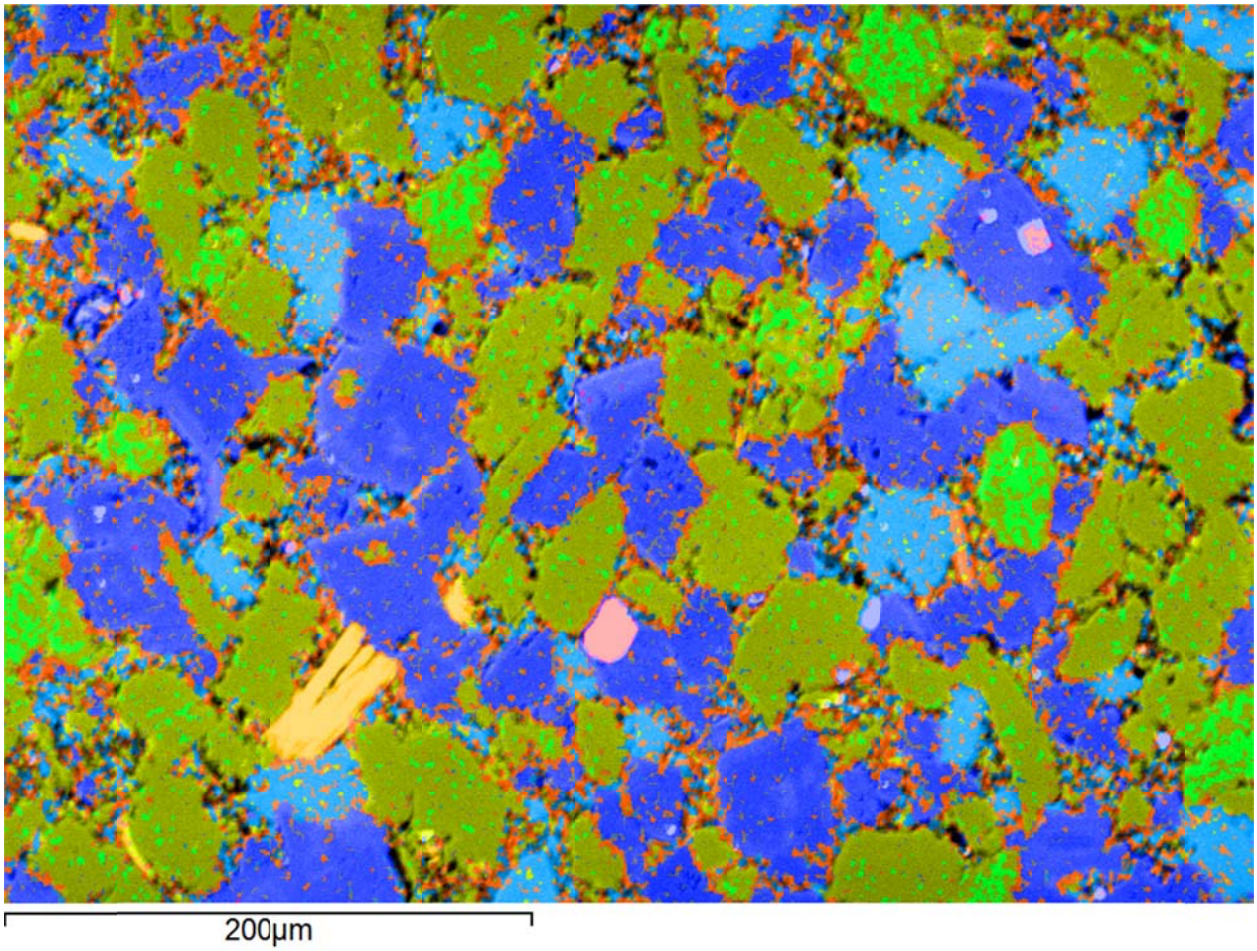

This page intentionally left blank.

EERC Energy & Environmental Research Center® Putting Research into Practice UND THE UNIVERSITY OF NORTH DAKOTA	**Applied Geology Laboratory**		ID: 116991
	Well Name: NDIC No. 9001	Middle Bakken 4	Rival Field
	API No.: 33-013-00877-00-03	Lithology: Argillaceous, dolomitic siltstone	Depth: 7392.4'

SAMPLE PHOTOGRAPH

PHYSICAL PROPERTIES

Porosity and Grain Density by Core Laboratories

Pycnometer Effective Porosity, vol%	Grain Density, g/cm^3
6.55	2.758

EERC Energy & Environmental Research Center® Putting Research into Practice UND THE UNIVERSITY OF NORTH DAKOTA	**Applied Geology Laboratory**		ID: 116991
	Well Name: NDIC No. 9001	Middle Bakken 4	Rival Field
	API No.: 33-013-00877-00-03	Lithology: Argillaceous, dolomitic siltstone	Depth: 7392.4'

PHOTOMICROGRAPHS

Transmission

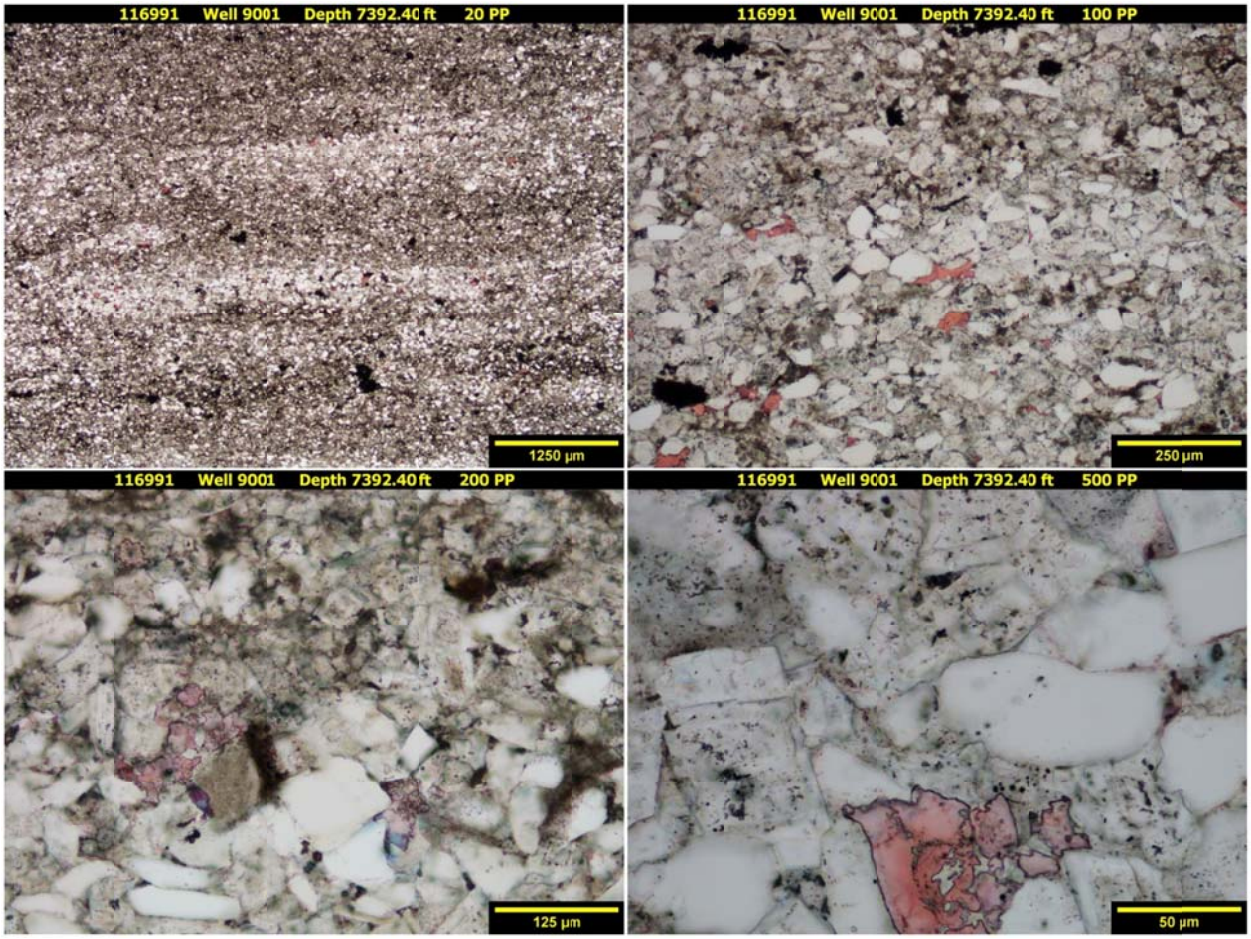

The sample from a depth of 7392.40 ft shows an argillaceous, dolomitic siltstone. Moderate burrowing and slightly wavy laminations are observed. Very fine grained, subangular to subrounded, monocrystalline quartz grains and trace amounts of muscovite and feldspars are disseminated throughout. Extensive anhederal to euhedral dolomitization has occurred throughout the sample. Abundant fine-grained crystalline dolomite occurs as replacement of precursor grains and mud. Trace levels of sparry calcite cement and non-skeletal grains remain. Disseminated pore-filling and replacement pyrite grains are observed throughout. The matrix is composed of a combination of clays and micro- to cryptocrystalline dolomite and occasional calcite cement. No open or closed fractures are observed. Inter-particle porosity is detected at trace amounts using standard optical techniques.

EERC Energy & Environmental Research Center® Putting Research into Practice UND THE UNIVERSITY OF NORTH DAKOTA	**Applied Geology Laboratory**		ID: 116991
	Well Name: NDIC No. 9001	Middle Bakken 4	Rival Field
	API No.: 33-013-00877-00-03	Lithology: Argillaceous, dolomitic siltstone	Depth: 7392.4'

Reflection

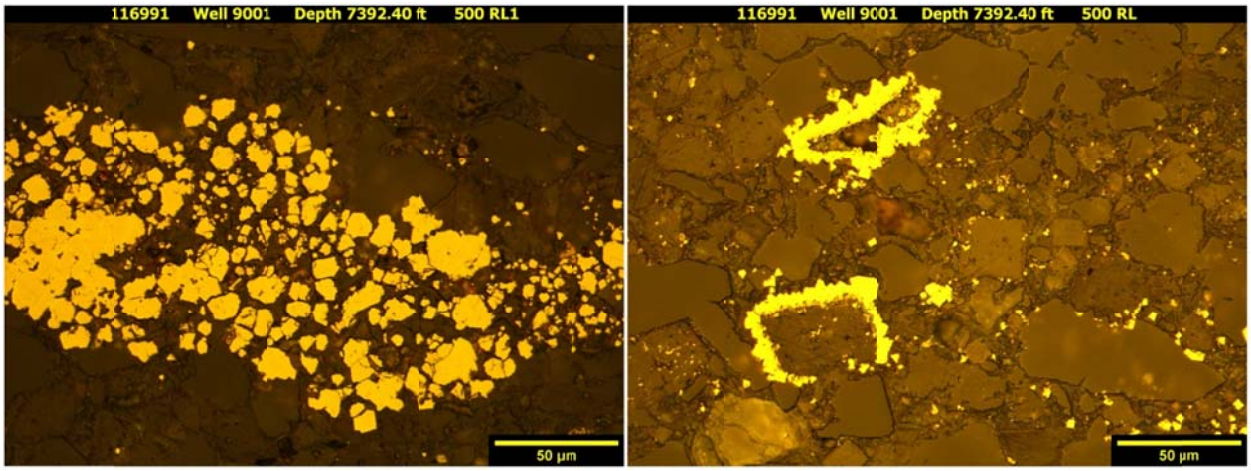

The sample from a depth of 7392.40 ft displays both euhedral and framboidal pyrite grains. Within this sample, euhedral grains are typically found within clay-rich areas. Partial to nearly complete euhdral pyritization of these precursor grains and organics have occurred. Framboidal grains are likely found within precursor pore and organic spaces. Occasional aggregates of semi-mature framboidal pyrite spheres are observed

EERC Energy & Environmental Research Center® Putting Research into Practice UND THE UNIVERSITY OF NORTH DAKOTA	**Applied Geology Laboratory**		ID: 116991
	Well Name: NDIC No. 9001	Middle Bakken 4	Rival Field
	API No.: 33-013-00877-00-03	Lithology: Argillaceous, dolomitic siltstone	Depth: 7392.4'

Transmission and Fluorescence Whole-Slide Images

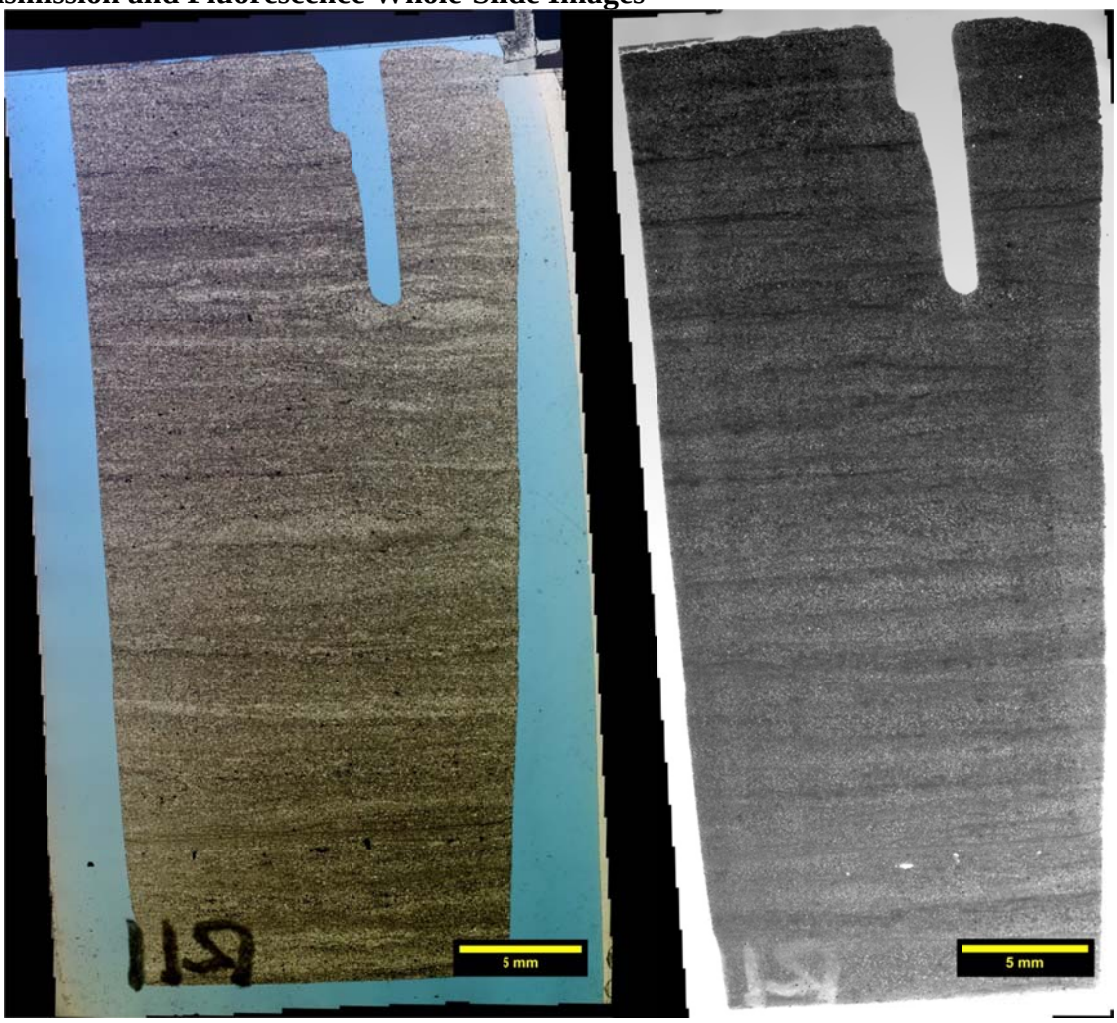

The image at a depth of 7392.40 ft shows a laminated sample. Effective porosity is reported at 6.55 vol%. Inter-particle-based porosity mainly exists within quartz and euhedral dolomite-rich laminations. Lesser amounts of porosity are noted within areas of small, mostly anhedral, dolomite grains and clay concentrations. Pore sizes appear to be very small. No natural or induced fractures are observed.

EERC Energy & Environmental Research Center® Putting Research into Practice UND THE UNIVERSITY OF NORTH DAKOTA	Applied Geology Laboratory		ID: 116991
	Well Name: NDIC No. 9001	Middle Bakken 4	Rival Field
	API No.: 33-013-00877-00-03	Lithology: Argillaceous, dolomitic siltstone	Depth: 7392.4'

XRF BULK CHEMICAL COMPOSITION

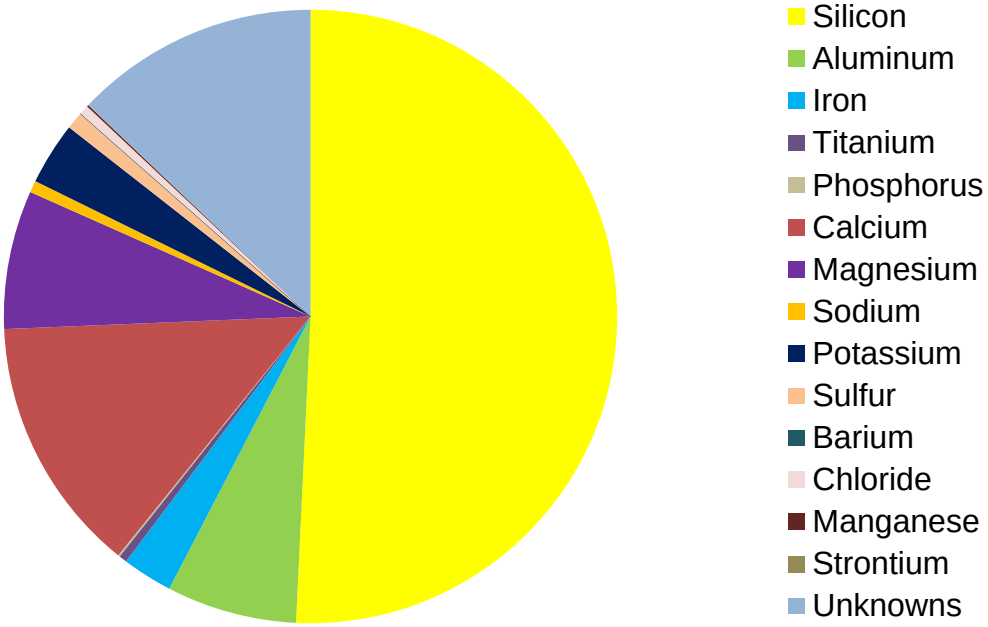

Element	Reporting Convention (Oxide)	Weight %
Si (silicon)	SiO_2	50.75
Al (aluminum)	Al_2O_3	6.87
Fe (iron)	Fe_2O_3	2.65
Ti (titanium)	TiO_2	0.43
P (phosphorus)	P_2O_5	0.09
Ca (calcium)	CaO	13.55
Mg (magnesium)	MgO	7.31
Na (sodium)	Na_2O	0.63
K (potassium)	K_2O	3.30
S (sulfur)	SO_3	0.92
Ba (barium)	BaO	0.00
Cl (chloride)	Cl	0.51
Mn (manganese)	MnO	0.09
Sr (strontium)	SrO	0.01
Unknowns	Due to the presence of carbonates	9.59
Total		100.01

EERC Energy & Environmental Research Center® Putting Research into Practice UND THE UNIVERSITY OF NORTH DAKOTA	**Applied Geology Laboratory**		ID: 116991
	Well Name: NDIC No. 9001	Middle Bakken 4	Rival Field
	API No.: 33-013-00877-00-03	Lithology: Argillaceous, dolomitic siltstone	Depth: 7392.4'

XRD MINERAL PHASE DISTRIBUTION

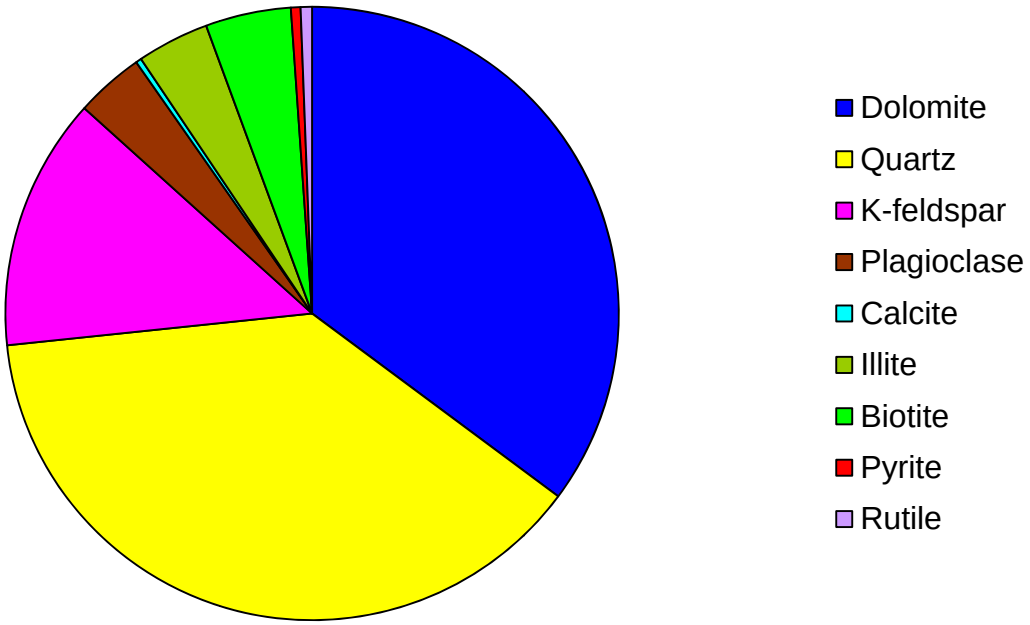

Mineral Phase	Formula	Weight %
Dolomite	$CaMg(CO_3)_2$	35.1
Quartz	SiO_2	38.1
K-feldspar	$KAlSi_3O_8$	13.3
Plagioclase	$Na_{0.5}Ca_{0.5}Al_{1.5}Si_{2.5}O_8$	3.6
Calcite	$CaCO_3$	0.3
Illite	$(K,H_3O)(Al,Mg,Fe)_2(Si,Al)_4O_{10}[(OH)_2,(H_2O)]$	3.8
Biotite	$K(Mg,Fe)_3[(OH)_2AlSi_3O_{10}]$	4.5
Pyrite	FeS_2	0.5
Rutile	TiO_2	0.6

Applied Geology Laboratory		ID: 116991
Well Name: NDIC No. 9001	Middle Bakken 4	Rival Field
API No.: 33-013-00877-00-03	Lithology: Argillaceous, dolomitic siltstone	Depth: 7392.4'

SEM

Observed Minerals

Mineral Phase	Mineral Phase
Calcite	Illite
Quartz	K-feldspar
Pyrite	Zircon
Dolomite	Apatite
Rutile	Albite

High-Magnification BSE Image Annotated with Examples of Mineral Phases Identified

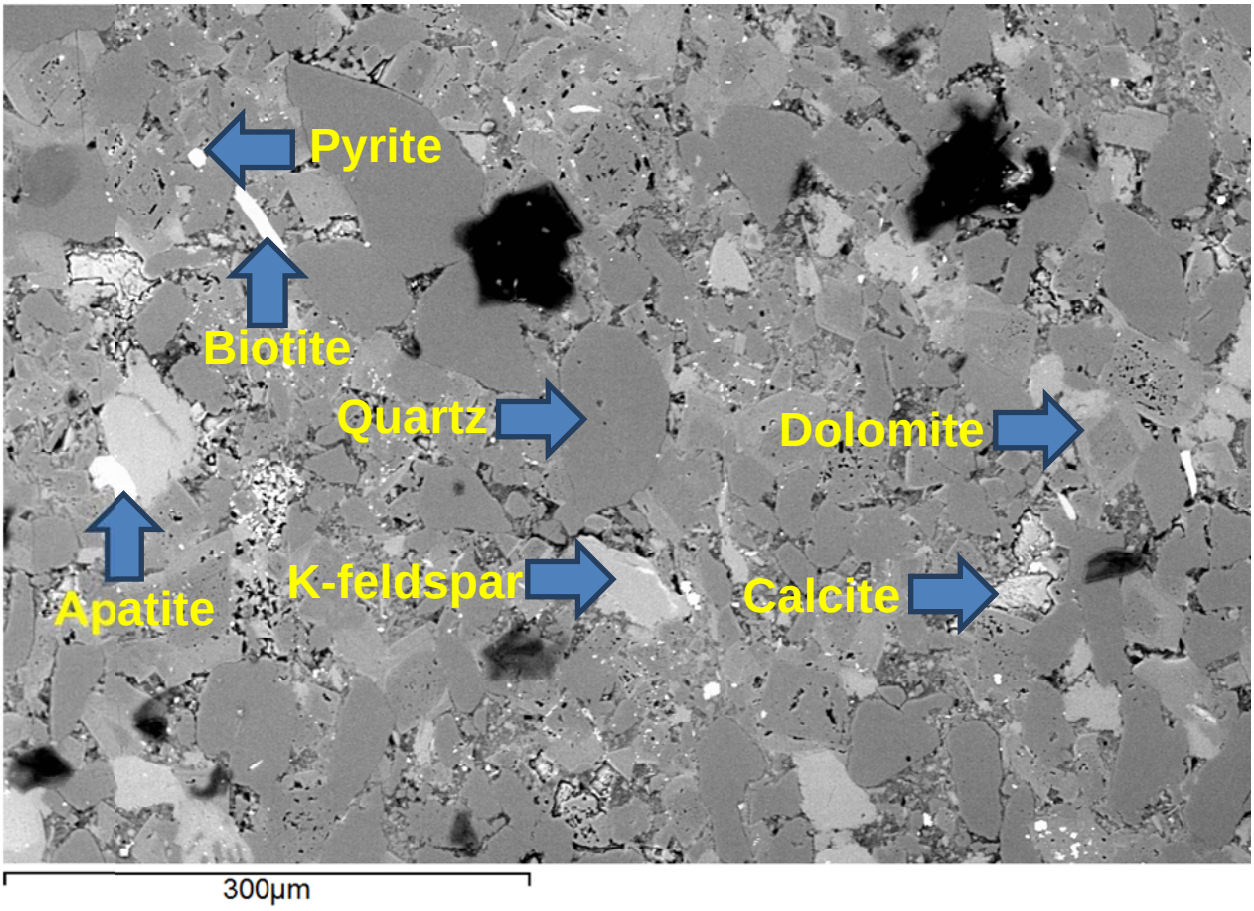

Additional High-Magnification BSE Images

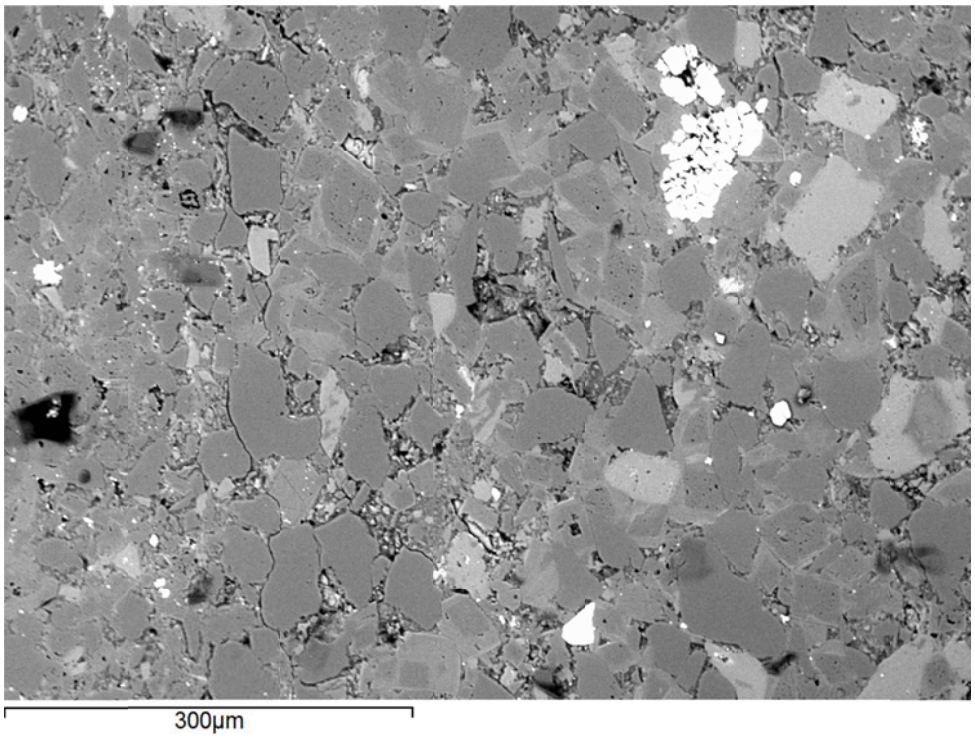

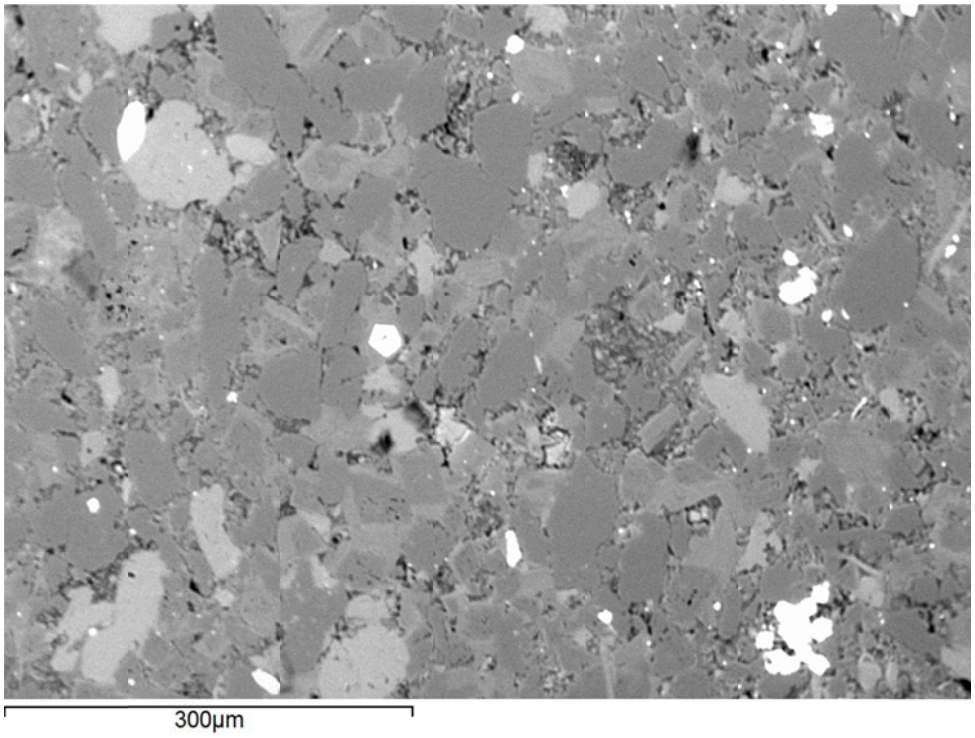

EERC Energy & Environmental Research Center® Putting Research into Practice UND THE UNIVERSITY OF NORTH DAKOTA	**Applied Geology Laboratory**		ID: 116991
	Well Name: NDIC No. 9001	Middle Bakken 4	Rival Field
	API No.: 33-013-00877-00-03	Lithology: Argillaceous, dolomitic siltstone	Depth: 7392.4'

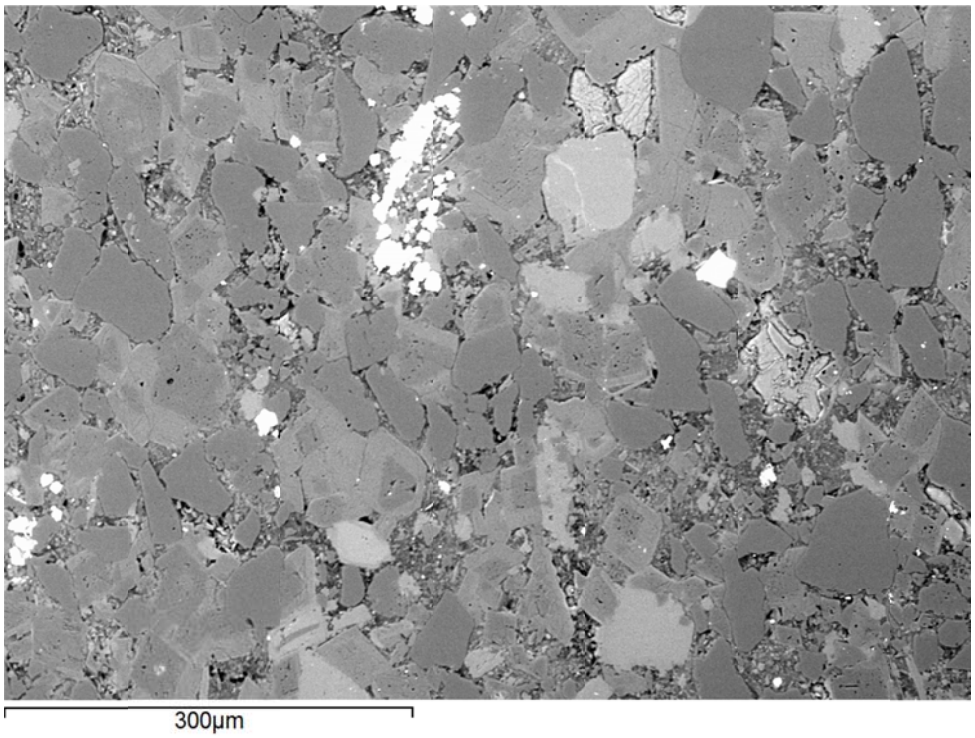

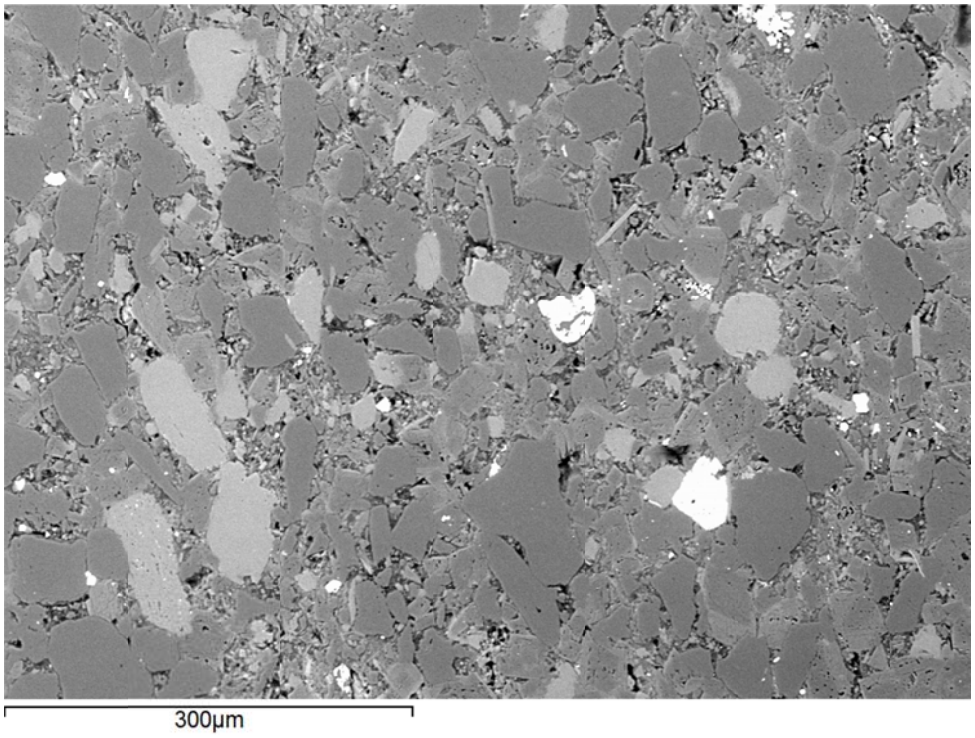

Applied Geology Laboratory		ID: 116991
Well Name: NDIC No. 9001	Middle Bakken 4	Rival Field
API No.: 33-013-00877-00-03	Lithology: Argillaceous, dolomitic siltstone	Depth: 7392.4'

SEM Digital Composite Mineral Map Image Overlaid on BSE Image with Mineral Phase 2D Area Percentages

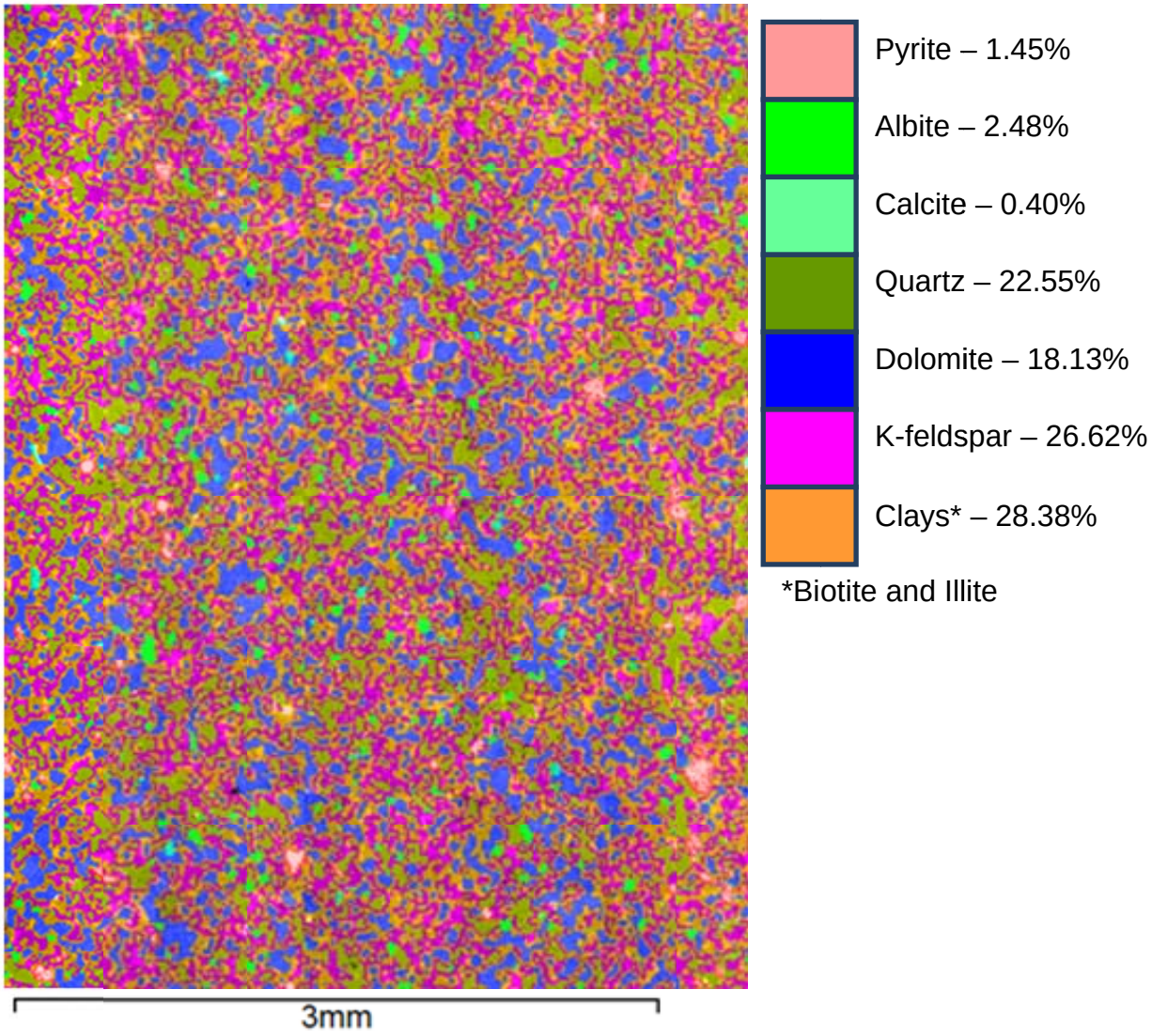

	Applied Geology Laboratory		ID: 116992
	Well Name: NDIC No. 9001	Middle Bakken 3	Rival Field
	API No.: 33-013-00877-00-04	Lithology: Dolomitic siltstone	Depth: 7394.8'

SAMPLE PHOTOGRAPH

PHYSICAL PROPERTIES

Porosity and Grain Density by Core Laboratories

Pycnometer Effective Porosity, vol%	Grain Density, g/cm^3
8.70	2.738

EERC Energy & Environmental Research Center® Putting Research into Practice UND THE UNIVERSITY OF NORTH DAKOTA	**Applied Geology Laboratory**		ID: 116992
	Well Name: NDIC No. 9001	Middle Bakken 3	Rival Field
	API No.: 33-013-00877-00-04	Lithology: Dolomitic siltstone	Depth: 7394.8'

PHOTOMICROGRAPHS

Transmission

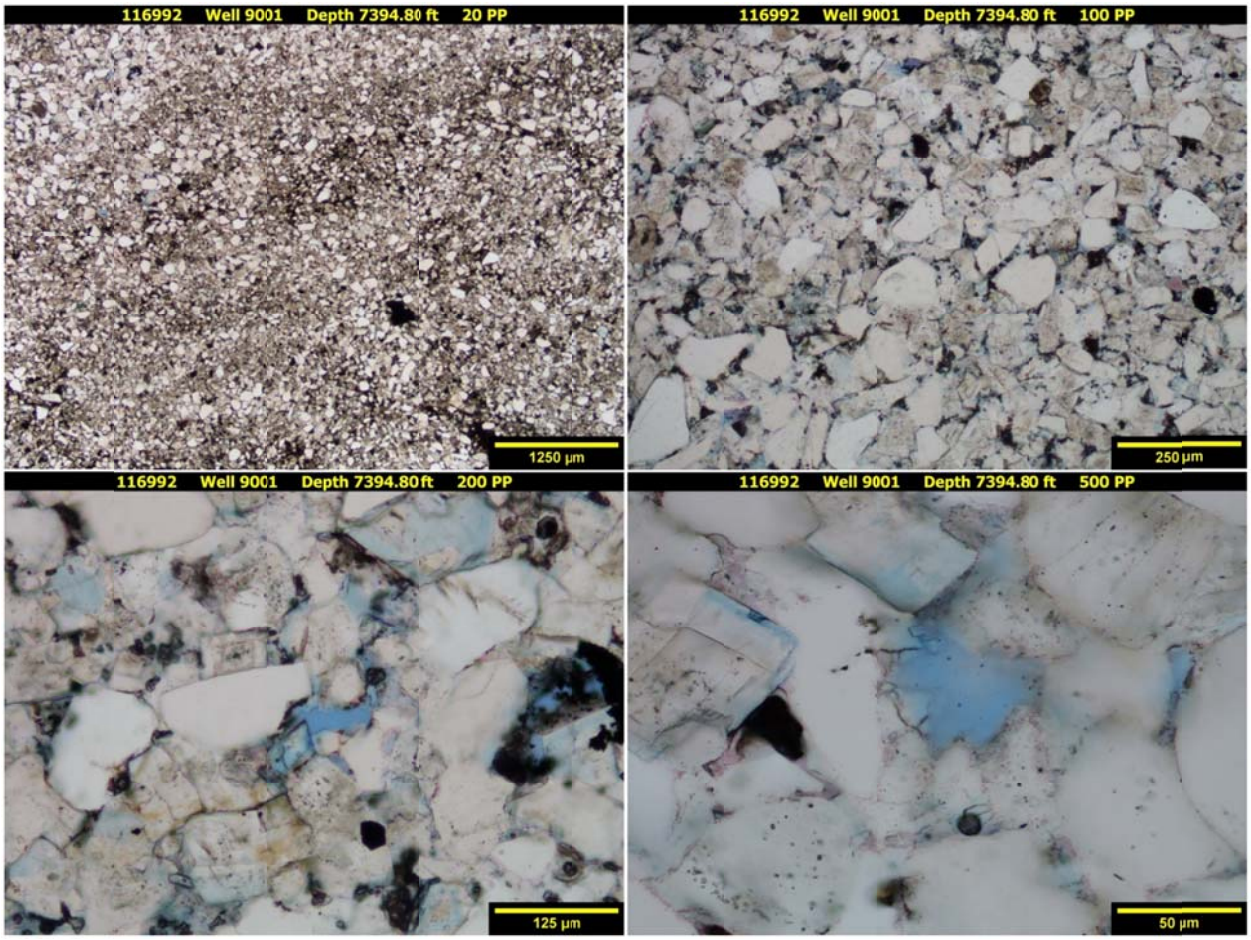

The sample from a depth of 7394.80 ft shows a moderately bioturbated dolomitic siltstone. Very fine to fine-grained, angular to subangular, monocrystalline quartz grains, lesser amounts of feldspar, and trace levels of muscovite and biotite are disseminated throughout. Extensive anhedral to euhedral dolomitization (trace ferroan) has occurred throughout the sample. No calcareous skeletal or non-skeletal grains remain. Disseminated pore-filling and replacement pyrite grains are present throughout. Clay is found at small quantities, assisting in creating faint, wavy laminations and lenses because of burrowing. No fractures are observed. Organics are typically associated with pyrite. A good amount (for Middle Bakken) of inter-particle porosity is observed using standard petrographic techniques.

	Applied Geology Laboratory		ID: 116992
	Well Name: NDIC No. 9001	Middle Bakken 3	Rival Field
	API No.: 33-013-00877-00-04	Lithology: Dolomitic siltstone	Depth: 7394.8'

Reflection

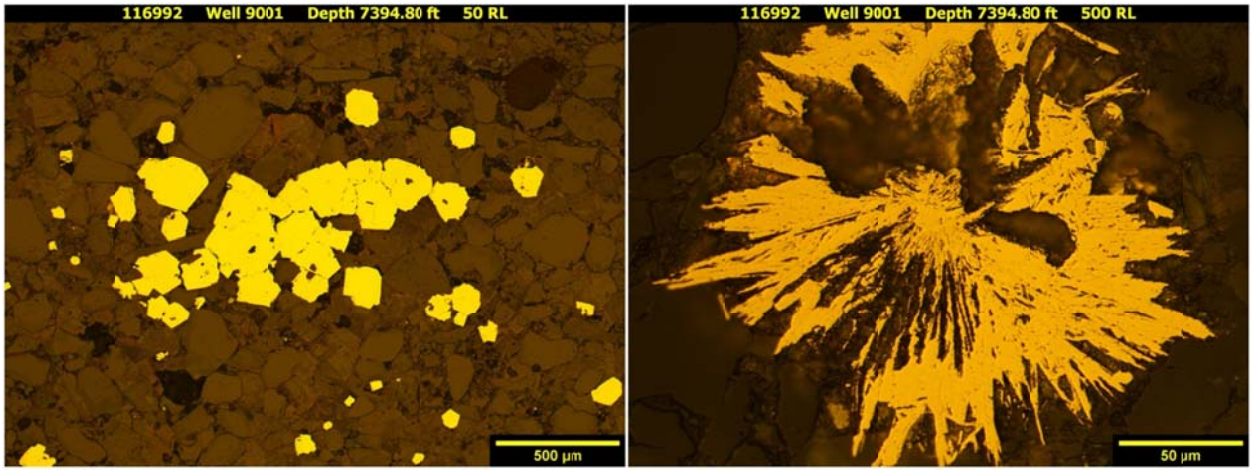

The sample from a depth of 7394.80 ft displays predominantly euhedral and trace amounts of framboidal pyrite growth. This diagenetic mineral acts predominantly as a grain replacer and pore filler. Euhedral grains are largely fine-grained. Aggregates of euhedral grains form to create larger medium-sized grains. Framboidal pyrite is very rare and represents some of the smallest grains within the sample. Partial to nearly complete pyritization of precursor grains and organics have occurred at some localities. Unique to this sample are the fiberous- or spinny-like pyrite species, possible replacement of carbonate concretions. Organics observed are typically associated with both euhedral and framboidal pyrite.

EERC Energy & Environmental Research Center® Putting Research into Practice UND THE UNIVERSITY OF NORTH DAKOTA	**Applied Geology Laboratory**		ID: 116992
	Well Name: NDIC No. 9001	Middle Bakken 3	Rival Field
	API No.: 33-013-00877-00-04	Lithology: Dolomitic siltstone	Depth: 7394.8'

Transmission and Fluorescence Whole-Slide Images

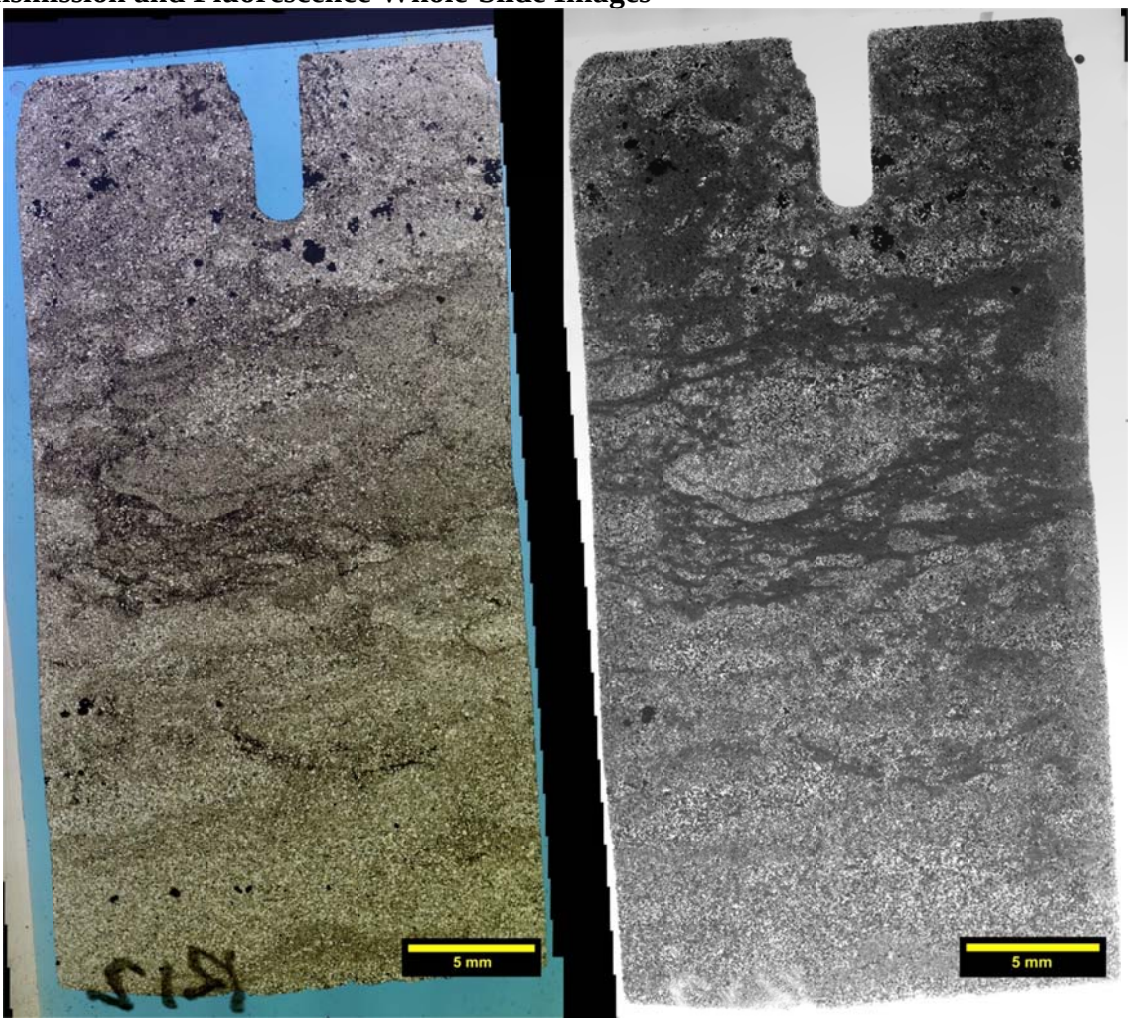

The image is moderately bioturbated, aiding in the heterogeneity of the sample. Effective porosity is reported at 8.70 vol%. The center to upper portion is finer-grained and more clay-rich. This combination of factors has limited inter-particle porosity. The upper zone shows more complete dolomitization and larger pyrite grains, perhaps revealing a more advanced diagenetical status. These factors can greatly reduce porosity. The bottom portion has coarser quartz and dolomite grains. The dolomite is more euhedral, thus allowing for micropores after replacement, and pyrite grains are small compared to the upper portion of the thin section. These characteristics have aided in increased porosity. No natural fractures were observed. The only induce fracture is at the upper left.

EERC Energy & Environmental Research Center® Putting Research into Practice UND THE UNIVERSITY OF NORTH DAKOTA	**Applied Geology Laboratory**		ID: 116992
	Well Name: NDIC No. 9001	Middle Bakken 3	Rival Field
	API No.: 33-013-00877-00-04	Lithology: Dolomitic siltstone	Depth: 7394.8'

XRF BULK CHEMICAL COMPOSITION

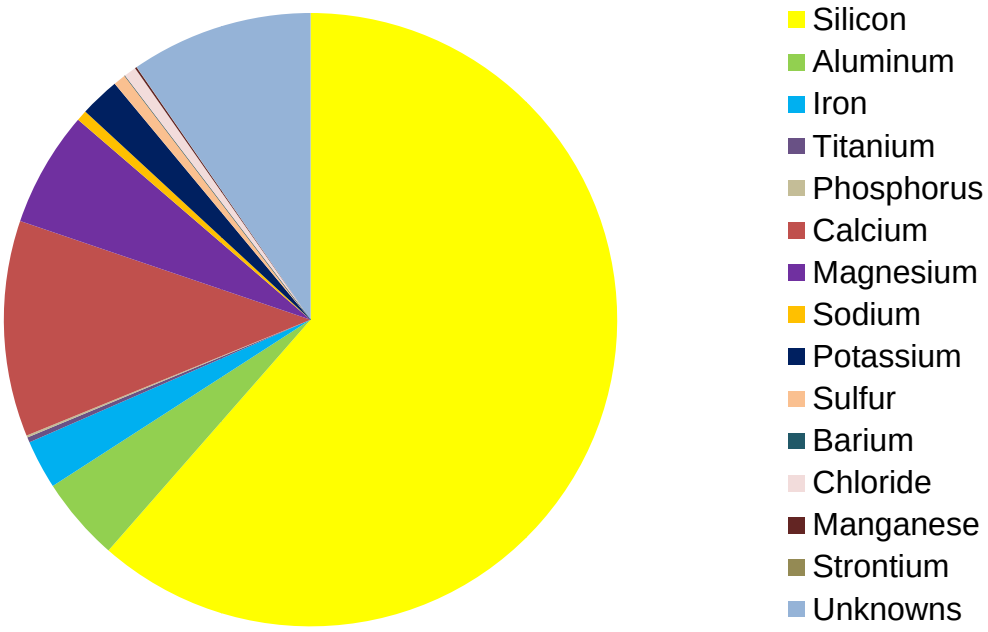

Element	Reporting Convention (Oxide)	Weight %
Si (silicon)	SiO_2	61.45
Al (aluminum)	Al_2O_3	4.44
Fe (iron)	Fe_2O_3	2.57
Ti (titanium)	TiO_2	0.27
P (phosphorus)	P_2O_5	0.11
Ca (calcium)	CaO	11.38
Mg (magnesium)	MgO	6.10
Na (sodium)	Na_2O	0.56
K (potassium)	K_2O	2.11
S (sulfur)	SO_3	0.67
Ba (barium)	BaO	0.00
Cl (chloride)	Cl	0.65
Mn (manganese)	MnO	0.10
Sr (strontium)	SrO	0.01
Unknowns	Due to the presence of carbonates	9.59
Total		100.01

	Applied Geology Laboratory		ID: 116992
EERC Energy & Environmental Research Center® Putting Research into Practice UND THE UNIVERSITY OF NORTH DAKOTA	Well Name: NDIC No. 9001	Middle Bakken 3	Rival Field
	API No.: 33-013-00877-00-04	Lithology: Dolomitic siltstone	Depth: 7394.8'

XRD MINERAL PHASE DISTRIBUTION

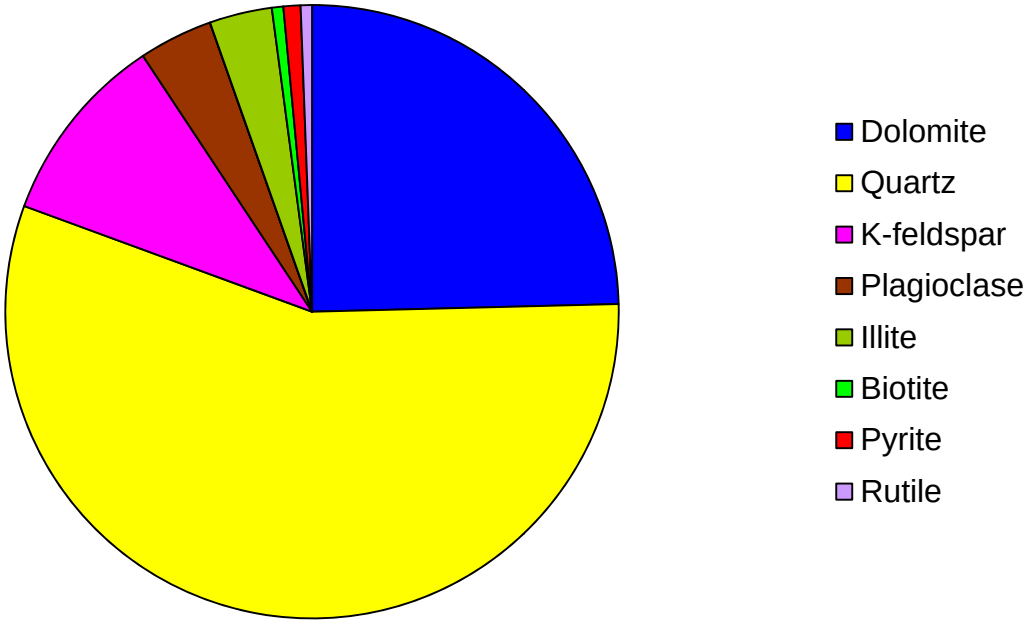

Mineral Phase	Formula	Weight %
Dolomite	$CaMg(CO_3)_2$	24.6
Quartz	SiO_2	56.0
K-feldspar	$KAlSi_3O_8$	10.1
Plagioclase	$Na_{0.5}Ca_{0.5}Al_{1.5}Si_{2.5}O_8$	3.9
Illite	$(K,H_3O)(Al,Mg,Fe)_2(Si,Al)_4O_{10}[(OH)_2,(H_2O)]$	3.3
Biotite	$K(Mg,Fe)_3[(OH)_2AlSi_3O_{10}]$	0.6
Pyrite	FeS_2	0.9
Rutile	TiO_2	0.6

Applied Geology Laboratory		ID: 116992
Well Name: NDIC No. 9001	Middle Bakken 3	Rival Field
API No.: 33-013-00877-00-04	Lithology: Dolomitic siltstone	Depth: 7394.8'

SEM

Observed Minerals

Mineral Phase	Mineral Phase
Pyrite	Zircon
Illite	Dolomite
Quartz	Apatite
K-feldspar	Biotite

High-Magnification BSE Image Annotated with Examples of Mineral Phases Identified

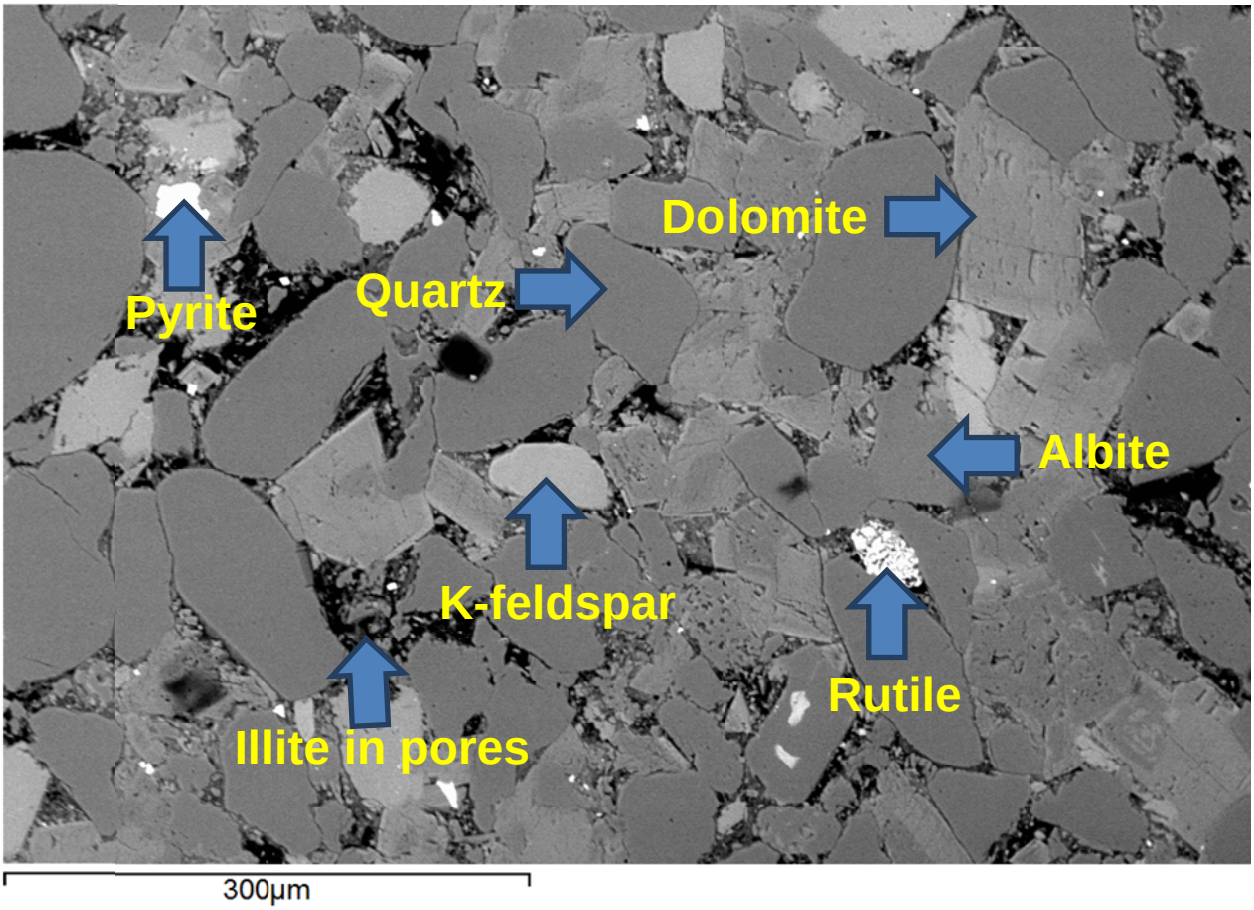

Additional High-Magnification BSE Images

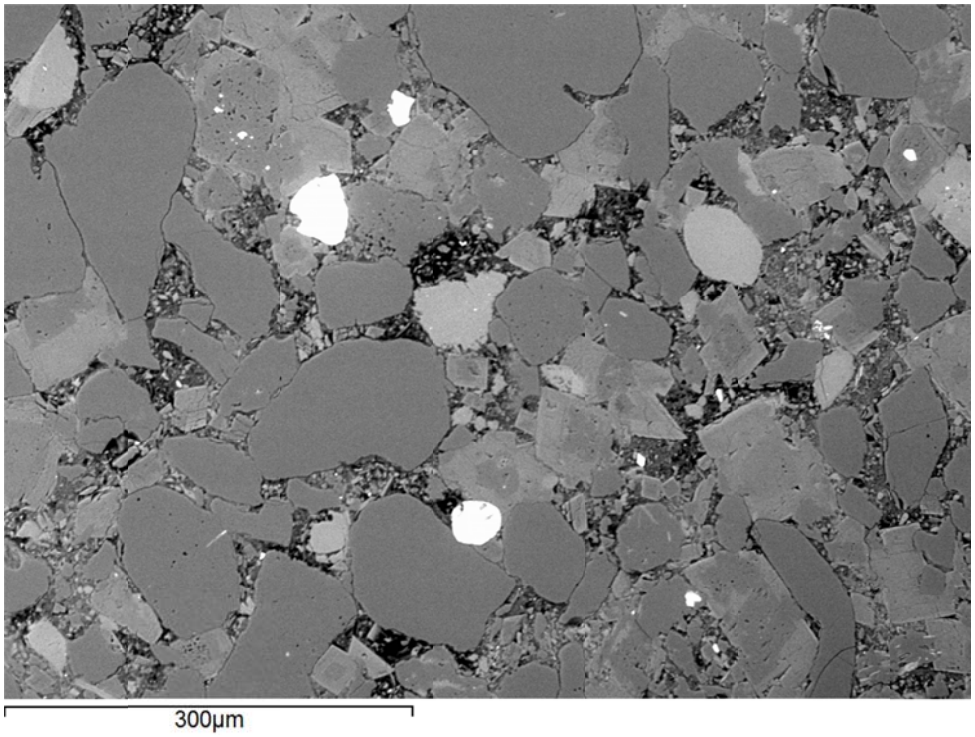

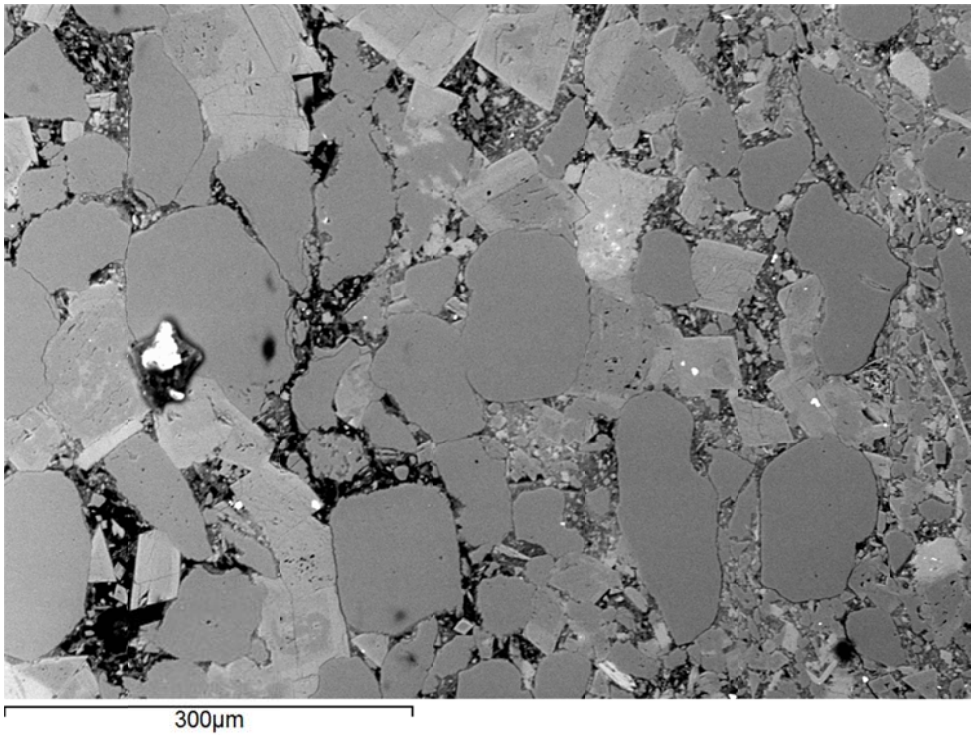

	Applied Geology Laboratory		ID: 116992
	Well Name: NDIC No. 9001	Middle Bakken 3	Rival Field
	API No.: 33-013-00877-00-04	Lithology: Dolomitic siltstone	Depth: 7394.8'

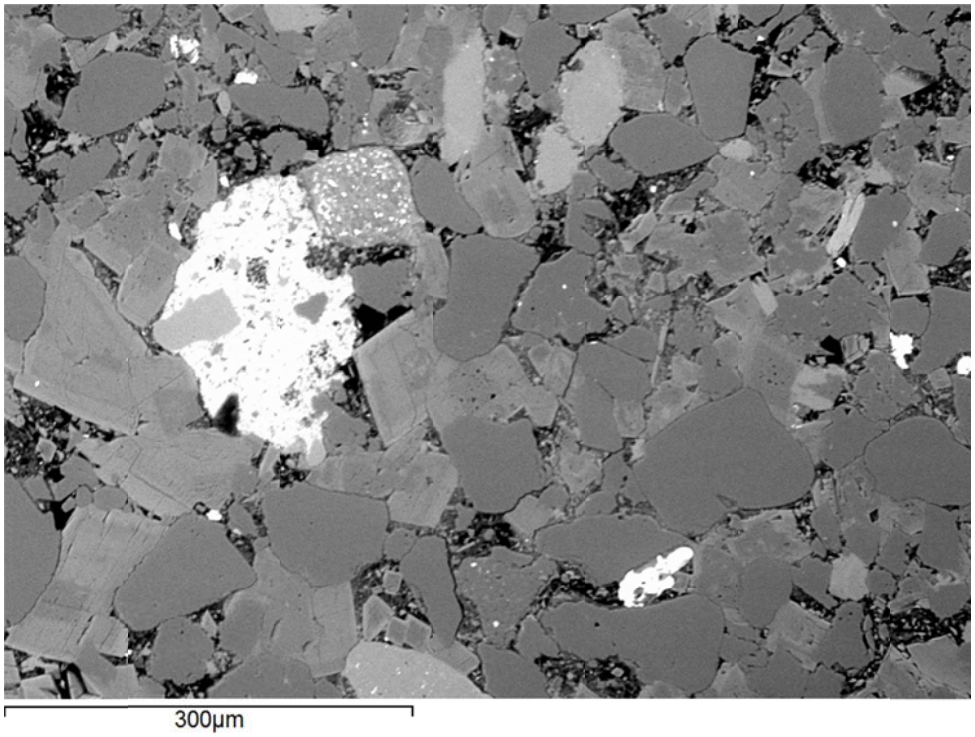

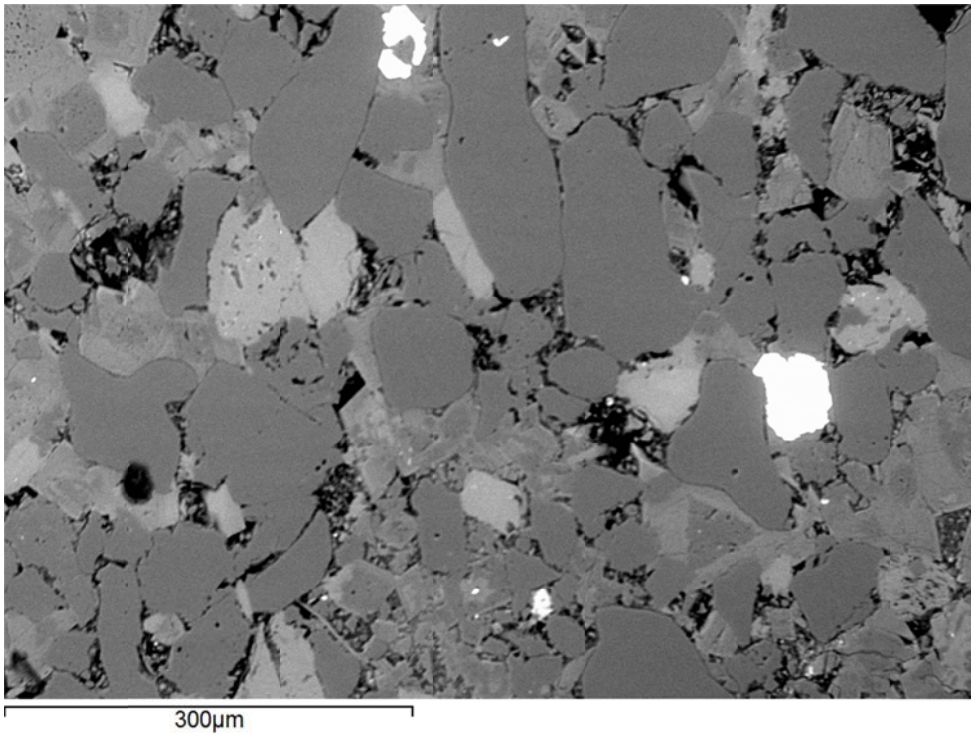

EERC Energy & Environmental Research Center® Putting Research into Practice UND THE UNIVERSITY OF NORTH DAKOTA	**Applied Geology Laboratory**		ID: 116992
	Well Name: NDIC No. 9001	Middle Bakken 3	Rival Field
	API No.: 33-013-00877-00-04	Lithology: Dolomitic siltstone	Depth: 7394.8'

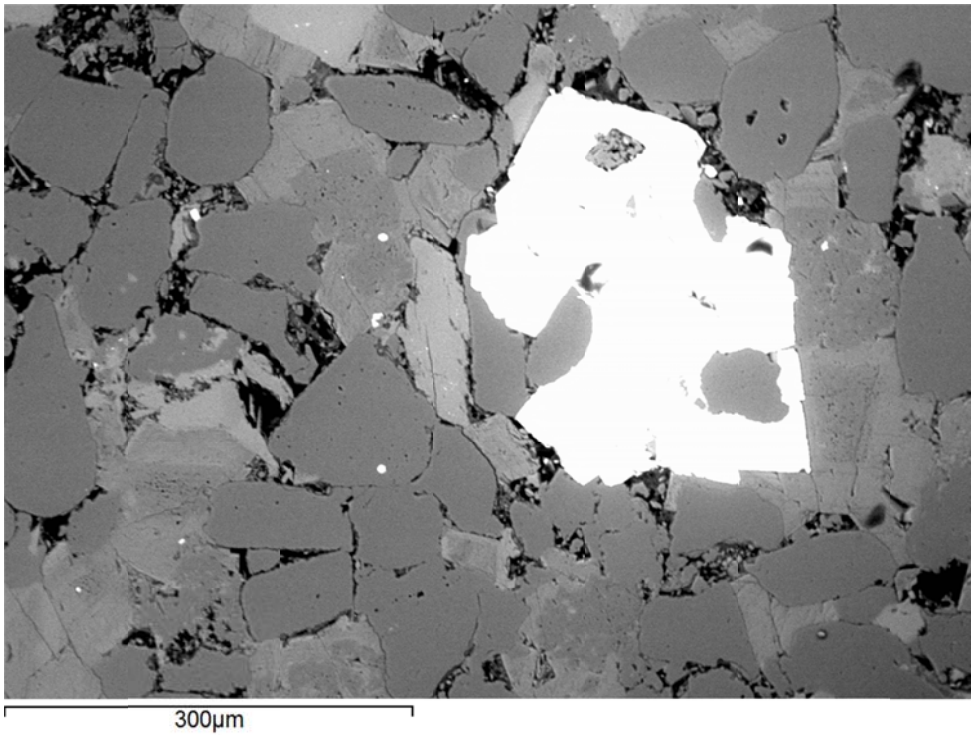

EERC Energy & Environmental Research Center® Putting Research into Practice UND THE UNIVERSITY OF NORTH DAKOTA	**Applied Geology Laboratory**		ID: 116992
	Well Name: NDIC No. 9001	Middle Bakken 3	Rival Field
	API No.: 33-013-00877-00-04	Lithology: Dolomitic siltstone	Depth: 7394.8'

SEM Mineral Map Image Overlaid on BSE Image with Mineral Phase 2D Area Percentages

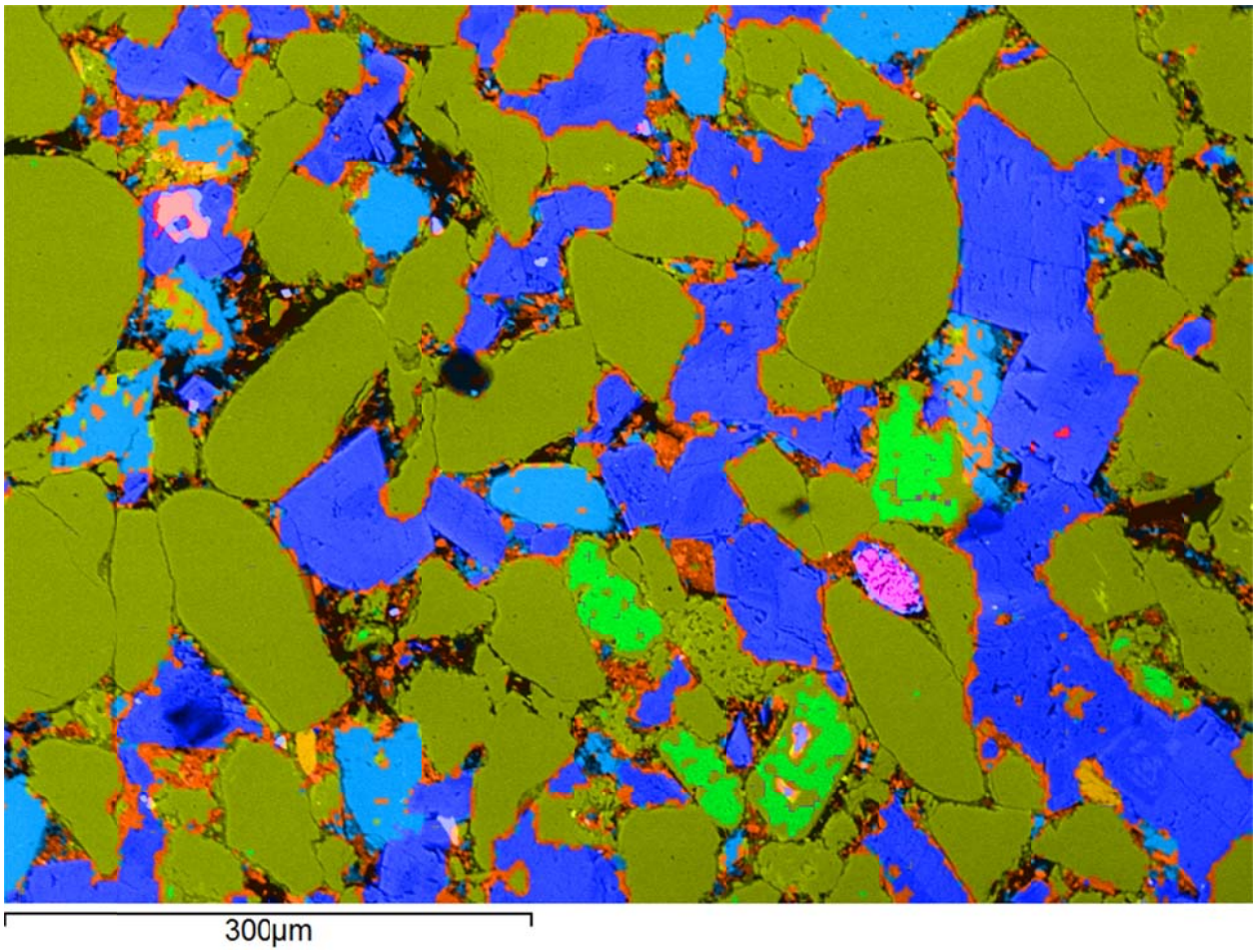

This page intentionally left blank.

EERC Energy & Environmental Research Center® Putting Research into Practice UND THE UNIVERSITY OF NORTH DAKOTA	**Applied Geology Laboratory**		ID: 116993
	Well Name: NDIC No. 9001	Middle Bakken 2	Rival Field
	API No.: 33-013-00877-00-05	Lithology: Calcareous siltsone	Depth: 7399.0'

SAMPLE PHOTOGRAPH

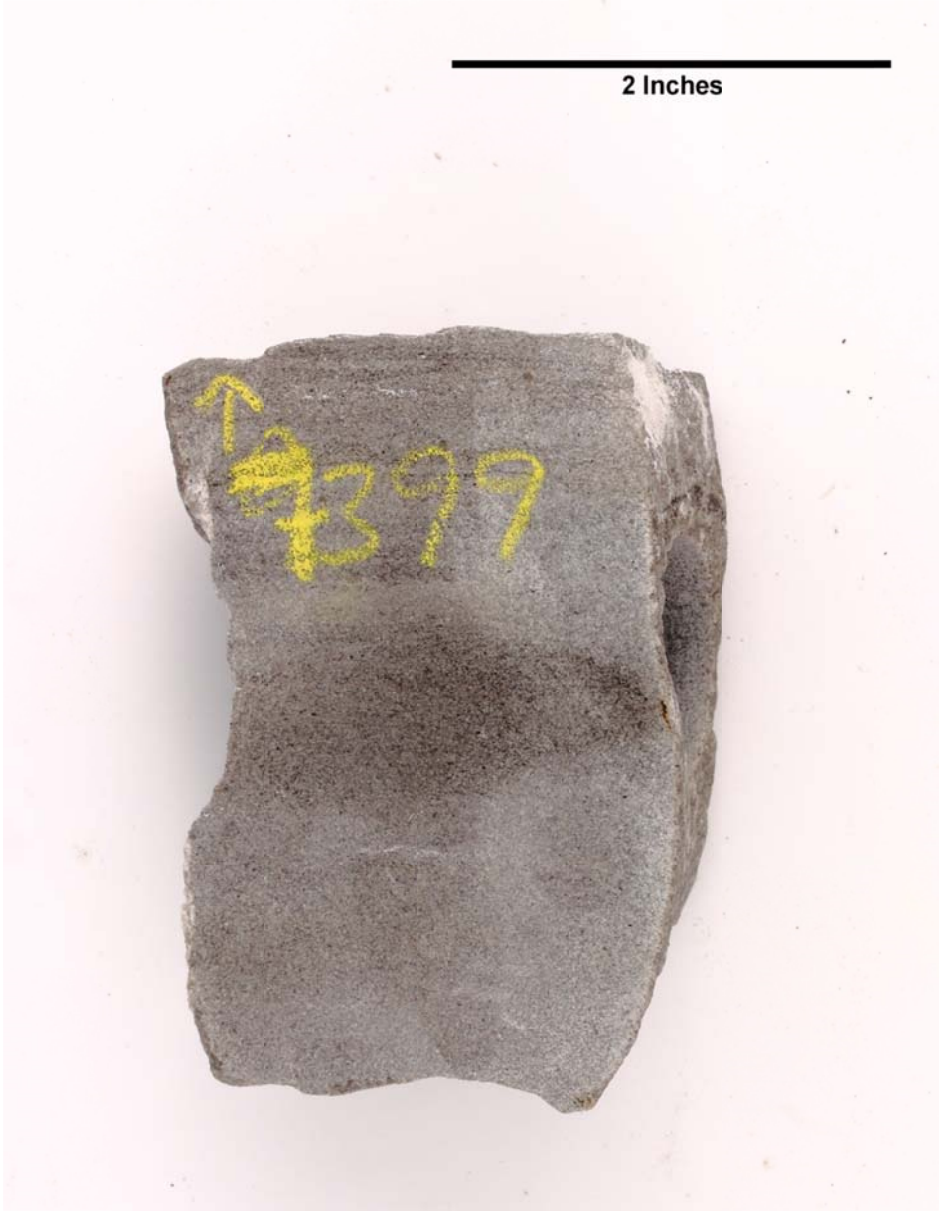

	Applied Geology Laboratory		ID: 116993
EERC Energy & Environmental Research Center® Putting Research into Practice UND THE UNIVERSITY OF NORTH DAKOTA	Well Name: NDIC No. 9001	Middle Bakken 2	Rival Field
	API No.: 33-013-00877-00-05	Lithology: Calcareous siltsone	Depth: 7399.0'

PHOTOMICROGRAPHS

Transmission

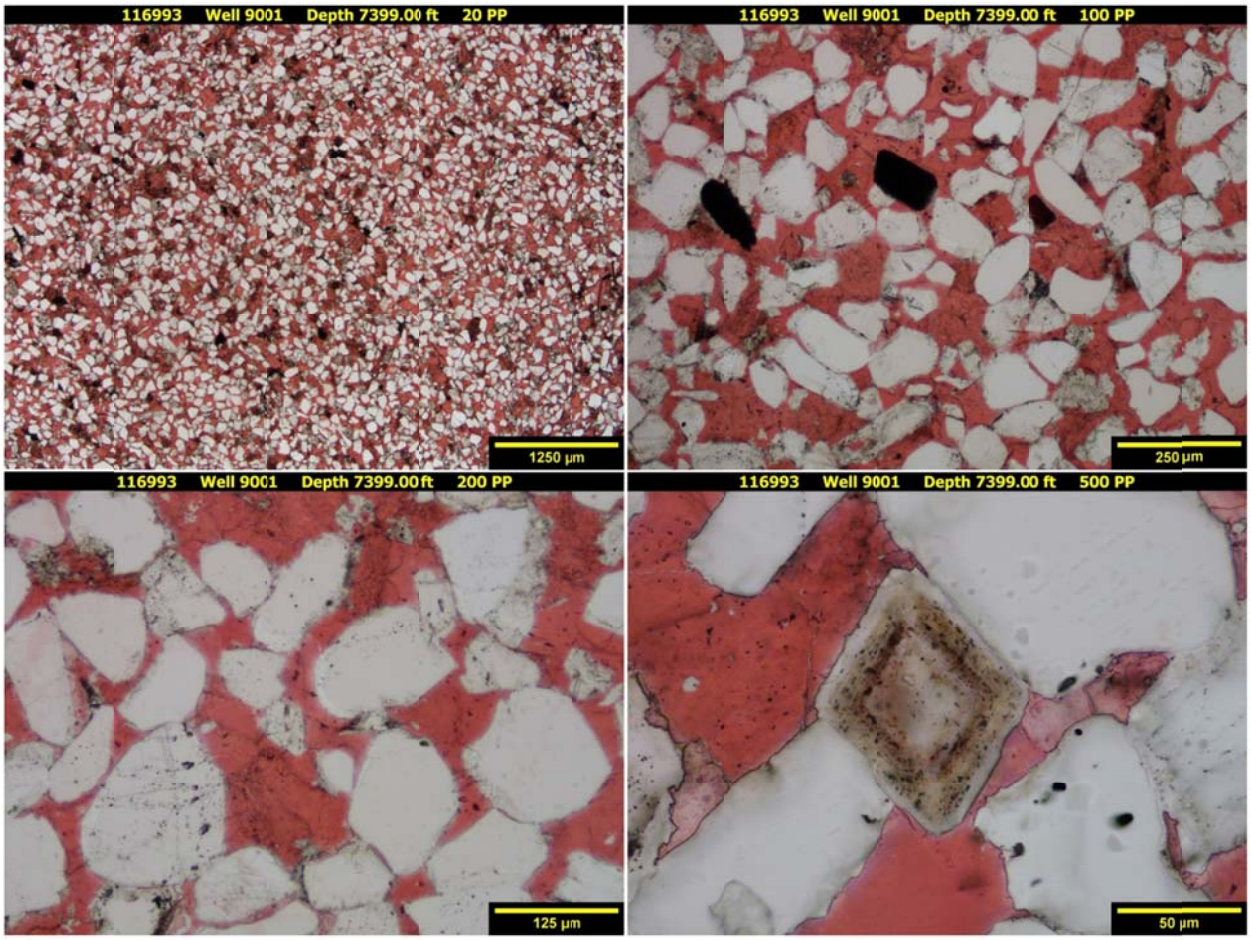

The sample captured at a depth of 7399.00 ft is a calcareous siltstone. It is a very massive sample expressing no bedding structures. Fine-grained, subangular to subrounded, monocrystalline quartz grains are prevalent. Trace amounts of muscovite, rutile, and feldspars are disseminated throughout. Euhedral dolomitization has occurred sparingly throughout the sample. Rare skeletal and common non-skeletal calcite remains. Disseminated pore-filling and replacement pyrite grains exist throughout. The matrix consists primarily of sparry calcite cement and rare levels of clay. Organics detection is usually associated with pyrite grains. No natural fractures or porosity are detected using standard optical techniques.

EERC Energy & Environmental Research Center® Putting Research into Practice UND THE UNIVERSITY OF NORTH DAKOTA	**Applied Geology Laboratory**		ID: 116993
	Well Name: NDIC No. 9001	Middle Bakken 2	Rival Field
	API No.: 33-013-00877-00-05	Lithology: Calcareous siltsone	Depth: 7399.0'

Reflection

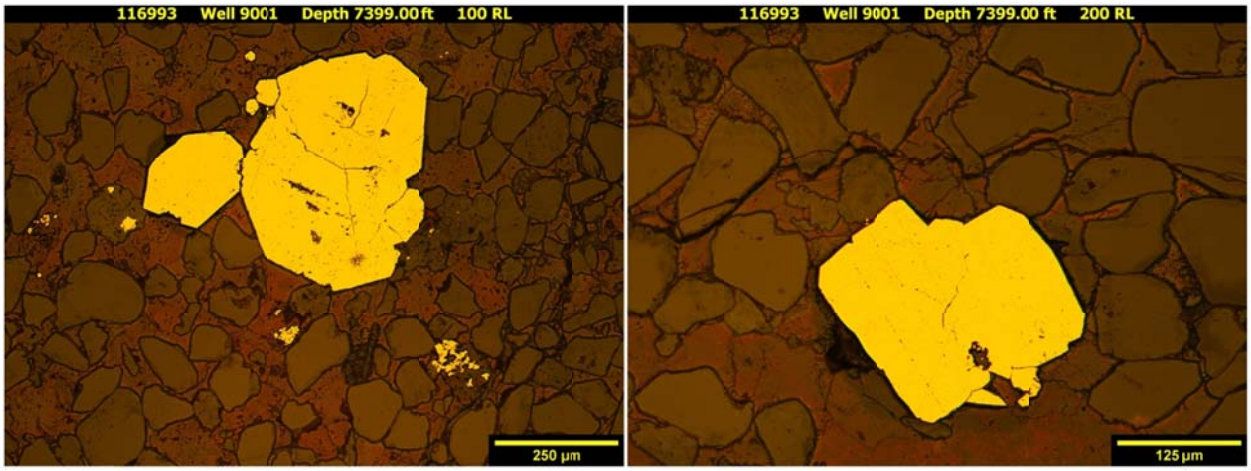

The sample from a depth of 7399.80 ft displays only euhedral framboidal pyrite growth. The sample reveals a lesser degree of pyrite. This diagenetic mineralization replaces precursor minerals and occupies pore space. Euhedral grains are fine- to medium-grained. Because of the rounded shape, some observed grains may be of a clastic nature.

EERC Energy & Environmental Research Center® Putting Research into Practice UND THE UNIVERSITY OF NORTH DAKOTA	**Applied Geology Laboratory**		ID: 116993
	Well Name: NDIC No. 9001	Middle Bakken 2	Rival Field
	API No.: 33-013-00877-00-05	Lithology: Calcareous siltsone	Depth: 7399.0'

Transmission and Fluorescence Whole-Slide Images

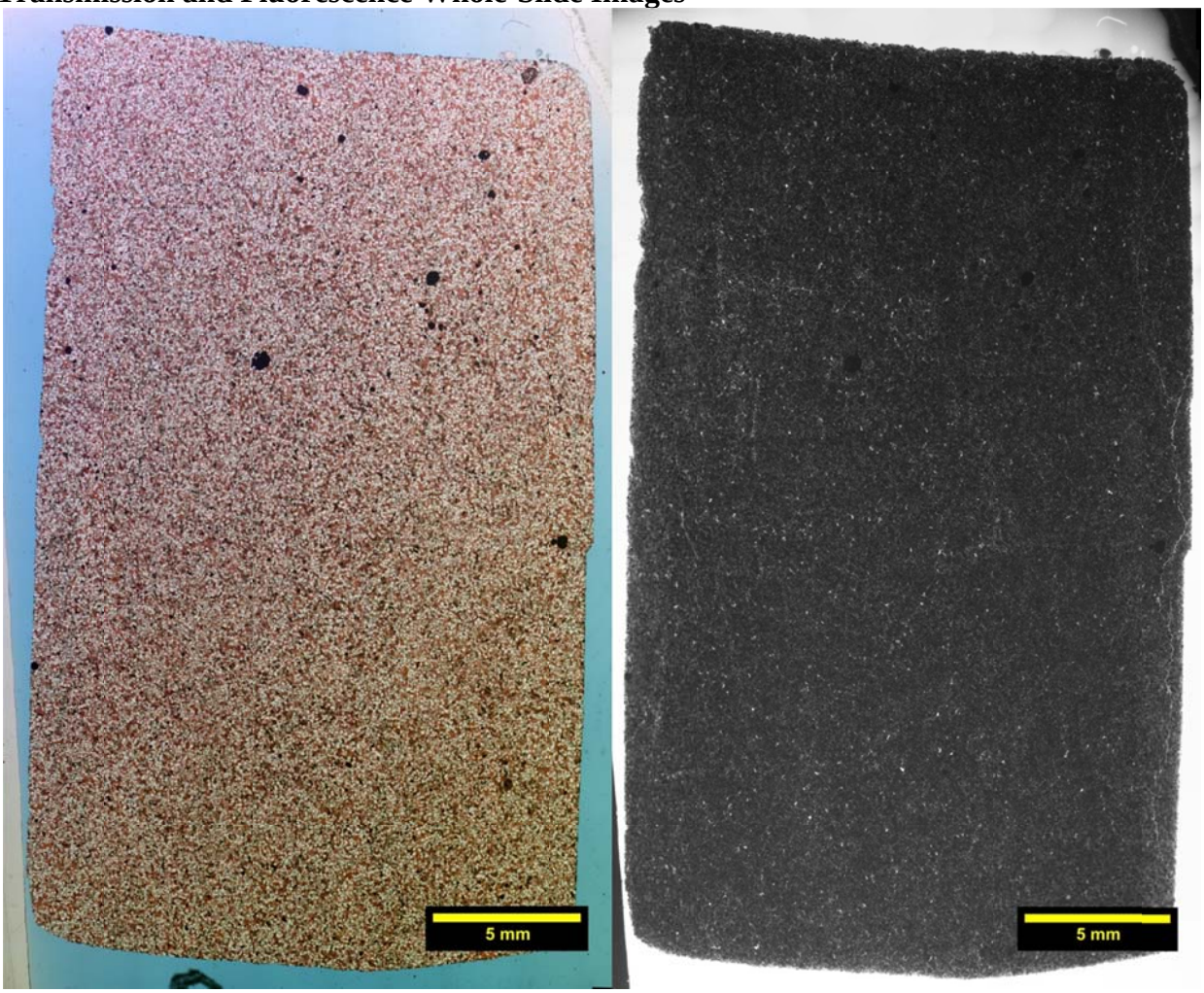

The sample collected at a depth of 7399.00 ft displays a relatively homogeneous calcareous siltstone lacking any bedding features. The sample is well-cemented with calcite spar. The observed limited micro-inter-particle porosity may be due to dolomitization, incomplete calcite cementation, and/or mineral dissolution (feldspar) or leaching (pyrite). No legitimate fractures are detected.

EERC Energy & Environmental Research Center® Putting Research into Practice UND THE UNIVERSITY OF NORTH DAKOTA	**Applied Geology Laboratory**		ID: 116993
	Well Name: NDIC No. 9001	Middle Bakken 2	Rival Field
	API No.: 33-013-00877-00-05	Lithology: Calcareous siltsone	Depth: 7399.0'

XRF BULK CHEMICAL COMPOSITION

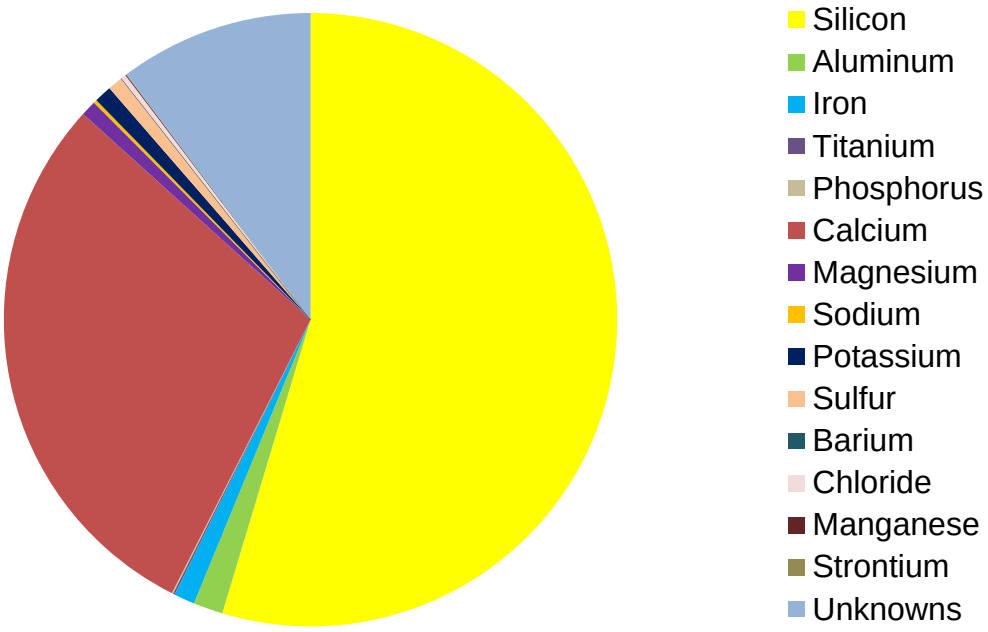

Element	Reporting Convention (Oxide)	Weight %
Si (silicon)	SiO_2	54.65
Al (aluminum)	Al_2O_3	1.56
Fe (iron)	Fe_2O_3	1.10
Ti (titanium)	TiO_2	0.09
P (phosphorus)	P_2O_5	0.07
Ca (calcium)	CaO	29.23
Mg (magnesium)	MgO	0.82
Na (sodium)	Na_2O	0.18
K (potassium)	K_2O	0.92
S (sulfur)	SO_3	0.80
Ba (barium)	BaO	0.00
Cl (chloride)	Cl	0.27
Mn (manganese)	MnO	0.05
Sr (strontium)	SrO	0.01
Unknowns	Due to the presence of carbonates	10.25
Total		100.00

EERC Energy & Environmental Research Center® Putting Research into Practice UND THE UNIVERSITY OF NORTH DAKOTA	**Applied Geology Laboratory**		ID: 116993
	Well Name: NDIC No. 9001	Middle Bakken 2	Rival Field
	API No.: 33-013-00877-00-05	Lithology: Calcareous siltsone	Depth: 7399.0'

XRD MINERAL PHASE DISTRIBUTION

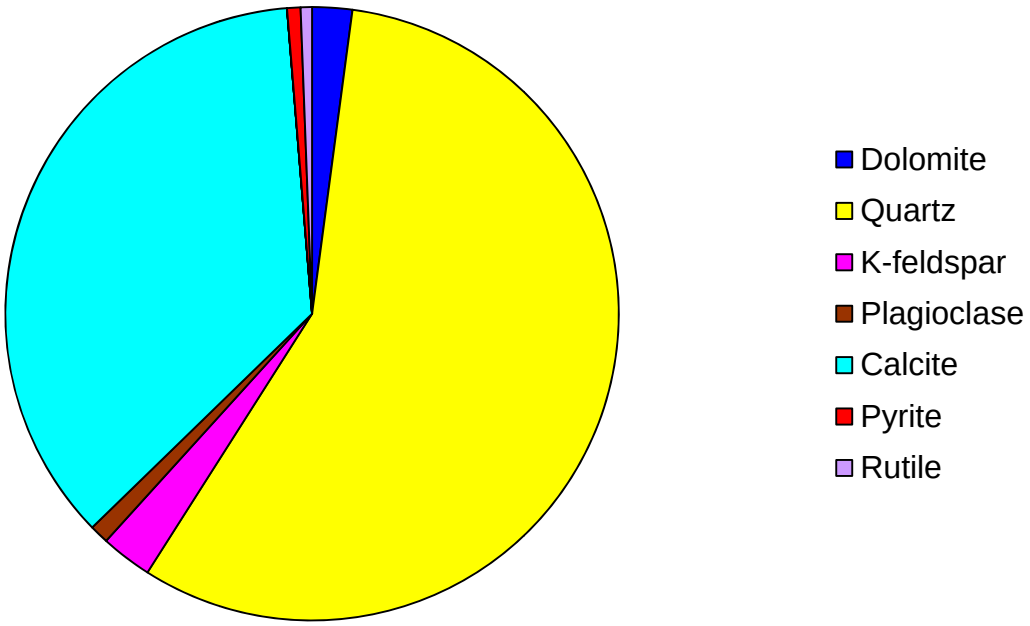

Mineral Phase	Formula	Weight %
Dolomite	$CaMg(CO_3)_2$	2.1
Quartz	SiO_2	56.8
K-feldspar	$KAlSi_3O_8$	2.7
Plagioclase	$Na_{0.5}Ca_{0.5}Al_{1.5}Si_{2.5}O_8$	1.0
Calcite	$CaCO_3$	35.9
Pyrite	FeS_2	0.7
Rutile	TiO_2	0.6

Applied Geology Laboratory		ID: 116993
Well Name: NDIC No. 9001	Middle Bakken 2	Rival Field
API No.: 33-013-00877-00-05	Lithology: Calcareous siltsone	Depth: 7399.0'

SEM

Observed Minerals

Mineral Phase	Mineral Phase
Calcite	Illite
Pyrite	K-feldspar
Dolomite	Rutile
Quartz	Albite
Apatite	Zircon

High-Magnification BSE Image Annotated with Examples of Mineral Phases Identified

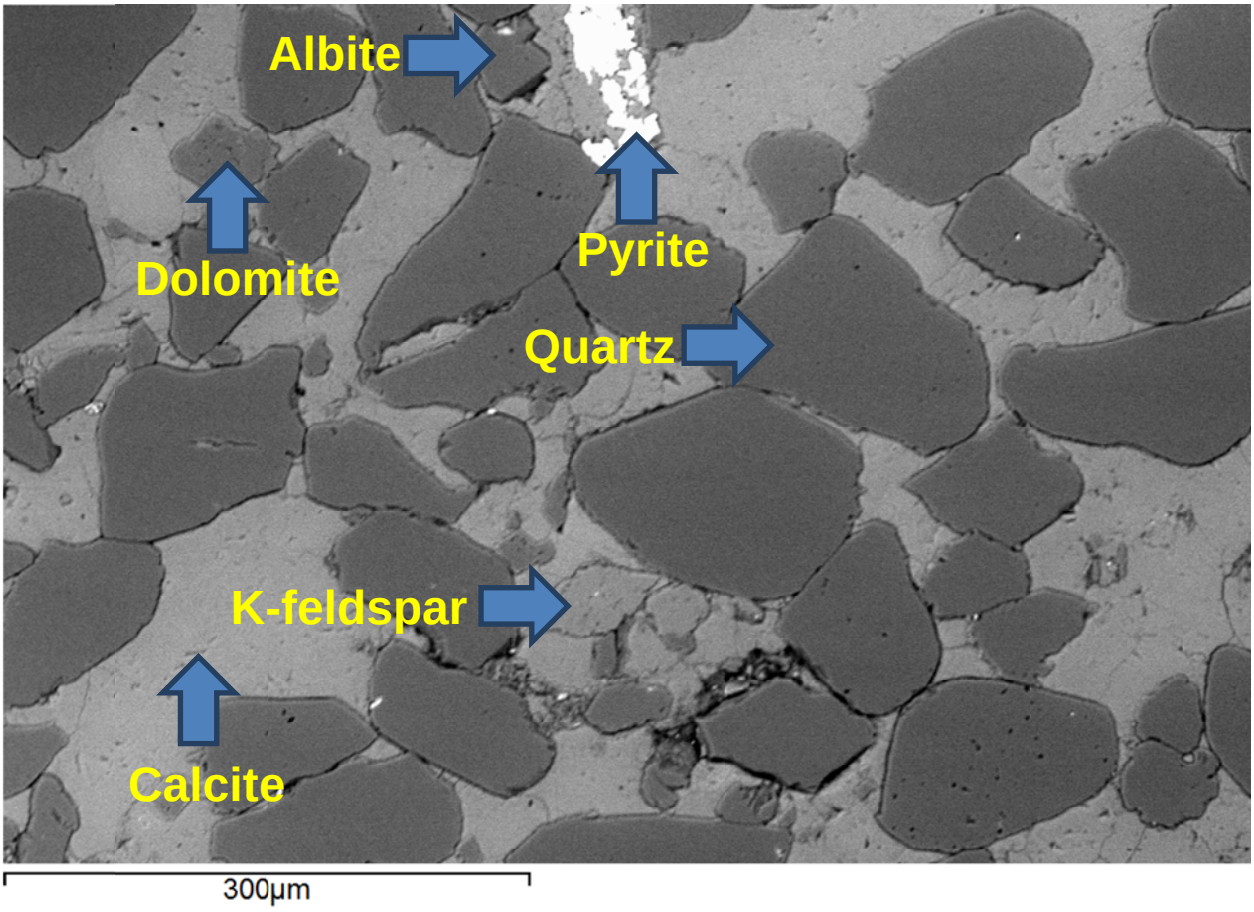

Additional High-Magnification BSE Images

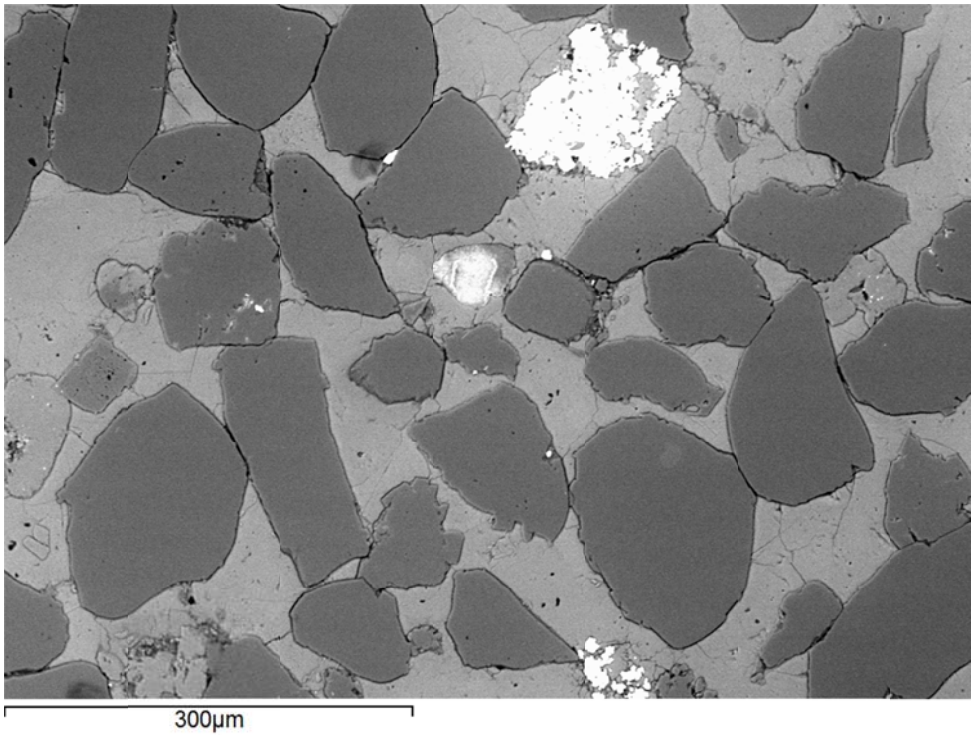

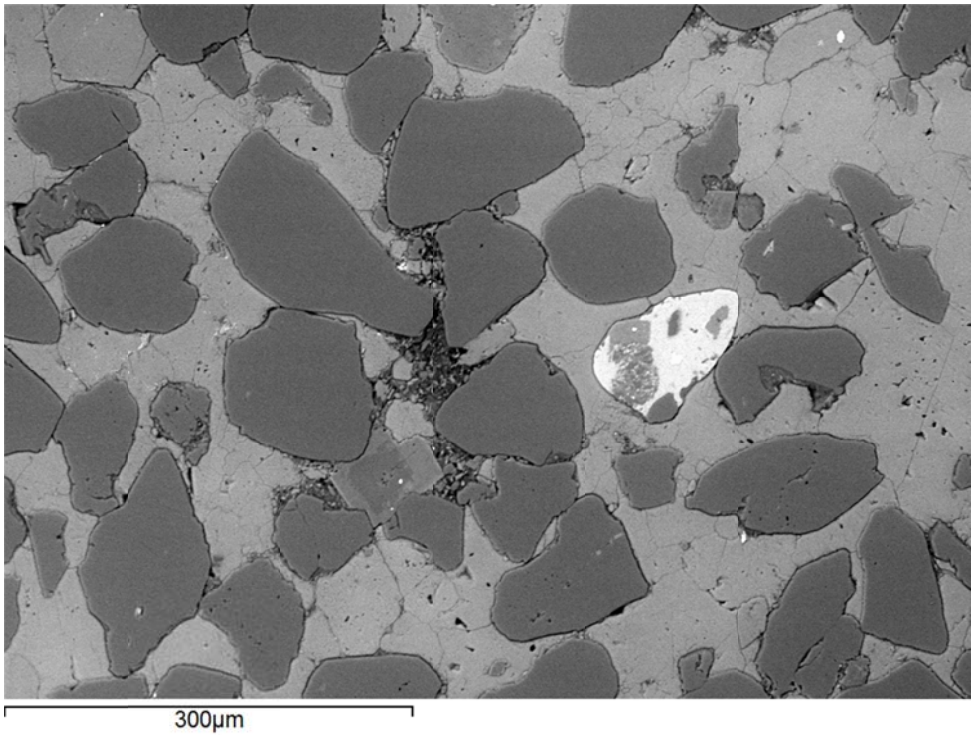

Applied Geology Laboratory		ID: 116993
Well Name: NDIC No. 9001	Middle Bakken 2	Rival Field
API No.: 33-013-00877-00-05	Lithology: Calcareous siltsone	Depth: 7399.0'

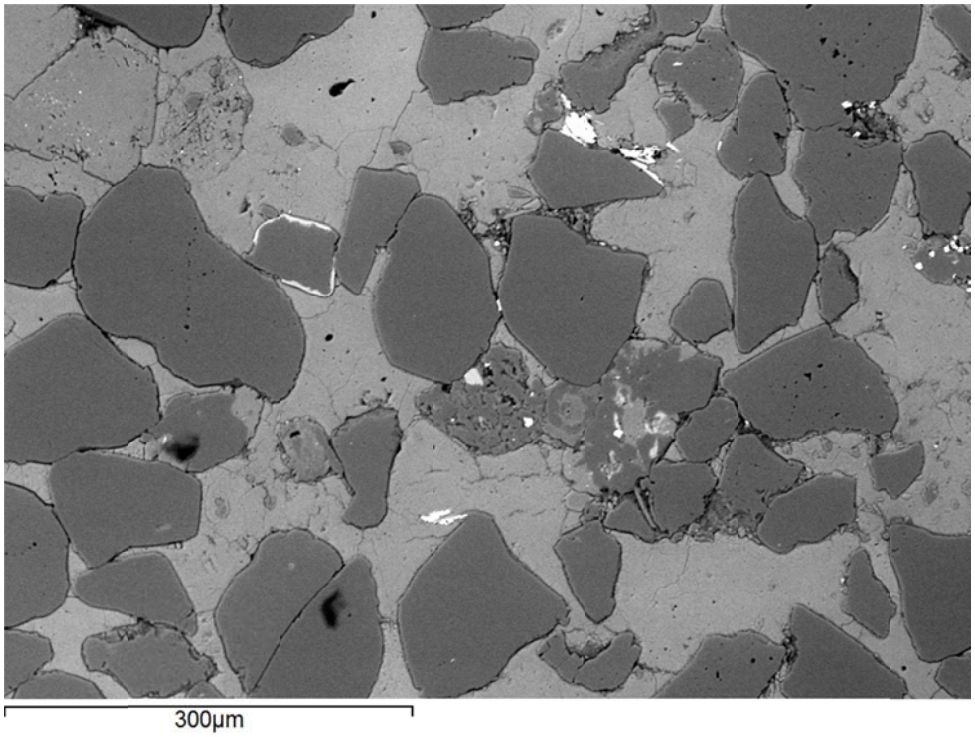

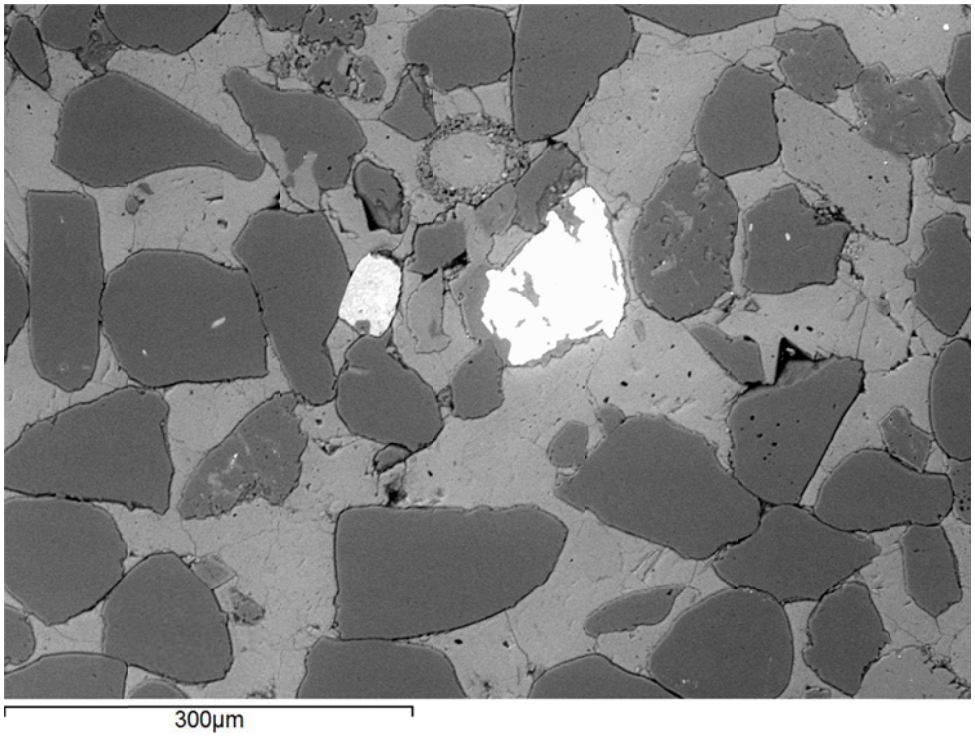

	Applied Geology Laboratory		ID: 116993
EERC Energy & Environmental Research Center® Putting Research into Practice UND THE UNIVERSITY OF NORTH DAKOTA	Well Name: NDIC No. 9001	Middle Bakken 2	Rival Field
	API No.: 33-013-00877-00-05	Lithology: Calcareous siltsone	Depth: 7399.0'

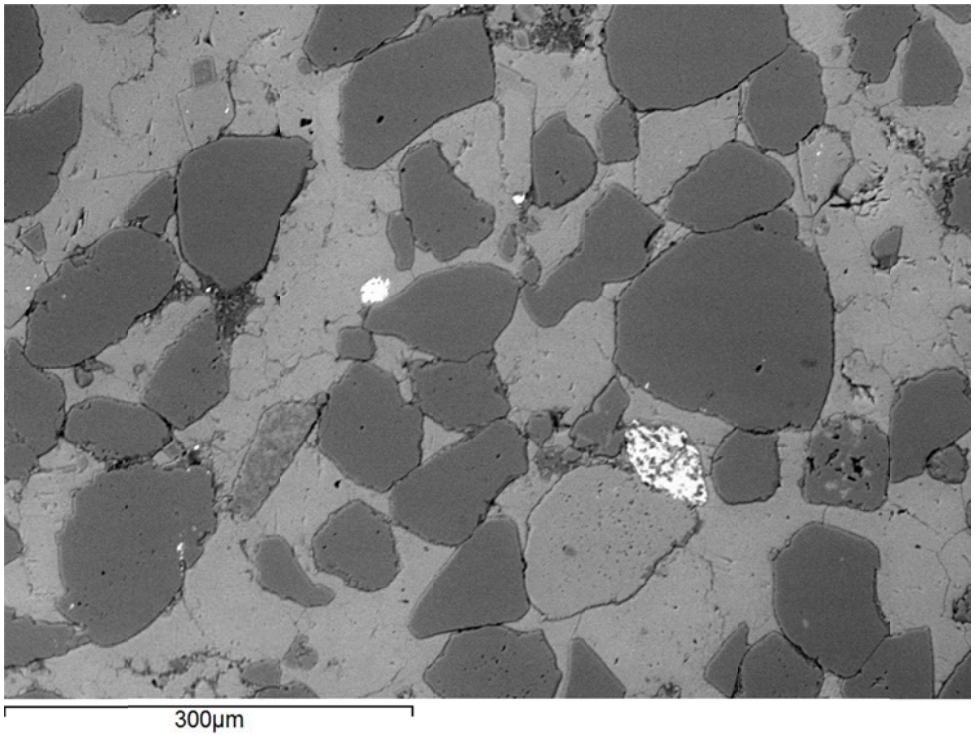

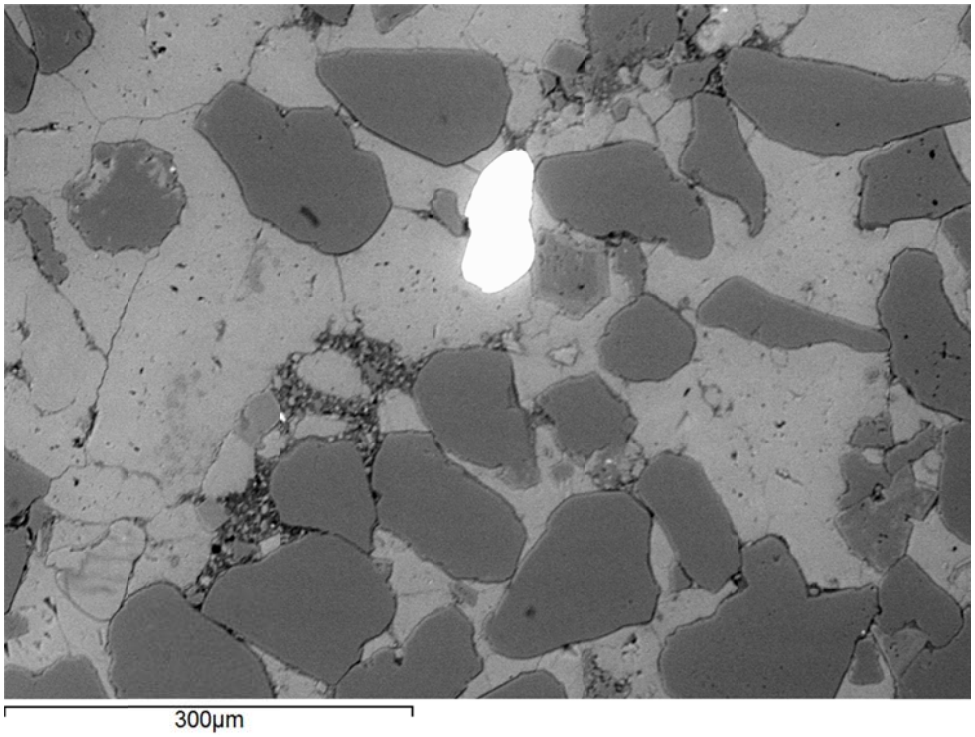

EERC Energy & Environmental Research Center® Putting Research into Practice UND THE UNIVERSITY OF NORTH DAKOTA	**Applied Geology Laboratory**		ID: 116993
	Well Name: NDIC No. 9001	Middle Bakken 2	Rival Field
	API No.: 33-013-00877-00-05	Lithology: Calcareous siltsone	Depth: 7399.0'

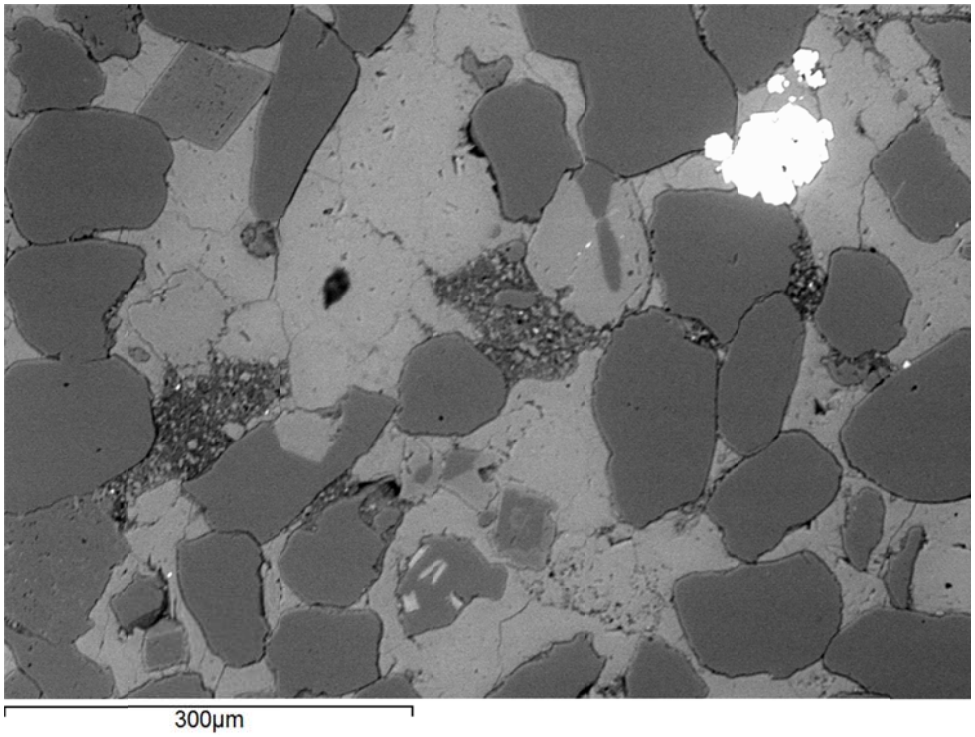

	Applied Geology Laboratory		ID: 116993
EERC Energy & Environmental Research Center® Putting Research into Practice UND THE UNIVERSITY OF NORTH DAKOTA	Well Name: NDIC No. 9001	Middle Bakken 2	Rival Field
	API No.: 33-013-00877-00-05	Lithology: Calcareous siltsone	Depth: 7399.0'

SEM Mineral Map Image Overlaid on BSE Image with Mineral Phase 2D Area Percentages

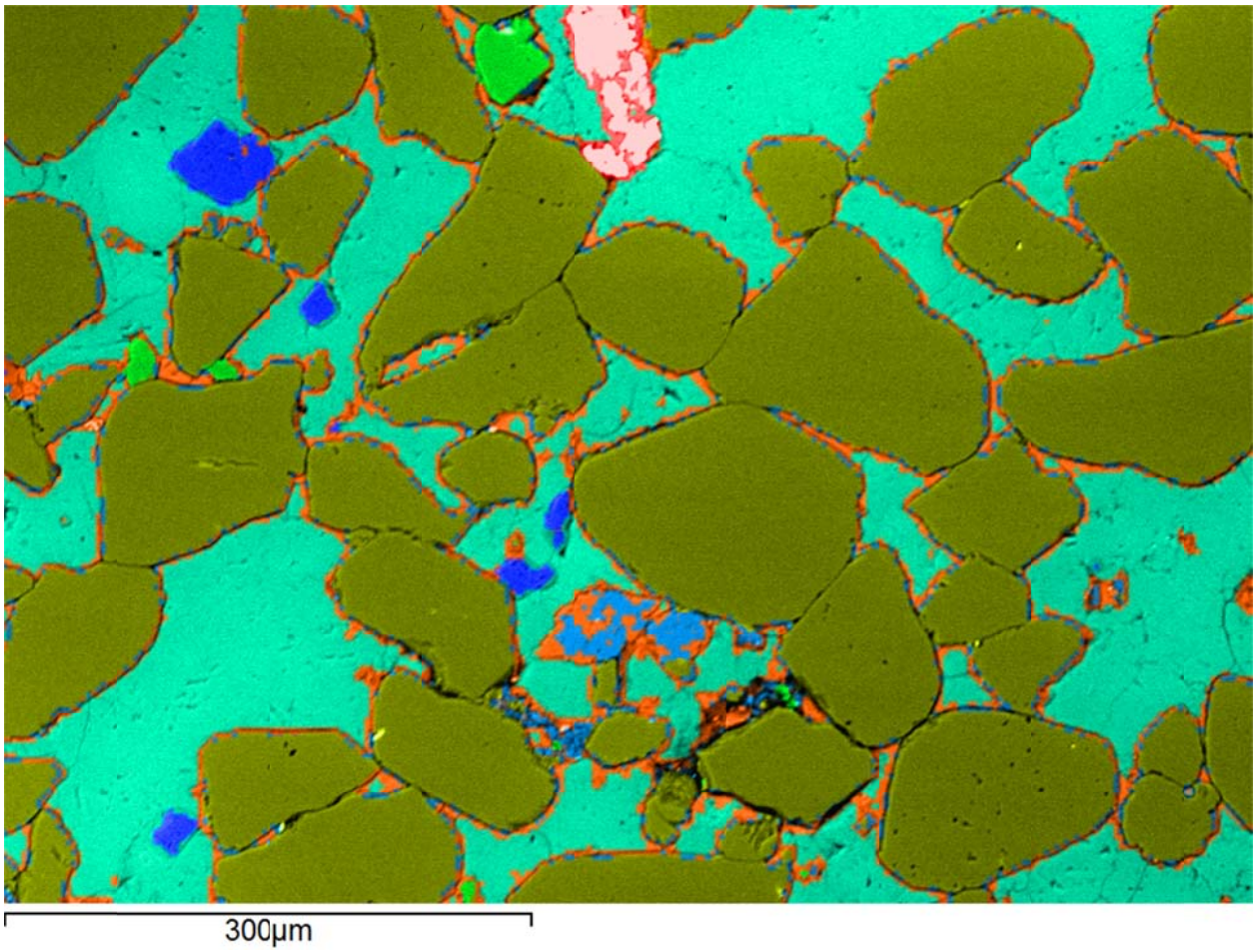

EERC Energy & Environmental Research Center® Putting Research into Practice UND THE UNIVERSITY OF NORTH DAKOTA	**Applied Geology Laboratory**		ID: 116994
	Well Name: NDIC No. 9001	Middle Bakken 1	Rival Field
	API No.: 33-013-00877-00-06	Lithology: Argillaceous, dolomitic siltstone	Depth: 7409.2'

SAMPLE PHOTOGRAPH

EERC Energy & Environmental Research Center® Putting Research into Practice UND THE UNIVERSITY OF NORTH DAKOTA	**Applied Geology Laboratory**		ID: 116994
	Well Name: NDIC No. 9001	Middle Bakken 1	Rival Field
	API No.: 33-013-00877-00-06	Lithology: Argillaceous, dolomitic siltstone	Depth: 7409.2'

PHOTOMICROGRAPHS

Transmission

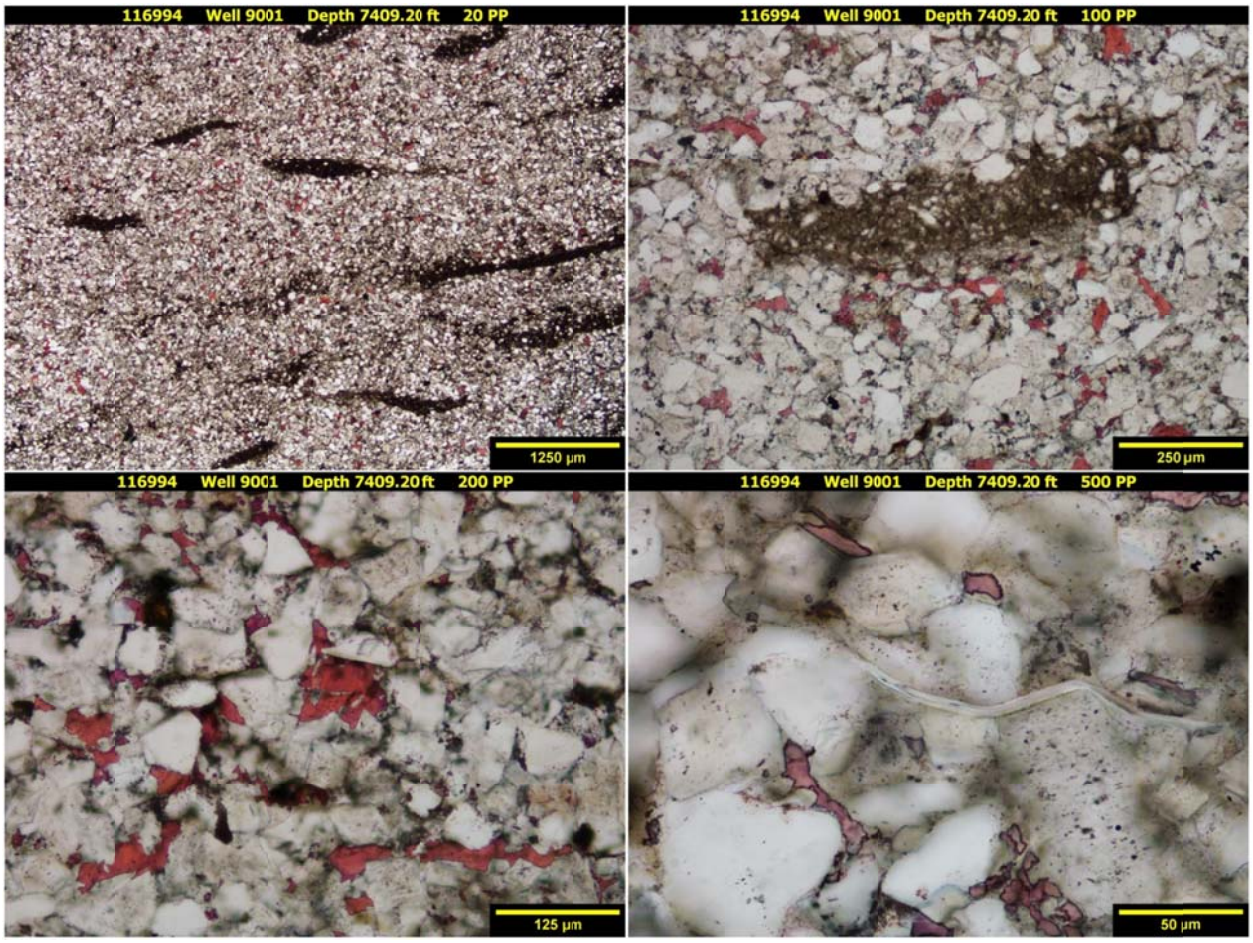

The sample from a depth of 7409.20 ft shows a silty dolostone. A heavy degree of burrowing and faint, wavy laminations are present. Very fine grained, angular to subrounded, monocrystalline quartz grains and trace amounts of muscovite are disseminated throughout. Mild quartz overgrowth is noted. Extensive anhederal to euhedral dolomitization has occurred throughout the sample. Occasional calcareous grains and sparry calcite remain. Disseminated pore-filling and replacement pyrite grains are present at much lesser quantities than in other samples within the well. An additional matrical component is clay, found at moderate quantities creating faint, wavy laminations, lenses, and burrowing structures. Open fractures, predominately horizontal, observed within burrows are likely the result of the sample process. Organics are rarely observed and typically associated with pyrite. No porosity is observed using standard petrographic techniques.

EERC Energy & Environmental Research Center® Putting Research into Practice UND THE UNIVERSITY OF NORTH DAKOTA	**Applied Geology Laboratory**		ID: 116994
	Well Name: NDIC No. 9001	Middle Bakken 1	Rival Field
	API No.: 33-013-00877-00-06	Lithology: Argillaceous, dolomitic siltstone	Depth: 7409.2'

Reflection

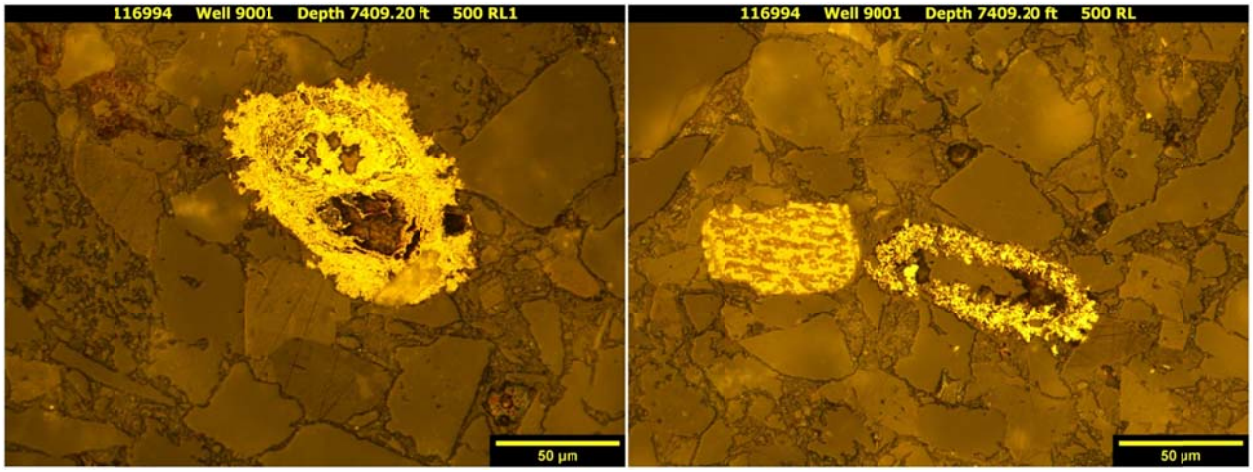

The sample from a depth of 7409.20 ft displays only trace euhedral pyrite growth. This diagenetic mineral acts predominantly as a grain replacer and pore filler. Partial to nearly complete pyritization of precursor grains and organics have rarely occurred.

EERC Energy & Environmental Research Center® Putting Research into Practice UND THE UNIVERSITY OF NORTH DAKOTA	**Applied Geology Laboratory**		ID: 116994
	Well Name: NDIC No. 9001	Middle Bakken 1	Rival Field
	API No.: 33-013-00877-00-06	Lithology: Argillaceous, dolomitic siltstone	Depth: 7409.2'

Transmission and Fluorescence Whole-Slide Images

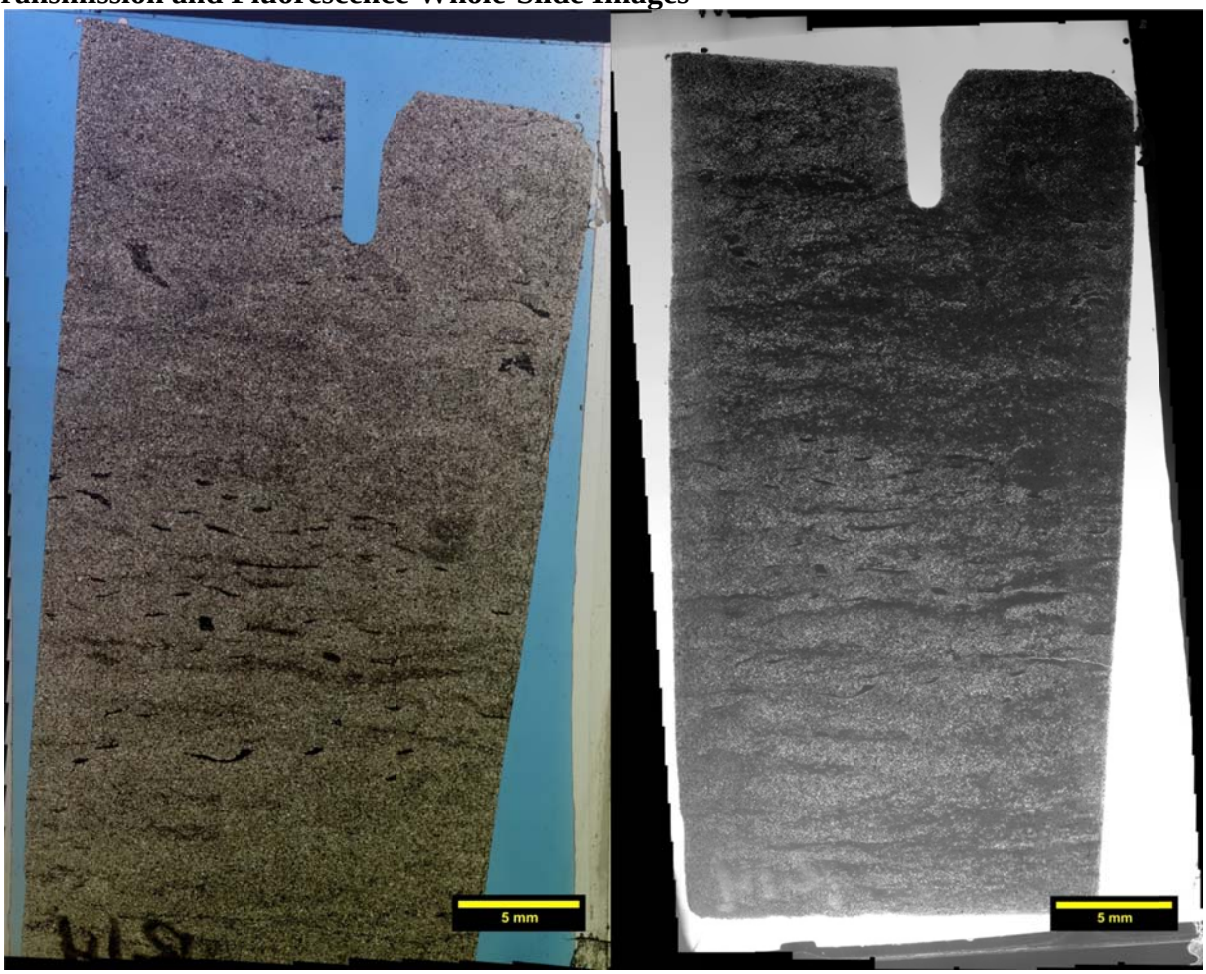

Images issues? The sample collected from a depth of 7409.20 ft depicts a burrowed dolomitic siltstone. Extensive anhedral to euhedral dolomite and calcite spar exist throughout the sample. Zones absent of burrowing, clay concentrations, and grains nearly completely interlocked by cements provide areas of highest porosity. No natural or induce fractures are observed.

EERC Energy & Environmental Research Center® Putting Research into Practice UND THE UNIVERSITY OF NORTH DAKOTA	**Applied Geology Laboratory**		ID: 116994
	Well Name: NDIC No. 9001	Middle Bakken 1	Rival Field
	API No.: 33-013-00877-00-06	Lithology: Argillaceous, dolomitic siltstone	Depth: 7409.2'

XRF BULK CHEMICAL COMPOSITION

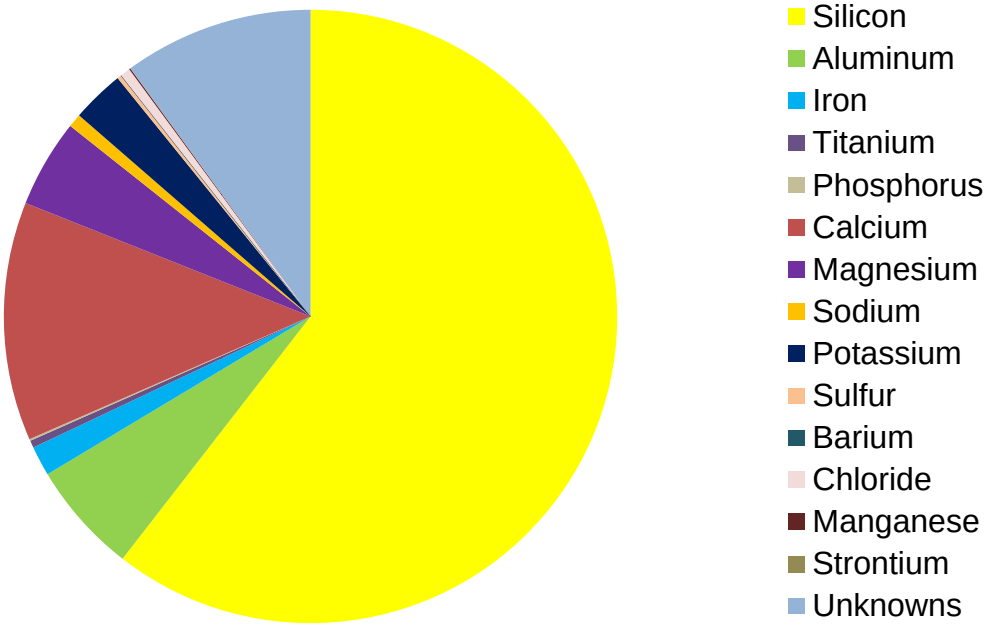

Element	Reporting Convention (Oxide)	Weight %
Si (silicon)	SiO_2	60.51
Al (aluminum)	Al_2O_3	5.90
Fe (iron)	Fe_2O_3	1.57
Ti (titanium)	TiO_2	0.38
P (phosphorus)	P_2O_5	0.09
Ca (calcium)	CaO	12.59
Mg (magnesium)	MgO	4.64
Na (sodium)	Na_2O	0.71
K (potassium)	K_2O	2.79
S (sulfur)	SO_3	0.23
Ba (barium)	BaO	0.00
Cl (chloride)	Cl	0.53
Mn (manganese)	MnO	0.07
Sr (strontium)	SrO	0.01
Unknowns	Due to the presence of carbonates	9.99
Total		100.01

	Applied Geology Laboratory		ID: 116994
EERC Energy & Environmental Research Center® Putting Research into Practice UND THE UNIVERSITY OF NORTH DAKOTA	Well Name: NDIC No. 9001	Middle Bakken 1	Rival Field
	API No.: 33-013-00877-00-06	Lithology: Argillaceous, dolomitic siltstone	Depth: 7409.2'

XRD MINERAL PHASE DISTRIBUTION

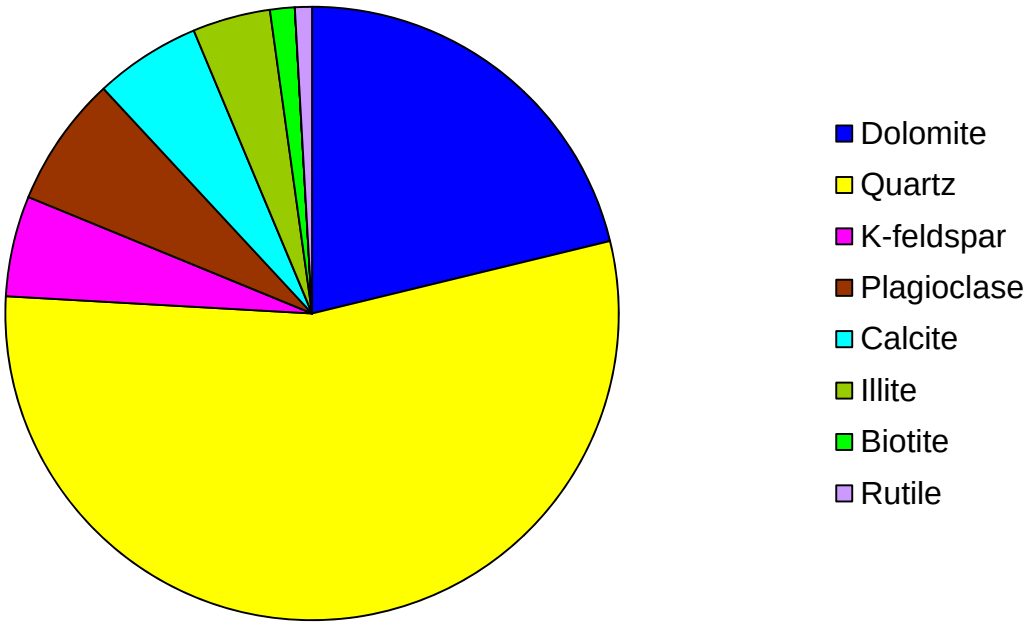

Mineral Phase	Formula	Weight %
Dolomite	$CaMg(CO_3)_2$	21.2
Quartz	SiO_2	54.7
K-feldspar	$KAlSi_3O_8$	5.3
Plagioclase	$Na_{0.5}Ca_{0.5}Al_{1.5}Si_{2.5}O_8$	6.9
Calcite	$CaCO_3$	5.6
Illite	$(K,H_3O)(Al,Mg,Fe)_2(Si,Al)_4O_{10}[(OH)_2,(H_2O)]$	4.1
Biotite	$K(Mg,Fe)_3[(OH)_2AlSi_3O_{10}]$	1.3
Rutile	TiO_2	0.9

Applied Geology Laboratory		ID: 116994
Well Name: NDIC No. 9001	Middle Bakken 1	Rival Field
API No.: 33-013-00877-00-06	Lithology: Argillaceous, dolomitic siltstone	Depth: 7409.2'

SEM

Observed Minerals

Mineral Phase	Mineral Phase
Quartz	Dolomite
Pyrite	Zircon
Apatite	Illite
K-feldspar	Biotite
Rutile	Albite

High-Magnification BSE Image Annotated with Examples of Mineral Phases Identified

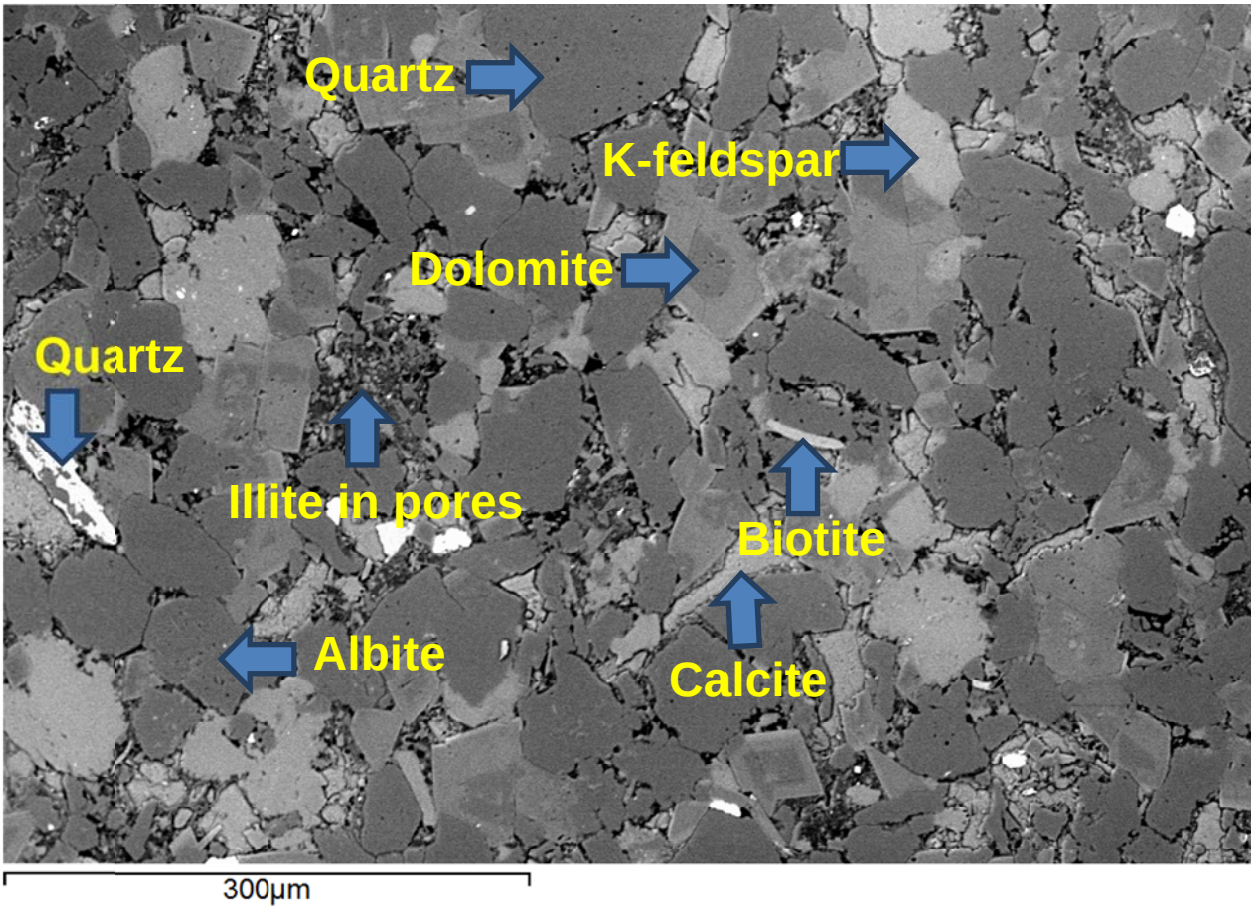

Additional High-Magnification BSE Images

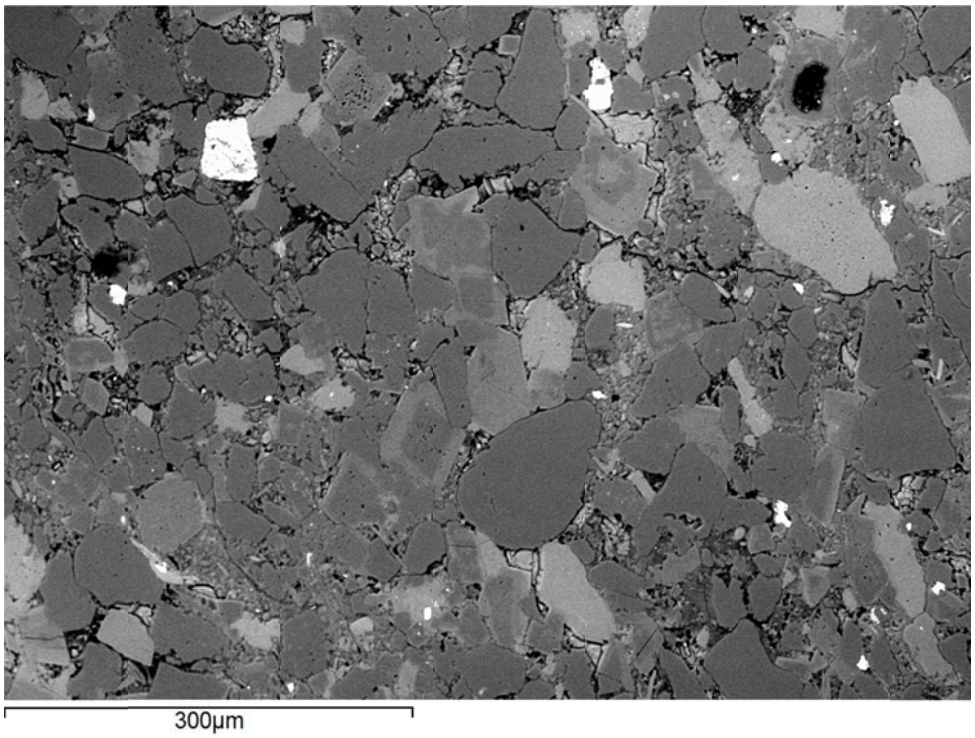

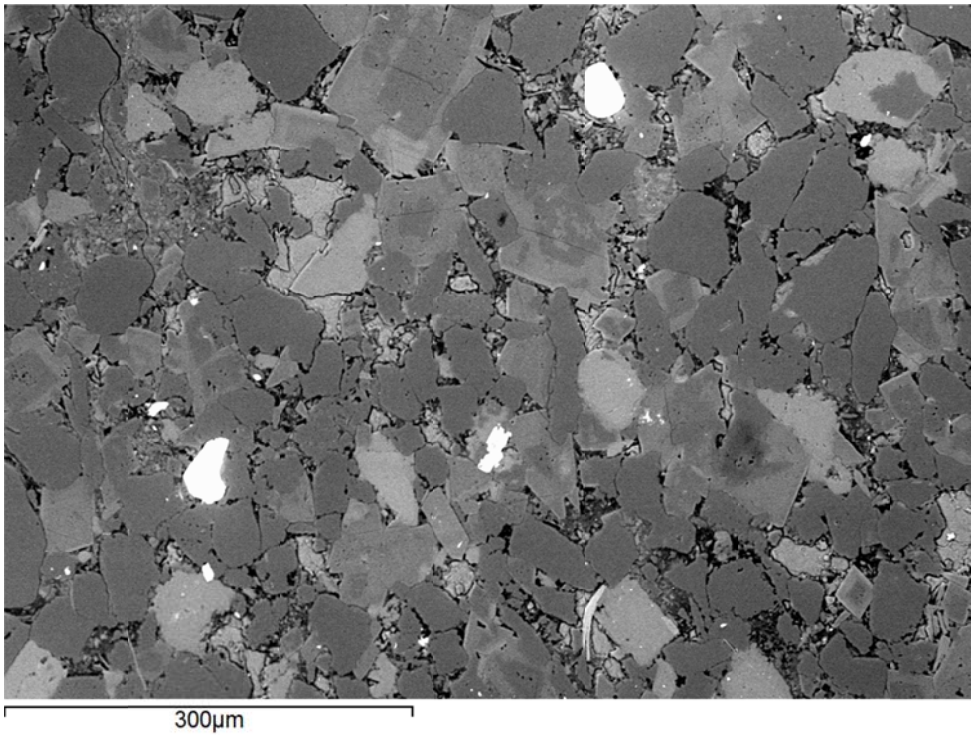

	Applied Geology Laboratory		ID: 116994
	Well Name: NDIC No. 9001	Middle Bakken 1	Rival Field
	API No.: 33-013-00877-00-06	Lithology: Argillaceous, dolomitic siltstone	Depth: 7409.2'

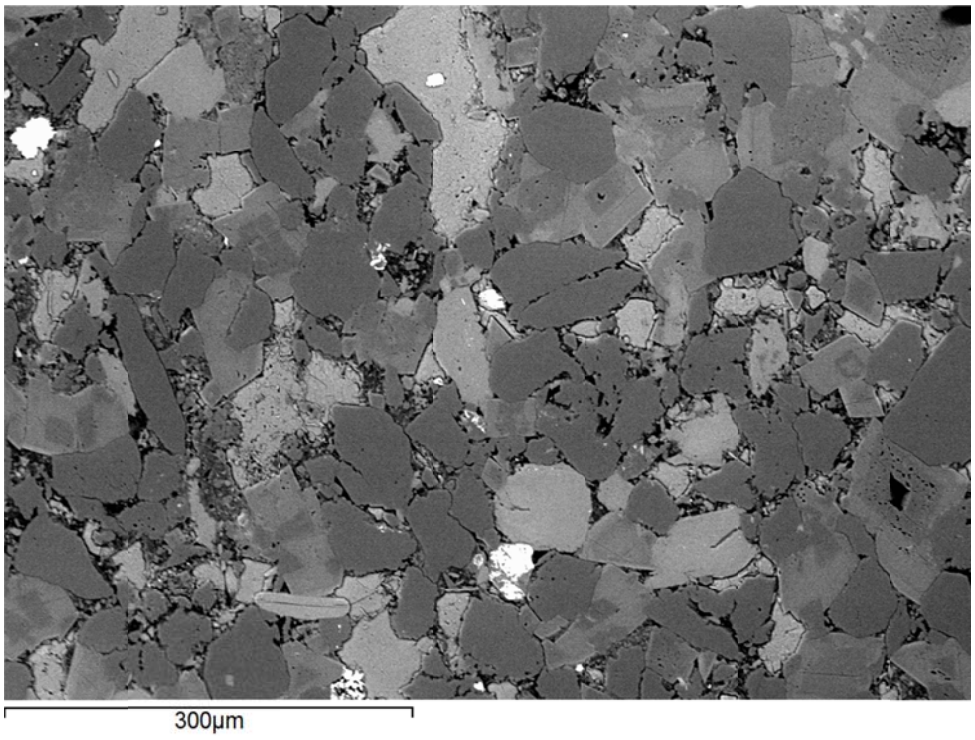

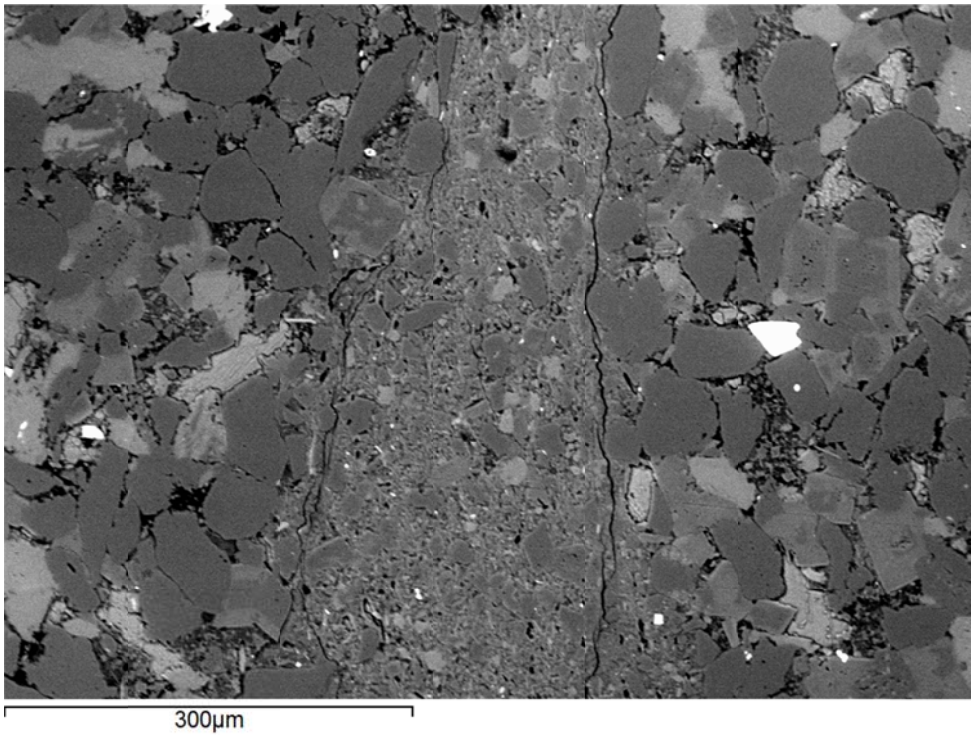

EERC Energy & Environmental Research Center® Putting Research into Practice UND THE UNIVERSITY OF NORTH DAKOTA	**Applied Geology Laboratory**		ID: 116994
	Well Name: NDIC No. 9001	Middle Bakken 1	Rival Field
	API No.: 33-013-00877-00-06	Lithology: Argillaceous, dolomitic siltstone	Depth: 7409.2'

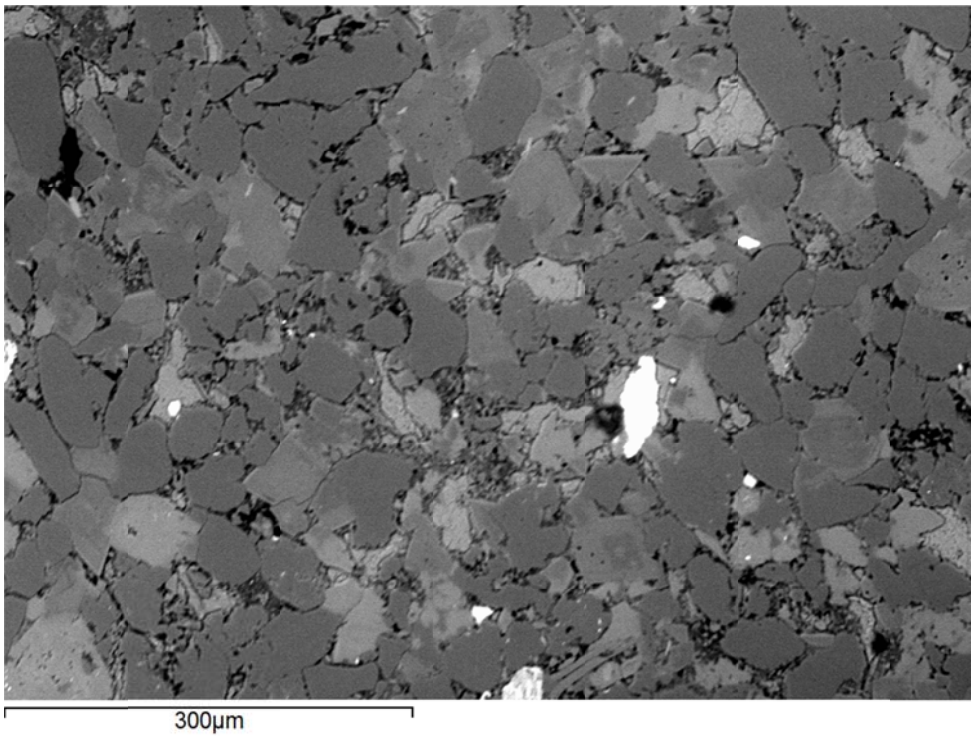

EERC Energy & Environmental Research Center® Putting Research into Practice UND THE UNIVERSITY OF NORTH DAKOTA	**Applied Geology Laboratory**		ID: 116994
	Well Name: NDIC No. 9001	Middle Bakken 1	Rival Field
	API No.: 33-013-00877-00-06	Lithology: Argillaceous, dolomitic siltstone	Depth: 7409.2'

SEM Mineral Map Image Overlaid on BSE Image with Mineral Phase 2D Area Percentages

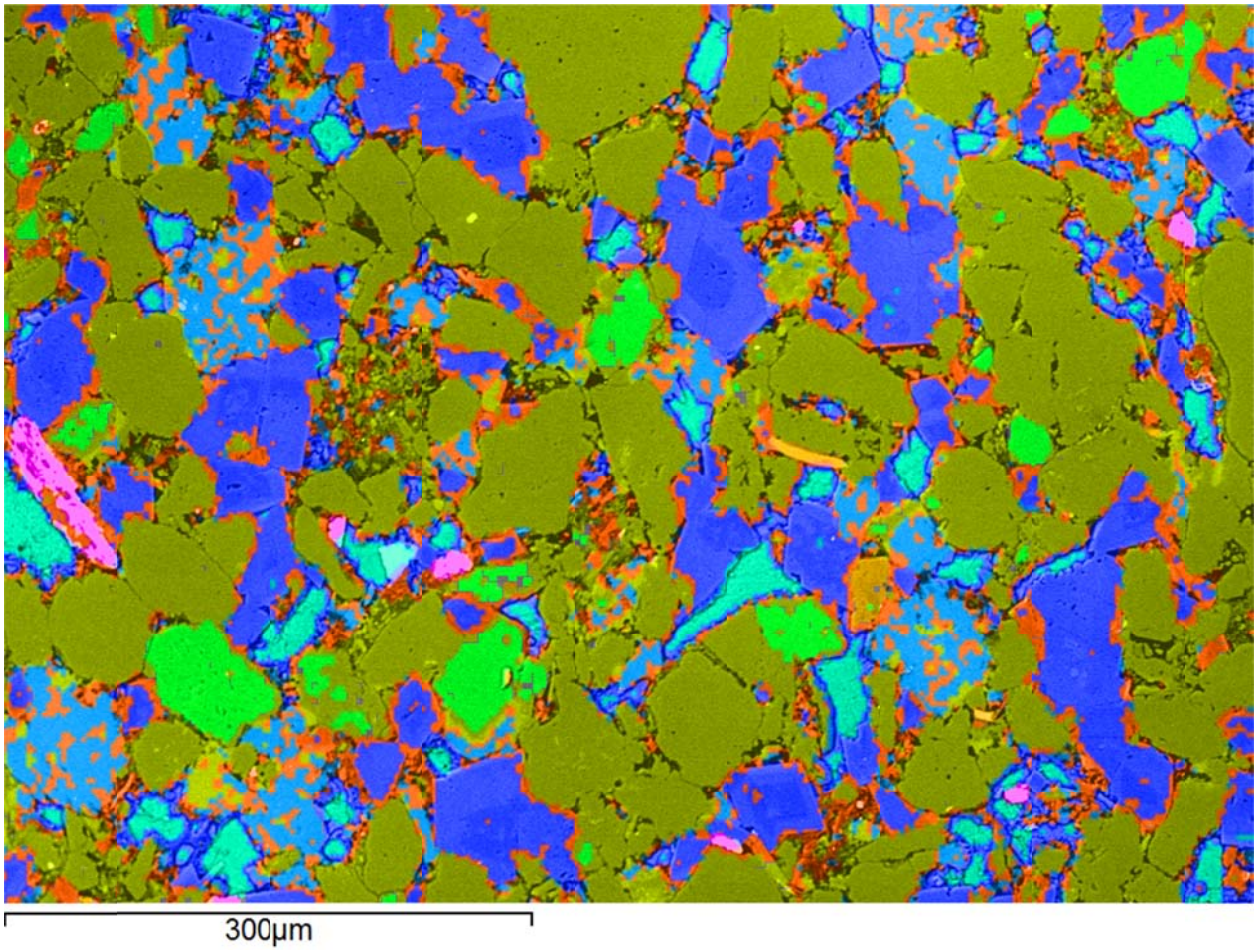

This page intentionally left blank.

EERC Energy & Environmental Research Center® Putting Research into Practice UND THE UNIVERSITY OF NORTH DAKOTA	**Applied Geology Laboratory**		ID: 116999
	Well Name: NDIC No. 17946	Middle Bakken 4	Grenora Field
	API No.: 33-061-00803-00-04	Lithology:	Depth: 8952.5'

SAMPLE PHOTOGRAPHY

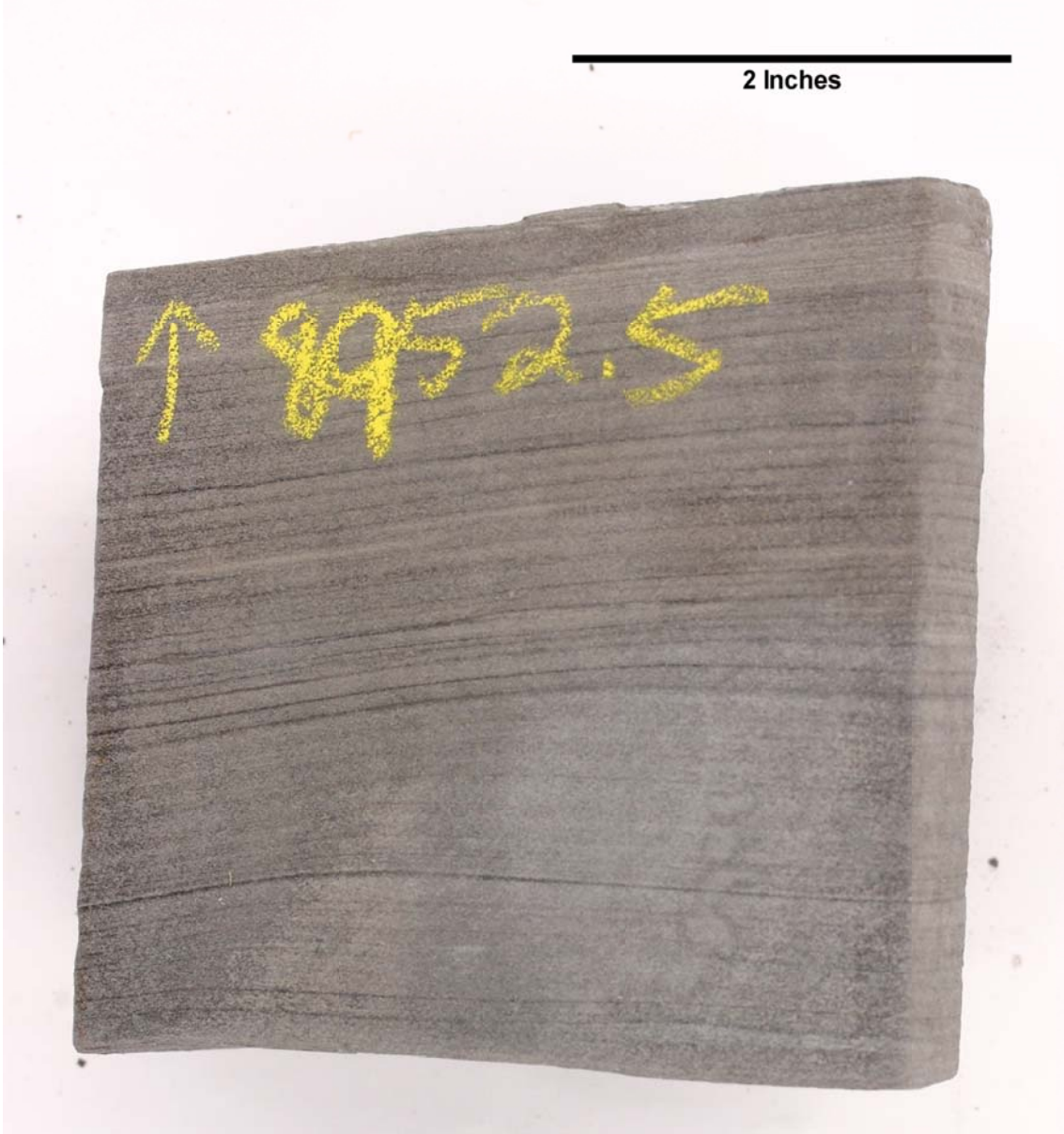

PHYSICAL PROPERTIES

Porosity and Grain Density by Core Laboratories

Pycnometer Effective Porosity, vol%	Grain Density, g/cm^3
5.00	2.717

This page intentionally left blank.

EERC Energy & Environmental Research Center® Putting Research into Practice UND THE UNIVERSITY OF NORTH DAKOTA	**Applied Geology Laboratory**		ID: 117000
	Well Name: NDIC No. 17946	Middle Bakken 3	Grenora Field
	API No.: 33-061-00803-00-05	Lithology:	Depth: 8956.5'

SAMPLE PHOTOGRAPH

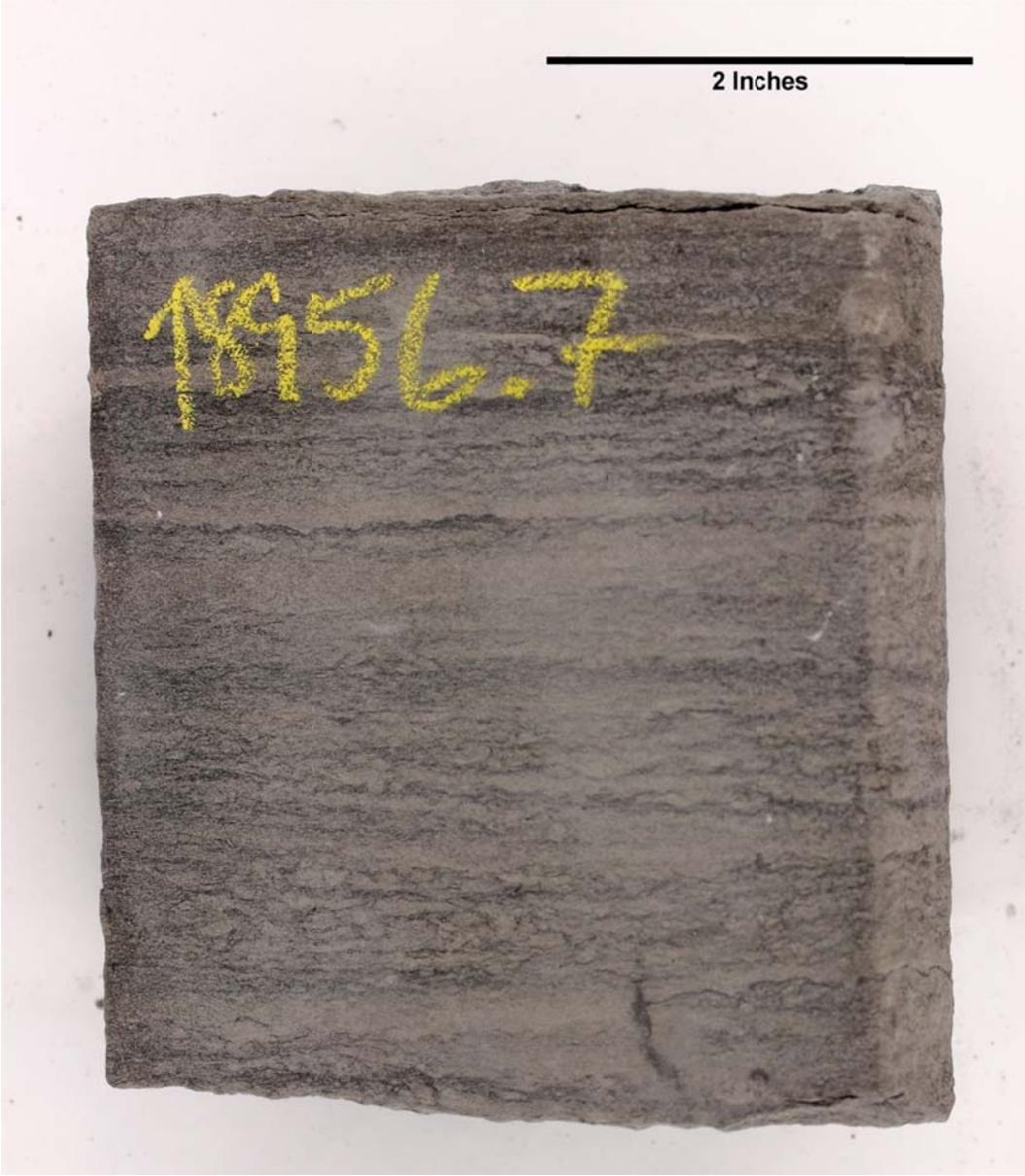

PHYSICAL PROPERTIES

Porosity and Grain Density by Core Laboratories

Pycnometer Effective Porosity, vol%	Grain Density, g/cm^3
8.01	2.721

This page intentionally left blank.

EERC Energy & Environmental Research Center® Putting Research into Practice UND THE UNIVERSITY OF NORTH DAKOTA	**Applied Geology Laboratory**		ID: 117001
	Well Name: NDIC No. 17946	Middle Bakken 2	Grenora Field
	API No.: 33-061-00803-00-06	Lithology:	Depth: 8964.5'

SAMPLE PHOTOGRAPH

PHYSICAL PROPERTIES

Porosity and Grain Density by Core Laboratories

Pycnometer Effective Porosity, vol%	Grain Density, g/cm^3
7.59	2.727

This page intentionally left blank.

EERC Energy & Environmental Research Center® Putting Research into Practice UND THE UNIVERSITY OF NORTH DAKOTA	**Applied Geology Laboratory**		ID: 117002
	Well Name: NDIC No. 17946	Middle Bakken 2	Grenora Field
	API No.: 33-061-00803-00-07	Lithology:	Depth: 8968.5'

SAMPLE PHOTOGRAPH

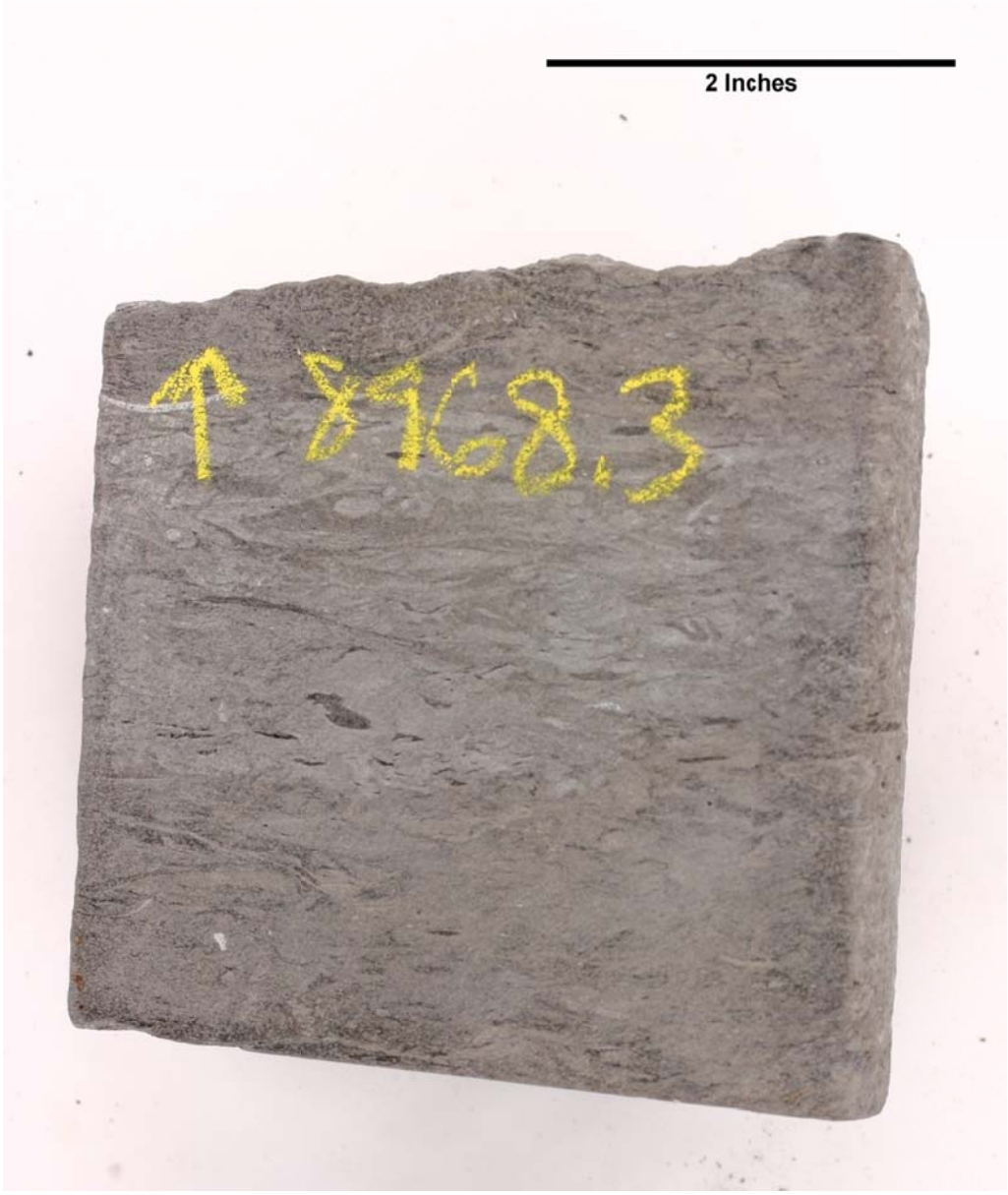

PHYSICAL PROPERTIES

Porosity and Grain Density by Core Laboratories

Pycnometer Effective Porosity, vol%	Grain Density, g/cm^3
6.12	2.718

This page intentionally left blank.

EERC Energy & Environmental Research Center® Putting Research into Practice UND THE UNIVERSITY OF NORTH DAKOTA	**Applied Geology Laboratory**		ID: 117004
	Well Name: NDIC No. 17946	Middle Bakken 2	Grenora Field
	API No.: 33-061-00803-00-09	Lithology:	Depth: 8977.0'

SAMPLE PHOTOGRAPH

PHYSICAL PROPERTIES

Porosity and Grain Density by Core Laboratories

Pycnometer Effective Porosity, vol%	Grain Density, g/cm^3
5.72	2.730

This page intentionally left blank.

EERC Energy & Environmental Research Center® Putting Research into Practice UND THE UNIVERSITY OF NORTH DAKOTA	**Applied Geology Laboratory**		ID: 117009
	Well Name: NDIC No. 20552	Middle Bakken 8	Grenora Field
	API No.: 33-105-02157-00-01	Lithology: Slightly silty, argillaceous limestone	Depth: 9613.0'

SAMPLE PHOTOGRAPH

PHYSICAL PROPERTIES

Porosity and Grain Density by Core Laboratories

Pycnometer Effective Porosity, vol%	Grain Density, g/cm^3
3.03	2.729

EERC Energy & Environmental Research Center® Putting Research into Practice UND THE UNIVERSITY OF NORTH DAKOTA	**Applied Geology Laboratory**		ID: 117009
	Well Name: NDIC No. 20552	Middle Bakken 8	Grenora Field
	API No.: 33-105-02157-00-01	Lithology: Slightly silty, argillaceous limestone	Depth: 9613.0'

PHOTOMICROGRAPHS

Transmission

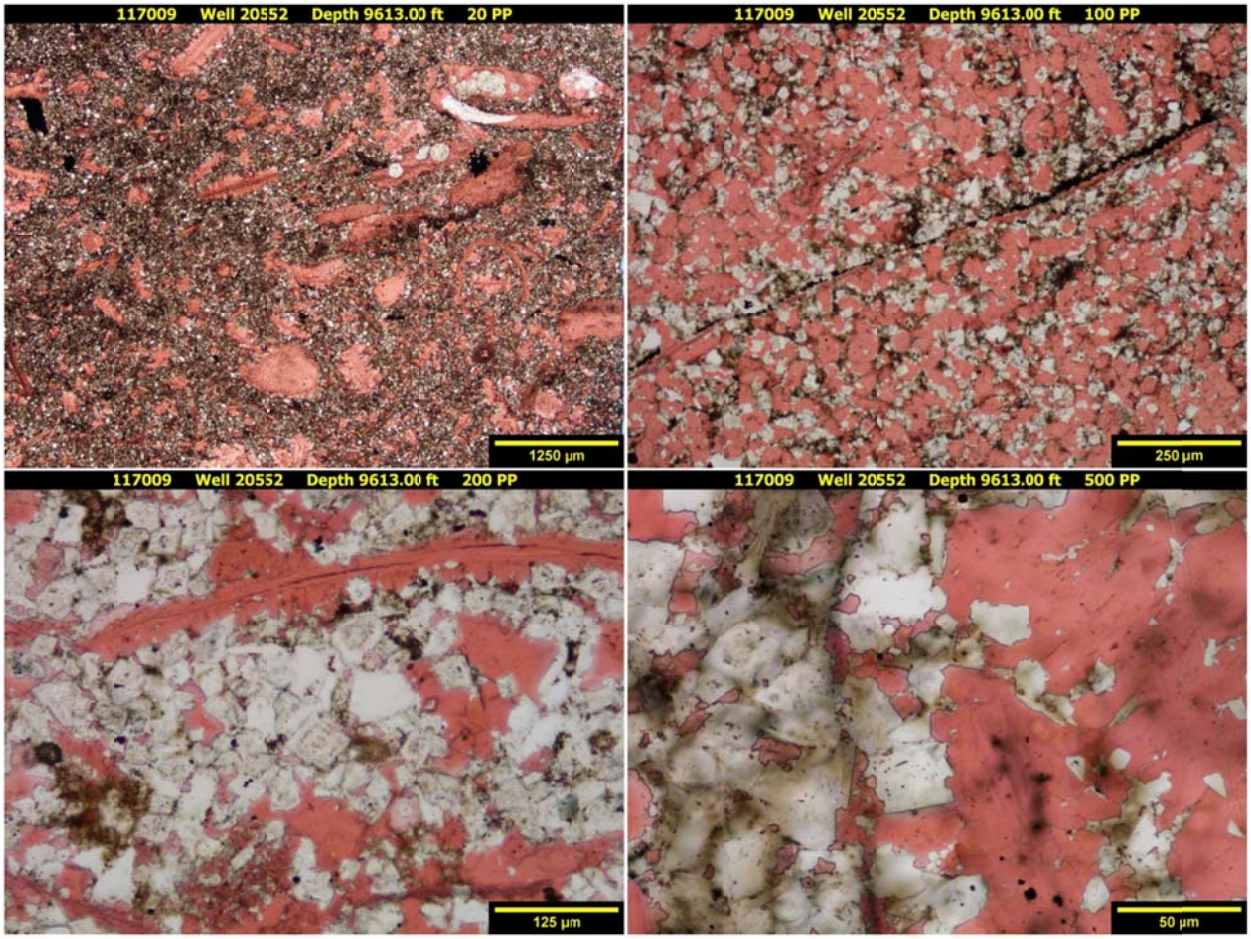

The sample from a depth of 9613.00 ft displays a slightly silty, argillaceous limestone. Very fine grained, angular to subangular, monocrystalline quartz is disseminated throughout the sample. Calcareous non-skeletal and skeletal clasts are abundant and observed with some gypsum and pyrite replacement. Rare amounts of microcrystalline dolomite exist within the sample matrix. Trace quantities of muscovite and feldspars are observed. Pore-filling, sparry calcite cement is prevalent and eliminates any observable inter-particle-based porosity in the thin section. Clay is found throughout the sample, concentrating in a few areas. Organics are rarely observed; when detected they are typically globular and associated with pyrite. Tiny, filled fractures are cemented with any combination of carbonates, pyrite, clays, and organics. No observable porosity is detected.

EERC Energy & Environmental Research Center® Putting Research into Practice UND THE UNIVERSITY OF NORTH DAKOTA	**Applied Geology Laboratory**		ID: 117009
	Well Name: NDIC No. 20552	Middle Bakken 8	Grenora Field
	API No.: 33-105-02157-00-01	Lithology: Slightly silty, argillaceous limestone	Depth: 9613.0'

Reflection

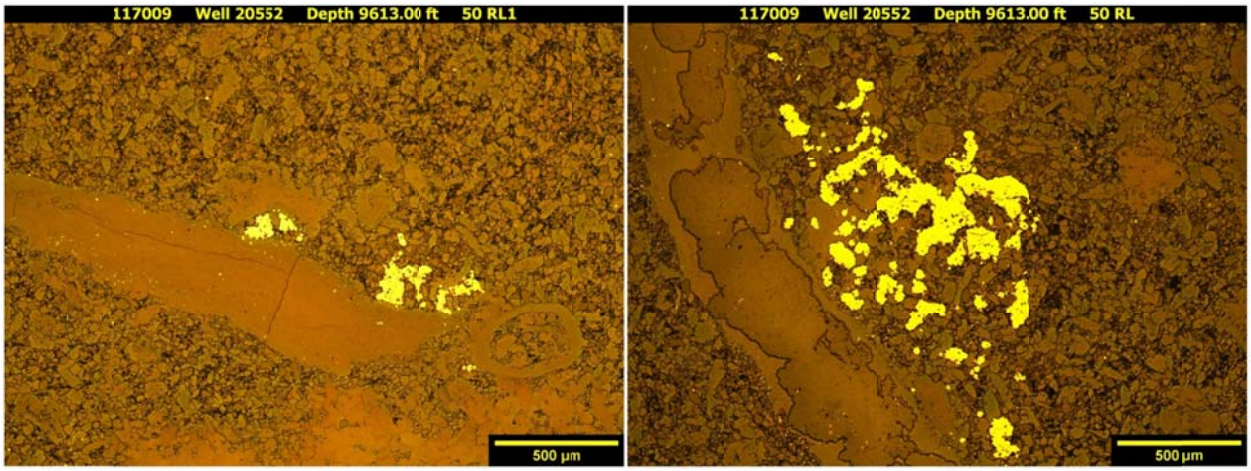

The sample from a depth of 9613.00 ft displays a small amount euhedral and trace levels frambodial pyrite growth. Euhedral mineralization is predominantly within calcareous skeletal and non-skeletal grains. Framboidal pyrite predominately is shown as individual spheres; no observed assemblages of spheres to create a larger, more mature sphere grouping are observed Euhedral grains are very fine grained and individual frambodial grains are observed at a fraction of that size. Organics observed are typically associated with both euhedral and framboidal pyrite.

EERC Energy & Environmental Research Center® Putting Research into Practice UND THE UNIVERSITY OF NORTH DAKOTA	**Applied Geology Laboratory**		ID: 117009
	Well Name: NDIC No. 20552	Middle Bakken 8	Grenora Field
	API No.: 33-105-02157-00-01	Lithology: Slightly silty, argillaceous limestone	Depth: 9613.0'

Transmission and Fluorescence Whole-Slide Images

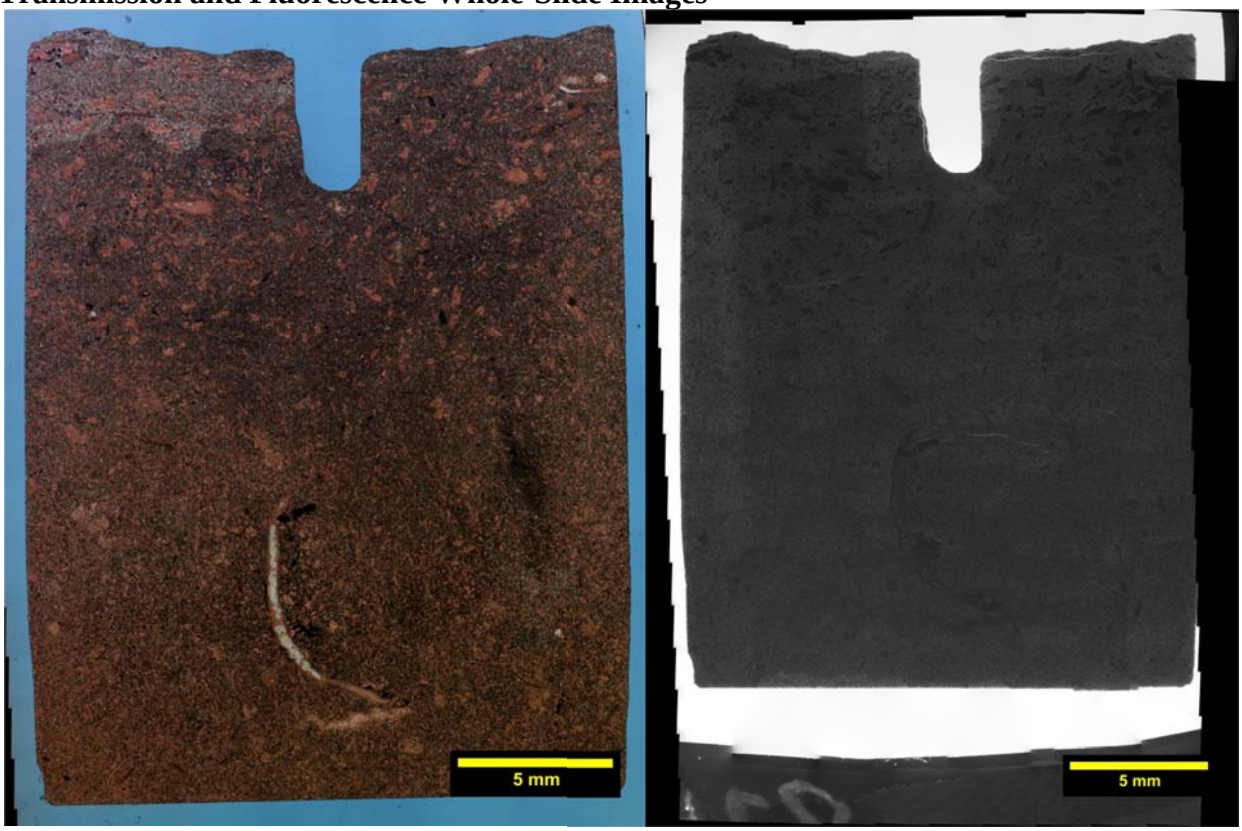

The sample collected from a depth of 9613.00 ft is a well-cemented slightly silty, argillaceous limestone. Effective porosity is reported at 3.03 vol%. No natural open fractures are observed. An occasional induce fracture is detected.

EERC Energy & Environmental Research Center® Putting Research into Practice UND THE UNIVERSITY OF NORTH DAKOTA	**Applied Geology Laboratory**		ID: 117009
	Well Name: NDIC No. 20552	Middle Bakken 8	Grenora Field
	API No.: 33-105-02157-00-01	Lithology: Slightly silty, argillaceous limestone	Depth: 9613.0'

XRF BULK CHEMICAL COMPOSITION

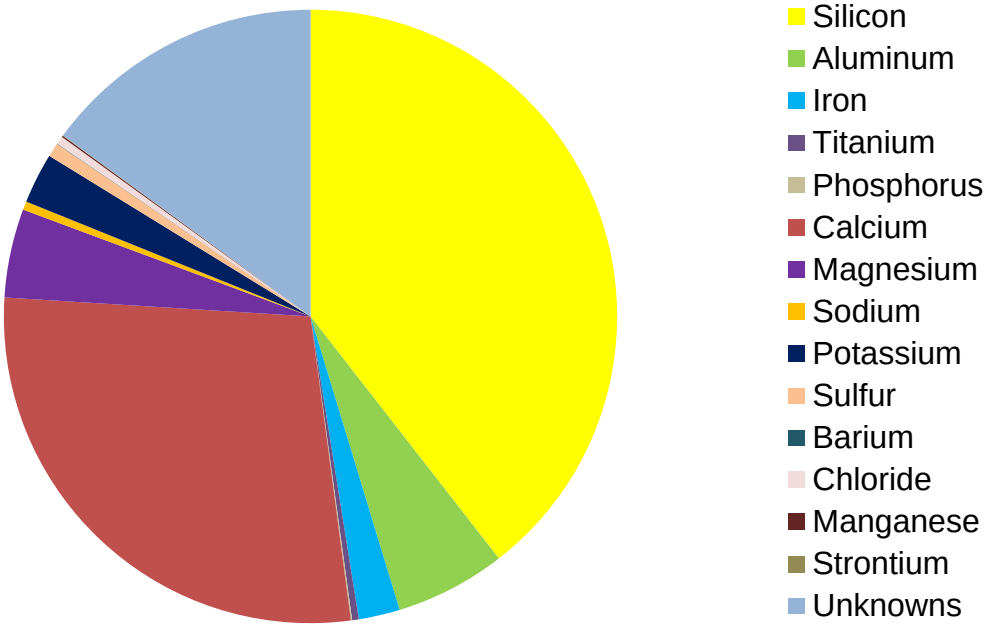

Element	Reporting Convention (Oxide)	Weight %
Si (silicon)	SiO_2	39.48
Al (aluminum)	Al_2O_3	5.83
Fe (iron)	Fe_2O_3	2.18
Ti (titanium)	TiO_2	0.35
P (phosphorus)	P_2O_5	0.07
Ca (calcium)	CaO	28.09
Mg (magnesium)	MgO	4.68
Na (sodium)	Na_2O	0.45
K (potassium)	K_2O	2.66
S (sulfur)	SO_3	0.74
Ba (barium)	BaO	0.02
Cl (chloride)	Cl	0.42
Mn (manganese)	MnO	0.08
Sr (strontium)	SrO	0.02
Unknowns	Due to the presence of carbonates	14.95
Total		100.02

	Applied Geology Laboratory		ID: 117009
EERC Energy & Environmental Research Center® Putting Research into Practice UND THE UNIVERSITY OF NORTH DAKOTA	Well Name: NDIC No. 20552	Middle Bakken 8	Grenora Field
	API No.: 33-105-02157-00-01	Lithology: Slightly silty, argillaceous limestone	Depth: 9613.0'

XRD MINERAL PHASE DISTRIBUTION

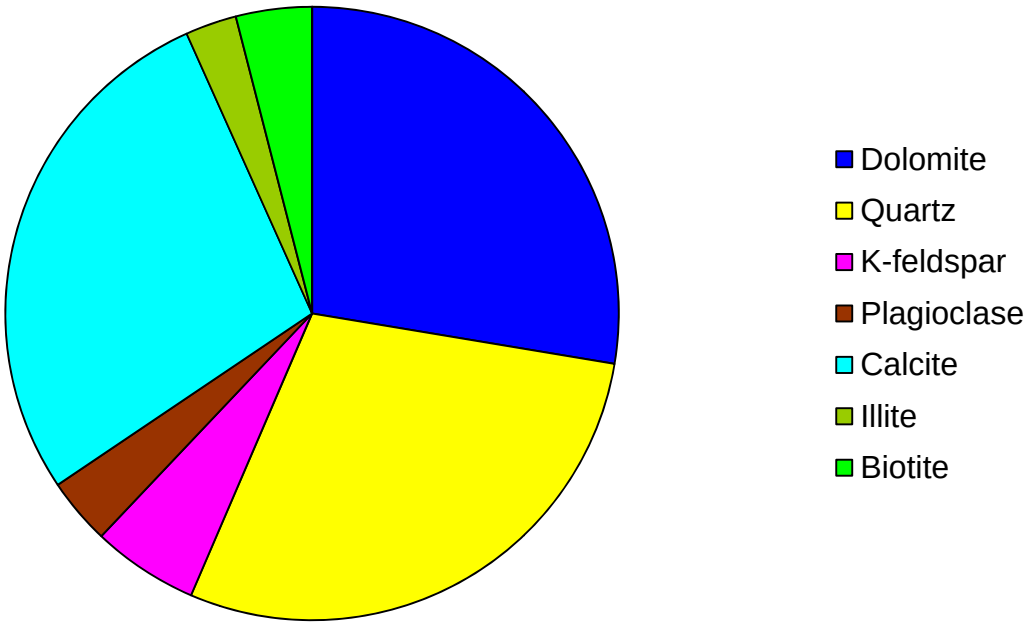

Mineral Phase	Formula	Weight %
Dolomite	$CaMg(CO_3)_2$	27.6
Quartz	SiO_2	28.8
K-feldspar	$KAlSi_3O_8$	5.6
Plagioclase	$Na_{0.5}Ca_{0.5}Al_{1.5}Si_{2.5}O_8$	3.5
Calcite	$CaCO_3$	27.7
Illite	$(K,H_3O)(Al,Mg,Fe)_2(Si,Al)_4O_{10}[(OH)_2,(H_2O)]$	2.7
Biotite	$K(Mg,Fe)_3[(OH)_2AlSi_3O_{10}]$	4.0

Applied Geology Laboratory		ID: 117009
Well Name: NDIC No. 20552	Middle Bakken 8	Grenora Field
API No.: 33-105-02157-00-01	Lithology: Slightly silty, argillaceous limestone	Depth: 9613.0'

SEM

Observed Minerals

Mineral Phase	Mineral Phase
Cacite	Rutile
Quartz	Albite
Dolomite	Biotite
Illite	Zircon
K-feldspar	Apatite
Pyrite	Chromite

High-Magnification BSE Image Annotated with Examples of Mineral Phases Identified

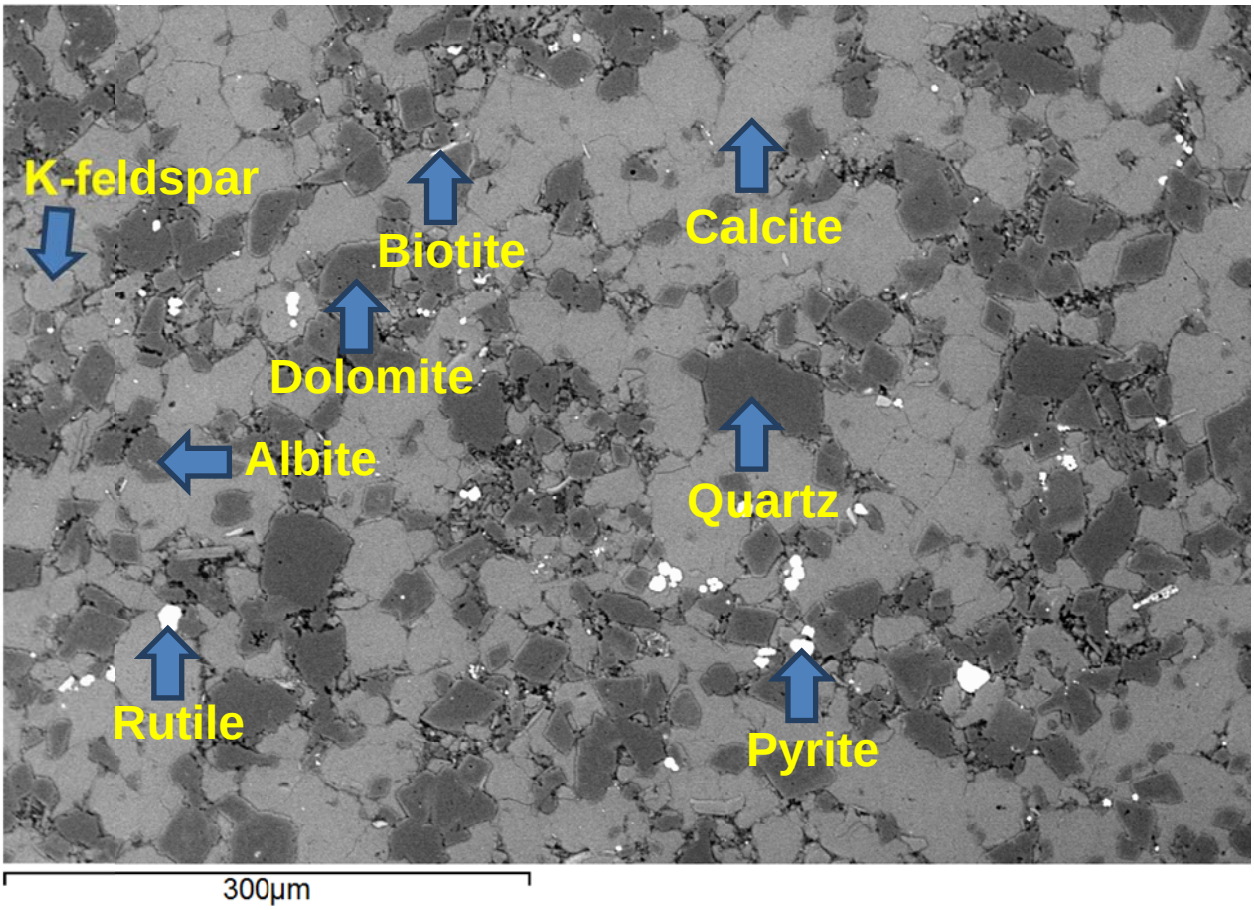

Additional High-Magnification BSE Images

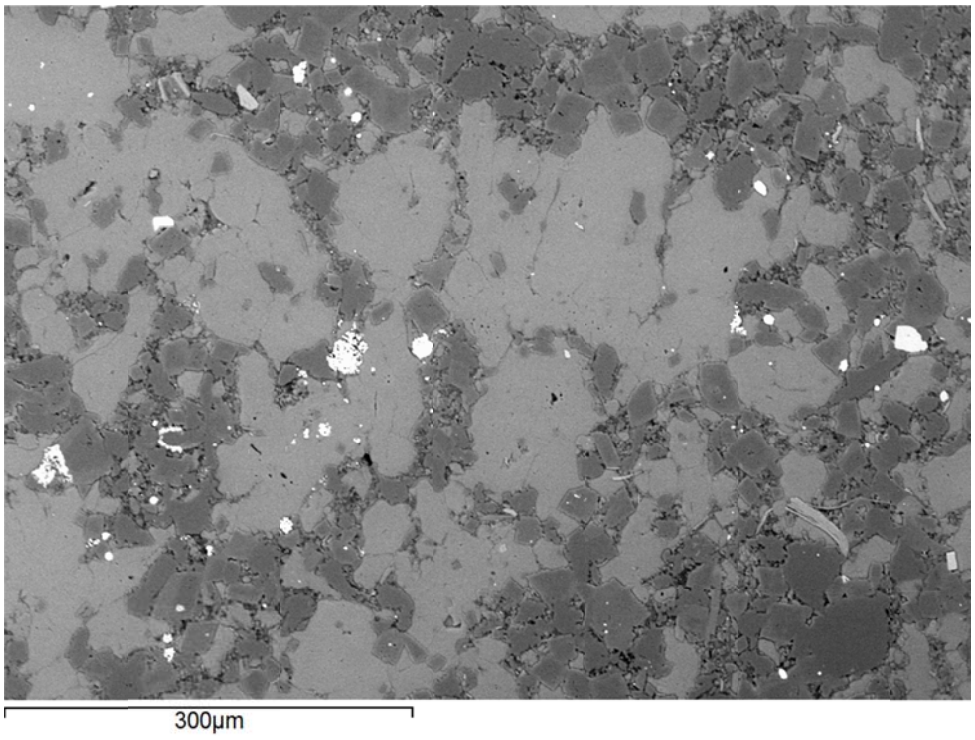

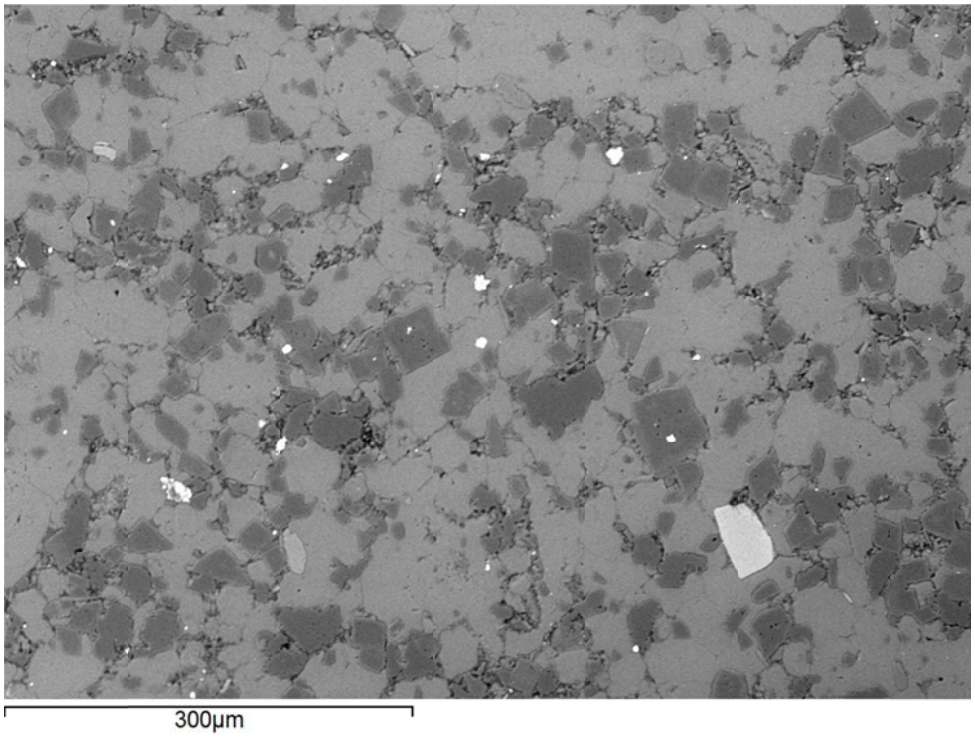

	Applied Geology Laboratory		ID: 117009
	Well Name: NDIC No. 20552	Middle Bakken 8	Grenora Field
	API No.: 33-105-02157-00-01	Lithology: Slightly silty, argillaceous limestone	Depth: 9613.0'

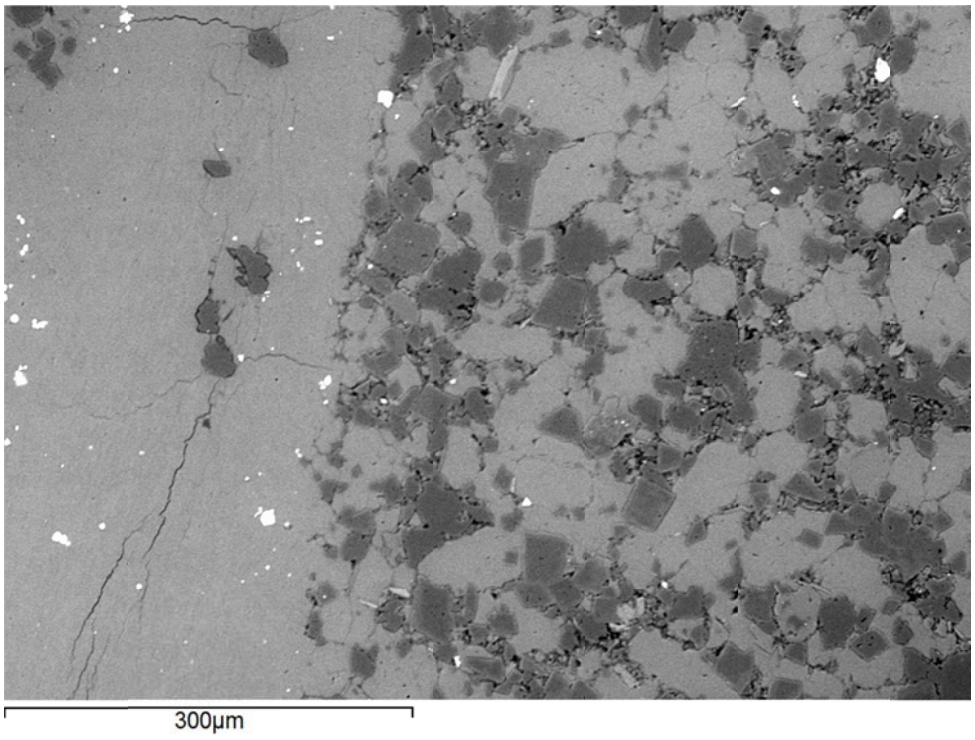

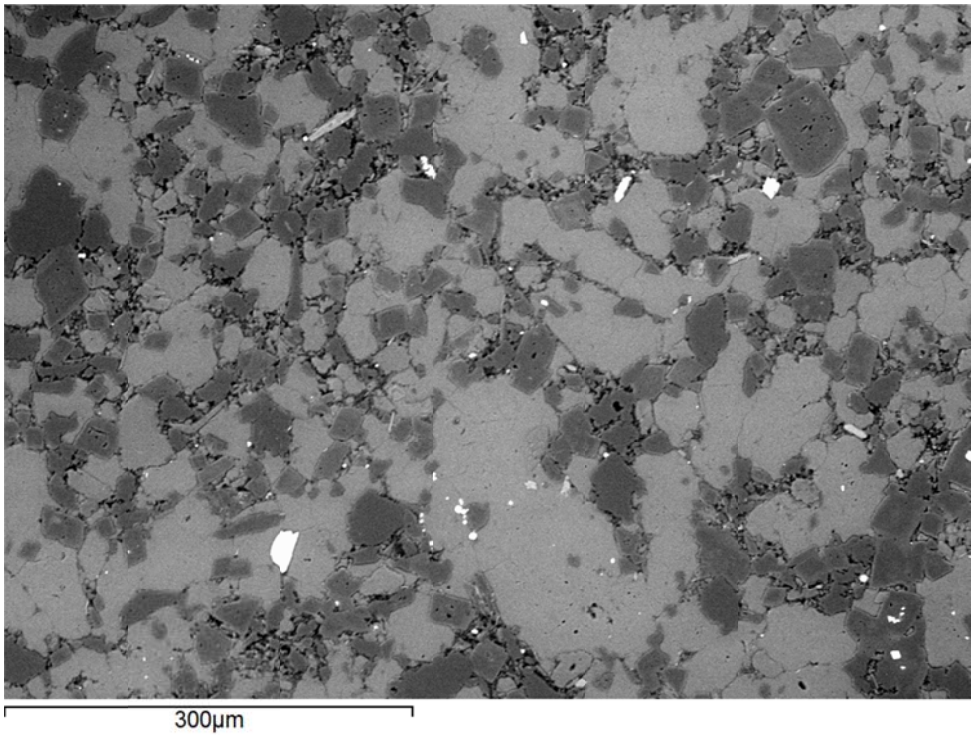

EERC Energy & Environmental Research Center® Putting Research into Practice UND THE UNIVERSITY OF NORTH DAKOTA	**Applied Geology Laboratory**		ID: 117009
	Well Name: NDIC No. 20552	Middle Bakken 8	Grenora Field
	API No.: 33-105-02157-00-01	Lithology: Slightly silty, argillaceous limestone	Depth: 9613.0'

SEM Mineral Map Image Overlaid on BSE Image with Mineral Phase 2D Area Percentages

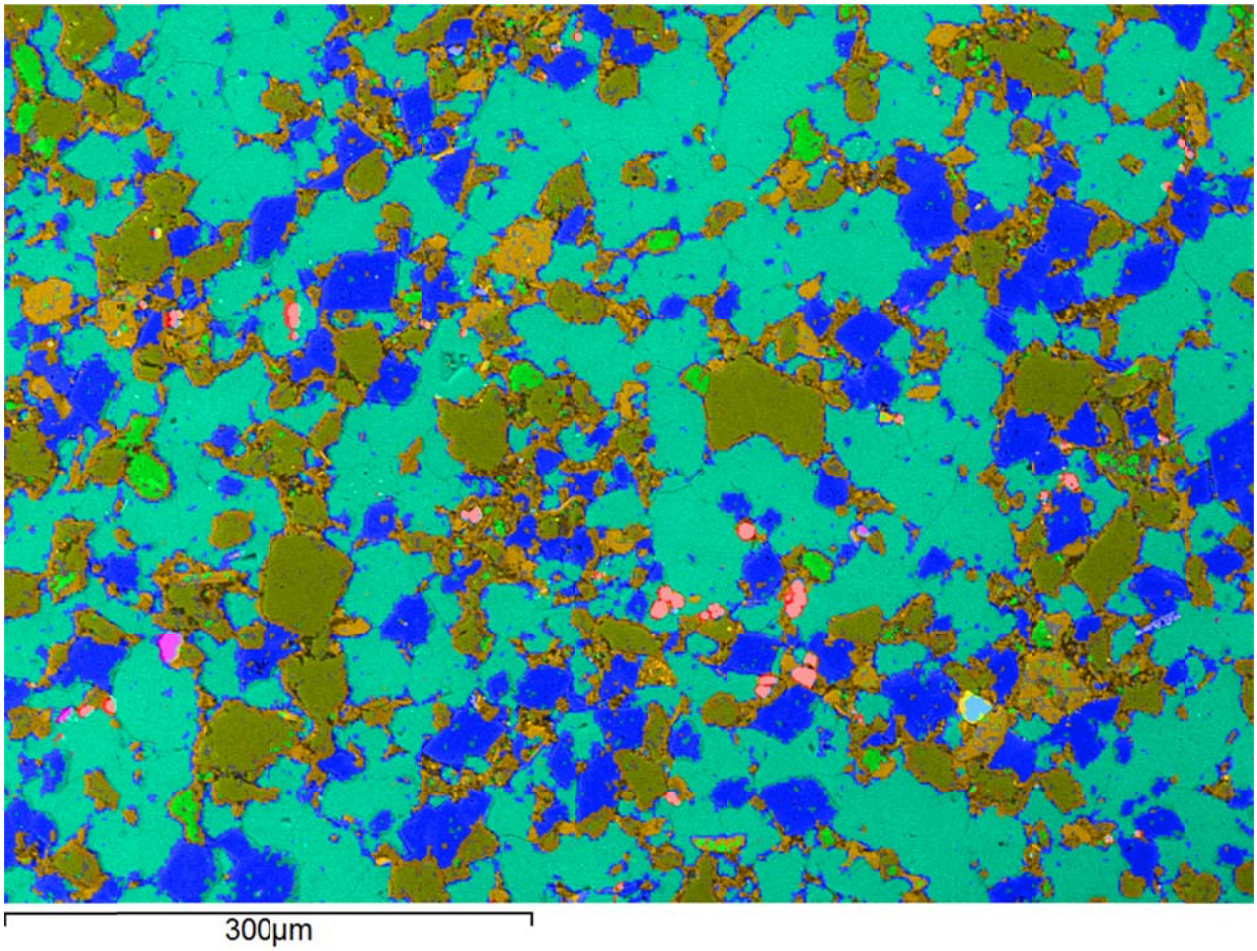

EERC Energy & Environmental Research Center® Putting Research into Practice UND THE UNIVERSITY OF NORTH DAKOTA	**Applied Geology Laboratory**		ID: 117010
	Well Name: NDIC No. 20552	Middle Bakken 8	Grenora Field
	API No.: 33-105-02157-00-02	Lithology: Silty, argillaceous dolostone	Depth: 9616.0'

SAMPLE PHOTOGRAPH

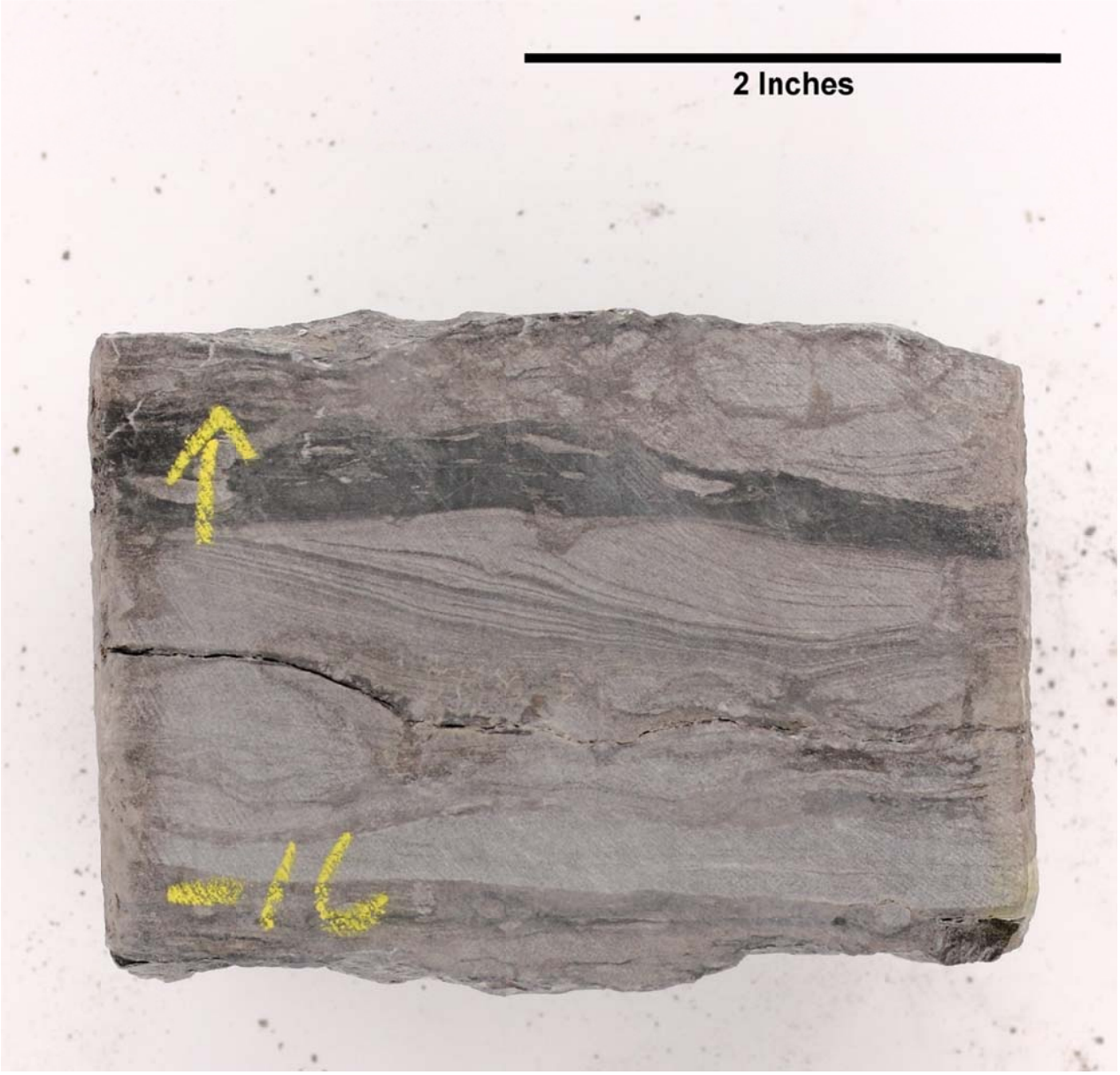

EERC Energy & Environmental Research Center® Putting Research into Practice UND THE UNIVERSITY OF NORTH DAKOTA	**Applied Geology Laboratory**		ID: 117010
	Well Name: NDIC No. 20552	Middle Bakken 8	Grenora Field
	API No.: 33-105-02157-00-02	Lithology: Silty, argillaceous dolostone	Depth: 9616.0'

PHOTOMICROGRAPHS

Transmission

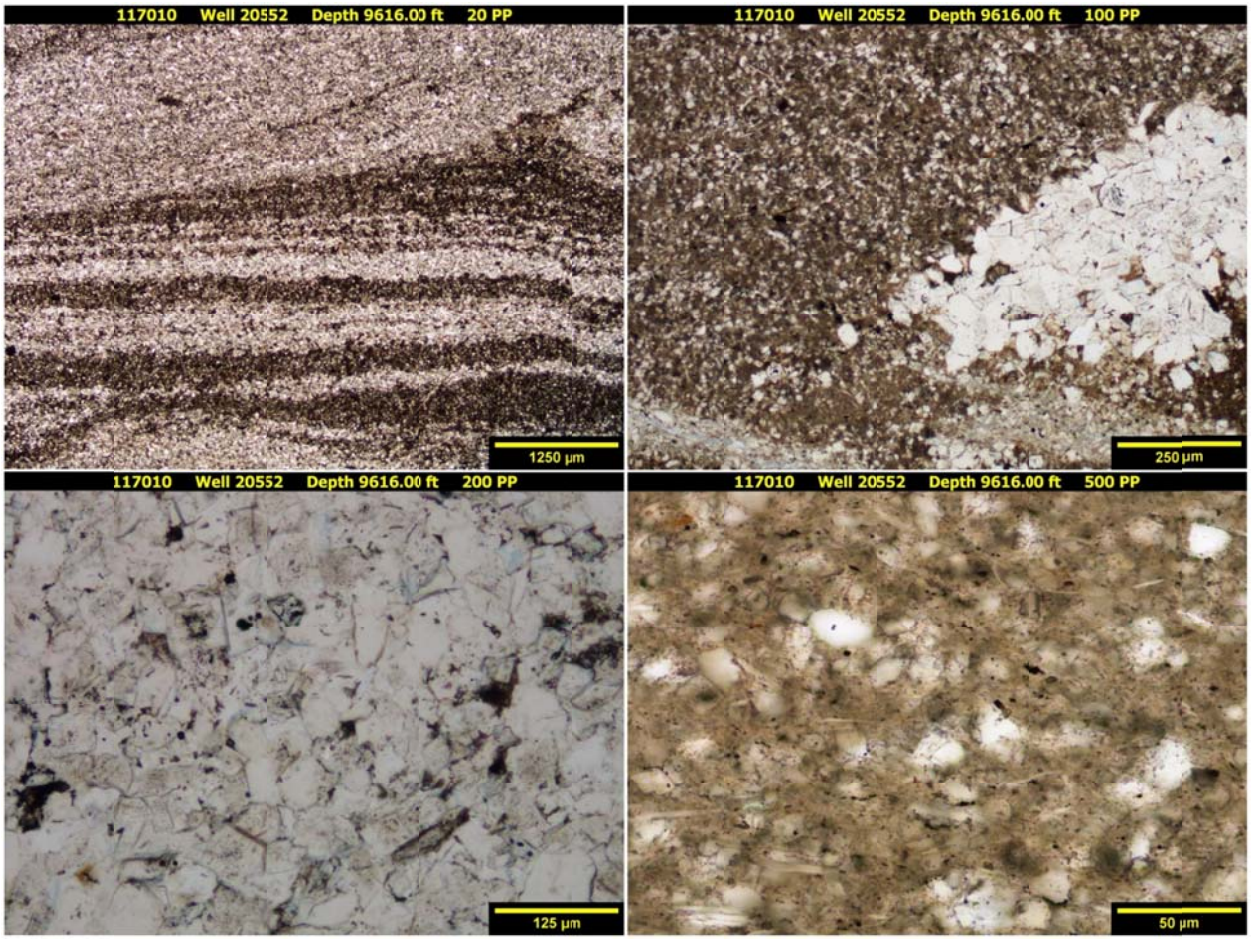

The sample from a depth of 9616.00 ft shows a silty, argillaceous dolostone. A high degree of bioturbation and localized laminations are present. It contains very fine grained, subangular to subrounded, monocrystalline quartz grains having moderately high overgrowths at a few localities where quartz grains are concentrated. Trace amounts of muscovite and feldspars are disseminated throughout. Extensive anhederal to euhedral dolomitization has occurred throughout the sample. No skeletal or non-skeletal calcareous grains remain. Disseminated pore-filling and replacement pyrite grains are observed throughout, concentrating in some areas. An abundant mineralogical component is clay, found throughout the sample creating a variety of burrowing features. Randomly-oriented filled and unfilled fractures are detected. Open fractures, predominately horizontal, observed are likely the result of the sample process. Filled fractures are more randomly-orientated and usually reside within the clay-rich areas. The infill is likely composed of organics, darker clays, and rare pyrite. A trace amount of inter-particle porosity is observed using standard petrographic techniques.

EERC Energy & Environmental Research Center® Putting Research into Practice UND THE UNIVERSITY OF NORTH DAKOTA	**Applied Geology Laboratory**		ID: 117010
	Well Name: NDIC No. 20552	Middle Bakken 8	Grenora Field
	API No.: 33-105-02157-00-02	Lithology: Silty, argillaceous dolostone	Depth: 9616.0'

Reflection

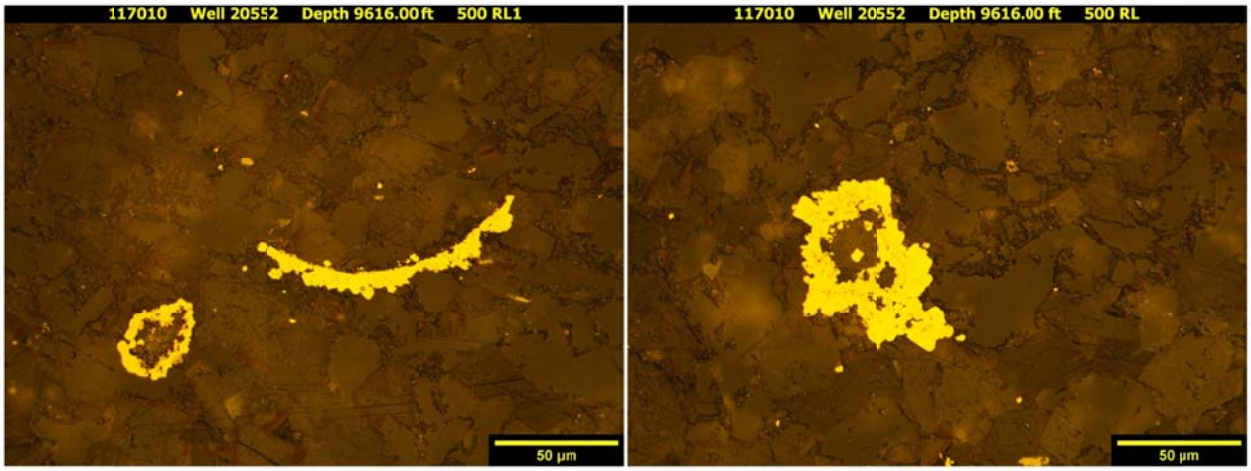

The sample from a depth of 9616.00 ft displays a moderate amount of euhedral and trace amounts of frambodial mineralization. Euhedral pyrite is observed largely as skeletal and non-skeletal grain replacement. Predominantly tiny individual spherical framboidal pyrite is observed as organic replacement found within clay concentrations. No larger, more mature sphereical framboidal occurrences are observed.

EERC Energy & Environmental Research Center® Putting Research into Practice UND THE UNIVERSITY OF NORTH DAKOTA	**Applied Geology Laboratory**		ID: 117010
	Well Name: NDIC No. 20552	Middle Bakken 8	Grenora Field
	API No.: 33-105-02157-00-02	Lithology: Silty, argillaceous dolostone	Depth: 9616.0'

Transmission and Fluorescence Whole-Slide Images

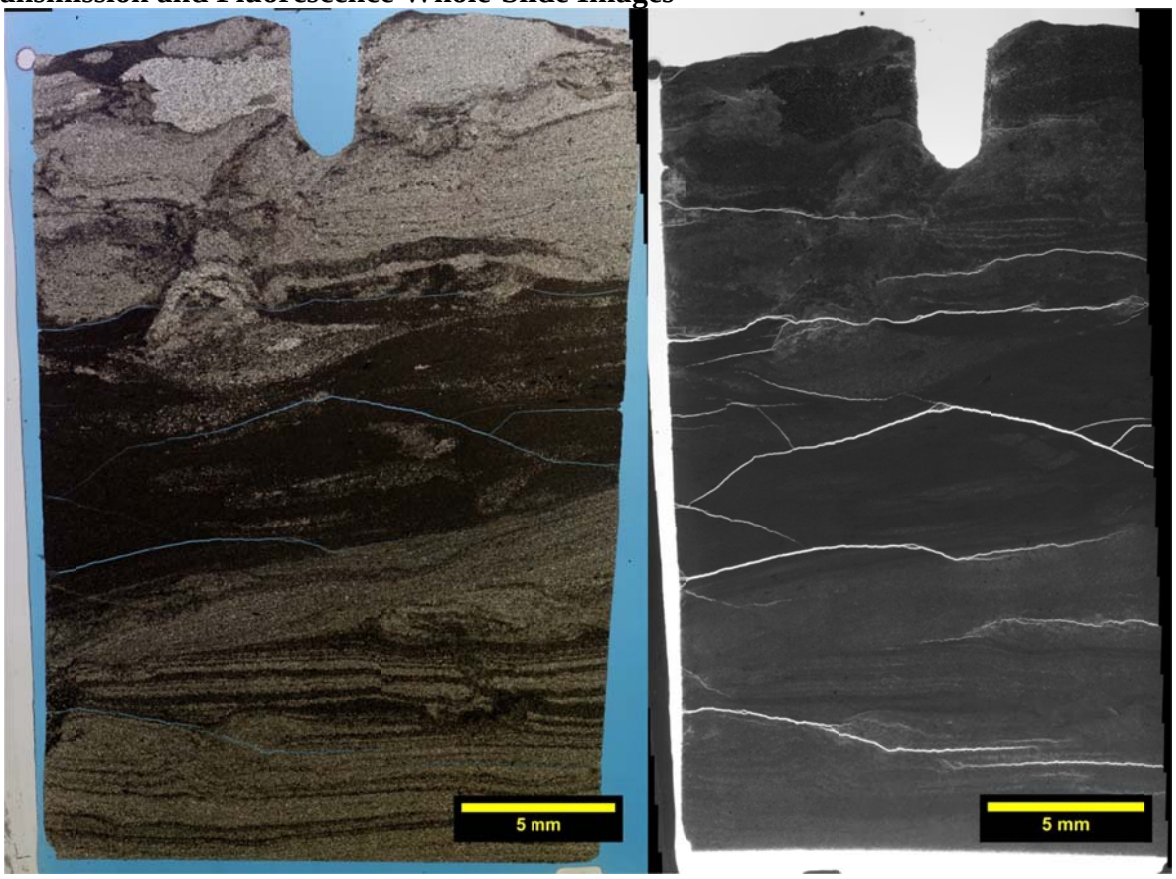

The sample collected at a depth of 9616.00 ft shows a predominantly bioturbated sample. Inter-particle-based micro-porosity exists inconsistently throughout the sample. Observed porosity typically concentrates within larger grained quartz and dolomite-rich zones. Lesser amounts of porosity are noted within areas of smaller grains and clay concentrations. Extensive interlocking anhedral to euhedral dolomitization and dispersed pyritization has occurred. These diagenetic events and very fine grain sizes are limiting factors of pore size and distribution. No natural fractures are likely observed. All open observed fractures are likely the result of sampling process, but may give insight to how the rock would perform under stress.

EERC Energy & Environmental Research Center® Putting Research into Practice UND THE UNIVERSITY OF NORTH DAKOTA	**Applied Geology Laboratory**		ID: 117010
	Well Name: NDIC No. 20552	Middle Bakken 8	Grenora Field
	API No.: 33-105-02157-00-02	Lithology: Silty, argillaceous dolostone	Depth: 9616.0'

XRF BULK CHEMICAL COMPOSITION

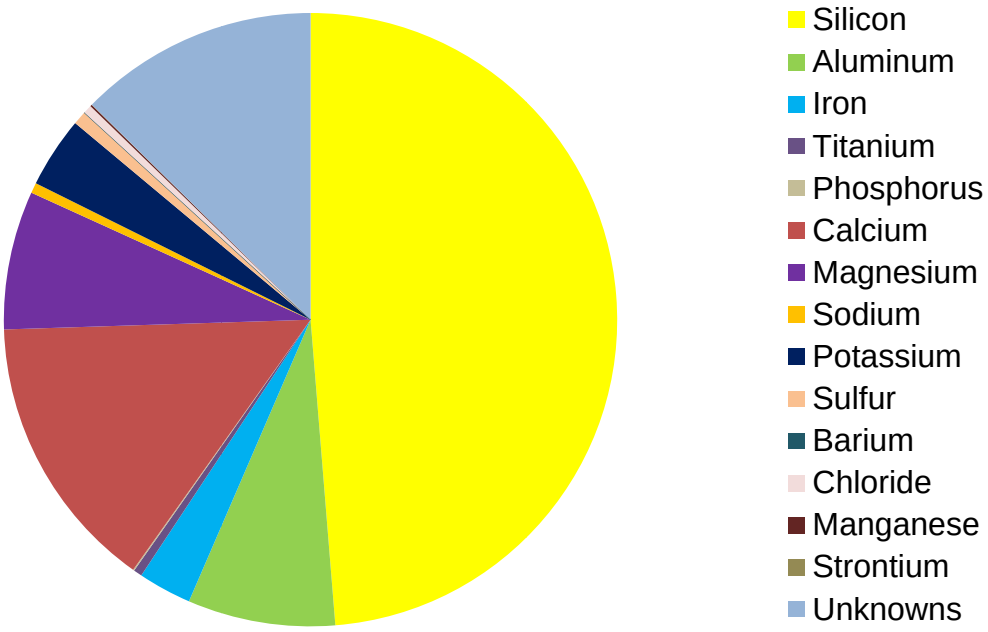

Element	Reporting Convention (Oxide)	Weight %
Si (silicon)	SiO_2	48.72
Al (aluminum)	Al_2O_3	7.78
Fe (iron)	Fe_2O_3	2.82
Ti (titanium)	TiO_2	1.45
P (phosphorus)	P_2O_5	0.06
Ca (calcium)	CaO	14.68
Mg (magnesium)	MgO	7.30
Na (sodium)	Na_2O	0.55
K (potassium)	K_2O	3.74
S (sulfur)	SO_3	0.72
Ba (barium)	BaO	0.00
Cl (chloride)	Cl	0.46
Mn (manganese)	MnO	0.09
Sr (strontium)	SrO	0.01
Unknowns	Due to the presence of carbonates	12.64
Total		100.02

	Applied Geology Laboratory		ID: 117010
EERC Energy & Environmental Research Center® Putting Research into Practice UND THE UNIVERSITY OF NORTH DAKOTA	Well Name: NDIC No. 20552	Middle Bakken 8	Grenora Field
	API No.: 33-105-02157-00-02	Lithology: Silty, argillaceous dolostone	Depth: 9616.0'

XRD MINERAL PHASE DISTRIBUTION

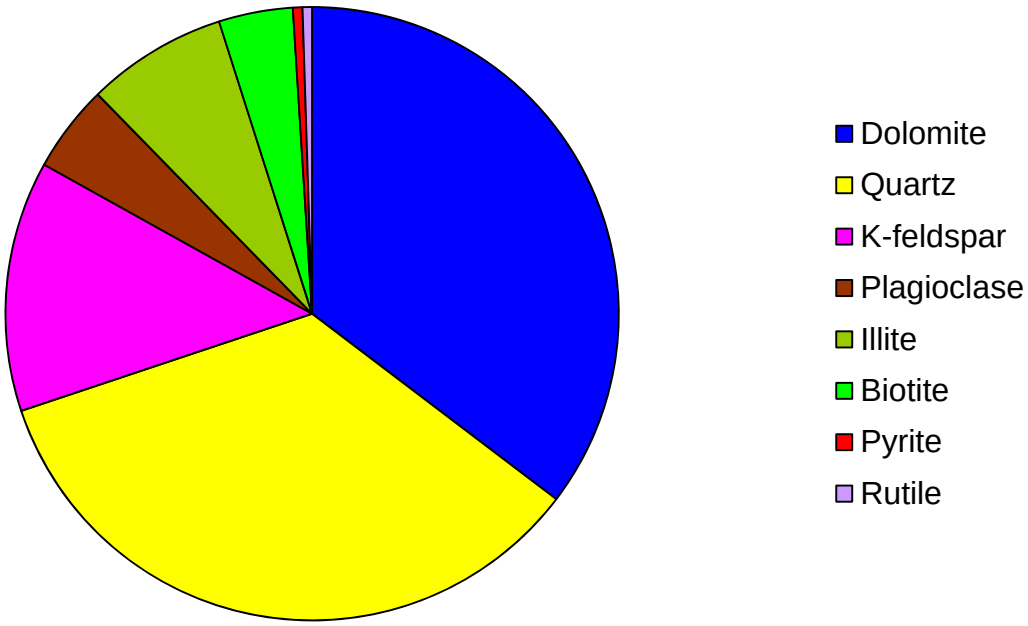

Mineral Phase	Formula	Weight %
Dolomite	$CaMg(CO_3)_2$	35.3
Quartz	SiO_2	34.5
K-feldspar	$KAlSi_3O_8$	13.2
Plagioclase	$Na_{0.5}Ca_{0.5}Al_{1.5}Si_{2.5}O_8$	4.6
Illite	$(K,H_3O)(Al,Mg,Fe)_2(Si,Al)_4O_{10}[(OH)_2,(H_2O)]$	7.4
Biotite	$K(Mg,Fe)_3[(OH)_2AlSi_3O_{10}]$	3.9
Pyrite	FeS_2	0.5
Rutile	TiO_2	0.5

EERC Energy & Environmental Research Center® Putting Research into Practice UND THE UNIVERSITY OF NORTH DAKOTA	**Applied Geology Laboratory**		ID: 117010
	Well Name: NDIC No. 20552	Middle Bakken 8	Grenora Field
	API No.: 33-105-02157-00-02	Lithology: Silty, argillaceous dolostone	Depth: 9616.0'

SEM

Observed Minerals

Mineral Phase	Mineral Phase
Dolomite	Illite
Pyrite	K-feldspar
Apatite	Biotite
Quartz	Rutile

High-Magnification BSE Image Annotated with Examples of Mineral Phases Identified

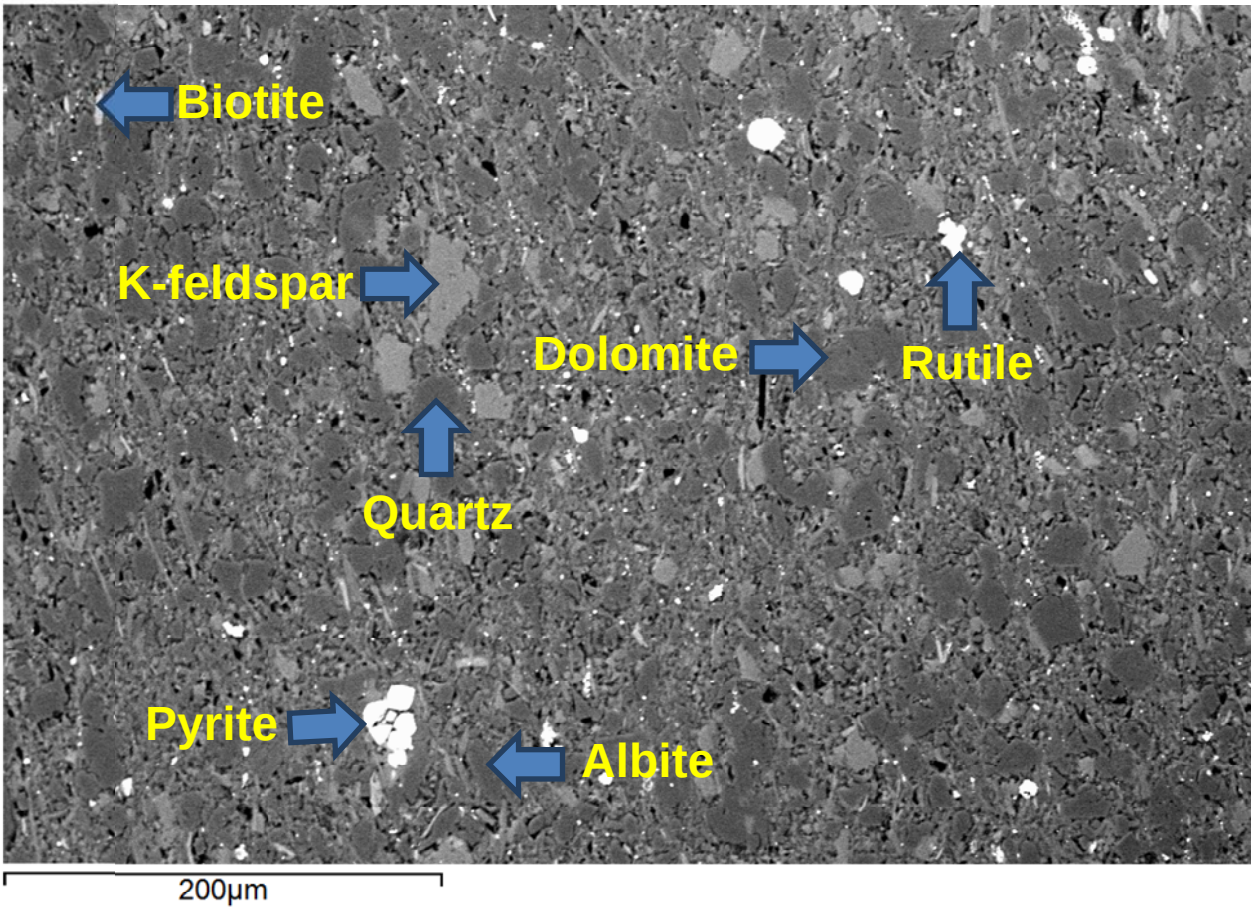

Additional High-Magnification BSE Images

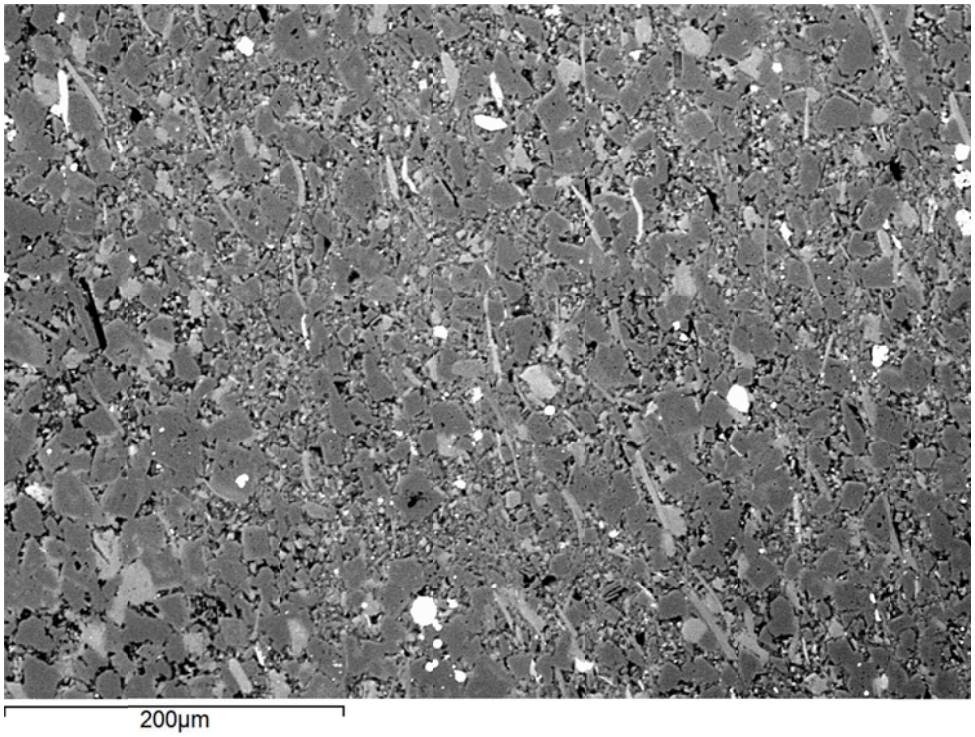

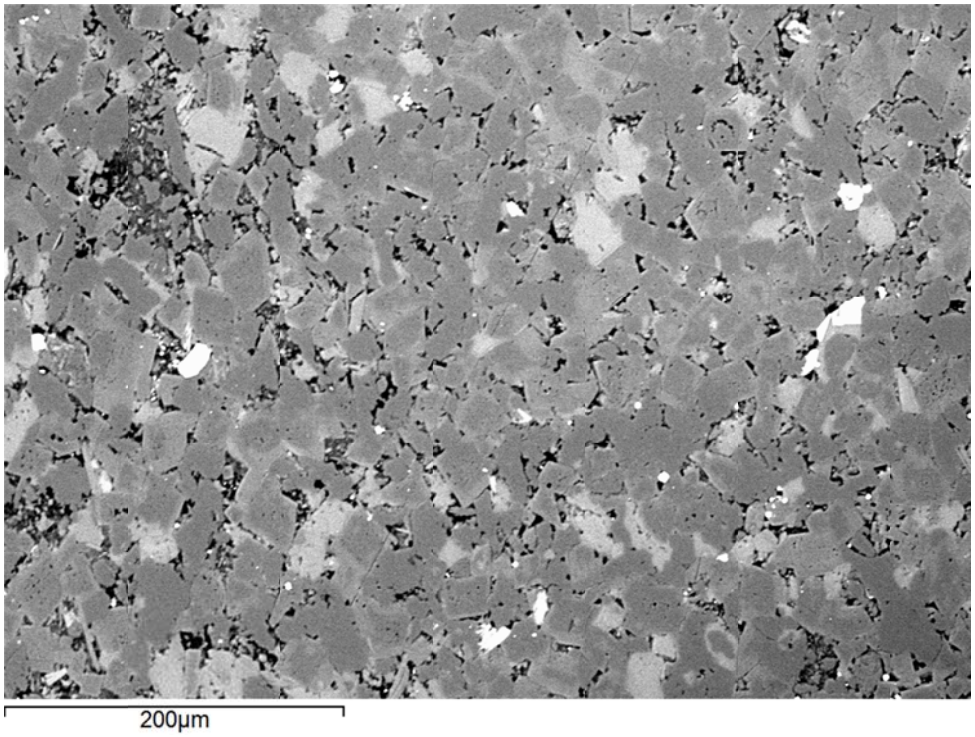

	Applied Geology Laboratory		ID: 117010
EERC Energy & Environmental Research Center® Putting Research into Practice UND THE UNIVERSITY OF NORTH DAKOTA	Well Name: NDIC No. 20552	Middle Bakken 8	Grenora Field
	API No.: 33-105-02157-00-02	Lithology: Silty, argillaceous dolostone	Depth: 9616.0'